FLAVOUR MIXING
and
CP VIOLATION

Moriond Workshop on Heavy Quark
Flavour Mixing and CP Violation

La Plagne - Savoie - France,
January 13-19, 1985

FLAVOUR MIXING AND CP VIOLATION

ISBN 2-86332-031-9

Editions Frontieres
B.P. 44
91190 GIF-SUR-YVETTE — France

Printed in Singapore by Kim Hup Lee
Printing Co. Pte. Ltd.

Proceedings of the

FIFTH MORIOND WORKSHOP

La Plagne – Savoie – France, January 13–19, 1985

FLAVOUR MIXING and CP VIOLATION

edited by
J. Tran Thanh Van

The Fifth Moriond Workshop on

FLAVOUR AND CP VIOLATION

was organized by

J.D. BJORKEN
G. KALMUS
L. MONTANET
L. OLIVER
E. PASCHOS
and J. TRAN THANH VAN

Associated Editors: L. Montanet
L. Oliver
A. Pottier

FOREWORD

The fifth Moriond Workshop of the XXth Rencontres de Moriond was held at La Plagne, Savoie, (France) from January 13 to January 19, 1985.

The main purpose of the Rencontres de Moriond is to discuss recent developments in contemporary physics and also to promote effective collaboration between experimentalists and theorists in similar fields. By bringing together a relatively small number of participants, we hope to develop better humain relations as well as a more thorough and detailed discussion of the contributions in an informal and friendly atmosphere.

The first workshop (1981) was devoted to Lepton pair production, the second one (1982) to New flavour production, the third one (1983) to Antiproton-proton physics and the W discovery and the fourth one (1984) to massive neutrinos and their implication in astrophysics and particle physics. This year, we focus the workshop on heavy quark production and decay properties, flavour mixing and CP violation. It is hoped that this confrontation of ideas between experimentalists and theorists in this rapidly evolving field allows to deepen our knowledge of the basic structure of matter.

I would like to thank the program committee members : K. Berkelman, J. D. Bjorken, J. Dorfan, G. Kalmus and especially the coordinators : L. Montanet, L. Oliver and E. Paschos for the hard work of organizing and preparing the scientific program and the conference secretaries J. Boratav, L. Norry, A. Pottier and Le Van Suu who have devoted much of their time and energy to the success of the fifth Moriond Workshop.

I am also grateful to Ms N. Pascualena who contributed through her hospitality and cooperation to the well-being of the participants, enabling them to work in a relaxed atmosphere.

J. Tran Thanh Van

CONTENTS

I – PRODUCTION PROPERTIES OF HEAVY FLAVOURS

II - DECAY PROPERTIES OF HEAVY FLAVOURS

III - STANDARD MODEL AND CP VIOLATION

UPSILON SPECTROSCOPY

Terrence Jensen
Department of Physics
The Ohio State University
Columbus, Ohio 43210

Abstract

Recent results on $b\bar{b}$ spectroscopy are presented. Searches by the CLEO collaboration for the inclusive decay $\Upsilon(1S) \to \gamma X$ and the exclusive decay $\Upsilon(1S) \to \gamma\pi^+\pi^-$ are discussed, and upper limits for these processes are presented. Evidence from CLEO and CUSB for the production of $\Upsilon(5S)$ and $\Upsilon(6S)$ resonances in e^+e^- collisions is presented.

Introduction

In this report, I discuss recent developments in $b\bar{b}$ spectroscopy, with emphasis on results obtained by the CLEO collaboration at the Cornell Electron Storage Ring (CESR).

The level diagram for the $b\bar{b}$ system is shown in Fig. 1. As indicated, a number of γ and 2π transitions among the bound states are predicted. Many of these transitions have been observed, and their measured properties found to be in fairly good agreement with theoretical expectations .[1] In Fig. 2 the $^3S_1$ states are observed as resonances in the total cross section for e^+e^- → hadrons. The widths of the first three resonances are determined by the spread in beam energies, whereas the fourth resonance, above the threshold for $B\bar{B}$ production, is noticably broader. The study of B decay is a separate subject which will be discussed later in this conference by my colleague T. Gentile.

The past year has seen little new information on the bound state spectroscopy; rather, the results presented below have come from the two extremes of the spectrum. At the low end there has been much interest concerning the possible existence of a radiative transition from the $\Upsilon(1S)$ to a narrow state at 8.3 GeV. The second topic concerns the recent observations by the CLEO and CUSB groups of new structure above the $B\bar{B}$ threshold.

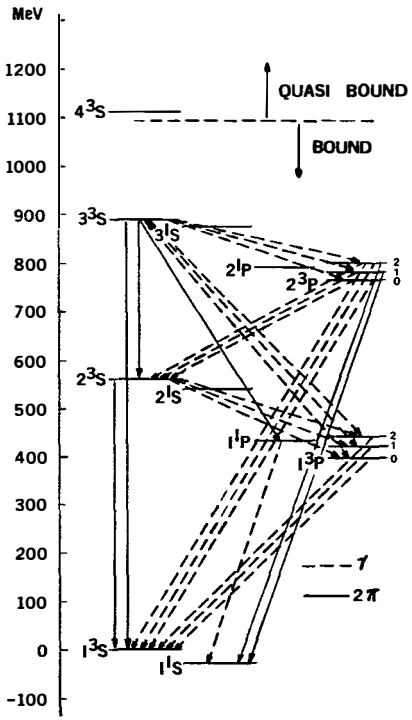

Fig. 1. Energy levels for the $b\bar{b}$ system showing some of the expected transitions.

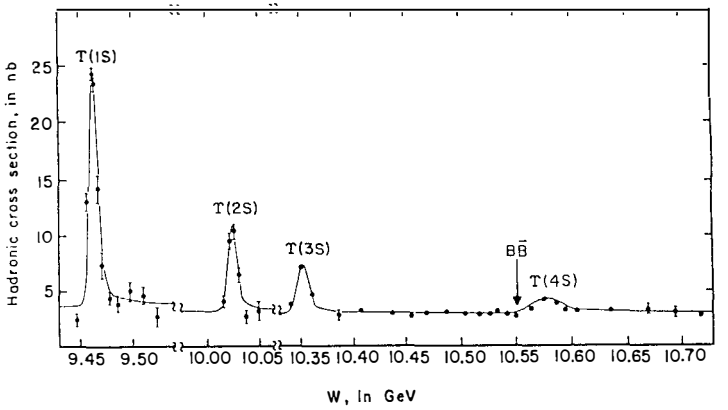

Fig. 2. The cross section for e^+e^- → hadrons in the upsilon energy range.

Search for Photon Transitions from the Υ(1S)

Much excitement was generated last summer when the Crystal Ball group reported evidence for a radiative decay, Υ(1S) → γζ, with the following properties:[2]

E_γ = (1071±8±21) MeV
M_ζ = (8322±8±24) MeV
Γ_ζ < 80 MeV
B[Υ(1S) → γζ] = (0.47±0.11±0.26)%.

The possibility that this was the long sought Higgs particle made it very desirable to seek confirmation of this result. Hence, CESR operated at the Υ(1S) energy from August to November 1984.

The CLEO detector, shown in Fig.3, is not optimized for photon detection. The shower counters, composed of lead and proportional tubes, have energy resolution $\delta E/E = 17\%/\sqrt{E}$. Therefore, we decided to insert a 10% lead converter between the vertex detector and the inner drift chamber, and use the drift chamber in the 1.0 Tesla magnetic field as a pair spectrometer. Using this technique, we achieve very good energy resolution ($\delta E/E = 1.4\%$ for a 1 GeV photon), but pay in terms of efficiency (2.5% after accounting for geometrical acceptance, reconstruction efficiency, and cuts to eliminate background).

Preliminary results from 308,000 hadronic events are shown in Fig. 4. We have fit the spectrum to a smooth background plus a Gaussian with a mean fixed at the value reported by Crystal Ball[2], and a width determined by our energy

resolution. This yields 11±15 events for a 90% C. L. upper limit of $B[\Upsilon(1S) \to \gamma\varsigma] < 0.45\%$. Unfortunately, this does not provide a very restrictive test of the Crystal Ball result.

If the ς were a Higgs, some models[3] would predict a large branching ratio for $\varsigma \to \tau^+\tau^-$. CLEO has searched for this signature by selecting events consistent with being a two-pronged τ-pair plus an associated photon. In order to reduce background, we required that one of the charged particles be identified as a muon, that the total charged energy be less than 8.0 GeV, and that at least one track have momentum less than 3.5 GeV/c. In these candidate events we searched for photons in the shower counters, limiting our search to regions away from charged-track trajectories, and eliminating photons which matched with another photon to form a π^0. Application of additional cuts to eliminate background from initial-state and final-state radiation and from cosmic rays reduced the overall efficiency to ~1%. From 202,000 resonant $\Upsilon(1S)$ decays we have observed two events which could be consistent with the decay $\Upsilon(1S) \to \gamma\varsigma(8.3) \to \gamma\tau^+\tau^-$. The first of these events has a photon energy of 752 MeV and the other has a photon energy of 1070 MeV. The preliminary result of this analysis is a 90% C. L. upper limit for the product branching ratio $B[\Upsilon(1S) \to \gamma\varsigma(8.3) \to \gamma\tau^+\tau^-] < 0.3\%$. Once again, this is not restrictive enough to be in contradiction with the original signal reported by Crystal Ball.

These searches by the CLEO group have suffered from low efficiency. By contrast, the CUSB detector, composed of sodium iodide and BGO crystals, has relatively good efficiency and resolution for photon detection. P. Franzini will report later at this conference on a more sensitive test of the Crystal Ball result.[4]

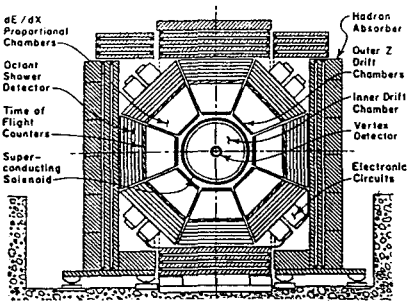

FIG. 3. End View of the CLEO detector.

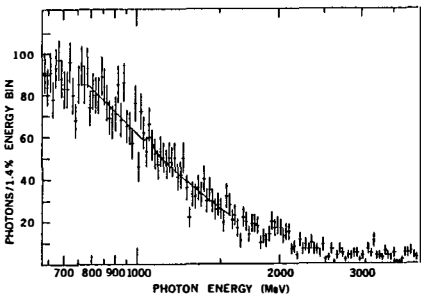

Fig. 4. Inclusive photon spectrum for $\Upsilon(1S)$ decays. (CLEO, preliminary)

New Structure Above $B\bar{B}$ Threshold

Figure 2 shows the cross section for e^+e^- → hadrons in the upsilon region as it was known a little over a year ago. Since that time CLEO has collected 70 pb^{-1}, and CUSB 123 pb^{-1} of data in the energy range $10.6 < W < 11.25$ GeV. The results[5,6] of this scan are presented in Figure 5 in terms of the variable $R = \sigma(e^+e^- \rightarrow \text{hadrons})/\sigma_{\mu\mu}$ (for the CUSB data, $R_{visible}$, which is not corrected for efficiency, is plotted). The scales for these plots are quite different from those of Fig. 2. The $\Upsilon(4S)$ is now the prominent feature followed by additional wiggles at higher energies. The two data samples show similar features: a shoulder just above the $\Upsilon(4S)$, a prominent bump near 10.9 GeV, and indications of another bump near 11.0 GeV (the latter being less prominent in the CUSB data).

From experiences in the charm sector[7], it is expected that the interpretation of this structure will be very complicated. Potential models predict that several S-state resonances will appear in this energy range.[8]

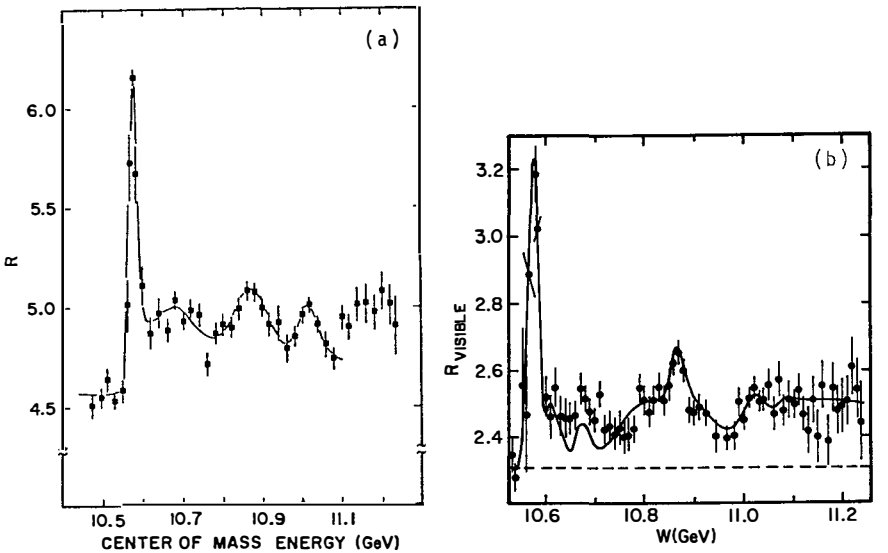

Fig. 5. (a) Corrected R ($\sigma_{had}/\sigma_{\mu\mu}$) versus center of mass energy as measured by CLEO. (b) R_{vis} versus center of mass energy as measured by CUSB. See text for description of curves.

However, predictions for the masses and leptonic widths of these resonances are not straightforward. It is generally agreed that there will be mass shifts caused by coupled-channel effects above the $B\bar{B}$ threshold.[9] The magnitude of these shifts will be influenced by S-D mixing as well as thresholds for B^*, $B_s\bar{B}_s$ and $B\bar{B}$ + nπ production. As will be discussed below, there is little experimental information regarding these thresholds. In addition, there has recently been speculation[10] concerning mixing of $b\bar{b}$ and $b\bar{b}g$ states.

In fitting the data, two different approaches have been followed. One method is to simply fit the structure to several Gaussians plus a continuum background. A more detailed fit requires predictions from a specific model.

Owing to the limited statistics and lack of experimental information on thresholds for higher mass B meson states, CLEO has chosen the first method for extracting information on this new structure.[5] We have corrected the hadronic cross section by extrapolating the continuum level below the Υ(4S) to the region above it and applying the 2-jet efficiency (80±2%) for this level. The excess was then corrected by using the $B\bar{B}$ efficiency (91±2%) calculated at the Υ(4S). We have fit the data between 10.5 GeV and 11.1 GeV to four Gaussians with radiative tails[11] and a single step in R. Data above 11.1 GeV have been excluded from the fit. The sharp rise in total cross section at this energy followed by a leveling off may be due to the onset of $B\bar{B}$ + nπ production. The results of the fit are plotted over the data in Fig. 5(a), and the parameters for the resonances are displayed in Table I. The leptonic width is calculated from the integrated hadronic cross section in the standard manner, $\Gamma_{ee} = (M^2/6\pi^2)\int dE\sigma_{had}$. The rather large systematic errors in these widths are a result of the insensitivity of the fit to the level of continuum background.

TABLE I. The parameters measured by CLEO for the four radiative Gaussians shown in Fig. 5(a).

Resonance	Mass (GeV)	Γ (MeV)	Γ_{ee} (keV)
Υ(4S)	10.5775 ± 0.0007 ± 0.004	20 ± 2 ± 4	0.192 ± 0.007 ± 0.038
	10.684 ± 0.010 ± 0.008	131 ± 27 ± 23	0.20 ± 0.05 ± 0.10
Υ(5S)	10.868 ± 0.006 ± 0.005	112 ± 17 ± 23	0.22 ± 0.05 ± 0.07
Υ(6S)	11.019 ± 0.005 ± 0.007	61 ± 13 ± 22	0.095 ± 0.03 ± 0.035

The CUSB group has used a coupled-channel model to fit their data.[6] They assume that the triplet S-wave states (4S,5S,6S,7S) decay mostly into $B\bar{B}$, $B\bar{B}^*$ + $B^*\bar{B}$, $B^*\bar{B}^*$, $B_s\bar{B}_s$, $B_s\bar{B}_s^*$ + $B_s^*\bar{B}_s$, and $B_s^*\bar{B}_s^*$ channels. In addition, they account for $B\bar{B}$ + nπ production by adding a smooth step in R. Estimates for the various thresholds are taken from theoretical predictions.[8,12] The results of the fit

are shown superimposed on the data in Fig. 5(b), and broken down according to the different contributions in Fig. 6. Table II gives the measured properties of the $\Upsilon(4S)$, $\Upsilon(5S)$, and $\Upsilon(6S)$ resonances. These parameters are in fairly good agreement with the results obtained by CLEO. The shoulder above the $\Upsilon(4S)$ is found by CUSB to be due primarily to production of excited B mesons. From the inclusive photon spectrum, CUSB has found evidence for B^* production at a mass difference $M_{B^*}-M_B = 50$ MeV.[13]

TABLE II. Summary of resonance properties as measured by CUSB.

Resonance	Mass (GeV)	Γ (MeV)	Γ_{ee} (keV)
$\Upsilon(4S)$	10.5774 ± 0.001	25 ± 2.5	0.283 ± 0.037
$\Upsilon(5S)$	10.845 ± 0.020	110 ± 15	0.365 ± 0.070
$\Upsilon(6S)$	11.02 ± 0.03	90 ± 20	0.156 ± 0.040

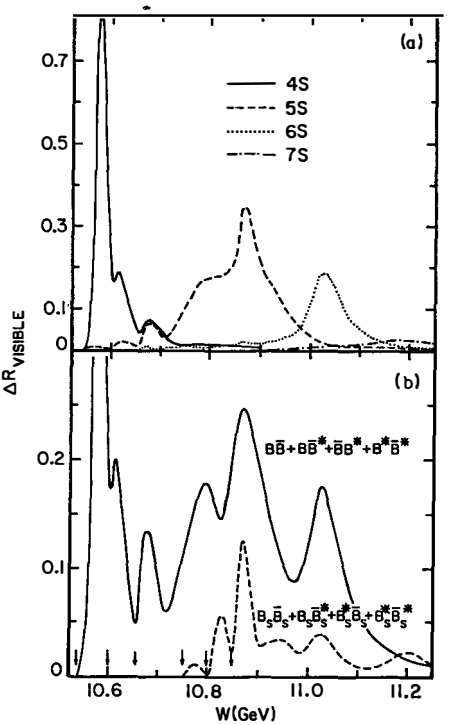

Fig. 6. (a) Contributions of the four Υ's to R for two-body decays. (b) Contribution to R from B mesons (solid curve) and strange B mesons (dashed curve). Arrows indicate thresholds; $B\bar{B}$(10.545 GeV), $B\bar{B}^*$(10.600 GeV), $B^*\bar{B}^*$(10.655 GeV), $B_s\bar{B}_s$(10.751 GeV), $B_s\bar{B}_s^*$(10.801 GeV), $B_s^*\bar{B}_s^*$(10.851 GeV).

So far it has not been possible to fully reconstruct a significant number of final states containing B mesons.[14] Therefore, one must turn to other methods to unravel the structure. Figure 7 shows the average charged multiplicity as a function of center of mass energy. The first point on this plot is from the continuum below the $\Upsilon(4S)$. The difference in average multiplicity above the $\Upsilon(4S)$ relative to below the $\Upsilon(4S)$ is consistent with the excess hadronic cross section above the $\Upsilon(4S)$ being dominated by B meson production. However, with the limited statistics it is not possible to say whether we have crossed a threshold for $B\bar{B} + n\pi$ production.

Another tool for determining the general nature of the final state is the event shape, which can be quantified, for example, in terms of the Fox-Wolfram variable[15], R_2 ($=H_2/H_0$). Figure 8 shows the cross section ratio, R, for those events satisfying $R_2 < 0.3$. This emphasizes spherical events expected for production of B mesons near threshold. Comparing with Fig. 5, we observe the same general structure, again suggesting that the excess hadronic production could be due to B meson decay.

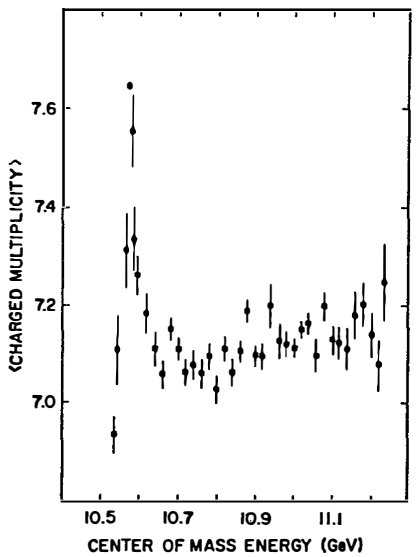

Fig. 7. Average observed charged multiplicity versus center of mass energy.

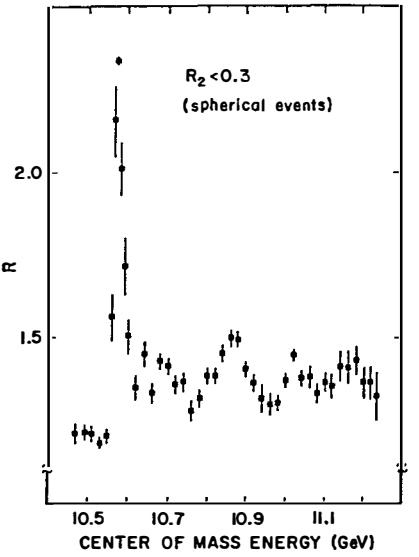

Fig. 8. Corrected R versus center of mass energy for events with $R_2<0.3$.

The CLEO detector has good efficiency for identifying electrons and muons.[16] In Fig. 9 we show the measured contribution to R from events containing a high energy lepton. For this plot we have chosen spherical events ($R_2 < 0.3$), and selected electrons with momenta greater than 1.0 GeV/c and muons with momenta greater than 1.2 GeV/c. The curve is of the same shape shown in Fig. 5(a), normalized to the height of the $\Upsilon(4S)$. The data follow the curve quite well, indicating that the decay products of the higher mass structure have semileptonic branching ratios comparable to those of the B meson.

The threshold for $B_s\bar{B}_s$ production is also expected to lie in this energy range. As evidence for B_s production, CLEO has looked for increases in the yields of K, Λ, ϕ, and F particles as a function of center of mass energy. Unfortunately, the efficiency for identifying these particles was too small to enable us to make a significant measurement.

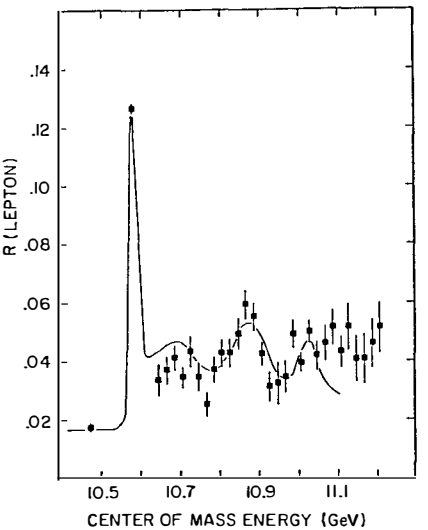

Fig. 9. Visible R for inclusive electron and muon production versus center of mass energy. The curve is the same as in Fig. 5(a) normalized to the height of the $\Upsilon(4S)$.

Summary

The subject of radiative transitions from the $\Upsilon(1S)$ remains somewhat controversial. The CLEO group sees no evidence for the $\zeta(8.3)$, but the upper limit does not exclude the original measurement by Crystal Ball. New results from CUSB are eagerly awaited.

Rich new structure above the $B\bar{B}$ threshold has been observed by CLEO and CUSB. The interpretation of the data is complicated by model dependent

parameters, but there is fair agreement on the existence of two new resonances, the $\Upsilon(5S)$ and $\Upsilon(6S)$. To make further progress in understanding this structure, higher statistics and better particle identification are required. Ongoing improvements to both the CLEO and CUSB detectors and to the CESR machine should make this possible in the near future.

These improvements should also aid in better understanding the bound-state spectroscopy. Notable gaps in the experimental knowledge are the properties of the singlet S states and the singlet P states.

Acknowledgements

I would like to thank my CLEO colleagues for their advice in preparing this talk, and especially R. Kass for proofreading this report. J. Lee-Franzini has provided me with the CUSB results on the structure above the $\Upsilon(4S)$. Finally I thank the conference organizers for an enjoyable and stimulating meeting.

This work was supported by the Department of Energy and the National Science Foundation.

References

1. For a review of bound-state spectroscopy see P. M. Tuts, Proc. 1983 International Lepton/Photon Symposium, Cornell University.
2. Crystal Ball group, H. J. Trost, XXII International Conference on High Energy Physics, Leipzig, East Germany, 1984.
3. See, for example, H. Georgi, A. Manohar, and G. Moore, Phys. Lett. 149B, 234 (1984); P. N. Pandita, Phys. Lett. 151B, 51 (1985).
4. P. Franzini, these proceedings.
5. D. Besson et al., Phys. Rev. Lett. 54, 381 (1985).
6. D. M. J. Lovelock et al., Phys. Rev. Lett. 54, 377 (1985).
7. E. Eichten et al., Phys. Rev. D21, 203 (1980).
8. See, for example, W. Buchmuller and S.-H. H. Tye, Phys. Rev. D24, 132 (1981), and references therein.
9. Examples of coupled-channel models can be found in reference 7, as well as K. Heikkila, N. A. Tornqvist, and S. Ono, Phys. Rev. D29, 110 (1984); N. A. Tornqvist, Phys. Rev. Lett. 53, 878 (1984). See also reports by Tornqvist and Ono in these proceedings.
10. S. Ono, LPTHE Orsay 84/13, and these proceedings.
11. J. D. Jackson and D. L. Scharre, Nucl. Instr. Meth., 128, 13 (1975).
12. E. Eichten et al., Phys. Rev. D17, 3090 (1978), and D21, 313 (1980); E. Eichten, Phys. Rev. D22, 1819 (1980).
13. P. Franzini, these proceedings.
14. For results on B meson decay see S. Behrends et al., Phys. Rev. Lett. 50, 881 (1983); also T. Gentile, these proceedings.
15. G. C. Fox and S. Wolfram, Phys. Rev. Lett. 41, 1581 (1978).
16. A. Chen et al., Phys. Rev. Lett. 52, 1084 (1984).

EXPERIMENTAL EVIDENCE FOR THE B^* MESON

Paolo Franzini
Columbia University, New York, N.Y..10027

ABSTRACT

We have have observed production of monochromatic low energy photons in e^+e^- hadronic annihilations between 10.6 and 11.2 GeV. This signal is associated with production of b-flavored mesons and gives the first experimental evidence for the existence of vector $b\bar{u}$, $b\bar{d}$ mesons, B^*. The B^*-B mass difference is $52\pm2\pm4$ MeV.

The discovery of the T's[1], bound states of a b quark and a $\bar{b}$ antiquark, suggests the existence of $(b\bar{u})$, $(b\bar{d})$ etc. mesons. These states, called B mesons, were first proved to exist by the CUSB and CLEO collaborations through the observation of their semileptonic decays[2]. More recently CLEO has observed a few examples of non-leptonic B decays[3].

While the mass of the lowest B meson cannot be accurately predicted, it should be of the order of $M_{T'''}/2$ or about 5.2 GeV. Heavy-light $q\bar{q}$ states in s-waves can have J=0 (spin singlet, pseudoscalar mesons) or J=1 (spin triplet, vector mesons). For B-mesons, just as for strange and charmed mesons, the pseudoscalar state, B, is expected to be the lightest. The vector state, B^*, was

predicted several years ago to be ≈50 MeV heavier than the B[4]. For such small value for $\Delta M = M_{B^*} - M_B$ we expect the B^* to decay dominantly (>>99%) according to $B^* \to B + \gamma$, with a photon energy, in the B^* rest frame, given by $(M_{B^*}^2 - M_B^2)/(2 \times M_B) \approx 0.995 \times \Delta M$.

The CUSB collaboration has reported sometime ago[5] negative results in a search for monochromatic photons of $30 < E_\gamma < 90$ MeV in a large sample of T''' decays. This result implies that $BR(T''' \to B\bar{B}) \geq 95\%$ and confirms that the mesons reconstructed by CLEO are indeed B's rather than B^*'s.

Recently a large amount of data was collected at CESR at energies above the T'''. The cross section for $e^+e^- \to$ hadrons shows complicated structure above the b-flavor threshold[6,7]. A prominent peak is visible at 10.85 GeV which can be identified as the fifth upsilon state, T(5S). The increase in the e^+e^- annihilation cross section into hadrons above the threshold with respect to the value observed below has been proved to be due to the production of "free" $b\bar{b}$ quark pairs. A simple coupled channel calculation[8] explains quite well the shape of the cross section as observed by CUSB[6] and clearly and uniquely resolves the contributions to the cross section from the decays of T(4S), T(5S) and T(6S) into the six two-body final states: BB, BB^*, B^*B^*, B_sB_s, $B_sB_s^*$ and $B_s^*B_s^*$. Here B_s stands for $(b\bar{s})$ mesons and the particle antiparticle distinction is dropped for simplicity. In particular one finds that 1.3 B^* mesons are produced in average per $b\bar{b}$ pair for $10.6 < W < 11.2$ GeV. While this yield is large, the search for B^* mesons through the observation of a "line" in the inclusive photon spectrum from e^+e^- hadronic annihilations is very difficult. This is due mostly to:

i). $b\bar{b}$ production is only ≈8% of the hadronic cross section.

ii). B^* produced in the energy range $10.6 < W < 11.2$ GeV have momenta up to 500 MeV, resulting in considerable Doppler smearing.

iii). The efficiency and resolution degrade very rapidly for photon energies below 100 MeV.

The first evidence for a broad excess of photons around 50 MeV was observed using low resolution and high efficiency search codes on the data taken above threshold. No excess was instead found at the T''' nor below threshold. Other search codes and B tagging means were developed, all showing a clear signal from B^* decay. In the following I will concentrate mostly in proving that the observed photon signal is uniquely associated with $b\bar{b}$ pair production above threshold employing different methods for enriching the $b\bar{b}$ contents of the analyzed sample. We can do this in three ways:

i). Thrust cuts can be used to enrich the $b\bar{b}$ contents of the sample.

ii). Choose selected regions in center of mass energy, corresponding

to maximum B^* production.

iii). Tag B production by the presence of a high energy lepton (E>1.3 GeV) from B semileptonic decay[9].

Fig. 1a shows the inclusive photon spectrum for all hadronic annihilation events with W> 10.6 GeV, fitted with a third order polynomial plus a gaussian which is a good rapresentation of our experimental resolution folded with the doppler smearing due to the B^* motion. The subtracted signal (i.e. data minus fitted polynomial) is shown in figure 1d with the expected shape superimposed, showing very good agreement. The observed signal is 2112±424 photons for a significance of 5 standard deviations.

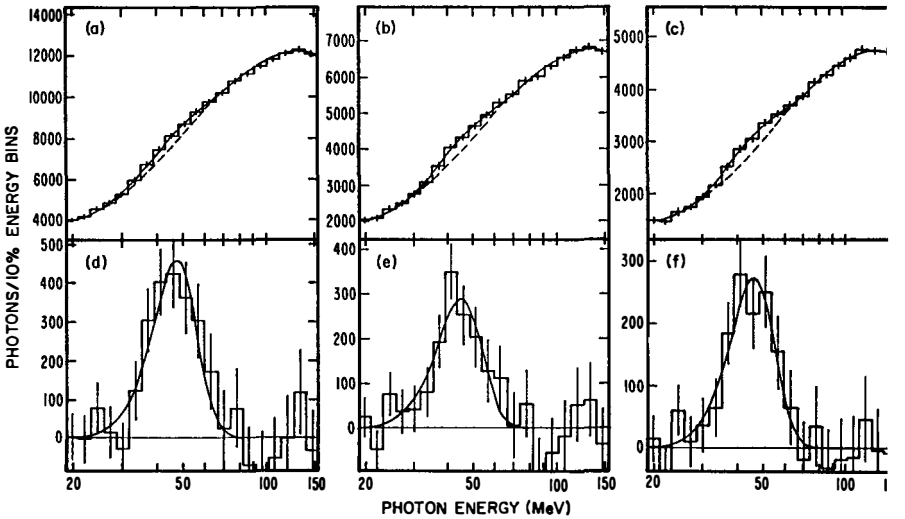

Figure 1. The inclusive photon spectrum from different data samples.

Figures 1b, 1e and 1c, 1f respectively show the signal for a thrust cut sample and for selected energy intervals. The results of applying these cuts are summarized in table I. In all three cases the quality of the fit is excellent and the fraction of observed photons is proportional to the amount of resonance production. Similar data sets from T''' decays and continuum annihilations below threshold do not show any excess above a third order polynomial fit.

Figure 2a shows the inclusive photon spectrum from hadronic annihilation events at center of mass energies greater than 10.6 GeV containing an electron or muon of energy greater than 1.3 GeV. Also shown is a composite sample of annihilations at the T''' peak plus continuum events with $W<M_{T'''}$ in order to dilute the "free" $b\bar{b}$ pair contents to the level above threshold, with the same requirement about the presence of a lepton. The $b\bar{b}$ pair contents above threshold

is increased from ≈8% to ≈33% by the requirement that a high energy lepton be present but the number of events is reduced by almost a factor 10. The photon spectrum from data above the T''' again shows a clear signal around 50 MeV, which is absent in the control sample. Figure 2b shows a bin by bin subtraction of the two spectra and a fit to the excess around 50 MeV with the computed resolution function mentioned above. In this way we obtain that the excess contains 123±28 counts for a statistical significance of 4.4 standard deviations.

All photon spectra shown are plotted versus the observed photon energy in the detector. Several correction are required to obtain the true photon energy, of which the largest (≈15%) is due to the inactive material between NaI layers in the detector.

Table I gives a summary of the observed counts, the corrected fraction of observed photons per $b\bar{b}$ produced pair and the corrected mean photon energy for the four data samples discussed.

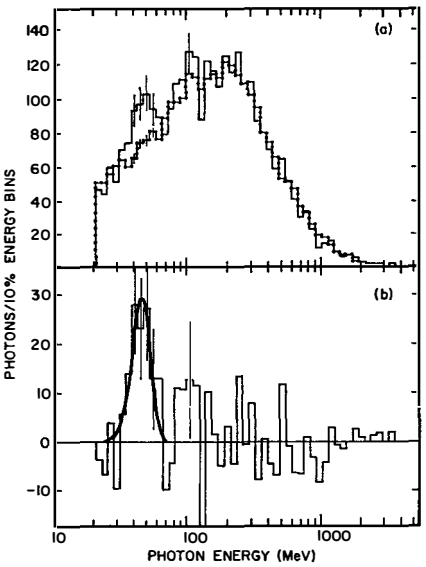

Figure 2. The inclusive photon from lepton tagged hadronic annihilations.

The first and last samples are essentially statistically independent and therefore we have observed production of monochromatic photons with a significance of 6.6 standard deviations, which we interpret as evidence for production of excited B mesons, B^*, in e^+e^- annihilations with $10.6<W<11.2$ GeV, followed by the decay $B^* \to B+\gamma$. These results also imply that 1.45 ± 0.35 B^* mesons per resonant events are produced in the above energy range, in good agreement with our coupled channel calculation.

TABLE I

	All data	T cut	W sel.	Lepton tag
N_{res}	25,100	20,620	15,400	1541
N_{res}/N_{tot}	0.081	0.149	0.158	0.51
N_γ	2112±424	1405±350	1286±272	123±28
N_γ/N_{res}	0.08±0.02	0.07±0.02	0.08±0.02	0.08±0.02
E_γ (MeV)	51.6±1.7	49.1±2.0	50.5±1.8	52

The signal, either by thrust cuts, energy region selection or lepton tag is clearly associated with production of $b\bar{b}$ pairs of sufficient energy to dress as B^* mesons, reinforcing the above conclusion. The best value for the B^*-B mass difference is $\Delta M=52\pm2\pm4$ MeV, in agreement with predictions. We conclude with a list of mass squared differences for vector-pseudoscalar mesons which show a remarkable narrow spread from the lightest to the heaviest known mesons.

$\Delta M^2(\rho-\pi)=0.574$ GeV^2	$\Delta M^2(F^*-F)=0.589\pm0.050$	Argus[10]
$\Delta M^2(K^*-K)=0.556$	" $=0.569\pm0.060$	TPC[10]
$\Delta M^2(D^*-D)=0.546$	$\Delta M^2(B^*-B)=0.551\pm0.043$	CUSB

Acknowledgements. I wish to acknowledge the efforts of all the members of the CUSB collaboration, in particular R. D. Schamberger and P. M. Tuts for keeping the CUSB detector always at peak performance. Most of these results would not have been obtained without the guidance and work of J. Lee-Franzini. Finally I wish to thank the organizers of this workshop for a very exciting and enjoyable week of physics and clean air.

References.

1). S. W. Herb et al., Phys. Rev. Lett. 39 (1977) 252
2). C. Bebek et al., Phys. Rev. Lett. 46 (1981) 84; L. J. Spencer et al., Phys. Rev. Lett. 47 (1981) 771.
3). S. Behrends et al., Phys. Rev. Lett. 50 (1983) 881
4). A. Martin, Phys. Lett. 103B (1980) 55; E. Eichten et al., Phys. Rev. D21 (1980) 203.
5). R. D. Schamberger et al., Phys. Rev. D 30 (1984) 1985; 26 (1982) 720.
6). D. M. J. Lovelock et al., Phys. Rev. Lett. 54 (1985) 377
7). D. Besson et al., Phys. Rev. Lett. 54 (1985) 381
8). J. Lee-Franzini, Proc. XXII Int. Conf. on High Energy Physics, Eds. A. Meyer and E. Wieczorek, Leipzig.
9). C. Klopfenstein et al, Phys. Lett. 130B (1983) 444.
10). As reported at this workshop.

HEAVY QUARK PRODUCTION IN e^+e^- ANNIHILATION AT 29 GeV

Hiroaki Aihara
University of Tokyo, Tokyo 113, Japan

(Representing PEP-4 TPC Collaboration)

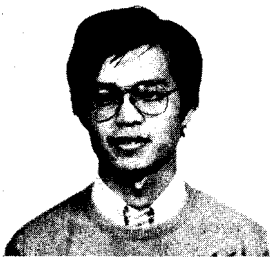

We present comprehensive studies on heavy quark production in e^+e^- annihilations using the PEP-4 TPC detector. The results include the measurements of b and c quark fragmentation functions and of the forward-backward asymmetries in $e^+e^- \to c\bar{c}$ and $b\bar{b}$, based on D* and prompt lepton events. We have observed F* meson via its radiative decay $F^* \to \gamma F$ followed by $F \to KK\pi$. Gluon emission from b quark is investigated using b quark events tagged by prompt leptons.

1. Introduction

In this talk we present results from D* and F* events and c and b events tagged by prompt leptons. The emphasis is put on the study of the flavor dependence of quark production and hadronization processes in e^+e^- annihilations. The data was collected with the PEP-4 time projection chamber (TPC) detector at a c.m. energy of 29 GeV at PEP storage ring. Details of the PEP-4 TPC detector are described elsewhere.[1] The data sample reported here consists of 29,000 hadronic events, corresponding to an integrated luminosity of 77 pb^{-1}.

2. D* meson

The $D^{*+}\to\pi^+D^0$ decays were detected in the $D^0\to K^-\pi^+$, $K^-\pi^+\pi^0$ and $K^-\pi^+\pi^-\pi^+$ decay modes. Both kaons and charged pions were identified based on the dE/dX measurement in the TPC. Neutral pions were reconstructed by the barrel electromagnetic calorimeter. The invariant mass of the D^0 decay candidates was constrained to the D^0 mass. Only D^0 decay candidates passing the mass-constrained fit at the 1% confidence level were retained. The mass difference $M(\pi D^0) - M(D^0)$ is formed by combining each D^0 candidate with pions of charge opposite to the charge of kaon. The distribution for each decay mode is shown in Figure 1. The requirement for $z(=E_{D^*}/E_{beam})$ is also shown. The yield of D* mesons in each decay mode was obtained by fitting the mass-difference plot with a gaussian plus a smooth background. The number of events found are 48.2±9.5 for $K^-\pi^+$ mode, 8.9±5.1 for $K^-\pi^+\pi^0$ mode and 12.9±5.1 for $K^-\pi^+\pi^-\pi^+$ mode.

Figure 2 shows the scaled cross section of D* with previous results[2] from PEP and PETRA. A fit to the Peterson[3] form of the fragmentation function yields a mean value of $\langle z_c\rangle=0.55\pm0.03$ and an ε parameter of $\varepsilon_c=0.25\pm0.11$. Here errors include statistical errors only. A value of the forward-backward asymmetry is obtained by measuring the distribution of D* with respect to the direction of beam e^+, shown in Figure 3. Only the $D^0\to K^-\pi^+$ decay mode was used to minimize the background. The distribution can be parameterized as $dN/d\cos\theta\propto(1+\cos^2\theta+\lambda_f\cos\theta)$. In the standard model, $\lambda_f=-4(a_e a_f/Q_f)\chi$, where $a_e(=-1)$ and a_f are the axial vector couplings of the neutral current to an electron and a quark of charge Q_f, respectively, and χ depends on $\sqrt{s}$ ($\chi\cong-0.04$ at 29 GeV). A maximum likelihood fit gives $a_c=1.8\pm1.8$, consistent with the standard model value of +1. By examining the wrong-sign combinations which would result from the sequence $D^*\to\pi D^0\to\bar{D}^0\to K^+\pi^-$, we have placed a limit of 16.6% (90% C.L.) on the rate for $D^0-\bar{D}^0$ mixing.

3. F* meson[4]

The F* mesons were detected via its radiative decay $F^*\to\gamma F$ followed by $F\to KK\pi$. We applied a similar technique as we did for D*. Kaons and pions were identified by the dE/dX in the TPC. Photons were detected either by the barrel calorimeter

or by the TPC as photon-converted e^+e^- pairs. The invariant mass of KKπ combination was constrained to the F mass[5] of 1.97 GeV/c^2. Those combinations (F candidates) passing the fit at the 10% confidence level were combined with photons to make KKπγ invariant masses. The mass-squared difference, $\Delta M^2=M^2(KK\pi\gamma)-M^2(KK\pi)$, was calculated for those combinations with $z_{F*}>0.5$ and is shown in Figure 4 (solid line). A control sample distribution (dashed line) was obtained by selecting KKπ combinations that give a good fit (C.L.>10%) when the mass was constrained to 1.67 GeV/c^2 or 2.27 GeV/c^2 but give a poor fit (C.L.<1%) to the F mass. The F-candidate distribution shows a clear peak while the control sample distribution shows no structure. The yield of F^* mesons and the peak of ΔM^2 were obtained by fitting both the F-candidate and control-sample ΔM^2 distributions to a smooth background, plus, for the F-candidate sample, a gaussian with fixed width of 0.13 $(GeV/c^2)^2$. The fit gives $\Delta M^2=0.569\pm0.037(stat)\pm0.041(syst)$ $(GeV/c^2)^2$ with 60±15 events in the peak. Fixing the F mass to be 1.97 GeV/c^2, the corresponding mass difference is $\Delta M=139.5\pm8.3\pm9.7$ MeV/c^2 and the F* mass is $M(F^*)=2110\pm8.3\pm9.7$ MeV/c^2.

As a check, we made the invariant mass distribution of all KKπ combinations for which the unconstrained mass-squared difference falls in the F* region, $0.4<\Delta M^2<0.8$ $(GeV/c^2)^2$, and in a control region, $0.9<\Delta M^2<1.4$ $(GeV/c^2)^2$. Figure 5 shows those distributions. The F*-candidate sample gives a clear peak at $M(KK\pi)=1.948\pm0.028\pm0.010$ GeV/c^2, consistent with the F mass of 1.97 GeV/c^2. The resulting yield of F mesons is 65±17. At the 90% confidence level we have placed an upper limit of 13% on the branching fraction for $F^+\to\phi\pi^+$, based on the $M(K^+K^-)$ distribution of the F* sample. This limit is consistent with previous measurements[5].

Our measured mass difference agrees well with the QCD-motivated potential model prediction, $\Delta M=132\pm6$ MeV/c^2, by K.Igi and S.Ono[6]. W.C.Haxton and L.Heller[7] predicted the F* mass as 2106 MeV/c^2 based on the MIT bag model. This value also agrees with our observed value. The ARGUS group at DORIS also found F* mesons[8], with the mass consistent with our observation.

We have determined the mean value of the c quark fragmentation function from the scaled cross section of F*, shown in Figure 6. We have obtained $\langle z_c\rangle=0.58\pm0.06$ with $\varepsilon_c=0.19^{+0.17}_{-0.08}$, which agrees with our D* result, $\langle z_c\rangle=0.55\pm0.03$ with $\varepsilon_c=0.25\pm0.11$, within errors.

4. Prompt leptons

In the following we present the results obtained from heavy quark (c and b) events tagged by prompt leptons. The selection of prompt electrons and muons are described in detail in Ref.9 and 10. Prompt electron sample contains 526 electrons with P>1 GeV/c and has the purity of about 70%. Prompt muon sample contains

644 muons with P>2 GeV/c and has the purity of about 73%. The c quark events and b quark events are separated based on the prompt lepton P_T (transverse momentum with respect to the jet axis).

Both P and P_T spectra were fitted with the contributions from primary ($b\to l$) and secondary ($b\to c\to l$) b quark decays, primary ($c\to l$) c quark decays and the background. The following four parameters were used: the branching fraction of $b\to l$, the branching fraction of $c\to l$ and the parameters ε_b and ε_c of the Peterson et al. heavy quark fragmentation functions. For electron data ε_c is fixed to 0.24±0.06. Figure 7 shows the background-subtracted muon spectra for $P_T<1$GeV/c and for $P_T>1$ GeV/c with the result of the fit. The muon data yields the mean values of z as $\langle z_c\rangle=0.60\pm0.06\pm0.04$ for c quark and $\langle z_b\rangle=0.80\pm0.05\pm0.05$ for b quark. The electron data yields $\langle z_b\rangle=0.74\pm0.05\pm0.03$. Combining the muon and electron results for b quark gives $\langle z_b\rangle=0.77\pm0.04\pm0.03$, which shows that the fragmentation function of b quark is harder than that of c quark.

Figure 8 shows the background-subtracted angular distributions of the thrust axis with respect to the initial e^- direction for prompt muon data: (a) the c-enriched sample ($P_T<1$GeV/c) and (b) the b-enriched sample ($P_T>1$GeV/c). The forward direction of the thrust axis is taken as the hemisphere containing μ^+. The solid curve shows the result of the fit to the data of angular distributions for $e^+e^-\to c\bar{c}$ and for $e^+e^-\to b\bar{b}$. The dashed curve shows the contribution from the minority source: for $P_T<1$GeV/c this is $e^+e^-\to b\bar{b}$ and for $P_T>1$GeV/c this is $e^+e^-\to c\bar{c}$. The resulting values of the axial vector couplings are $a_c=1.7\pm1.4\pm0.5$ and $a_b=-1.3\pm1.0$ 0.3. The electron data gives $a_c=2.3\pm1.4\pm1.0$ and $a_b=-2.0\pm1.9\pm0.5$. Combining results from the muon and electron data, we find $a_c=2.0\pm1.0\pm0.4$ and $a_b=-1.4\pm0.9$ ±0.3. These values are consistent with the standard model values: $a_c=+1$ and $a_b=-1$.

In QCD the quark-gluon coupling is assumed to be flavor independent. In order to check this assumption we have looked for evidence of gluon emission from b quark using the b-enriched sample. Here b-enriched events were selected by requiring prompt leptons with P>2GeV/c and $P_T>1$GeV/c. There are 69 events from electron data and 155 events from muon data. About 80% of those events are estimated to be originated from b quark. Figure 9 shows the background-subtracted P_T^2(in) and P_T^2(out) spectra of tracks contained in the jets opposite to the the prompt leptons. Here P_T(in) and P_T(out) are transverse momenta within and out of the event plane, respectively. The event axis and event plane were reconstructed using all charged tracks. Also shown in Figure 9 are Monte Carlo predictions for b quark events with (dashed line, $\alpha_s=0.2$) and without (solid line, $\alpha_s=0$) gluon emissions. The clear discrepancy between the data and Monte Carlo data without gluon emission is seen. The Monte Carlo events were generated using LUND[11] of version 5.3. We have verified that Monte Carlo reproduces the B meson

decay properties measured by CLEO group at CESR. The discrepancy indicates the existance of gluon emission from b quark. The work to determine α_s and more checks are in progress.

5. Conclusion

Comprehensive studies of heavy quark production in e^+e^- annihilation by the PEP-4 TPC group have been presented with the emphasis on the flavor dependence of quark production and hadronization mechanism. The obtained results are;

1) the measurements of the heavy quark fragmentation functions,

$\langle z_c \rangle = 0.55 \pm 0.03$ (by D*),
$= 0.58 \pm 0.06$ (F*),
$= 0.60 \pm 0.06 \pm 0.04$ (prompt muon),
$\langle z_b \rangle = 0.74 \pm 0.05 \pm 0.03$ (prompt electron),
$= 0.80 \pm 0.05 \pm 0.05$ (prompt muon),

2) observation of F* meson via its radiative decay and
$\Delta M(F^*-F) = 139.5 \pm 8.3 \pm 9.7$ MeV/c^2,

3) the determination of the axial vector couplings of the neutral current to the heavy quarks,

$a_c = +1.8 \pm 1.8$ (D*),
$= +1.7 \pm 1.4 \pm 0.5$ (prompt muon),
$= +2.3 \pm 1.4 \pm 1.0$ (prompt electron),
$a_b = -1.3 \pm 1.0 \pm 0.3$ (prompt muon),
$= -2.0 \pm 1.9 \pm 0.5$ (prompt electron),

4)the investigation of gluon emission from b quark using lepton-tagged heavy quark events.

References

1) H.Aihara et al. (TPC), IEEE Trans. Nucl. Sci. NS30, 63,67,76,153,162 (1983); H.Aihara et al. (TPC), Nucl. Instr. and Meth. 217, 259 (1983)
2) M.Derrick et al. (HRS), Phys. Lett. 146B, 261 (1984); M.Altoff et al. (TASSO), Phys. Lett. 126B, 493 (1983); W.Bartel et al. (JADE), Phys. Lett. 146B, 121 (1984)
3) C.Peterson et al., Phys. Rev. D27, 105 (1983)
4) H.Aihara et al. (TPC), Phys. Rev. Lett. 53, 2465 (1984)
5) A.Chen et al. (CLEO), Phys. Rev. Lett. 51, 634 (1983); M.Altoff et al. (TASSO), Phys. Lett. 136B, 130 (1984)
6) K.Igi and S.Ono, University of Tokyo preprint, UT-446, November 1984
7) W.C.Haxton and L.Heller, Phys. Rev. D22, 1198 (1980)
8) H.Albrecht et al. (ARGUS), Phys. Lett. 146B, 111 (1984)
9) H.Aihara et al. (TPC), Z. Phys. (in press)
10) H.Aihara et al. (TPC), submitted for publication
11) T.Sjoestrand, Comput. Phys. Commun. 27, 243 (1982), 28, 229 (1983)

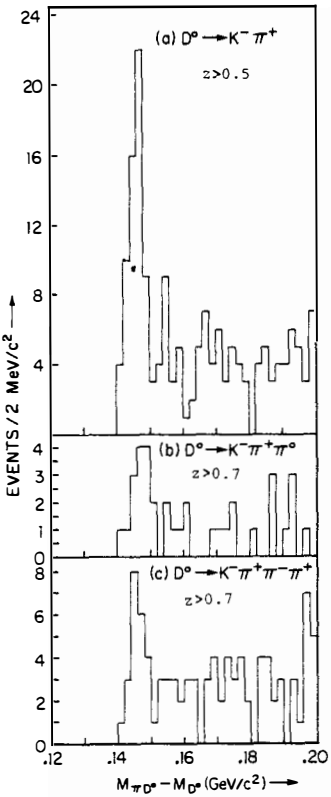

Fig.1. Mass difference distribution

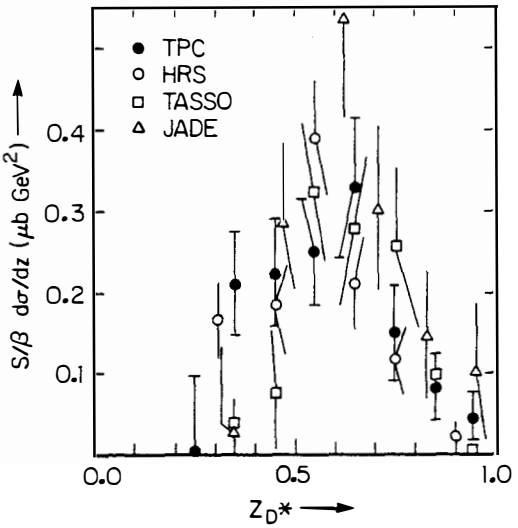

Fig.2. Scaled cross section of $e^+e^- \to D^{*\pm}X$

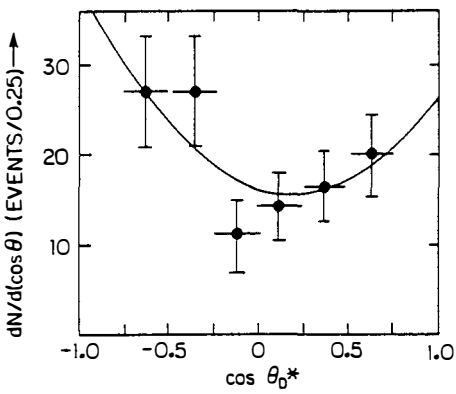

Fig.3. Angular distribution of produced D*

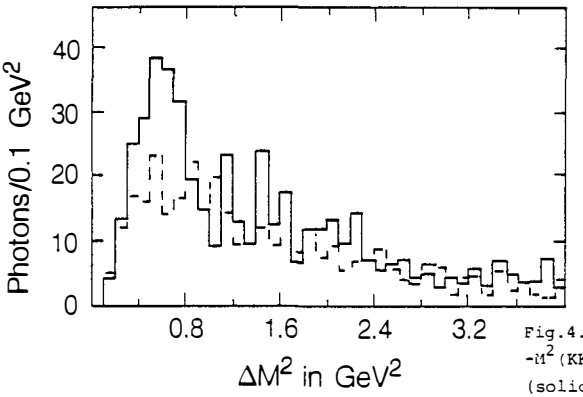

Fig.4. Distributions of $\Delta M^2 = M^2(KK\pi\gamma) - M^2(KK\pi)$ for the F-candidate sample (solid line) and for the control sample (dashed line)

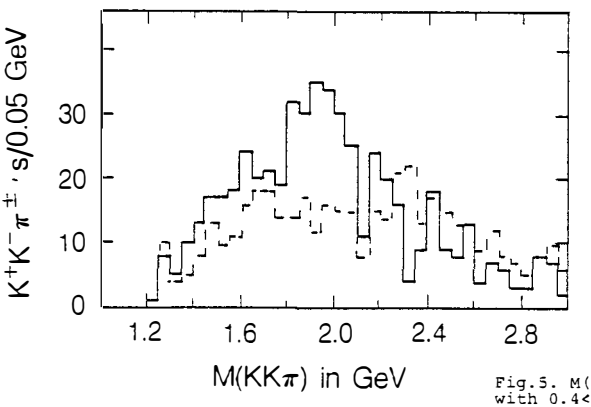

Fig.5. $M(KK\pi)$ for $KK\pi\gamma$ combinations with $0.4<\Delta M^2<0.8 GeV^2$ (solid line) and for those with $0.9<\Delta M^2<1.4 GeV^2$ (dashed line)

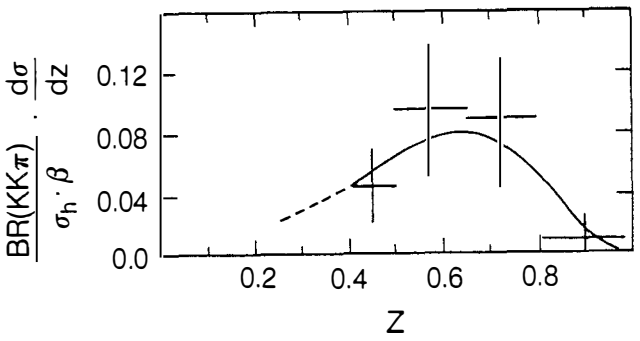

Fig.6. Differential cross section of F* production

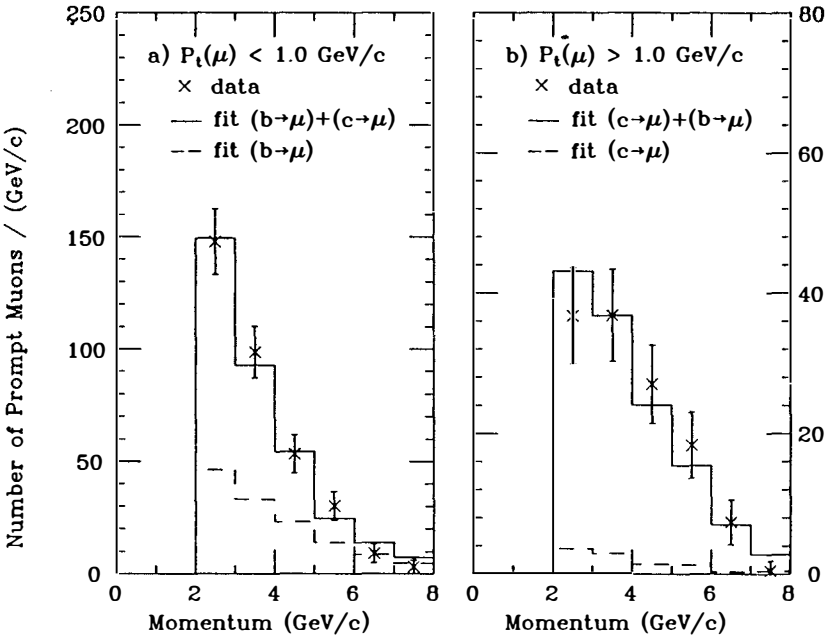

Fig.7. Background-subtracted prompt muon spectra (2<p<8GeV/c): a) for Pt<1 GeV/c and b) for Pt>1GeV/c. The solid line is the result of the fit to the data and includes the heavy quark decay contributions b→μ, b→c→μ, and c→μ. The dashed line shows the contribution for the minority source: for Pt<1GeV/c this is the sum of b→μ and b→c→μ decays, for Pt>1GeV/c this is the contribution of c→μ decays.

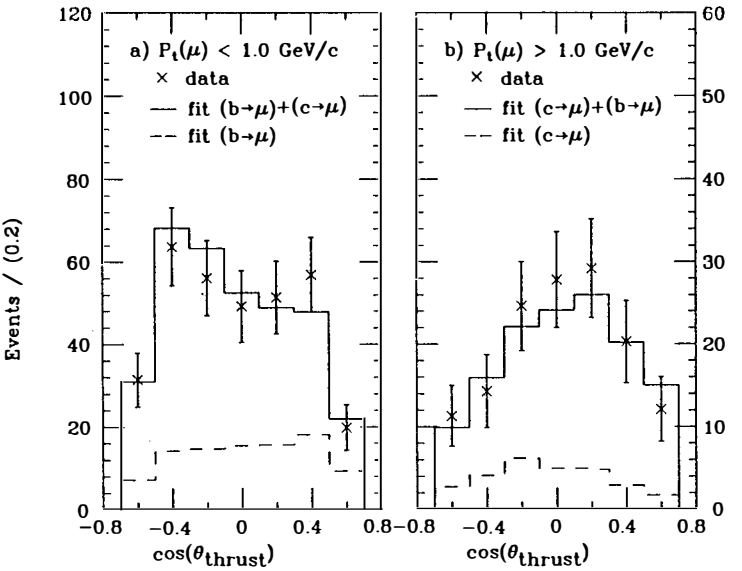

Fig.8. Background-subtracted angular distribution of the thrust axis for events a) in the c enriched (Pt<1GeV/c) and b) in the b enriched (Pt>1GeV/c) samples. The solid curve is the result of the fit to the data of angular distributions for e+e- -> $c\bar{c}$ and for e+e- -> $b\bar{b}$. The dashed curve shows the contribution from the minority source.

Preliminary

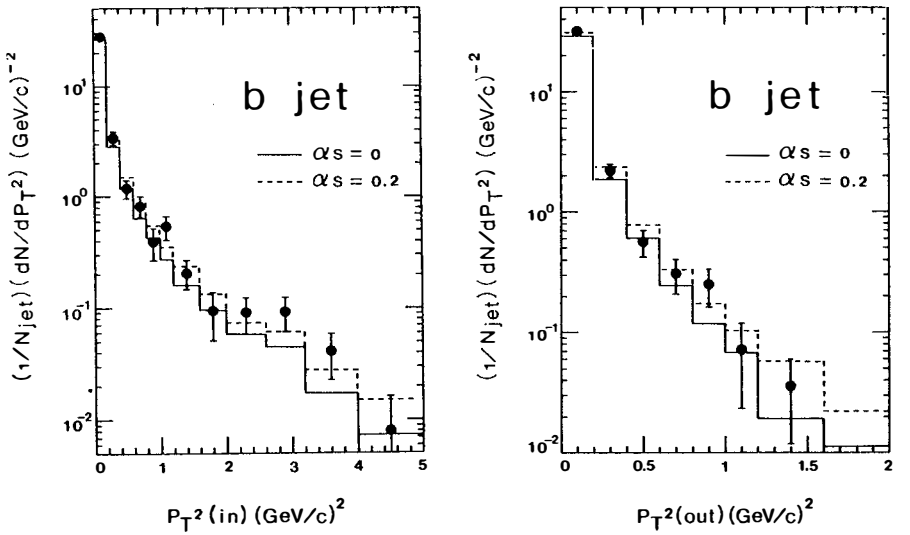

Fig.9. Background-subtracted P_T^2(in) and P_T^2(out) spectra of tracks contained in the jet opposite to the prompt leptons.

CHARM HADROPRODUCTION IN THE ACCMOR COLLABORATION

ACCMOR Collaboration[1)]

presented by: Gijs de Rijk

NIKHEF-H, Amsterdam
The Netherlands

ABSTRACT: The present status of the experiment NA11/NA32 is discussed. For 1982 final numbers for the D lifetimes are presented. A partial analysis ofthe 1984 data has yielded F candidates for a lifetime measurement.

The charm program with the ACCMOR spectrometer, using a Si-microstrip vertex telescope has been running since 1982 (Fig. 1). In 1982 the telescope consisted of 6 counters arranged in 2 views with 4.5 μm (7.9 μm) resolution in the inner (outer) regions.

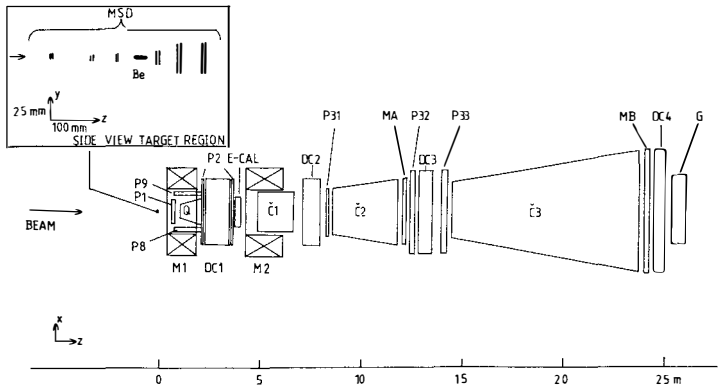

Fig. 1 Top view of the ACCMOR spectrometer in 1982, showing target (Be), Si microstrip detectors (MSD), magnets (M), drift chambers (DC), Cerenkovs (Q,C), multiwire proportional chambers (P), scintillator arrays (MA,MB), and electron (photon) calorimeters (E-CAL,G).

Data were taken with 2 different triggers. A single electron trigger, triggering on the electron from the semileptonic decay of an associated produced charmed particle, and a ϕ trigger, triggering on a K^+K^- pair from the decay of a ϕ meson.

The single electron trigger data has been used to measure the lifetime of D mesons. 54 D-decays, with all decay products fully reconstructed and identified, have been observed (Fig. 2):

$$9 \quad \bar{D}^0 \to K\pi,$$

$$17 \quad \bar{D}^0 \to K\pi\pi\pi,$$

$$28 \quad D^{\pm} \to K\pi\pi,$$

From these events the $\bar{D}^0$ and $D^{\pm}$ lifetimes have been determined. The final results are[2]:

$$\tau(\bar{D}^0) = 3.7^{+1.0}_{-0.7} \cdot 10^{-13} \text{ s},$$

$$\tau_{D^\pm} = 10.6^{+3.6}_{-2.4} \cdot 10^{-13} \text{ s}.$$

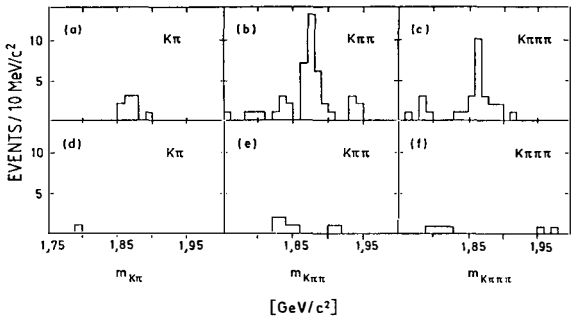

Fig. 2 Invariant mass plots of single electron trigger D candidates used for the lifetime determination:
a,b,c : e-K same charge
d,e,f : e-K opposite charge.

Both the e-trigger data and the ϕ trigger data (±200, +120, -100 GeV/c) have been used to search for F-mesons in the KKπ decay. A complete description of the data analysis for part of the data is given in Ref. 3. In total we observe 35 events distributed over the different data samples. Figure 3 gives the KKπ mass spectrum for the selected data sample, clear signals are observed at the D and F mass. The shoulder at the low side of the D-mass is still under investigation. It could be caused by an F→KKπ decay with a missing π^0. For the events in the mass interval 1.95-1.99 GeV a maximum likelihood fit for the mass gives m = 1972±2 MeV. The presence of one or more strange particles is further confirmation that the decay originates from a charmed particle. We therefore show events which have a well-identified additional strange particle hatched in Fig. 3. For the average lifetime of the 12 events in the mass range $1.95 < m(KK\pi) < 1.99$ GeV we obtain $(3.1^{+1.2}_{-0.8}) \cdot 10^{-13}$s.

In 1984 the original Beryllium target was replaced by an active target, consisting of 14 Si-microstrip detectors. The target provides a very precise interaction point $(\sigma_x, \sigma_y, \sigma_z) = (21,5,81)\mu m$, and can serve as a tracking device in the region of production and decay vertices (Fig. 4).

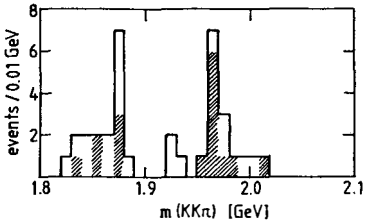

Fig. 3 KKπ mass spectrum for VMSD selected events. No distinction is made for the energy and identity of incident beam particle. The hatched events have a well-identified additional strange particle.

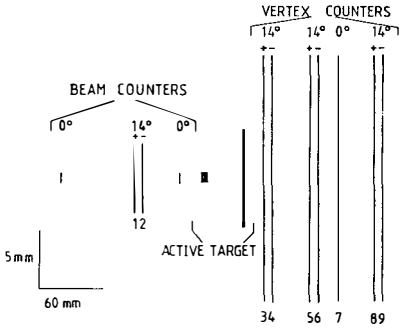

Fig. 4 NA32 target area (side view) consisting of:

beam counters	2	48 strip counters	20 μ pitch
	2	120 strip counters	60 (120) μ pitch
active target	14	48 strip counters	20 μ pitch
	2	24 strip counters	400 μ pitch
vertex telescope	7	240 strip counters	60 (120) μ pitch

With this setup using an interaction trigger the following data were recorded onto tape :

$22 \cdot 10^6$ π^-,
$11 \cdot 10^6$ p,
$5.5 \cdot 10^6$ K^- triggers, at 200 GeV/c momentum.

A preliminary analysis of 10% of the π^- data has yielded a sample of 20 D candidates. This confirms our expectation of obtaining a total sample of > 200 D's.

Most of the recent analysis efforts have been concentrated on the K^- incoming beam data, to obtain a sample of F's for lifetime and cross-section measurement. The K^- beam data are used guided by the theoretical prejudice that F^- production in a K^- beam might be enhanced above that in a π^- beam.

Up to now the preliminary analysis has shown a sample of 4 F candidates in a fraction of the data. An example of such an event is shown in Fig. 5.

The continuation program for 1985 aims at obtaining a high statistics sample of F's and Λ_c's for lifetime measurement and cross-section measurement[4].

Use will be made of 2 proven techniques :

1) A vertex telescope updated with high resolution Charged Coupled Devices giving space coordinates with errors $(\sigma_x, \sigma_y) = (5,5)\mu m$, for a precise vertex measurement[5].

2) A trigger on KK or pK pairs in the downstream spectrometer using the FAMP microprocessor system[6].

The Λ_c's and F's will be searched for in the decay channels

$$F^{\pm} \rightarrow K^+K^-\pi^{\pm},$$

$$\Lambda_c \rightarrow K^-p\pi^+.$$

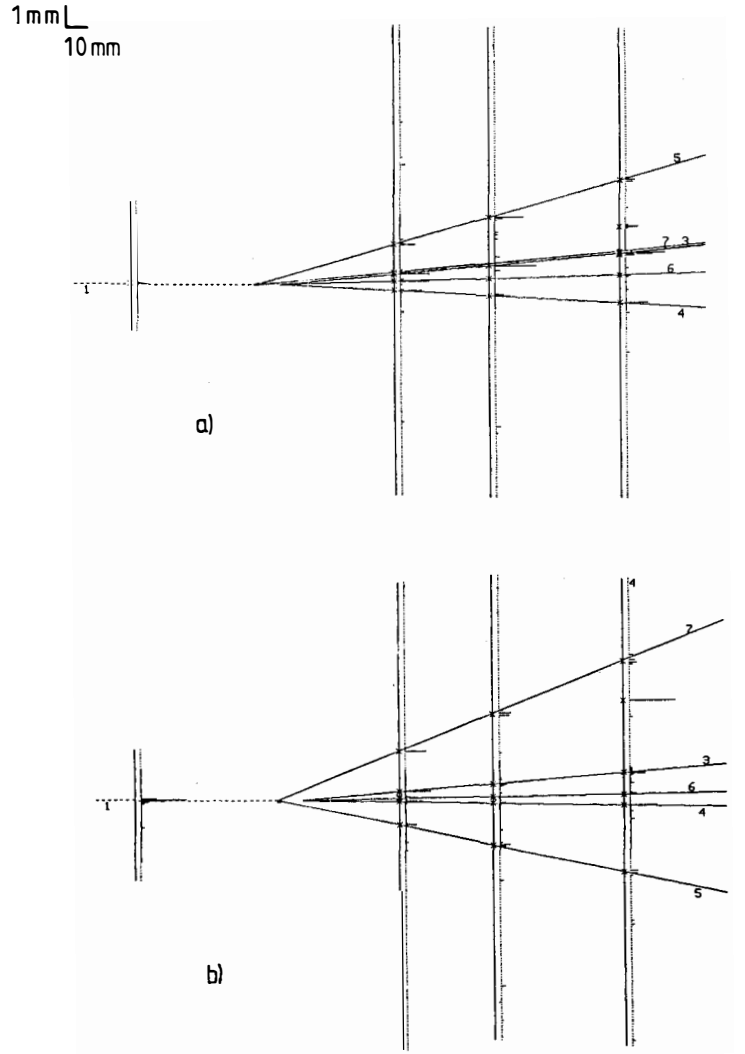

Fig. 5 Display of F^- candidate: a) view 1, b) view 2.
Track 3 : 33.8 GeV/c K^-; 6 : 29.3 GeV/c K^+; 4 93.7 GeV/c π^-;
Δz decay = 11.3 mm; $M_{KK\pi}$ = 1.978 GeV/c^2.

REFERENCES

1) R. Bailey[6], E. Belau[5], T. Böhringer[3], M. Bosman[3], V. Chabaud[3], C. Damerell[6], C. Daum[1], G. De Rijk[1], H. Dijkstra[1], S. Gill[6], A. Gillman[6], R. Gilmore[2], Z. Hajduk[4], C. Hardwick[1], W. Hoogland[1], B.D. Hyams[3], R. Klanner[5], U. Koetz[3], S. Kwan[2], G. Lütjens[5], G. Lutz[5], J. Malos[2], W. Männer[5], E. Neugebauer[5], M. Pepé[6], J. Richardson[6], M. Rozanska[4], K. Rybicki[4], H.J. Seebrunner[5], U. Stierlin[5], R.J. Tapper[2], H.G. Tiecke[1], M. Turala[4], G. Waltermann[5], S. Watts[6], P. Weilhammer[3], F. Wickens[6], L.W. Wiggers[1], A. Wylie[5], and T. Zeludziewicz[5]

Amsterdam[1]-Bristol[2]-CERN[3]-Cracow[4]-Munich[5]-Rutherford[6]

2) E. Belau et al., Measurement of the Lifetime of Charged and Neutral D-Mesons with High Resolution Silicon Strip Detectors, to be published.

3) R. Bailey et al., Phys. Lett. 139B (1984) 320.

4) NA32 Collaboration Memo to SPSC, CERN/SPSC/85-8.

5) R. Bailey et al., Nucl. Instrum. Methods 213 (1983) 201.

6) C. Daum et al., Nucl. Instrum. Methods 217 (1983) 361.

PRODUCTION OF ϕ AND F(1970)$\rightarrow\phi\pi$ IN e^+e^- ANNIHILATION AT 29 GeV

Ivano Beltrami
Purdue University
Representing the HRS Collaboration

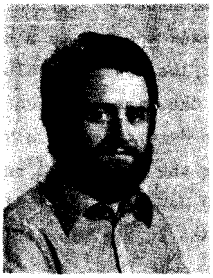

Data corresponding to an integrated luminosity of 176 pb^{-1} from the High Resolution Spectrometer at PEP has been used to study the inclusive production of ϕ-mesons and $F^{\pm}$ mesons decaying into $\phi\pi^{\pm}$. Fragmentation functions and cross sections are presented and compared to existing data. The total ϕ cross section is 40 ± 6 pb. The rate of F production in the region $z > 0.4$, assuming $R(F)/(R(F)+R(D)) = 0.15$, corresponds to an $F \rightarrow \phi\pi$ branching ratio of (2.0 ± 0.8)%.

The hadronic events used in the analysis come from an integrated luminosity of 176 ± 6 pb^{-1} obtained using the High Resolution Spectrometer (HRS) at PEP. Hadronic events were selected by demanding more than 5 vertex-fitted tracks and that the visible energy be greater than 13 GeV.

To search for ϕ production in these events all possible K^+K^- mass combinations were formed. To reduce the pion background in the kaon sample, all track candidates with momenta less than 1.5 GeV/c and flight times inconsistent with a kaon interpretation were rejected. In addition, the absence of a Cerenkov signal was required for kaon candidates with momenta below the kaon threshold.

The K^+K^-invariant mass distribution is shown in Fig. 1a for $z_{KK} > 0.1$ and in Fig. 1b for $z_{KK} > 0.4$, where $z_{KK} \equiv 2 \cdot E_{KK}/\sqrt{s}$. A clear signal corresponding to ϕ production is observed with an excellent signal to noise ratio in the higher momentum selection. The ϕ signal was determined by fitting the mass spectra to a smooth background and a resonance contribution described by a convolution of a p-wave Breit-Wigner with FWHM 4.1 MeV/c^2 and a Gaussian representing the spectrometer resolution. The latter, as determined by a Monte-Carlo calculation, averages 7 MeV/c^2 FWHM over the ϕ momentum range. The resulting composite FWHM is 9.5 ± 2.0 MeV/c^2. The ϕ signal displayed in Fig. 1a contains 948 ± 102 events and in Fig. 1b 217 ± 25 events.

The differential cross section was determined from a series of fits to the K^+K^- mass spectra for several intervals of z. In these fits the ϕ mass was fixed at 1019.6 MeV/c^2 and the width was set as described above. The detector acceptance was determined by a similar series of fits to ϕ events generated by a Monte-Carlo simulation. Our precise data are in good agreement in magnitude and shape with the ϕ fragmentation in the LUND Monte-Carlo simulation and with results from the TPC collaboration.[1]

The inclusive ϕ production cross section measured for $z > 0.1$ is 39 ± 6 pb. A linear extrapolation to the threshold of $z_{th} = 0.07$ yields a total ϕ production cross section $\sigma(\phi) = 40 \pm 6$ pb. Dividing by the μ pair cross section for $\sqrt{s} = 27.3$ GeV to correct for initial state radiation gives $R(\phi) = 0.34 \pm 0.05$.

To search for the decay mode $F \to \phi\pi$, each K^+K^- combination in the ϕ mass band (1019.6 ± 10) MeV/c^2 was combined with each other track in the

event taken as a pion. An enchancement is observed in the resulting $\phi\pi$ effective mass spectrum shown in Fig. 3a for $0.2 < z(\phi\pi) < 0.4$ and in the upper part of Fig. 3b for $z(\phi\pi) > 0.4$, where $z(\phi\pi) \equiv 2 \cdot E(\phi\pi)/\sqrt{s}$. The separation of the data into two regions of z is motivated by the different mechanisms expected for F production. The region $z > 0.4$ is dominated by direct charm whereas the data with $0.2 < z < 0.4$ contain the majority of the events from B decay. The fit shown by the full line in Fig. 3b yields 37 ± 13 events centered at a mass of 1967 ± 5 MeV/c^2 and with a width of 25 ± 6 MeV/c^2. The observed width is consistent with the calculated spectrometer resolution of 19 ± 1 MeV/c^2. The spectrum of Fig. 3a was fitted with a Monte-Carlo resolution of 15 MeV and yielded a peak of 70 ± 18 events centered at a mass of 1975 ± 2 MeV/c^2. When the width was permitted to vary in the fit, a value of 9 ± 2 MeV/c^2 was obtained.

The z dependence of the F production was determined by a series of fits to the $\phi\pi$ mass spectrum for successively larger z selections. The fits were made using widths determined by Monte-Carlo calculation. The data were corrected for acceptance and the resulting fragmentation function $D(z) \equiv s/\beta \cdot d\sigma/dz$ is shown in Fig. 4. Data from the TASSO collaboration,[2] also plotted in Fig. 4, give a higher cross section. The solid curve in Fig. 4 represents our measured fragmentation function for D* mesons[3] in the region $z > 0.4$, normalized to our $\phi\pi$ data in the same region.

The F cross section and z-distribution observed above $z = 0.4$ is lower than, but consistent with, that extrapolated from the CLEO measurements.[4] Below $z = 0.4$ the F signal exceeds that expected. Suzuki[5] has estimated the contribution to F production from B meson decay to be 21% of the b quark production rate. This estimate includes a contribution from the $c\bar{s}$ decay of the W. The dashed curve in Fig. 4 is the sum of this prediction (using our measurement of the $F \to \phi\pi$ branching ratio) and the solid curve of Fig. 4. The dashed curve predicts 23 events for $0.2 < z < 0.4$ as compared to 70 ± 18 events observed.

The enchancements in both z regions were tested for consistency with a 0^- spin assignment of the F. The events were divided into two regions, $|\cos(\theta)| < 0.5$ and $|\cos(\theta)| > 0.5$, where θ is the angle between the F (ϕ) direction in the Lab (F) system and the ϕ (K) direction in the F (ϕ) center of mass. Equal populations are expected for the $F(0^-) \to \phi\pi$ decay and a $\cos^2(\theta)$ distribution in the helicity frame of the ϕ for the

subsequent ϕ ($1^- \to 0^-0^-$) decay. Table I contains the event counts, errors and probabilities that the observed events result from the decay of a 0^- particle into $\phi\pi$.

		$0.2<z<0.4$	$z > 0.4$
$\phi\pi$	$\cos(\theta) < 0.5$	10 ± 10	15 ± 8
	$\cos(\theta) > 0.5$	60 ± 15	22 ± 10
	Probability	0.5%	58%
ϕ	$\cos(\theta) < 0.5$	32 ± 12	0 ± 7
	$\cos(\theta) > 0.5$	38 ± 13	37 ± 11
	Probability	1%	48%

Table I

Above $z = 0.4$ the peak is entirely consistent with the 0^- interpretation. If the data are restricted to decay region $|\cos(\theta)| > 0.5$ for the ϕ decay and $|\cos(\theta)| < .7$ for the $\phi\pi$ decay, the histogram in the lower part of Fig. 3b is obtained. The fit shown by the dashed line gives a signal of 30 ± 8 events over a small background.

Below $z = 0.4$ the probability that the peak is due to a 0^- decay is $\leq 1\%$. This low probability along with the unexpectedly large cross section suggest that the peak in the $0.2 < z < 0.4$ region is not entirely due to F production. Restricting the decay angular ranges as described in the previous paragraph, as a means of enhancing the 0^- component, the histogram in the lower part of Fig. 3b is obtained. The fit shown by the dashed line gives a signal of 23 ± 11 events and yields $B(F\to\phi\pi)\cdot s/\beta\cdot d\sigma/dz = 6.7 \pm 3.2$ (nb·GeV^2). This cross section is consistent with that expected for the sum of direct charm production and B meson decay.

The product of the total cross section and branching ratio for $z > 0.4$ is $\sigma(F^+F^-)\cdot B(F\to\phi\pi) = 0.93 \pm 0.33$ pb, which corresponds to $R(F^+F^-)\cdot B(F\to\phi\pi) = 0.0080 \pm 0.0028$. Comparing this result to our measurement of $R(D\bar{D}) = 2.2 \pm 0.5$ in the same z region yields $R(F)\cdot B(F\to\phi\pi)/R(D) = 0.0036 \pm 0.0015$. This leads to a branching ratio $B(F\to\phi\pi) = (2.0 \pm 0.8)\%$, assuming $R(F)/(R(D)+R(F)) = 0.15$.

REFERENCES

1. H. Aihara et al., Phys. Rev. Lett. 52, 2201 (1984).
2. M. Althoff et al., Phys. Lett. B 136, 130 (1984).
3. M. Derrick et al., Phys. Lett. B 146, 261 (1984).
4. A. Chen et al., Phys. Rev. Lett. 51, 634 (1983).
5. M. Suzuki, UCB-PTH-84/32 (1984); Phys. Lett. B 142, 305 (1984).

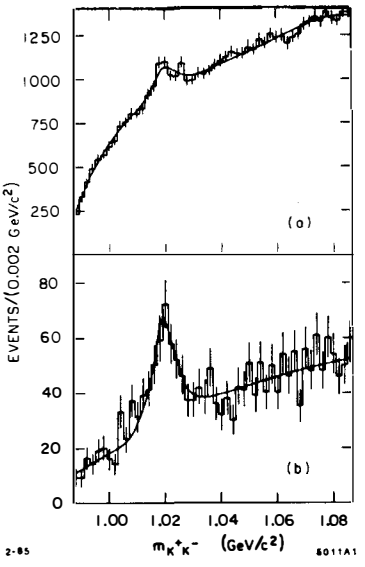

Figure 1. The K^+K^- mass spectrum for
(a) $z(K^+K^-) > 0.1$
(b) $z(K^+K^-) > 0.4$

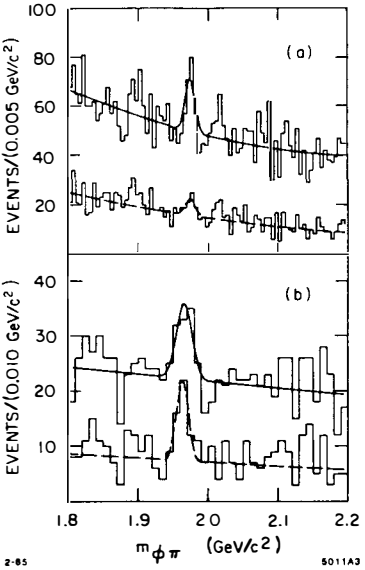

Figure 3. The $\phi\pi$ mass spectrum for
(a) $0.2 < z(\phi\pi) < 0.4$
(b) $z(\phi\pi) > 0.4$

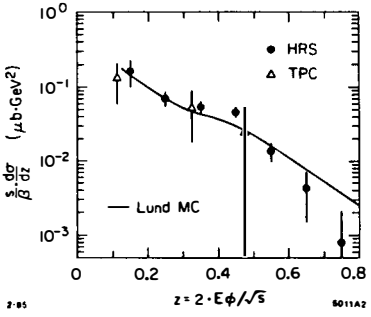

Figure 2. The ϕ fragmentation function.

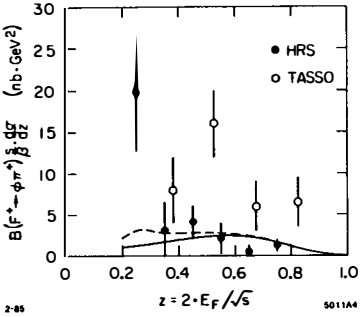

Figure 4. The F fragmentation function.

ARGUS RESULTS ON CHARM PRODUCTION

Klaus R. SCHUBERT
Institut für Hochenergiephysik
Universität Heildelberg

ABSTRACT

Using the ARGUS detector at the DORIS II storage ring at DESY, we collected 80 events/picobarn in the energy range of the Υ resonances. Results on production and decay of the charmed mesons D^0, D^{*+}, F^+ and F^{*+} are presented and discussed.

The ARGUS detector at the DORIS II storage ring started to take data in March 1983 and accumulated 80 events/picobarn during its first two years of operation. These e^+e^- annihilation data were mainly obtained on the T(9460) and T'(10023) resonances, some of them also on the T'''(10577) and in the nearby continuum.

The detector is shown in fig. 1, its main properties are as follows : the normal conducting coil produces a solenoidal field of 0.8 T. The cylindrical drift chamber with 5940 celles in 36 layers gives a momentum resolution of $\sigma(p)/p = 0.012. \sqrt{1 + p^2c^2/\ GeV^2}$ and dE/dx information with $\sigma(dE)/dE = 0.045$. The time-of-flight scintillator system has a resolution of $\sigma(ToF) = 220$ psec, and the shower counter system has reached a resolution of $\sigma(E)/E = 0.07 \sqrt{1 + 1\ GeV/E}$. The muon detection tubes have 5.1 absorption lenghts in front of them.

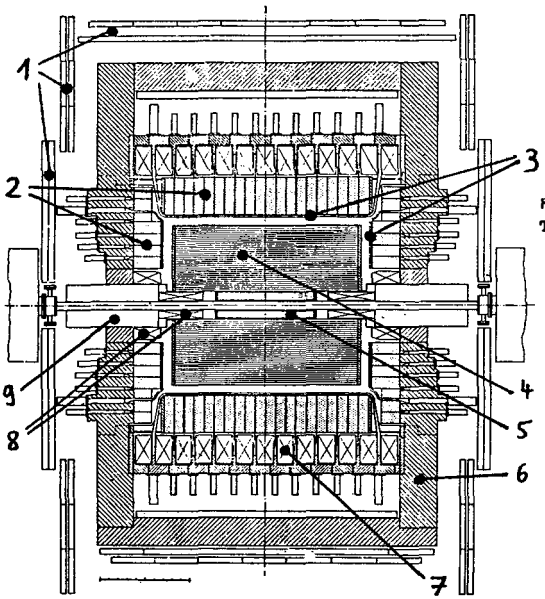

Fig. 1
The ARGUS Detector
1 = muon tubes
2 = shower counters
3 = time-of-flight counters
4 = main drift chamber
5 = vertex drift chamber
6 = iron yoke
7 = main coil
8 = compensation coils
9 = mini-β-quadrupoles

The ARGUS operation was very satisfactory, and a number of results have been obtained so far. This report concentrates on the charmed meson production. There is no evidence for charm production in the direct decays of T'(9460) and T'(10023) mesons. All or data, though they are mainly taken at the resonance energies, are compatible with production in the e^+e^- continuum. The ARGUS author list is given in ref. 1.

D^{**} (2010) production

The results on D^{*} production are published in ref. 1 ; they are obtained from the first year's data with 40 events/pb. I would like to summarize the results :

$m(D^{o}) = (1865 \pm 2 \pm 3)$ MeV,

$m(D^{*+}) - m(D^{o}) = (145.46 \pm 0.07 \pm 0.03)$ MeV,

$BR(D^{o} \to K^{-}\pi^{+}\pi^{+}\pi^{-})/BR(D^{o} \to K^{-}\pi^{+}) = 2.17 \pm 0.28 \pm 0.23$,

$\Gamma(D^{o} \to D^{o} \to \text{decay})/\ \Gamma(D^{o} \to \text{decay}) < 0.11$(90 % CL).

Fig. 2 shows the D^{*+} fragmentation function $s.d\sigma/dx_p$ as a function of x_p $p(D^{*})/p(D^{*},\ max)$. It is not corrected for gluon and photon radiation. The two curves are the best fits of the parametrisations following Peterson et al. [2] and Kartvelishvili et al. [3]. The former with $s.d\sigma/dx_p \sim x_p^{-1}.[1-1/x_p-\epsilon/(1-x_p)]^{-2}$ yields $\epsilon = 0.19 \pm 0.03$ with $\chi^2 = 19.2$ for 6 degrees of freedom, whereas the latter with $s.d\sigma/dx_p \sim x_p^{\alpha}.(1-x_p)$ gives $\alpha = 1.5 \pm 0.2$ with $\chi^2 = 7.4$ for 6 d.o.f.. The fact that the Peterson form leads to a much poorer fit comes predominantly from the highest x_p bin. There exists a disagreement which cannot be solved by radiative corrections. These would shift the data points for high x_p even higher.

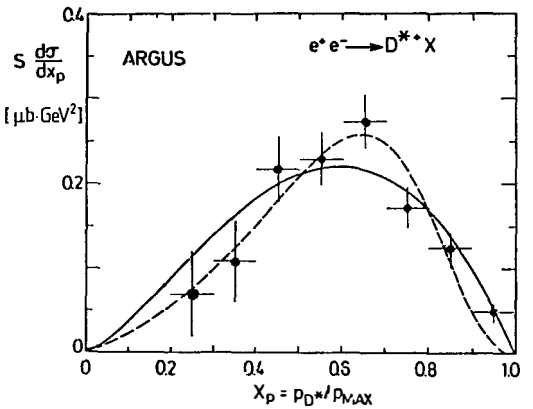

Fig. 2 The D^{*} fragmentation function. The dashed curve is the best fit of the Peterson parametrisation, the solid curve the best fit of the Kartvelishvili parametrisation

$F^+(1970)$ Production

ARGUS observes the "new" F meson in two decay channels. The final results form the first 63/pb luminosity were published in the end of 1984 [4]. The two channels are $\Phi\pi^\pm$ and $\Phi\pi^+\pi^-\pi^\pm$, where the $\Phi(1020)$ is identified through its K^+K^- mode. Fig. 3 shows the obtained Φ signal with 5080 ± 280 events in the peak. Mass and width are as expected. The particle identification capabilities of ARGUS through time-of-flight and specific ionisation in the drift chamber play an essential role.

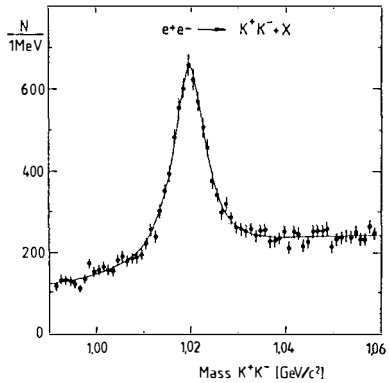

Fig. 3
The K^+K^- invariant mass distribution

Selecting in multihadron events all $KK\pi$ and $KK3\pi$ combinations with $|m(KK)-m(\Phi)| < 15$ MeV, $p(KK\pi) > 1.5$ GeV/c, $p(KK3\pi) > 2.2$ GeV/c and -for the $KK\pi$ only- $\cos\theta^*_\pi$ between -0.8 and +1.0 to exclude backward pions in the $KK\pi$ rest frame, one obtains the invariant mass plots in fig. 4. Both channels show a clear signal at 1970 MeV, $\Phi\pi$ with 4.7 standard deviations and $\Phi 3\pi$ with 4.0 s.d.. The results are as follows :

$$m(F) = (1973.6 \pm 2.6 \pm 3.0)\ \text{MeV},$$
$$BR(F^+ \to \Phi\pi^+\pi^+\pi^-)/BR(F^+ \to \Phi\pi^+) = 1.11 \pm 0.37 \pm 0.28,$$
$$R(F).BR(F^+ \to \Phi\pi^+) = (1.47 \pm 0.32 \pm 0.20)\%.$$

The mass agrees well with the CLEO result [5] and with all following observations of the new F [6,7,8]. Results on the R.BR. value, where $R(F) = \sigma(e^+e^- \to F + \text{anything})/\sigma(e^+e^- \to \mu^+\mu^-)$, are not so well in agreement. CLEO [5] finds (2.0 ± 0.5)%, TASSO [6] finds (6.4 ± 2.3)%, where both values, like ours, are extrapolated over the full momentum range of F production in e^+e^- annihilation. Because of the poor agreement I would like to use the ARGUS result alone for deriving a branching ratio estimate.

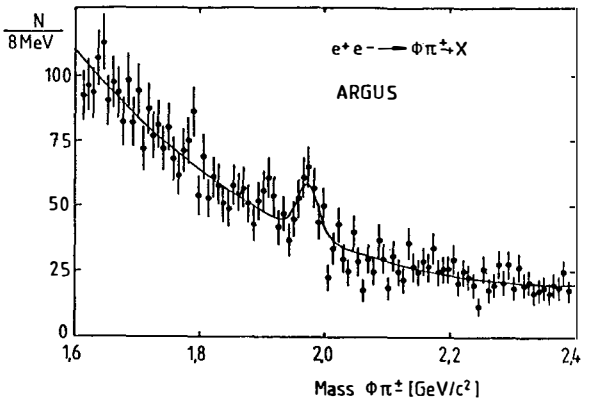

Fig. 4a
The invariant mass distribution of $\Phi\pi^{\pm}$ with cuts $p(\Phi\pi) > 1.5$ GeV/c and $\cos\theta_{\pi}$ between −.8 and +1

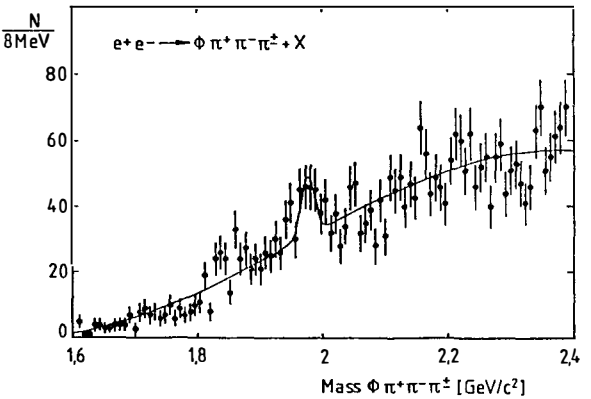

Fig. 4b
The invariant mass distribution of $\Phi\pi^{+}\pi^{-}\pi^{\pm}$ with the cut $p(\Phi 3\pi) > 2.2$ GeV/c

The R value for charm production is $3.4/9.(1+\alpha_s/\pi)$, and there are two charmed particles per event. Neglecting fragmentation into baryons and assuming u:d:s = 1:1:0.36, there are 2.0.36/2.36 F and F^* mesons per charm event. Since all F^* have to decay into F, this estimate leads to R(F) = 0.43. From our R.BR value quoted above, we obtain :

$$BR(F^+ \to \Phi\pi^+) = (3.4 \pm 0.9)\%.$$

This estimate may be combined with recent life time measurements of the F meson to obtain a partial decay rate. The E531 group [9] finds $(2.6 + 1.2 - 0.8).10^{-13}$ s from 8 decays, and the ACCMOR group [7] finds $(3.2 + 3.0 - 1.3).10^{-13}$ s from 4 decays. Averaging leads to :

$$\tau(F^+) = (2.8 + 1.1 - 0.7).10^{-13}\ s,$$
$$\Gamma(F^+ \to \Phi\pi^+) = (1.2 \pm 0.5).10^{-11}\ s^{-1}.$$

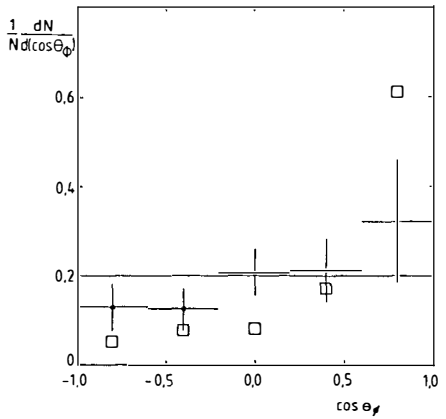

Fig. 5a
Angular distribution of the Φ in the F rest frame with respect to the F boost direction (points). The solid line is the expected isotropic distribution. The open squares show the corresponding distribution of the background.

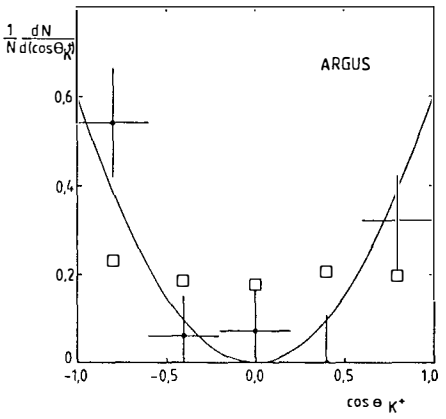

Fig. 5b
Angular distribution of the K^+ in the Φ rest frame with respect to the Φ boost direction (points). The solide curve is the expected $\cos^2\Theta$ distribution. The open squares show the corresponding distribution of the background

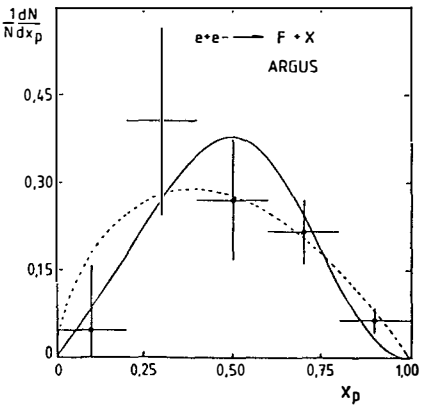

Fig. 6
Fragmentation function of the F meson from a combination of both observed decay channels. $X_p = p(F)/p(F,max)$. The solid curve is the best fit of the Peterson parametrisation, the dashed curve is the best fit of the Kartvelishvili parametrisation.

The partial rate is in surprisingly good agreement with a spectator model calculation of Fakirov and Stech 1978 [10] which gave :

$$\Gamma(F^+ \to \Phi\pi^+) = 1.3 \cdot 10^{-11}\ s^{-1}.$$

ARGUS has additional evidence that the observed $\Phi\pi$ and $\Phi 3\pi$ decays originate from a charmed pseudoscalar meson. The angular distributions of the Φ in the $\Phi\pi$ rest frame and of the K^+ in the Φ rest frame support the 0^- assignment, see fig. 5, and the fragmentation function supports the charm assignment, see fig. 6. The fragmentation function is softer than for the D^* as shown in fig. 2. The fits give ϵ(F, Peterson) = 0.50 + 0.22 − 0.14 and α(F, Kartvelishvili) = 0.64 ± 0.22. Within the given statistics, both fits are equally good.

Evidence for the F^+ Meson

Including the F meson at 1979 MeV, all 16 pseudoscalar mesons from u,d,s and c quarks are now well established. There are only 15 well established (ground-state) vector mesons and no strong evidence for the $F^* = cs(1^-)$. There were some hints from DASP [11], but they were based on the $\eta\pi^+$ decay mode of the F. The quoted mass was (2140 ± 60) MeV. A relativistic quarkonium potential model of Klima and Maor [12] predicts a mass of 2100 MeV for the F^*.

Last summer, the ARGUS group [13] has observed a candidate for the F^* meason with a mass near 2110 MeV. Fig. 7a shows the invariant mass distribution of all $K^+K^-\pi^\pm$ combinations in the reaction $e^+e^- \to (K^+K^-\pi^\pm)X$ at $s = 10$ GeV, which have K^+K^- in a narrow mass band around the Φ mass and $p(KK\pi) > 1.65$ GeV/c. There is a weak F signal near 1970 MeV. If those $K^+K^-\pi^\pm$ combinations are selected which have a photon in the event and form a $KK\pi\gamma$ mass between 2080 and 2170 MeV, the F signal is strongly enhanced as seen in fig. 7b. The strength of the F signal varies with the $KK\pi\gamma$ mass. Fig. 8 shows the fitted number of F mesons as a function of this mass, the spectrum shows a clear peak near 2110 MeV.

Since F^* production is expected to be at least as abundant in e^+e^- annihilation as direct F production and since $F\gamma$ is the dominant decay mode of the F^* ($F\pi^0$ is forbidden by isospin conservation), the observed peak is a good candidate to be the F^* meson. The ARGUS result for the F^*–F mass difference is Δm = (144 ± 9 ± 7)MeV. Combining it with the more recent F mass of 1973.6 MeV quoted above, we obtain :

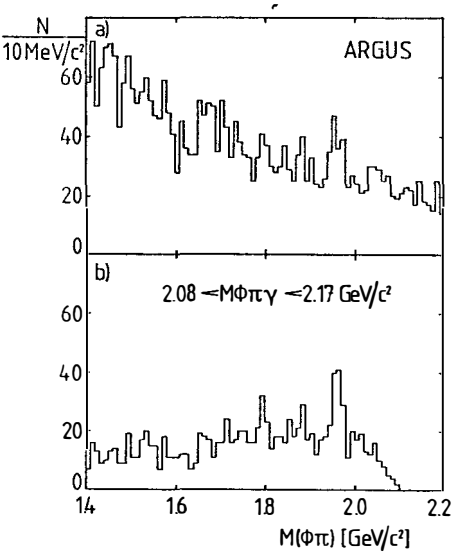

Fig. 7
a) the $\Phi\pi$ invariant mass spectrum for $p(\Phi\pi) > 1.65$ GeV/c without requiring an extra photon,

b) the same spectrum, but with the requirement that there are photons in the event which give a $\Phi\pi\gamma$ invariant mass in the F^* region

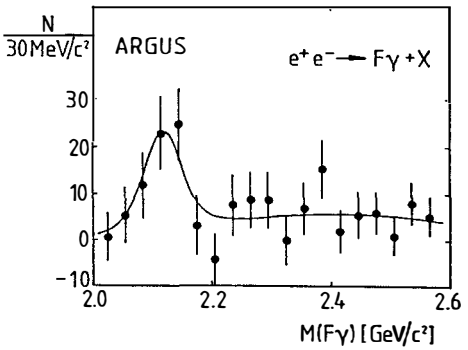

Fig. 8
The background subtracted number of F mesons as a function of the $F\gamma$ mass.

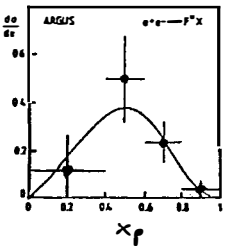

Fig. 9
The F^* fragmentation function. The curve is the best fit of the Peterson parametrisation.

$m(F^{*+}) = (2118 \pm 9 \pm 8)$MeV.

Fig. 9 shows the F^* fragmentation function, it is slightly softer than for the D^*. The solid curve is a fit following the Peterson parametrisation. We obtain $\epsilon = 0.49 + 0.30 - 0.16$, but there is not enough statistics to discuss differences between the two parametrisations like in the D^* case.

Further evidence for the F^* has recently been reported by the TPC group at PEP [14] with $\Delta m(F^*-F) = (139.5 \pm 8.3 \pm 9.7)$ MeV and by a neutrino experiment at Serpukhov [15] with $\Delta m(F^*-F) = (150 \pm 15)$ MeV.

References

1] H. Albrecht, U. Binder, G. Drews, G. Harder, H. Hasemann, A. Philipp, W. Schmidt-Parzefall, H. Schroder, H.D. Schulz, F. Selonke, R. Wurth (DESY), A. Drescher, B. Gräwe, U. Matthiesen, H. Scheck, J. Spengler, D. Wegener (Dortmund), R. Heller, K.R. Schubert, J. Stiewe, R. Waldi, S. Weseler (Heidelberg), K.W. Edwards, W.R. Frisken, Ch. Fukunaga, M. Goddard, P.C.H. Kim, R.Kutschke, D.B. MacFarlane, J.A. McKenna, K. McLean, A. Nilsson, R.S. Orr, P. Padley, P.M. Patel, J.D. Prentice, H.C.J. Seyward, B.J. Stacey, T.S. Yoon, J.C. Yun (IPP Canada), R. Ammar, D. Coppage, R. Davis, S. Kanekal, N. Kwak (Kansas), P. Böckmann, L. Jonsson, Y. Oku (Lund), M. Danilov, L. Lubimov, V. Matveev, V. Nagovitsin, V. Ryltsov, Yu. Semenov, V. Shevchenko, V. Soloshenko, V. Sopov, I. Tichomirov, Yu. Zaitsev (Moscow), R. Childers, C.W. Darden, and H. Gennow (South Carolina),
Phys. Lett. 150B (1985) 235

2] C. Peterson et al., Phys. Rev. D27 (1983) 105

3] V.G. Kartvelishvili et al., Yad. Fiz 38 (1983) 105,

4] H. Albrecht et al. (ARGUS), DESY preprint 84-043

5] A. Chen et al. (CLEO), Phys. Rev. Lett. 51 (1983) 634

6] M. Althoff et al. (TASSO), Phys. Lett. 139B (1984) 130

7] R. Bailey et al. (ACCMOR), Phys. Lett. 139B (1984) 320

8] J.M. Weiss et al. (HRS), Proc. Leipzig Conf. 1984, vol. 1, p. 316
I. Beltrami, talk presented at this workshop

9] N.W. Reay (E531), Proc. Physics in Collision, Como 1983, p. 223

10] D. Fakirov and B. Stech, Nucl. Phys. B133 (1978) 315

11] R. Brandelik et al. (DASP), Phys. Lett. 70B (1977) 132

12] B. Klima and U. Maor, DESY preprint 84-029

13] H. Albrecht et al. (ARGUS), Phys. Lett. 146B (1984) 111

14] H. Aihara et al. (TPC), Phys. Rev. Lett. 53 (1984) 2465

15] A.E. Asratyan et al. (Serpukhov), preprint ITEP-99 (1984).

EVIDENCE FOR THE CHARMED DOUBLE STRANGE BARYON T^0 AT 2.74 GEV/C^2 FROM THE WA62 COLLABORATION[1)]

[BRISTOL-GENEVA-HEIDELBERG-LAUSANNE-LONDON(QMC)-RAL]

R M Brown
Rutherford Appleton Laboratory, Chilton, Didcot, OXON, ENGLAND

ABSTRACT

In an experiment performed at the CERN-SPS hyperon beam, first evidence for the baryon T^0 with quark content (css) has been obtained in the reaction $\Sigma^- + Be \rightarrow (\Xi^- K^{*0}(890)\pi^+) + X$. The signal contains 3 events without any background. The measured decay lengths of these events are consistent with a mean lifetime of several times 10^{-13}s.

The conclusion that these events arise from a Cabibbo favoured decay of the T^0 is based on the observed lifetime and the quantum numbers of the final state : baryon number B = 1, strangeness S = -3 and electrical charge Q = 0.

The mass of the new state is determined to be 2740 ± 20 MeV/c^2.

1) APPARATUS AND TRIGGER

The experiment was designed to accept charmed strange baryons produced in the forward direction in Σ^--Be collisions and to identify them by studying the effective mass distributions of combinations of particles. It was performed at the CERN SPS in the charged hyperon beam[2] which, for this measurement, was tuned to its maximum momentum of 135 GeV/c.

A differential Cherenkov counter (DISC) selected 2 x 10^4 incident Σ^- in each 1.5 s beam pulse of 1.5 x 10^6 particles (mainly π^-). The trajectories of the beam particles were measured in multiwire proportional chambers (MWPCs) located upstream and downstream of the DISC (Fig. 1). The Σ^- struck an 8 cm long Be target, located downstream of the DISC. Charged particles produced in the forward direction were tracked in a double magnet spectrometer equipped with MWPCs and drift chambers (DCs)[1]. Protons, kaons and pions with sufficient momentum to pass through both magnets were identified in two multicell Cherenkov counters, C1 and C2, which had pion thresholds of 14 GeV/c and 10 GeV/c, respectively.

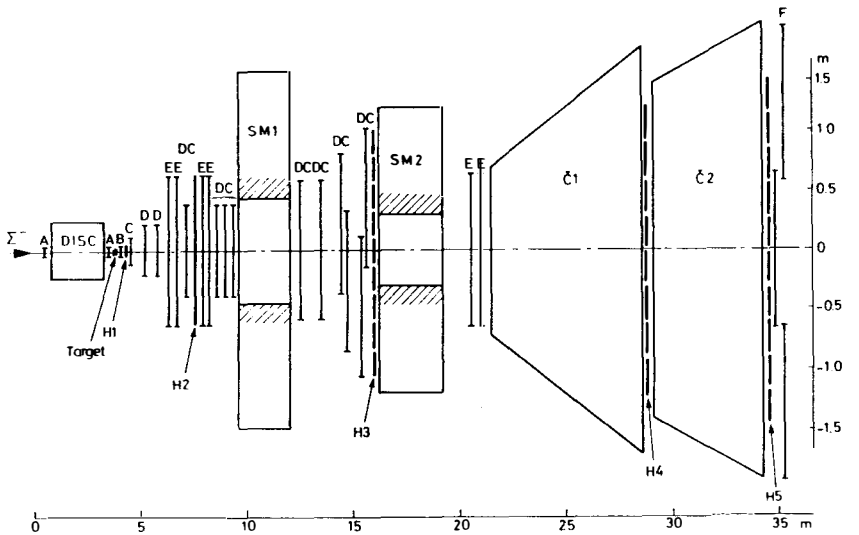

FIG. 1 LAYOUT OF APPARATUS. A-F = MWPC CLUSTERS; DC = DRIFT CHAMBER CLUSTERS; SM1, SM2 = MAGNETS; C1, C2 = GAS CHERENKOV COUNTERS; H1-H5 = SCINTILLATOR HODOSCOPES.

The trigger used in the experiment was aimed at selecting final states of strangeness -2 or -3, with zero or positive charge. It therefore required among the produced particles, a Λ and a K^- together with at least one more charged particle. This restricted choice was made because the data recording system had a capacity of 250 events per beam spill, which at the full Σ^- rate of 20000 per spill was not sufficient to accept all possible decay channels.

2) EVIDENCE FOR THE T^0

This experiment has already yielded results on the $A^+(csu)$ baryon, observed as a narrow peak in the $\Lambda K^-\pi^+\pi^+$ channel[1] which has S = -2. Using the same sample a search was made for events where the Λ was produced indirectly via the decay $\Xi \to \Lambda\pi^-$, indicating an S = -3 final state. Fig. 2 shows the $\Lambda\pi^-$ effective mass distribution obtained from events with an additional negative track, assumed to be a π^-, which intersected the Λ line of flight downstream of the target. A clear signal of 20 events is visible within $\pm$ 7 MeV/c^2 of the Ξ^- mass. None of these events contributed a $\Lambda K^-\pi^+\pi^+$ mass combination to the A^+ peak.

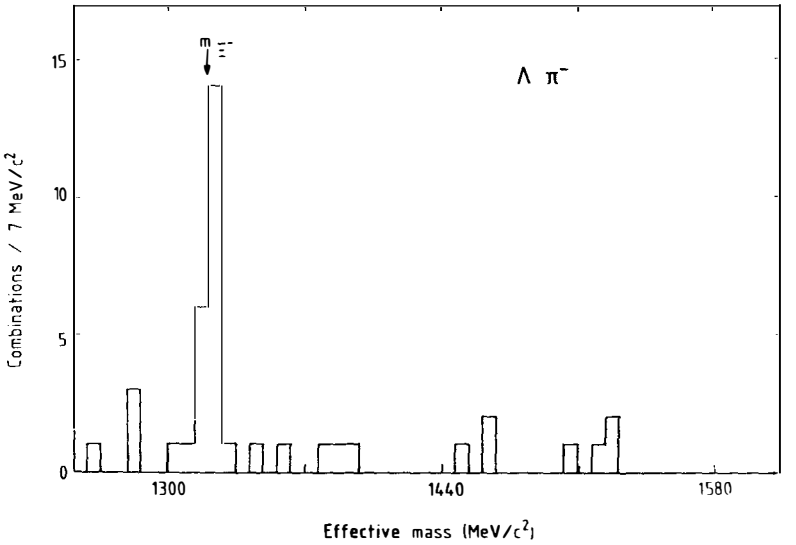

Fig. 2 : The $\Lambda\pi^-$ effective mass distribution for $(\Lambda K^-\pi^+\pi^+)$ events with a $\Lambda\pi^-$ decay vertex downstream of the target.

The $\Xi^-K^-\pi^+\pi^+$ effective mass was calculated for these 20 events, yielding 26 such combinations (Fig. 3a). Fig. 3b shows the mass distribution for events which had additional tracks in the chambers just downstream of the target,

thereby permitting the reconstruction of the production vertex. This requirement was suggested by the observation that the ratio of signal to background for the $A^+ \to \Lambda K^-\pi^+\pi^+$ channel increased from 82/147 to 53/59 when the same condition was imposed. This sample contained 15 combinations from 10 events.

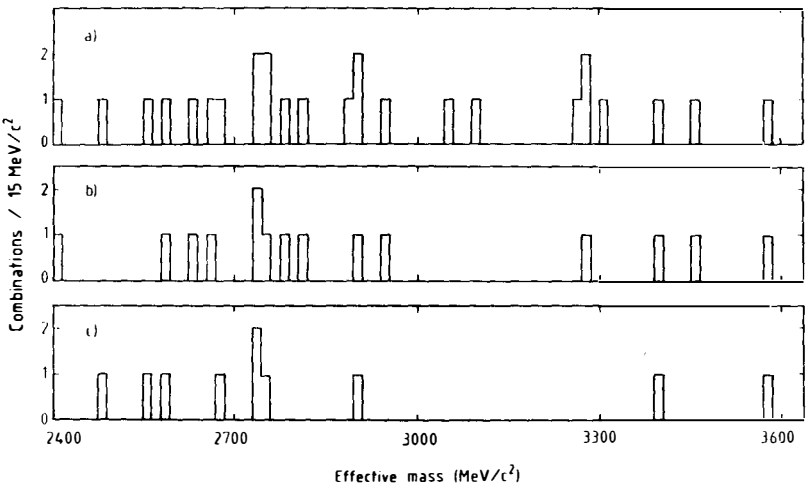

Fig. 3 : The $\Xi^-K^-\pi^+\pi^+$ effective mass distributions.
a) all events. b) events for which the interaction vertex was reconstructed. c) events which were compatible with the decay $K^* \to K^-\pi^+$.

The events shown in Fig. 3c were required to have a $K^-\pi^+$ combination with an effective mass compatible with a $K^{*o}(896)$, i.e. $0.85 < M(K^-\pi^+) < 0.95$ GeV/c^2. Ten combinations from seven events remain. The main motivation for this requirement was to strengthen the S = -3 assignment of the final state by removing K^+ and π^- which had been misidentified as π^+ or K^-, respectively.

The requirement of both a reconstructed production vertex and a $K^{*o}(896)$ resulted in a $\Xi^-K^-\pi^+\pi^+$ effective mass distribution (Fig. 4) with six combinations from four events. Three events have a mass combination near 2740 MeV/c^2, which is in the region where the T^0 is expected[4].

The spread of the masses of the three events around 2740 MeV/c^2 is fully compatible with the mass resolution of the apparatus, which we estimated from Monte Carlo calculations to be 25 MeV/c^2 (FWHM). The mass of this state was determined to be (2740 ± 20) MeV/c^2, where the error was dominated by the systematic uncertainty in the mass scale.

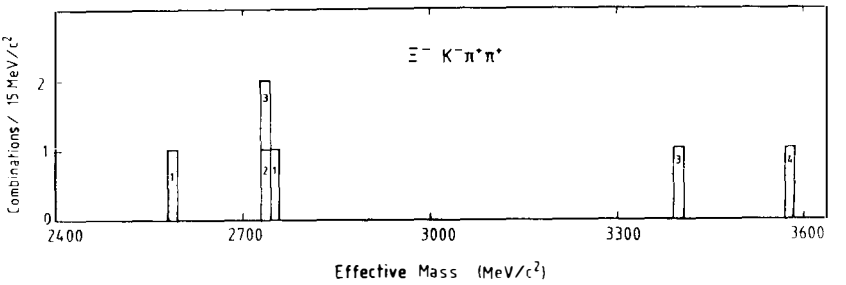

Fig. 4 : The $\Xi^-K^-\pi^+\pi^+$ effective mass distribution for T^0 candidates. The four events are numbered to indicate their combinatorial entries into this plot. Hatched entries have negative Δz.

The reconstructed production vertex in these events allowed a measurement of the distance Δz between the production and the decay of the $\Xi^-K^-\pi^+\pi^+$ system with a resolution of 6 mm (r.m.s.). A mean Δz of this magnitude would correspond to a T^0 lifetime of about 6×10^{-13}s. Two of the combinations (shown shaded in Fig. 4) have negative values of Δz, corresponding to a reconstructed decay vertex upstream of the reconstructed production vertex. On the other hand Δz is positive for all three combinations with a mass near 2740 MeV/c^2, the Δz values being 2, 0.5 and 1.5 standard deviations away from zero, respectively. This is an indication that these events result from a weak decay. We therefore conclude that we have observed evidence for the T^0 baryon decaying in a Cabibbo-favoured mode.

3) DISCUSSION

Although the branching ratio of $T^0 \to \Xi^-K^{*o}(896)\pi^+$ is unknown, some qualitative comments on the T^0 cross section may be made. Assuming similar momentum spectra for the T^0 and the A^+, the acceptance of the apparatus for the T^0 is approximately one half that for the A^+, mainly because of the additional Ξ^- decay length. Furthermore it can be expected that in Σ^-N collisions T^0 are produced with a lower rate than A^+ because of the additional strange quark contained in the T^0. In 200 GeV/c pN collisions, for example, the ratio of Σ^- and Ξ^- produced at $x = 0.66$ is 20[2]. Therefore the observation of three T^0 decays, as compared to 53 A^+ decays is not unreasonable.

It is more meaningful to consider the mass differences between Λ_c^+, A^+, and T^0 instead of the absolute values when comparing with theoretical work on charmed baryons, since most authors have used the then current value of the Λ_c^+ mass to fix their mass scale. We use the 1984 world average of the Λ_c^+ mass[3],

$m = (2282 \pm 3)$ MeV/c^2 to calculate mass differences Δm (Λ_c^+,A^+) and Δm (Λ_c^+,T^0). It should be kept in mind, however, that the experimental situation with respect to the Λ_c^+ mass is not yet satisfactory. In the table various predictions for the mass differences between Λ_c^+, A^+ and T^0 are compiled[4]. Three of these predictions [4a,4c,4d] are in agreement with the experimental values for both A^+ and T^0.

Comparison of mass differences predicted by various models with experimental results (units are MeV/c^2)

Authors [Ref. 4]	Δm (Λ_c^+,A^+)	Δm (Λ_c^+,T^0)	Δm (A^+,T^0)
De Rujula et al (1975)	220	480	260
Fuchs and Scadron (1979)	110	550	440
Körner et al (1979)	210	470	260
Maltman and Isgur (1980	220	470	250
Sakharov (1980)	235	500	265
Vaisenberg (1982)	110	470	360
Richard and Taxil (1983)	180	380	200
This experiment	180 ± 15	460 ± 20	280 ± 10*

*Some sources of systematic error are common to both the A^+ and T^0 mass measurements in this experiment, hence the error on Δm (A^+,T^0) is smaller than that on Δm (Λ_c^+,A^+) or Δm (Λ_c^+,T^0).

1) a) S F Biagi, M Bourquin, A J Britten, R M Brown, H J Burckhart, A A Carter, Ch Dore, P Extermann, M Gailloud, C N P Gee, W M Gibson, J C Gordon, R J Gray, P Igo-Kemenes, P Jacot-Guillarmod, W C Louis, T Modis, Ph Rosselet, B J Saunders, P Schirato, H W Siebert, V J Smith, K -P Streit, J J Thresher, S N Tovey and R Weill. Phys. Lett. 122B (1983) 455.
   b) H J Burckhart, Ph.D. Thesis, Heidelberg (1983).
   c) S F Biagi et al., Phys. Lett. 150B (1984), 230.
2) M Bourquin et al., Nucl. Phys. B153 (1979) 13.
3) Particle Data Group, Rev. Mod. Phys. 56 (1984) No. 2, II.
4) a) A De Rujula et al., Phys. Rev. D12 (1975) 147.
   b) N H Fuchs and M D Scadron, Phys. Rev. D20 (1979) 2421.
   c) J G Körner et al., Z. Phys. C2 (1979) 117.
   d) K Maltman and N Isgur, Phys. Rev. D22 (1980) 1701.
   e) A D Sakharov, SLAC Trans. 0191 (1980), preprint ITEF 82-005.
   f) A O Vaisenberg, DESY L-Trans-264 (1982).
   g) J M Richard and P Taxil, CNRS Marseille preprint, IPNO/TH 83-11.

HEAVY LIGHT MESONS

Jean-Marc Richard[+]
Institut Laue-Langevin
156X
38042 Grenoble Cedex, France

Abstract

A review is presented of theoretical and phenomenological studies of the spectroscopy of mesons with open heavy flavour. The non-relativistic quark model is often used for illustration, but more elaborated treatments of the quark dynamics are also listed and commented upon. Hybrid and multiquark states with open flavour are also discussed.

Résumé

Cet exposé contient une revue des travaux théoriques et phénoménologiques sur la spectroscopie des mésons avec saveur lourde ouverte. Le modèle des quarks non relativiste est souvent utilisé à titre d'exemple, mais les traitements plus élaborés de la dynamique des quarks sont également recensés et commentés. La discussion porte également sur les états hybrides ou multiquarks avec saveur nue.

1. Introduction

One should first acknowledge that during recent months there has been no spectacular development in the theoretical description of the $(Q\bar{q})$ states, those mesons consisting of a heavy quark Q bearing charm or beauty and a light antiquark $\bar{q}$ which can be $\bar{u}$, $\bar{d}$ or $\bar{s}$. In presenting this review of sometimes relatively old theoretical work, our motivation is essentially twofold. Firstly, we discuss the recent results concerning the F and B mesons. Secondly, we emphasize the points where the situation is controversial for theorists and experimental progress could help in our understanding of the quark dynamics. This includes the P-wave mesons with charm, the $(Q\bar{q}g)$ hybrids with heavy flavour and the multiquark sector.

The $(Q\bar{q})$ systems are both extreme and intermediate within meson spectroscopy. On the one hand it should be noted that the light constituent $\bar{q}$ is more relativistic in $(Q\bar{q})$ than in $(q\bar{q})$. If, for example, one uses the non-relativistic quark model (NRQM) with universal potential $V = k\, r^{\nu}$, one easily obtains the ratio of the $\bar{q}$ velocities for $Q \to \infty$ from the standard scaling laws[1)]

$$v(Q\bar{q}) \,/\, v(q\bar{q}) = 2^{1/(2+\nu)} \qquad (1)$$

This is the well-known effect that the electron moves faster in the hydrogen atom than in positronium. As a consequence, when considering $(Q\bar{q})$ spectroscopy, one is tempted to worry much on relativistic effects and to adopt for instance the picture of a Dirac particle $\bar{q}$ moving around a static potential source Q.

On the other hand, the flavoured $(Q\bar{q})$ mesons represent in many respects a configuration intermediate between the heavy quarkonia $(Q\bar{q})$ and the ordinary mesons $(q\bar{q})$. From this point of view, it is highly desirable that the models used remain flexible enough to allow for uniform treatment of all mesons in order to test the universality of the dynamics. In addition to the NRQM, there have already been some attempts to produce relativistic models. These different approaches will be discussed in Section 5.

2. Convexity properties

In QCD, the quark-gluon coupling is universal, so that, apart from recoil corrections affecting in particular the spin dependent components, the quark-antiquark potential is expected to be flavour independent. Assuming this property to be strictly true leads to the inequality

$$M(Q\bar{Q}) + M(q\bar{q}) < 2M(Q\bar{q}) \qquad (2)$$

In the NRQM, the proof[2] is most easily achieved by first removing the motion of the centre-of-mass. The hamiltonian depends linearly on the inverse reduced mass μ^{-1} and the ground state energy varies as a concave (and obviously increasing) function of μ^{-1}. The inequality also holds for the ground levels with a given angular momentum and for the sum of the masses of the first n states in any partial wave[3]. E. Lieb[4] recently generalized the formulation of (2) so that, in particular, a relativistic form $\sqrt{\vec{p}^2 + m^2}$ of the individual kinetic energy can be used instead of the non relativistic form $m + \vec{p}^2/2m$. There have also been proofs of (2) directly from QCD, with, however, some restrictions on the effect of quark annihilation[3,5].

Experimentally the inequality (2) is quite well satisfied for the spin averaged ground states, so that no dramatic departure from flavour independance is observed. Using π and ρ to estimate the mass of the $(n\bar{n})$ state, where n means u or d, we check for instance that

$$n\bar{n} + c\bar{c} \simeq 3.71 \text{ GeV} < 2(c\bar{n}) \simeq 3.94 \text{ GeV} \tag{3}$$

One can also predict for the spin-averaged $b\bar{s}$ state a mass

$$b\bar{s} > \frac{3}{8}\gamma + \frac{1}{8}\eta_b + \frac{3}{8}\phi + \frac{1}{8}s\bar{s}(0^{-+}) > 5.2 \text{ GeV} \tag{4}$$

assuming $\gamma - \eta_b = 50$ MeV and 0.96 GeV (η') as an upper limit for the last term.

Clearly, the inequality (4) is not very constraining, maybe because it relates systems with quite different average quark velocity and interquark separation. The flavour independence of the potential also induces inequalities which deal only with heavy-light systems such as D, F, B and B_s.

In the figure, we plot the ground-state energy E as a function of the inverse reduced mass μ^{-1}, for various $Q\bar{q}$ systems. From the convexity of $E(\mu^{-1})$, one obtains for instance

$$E(c\bar{n}) - E(b\bar{n}) < E(c\bar{s}) - E(b\bar{s})$$

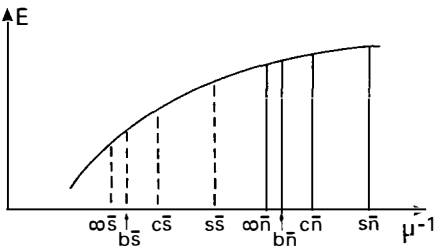

i.e.

$$M(b\bar{s}) - M(b\bar{n}) < M(c\bar{s}) - M(c\bar{n}) \tag{5}$$

and other similar inequalities. Experimentally, considering the spin-averaged masses (5) most probably works for $s\bar{s} - s\bar{n}$ ($\lesssim$ 206 MeV) versus $c\bar{s} - c\bar{n}$ ($\simeq$ 78 MeV).

+On leave of absence from the Université Pierre et Marie Curie, Paris

One also finds the interesting constraint for the spin averaged $b\bar{s}$ state

$$b\bar{s} < b\bar{n} + c\bar{s} - c\bar{n} = 5.41 \text{ GeV} \tag{6}$$

3. Hyperfine splittings

Within the NRQM, a very naive but successful[6] treatment of the hyperfine splittings consists of following the analogy with the Breit-Fermi corrections in atoms. This gives, with obvious notations

$$M(^3S_1) - M(^1S_0) = \frac{32\pi}{9} \alpha_s \frac{|\phi(0)|^2}{m_1 m_2} \tag{7}$$

Neglecting the variations of the wave-function at the origin, $\phi(0)$, would lead to the prediction that $(D^* - D)/(F^* - F) \simeq 2 - 3$, in contradiction with experiment. In fact, in most realistic models, the interquark separation scales approximately as in the case of a logarithmic potential[1], i.e. as $\mu^{-1/2}$ where μ is the reduced mass, so $|\phi(0)|^2$ varies like $\mu^{3/2}$ and the naive formula (7) now gives $D^* - D \simeq F^* - F$ in surprising agreement with experiment. If the charmed quark is now changed into a bottom quark, this reduces only marginally the size of the wave-function, so that it can be predicted quite safely that

$$B_s^* - B_s \simeq B^* - B \simeq (D^* - D) \frac{m_c}{m_b} \tag{8}$$

This is in agreement with the recent result[7] that $B^* - B \simeq 50$ MeV. This also shows, in conjunction with (6) that the B_s should lie just above the B^* (at 50 MeV or less). For instance, the NRQM of ref. 8) gives $B_s = 5.35$ GeV and $B_s^* = 5.41$ GeV whereas ref. 9) predicts $B_s - B^* \simeq 0.02$ GeV.

Note that the rule stating that the quantity $M^2(^3S_1) - M^2(^1S_0)$ remains constant within the whole meson spectroscopy works surprisingly well. This was studied recently in some detail[10].

4. The fine structure of the $(Q\bar{q})$ P-states

A major progress in the understanding of the quark dynamics was achieved by Gromes[11] who clarified the controversy between Eichten, Buchmüller, himself and others concerning the most plausible spin dependence of the linear confining potential which presumably arises from QCD[12]. The theory was hesitating between a positive and a negative spin-orbit potential. Ref. 11) gives a strong argument for the latter sign, in agreement with the phenomenology, which favours a confining potential behaving like a Lorentz scalar.

Note that, in principle, $Q\bar{q}$ systems give unique information on the spin-dependent hamiltonian, since they permit a distinction to be made between $(m_1\ m_2)^{-1}$, m_1^{-2} and m_2^{-2} types of terms which coincide for equal mass quarkonia. In practice, however, the situation is not as clear as for the χ states. The charmed mesons with negative parity are presumably broad and shifted by their coupling to their decay channels[13]. The P-states of the F meson might be better in this respect, since they probably decay less strongly via for instance $(c\bar{s})_P \to (c\bar{n})_s + K$ or $(c\bar{s})_s + \pi\pi$.

The ordering of the P-states of the D-meson is highly controversial in the literature, due to their situation intermediate between dominant short-range and dominant long-range interaction. In a $(Q\bar{q})$ system the total spin s of the quarks is not conserved, but one can still use the standard spectroscopic notation $^{2s+1}L_J$ by referring to the dominant piece of the wave-function, or, alternatively $L_J^{(j)}$, where $\vec{j} = \vec{l} + \vec{s}_2$ is the total moment of the antiquark. The Coulomb interaction favours a "normal" order $^3P_0 < {}^3P_1 < {}^1P_1 < {}^3P_2$. The long-range force, with its negative spin-orbit component, tends to invert this order. This was underlined by Schnitzer[14] and confirmed, e.g. by Henriques[15] who predicts $^1P_1 < {}^3P_0 < {}^3P_2 < {}^3P_1$ for $c\bar{n}$ and $^1P_1 < {}^3P_2 < {}^3P_0 < {}^3P_1$ for $b\bar{n}$. On the other hand, Pignon and Piketty[16] obtained $^3P_0 < P_1(3/2) < {}^3P_2 < P_1(1/2)$. More recently, Klima and Maor[17]) also found a quite normal ordering for both $c\bar{n}$ and $b\bar{n}$ P-states.

5. Specific models

As emphasized in the introduction, the NRQM hardly remains non-relativistic in handling the $Q\bar{q}$ spectroscopy. A dramatic illustration arises when studying the resultant mass $M_T(M,m)$ as a local function of the light mass m for a flavour independent interaction. (This variation enters in the estimate of the electromagnetic mass differences like $D^+ - D^0$). One sometimes finds the surprising and probably non-physical result $\partial M_T/\partial m < 0$[18].

For $Q \to \infty$, the Dirac equation is certainly very suitable. It was adopted in refs. 16 and 19 for quantitative studies in the charm sector. These calculations reproduce quite well the experimental results, and in particular the property that $F^* - F \simeq D^* - D$. Note that the Dirac equation should exhibit its superiority over the NRQM more clearly in decay matrix elements than in mass spectra.

More ambitious are the models where both particles are treated relativistically. In a first group of papers, the kinetic energy $\vec{p}^2/2m$ is replaced by $\sqrt{\vec{p}^2 + m^2} - m$ for each particle, leading to an interesting phenomenology, where all mesons, light and heavy, are treated simultaneously[20]. The most extensive

study, in this category, is probably that of ref. 9, where the decay properties of the mesons are also systematically studied, in addition to their mass spectrum. Besides these models, there are attempts to incorporate ab initio all the spin effects in a relativistic way. This means solving the Bethe-Salpeter equation or at least obtaining a decent approximation. Some works are listed in ref. 21, but there are many others of interest. Generally, these relativistic calculations reproduce on firmer ground the results obtained using the Schrödinger equation supplemented by suitable Breit-Fermi corrections.

In the bag model phenomenology, there are two simple limits. The first one is the fixed cavity approximation adopted by the MIT group to get a fit of all light hadrons in the ground state[22]. This model has given rise to hundreds of papers dealing with centre-of-mass corrections, pionic cloud corrections, breathing modes, etc. In the MIT bag, the quarks oscillate freely into a spherical canty, and the radius is adjusted to minimize the mass of the hadron. The second limit deals with heavy quarks, for which the bag model is used in the so-called adiabatic approximation similar to the Born-Oppenheimer treatment of the molecular binding. For fixed interquark separation r, the bag shape is adjusted to minimize the energy, and this minimum is used as the $Q\bar{Q}$ potential V(r) in the Schrödinger equation[23]. For heavy light systems, Izatt et al[24] used the compromise of a light antiquark $\bar{q}$ oscillating relativistically into a cavity centered at the position of the heavy quark Q. They obtained a good agreement with experiment.

In lattice QCD, there are also different strategies which are to some extent similar to those employed by bag modelists. For light hadrons, the masses are estimated directly from the lattice[25]. On the other hand, for heavy quarks, the lattice is used to compute the interquark potential[26], which (when corrected for the omitted quark loop effects) can be inserted into the Schrödinger equation. Perhaps heavy-light systems deserve special treatment, where a static colour source Q is attached to the lattice and the $\bar{q}$ motion is studied by an appropriate Monte-Carlo algorithm.

Finally the QCD sum rules should be mentioned, an approach where known perturbative properties and the assumed mathematical properties are tentatively incorporated[27]. In practice this method is restricted to the lowest state for each set of quantum numbers. For light mesons, the sum rules are controlled by gluon or quark condensates whereas the perturbative terms dominate for heavy quarkonia. Among the results obtained so far for mesons with open beauty[28], one may note

i) $B_s^* - B_s \simeq 0.04$ GeV $< B^* - B \simeq 0.07$ GeV

ii) $M(0^{++}) < M(1^{++})$, i.e. a normal ordering

iii) a large S-P splitting.

It would be interesting to test whether these properties are stable against variations of the computation procedure within this approach.

6. Hybrids

The literature is already rich in so-called hybrids or hermaphrodites, these hadrons where the usual quarks are supplemented by constituant gluons to achieve a colour singlet configuration[29]. Light ($n\bar{n}g$) and heavy ($Q\bar{Q}g$) hybrid mesons have been studied, but none has never been definitely discovered. If gluons and hybrids with hidden flavour exist, they are certainly hybrids with naked flavour, i.e. ($Q\bar{q}g$). The problem is to guess which of these new hadronic states has the best chance to show up in the spectrum with a clean signal. Maybe constituant gluons appear only in the strong colour field produced by a static heavy quark Q. Perhaps in $Q\bar{Q}$, this field is too efficiently screened, leaving $Q\bar{q}g$ as the best candidate for hybrids ? This should be studied less naively in specific models and we may anticipate controverses. Remember that the bag model gives relatively low ($b\bar{b}g$) states[23], whereas a recent estimate with QCD sum rules predicts much higher masses[30].

7. Multiquarks

The question of the existence of multiquarks is still open, although not very fashionable in this year 1985. The LEAR results have not produced so far any strong evidence for baryonium[31]. The situation is also not fully clarified in the dibaryon sector[32]. If one insists on killing the multiquarks, one has to find a good mechanism of saturation such that when a quark and an antiquark form a meson or three quarks form a baryon, no additional quark or antiquark can be inserted to produce a heavier stable system.

The situation with the present models is, however, far from being settled. It has often been emphasized that special spin-flavour configurations give coherent attraction in the chromomagnetic forces[33]. Also, assymetric mass configurations like $QQ\bar{q}\bar{q}$ with $M/m \gg 1$ might favour collective binding[33]. Perhaps some $cs\bar{n}\bar{n}$ states could combine the two effects and lie below their dissociation threshold D + K. In most studies, however, a naive additive rule is assumed for the flavour independent confining potential, namely $V = \sum F_i F_j V_o(r_{ij})$, where the F's are the SU(3) colour generators. More elaborate ansatz should also be considered, based e.g. on the string[34] or the bag[35] pictures, in order to test the model dependence of the multiquark spectrum.

Acknowledgements

I would like to thank L. Oliver and H. Rubinstein for discussions during the workshop, and D. Gray for comments on the manuscript.

References

1) C. Quigg and J.L. Rosner, Phys. Rep. 56, 167 (1979)
2) R. Bertlmann and A. Martin, Nucl. Phys. B168, 111 (1980)
3) S. Nussinov, Phys. Rev. Lett. 52, 966 (1984)
4) E. Lieb, "Baryon mass inequalities in quark models", Princeton preprint, 1985
5) E. Witten, Phys. Rev. Lett. 51, 2351 (1983)
6) A. de Rujula, H. Georgi and S.L. Glashow, Phys. Rev. D12, 147 (1975)
7) P. Franzini, Contribution to this Workshop
8) A. Martin, Phys. Lett. 100B, 511 (1981)
9) S. Godfrey and N. Isgur, "Mesons with chromodynamics", University of Toronto preprint, July 1984
10) K. Igi and S. Ono, "Hyperfine splitting of quarkonium", Tokyo preprint UT 446 (1984). See also the contribution by S. Ono at this Workshop.
11) D. Gromes, Z. Physik C26, 401 (1984) and references therein
12) For a review, see J.L. Rosner, "Spin dependent forces in quark models", Chicago preprint 84133, talk at the 6th Int. Symp. on High Energy Spin Physics, Marseille, 12-19 Sept.84, to appear in J. de Physique
13) See, e.g., the contribution by N. Törnqvist at this Workshop
14) H.J. Schnitzer, Phys. Lett. 76B, 461 (1978) and 149B, 408 (1984)
15) A.B. Henriques, Z. Physik C11, 31 (1981)
16) D. Pignon and C.A. Piketty, Phys. Lett. 81B, 334 (1979)
17) B. Klima and U. Maor, work quoted in ref. 12
18) J.M. Richard and P. Taxil, Z. Physik C26, 421 (1984)
19) See, for instance, N. Barik and S.N. Jena, Phys. Lett. 101B, 282 (1981), M. Kaburagi et al, Z. Physik C9, 213 (1981), etc.
20) D.P. Stanley and D. Robson, Phys. Rev. D21, 3180 (1980); J.L. Basdevant and S. Boukraa, "Successes and difficulties of unified quark-antiquark potential models", Paris preprint PAR LPTHE 84-21 (June 1984) to appear in Z. Physik C; D.B. Lichtenberg et al, Phys. Lett. 113B, 267 (1982); etc.
21) A.B. Henriques, B.M. Kellett and R.G. Moorhouse, Phys. Lett. 64B, 85 (1976); M. Bander et al, Phys. Rev. D29, 2038 (1984); H.W. Crater and P. van Alstine, Phys. Rev. Lett. 53, 1527 (1984); A. le Yaouanc et al, Phys. Rev. Lett. 54, 506 (1985)
22) T. de Grand et al, Phys. Rev. D12, 2060 (1975)
23) P. Hasenfratz et al, Phys. Lett. 95B, 299 (1980)
24) D. Izatt et al, Nucl.Phys. B199,269(1982).W.Wilcox et al, P.R. D31,1081 (1985)
25) See, e.g., B. Berg, in "PANIC 84", Nucl. Phys. A 434, 151c (1985)
26) D. Barkai et al, Phys. Rev. D30, 1293, 2201 (1984)
27) H.R. Rubinstein et al, Phys. Rep. (in the press)
28) L.J. Reinders et al, Phys. Lett. 104B, 305 (1981)
29) See, e.g., F. Close, in Proc. Eur. Conf. on High Energy Physics, Brighton, 1983
30) J. Govaerts et al, "Hybrid quarkonia from QCD sum rules", Nucl. Phys. B248, 1 (1984)
31) Proc. of the Third LEAR Workshop, Tignes, Jan. 1985, Editions Frontières, to appear
32) A. Svarc, in "PANIC 84", Nucl. Phys. A 434, 329c (1985)
33) See, e.g., J.M. Richard, in Proc. XIX Rencontre de Moriond, Vol. II, p. 515, ed. by J. Tran Thanh Van (Editions Frontières)
34) N. Isgur and J. Paton, "A flux tube model for hadrons in QCD", Toronto preprint (1984)
35) L. Heller and J.A. Tjon, "On bound states of heavy $Q^2\bar{Q}^2$ systems", Los Alamos preprint 84.3219

A REVIEW OF SOME RECENT QUARK MODEL CALCULATIONS

FOR HEAVY BARYONS

P. TAXIL
CENTRE DE PHYSIQUE THEORIQUE
C.N.R.S. Luminy Case 907
13288 MARSEILLE Cedex 9

ABSTRACT

A review is presented of the theoretical situation concerning the heavy baryon masses from the point of view of potential models. A few model independent results are emphasized and a comparison is made between the prediction of various models in the sector of the newly discovered charmed strange states.

INTRODUCTION

This short review is covering some aspects of the theoretical situation concerning the heavy baryon masses, from the point of view of potential models mainly. By heavy baryon, one means a baryon containing some heavy flavoured quark c or b. Note that some authors [1,2] have also considered the strange quark s as an heavy one with some success.

In fact, in view of the experimental situation, the comparison between theory and experiment can be done only in a narrow region of the charmed baryon sector : a few objects have been discovered and all of them contain only one heavy quark. The Λ_c^+ (quark content u d c) and the Σ_c^{++} (u u c) have been established at 2282 ± 3 MeV and around 2450 MeV respectively [3] ; the discovery of the A^+ (usc) at 2460±15 MeV has been reported in 1983 at Moriond [4] and now there is some evidence for the T° (ssc) state at 2740 ± 25 MeV[5]. We are still waiting for baryons with beauty, for instance the Λ_b is not firmly established[3], and of course baryons containing the top quark must exist but such objects have little chance to be discovered in the near future.

I. Model independent results :

Before giving a comparison between the predictions of various models it is instructive to remain at a more model independent level and to recall some consequences of general principles for the baryon states. A few topics will be stressed, somewhat arbitrarily chosen, which from my point of view present some interest for experimental searches.

a) Flavour independence :

Flavour independence (F.I.) is an important consequence of the idea of an universal interaction between the quarks. In QCD the basic interaction is flavour independent. Although it is not proven that the confining part of the interaction does not contain a remnant flavour dependence, it seems that the F.I. hypothesis is well satisfied in the heavy meson sector. The baryon sector is also a laboratory for testing this property or any departure from it.

In non relativistic potential models, the F.I. hypothesis implies that :

- the interquark potential itself does not depend explicitely upon the masses
- the heavy quark mass m_Q will be the only characteristic of the heavy flavoured quark
- it appears only in the kinetic energy $P^2/2m_Q$ and in the spin-spin force which is due to one gluon exchange (OGE) at short distance as introduced by De Rujula, Georgi and Glashow[6]

$$H_{S_i S_j} = C \frac{\vec{S}_i \cdot \vec{S}_j}{m_i \quad m_j} \delta^3 (r_{ij}) \qquad (1)$$

with $C = 2/3\, \alpha_S \cdot 8\pi/3$ for OGE between two quarks in a colour singlet baryon (for a meson 2/3 becomes 4/3).

A direct consequence of this mass dependence for a qqQ system (q = light quark ; Q = heavy quark) is that the hamiltonian for such a system can be written in the form :

$$H = \frac{H_1}{m_Q} + H_2 \qquad (2)$$

Then, it has been noticed[7] that the ground state energy of H will be a concave function of $1/m_Q$, and extrapolating from lighter baryons A. Martin obtained the bounds[7] :

$$\begin{aligned} \Lambda_b &\leqslant 5630 \quad \text{MeV} \\ \Sigma_b &\leqslant 5825 \quad \text{MeV} \end{aligned} \qquad (3)$$

Note that these bounds are respected by explicit calculations[8] using particular models and also that, with power law potentials, the binding energy is almost linear in $1/m_Q$ as conjectured in [7].

Other concavity properties could be verified by the baryon states in the framework of F.I. additive potentials. By analogy to the two body meson case[9,10] some inequalities have been conjectured[8] between the (spin averaged) masses of different systems, namely :

$$(qqq) + (qQQ) \lesssim 2\,(qqQ) \qquad (4)$$

These inequalities cannot be proved easily by simple arguments[22] and a rigorous derivation is still lacking,[23] but they have been verified numerically with a large class of potentials[8,11]. Note that, with ordinary quarks this could give an explanation to the negative sign of the Gell-Mann-Okubo combination (after adding the spin-spin forces) : $2\,(N+\Xi) - \Sigma - 3\Lambda < 0$ (Exp : -25 ± 5 MeV).

In the charm sector one gets :

$$\begin{aligned} (qqq) + (qcc) &\lesssim 2\,(qqc) \\ (ccc) + (cqq) &\lesssim 2\,(ccq) \\ (ccc) + (css) &\lesssim 2\,(ccs) \\ (sss) + (scc) &\lesssim 2\,(ssc) \end{aligned} \qquad (5)$$

and similar relations in the beauty sector.

b) Spin shifts for systems with one heavy quark :

As recalled recently in an extensive review by D. Gromes[12] there is an interesting mass effect in the spin shifts for the qqQ system. The various states are of Λ, Σ, or Σ^* type :

$$\begin{aligned} \Lambda_Q &= ((qq)_{j=0}\ Q)_{j=1/2} \\ \Sigma_Q &= ((qq)_{j=1}\ Q)_{j=1/2} \\ \Sigma^*_Q &= (qq\,Q)\ j=3/2 \end{aligned} \tag{6}$$

i) The $\Sigma_Q - \Lambda_Q$ mass difference is sensitive mainly to the hyperfine interaction between the two light quarks. The splitting increases when m_Q increases up to an asymptotic value for m_Q going to infinity.

ii) On the contrary $\Sigma^*_Q - \Sigma_Q$ is sensitive only to the spin-spin interaction between the light quarks and the heavy one, consequently it decreases as m_Q increases.

This behaviour is very general and is obeyed by various potential as well as bag model calculations.

For comparison the situation in the various sectors is the following :

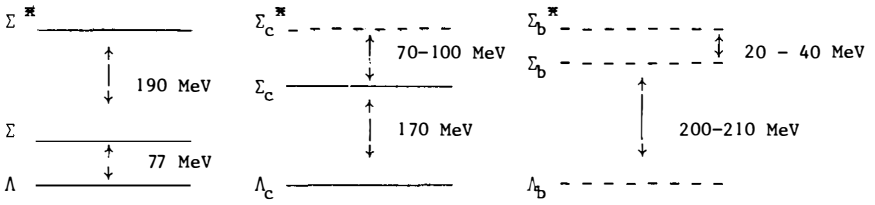

where the predictions (dashed lines) are those obtained using the models we discuss in the following. Note that Σ^*_b and Σ_b being predicted above the $\Lambda + \pi$ threshold and very close to each other, they will be difficult to separate.

c) The link between mesons and baryons :

The rule giving the $Q\bar{Q}$ potential inside a baryon from the QQ potential inside a meson is :

$$V_{QQ} = \frac{1}{2}\ V_{Q\bar{Q}} \tag{7}$$

This is suggested by what happens for OGE or more generally colour octet exchange. This rule has to be applied with some caution (see e.g. the reviews[12,13] and references therein). Note that it is not in contracdiction with the string picture[14] and it is supported by recent lattice calculations[15].

If taken seriously, by variational arguments, this rule leads to[16] :

$$M(QQQ) \geq \frac{3}{2} \quad M(Q\bar{Q}) \tag{8}$$

For instance, incorporating the spin-spin force (in the triplet state) into the potential, one gets :

$$\begin{aligned} M(ccc) &\geq \frac{3}{2} \quad J/\psi \\ M(bbb) &\geq \frac{3}{2} \quad \Upsilon \end{aligned} \tag{9}$$

Note that this inequality is already verified for lighter systems : Ω (1672) > 3/2 Φ (1530) and Δ (1232) > 3/2 ρ (1155). These inequalities can be generalized to systems made with quarks of different flavours[17]:

$$M(Q_1Q_2Q_3) \geq \frac{1}{2} \; M(Q_1\bar{Q}_2) + M(Q_2\bar{Q}_3) + M(Q_3\bar{Q}_1) \tag{10}$$

this gives in the charmed sector :

$$\begin{aligned} \Sigma_c^{*}(cqq) &\geq D^{*} + \frac{1}{2}\,\rho && = 2.39 \text{ GeV} \\ S^{*}(csq) &\geq \frac{1}{2}F^{*} + \frac{1}{2}D^{*} + \frac{1}{2}K^{*} && = 2.50 \text{ GeV} \\ T^{*}(ssc) &\geq F^{*} + \frac{1}{2}\,\Phi && = 2.65 \text{ GeV} \end{aligned} \tag{11}$$

II. Comparison between experiment and some model calculations :

For a comparison between theory and experiment in the sector of the newly discovered charmed-strange states I have chosen a few models which seem representative enough of the theoretical situation.

a) Harmonic oscillator model :

This well known model has been extensively used by Isgur, Karl and collaborators[18] : the quarks are bounded in an harmonic oscillator potential supplemented by standard hyperfine interaction. The parameters are fixed from extensive calculations of the spectrum of ordinary baryons and the charmed quark mass is fixed from that of the Λ_c^{+} around 1.9 GeV (a strategy common to all the models).

b) Smooth quasi logarithmic potential[8,19] :

$$V = \frac{1}{2} \sum_{i<j} A + B \; r_{ij}^{0.1} \tag{12}$$

the hyperfine interaction being given by Eq (1). The parameters are also fixed from a fit of the ordinary baryons. They are not very different from those of A. Martin's potential for heavy quarkonia[1] (taking into account the 1/2 factor) apart for the hyperfine constant which has been adjusted to reproduce the Δ - N splitting and is certainly overestimated for the heavy quark sector.

c) A potential introduced by S.Ono and F. Schoberl[20]

This potential which is essentially coulombic (vector) at short distance and linear (scalar) at large distance, has been used to fit the whole spectrum of mesons and baryons. Note a particularity of this approach : the short distance vector part of the potential is enhanced in baryons (the 1/2 factor of Eq.7 becomes 3/2), a procedure which has no theoretical justification but seems necessary to get a good fit.

In the following table are also displayed for comparison the older results of De Rujula, Georgi and Glashow (DGG)[6] and those obtained in a version of bag model suited for heavy quarks[21] (concerning this model see also[10]). In this table the S is a (csq) state with the (sq) pair mostly in a spin triplet state instead of a spin singlet as in the A , S^* and T^* being the spin 3/2 partners of the S and T respectively. All the masses are in MeV.

State	Exp	Isgur et al	Richard Taxil	Ono Schoberl	Bag	DGG
A (qsc)	2460 ± 15	2495	2457	2460	2430	2420
$A-\Lambda_c$	180 ± 15	220	175	194	150	220
S (qsc)	-	2590	2558	2578	2500	2510
S - A	-	90	98	118	70	90
S^*	-	2660	2663	-	2600	2560
$S^* - A$	-	160	200	-	170	140
T (ssc)	2740 ± 25	2745	2664	2759	2610	2680
$T - \Lambda_c$	460 ± 25	470	380	490	330	480
T^*	-	2805	2775	-	2710	2720
$T^* - T$	-	60	110	-	100	40

A few comments are in order :

- Since in all the models the mass scale is fixed on the Λ_c^+ , it is more instructive to consider the mass differences between the various states as displayed in the table.
- One can see that the agreement between models and experiment is not bad, sometimes very good - even for the simplest approach of DGG ! - apart for the bag model results which are systematically too low. Note that with a smooth potential like in[19] but with a smaller hyperfine constant adjusted from charmonium splittings as in[1], one gets a better value for the T (ssc) : 2710 MeV instead of 2664 MeV.
- Concerning the states to be discovered :

  i) for the S(qsc), the various predictions do not differ by more than 30 MeV in

potential models. This state is predicted to be stable against $S \to A + \pi$.

ii) in the harmonic oscillator model the S^* is just above the threshold $A + \pi$, this is different with a smooth potential.

iii) in all the models the T^* will be stable against

$T^* \to T + \pi$

Certainly more data are needed to discriminate between the various models and of course data on the beauty states would be very interesting.

III. Excited states :

An interesting question is : can we expect a rich spectroscopy of stable excited heavy baryonic states ? Here "stable" is meant in the same sense as the excitations of Ψ or γ systems which lie below their Zweig allowed threshold. A first estimation - in the framework of a smooth potential - is not very optimistic. Indeed, the π (and also the K) are so light that it is difficult for an heavy ground state baryon containing a light or strange quark to have an excitation below the "Zweig allowed" threshold. On the contrary a rough estimate shows that some excitations of (ccc) would be stable (and a fortiori excitations of heavier states made with c or b quarks only). The situation may be quite different with a steepest potential like the harmonic oscillator model where it has been noticed[18] that the radially excited (ssc) or even an orbital excitation of the Λ_c could be stable against strong decay.

Acknowledgements

I am indebted to J.M. Richard for many discussions and advices, to S. Ono for an informative discussion and to J. Soffer for a careful reading of the manuscript.

REFERENCES

(1) A Martin, Phys. Lett. 100 B, 511 (1981)
(2) J.M. Richard, Phys. Lett. 100 B, 515 (1981)
(3) Particle Data Group Rev. Mod. Phys. 56 n° 2 (April 1984)
(4) K.P. Streit, in "Gluons and Heavy Flavours", Proc. XVIII Rencontre de Moriond, La Plagne, 1983, ed. : Tran Thanh Van (ed. Frontières)
S.F. Biagi et al. Phys. Lett 122B,455 (1983)
(5) R.M. Brown : these procedings and S.F. Biagi et al. CERN-EP/84-154
(6) A. De Rujula, H. Georgi and S.L. Glashow, Phys. Rev.D12,147(1975)
(7) A. Martin, Phys. Lett. 103B,51 (1981)
(8) J.M. Richard and P. Taxil, Ann. Phys (NY) 150,267 (1983)
(9) R. Bertlmann and A. Martin, Nucl. Phys. B168, 111 (1980)
(10) J.M. Richard : these proceedings.
(11) N. Papanicolaou and P. Spathis, Whashington University (St Louis) preprint, May 1984.

12) D. Gromes ; lectures given at the Yukon Advanced Study Institute, Heidelberg preprint HD-THEP 84-21 ; see also A. Martin in Proc. 1981 Lisbon EPS Intern. Conf. on High energy physics eds : J. Dias de Deus and J. Soffer.

13) J.M. Richard in "Heavy flavours and Hadron Spectrosocopy", Proc. XVI "Rencontre de Moriond", Les Arcs, 1981, ed. Tran Thanh Van (ed. Frontières)

14) H.G. Dosch and V.F. Muller, Nucl. Phys. B116,470 (1976)

15) R. Sommer and J. Wosiek, Phys. Lett. 149B,197 (1984)

16) J.P. Ader, J.M. Richard and P. Taxil, Phys Rev D25, 2370 (1982)

17) J.M. Richard, Phys. Lett. 139B,408 (1984) ; S. Nussinov, Phys.Rev.Lett. 51, 2081 (1983). See also J.M. Richard in "New Particle Production". Proc. XIX Rencontre de Moriond, La Plagne, 1984, ed : Tran Than Van (ed. Frontières).

18) See for a review of the model, e.g. N. Isgur in "Heavy flavours and Hadron Spectroscopy", op. cit. and for heavy baryons : L.A. Copley, N. Isgur and G. Karl, Phys. Rev. D20, 768 (1979) and K. Maltman and N. Isgur. Phys.Rev. D22, 1701 (1980)

19) J.M. Richard and P. Taxil, Phys. Lett. 128B,453 (1983)

20) S. Ono and F. Schoberl, Phys. Lett. 118B,419 (1982) ; Phys. Rev. D30,603 (1984)

21) D. Izatt, C. Detar and M. Stephenson, Nucl. Phys. B199,269 (1982).

22) See J.M. Richard and P. Taxil, Phys.Rev.Lett 54,847 (1985) and references therein.

23) After this review has been completed we have learnt from E. Lieb that such inequalities can be proved with a large class of potentials and also that some counterexamples can be found in some extreme cases. See : E. Lieb. "Baryon mass inequalities in quark models", Princeton University preprint, submitted to Phys.Rev.Letters,

THE SPECTROSCOPY OF HEAVY QUARKONIUM SYSTEMS

Seiji Ono
Physics Department
University of Tokyo
Tokyo 113, Japan

ABSTRACT: The anomalies in $c\bar{c}$ and $b\bar{b}$ spectra and their theoretical interpretations are reviewed. Phenomenological analysis for $q\bar{Q}$ and $t\bar{t}$ spectra are also presented.

(A) Anomalies in $c\bar{c}$ and $b\bar{b}$ spectra and the theoretical interpretations

There are several difficulties which cannot be easily accomodated in the standard potential models. We make the list of these anomalies[1,2]

(i) The mass difference between T(4S) and T(5S) is too large. This is even larger than 3S-4S difference.

(ii) There is some structure between T(4S) and T(5S) which is unexpected in the potential model.

(iii) For most potential models the mass of $\psi(4030)$ (usual assignment is 3S) is too low and $\Gamma_{ee}(3S)/\Gamma_{ee}(1S)$ is around one half of the theoretically expected value.

(iv) $\psi(4159)$ is usually assigned as 2D, $c\bar{c}$ state, which couples to e^+e^- through S-D mixing. However, even the coupled channel model predicts only $\sim 1/20$ of the observed $\Gamma_{ee}(4159)$.

(v) $\Gamma_{ee}(4415)/\Gamma_{ee}(1S)$ is much smaller than theoretically expected if $\psi(4415)$ is 4S, $c\bar{c}$.

We show three possible explanations for these anomalies.

(I) The $Q\bar{Q}$-$Q\bar{Q}g$ mixing model[1,2]

It is shown[1,2] that if we assume $\psi(4030) \approx (\psi(3S,c\bar{c}) - \psi(c\bar{c}g))/\sqrt{2}$ and $\psi(4159) \approx (\psi(3S,c\bar{c}) + \psi(c\bar{c}g))/\sqrt{2}$ we can explain anomalies (iii), (iv) and (v) naturally. Theoretically the lowest 1^{--}, $c\bar{c}g$ state is indeed predicted around 3S, $c\bar{c}$ state[3,4] (see also refs. 1,2) and excited $c\bar{c}g$ states around or above 4S, $c\bar{c}$ state.

As for bottonium states 1^{--}, $b\bar{b}g$ state is predicted just above T(4S). It has been known for some time that the measured mass of T(4S) is lower than the theoretical one by 20-50 MeV and measured $\Gamma_{ee}(4S)$ is slightly smaller than the theoretical one. Motivated by these three facts it was suggested[1] that a 1^{--}, $b\bar{b}g$ state might be just above T(4S). Due to the mixing T(4S) is pushed down and $\Gamma_{ee}(4S)$ decreases. After this proposal experimentalists indeed found a structure between T(4S) and T(5S). The mass difference T(5S) - T(4S) is found to be abnormally large.

Let us consider a simple mixing model

$$\begin{pmatrix} m_{4S}^{(0)} & \delta_1 & 0 \\ \delta_1 & m_H^{(0)} & \delta_2 \\ 0 & \delta_2 & m_{5S}^{(0)} \end{pmatrix} \psi = E\psi \qquad (1)$$

Let us assume masses before mixing $(m_{4S}^{(0)}, m_H, m_{5S}^{(0)}) = (10.61, 10.66, 10.86)$ with mixing parameter $\delta_1 = \delta_2 = 0.05$ GeV. Due to mixing 4S is pushed down and 5S is pushed up, thus we can explain anomaly (i). One finds $(m_{4S}, m_H, m_{5S}) = (10.577, 10.681, 10.872)$,

$$
\begin{aligned}
T('4S') &= 0.827|4S,b\bar{b}> + 0.56|H> + 0.046|5S,b\bar{b}> \\
T('H') &= -0.55|4S,b\bar{b}> + 0.80|H> + 0.24|5S,b\bar{b}> \\
T('5S') &= 0.10|4S,b\bar{b}> - 0.22|H> + 0.97|5S,b\bar{b}>
\end{aligned} \tag{2}
$$

Combining with the quark pair creation model[5,6] one finds the total width

		theory	experiment
$\Gamma('4S')$	=	26 MeV	20 ± 6 MeV
$\Gamma('H')$	=	94 MeV	131 ± 50 MeV
$\Gamma('5S')$	=	35 Me V	112 ± 40 MeV

(3)

where the width of H before mixing is assumed to be zero ($\Gamma^{(0)}(H) = 0$) since it is shown[7] that hybrid states are narrow. One can increase the widths by assuming non zero $\Gamma^{(0)}(H)$, but $\Gamma('4S')$ and $\Gamma('H')$ are already large enough. We find rather small $\Gamma('5S')$ but the coupled channel effects might affect the width (see ref.8).

Combining predictions by Richardson potential model[9] $\Gamma_{ee}(4S)/\Gamma_{ee}(1S) = 0.27$, $\Gamma_{ee}(5S)/\Gamma_{ee}(1S) = 0.22$ with eq.2 one obtains

	theory	experiment (CLEO[10])
$\Gamma_{ee}('4S')/\Gamma_{ee}(1S)$	0.185	$0.192 \pm 0.04/(1.3 \pm 0.13)$
$\Gamma_{ee}('H')/\Gamma_{ee}(1S)$	0.094	$0.2 \pm 0.15/(1.3 \pm 0.13)$
$\Gamma_{ee}('5S')/\Gamma_{ee}(1S)$	0.214	$0.22 \pm 0.12/(1.3 \pm 0.13)$

(4)

Larger value for $\Gamma_{ee}(5S)/\Gamma_{ee}(1S)$ ($\sim$0.32) is found by CUSB group[11] where the background is subtracted in a different way.

We conclude that $Q\bar{Q}$-$Q\bar{Q}g$ mixing hypothesis provides natural explanations for all anomalies ((i) - (v)) in heavy quarkonium systems. It is recently shown[7] that the mixing parameters used for $b\bar{b}$-$b\bar{b}g$ and $c\bar{c}$-$c\bar{c}g$ are reasonable.

(II) Unitarized quarkonium model[8,12] (or coupled channel model[13]).

It is shown that the inclusion of coupled channel effects removes difficulties (ii) - (v), but not completely. Especially the anomaly in $\Gamma_{ee}(4159)/\Gamma_{ee}(1S)$ remains unsolved[12,13]. Recently Törnqvist has extended[8] the calculation of ref. 12 and found an interpretation for anomalies (i) and (ii). We omit the detail of this analysis since this will be included in the talk by Törnqvist. We will just make some comments on his calculation.

(a) In this calculation only six thresholds ($B\bar{B}$, $B\bar{B}^*+B^*\bar{B}$, $B^*\bar{B}^*$, $B_s\bar{B}_s$, $B_s\bar{B}_s^*+B_s^*\bar{B}_s$, $B_s^*\bar{B}_s^*$) which make the difference T(5S) - T(4S) larger are included. Other thresholds e.g., $B_p\bar{B}$, $B_p\bar{B}^*$ (B_p = 1P state of $\bar{u}b$) which make the difference T(5S) - T(4S) smaller should also be included. We are now planning to make more complete analysis to check if the UQM can explain the T(5S) - T(4S) anomaly.

(b) If the coupled channel effects are as large as 50 MeV even for $b\bar{b}$ this will ruin the success of the potential model since these effects disturb the $c\bar{c}$

spectrum by the order of 200 MeV and light quark spectra by the order of 1 GeV. One must note that coupled-channel effects are much more important for lighter quark systems than for heavy quarkonium systems. Are light quark spectra disturbed so violently? No! By neglecting coupled channel effects we can still have excellent fits[14-16] from light quarkonium to $b\bar{b}$. As an example let us consider the flavor independent potential model by Ono and Schöberl[14]. One might say that this is just a parameter fit. However, one can see the quality of fit by considering only data which were measured after the publication of this paper. $F = 1963\ (1971 \pm 6)$MeV, $F^* - F = 136\ (139.5 \pm 18,\ 144 \pm 16)$, $B^* - B = 49\ (52 \pm 6)$, $A = 2460\ (2460 \pm 15)$. Thus we cannot see any trace of violent disturbance due to the coupled-channel effects. If coupled-channel effects are so small for these states, they must be even smaller for $b\bar{b}$ systems. Therefore, one is forced to chose either of the following conclusions.

(i) Coupled-channel effects are small or can be included in the effective potential for all quarkonium systems including T(5S) - T(4S). Thus, the potential model analysis is meaningful.

(ii) One believes that mass shifts due to such effects are as large as the ones given in refs. 8, 12. In this case any success of the potential model is accidental. If so one must try to find other anomalies in quarkonium spectra which can only be explained by coupled channel model.

(III) Tailed potential model

Due to light quark pair creation the string between Q and $\bar{Q}$ breaks. Thus, the potential for large R does not rise as fast as linear one but it is tailed somewhere. Martin potential[17] $V = -8.064 + 6.8698\ r^{0.1}$ is an example of a tailed potential since it becomes $V \sim r^{0.1}$ for large r. Let us change the parameters of this potential slightly.

$$V = -7.908 + 6.8698\ r^{0.096}$$
$$m_c = 1.737, \quad m_b = 5.1 \text{ GeV} \tag{5}$$

We call this "modified Martin potential". In the following table we compare the results of this model with experimental data.

$b\bar{b}$	theory	data
$\Gamma_{ee}(2S)/\Gamma_{ee}(1S)$	0.495	0.46 ± 0.03
3S	0.332	0.33 ± 0.03
4S	0.251	0.23 ± 0.03
5S	0.199	
6S	0.167	
7S	0.144	

$c\bar{c}$	theory	data
$\Gamma_{ee}(2S)/\Gamma_{ee}(1S)$	0.394	0.45 ± 0.08
3S	0.236	0.16 ± 0.04
4S	0.166	
5S	0.127	0.11 ± 0.04
6S	0.102	

One should note that we have here unconventional assignments for T(10868), T(11019), ψ(4415). In this model T(10868) is not T(5S) but T(6S), thus the large mass difference between 4S and "5S" is understandable. A difficulty of this model is that we have to assign ψ(4159) = $c\bar{c}$, 4S where predicted value is 100 MeV higher than the measured value. On the other hand $\Gamma_{ee}(4159)/\Gamma_{ee}(4030)$ is not so bad since ψ(4030) and ψ(4159) are both S-states.

	$b\bar{b}$		$c\bar{c}$	
	theory	data	theory	data
1S	9460	9460	3096	3097
2S	10011	10021	3675	3686
3S	10331	10353	4012	4030
4S	10560	10578	4252	
5S	10740	10684	4441	4415
6S	10888	10868	4597	
7S	11015	11019	4730	
8S	11125		4846	
1P	9858	9901	3515	3521
2P	10225	10256	3900	
1D	10119		3789	3770
2D	10396		4080	

(B) $q\bar{Q}$ systems

Recently $F^* - F$ and $B^* - B$ are measured experimentally[18]. The phenomenological relation

$$\rho^2 - \pi^2 = K^{*2} - K^2 = D^{*2} - D^2 = F^{*2} - F^2 = B^{*2} - B^2 = \ldots \quad (6)$$

works nicely. By using the Breit Fermi Hamiltonian even more precise relation

$$[M(^3S_1)]^2 - [M(^1S_0)]^2 \simeq \kappa \cdot 64\pi\alpha_s |\psi(0)|^2/9\mu \quad (7)$$

$$\alpha_s(Q^2) = 12\pi/\{(33 - 2n_f)\ln(Q^2/\Lambda^2)\}$$

$$Q = m(q\bar{q}) \sim 2m_q \sim 4\mu$$

is found[19]. Comparing with the data one finds $\Lambda = 140 \pm 60$ MeV. From eq.7 one finds $F^* - F = 132 \pm 6$ MeV (theory), 139.5 ± 18 MeV (PEP4), 144 ± 16 MeV (Argus); $B^* - B = 49.7 \pm 1.2$ MeV (theory), 52 ± 6 MeV (CUSB). For $m_t = 40$ GeV eq.7 predicts $T^* - T = 6.6$ MeV and $T_s^* - T_s = 7.1$ MeV.

For completeness we show complete open top meson spectrum,

$$\mathrm{cog}(T_s^*, T_s) - \mathrm{cog}(T^*, T) \cong 60 \text{ MeV} \quad \text{(ref.20)} \quad \text{for } m_t \gtrsim 30 \text{ GeV}$$

$$T^+ - T^0 \cong D^+ - D^0 = 4.7 \pm 0.3 \text{ MeV}, \quad (8)$$

$$T^{*+} - T^{*0} \cong D^{*+} - D^{*0} = 2.9 \pm 1.3 \text{ MeV}.$$

Similar spectrum was found by Eichten[21].

(C) $t\bar{t}$ systems

The UA1 group found evidence for the top quark with the mass $m_t = 40 \pm 10$ GeV[22]. For this mass the $Q\bar{Q}$ potential inside 0.1 fm becomes important. From the spectra of $c\bar{c}$ and $b\bar{b}$ states we find the shape and flavor independence of the potential between 0.1 and 1 fm. Through perturbative two loop calculation it is shown[23] that the potential has an asymptotic behaviour for $r < 0.01$ fm. The substantial part of the low lying toponium wave functions are in this unknown region (0.01 - 0.1 fm). The potential behaviour in this region (and spectra below 3S-state) is very model dependent.

For example, let us consider the case $m_t = 40$ GeV. We find $E(2S) - E(1S) = 640$ MeV for Kühn Ono potential[24], 519 MeV for Martin potential[17] and 2104 for Coulomb plus linear potential[13]. At present it is not possible to determine the differences $E(3S) - E(2S)$ and $E(2S) - E(1S)$ very precisely from QCD. If these are determined experimentally we can fix the potential behaviour for $r < 0.1$ fm and check if QCD motivated models such as refs. 23, 24 are correct.

As for Γ_{ee} we have even more serious model dependence. $\Gamma_{ee}(1S)$ by linear plus Coulomb potential is around 30 times as large as that of Martin potential. Even for higher excited S-state the former is several times larger than the latter.

Γ_{ee} is much affected by the presence of the Z^0 pole. As the $t\bar{t}$ state gets close to Z^0, Γ_{ee} increases. If the lowest $t\bar{t}$ state is slightly (2-5 GeV) lower than Z^0, Γ_{ee} for higher excited states are relatively enhanced since they are nearer to Z^0. Numerically we find the relation $\Gamma_{ee}(5S) \gtrsim \Gamma_{ee}(6S) \gtrsim \Gamma_{ee}(7S) \gtrsim \cdots$. On the other hand if toponium ground state is above Z^0, Γ_{ee} decreases rapidly as we go to higher excited state. However, Γ_{ee} defined here does not have the same meaning as that for $b\bar{b}$ and $c\bar{c}$ if $t\bar{t}$ is very near Z^0 (see ref.25).

Acknowledgement

The computer calculation for this work has been financially supported by Institute for Nuclear Study, University of Tokyo.

References

1. S. Ono, Orsay preprint LPTHE Orsay 83/32 (1983).
2. S. Ono, Proc. of XIXth Rencontre de Moriond, New Particle Production at High Energies, La Plagne, March 4-10, 1984; Zeit. f. Physik C26 307 (1985).
3. P. Hasenfratz et al., Phys. Lett. 22B 299 (1980).
4. T. Kitazoe et al., Zeit. f. Physik C24 143 (1984).
5. A. Le Yaouanc et al., Phys. Rev. D8 2223 (1973).
6. S. Ono, Phys. Rev. D23 1118 (1981); D26 3266 (1982).
7. A. Le Yaouanc et al., LPTHE 84/35, Zeit. f. Physik C to be published.

8. N. A. Törnqvist, Phys. Rev. Lett. 53 878 (1984); talk at this workshop.
9. J. L. Richardson, Phys. Lett. 83B 272 (1979).
10. T. Jensen, talk at this workshop; D. Besson et al. CLNS 84/629, CLEO 84-8, Oct. 1984.
11. J. Lee-Franzini, talk at this workshop; D. M. J. Lovelock et al., contributed to XXII Int'l Conf. on High En. Phys. Leipzig 1984.
12. K. Heikkilä, S. Ono, N. A. Törnqvist, Phys. Rev. D29 110 (1984); S. Ono, N. A. Törnqvist, Zeit. f. Physik C23 59 (1984).
13. E. Eichten et al. Phys. Rev. D21 203 (1980).
14. S. Ono and F. Schöberl, Phys. Lett. 118B 419 (1982).
15. D. P. Stanley and D. Robson, Phys. Rev. D21 3180 (1980).
16. S. Godfrey, N. Isgur, Toronto Univ. preprint July 1984.
17. A. Martin, Phys. Lett. 100B 511 (1981).
18. H. Aihara et al., Phys. Rev. Lett. 24 2465 (1984); H. Albrecht et al., Phys. Lett. 146B 111 (1984), talk at this workshop by H. Aihara and K. Schubert.
19. K. Igi and S. Ono, UT-446, submitted for publication.
20. S. Ono, Phys. Rev. D29 2975 (1979).
21. E. Eichten, Lecture at SLAC Summer Institute, July 1984.
22. P. Erhard, talk at this workshop.
23. W. Buchmüller and S. -H. H. Tye, Phys. Rev. D24 132 (1981).
24. J. H. Kühn, S. Ono, Zeit. f. Physik C21 395 (1984); C24 404 (1984).
25. J. H. Kühn, talk at this workshop.

PROPERTIES OF TOPONIUM

J.H. Kühn
CERN, Geneva, Switzerland

ABSTRACT

We discuss the properties of toponium states, with special emphasis on their appearance in e^+e^- collisions. We describe their relevance for the determination of the quarkonium potential and the interplay between electromagnetic and weak interactions in their production and decay. Finally, we comment on their role in the search for Higgs particles or for supersymmetry.

1. INTRODUCTION

With the three e^+e^- colliders TRISTAN, SLC, and LEP, at present under construction (or even nearing completion), a new energy range is opened up in the search for toponium. The present lower limit on its mass[1] of 46 GeV necessarily places the toponium system in a region where its appearance will be rather different from the expectations for the 'low' mass range of PETRA or PEP. For bound state masses below 50 GeV, weak interactions were to be considered as small perturbations of a system which would have been dominated by strong and electromagnetic interactions. For higher masses, however, which are also suggested by the recent UA1 results[2], weak decays and electroweak interferences become equally important.

Toponium will thus become a unique system, where all aspects of the standard model come into play and can be studied in a clean environment: long- and short-distance aspects of QCD through the potential; perturbative QCD through strong decays; electromagnetic and neutral-current interactions through decays into fermion-antifermion pairs; and last but not least, charged-current interactions through single quark decays (SQDs). Furthermore, it is well known that the search for the Higgs particle is particularly promising through the Wilczek mechanism $V \to H + \gamma$. In addition, toponium may be well suited to the study of various aspects of 'new physics' outside the realm of the standard model, among which supersymmetry or additional charged or neutral Higgs bosons are only the most outstanding examples. I will now discuss the various aspects in turn.

2. THE POTENTIAL*)

As far as the potential is concerned, the difference between a 50 GeV and a 100 GeV system is not drastic. The 1S together with 1P and the 2S states will serve to probe the potential for distances of less than 0.1 down to $\sim$ 0.03 fm. Even various QCD-inspired potentials with a short-distance behaviour of $\sim 1/(r \ln r)$ lead to rather different predictions for the energy levels of the 1S and 2S states and for $\Gamma_{e^+e^-}$. Calculations, based on a more singular short-distance behaviour of $\sim 1/r$, or on the rather soft $r^{0.1}$ potential, would of course lead to even more drastic deviations.

For intermediate and large distances, the potential has already been explored by the charmonium and $(b\bar{b})$ system, and the levels of higher radial excitations are thus predicted quire unambiguously. Nevertheless, it is of great interest to have an experimental check of this expectation. The verification of flavour independence would not only confirm the obvious expectation from QCD -- an independent measurement of V(r) for larger distances would also lead to a more refined understanding of the role of relativistic corrections for the lighter quarkonia.

*) For reviews with references to the original literature, see Ref. 3.

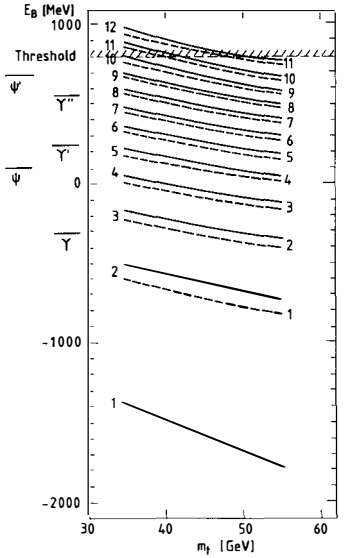

Fig. 1 Energy levels of the 12 lowest S and P states as calculated with the Richardson potential (from Ref. 5c) together with the ($c\bar{c}$) and ($b\bar{b}$) states below threshold.

A rough idea of the complexity of toponium can be gained from Fig. 1, which gives the binding energies of the 12 lowest S and P states as a function of m_t, together with the ($c\bar{c}$) and ($b\bar{b}$) levels below threshold. For $m_t \approx 40$ GeV, all states up to 10S are below the open top threshold. A theorem given by Baumgartner et al.[4] on the level ordering of orbital and radial excitations tells us that it is between the level ordering of the hydrogen atom and the harmonic oscillator, in the sense that

$$E_{n+1,l} \gtrsim E_{n,l+1} \gtrsim E_{n+1,l-1} \cdot \qquad (1)$$

Including fine and hyperfine splitting and all orbital excitations, the total number of toponium levels up to nS (and thus up to at least $l = n-1$) is given by

$$n + n + (n-1) + 3(n-1) + (n-2) + 3(n-2) + \ldots + 1 + 3 = 2n^2 \ . \qquad (2)$$

If, for example, 10S happens to be the highest state below threshold, this amounts to <u>at least</u> 200 different narrow resonances. As the maximal number, one finds*) $2(2n^2-1)$. Although one will not be able to explore all these states in the near or even distant future, a detailed study of most of the $^3S_1$ levels and

*) I thank A. Khare for a discussion on this point.

perhaps also of the lowest ^3P_J states is experimentally feasible and will thus completely fix the potential down to a distance of less than 0.1 fm, beyond which it is predictable by perturbation theory.

3. Z-γ-W INTERFERENCE*)

One of the great surprises in the study of charmonium was the observation that strong and electromagnetic decays are of comparable strength. With increasing mass -- for toponium, say between 35 and 60 GeV -- production and decay through the virtual Z leads firstly to minute contributions to the amplitude, which could be observed in the study of various asymmetries through its interference with the dominant electromagnetic term. For masses above 60 GeV the neutral-current amplitude becomes more important, and above 80 GeV it is dramatically enhanced by the Z^0 propagator. On the other hand, the rate for three gluons and for two gluons plus a photon remains largely mass-independent. The study of these modes, which could provide interesting information on gluon properties and the three-gluon coupling[17] thus becomes more and more difficult (Fig. 2).

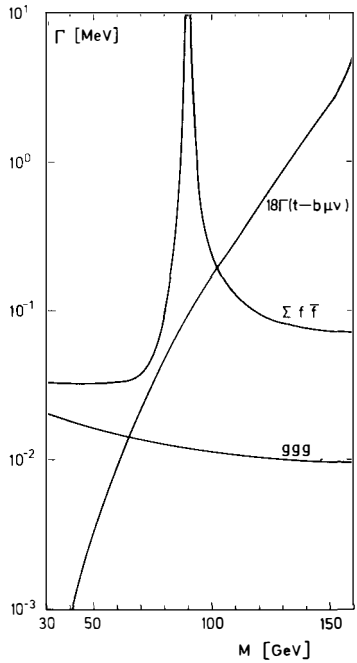

Fig. 2 Comparison of rates for SQDs, hadronic decays, and fermionic decays as a function of m_V for $\Gamma(V \xrightarrow{\gamma^*} e^+e^-) = 5$ keV (Ref. 13).

*) This part is based on work done in collaboration with S. Güsken and P. Zerwas (Ref. 5). For related papers, see Refs. 6 and 7. Earlier work can be found in Refs. 8 to 16.

The Z-γ interference has a drastic effect on the production in e^+e^- annihilation. Since all contributions are proportional to the wave function at the origin, their relative strength and the asymmetries are potential-independent. Furthermore, since $^3S_1$ is by construction a vector state, one is only sensitive to the vector part of the neutral-current coupling to top quarks.

One simple direct consequence*) is a difference in the production rate for right-handed versus left-handed polarized beams

$$\alpha(RL)^{on} = \frac{\sigma_R - \sigma_L}{\sigma_R + \sigma_L} = - \frac{2\ \mathrm{Re}\ (\lambda_e^* \lambda_e')}{|\lambda_e|^2 + |\lambda_e'|^2} , \tag{3}$$

with

$$\lambda_f = \frac{e^2 e_f e_t}{s} + \left(\frac{e}{y}\right)^2 \frac{v_f v_t}{s - m_Z^2 + i m_Z \Gamma_Z} ,$$

$$\lambda_f' = \left(\frac{e}{y}\right)^2 \frac{a_f v_t}{s - m_Z^2 + i m_Z \Gamma_Z} , \tag{4}$$

$$v_f = 2I_3^f - 4e_f \sin^2 \theta_W ; \qquad a_f = 2I_3^f ; \qquad y = 2 \sin 2\theta_W ;$$

this amounts to 100% for a toponium mass close to 80 GeV (Fig. 3). For unpolarized beams this implies that toponium will be produced with a preferred spin direction,

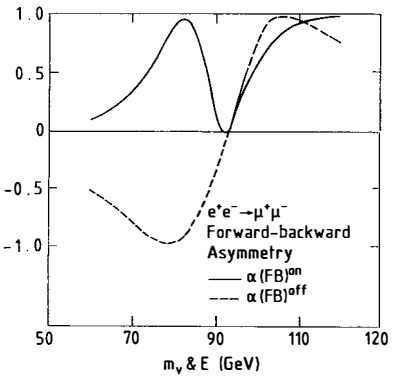

Fig. 3 Polarization asymmetry α_{RL} on and off resonance as a function of m_v (full curve) and E (dashed curve) (Ref. 5c).

*) For a more detailed discussion, which takes into account the interference with the continuum, see Ref. 5c.

$$\langle \vec{S}_V \cdot \vec{n}_e \rangle = \alpha(RL) \qquad (5)$$

and this in turn could be observed in weak decays, as discussed below.

Similar to the situation off resonance, for toponium one also expects a forward-backward asymmetry for fermion-antifermion final states, which is most easily measured for muons and tau leptons. As far as the contribution from toponium is concerned, polarization and forward-backward asymmetries are simply related[18]:

$$\frac{\sigma_F - \sigma_B}{\sigma_F + \sigma_B} = \frac{3}{4} \alpha_{FB} ,$$

$$\alpha_{FB}(f) = \alpha_{RL}(e) \cdot \alpha_{RL}(f) , \qquad (6)$$

and similar relations can be obtained for the azimuthal asymmetries discussed in Ref. 5c. This factorization follows from the fact that the reaction proceeds through one single resonance with definite spin. In Ref. 5c it is demonstrated that for toponium sufficiently far away from Z^0 the incoherent summation of resonance and continuum is indeed appropriate, once the energy spread of the beam has been taken into account.

Among the decays into quark-antiquark, those into $b\bar{b}$ are of particular interest. Since t and b are members of one isodoublet, $(t\bar{t}) \to b\bar{b}$ may also proceed by the exchange of a W. Rate and angular distribution are thus quite distinct from those of the other down-type quarks $d\bar{d}$ or $s\bar{s}$. Compared with the γ and Z-amplitude, the relative weight of W exchange depends on different colour factors, such that the measurement of, for example, the $b\bar{b}$ rate or of the angular distribution, gives a nice check on the whole approach. It goes without saying that $b\bar{b}$ jets are also particularly attractive from the experimental point of view, since B mesons could be tagged either through their characteristic decay modes or even through the observation of their decay vertex.

A rather peculiar situation occurs for toponium very close to the Z (Ref. 5a). Production and decay are then completely dominated by the intermediate boson. However, since the widths of V and Z are so drastically different (before and after mixing) and the V-Z coupling is small compared to $\Gamma_Z - \Gamma_V$, it is still legitimate to use lowest-order perturbation theory. For toponium very close to the Z, the mass shift and width are approximately given by*)

*) For a more detailed treatment, see Ref. 5c.

$$m_V - m_{V^0} = \left(\frac{ev_t f_V m_V^2}{y}\right)^2 \frac{\left[m_{V^0} - m_{Z^0}\right]}{\left[m^2_{V^0} - m^2_{Z^0}\right]^2 + \left[m^2_{Z^0}\Gamma_{Z^0}\right]^2},$$

$$\Gamma_V = \left(\frac{ev_t f_V m_V^2}{y}\right)^2 \frac{\Gamma_Z}{\left[m^2_{V^0} - m^2_{Z^0}\right]^2 + \left[m^2_{Z^0}\Gamma_{Z^0}\right]^2}, \qquad (7)$$

This amounts to an increase of Γ_V up to ~ 20 MeV and a mass shift up to ~ 5 MeV. The contribution from one state to the shift in the mass and width of the intermediate boson Z is equal in magnitude but opposite in sign. Although Z^0 receives contributions from all states, the total effect on m_Z shown in Fig. 4 is still below the experimental accuracy, and the same is true for the change in width.

So far we have discussed V and Z as separate entities. It has been customarily assumed (for example, Ref. 19) that it is legitimate to add their contributions to the cross-section incoherently, once the real cross-section has been folded with the inherent beam energy spread of e^+e^- machines. However, this is

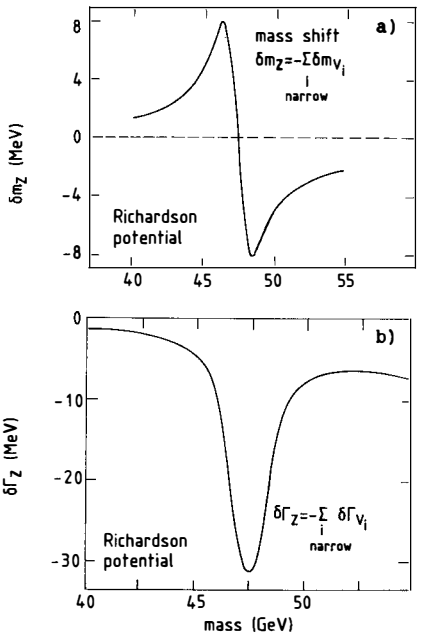

Fig. 4 Shift of the Z mass (a) and the Z width (b) due to all narrow toponium states for a given top quark mass.

no longer true if toponium is sufficiently close to the Z. Ignoring interference effects and radiative corrections, the integrated cross-section from a resonance is simply given by

$$\int dE\ \sigma_{res}(E) = \frac{6\pi^2}{m_V^2}\,\Gamma_{ee} = \frac{4\pi}{3}\,\frac{\alpha^2}{m_V^2}\,\mathcal{J}(2\pi)\delta W R_V \ . \tag{8}$$

with

$$R_V(\text{incoh.}) \equiv \frac{9\pi}{2\alpha^2}\,\frac{\Gamma_{ee}}{\mathcal{J}(2\pi)\delta W} \ . \tag{9}$$

For J/ψ and Υ production this remains true even if interference effects are taken into account. In these cases the difference in phase between the even part of the Breit-Wigner amplitude (which contributes to the integral) and the background is $\pi/2$, so that they do not interfere. The odd part of the resonant amplitude does interfere and leads, for example, to the well-known dip of the μ-pair cross-section below the J/ψ, but is irrelevant for the integral.

However, if the difference between the toponium and Z^0 masses and the width of Z are of comparable magnitude, the situation changes drastically. If we assume that toponium is very close*) to the Z^0, the combined amplitude for $f\bar{f}$ final states in the neighbourhood of toponium is given by

$$A_{Z+V} \propto \frac{1}{m_V^2 - m_Z^2 + im_Z\Gamma_Z} + \frac{1}{(m_V^2-m_Z^2+im_Z\Gamma_Z)}\,\frac{(ev_t f_V m_V^2/y)^2}{(S-m_V^2+im_V\Gamma_V)}\,\frac{1}{(m_V^2-m_Z^2+im_Z\Gamma_Z)} \ . \tag{10}$$

For the extreme case of complete mass degeneracy,

$$A_{Z+V} \propto \frac{1}{im_Z\Gamma_Z} + \left(\frac{1}{im_Z\Gamma_Z}\right)^2 \frac{(ev_t f_V m_V^2/y)^2}{(S-m_V^2+im_V\Gamma_V)} \ . \tag{11}$$

In this case it is the even part of the toponium amplitude which interferes with the Z 'background', and this interference is evidently destructive. The contribution to the integrated cross-section from the resonance becomes negative, and hence one expects a dip instead of a bump, even after the energy smearing is

*) For the general case, see Ref. 5c.

taken into account. For toponium in the neighbourhood of Z, one may still take the (slightly) idealized case of Z dominance and find for the cross-section after smearing,

$$\langle R_{V+Z} \rangle \equiv \int R_{V+Z}(W')\, r\left(\frac{W-W'}{\delta W}\right) dW' \tag{12}$$

$$= R_V(\text{incoh.}) \left[\frac{(m_V^2-m_Z^2)^2 - (m_Z\Gamma_Z)^2}{(m_V^2-m_Z^2)^2 + (m_Z\Gamma_Z)^2}\, r'\left(\frac{W-m_V}{\delta W}\right) + \frac{2\Gamma_Z m_Z (m_V^2-m_Z^2)}{(m_V^2-m_Z^2)^2 + (m_Z\Gamma_Z)^2}\, r''\left(\frac{W-m_V}{\delta W}\right) \right] + R_Z \ ,$$

with

$$r' = \sqrt{(2\pi)}\,\delta W\, r \ ; \quad r'' = \int \frac{dW'}{W'}\, r'\left(\frac{W-W'}{\delta W}\right) \ ;$$

$R_V(\text{incoh.})$ is defined in Eq. (9), and r denotes the resolution function, which one may choose as Gaussian distribution or in more elaborate forms if the effects of radiative corrections are to be taken into account.

The resulting shape of R in the neighbourhood of m_V is shown in Fig. 5 for three characteristic cases. For $m_V = m_Z$ one finds a dip with the size and shape

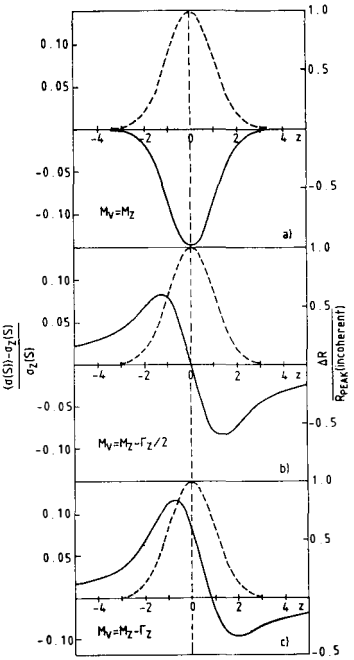

Fig. 5 Energy dependence of the resonance excitation cross-section for a toponium mass of a) $m_V = m_Z$, b) $m_Z - \Gamma_Z/2$, and c) $m_Z - \Gamma_Z$. The dashed line shows the cross-section without the interference terms being taken into account.

of the bump expected from incoherent summation. For $m_V = m_Z \pm \Gamma_Z/2$ the integrated cross-section vanishes; however, the asymmetric part still leads to a sizeable variation of the cross-section in the resonance region. Thus also in this case toponium would be easily detected by experiment. For $m_V = m_Z + \Gamma_Z$ the line shape already has a closer resemblance to the incoherent sum, although some distortion is still clearly visible.

For direct toponium decays, such as SQDs, ggg, or $H\gamma$, no interfering continuum exists and their contribution just adds incoherently

$$R_{direct} = R_V(\text{incoh.}) \cdot Br(\text{direct}) \cdot r\left(\frac{W - m_V}{\delta W}\right) . \qquad (13)$$

4. SINGLE QUARK DECAYS[8,13,20]

A mode which is specific for toponium is the weak decay of a top quark inside toponium with a rate

$$\Gamma_{SQD} = 18 \frac{G_F^2 m_t^5}{192\pi^3} f\left(\frac{m_t^2}{m_W^2}, \frac{m_b^2}{m_t^2}\right) , \qquad (14)$$

$$f(\varrho,\mu) = 2 \int_0^{(1-\sqrt{\mu})^2} \frac{du}{(1-u\varrho)^2} [(1-\mu)^2 + u(1+\mu) - 2u^2][1+\mu^2+u^2 - 2(\mu u+\mu+u)]^{1/2} .$$

For charmonium and bottomonium this decay mode is completely negligible. As it increases proportionally to m_t^5, it becomes comparable to the other channels for m_V close to 80 GeV. For masses close to m_Z, annihilation decays are again enhanced owing to the Z propagator. Roughly 10 GeV beyond the Z, SQDs become, and remain, dominant.

The striking topology of SQDs -- six jets in two planes -- or hard isolated leptons, enables them to be selected quite easily from all other decay modes. This same property can be used to reduce the continuum background in the scan for toponium. Whilst this feature is a welcome asset in the mass range below m_Z, it becomes the crucial tool at higher masses[14,21].

However, SQDs are interesting in their own right[20]. The total toponium decay rate is given by the μ-pair branching ratio together with Γ_{ee}, as is standard practice for charmonium and bottomonium. A measurement of the branching ratio for SQDs then leads to a direct determination of the t-quark lifetime.

Leptons from SQDs are also a very useful tool for obtaining information on the bound state. As a characteristic example, let us consider the spin of a $^3S_1$ state. The spins of the t and $\bar{t}$ quarks are aligned with the spin of toponium.

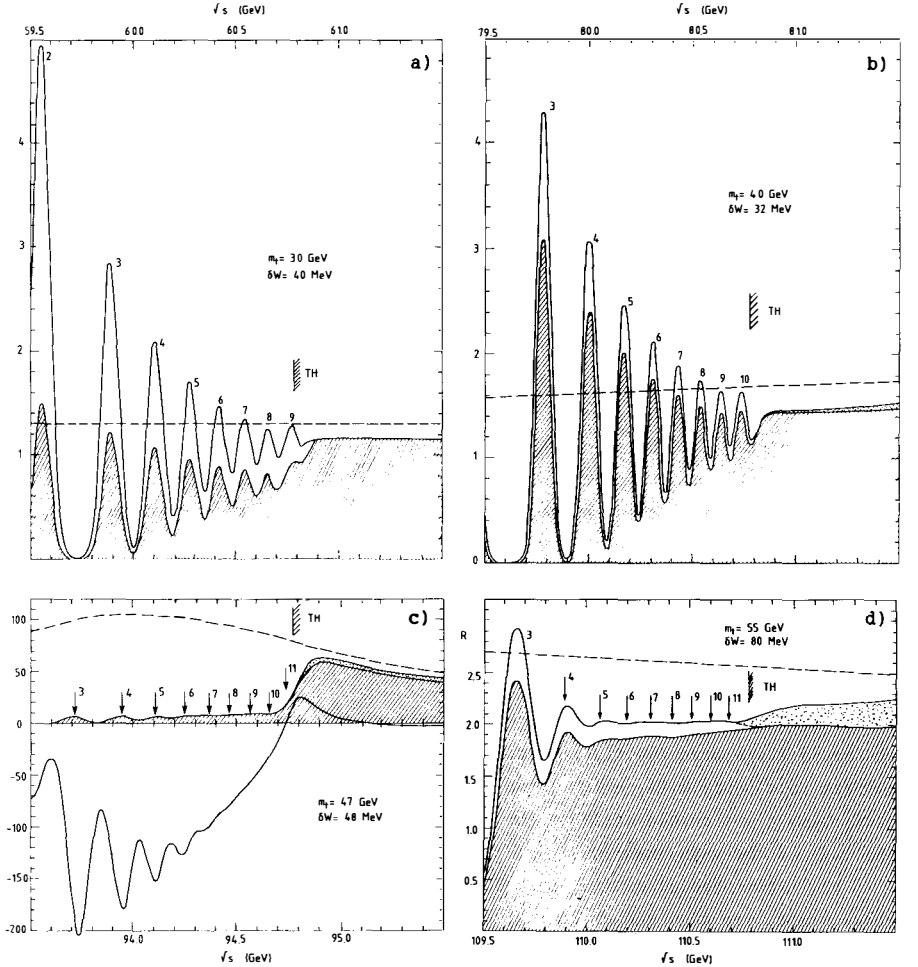

Fig. 6 Threshold behaviour of toponium and open top production, including neutral-current effects. The dashed area indicates the fraction of SQD events. The contribution to the continuum from axial-vector current is indicated by the dotted area. The dashed curve gives the production rate due to the electromagnetic current and the vector part of the neutral current for top quarks without QCD corrections and mass effects. a) $2m_t$ = 60 GeV, δW = 40 MeV; b) $2m_t$ = 80 GeV, δW = 32 MeV; c) $2m_t$ = 94 GeV, δW = 48 MeV [the solid line denotes the change of the fermion-antifermion cross-section alone, normalized to $\sigma(e^+e^- \to \gamma \to \mu^+\mu^-)$]; d) $2m_t$ = 110 GeV, δW = 80 MeV.

The degree of longitudinal polarization of the spins of top quarks and of toponium is thus identical. In addition, the angular distribution of leptons is independent of the energy, and for fully polarized quarks it is given by

$$\frac{dN}{d\cos\theta} \sim (1 + \cos\theta) \ , \tag{15}$$

with

$$\cos\theta = \vec{n}_l \vec{S} \ .$$

The resulting asymmetry thus allows a direct measurement of the bound-state polarization. It should be taken into account that only 50% of the prompt, first-generation leptons originate from the decay of a t quark inside toponium, and 50% from the decay of the T or T^* which decays only subsequently. The two sources can in practice not be separated, and only 50% of the polarization is retained in the second step[20]. The resulting asymmetry is finally given by

$$\frac{N_F - N_B}{N_F + N_B} = \frac{1}{2}\left(\frac{1}{2}\alpha_{RL} + \frac{1}{4}\alpha_{RL}\right) = \frac{3}{8}\alpha_{RL} \ .$$

The leptons could also be used for a diagnosis of the momentum distribution of the bound-state wave function. We note that the dispersion of the velocity amounts to roughly 0.01, which leads to a smearing of the lepton spectrum by $\pm$10%, with a noticeable shift of the end-point, not to speak of the effects of the tail of the wave function.

For higher radial excitations, SQDs are relatively more important. Since these states are also rather densely packed, it will not be easy to distinguish between the regions above and below threshold, as is indicated in Fig. 6 for some characteristic cases.

5. THE QUEST FOR THE HIGGS PARTICLE

Toponium will be an excellent place to look for new physics. In particular, it will play an eminent role in the search for the Higgs particle. Since this has already been discussed extensively in the literature[22], I will mention only the most important aspects. The branching ratio for $H\gamma$, shown in Fig. 7 for fixed m_H = 10 GeV as a function of the toponium mass[23], remains high throughout nearly the whole range accessible, for example by LEP. Since the suppression by the phase-space factor $(1-M_H^2/m_V^2)$ is not very severe, a standard Higgs particle with mass up to m_V - 10 GeV would be accessible in this way[24]. For toponium

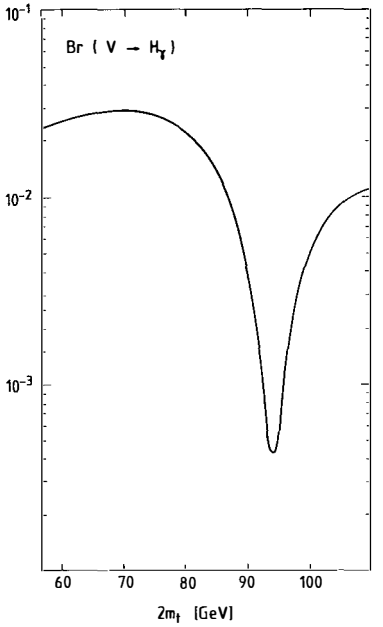

Fig. 7 Branching ratio into Hγ for $\Gamma(V \xrightarrow{\gamma^*} e^+e^-) = 5$ keV.

masses very close to m_Z, the branching ratio is drastically reduced owing to the overwhelming rate for Z^0-mediated decays. However, even in this region toponium competes well with Higgs production in Z decays, at least for a machine with the energy spread of LEP ($\delta W \sim 50$ MeV). Close to the Z^0 one finds, on top of the resonance,

$$R(e^+e^- \to V \to H\gamma) = \frac{9\pi}{2\alpha^2} \frac{\Gamma_{ee}}{\sqrt{(2\pi)}\delta W} Br(V \to H\gamma) = \frac{9\pi}{2\alpha^2} \frac{\Gamma(V \to H\gamma)}{\sqrt{(2\pi)}\delta W} Br(Z \to e^+e^-) \approx 0.2$$

which compares favourably with the continuum cross-section for Hγ even on top of the Z:

$$R(e^+e^- \to Z \to H\gamma) \approx 0.01 \ .$$

Even the mode $Z \to H\mu^+\mu^-$ leads to a smaller rate, at least as long as $m_H \gtrsim 30$ GeV.

We have shown above that the dominant contributions from V and Z decay interfere destructively for m_V close to m_Z. A reduction of the energy spread would thus lead to a very remarkable effect: the cross-section would be enhanced for H + γ and depleted for $f\bar{f}$.

6. TOPONIUM AND SUPERSYMMETRY*)

If supersymmetry partners of conventional particles exist with masses comparable to m_t, supersymmetry could play an important role for toponium; conversely, information on SUSY particles could be obtained which would be hard to get elsewhere. Depending on the masses of the various hypothetical particles, a large variety of decay modes can be envisaged. Various possibilities are summarized in Figs. 8a and 8b, taken from my recent review article[25]. If $m_{\tilde{t}} + m_{gaugino} < m_t$, the single quark decay $t \to \tilde{t}$ + gaugino is dominant and alters the appearance of toponium completely[26]. However, these decays would also dominate the weak decay

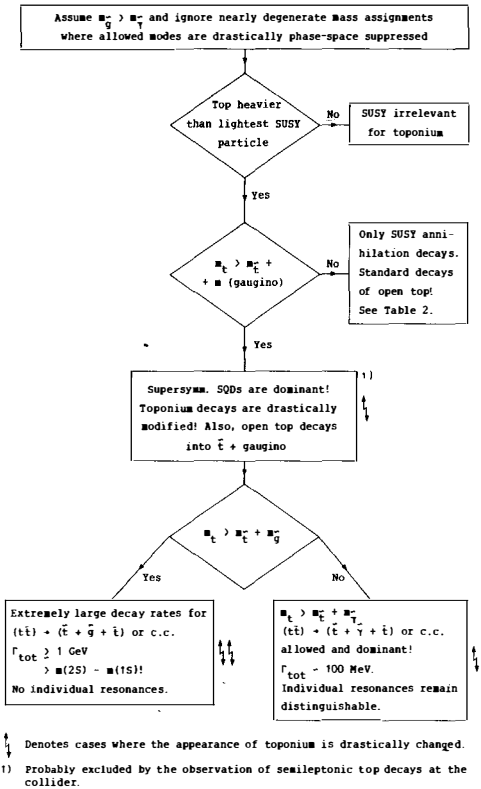

Fig. 8a Overview of toponium decays into SUSY particles through decays of the top quark.

*) For a review and the original references, see Ref. 25, where also the consequences of non-linear realizations of SUSY (Ref. 26) are discussed.

of top mesons. Considering the evidence for semileptonic top decays presented by the UA1 Collaboration[2], we tentatively ignore this possibility, which leaves us with the annihilation decays shown in Fig. 8b. For the narrow mass interval $m_t - m_\gamma < m_{\tilde{t}} < m_t$, the mode $(t\bar{t}) \to \tilde{t}\,\bar{\tilde{t}}$ through gluino exchange could be important. If $m_{\tilde{g}} < m_t$ and if parity is violated (i.e. $m_{\tilde{R}} \neq m_{\tilde{L}}$), toponium will dominantly decay into a pair of gluinos[27]. In this case most of our previous discussion on toponium properties would be irrelevant. The integrated cross-section would still be given by Γ_{ee}; the final state, however, would consist only of four jets and missing energy. One could then select a rather clean sample of gluino pairs, and various methods can be devised for measuring the gluino mass[28] quite accurately.

If, on the other hand, the masses of both gluino and of stop turn out to be larger than m_t, the mode $(t\bar{t}) \to \tilde{g}\tilde{\gamma}g$ will give access to rather heavy gluinos. However, the experimental isolation of this channel might be difficult[28].

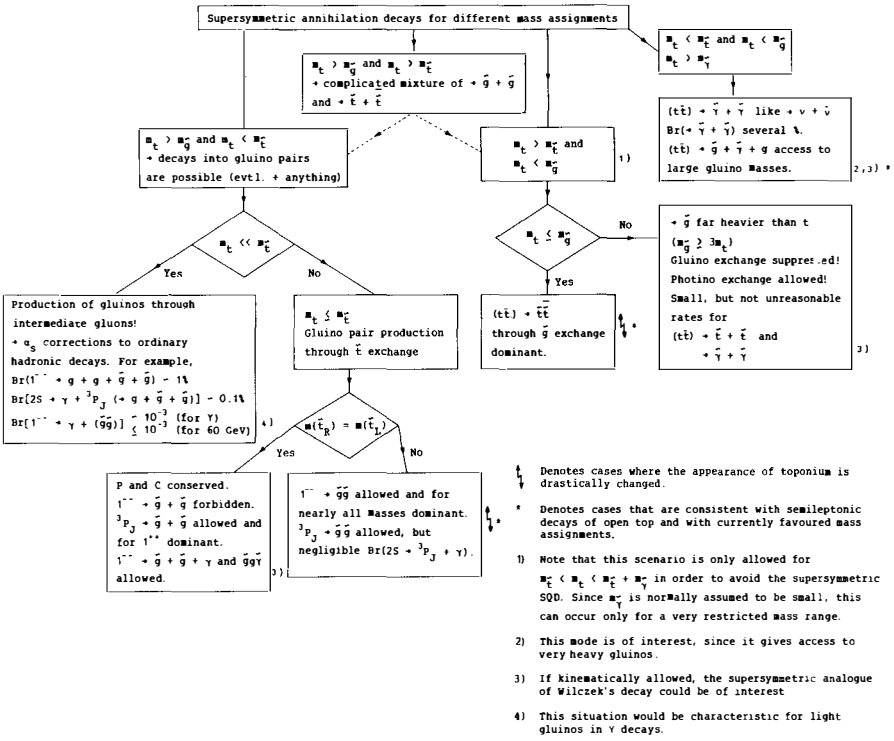

Fig. 8b Overview of toponium decays into SUSY particles through annihilation decays.

7. SUMMARY

Recent UA1 results on the observation of top mesons suggest that toponium should be found at e^+e^- colliders, which are at present under construction. For the whole mass region under consideration, one expects a variety of interesting and experimentally accessible effects even within the standard model, which predicts a unique interplay between strong and electroweak forces. Furthermore, toponium gives easy access to some aspects of physics beyond the standard model.

Acknowledgements

I am indebted to S. Güsken, S. Ono, K.H. Streng and P. Zerwas for an enjoyable collaboration on various aspects of toponium physics. Instructive discussions with W. Buchmüller, G. Coignet, F. Richard and H. Takeda are gratefully acknowledged.

REFERENCES

[1] P. Schacht, Munich preprint MPI-PAE/Exp.E1.139, to be published in Proc. 22nd Int. Conf. on High-Energy Physics, Leipzig, 1984.

[2] G. Arnison et al. (UA1 Collaboration), Phys. Lett. 147B, 493 (1984).

[3] C. Quigg and J.L. Rosner, Phys. Rep. 56, 167 (1979).
H. Grosse and A. Martin, Phys. Rep. 60, 341 (1980).
M. Peskin, Stanford preprint SLAC-PUB-3273 (1983).
W. Buchmüller, preprint CERN TH.3938/84 (1984).

[4] B. Baumgartner, H. Grosse and A. Martin, preprint CERN TH.4084/84 (1984).

[5a] J.H. Kühn and P.M. Zerwas, preprint CERN TH.4089/85 (1985).

[5b] S. Güsken, J.H. Kühn and P.M. Zerwas, preprint CERN TH.4106/85 (1985).

[5c] S. Güsken, J.H. Kühn and P.M. Zerwas, SLAC-PUB-3580 (1985) [CERN TH.4125/85 (1985)].

[6] P.J. Franzini and F.J. Gilman, SLAC-PUB-3541 (1985).

[7] L.J. Hall, S.F. King and S.R. Sharpe, Harvard preprint HUTP-85/A012 (1985).

[8] K. Fujikawa, Prog. Theor. Phys. 61, 1186 (1979).

[9] J. Ellis and M.K. Gaillard, CERN 76-18 (1976) and 79-01 (1979).

[10] I.Y. Bigi, J.H. Kühn and H. Schneider, Munich preprint MPI-PAE/PTh 28/78 (1978).

[11] J. Kaplan and J.H. Kühn, Phys. Lett. 78B, 252 (1979).

[12] J.H. Kühn, Acta Phys. Polon. B12, 347 (1981).

[13] J.H. Kühn, Acta Phys. Austriaca, Suppl. XXIV, 23 (1982).

[14] G. Goggi and G. Penso, Nucl. Phys. B165, 429 (1980).

[15] L.M. Sehgal and P.M. Zerwas, Nucl. Phys. B183, 417 (1981).

[16] I.Y. Bigi and H. Krasemann, Z. Phys. C7, 127 (1981).

[17] K. Koller, K.H. Streng, T. Walsh and P.M. Zerwas, Nucl. Phys. B193, 61 (1981) and B206, 273 (1982).

[18] A. Martin, private communication.

[19] J.D. Jackson, S.L. Olsen and S.H.H. Tye, Proc. of the 1982 Summer Study on Elementary Particles and Fields, Snowmass, eds. R. Donaldson et al. (Amer. Inst. Phys., New York, 1983), p. 175.

[20] J.H. Kühn and K.H. Streng, Nucl. Phys. B198, 71 (1982).

[21] F. Richard and L. Rolandi, Contributions to the LEPC Working Group on Toponium Physics (1984), to be published.

[22] F. Wilczek, Phys. Rev. Lett. 39, 1304 (1977).
M.I. Vysotsky, Phys. Lett. 97B, 159 (1980).
J. Polchinski, S.R. Sharpe and T. Barnes, Harvard preprint HUTP-84/A064 (1984).
J. Pantaleone, M.E. Peskin and S.-H.H. Tye, Stanford preprint SLAC-PUB-3439 (1984).
W. Bernreuther and W. Wetzel, Heidelberg preprint HDTHEP 85-2 (1985).
G. Barbiellini et al., preprint DESY 79/27 (1979).

[23] W. Buchmüller and J.H. Kühn, Contributions to the LEPC Working Group on Toponium Physics (1984), to be published.

[24] G. Coignet, Contribution to the LEPC Working Group on Toponium Physics (1984), to be published.

[25] J.H. Kühn, preprint CERN-TH.4083/84 (1984).

[26] J. Wess, *in* Quantum Theory of Particles and Fields (Birthday volume dedicated to Jan Lopuszanski), eds. B. Jancewicz and J. Lukierski (World Scientific Publishers, Singapore, 1983).

[27] J. Ellis and S. Rudaz, Phys. Lett. 128B, 248 (1983).

[28] F. Richard, Contribution to the LEPC Working Group on Toponium Physics (1984), to be published.

THE UPSILON AND BARYON MASS SPECTRA AND NONPERTURBATIVE UNITARITY EFFECTS*

Nils A. Törnqvist
Department of High Energy Physics, University of Helsinki,
Siltavuorenpenger 20 C, SF-00170 Helsinki, Finland

Piotr Żenczykowski
Institute for Nuclear Physics, Radzikowskiego 152,
31-343 Krakow, Poland

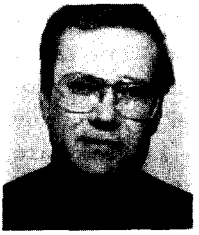

ABSTRACT

We comment on some recent results in applying the unitarised quark model (UQM) to the upsilons above the $B\bar{B}$ threshold and to the mass spectrum of the S- and P-wave baryons. In particular we discuss the $\Upsilon(5S)$ mass, the $\Lambda - \Sigma - \Sigma^*$ and $\Lambda(5/2) - \Sigma(5/2)$ mass splittings.

* Presented by N.A. Törnqvist

1. INTRODUCTION

This is already the fifth (!) time I or one of my collaborators[1] speak at a Moriond conference on questions related to non-perturbative unitarity effects in hadron spectroscopy. You may wonder why we continue pursuing this line of research, and not spend our energy on a more fashionable subject such as lattice gauge theory or superstrings. The reasons are several: (i) Many currently popular models neglect, without justification, these effects entirely[2], (ii) We are convinced they are important, and often even the dominant effect causing the mass splittings of light hadrons, (iii) Any reasonable theory must be unitary and eventually when these effects are calculable directly from a fundamental theory (without phenomenology) the calculation must (explicitly or implicitly) include the effects which we are talking about.

Thus we are quite confident that given enough time our efforts will not be proven worthless. In fact, although at present we must of course invoke some amount of phenomenology, in particular for the hadron form factors, we believe our approach has many advantages (compared e.g. to a future lattice calculation including quark loops in a reasonable approximation). It shows explicitly which threshold singularities are the most important.

Let us begin by giving a simple and essentially model independent argument why these effects must be large: The width of a typical OZI-allowed decay is $\sim$ 100 MeV for a resonance about 100 MeV above threshold (c.f. Fig. 1). Therefore, the variation of the imaginary part of the mass matrix is

$$\frac{d}{d\sqrt{s}}(2\,\mathrm{Im}\,M(s)) = O(1) \ , \tag{1}$$

from which almost inevitably follows, through analyticity, that the variation in the real part is of same order of magnitude:

$$\frac{d}{d\sqrt{s}}(\mathrm{Re}\,M(s)) = O(1) \ . \tag{2}$$

Thus the mass of a resonance depends sensitively on where the thresholds are. A state, say, 200 MeV below or above a threshold is shifted differently from a similar state at the threshold. It follows that the contribution to the mass splitting of the two states can be large, i.e. of the order 100 MeV. There are in addition many thresholds (both open and closed) to be summed over, the

contribution of which need not cancel. Typically, thresholds are separated by ∿ 100 MeV or more, so the cancellations cannot be complete apart from accidents in particular situations. Thus the hadronic nonperturbative mass shifts lead, in general, to substantial mass splittings in the physical spectrum. In which direction do the effects go? Are they similar to the observed experimental splittings?

In a large number of applications[3] ranging from the light mesons and baryons to the heavy upsilon states we have found that these nonperturbative unitarity effects generally enhance substantially the effect of a perturbation, such as that from the quark mass splitting $m_s - m_d$, or the one-gluon exchange. Because of the often highly nonlinear relations involved, the effects are not describable by only a simple overall enhancement factor. One also obtains a range of other phenomena such as: resonance mixing, distorted resonance shapes, an anomalously heavy T(5S) mass etc., which generally cannot be described by naive nonunitary models.

As an example which demonstrates the importance of these unitarity effects we[4] took the width model of Isgur and Koniuk[5] for the light baryons, and calculated with exactly their parameters the associated mass shifts and mixing matrices. The resulting mass spectrum is quite different from the input and would completely destroy the agreement of the naive one-gluon exchange mechanism (with large α_s of order unity) as calculated by Isgur and Karl[6]. In fact, a better agreement with data is then obtained if one neglects the one-gluon exchange entirely, or lets α_s have a smaller, more reasonable value around 0.3 instead of near 1. We have showed[4,7] that by improving the width model, i.e. using the $^3P_0$ model as a guide and supplementing it with very few phenomenological parameters in order to fit the experimental widths, one obtains an equally good fit to the S and P wave baryons with negligible one-gluon exchange and instead with dominance of unitarity effects. We return to this in section 3 below.

2. THE UPSILON MASS SPECTRUM

For heavy quarkonium such as $b\bar{b}$ the application of the unitarized quark model (UQM) is the most reliable since here (i) one has the remarkably successful "naive" potential model as a reference model, which serves as a first approximation and, (ii) relativistic

corrections are not very large. On the other hand, the effects of quark loops can often be absorbed into the naive potential by "renormalizing" its parameters.

But, in $b\bar{b}$ spectroscopy the last remark does not apply, to the 5S state[8] since being well above the first thresholds involving B,B*,B_s and B_s^* mesons it is shifted very differently compared to the 4 lighter S-states. Thus, while any naive model predicts a monotonically decreasing sequence for the 2S-1S, 3S-2S etc. mass splittings, the unitarized model predicts the mass splitting between the 5S and 4S states to be anomalously large $\simeq$ 80 MeV larger than in naive models (c.f. Fig. 2). The reason for this effect is essentially model independent. Above a threshold the mass shift due to the continuum ($B\bar{B}$ etc.) with energy below the resonance mass has the opposite sign compared to the higher energy continuum above the resonance. This causes in the $b\bar{b}$ case a rapid turnover of the mass shift, which is always negative for states below the threshold, to an even positive mass shift for a resonance well above the significant thresholds. Thus the 5S state will be considerably heavier than naively expected, a fact which is supported by the recent CUSB and CLEO experiments.

One common objection to these arguments is: What about higher thresholds? Three and multibody states can with good amount of confidence be neglected, (or rather, one assumes them to be dominated by two-body channels). This is supported both by theoretical models (e.g. dual models) and by experiment (c.f. $\varphi \to 3\pi$ or $\omega \to 3\pi$, which are known to be dominated by $\rho\pi$). The next group of thresholds involve P-wave B-mesons $B\bar{B}_p$ etc. should open up around 11 GeV, quite well separated from the S-wave B,B* etc. channels considered above. Similarly as the mass shifts of the 1S-4S upsilons in Fig. 2 fall on a nearly linear line,one on very general grounds expects the mass shifts due to $B\bar{B}_p$ etc. for the 1S to 5S states to also fall on a nearly linear line. Such mass shifts are easily absorbed into the parameters of the naive potential, while the 6S and in particular the 7S mass should increase. These higher thresholds should therefore not modify the conclusion of the anomalously high 5S-4S mass splitting.

As to the behaviour of the ratio R above the $B\bar{B}$ threshold a coupled channel model predicts a lot of structure <u>not</u> due to resonances[8]. This is shown in fig. 3 where the theoretical curve was computed <u>before</u> the experimental data[9] appeared. The extra

bumps, also seen in the recent CUSB and CLEO data, should thus not be interpreted as due to glueballs, hybrid states or any other even more speculative states. Similar results have also been reached by the CUSB group[10] using the Cornell model of Eichten et al.[11]. The bumps at 10.62 and 10.70 GeV come from the combined effects from the opening of the various thresholds and from the nodes in the decay amplitudes, which again are reflections of the radially excited quantum numbers of the upsilons. Thus the resonances have quite distorted shapes, with strongly energy dependent widths, compared to conventional naive Breit-Wigners. Furthermore there is a "background" due to all the other resonances, which interferes with the dominant resonance, slightly modifying its shape.

3. THE BARYON MASS SPECTRUM

The currently popular explanation of the baryon mass splittings is to attribute these to a simple one-gluon exchange mechanism as described by the Breit-Fermi Hamiltonian. The most extensive analysis of this kind is the "soft QCD" analysis performed by Isgur and Karl[6], who no doubt obtained some quite impressive fits to the data. However, the fact that they, ad hoc, had to omit the spin-orbit term (being less than one tenth in magnitude compared to the theoretical expectation), and the fact that their effective coupling constant α_s is near one is disturbing.

In a recent detailed analysis of the ground state and P-wave baryons we have found[7] an equally good description of the data with negligible direct one-gluon exchange. Instead the mass splittings are generated by nonperturbative quark loops. In principle, given a good model for the widths this is a zero-parameter fit, since the widths fix through analyticity the real parts of the mass matrix. In fact, using the width model of Isgur and Koniuk one obtains, as already mentioned in the introduction, large mass splittings not in too bad disagreement with experiment, even when one-gluon exchange is completely neglected.

The remaining discrepancies could not be explained by one-gluon exchange. Instead, since they mainly appear for the P-wave baryons with nearby strong S-wave thresholds,we are able to account for these by an improved model for the S-wave widths. In short in order to fit the P-wave baryon masses and mixing matrices we used the following parameters:(i) An overall quark pair creation

strength parameter which can be fixed either by the widths or by the NNπ coupling constant and the internal symmetry relations of the $^3P_0$ model, (ii) A cutoff parameter related to hadron size. We used essentially the same value (0.68 GeV) as Isgur and Koniuk corresponding to an R^2 of 8 and 6 GeV^{-2} for baryons and mesons respectively. (iii) One parameter parametrizing the S-wave widths, and one (or two) parameter(s) breaking the $^3P_0$ model prediction relating the various couplings. These are necessary in order to obtain a detailed fit to the various experimental widths. (If we normalize the overall strength parameter in (i) to the NNπ coupling constant we need a second $^3P_0$ model breaking parameter, which enhances the widths compared to the prediction from NNπ).

For a detailed description of these results we refer to our original papers[4,7]. Here we only discuss shortly the mass splittings of the Λ - Σ - Σ^* states, which serve as an illustrative example for how the mechanism works.

In Fig. 4 we show the position and strength of the $SU6_W$ related thresholds coupled to the ground state Λ, Σ or Σ^* baryons. The vertical lines have a length proportional to the weight (square of the effective coupling constant). The positions of the Λ,Σ or Σ^* masses on the energy axis are also shown. Note, in particular, the very large number of (mainly closed) thresholds with strengths which vary within quite large limits. It is easy to see by glancing at this figure that for Λ there are more nearby thresholds of large weight than for Σ, while for Σ^* the strong thresholds are the most distant. Since by positivity, a closed threshold shifts the resonance mass down, one easily sees that the ordering in mass shifts of the three states coincides with the experimental order of the masses. A more quantitative analysis (using a "linearized model") relates the mass shifts to a weighted sum of meson and baryon masses in the loop. In the detailed numerical fits[7] one puts in much more information about phase space, form factors etc., but qualitatively the effect which one can see already from Fig. 4 explains why the nonperturbative unitarity effects work in the right direction. In the case of the P-wave baryons, in particular the $\Lambda(5/2^-)$ - $\Sigma(5/2^-)$ mass splitting has the opposite sign compared to the ground state baryons. Remarkably enough, the unitarity effects also work in this direction. Thus the mechanism of Isgur and Karl involving different λ- and ρ-oscillator energies due to the strange-nonstrange quark mass difference need not explain the whole mass

splitting.

4. CONCLUDING REMARKS

Why has one not previously derived our results, although it has been recognized for a long time that unitarity effects must be present, and most likely are very important? We believe the reasons are several: (i) One needs a reasonable model like the $^3P_0$ model, or at least $SU6_W$, by which one can roughly estimate also the effects of many closed channels, (ii) One must sum over a very large number of intermediate states belonging to the same multiplet. This means for baryons typically over 20 thresholds per resonance (c.f. Fig. 4). Then one effectively perturbs around the comparatively small differences in threshold positions (iii) To obtain reliable results one must study simultaneously many mass splittings (or better ratios of mass splittings), where the largest uncertainties due to the cutoff parameter cancel (c.f. subtracted dispersion relations).

The overall total mass shift can be very large in models like ours, but it is quite uninteresting as it can be absorbed into the bare mass by renormalization. When one sums over complete multiplets in the intermediate states all states are shifted by essentially the same amount. Clearly if one does not include such complete sums the results can be quite arbitrary. Thus e.g. if one, as in the old days, would consider only $\Delta \to N\pi \to \Delta$ or $\rho \to \pi\pi \to \rho$ not much useful predictions could be derived.

REFERENCES

1) N.A. Törnqvist XIVth Rencontre de Moriond (1979, Quarks, Gluons and Jets) p. 633,
XVIth Rencontre de Moriond (1981, New Flavours and Hadron Spectroscopy) p. 311,
K. Heikkilä, S. Ono and N.A. Törnqvist
XVIIIthe Rencontre de Moriond (1983, Gluons and Heavy Flavours) p. 361,
P. Żenczykowski and N.A. Törnqvist, XIXth Rencontre de Moriond (1984, New Particle Production) p. 867.

2) However,the situation is rapidly changing, the latest application of the unitarized quark model comes from Peking: Guo-Zhong Li (李国忠) and Yu-Ping Kuang (邝宇平), Tsinghua University preprint TUTP.84/1 (October 1984).

3) For a review see N.A. Törnqvist, Helsinki University preprint HU-TFT-84-47 (Zakopane lectures) to be published in Acta Physica Polonica, June 1985.

[4] N.A. Törnqvist and P. Żenczykowski, "The Spectrum of the P-wave Baryons", Helsinki preprint HU-TFT-85-10.

[5] N. Isgur and R. Koniuk, Phys. Rev. D21 1868 (1980).

[6] N. Isgur and G. Karl, Phys. Lett. 72B 109 (1977), Phys. Rev. D18 4187 (1978).

[7] N.A. Törnqvist and P. Żenczykowski, Phys. Rev. D23 2139 (1984) P. Żenczykowski, Z. Physik C22, 441 (1984).

[8] N.A. Törnqvist, Phys. Rev. Lett. 53 (1984) 878.

[9] D. Besson et al. "Observation of New Structure in the e^+e^- Annihilation Cross Section" Cornell preprint (1984) CLNS 84/629, CLEO 84-8

[10] D.M.J. Lovelock, "Masses, Widths and Leptonic Widths of the Higher Upsilon Resonances, Paper presented at the XXII the Int. Conference on High Energy Physics, Leipzig (1984).

[11] E. Eichten et al., Phys. Rev. D17, 3090 (1978), D21, 313 (1981), D21, 203 (1981).

FIGURE CAPTIONS

Fig. 1. The qualitative behaviour of the width (Im M(s)) and the mass shift (Re M(s)) in the region of a threshold. Note that the variation in the mass shift is similar to that of the width ($\sim$ 100 MeV over an interval of $\sim$ 100 MeV).

Fig. 2. The contribution to R in e^+e^- from thresholds involving B,B*,B_s and B_s^* mesons. Note that the small bumps do not correspond to resonances. The CUSB data, which appeared after the model calculation, are also shown.

Fig. 3. The mass shift of the S and D wave states for $c\bar{c}$ states (a) and $b\bar{b}$ states (b). The curves are shown to guide the eye. Note in particular the sharp increase in the upsilon mass shift at the opening of $B\bar{B}$ etc. which explains the anomalously heavy 5S state. In $c\bar{c}$ (as well as for light quarkonium) the thresholds are relatively much more spread out and only one state is below the $D\bar{D}$ threshold. Therefore the unitarity effects are more easily tested in $b\bar{b}$ although the overall mass shifts are smaller.

Fig. 4. The weights (lengths of vertical lines) and positions of the SU6 related thresholds coupled to the Λ,Σ and Σ^* baryons. Note that the center of gravity of the thresholds is nearest for the Λ, followed by the Σ and Σ^*. This splits the Λ-Σ-Σ^* masses in the same direction as the experimental splittings.

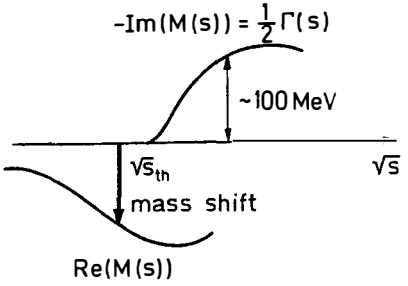
-Im(M(s)) = 1/2 Γ(s)
~100 MeV
√s_th
mass shift
√s
Re(M(s))

Fig.1.

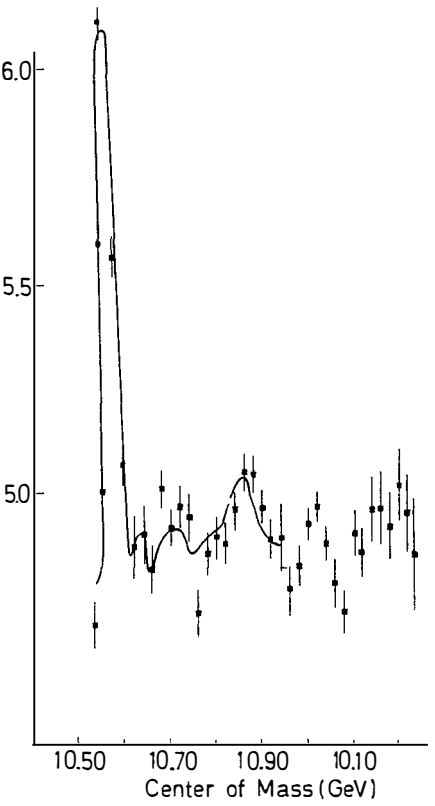
6.0
5.5
5.0
10.50
10.70
10.90
10.10
Center of Mass (GeV)

Fig.2.

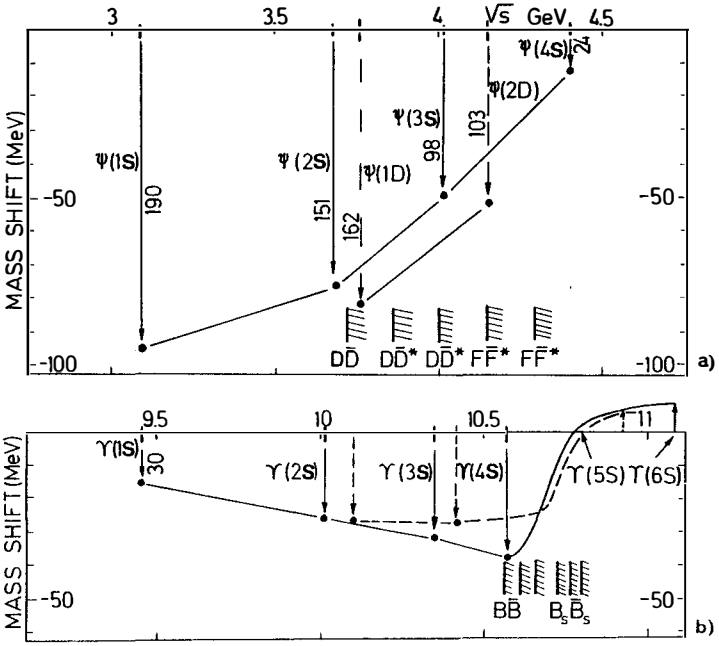
3
3.5
4
√s GeV
4.5
MASS SHIFT (MeV)
-50
-100
Ψ(1S)
Ψ(2S)
Ψ(1D)
Ψ(3S)
Ψ(4S)
Ψ(2D)
190
151
162
98
103
24
DD̄
DD̄*
DD̄*
FF̄*
FF̄*
a)
9.5
10
10.5
11
Υ(1S)
30
Υ(2S)
Υ(3S)
Υ(4S)
Υ(5S)
Υ(6S)
BB̄
BsB̄s
b)

Fig. 3.

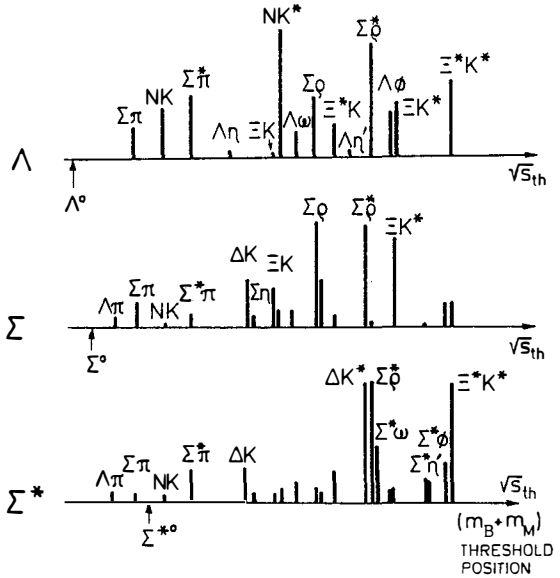
Λ
Σ
Σ*
Λ°
Σ°
Σ*°
√s_th
(m_B+m_M)
THRESHOLD
POSITION

Fig. 4.

EXCLUSIVE QUARKONIUM DECAY AND ENERGY DEPENDENCE OF OZI-FORBIDDEN PROCESSES

G. Karl and W. Roberts
Guelph Waterloo Program for Graduate Work in Physics
Department of Physics, University of Guelph, Guelph, Canada

and

N. Zagury
Departamento de Fisica, Pontificia Universidade Catolica,
Rio de Janeiro, Brazil

ABSTRACT
Recent work on the energy dependence of sequential quark pair creation in exclusive processes is being reviewed.

The work reported here was motivated by the very puzzling observation of Franklin et al[1] that the decay rate of ψ' (3685) into the $\rho\pi$ final state is very much smaller than the corresponding rate of decay of J/ψ:

$$\frac{\Gamma(J/\psi \to \pi\rho)}{\Gamma(\psi' \to \pi\rho)} > 46$$

This is very surprising given the small increase in the overall centre of mass energy between J/ψ and ψ' and their comparable leptonic widths. These decays, like all other $c\bar{c}$ decays into light systems are OZI-violating. Thus, it is tempting to suppose that OZI-violating processes are very energy dependent.

The mechanism we proposed[2] to accommodate this fact assumes that the light quark pairs needed to form the final state are produced sequentially, namely there is a certain time delay between the creation of the first pair and the creation of the second pair. This delay in time corresponds to an oscillatory behaviour in energy.

The amplitude for a process is usually computed by taking the overlap integral between the initial state and the final state. In hadron physics we are interested in processes of creation of a quark-antiquark pair - in these cases the number of fermions is not the same in the initial and final state. The amplitude for such processes was formulated by Micu[3], Le Yaouanc, Oliver, Pène, Raynal[4] and others[5] to explain the behavior of hadronic processes and form factors.

We have used the formalism of Cottingham et al[6], who consider a string model as the physical description of a decaying quark-antiquark system. In this formalism, the amplitude for the process $q\bar{q} \to \text{Meson}_1 + \text{Meson}_2$ has the form:

$$(1) \qquad A_\ell = \text{const} \int_0^\infty r^3 \, dr \Big[\int_0^1 d\sigma \, \phi_1(\sigma r) \, \phi_2((1-\sigma)r) \Big] \, \Psi_{in} \, j_\ell(k_f r/2)$$

In this formula ϕ_1 and ϕ_1 are the radial wavefunctions of the two final state mesons and j_ℓ is a spherical Bessel function describing the orbital motion of the two mesons relative to each other. We have assumed that all quarks have the same mass so that the distance between the two mesons $(r/2)$ is half the distance r between the two initial quarks. The final state momentum is k_f and the string is broken, by a $q\bar{q}$ pair at the point σr. The wave function of the initial $q\bar{q}$ pair is Ψ_{in}. In the application to OZI-allowed processes[4], for which the formula (1) was set up, the initial wavefunction Ψ_{in} is a bound state wavefunction, say of a $c\bar{c}$ system which later on decays into $(c\bar{d} + d\bar{c})$ the two final state mesons.

In the application of the formula (1) to OZI-forbidden processes we

have to prescribe the wavefunction appropriate to the first quark-antiquark pair created after the heavy quark and antiquark have annihilated. We have taken a semiclassical wavefunction which satisfies boundary conditions appropriate to a source at the origin - in other words, an outgoing wave near r=0, where the first pair is produced.

An example of such a form is:

$$\Psi_{in}(r) = \frac{1}{r} e^{i\left(k_o r - K r^2/2\right)} \tag{2}$$

In this formula K_o is the initial momentum of a quark (or antiquark), so that the total C of M energy is $2k_o$ for massless quarks, and K is the tension of the string between these two initial fermions.

The amplitude A_ℓ depends on the total energy through k_o in (2) and k_f in (1). The oscillatory behaviour can be understood since the only contribution of (2) in the integral (1) comes from the neighbourhood of the classical turning point r_t:

$$2k_o = K r_t$$

which at some energies, happens to be near a zero of the final state orbital wave function:

$$J_\ell\left(\frac{k_o k_f}{K}\right) \simeq 0$$

At such energies the amplitude of the process is small.

For example, if we take $2k_o \simeq 3.68$ GeV, the mass of the ψ' state, and $\ell=1$ as appropriate to decay into $\pi\rho$, $k_f \simeq 1.76$ we find

$$K = \frac{(1.76) \times (1.84)}{4.493} \simeq .72 \text{ GeV}^2$$

which is the solution proposed in reference 2. This value of K gives a reasonable prediction for the ratio $(\psi/\psi')_{\pi\rho}$ namely 324 and also for the similar ratio of decay into $\bar{K}K^*$ which is also observed[1] to be suppressed at the ψ'. Unfortunately this value of K is much larger than spectroscopy determinations which are about .2 GeV^2. It is also possible to fit the experimental data using higher zeros of the spherical Bessel function j_1. Thus with $K = .1$ GeV^2 the ratio $(\psi/\psi')$is about 20 which is not too far from the experimental data.

Another problem with the fit of reference 2 is that the $\pi\pi$ channel is also expected to be suppressed in the decay of the ψ' whereas experiment apparently gives similar rates for the decays $J/\psi \to \pi\pi$ and $\psi' \to \pi\pi$. It is not yet clear whether the mechanism of reference 2 is the correct explanation of the

suppression observed at ψ'. An additional test, not discussed in that reference would be provided by the observation of the decay ψ'' (4.03 GeV) into the $\pi\rho$ channel. That observation would demonstrate directly that one is dealing with a "zero" as a function of energy. Unfortunately, there is no data available at the moment at this resonance about the decay into $\pi\rho$. According to Fig. 1 of reference 2 one expects a rate of the same order of magnitude as in the $J/\psi \to \pi\rho$ decay (actually a factor two smaller).

In the absence of this data, it is possible[7] to apply this mechanism to other processes which are OZI forbidden, such as the production of $\phi\phi$ pairs in πp collisions, studied by Lindenbaum and his collaborators[8] at B.N.L. One can interpret the mass spectrum observed by these authors as a reflection of the energy dependence expected in sequential fragmentation. In this case the relevant process is the sequential production of two ss pairs, required to form the $\phi\phi$ final state. We discuss here the angular momentum quantum numbers expected in this process.

We assume that the final state pair is produced through a two gluon intermediate state, and therefore has positive charge conjugation as required. The annihilating $\bar{u}u$ pair must have $C = + = (-)^{\ell+S}$ and the total spin S=1 since the energy is high compared to the mass of the quarks. Therefore the orbital angular momentum is odd and the parity is even. Thus, the lowest J^P accessible to the two gluon system is 2^+, and the initial $s\bar{s}$ pair must be in a $^3P_2$ state. (At higher energies we could also have $^3F_2$, $^3F_3$, $^3F_4$ etc.) This initial $s\bar{s}$ pair forms a $\phi\phi$ system which must also have $J^P = 2^+$. In the $\phi\phi$ channel we can have the partial waves $^1D_2$, $^5D_2$ and $^5S_2$ for the total angular momentum and parity 2^+. It can be shown, using the formalism of Cottingham et al[6] or directly by assuming $^3P_0$ quantum numbers for the second $s\bar{s}$ pair produced, that the mechanism of sequential quark pair formation predicts the ratios

$$^5S_2 : {}^1D_2 : {}^5D_2 = 10:1:7$$

These weights, which multiply the squares of radial integrals (1) are in reasonable agreement with the experimental data. Even roughly, the experimental data[9] show that the dominant partial waves are $^5S_2$ and $^5D_2$. It should be stressed that this agreement only checks that the $\phi\phi$ pairs are produced through a mechanism of sequential quark pair formation, as was assumed in reference 7.

At higher energies one expects that higher partial waves, eg $J^P = 3^+$, of the two gluon system will be excited and these can also be observed in the $\phi\phi$ final state as $^5D_3$ or $^5G_3$. The relative ratio expected is

$$^5D_3 : {}^5G_3 = 9 : 5$$

and the maxima of the production mechanism are predicted at higher mass for the G wave, but at the same mass in the $^5D_3$ wave as in the $^5D_2$ wave. A more detailed calculation, which takes into account the momentum distribution of the quarks in the initial projectile and target, as well as the mechanism of production of the first $s\bar{s}$ pair is still underway.

Acknowledgements: Much of this work was done while the authors were in the Department of Theoretical Physics, Oxford whose hospitality they wish to thank. One of us (GK) wishes to thank the organizers of this meeting for their hospitality.

References

1) M.E.B. Franklin et al., Phys. Rev. Letters 51, 963 (1983)
2) G. Karl and W. Roberts, Physics Letters 144B 263 (1984)
3) L. Micu, Nucl. Physics B10, 521 (1969)
4) A. Le Yaouanc, L. Oliver, P. Pene and J.C. Raynal, Phys. Rev. D8, 2223 (1973), Phys. Letters 71B, 397 (1977), Phys. Letters 72B, 57 (1977)
5) R. Carlitz and M. Kisslinger, Phys. Rev. D2, 336 (1970)
6) J.W. Alcock, M.J. Burfit and W.N. Cottingham, Z. Phys. C. (1984)
7) G. Karl, W. Roberts and N. Zagury, Phys. Letters 149B, 403 (1984)
8) C. Edwards et al., Phys. Rev. Letters 48, 458 (1982)
9) R.S. Longacre in 'Experimental Meson Spectroscopy - 1983', AIP Conference Proceedings No. 113 (A.I.P. New York 1984) p. 51

THE LATEST D DECAYS*

Jay Hauser
California Institute of Technology

(Representing the Mark III Collaboration[1])

ABSTRACT

New, largely preliminary results on hadronic and semileptonic decays of D mesons are presented, based on a large data sample taken at the Ψ'' resonance by the Mark III detector.

1. Introduction

The first and simplest model of weak charmed particle decay is the light quark spectator model, in which the decay proceeds as if the charmed quark were a free particle. This picture leads to a prediction of equal lifetimes and equal semileptonic branchings ratios for all charmed particles. Experimental observation, first that the D^+ and D° semileptonic branching ratios are not equal,[2,3] and secondly that the D^+ and D° lifetimes are also different,[4] has led to the proposal of other, more detailed models for charm decay. Perhaps the most popular of these is the W-exchange model, in which the hadronic decays of the D°, but not the D^+, are enhanced by the presence of "non-spectator" diagrams involving the light quark. Another approach is taken in the quark cluster model, which suppresses the hadronic decays of the D^+ only by allowing destructive interference between different diagrams which lead to identical final states. An exhaustive review of the various models may be found in Reference 5.

*Work supported by U.S. Department of Energy Contract No. DE-AC03-81-ER40050.

In this paper, we content ourselves with a presentation of the new Mark III data on D meson decays, particularly as another contribution to these proceedings (B. Stech) is devoted to the interpretation of these results.

2. The Mark III Detector and Ψ'' Data Sample

From its beginning, the Mark III detector was optimized for the study of decays of charmed particles to exclusive final states. The following describes some of the salient features of the detector. Drift chamber reconstruction of charged particle trajectories is performed over 93% of 4π sr, with momentum resolution of 2% at 1 GeV/c over 85% of 4π sr attained in the 0.4 T magnetic field. The 48 time-of-flight (TOF) counters cover 80% of the 4π solid angle, providing more than 2σ π–K separation up to 1 GeV/c, and good π–e separation below 0.3 GeV/c. Outside of the TOF counters, the barrel shower counter furnishes good low-energy photon detection efficiency (75% at 75 MeV, ~100% for $\geqslant$ 100 MeV) by virtue of its placement within the magnet coil, excellent angular resolution of about 10 mr in both φ and θ, and good π/e separation above 0.3 GeV/c. Endcap shower counters of similar design and performance extend the total angular coverage of the shower counters to 95% of 4π sr.

The Ψ'' is a source of $D\bar{D}$ pairs with a cross-section of about 6 nb. The D mesons are produced with energy equal to the beam energy, furnishing a nice kinematic handle on their decay products. Mark III has collected data near the peak of the Ψ'' in three runs during 1982-1984, comprising 8650 nb^{-1} total integrated luminosity. Measurements presented herein on hadronic decay modes use ~8100 nb^{-1} and are to be regarded as preliminary. The measurements of D^+ and D° semileptonic branching ratios use the full data sample, and are final.

3. D^+ and D° Semileptonic Branching Ratios[61]

The study of both inclusive and exclusive semileptonic D decays is made considerably easier by searching for them in the recoil from fully reconstructed hadronic decays. Inclusively, this determines whether the event is $D^\circ\bar{D}^\circ$ or D^+D^-, fixes the expected lepton charge as opposite to the charm of the reconstructed D, as well as reducing the level of non-charm backgrounds. Exclusively, this allows a determination of the direction and energy of the missing neutrino. For the determination of inclusive D^+ and D° semileptonic branching ratios we use the large hadronic decay signatures shown in Figure 1. In each

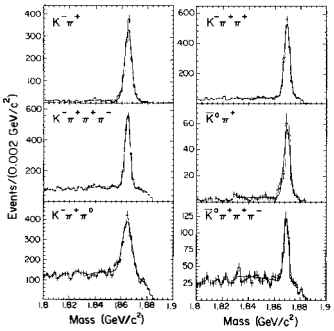

Figure 1. Hadronic D decay signals used in derivation of D^+ and D° semileptonic branching ratios.

mass plot a signal region centered on the D mass and a control region used to correct for background events under the signal are defined. The D° signal regions contain 4541 events, of which 1106 ± 39 are background, while the D^+ signal regions contain 2062 events, of which 333 ± 20 are background.

Candidate electron tracks recoiling from these reconstructed D mesons are required to lie within $|\cos\theta| < 0.77$, in which charged kaons are easily rejected by TOF. The remaining tracks are then required to have momentum greater than 150 MeV/c, originate near the event's primary vertex within 0.01 m perpendicular and 0.15 m parallel to the beam axis, and to deposit energy in the barrel shower counter. Most of the electrons arising from gamma conversions and Dalitz decays are removed by requiring candidate electron tracks to have opening angles larger than 8° with any other oppositely charged track in the event. Separation of electrons from pions is then accomplished using cuts on TOF and shower counter information. The misidentification rates which result from these cuts are shown in Figure 2, as measured for pions from K_s° decay and electrons from radiative Bhabha events.

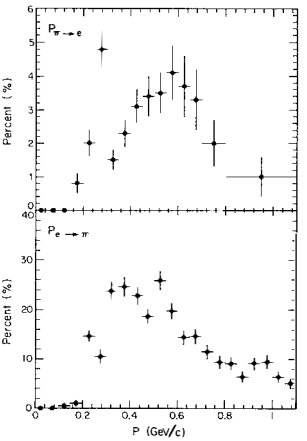

Figure 2. Misidentification probabilities for pions and electrons. For $p < 300$ MeV/c, only TOF is used for particle identification. For $p > 300$ MeV/c, both TOF and shower information are used.

The charm of the reconstructed D determines the charge of the recoil electron from semileptonic decay. This allows a subtraction of charge-symmetric sources of electrons such as remaining gamma conversions and Dalitz decays, and misidentification of equal numbers of plus- and minus-charged pions, to be made by subtracting the number of "wrong-sign" candidate electrons from the number of "right-sign" candidates. The major source of background which is not charge-symmetric is misidentification of a net number of right-sign pions. This amounts to 20% of the apparent right-sign electrons for D^+ and 14% for D°. The true numbers of electrons and pions are obtained from the observed numbers by inversion of the known misidentification matrix. Small corrections are then made for background events under the hadronic decay signals, TOF misidentification of both K and π in the $D^\circ \to K^-\pi^+$ channel, and K_{e3} decays. The efficiency for an electron to pass all cuts, which averages about 70% with

TABLE I

Recoil Electron Identification

Source	Signal Events (Tags)	Right Sign Recoil Electrons	Wrong Sign Recoil Electrons	Control Region Electrons	Net Signal Electrons	Signal Electrons Corrected for Efficiency
D°	3435 ± 39	193 ± 13.9	57.0 ± 7.5	5.2 ± 4.5	136.6 ± 20.4	257.5 ± 37.9
D^+	1729 ± 20	177 ± 13.3	14.0 ± 3.7	2.5 ± 2.9	158.2 ± 17.6	294.0 ± 32.6

a slight momentum dependence, is determined by Monte Carlo simulation. Table I summarizes this procedure. The resulting electron spectra are shown in Figure 3, along with those expected from $Ke\nu$ and $K^*e\nu$ decays.[71]

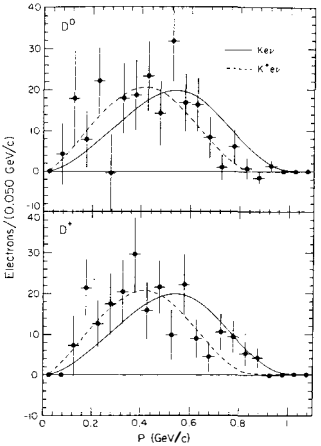

Figure 3. D° and D^+ electron spectra. The curves represent the shape of spectra expected from $Ke\nu$ and $K^*e\nu$ decays.

The numbers of recoil electrons of correct sign relative to the number of events lead to the branching fractions:

$$B(D^+ \to e^+ + X) = (17.0 \pm 1.9 \pm 0.7)\ \% \tag{1}$$

$$B(D^\circ \to e^+ + X) = (7.5 \pm 1.1 \pm 0.4)\ \%\ ,$$

and thus to the ratio

$$\frac{B(D^+ \to e^+ + X)}{B(D^\circ \to e^+ + X)} = 2.3^{+0.5+0.1}_{-0.4-0.1} \tag{2}$$

which has a negative log likelihood function shown in Figure 4. Several systematic errors cancel in the ratio of branching fractions.

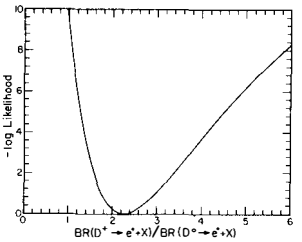

Figure 4. The negative log likelihood function for the ratio of D^+ to D° semileptonic branching ratios.

These measurements yield an average D semileptonic branching ratio at the Ψ'' of $(11.7 \pm 1.0 \pm 0.5)\%$, using the expected 56/44% ratio of $D^\circ\overline{D^\circ}$ to D^+D^- production, which is consistent with the Mark II value[21] of $(10.0 \pm 3.2)\%$ obtained by the same technique, but higher than the DELCO and LGW determinations of $(8.0 \pm 1.5)\%$ and $(7.2 \pm 2.8)\%$, respectively. Our result is an absolute measurement, while the DELCO and LGW results rely on normalization of the electron signal to the Ψ'' cross-section. Indications that the Ψ'' cross-section may have been overestimated in the past, and hence the D branching ratios underestimated, come also from the study of fully reconstructed events discussed in the next section.

4. Absolute Determination of Branching Ratios

In the past, the only method available for deriving D meson branching ratios was to fit the plot of R in e^+e^- collisions to obtain the Ψ'' cross-section, assume that the Ψ'' decays only to $D\overline{D}$ pairs, and use the 56/44% ratio of $D^\circ\overline{D^\circ}$ to D^+D^- pair production expected from p-wave phase space, the mass difference between D^+ and D°, and the Ψ'' effective interaction radius, to determine σ_{D° and σ_{D^+}. These cross-sections are then used to normalize the observation of D decays in specific final states at the Ψ''. Because of our large data sample, we have been able to employ an alternate technique which is free of the uncertainties and assumptions implicit in the previous method.

This technique compares the number of events in which both D mesons are reconstructed in charge-conjugate decay modes (double tags), to the number of decays reconstructed in that mode independent of the other half of each event (single tags). One can write the numbers of events as

$$(\#\ \text{doubles}) = \varepsilon_t \cdot \varepsilon_r \cdot B^2 \cdot N_D \tag{3}$$

$$(\#\ \text{singles}) = \varepsilon_t \cdot B \cdot N_D \ ,$$

where ε_+ is the efficiency for reconstructing a "tag", ε_r is the efficiency for reconstructing the recoil decay, B is the branching ratio, and N_D is the number of produced D mesons of the appropriate charge. Dividing these two numbers yields

$$\left(\frac{\#\ \text{doubles}}{\#\ \text{singles}} \right) = \varepsilon_r B \ . \tag{4}$$

Because of the cleanliness of these double tag events, detection of the recoil D needs only use the drift chamber momentum measurements, so that ε_r can be easily and accurately determined by Monte Carlo.

This technique has been applied to the decay modes $D^\circ \to K^-\pi^+$ and $D^+ \to K^-\pi^+\pi^+$. Figure 5 shows the double tag signals, with the mass of the recoil system plotted against the tag mass.

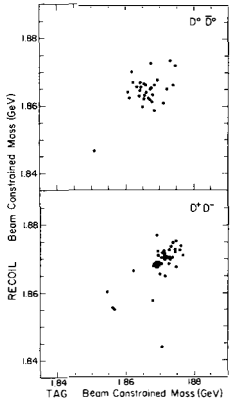

Figure 5. Scatterplots of a) tagged $D^\circ \to K^-\pi^+$ versus $\overline{D^\circ} \to K^+\pi^-$, b) tagged $D^+ \to K^-\pi^+\pi^+$ versus $D^- \to K^+\pi^-\pi^-$.

A summary of the numbers which lead to the branching ratios of (4.9 ± 0.9 ± 0.5)% for $D^\circ \to K^-\pi^+$ and (9.1 ± 1.5 ± 0.9)% for $D^+ \to K^-\pi^+\pi^+$ is contained in Table II.

TABLE II

Double Tag Analysis

Channel	Singles	Doubles	Background	ε (recoil)	Br (%)
$D^\circ \to K^-\pi^+$	978 ± 33	29 ± 6	1.7	.61	4.9 ± 0.9 ± 0.5
$D^+ \to K^-\pi^+\pi^+$	1109 ± 37	46 ± 7	2.2	.45	9.1 ± 1.5 ± 0.9

These measurements can be used in conjunction with $\sigma \cdot B$ measurements from single tags to derive the production rates

$$\sigma(D^\circ) = 5.7 \pm 1.1 \pm 0.9 \text{ nb} \quad \sigma(D^+) = 4.6 \pm 0.8 \pm 0.7 \text{ nb} \tag{5}$$

for D mesons in our data sample.

The $\sigma \cdot B$ and B measurements made by LGW, Mark II, and Mark III (by this technique) are compared in Figure 6. It is clear that the branching ratios determined in this absolute way are significantly higher than those which rely on normalization using the Ψ'' cross-section, although the production rates for these decays ($\sigma \cdot B$) were comparable. While our preliminary measurements have large statistical errors, we expect a great improvement with application of kinematic fitting and by using other decay modes.

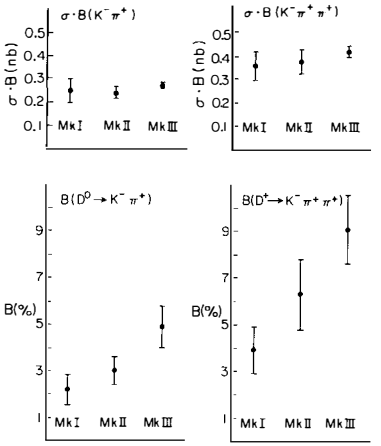

Figure 6. Comparison of production rates and branching ratios for $D^\circ \to K^-\pi^+$ and $D^+ \to K^-\pi^+\pi^+$.

assumptions. Insofar as the three-body $K\pi\pi$ modes occur through $K\rho$ or $K^*\pi$, these modes are interesting as well.

Our signal for $D^\circ \to \bar{K}^\circ\pi^\circ$ is shown in Figure 7a. A fit to this plot yields 68 ± 11 events, as compared to the previous Mark II observation[21] of 9 ± 4 events in this mode. Three-body signals not contained in Figure 1 are shown for completeness in Figures 7b and 7c for $D^\circ \to \bar{K}^\circ\pi^+\pi^-$ and $D^+ \to \bar{K}^\circ\pi^+\pi^\circ$.

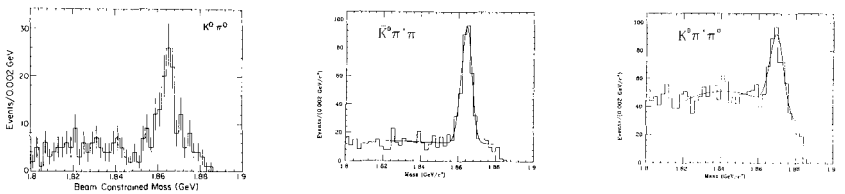

Figure 7. Beam constrained mass distributions for a) $D^\circ \to \bar{K}^\circ\pi^\circ$, b) $D^\circ \to \bar{K}^\circ\pi^+\pi^-$, and c) $D^+ \to \bar{K}^\circ\pi^+\pi^\circ$.

5. Cabibbo-allowed Hadronic D Decays

In addition to the six large D decay modes shown in Figure 1, we observe other Cabibbo-allowed two- and three-body modes. The two-body modes are especially interesting because they can be easily related to theoretical predictions within each of the contending models of D decay, under certain

A maximum likelihood fit is performed to the Dalitz plots of the $K\pi\pi$ systems to extract the K^* and ρ content. The matrix elements use P-wave Breit-Wigner line shapes having energy dependent widths and arbitrary phases, plus a non-resonant phase space contribution. The distribution of background events under the D signals is taken into account by using the sidebands of lower mass. This simple technique fails to give an acceptable fit to the Dalitz plot of $D^+ \to K^-\pi^+\pi^+$ shown in Figure 8 with one of the $K^-\pi^+$

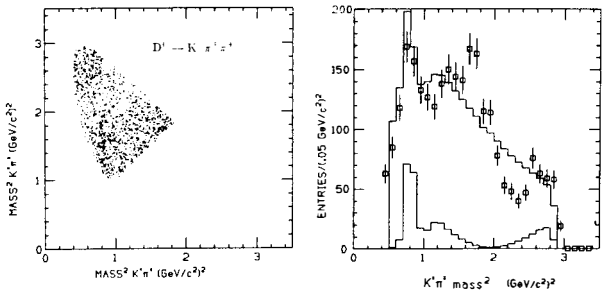

Figure 8. Dalitz plot of the decay $D^+ \to K^-\pi^+\pi^+$.

mass projections. However, it works adequately for the Dalitz plots of $D^\circ \to K^-\pi^+\pi^\circ$, $D^\circ \to \overline{K}^\circ\pi^+\pi^-$, and $D^+ \to \overline{K}^\circ\pi^+\pi^\circ$ which are shown in Figures 9-11, with interesting mass projections. Results from all of the major Cabibbo-allowed hadronic decays discussed thus far are listed in Table III. It should be noted, however, that the $\sigma \cdot B$ measurements of $D^\circ \to K^-\pi^+\pi^\circ$ and $D^+ \to \overline{K}^\circ\pi^+\pi^\circ$ use efficiencies determined by Monte Carlo assuming flat phase space production. We expect these measurements to increase substantially when the substructure is properly taken into account.

TABLE III

Measurements of Cabibbo-allowed Hadronic Modes

	Mode	$\sigma \cdot B$	Fraction
$D^\circ \to$	$K^-\pi^+$	.28 ± .01 ± .03	
	$\overline{K}^\circ\pi^\circ$	.10 ± .02 ± .02	
	$K^-\pi^+\pi^\circ$	.53 ± .05 ± .10	0.0 ± 4.5 ± 3.0%
	$K^-\rho^+$		77.1 ± 4.9 ± 5.0%
	$\overline{K}^{*\circ}\pi^\circ$		5.4 ± 2.0 ± 2.0%
	$K^{*-}\pi^-$		17.5 ± 3.0 ± 2.0%
	$\overline{K}^\circ\pi^+\pi^-$	.40 ± .04 ± .03	17.0 ± 8.1 ± 3.0%
	$K^{*-}\pi^+$		66.6 ± 8.0 ± 5.0%
	$\overline{K}^\circ\rho^\circ$		16.4 ± 5.1 ± 2.0%
	$K^-\pi^+\pi^+\pi^-$	.56 ± .03 ± .06	
$D^+ \to$	$\overline{K}^\circ\pi^+$	.15 ± .02 ± .01	
	$K^-\pi^+\pi^+$	.42 ± .02 ± .04	?
	$\overline{K}^{*\circ}\pi^+$		?
	$\overline{K}^\circ\pi^+\pi^\circ$	.45 ± .07 ± .07	7.4 ± 5.4 ± 4.5%
	$\overline{K}^\circ\rho^+$		84.0 ± 8.5 ± 4.0%
	$\overline{K}^{*\circ}\pi^+$		8.6 ± 4.7 ± 4.0%
	$\overline{K}^\circ\pi^+\pi^+\pi^-$	.38 ± .05 ± .04	

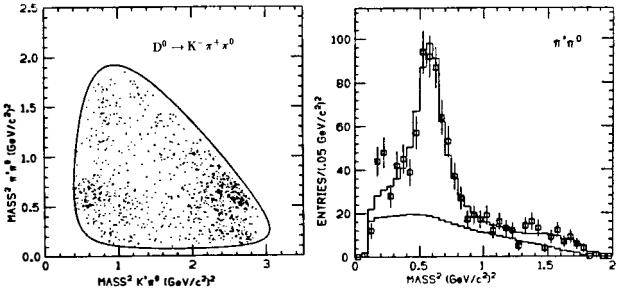

Figure 9. Dalitz plot of the decay $D^\circ \to K^-\pi^+\pi^\circ$.

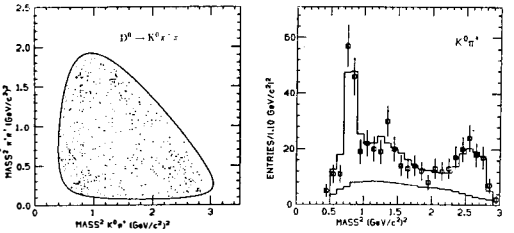

Figure 10. Dalitz plot of the decay $D^\circ \to \overline{K}^\circ\pi^+\pi^-$.

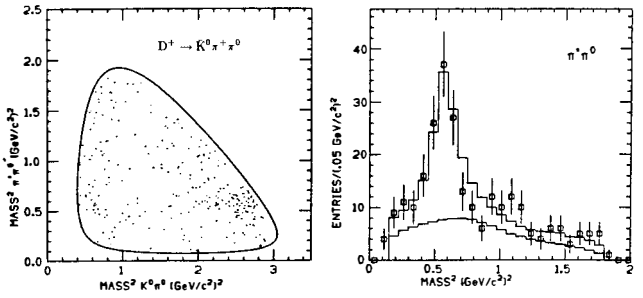

Figure 11. Dalitz plot of the decay $D^+ \to \overline{K}^\circ\pi^+\pi^\circ$.

6. Cabibbo-suppressed Hadronic D Decays

One expects to see Cabibbo-suppressed hadronic D decays either to final states with two kaons or to states with no kaons. The former is associated with the ordinary sine of the Cabibbo angle, while the latter is associated with the V_{cd} element of the weak quark mixing matrix, which is roughly equivalent to the sine of the Cabibbo angle in the present picture of the mixing matrix. Definite predictions for Cabibbo-suppressed decay modes are made by several models. In the quark cluster interference model, for instance, suppression of allowed hadronic decays should lead to a relatively large proportion of D^+ hadronic decays which are Cabibbo-suppressed. Ordinary flavor SU(3) predicts the rates for D° decay to K^+K^- and $\pi^+\pi^-$ to be both equal to $\tan^2\theta_c \approx 0.05$ of the rate into $K^-\pi^+$. It was a great surprise in 1979 when Mark II reported these rates[9] as 0.113 ± 0.030 for K^+K^-, and 0.033 ± 0.015 for $\pi^+\pi^-$ relative to $K^-\pi^+$ decay.

Invariant mass distributions in the final states K^+K^-, $K^-\pi^+$, and $\pi^+\pi^-$ are shown in Figure 12. The shape of the background in each plot is determined by smoothing data from sidebands in total momentum away from the expected D momentum. Feeddown from the dominant $K^-\pi^+$ decay into the K^+K^- and $\pi^+\pi^-$ plots because of TOF misidentification results in the bumps at 1.980 and 1.740 GeV/c^2, respectively. Fits which include the smoothed background shape plus Gaussians to represent the D° signals and misidentification peaks yield 75 ± 10 K^+K^- events, 889 ± 35 $K^-\pi^+$ events, and 33 ± 9 $\pi^+\pi^-$ events. The detection efficiency for K^+K^- is actually somewhat lower than that for the $\pi^+\pi^-$ mode because of kaon decays in flight. We thus confirm the inequality observed by Mark II with much better precision.

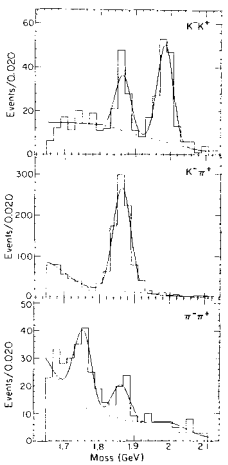

Figure 12. Invariant mass plots and fits for D° decays to a) K^+K^-, b) $K^-\pi^+$, and c) $\pi^+\pi^-$.

The same technique is used to determine the background shape in the D^+ decay modes $\overline{K^\circ}K^+$ and $\overline{K^\circ}\pi^+$. Fits to the mass plots shown in Figure 13 yield 29 ± 6 $\overline{K^\circ}K^+$ events and 141 ± 13 $\overline{K^\circ}\pi^+$ events. The technique is repeated again for the three-body D^+ decay modes $K^+K^-\pi^+$, $K^-\pi^+\pi^+$, and $\pi^+\pi^+\pi^-$, which are shown in Figure 14. In the case of $K^+K^-\pi^+$, there is a significant contribution to this final state from $D^+ \rightarrow \varphi\pi^+$. Figure 15 shows the distribution of K^+K^- mass within the $K^+K^-\pi^+$ signal.

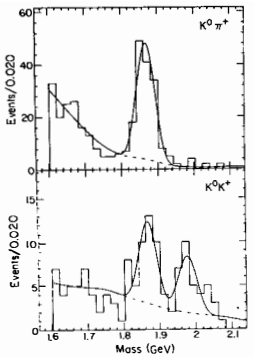

Figure 13. Invariant mass plots and fits for D^+ decays into a) $\overline{K}^0K^+$ and b) $\overline{K}^0\pi^+$.

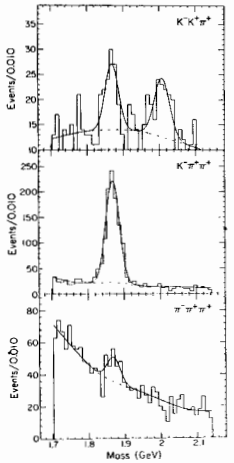

Figure 14. Invariant mass plots and fits for D^+ decays into a) $K^+K^-\pi^+$, b) $K^-\pi^+\pi^+$, and c) $\pi^+\pi^+\pi^-$.

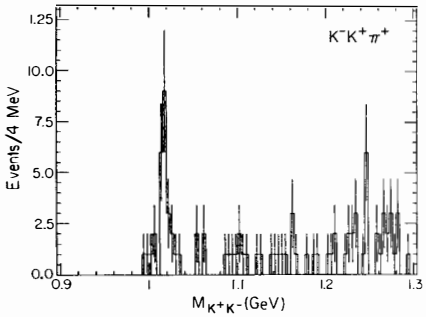

Figure 15. The K^+K^- submass within the $D^+ \rightarrow K^+K^-\pi^+$ signal.

The results of these analyses are quoted as ratios of Cabibbo-suppressed to similar allowed decays. This usually allows cancellation of certain systematic errors, as well as being easier to relate to the theoretical predictions. The contribution from $\varphi\pi^+$ is substracted from the measurement of $D^+ \to K^+K^-\pi^+$:

$$\frac{\Gamma(D^\circ \to K^+K^-)}{\Gamma(D^\circ \to K^-\pi^+)} = 0.125 \pm 0.018 \pm 0.010$$

$$\frac{\Gamma(D^\circ \to \pi^+\pi^-)}{\Gamma(D^\circ \to K^-\pi^+)} = 0.038 \pm 0.010 \pm 0.005$$

$$\frac{\Gamma(D^+ \to \bar{K}^\circ K^+)}{\Gamma(D^+ \to \bar{K}^\circ\pi^+)} = 0.294 \pm 0.074 \pm 0.051$$

$$\frac{\Gamma(D^+ \to K^+K^-\pi^+)}{\Gamma(D^+ \to K^-\pi^+\pi^+)} = 0.072 \pm 0.024 \pm 0.015$$

$$\frac{\Gamma(D^+ \to \varphi\pi^+)}{\Gamma(D^+ \to K^-\pi^+\pi^+)} = 0.083 \pm 0.023 \pm 0.012$$

$$\frac{\Gamma(D^+ \to \pi^+\pi^+\pi^-)}{\Gamma(D^+ \to K^-\pi^+\pi^+)} = 0.059 \pm 0.016 \pm 0.010$$

In general, these ratios are not greatly different from the expectations of about 5%. Consideration of isospin amplitudes for D° decay to $K^-\pi^+$ and $\bar{K}^\circ\pi^\circ$ relative to $D^+ \to \bar{K}^\circ\pi^+$ indicates that the large ratio of $D^+ \to \bar{K}^\circ K^+$ relative to $\bar{K}^\circ\pi^+$ is due to suppression of the $\bar{K}^\circ\pi^+$ rate rather than any particular enhancement of the $\bar{K}^\circ K^+$ rate. While this might be construed as supportive evidence for the quark cluster interference model previously mentioned, the other D^+ Cabibbo-suppressed decays do not show particular enhancement.

7. W-Exchange Final States

The best evidence for W-exchange in D° decays would be the observation of final states which contain no u or $\bar{u}$ quark content. Very few such states are experimentally accessible, the best possibilities being $\bar{K}^\circ\varphi$ and $K^\circ\bar{K}^\circ$. The latter decay occurs at a Cabibbo-suppressed level.

The $\bar{K}^\circ\varphi$ decay is observable in the $\bar{K}^\circ K^+K^-$ final state. The mass distribution of such combinations shown in Figure 16 shows a very distinct signal at the D° mass. The $K^\circ K^+K^-$ Dalitz plot formed from this signal is shown in Figure 17, and does indeed show an accumulation of events at low K^+K^- mass. However, the width of the K^+K^- mass distribution is far wider than our φ mass resolution, and in addition, does not show the accumulation of events at very high and very low $\bar{K}^\circ K^+$ masses which would be expected from the pseudoscalar-vector $\bar{K}^\circ\varphi$ decay. The Dalitz plot appears to be more consistent with the hypothesis $D^\circ \to K^-\delta^\circ$ where $\delta^\circ \to K^+K^-$, although the lack of a $D^\circ \to \bar{K}^\circ\delta^+$ ($\delta^+ \to K^+\bar{K}^\circ$) signal in the same Dalitz plot is surprising. The decay $D^\circ \to \bar{K}^\circ S^{*\circ}$ is ruled out because the decay $S^* \to \pi^+\pi^-$ should show prominently in the $\bar{K}^\circ\pi^+\pi^-$ Dalitz plot and is not observed. The 4 events having K^+K^- mass within 2σ of the φ mass furnish an upper limit $\sigma \cdot B < 0.13$ nb at 95% confidence level for the decay $D^\circ \to \bar{K}^\circ\varphi$.

The $K^\circ\bar{K}^\circ$ final state is isolated by tight cuts on the vertex displacement of the K° candidates to reject contamination from the large decay $D^\circ \to \bar{K}^\circ\pi^+\pi^-$, where the $\pi^+\pi^-$ mass happens to lie close to the K_s°

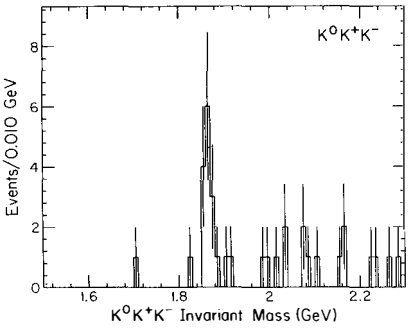

Figure 16. Invariant mass distribution for $\overline{K^0}K^+K^-$ combinations.

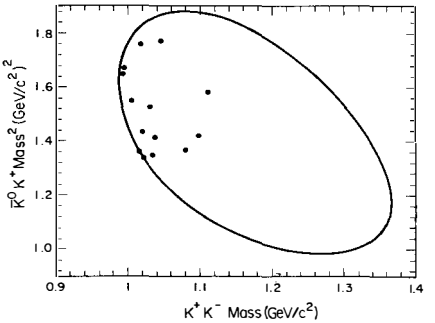

Figure 17. Dalitz plot of the decay $D^\circ \to \overline{K^0}K^+K^-$.

mass. Figure 18 shows one event within 2σ of the correct D° beam-constrained and invariant masses. Based on this one event, we quote the limit $\frac{\Gamma(D^\circ \to K^0\overline{K^0})}{\Gamma(D^\circ \to K^-\pi^+)} < 0.11$ at 95% confidence level. It should be noted that this decay is strictly forbidden in the limit of exact SU(3) symmetry.

8. Conclusions

The Mark III data presented here considerably extends our knowledge of D meson decays. The lifetime ratio between D^+ and D°, once the object of controversy, seems to have settled down to a value between 2 and 3, in agreement with the semileptonic branching ratios measured herein. Although the D° semileptonic branching ratio of 7.5% is well below perturbative QCD estimates within the light quark spectator model, thus favoring the existence of W-exchange diagrams, experimentally we have not yet found direct evidence to support this. In fact, certain features of the data, such as the large $D^+ \to \overline{K^0}K^+$ rate relative to $D^+ \to \overline{K^0}\pi^+$, tend to favor quark cluster interference as the source of the lifetime difference. If this were true, significant contributions from non-perturbative effects must be present to lower the D° semileptonic branching ratio. Some of the other interesting measurements presented are the confirmation of the

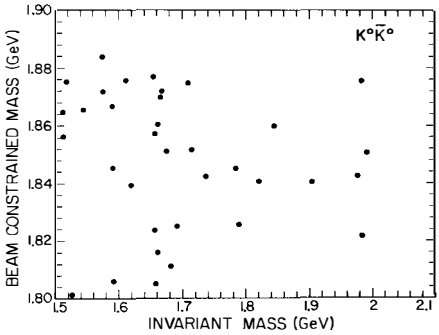

Figure 18. Beam-constrained mass versus invariant mass for $K_s°K_s°$ combinations.

inequality of $D° \to K^+K^-$ and $D° \to \pi^+\pi^-$ rates (apparently because of large flavor SU(3) breaking), the observation of the "color-suppressed" decay $D^+ \to \phi\pi^+$, and the measurement of significantly larger branching ratios by a new, absolute technique than were previously measured using the apparent Ψ'' cross-section for normalization.

References

1] Members of the Mark III collaboration are: R. M. Baltrusaitis, D. Coffman, G. Dubois, J. Hauser, D. G. Hitlin, J. D. Richman, J. J. Russell, and R. H. Schindler, California Institute of Technology; K. O. Bunnell, R. E. Cassell, D. H. Coward, S. Dado, K. F. Einsweiler, L. Moss, R. F. Mozley, A. Odian, J. R. Roehrig, W. Toki, F. Villa, N. Wermes, and D. E. Wisinski, Stanford Linear Accelerator Center; D. E. Dorfan, R. Fabrizio, F. Granegagnolo, R. P. Hamilton, C. A. Heusch, L. Koepke, W. Lockman, R. Partridge, J. Perrier, H. F. Sadrozinski, T. L. Schalk, A. Seiden, and A. Weinstein, University of California at Santa Cruz; J. J. Becker, G. T. Blaylock, B. Eisenstein, G. Gladding, S. A. Plaetzer, A. L. Spadafora, J. J. Thaler, B. Tripsas, A. Wattenberg, and W. J. Wisniewski, University of Illinois, Champaign-Urbana; J. S. Brown, T. H. Burnett, V. Cook, C. Del Papa, A. L. Duncan, P. M. Mockett, A. Nappi, J. C. Sleeman, and H. J. Willutzki, University of Washington, Seattle.

2] R. H. Schindler *et al., Phys. Rev.* **D24**, 78 (1981).

3] W. Bacino *et al., Phys. Rev. Lett.* **45**, 329 (1980).

4] For a review of these measurements, see R. Klanner, *Proceedings of the XXII International Conference on High Energy Physics* (Leipzig, 1984).

5] R. Rückl, Habilitationsschrift, University of Munich (1983).

6] For a more detailed explanation of the analysis, see R. M. Baltrusaitis *et al.*, SLAC-PUB-3532, submitted to *Phys. Rev. Lett.*.

7] A. Ali, *Phys. Lett.* **65B**, 275 (1976).

8] W. Bacino *et al., Phys. Rev. Lett.* **43**, 1073 (1979);
J. M. Feller *et al., Phys. Rev. Lett.* **40**, 274 (1978).

9] G. S. Abrams *et al., Phys. Rev. Lett.* **43**, 481 (1979).

CHARMED MESON LIFETIMES FROM 20 GEV PHOTOPRODUCTION

James E. Brau
University of Tennessee
Knoxville, TN USA

(representing the SLAC Hybrid Facility Photon Collaboration)

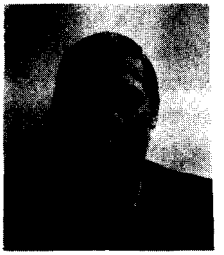

A sample of 134 events containing 159 visible multiprong charm decays has been obtained from the 20 GeV charm photoproduction experiment at the SLAC Hybrid Facility. Following a selection procedure which ensures high and uniform detection efficiency for selected events, 47 charged, 46 neutral and five topologically ambiguous decays remain. These decays yield preliminary lifetimes of

$$\tau_{D^{\pm}} = (9.2 \pm 1.5 \pm 0.5) \times 10^{-13} \text{ secs}$$

$$\tau_{D^{\circ}} = (6.1 \pm 1.1 \pm 0.4) \times 10^{-13} \text{ secs}$$

and a ratio

$$\frac{\tau_{D^{\pm}}}{\tau_{D^{\circ}}} = 1.5^{+0.6}_{-0.3} \pm 0.1$$

One fully reconstructed four-body $\bar{D}^{\circ}$ decay has a proper flight time of 55×10^{-13} seconds.

Introduction

The SLAC Hybrid Facility Photon Collaboration[1] has recently completed the scanning and preliminary analysis of 3.6 million bubble chamber pictures taken with a high resolution camera capable of detecting charmed particle decays (Experiments BC72-73 and BC75). A comparison of charged and neutral D meson lifetimes is interesting since it reveals the role of non-spectator processes in the decay (these processes being Cabibbo suppressed for the D^+ meson).[2] The absence of non-spectator processes (a simple spectator model) would predict equal charged and neutral D lifetimes.

The Experiment

The experiment was performed at the SLAC Hybrid Facility with a backward scattered laser beam incident on the 1 m hydrogen bubble chamber operated at 10-12 Hz. The beam was 3 mm in diameter, peaked at 20 GeV with a FWHM of 2 GeV, and contained an average of 25 photons per pulse. Following the bubble chamber were four sets of multiwire proportional chambers (MWPC), two atmospheric pressure Cerenkov counters, and a lead-glass wall. The Cerenkov counters (filled with Freon) separated pions from kaons and protons in the momentum range 3 GeV/c to 10.7 GeV/c during BC72/73 and from 2.6 GeV/c to 9.3 GeV/c during BC72/73. The lead glass wall measures pi zeros with a mass resolution of about 10 MeV/c. Details of the apparatus are described in Reference 1.

In order to detect charm decays near the interaction vertex, a fourth camera with high resolution optics (HRO) was used. This camera resolved 55 micron bubbles over a depth of field of ± 6 mm for BC72/73 and 40 micron bubbles over ±3mm for BC75 when a new camera employing two lenses was installed. Each lens viewed approximately one-half of the bubble chamber. The bubble chamber was operated at an elevated temperature of 27°K to give a high bubble density of 60 per cm but a slow bubble growth to allow sufficient time to trigger the camera.

The cameras were triggered on either of two conditions. The first condition was the passage through three MWPC stations of any charged particles originating in the fiducial volume of the bubble chamber. The required calculation was performed by a 168/E processor. The second trigger condition was based on the energy deposited in the lead-glass wall. With this combination, we triggered on 88 ± 6 percent of the charm cross section as indicated by untriggered data and by Monte Carlo studies.

The Data

The results presented here are based on approximatly 678,000 hadronic interactions within a useable fiducial volume. The fiducial volume has been

restricted to ensure a high and uniform detection efficiency, to ease interpretation, and to yield good momentum measurements. All hadronic events were closely examined at least twice for the decays of short-lived particles within 1 cm of the interaction vertex. For BC75 the search was extended to 1.5 cm. In order for an event to be considered a charm candidate, either the decay point had to be visible or the backward projection of one of the tracks in the event had to miss the production vertex by an impact distance of at least one track width. Only decays having two or more charged tracks are considered here. Decays consistent with strange particle hypotheses were eliminated. One hundred thirty-four events remained with one hundred fifty-nine visible multiprong charmed particle decays. Examples of events from this experiment with charmed particle decays have been published.(1)

Three cuts were imposed on all events:

1. An impact distance greater than 110 μm (2-3 track widths) was required for at least one track in each event to ensure high efficiency for finding charged and neutral decays. This defines d_{max}.
2. A second track from the same decay vertex was required to have an impact distance of at least 40 μm to select multiprong decays. This is d_2.
3. A minimum decay length cut of 600 μm was imposed to allow a clean separation of the charged and neutral decays.

We have investigated possible sources of background which would simulate charmed particle decays. These studies, based on calculations and searching for decays at distances greater than 1 cm, show that backgrounds from all sources are small compared to 1 event.

After imposing the three cuts, ninety-two events remain containing ninety-eight decays satisfying all three conditions. These included forty-six neutral (twenty-one two-prongs and twenty-five four-prongs), sixteen positive (one five-prong and one three-prong with an additional Dalitz pair), thirty-one negative (twenty-nine three-prongs and two five-prongs) and five charge/neutral ambiguous decays.

Results

The lifetime for a D meson which travels a distance ℓ and has a momentum P is

$$\tau = \frac{\ell M_D}{P\,c}$$

where M_D is the D meson mass and c is the speed of light. For the purpose of determining the lifetime of the D meson from a sample of decays we must measure the proper flight time of each decay beyond the point at which it would pass all cuts described above. We therefore replace ℓ with ℓ_{eff}, where

$$\ell_{eff} = \min\left[\left(1 - \frac{110\mu m}{d_{max}}\right)\ell,\ \left(1 - \frac{40\mu m}{d_2}\right)\ell,\ \ell - 600\ \mu m\right] .$$

In order to estimate p for all decays which pass the cuts described above we use p_{vis}, the momentum obtained from the charged tracks and m_{vis}, the visible mass obtained by assuming all charged tracks are pions. We then determine the relationship between m_{vis} and the actual visible mass, m_{vis}^{actual} by a Monte Carlo which incorporates the current best knowledge of D decay branching ratios. This study yields for decays that have missing neutrals or are Cabibbo suppressed, $\alpha = \left\langle \frac{m_{vis}^{actual}}{m_{vis}} \right\rangle = 1.10 \pm .02$ where the error indicates the uncertainty due to errors in the branching ratios. The standard deviation of α on an event to event basis is 0.13, indicating the level of uncertainty in estimating m_{vis}^{actual} from m_{vis}. The lifetime estimation is then

$$\tau_{est} = \frac{\ell_{eff}\,\alpha\, m_{vis}}{p_{vis}\, c}$$

and it is only dependent on decay model assumptions (with an uncertainty of less than two per cent) and is independent of particle momentum (and consequently production model). It is also reasonably insensitive to the specific cuts used to select data, as long as the cuts chosen ensure uniform detection efficiency as a function of length, as ours do.

The total sample of forty-seven charged and forty-six neutral decays have distributions of τ_{est} shown in Figures 1 and 2. The mean proper flight times

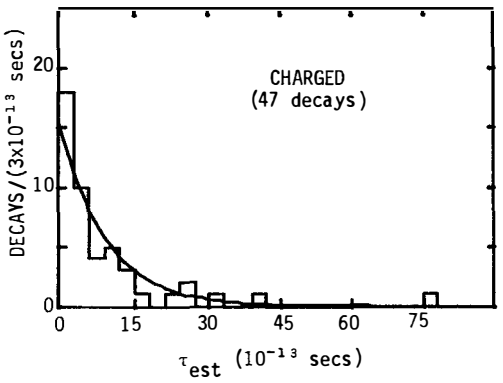

Figure 1) The τ_{est} distribution for charged decays. The curve is an exponential with lifetime of 9.1×10^{-13} seconds normalized to 46 decays.

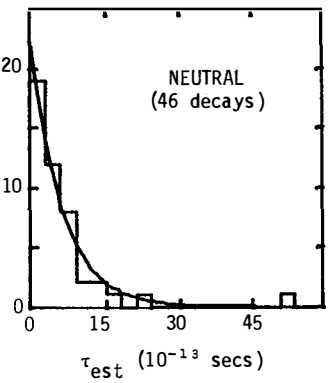

Figure 2) The τ_{est} distribution for neutral decays. The curve is for a lifetime of 6.2×10^{-13} seconds normalized to 47 decays.

are 9.1 x 10^{-13}s and 6.2 x 10^{-13}s.[3] These must be corrected for the loss of decays to the charged/neutral ambiguous sample. To estimate this effect, we have considered the 32 possible assignments of the five ambiguous decays between charged and neutral. For each event ℓ_{eff} is independent of this choice but p_{vis} and m_{vis} depend on it. The effect of the ambiguous decays is to shift our best estimates downward to 8.8 x 10^{-13}s and 6.1 x 10^{-13}s.

One additional correction is needed to convert the lifetimes to D-meson lifetimes: the contamination of Λ_c^+ and F decays within the charged decay sample must be corrected for. When this is done, we find

$$\tau_{D^\pm} = (9.2 \pm 1.5 \pm 0.5) \times 10^{-13} \text{ sec}$$

$$\tau_{D^\circ} = (6.1 \pm 1.1 \pm 0.4) \times 10^{-13} \text{ sec}$$

and the charged to neutral lifetime ratio is

$$\frac{\tau_{D^\pm}}{\tau_{D^\circ}} = 1.5^{+0.6}_{-0.3} \pm 0.1$$

This measurement of the $D^\pm$ lifetime is fully consistent with the two world average lifetimes reported in the Leipzig Conference[4] Proceedings (~9.0 ± 1.0 x 10^{-13}s), while the neutral lifetime is just over one standard deviation above the world average value of ~ (4.2 ± 0.4) x 10^{-13}s. This is not particularly alarming, but one of the neutral decays in the experiment is extremely long, highly unlikely to have emerged from a lifetime of 4.2 x 10^{-13}s. This event, shown in Figure 3, contains two charm decays, one of which is a four prong decay 9.0 mm from the production vertex. The decay is identified as $K\pi\pi\pi$, either by

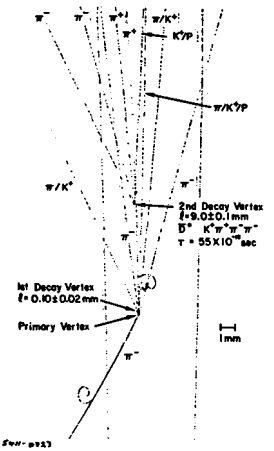

Figure 3) A photograph showing an event with a $\bar{D}^\circ$ decay after 9 mm. The proper flight time for this $D^\circ \to K^+\pi^+\pi^-\pi^-$ decay is 55 x 10^{-13}s.

information from the Cerenkov counter or ionization in the bubble chamber (although the K is ambiguous with p and the pions with e or μ). It has an effective mass of 1862 ± 8 MeV/c^2. Further details on the event are given in reference 5 where it is shown that the background sources for this event are extremely small (less than 1 in 6 x 10^7 experiments of our size). Figure 4 shows the relative probability that the event would appear in an experiment the size of ours as a function of the charm lifetime. The $D^0/\bar{D}^0$ is required to decay to $K^{\mp}\pi^{\pm}\pi^{+}\pi^{-}$ (with a 7.5% branching ratio) and to decay after 55 x 10^{-13} seconds. The probability for an experiment of our size to see a D^0 surviving 55 x 10^{-3} seconds when the D^0 lifetime is 6.1 x 10^{-13} seconds is about two percent while it would be about 3 x 10^{-4} if the D^0 lifetime were 4.2 x 10^{-13} seconds.

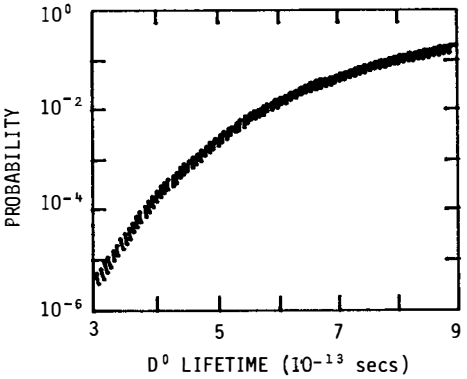

Figure 4) Probability that an experiment of this size would contain an acceptable $D^0/\bar{D}^0$ with proper flight time > 55 x 10^{-13} seconds.

References

1. K. Abe et al., "Charm Photoproduction at 20 GeV," Physical Review D30, 1 (1984).
2. N. Cabibbo and L. Maiani, Phys. Lett. 79B, 109 (1978); N. Cabibbo, G. Corbo, and L. Maiani, Nucl. Phys. B115, 93 (1979); B. Guberina et al., Phys. Lett. 89B, 111 (1979); W. Bernreuther, O. Nachtmann, and B. Stech, Z. Phys. C 4, 257 (1980); H. Fritzsch and P. Minkowski, Phys. Lett. 90B, 455 (1980); M. Bander, B. Silverman, and A. Soni, Phys. Rev. Lett. 44, 7 (1980).
3. This procedure for determining lifetimes is preferred over that used in reference 1 since it is more direct while retaining the model independence of our earlier method. The latter, based on a comparison of the parameters ℓ, ℓ_{eff}, d_{max}, and τ_{eff} to Monte Carlo events on an event by event basis, yields for the present data sample (ignoring the ambiguous decays) a charged lifetime of 8.1 ± 1.2 x 10^{-13}s and a neutral lifetime of $6.2^{+1.1}_{-0.9}$ x 10^{-13}s (statistical errors only). These numbers are well within the errors of our current method.
4. E. DiCapua, "Review of Charm Lifetime Experiments", Proceedings of the XXII International Conference on High Energy Physics, vol. I, p. 177 (1984); R. Klanner, "Weak Decays of Leptons and Quarks", Proceedings of the XXII International Conference on High Energy Physics, vol. II, p. 201 (1984).
5. K. Abe et al., "Observation of a Very Long-Lived D^0 Decay to $K^+\pi^+\pi^-\pi^-$ With a Proper Flight Time of 55 x 10^{-13} Seconds", SLAC-PUB-3493, (also RAL-84-110), October, 1984.

DECAY PROPERTIES OF D-MESONS PRODUCED IN 360 GeV/c π^-p INTERACTIONS

(LEBC-EHS Collaboration)

Presented by Peter R.S. Wright
Nuclear Physics Laboratory, Oxford University,
1 Keble Road, Oxford OX1 3RM, United Kingdom

ABSTRACT

Results are presented on lifetimes and decay branching ratios of neutral and charged D-mesons, produced in 360 GeV/c π^-p interactions.

1. DATA SAMPLE

In spring 1982 the NA27 Collaboration took ∿ 900,000 pictures using the LEBC-EHS setup, exposed to a 360 GeV/c π^- beam at the CERN SPS. The results presented here are based on the final sample of ∿ 270,000 interactions, corresponding to a sensitivity of 15.8 events/μb.

The Lexan Bubble Chamber, LEBC, filled with hydrogen, with a resolved bubble diameter of ∿ 15 μm, and a bubble density of ∿ 80 bubbles/cm, is sensitive to decay times down to ∿ 1 x 10^{-13}s. The two lever arm spectrometer, EHS, provides momentum measurement to a precision better than 1% over the whole momentum range, with very high acceptance for D-mesons produced with Feynman x > 0. Particle identification is provided by ISIS [1], and $\gamma + \pi^0$ detection is provided by two lead glass shower counters, IGD and FGD [2]. These devices also provide some electron/hadron discrimination.

All the film was scanned twice for decay vertices within ±2mm transverse to the incident beam, subjected to a physicist checkscan, and the resulting charm decay candidates measured and reconstructed. After eliminating strange particles, the charm events were remeasured on the Strasbourg HPD [3], which provides clean, high precision measurements, with a minimum detectable impact parameter of 7 μm. After this procedure the final data sample consisted of 114 events containing 197 decays; 83 events have two decays and 31 have only one. The topological classification of these decays is shown in Table 1.

TABLE 1

Topological classification of the decays

Charged Multiplicity of the decay	Neutral Decays	Charged Decays
1 ("C1")		27
2 ("V2")	86	
3 ("C3")		56
4 ("V4")	24	
5 ("C5")		4

The information from ISIS and the gamma detectors was then added and the events passed through a kinematics program.

2. LIFETIMES

In order to define a clean sample for computing lifetimes we consider only the V2, C3, V4 and C5 topologies. The C1 decays have a low reconstruction efficiency as there is always a missing neutral particle. We then make the following cuts:

3C fits are kept only if the kinematic χ^2 probability is > 0.1%.
2C, 1C fits are kept only if > 1% probable, and if there is no Cabibbo favoured 3C fit.
Cabibbo unfavoured fits are kept only if they are 3C, and there are no 3C Cabibbo favoured fits.
The particle identification probability is required to be > 1% for all tracks that have identification information.
Semileptonic fits are kept only if the electron is unique.
If there is a D/F/Λ_c ambiguity, a Cabibbo favoured D is chosen before an F or Λ_c.
Energy and charm conservation are imposed.

If the decay still has ambiguous fits, it is only accepted if all the fits are "close" i.e.:

$\Delta(x_F) < 0.1$ for all solutions
$\Delta(P_T) \leq 0.2$ GeV/c for all solutions
$\Delta(\tau) < 0.4 \times 10^{-13}$s for all solutions.

After these cuts we are left with 12 V2s, 10 C3s, 11 V4s and 2 C5s.

For each decay we compute the minimum (ℓ_{min}) and maximum (ℓ_{max}) decay length that the decay could have had and still be seen; ℓ_{min} depends on the configuration of the other tracks in the event, and ℓ_{max} on the location of the events in the chamber. A maximum likelihood fit is then performed to the decay time distribution; those decays with $t < t_{min}$ (3 V2s and 1 V4) being rejected, and the rest being weighted by their individual t_{min} and t_{max} (the times corresponding to ℓ_{min} and ℓ_{max}). The resulting lifetimes are:

$$\tau(D^\circ/\bar{D}^\circ) = 3.5^{+0.9}_{-0.7} \times 10^{-13} \text{ s} \qquad (19 \text{ decays})$$

$$\tau(D^+/D^-) = 10.1^{+5.0}_{-2.8} \times 10^{-13} \text{s} \qquad (12 \text{ decays})$$

with the corresponding ratio of the charged to the neutral lifetime being:

$$\frac{\tau(D^+/D^-)}{\tau(D^\circ/\bar{D}^\circ)} = 2.9^{+1.7}_{-0.8}$$

These results are stable with respect to any changes in the method of determining ℓ_{min}, and the selection of ambiguous fits; no systematic error is detectable.

3. SEMIELECTRONIC BRANCHING RATIOS

Starting from our sample of decays as defined in Table 1, we select only those events with unambiguous topologies. V2s with opening angle compatible with zero, and decays of uncertain charge are eliminated. This results in a sample of 56 V2s and 39 C3s, with essentially no contamination from $\gamma \to e^+e^-$ in the V2s, and no contamination from the charged into the neutral decays, or vice versa. Again, we ignore the C1s for the same reason as for the lifetime analysis. We require that all tracks from the decays enter ISIS, so that they have a chance of being identified, and for the V2s we additionally require that at least one track has a P_T of > 250 MeV/c, to eliminate any residual strange contamination. This leaves us with 43 V2s and 23 C3s.

In this sample we observe 5 V2s and 2 C3s with an e^+ or e^- identified by ISIS. In addition, 4 of the electrons also hit the IGD, where their identity is confirmed, by comparing the energy deposited to the measured momentum. We also observe that one of the V2 and both C3s have a $K\pi$ mass consistent with the decay going via a K^*_{890}.

We have computed via Monte Carlo the efficiency for identifying electrons from semielectronic D decays; for the V2s we obtain an efficiency of 85±5%, and for the C3s 78±5%. For the neutral Ds, applying all corrections, and using the topological branching ratio for $D^\circ \to$ V2 of 67±8% [4] we obtain:

$$BR(D^\circ/\bar{D}^\circ \to e^{\pm}h^{\mp}\nu) = 8.8^{+5}_{-3} \ \% \ (68\% \ CL)$$

We also have a semielectronic V4 and estimate its contribution to the total semielectronic branching ratio to be $\sim$ 1%, giving:

$$BR(D^\circ/\bar{D}^\circ \to e^{\pm}\nu + X) = O(10\%)$$

For the charged decays, using the topological branching ratio for $D^{\pm} \to C3$ of 43% [4] we obtain:

$$BR(D^+/D^- \to K^{\mp}\pi^{\pm}e^{\pm}\nu) = 4.7^{+7}_{-5} \ \% \quad (68\% \ CL)$$

As both C3s are compatible with the decay $D^{\pm} \to K^{*0}_{890}e^{\pm}\nu$ we make this assumption and hence can compute the total semielectronic branching ratio. From Clebsch-Gordon we have $K^{*0} \to K^{\pm}\pi^{\mp} = 2/3$, and from DELCO [5] we have $D^{\pm} \to Ke\nu/D^{\pm} \to K^*e\nu = 1.5\pm0.7$. Applying these corrections we obtain:

$$BR(D^+/D^- \to e^{\pm}\nu + X) = 19.2^{+20}_{-10} \ \% \quad (68\% \ CL)$$

Please note that these results are PRELIMINARY.

CONCLUSIONS

We have measured the lifetimes of the neutral and charged D-mesons in a clean manner, with no systematic bias. The results are:

$$\tau(D^\circ/\bar{D}^\circ) = 3.5^{+0.9}_{-0.7} \times 10^{-13}\text{s}$$

and $$\tau(D^+/D^-) = 10.1^{+5.0}_{-2.8} \times 10^{-13}\text{s}$$

We have also obtained preliminary measurements of the semielectronic branching ratios of the neutral and charged Ds:

$$BR(D^\circ/\bar{D}^\circ \to e^{\pm}\nu + X) = 0(10\%)$$

$$BR(D^+/D^- \to e^{\pm}\nu + X) = 19.2^{+20}_{-10} \ \%$$

REFERENCES

1) W.W.M. Allison et al., NIM 224 (1984) 396.

2) B. Powell et al., NIM 198 (1982) 217.

3) J.R. Lutz and A. Michalon, IInd Vezelay Workshops on EHS, CERN/EP/EHS/PH 80-2 (1980).

4) I. Peruzzi et al., Phys. Lett. 39 (1977) 1301.
R.H. Schindler et al., Phys. Rev. D24 (1981) 78.,
G.M. Trilling, Phys. Reports 75 (1981) 57.

5) Bacino et al., Phys. Rev. Lett. (1979) 1073.

WEAK TWO-BODY DECAYS OF HEAVY MESONS

Berthold Stech
Institut für Theoretische Physik der
Universität Heidelberg

ABSTRACT

Two-body decays of D, F and B-mesons are discussed and analysed. The factorization approximation appears to be appropriate. Information on QCD-factors, on the suppression of D^+-decay modes, and on final-state interactions is obtained.

1. Introduction. Non-leptonic weak decays are of particular interest because of the interplay of weak and strong interactions. New data on exclusive D-decays are now available from the Mark III collaboration[1]. Because the D-lifetimes[2] have been measured too, several non-leptonic transition rates are known within reasonable error limits. In this talk I will describe the theoretical expectations for two-body heavy meson decays and draw some conclusion from the data.

The influence of short and long-range QCD forces on weak amplitudes make detailed predictions of non-leptonic decays notoriously difficult. For example, the $|\Delta\vec{I}| = 1/2$ enhancement in strange particle decays has never been understood in a satisfactory way. However, for energetic two-body decays of heavy mesons (D, F, B, ...) the situation is simpler[3-5]. It appears to be possible to replace in the effective quark Hamiltonian the product of quark currents by the normal-ordered product of the corresponding hadron currents formed by the physical hadrons involved[6]. I will use here this factorization approximation[7,8] as a working hypothesis. I expect it to be a reasonable approximation in cases where the final mesons are fast and their final-state interaction is a purely on-mass-shell hadron scattering effect[F1]. The following discussion is based on the paper by Fakirov and the author[4] where factorization was used for detailed predictions of F and D-decays and follows closely a recent letter by M. Bauer and the author[6].

2. The hadron currents. For semi-leptonic and non-leptonic exclusive transitions it is necessary to express the colour singlet quark currents in terms of the hadron fields which participate in the decay process. We denote these hadron currents by an index H on the quark currents $(\bar{u}d)_H$, $(\bar{s}c)_H$, $(\bar{s}d)_H$, etc.. The explicit form (in general non-local because of formfactors) can be obtained from one, two, .. particle matrix elements of the quark currents. The one-particle part of $(\bar{u}d)_H$ is, for example

$$i\, f_\pi\, \partial_\mu\, \pi^- + f_\rho\, m_\rho^2\, \rho_\mu^- + \ldots \qquad (1)$$

$(f_\pi \cong 133$ MeV, $f_\rho\, m_\rho \cong 221$ MeV).

The two particle matrix elements of currents containing heavy quarks are not yet known well enough. I determined them using two assumptions:

1. The values at $q^2 = 0$ are obtained by taking the space integrals of the time and space components of the quark currents as generators of a collinear algebra at infinite momentum[9,10].
2. The q^2-dependence is obtained from nearest pole dominance and asymptotic current conservation in the $q^2 \to \infty$ limit. As an example I give the result for the $(\bar{s}c)$ current:

$$\langle K|(\bar{s}c)_\mu|D\rangle \cong (K_\mu + D_\mu - \frac{m_D^2 - m_K^2}{q^2} q_\mu) \frac{1}{1-q^2/m^2_{F(1^-)}} + \frac{m_D^2 - m_K^2}{q^2} q_\mu \frac{1}{1-q^2/m^2_{F(0^+)}} \quad (2)$$

and

$$\langle K^*|(\bar{s}c)_\mu|D\rangle \cong \frac{2}{m_D + m_{K^*}} \varepsilon_{\mu\nu\rho\sigma} \overset{*}{\varepsilon}{}^\nu \overset{*}{K}{}^\rho D^\sigma \frac{1}{1-q^2/m^2_{F(1^-)}} +$$

$$+i \left\{ \overset{*}{\varepsilon}_\mu (m_D + m_{K^*}) - \frac{\overset{*}{\varepsilon}\cdot D}{m_D + m_{K^*}} (D_\mu + K^*_\mu) - \frac{\overset{*}{\varepsilon}\cdot D}{q^2} 2m_{K^*} q_\mu \right\} \frac{1}{1-q^2/m^2_{F(1^+)}}$$

$$+ 2m_{K^*} i \frac{\overset{*}{\varepsilon}\cdot D}{q^2} q_\mu \frac{1}{1-q^2/m^2_{F(0^-)}} \quad (3)$$

The leading power in the infinite particle momentum fixes the scale factor of the time component in (2) (3)[F2]. The next-to-leading power determines[F3] (less reliably) the relative strengths of the first three covariants in (3). The longitudinal terms follow from the requirement for the cancellation of the $q^2 = 0$ poles. In the same approach the formfactors for $D \to \kappa(0^+)$ and $D \to K_A(1^+)$ vanish at $q^2 = 0$. Of course, the complete overlap of heavy and light meson wave functions at infinite momentum implied by (2) and (3) is not likely. A reduction factor $h \leq 1$ which depends on the initial and final particle should be introduced. Furthermore, the simple pole-type formfactors needed here in the time-like region can at most be used for small q^2. It is highly desirable to test and improve the formulae of the type (2) and (3) in semi-leptonic decays of D, F, and B-mesons and to determine the overlap factors h (in particular $h(D \to K)$ and $h(D \to K^*)$).

3. The effective Hamiltonian. For non-leptonic charm decays the hard-gluon corrected quark Hamiltonian is[11,12]

$$H_W = \frac{G}{\sqrt{2}} \left\{ c_1(\mu)\ (\bar{u}d')\cdot(\bar{s}'c) + c_2(\mu)\ (\bar{s}'d')\cdot(\bar{u}c) \right\} \qquad (4)$$

In this expression $d' = \cos\theta\ d + \sin\theta\ s$, $s' = \cos\theta\ s - \sin\theta\ d$ where θ denotes the Cabbibo angle[F4]. $c_1(\mu)$ and $c_2(\mu)$ are related to the QCD short-distance coefficients $c_+(\mu)$ and $c_-(\mu)$, $c_+(\mu) \cong (c_-(\mu))^{-1/2}$ by $c_1(\mu) = 1/2\ (c_+ + c_-)$, $c_2(\mu) = 1/2(c_+ - c_-)$.

According to the working hypothesis mentioned in the introduction the colour singlet V-A currents will now be replaced by V-A hadron currents giving an effective Hamiltonian[6]

$$H_{eff} = \frac{G}{\sqrt{2}} : \left\{ a_1(\bar{u}d')_H\cdot(\bar{s}'c)_H + a_2(\bar{s}'d')_H\cdot(\bar{u}c)_H \right\} : \qquad (5)$$

The normal ordered current product describes in fact a non-local interaction because of the (pole-type) formfactor dependence of the hadron currents. In (5) quark and colour exchange effects are absorbed into the real coefficients (by T-invariance) a_1 and a_2. The relation between a_1, a_2 and the scale-dependent coefficients $c_1(\mu)$, $c_2(\mu)$ may be quite involved. However, if factorization is a good approximation at a specific energy scale μ one finds

$$a_1 = c_1(\mu) + \xi\, c_2(\mu) \qquad a_2 = c_2(\mu) + \xi\, c_1(\mu) \qquad (6)$$

The quantity ξ introduced here arises from Fierz-reordering of the quark current product in (4) before saturation. From colour matching one expects $\xi = 1/3$. In the following, however, a_1 and a_2 are treated as parameters and the comparison with (6) is postponed to section 6.

4. The decay amplitudes. With the hadron currents given in section 2 it is now easy to compute two-body decay amplitudes. For the moment the final-state interaction between the outgoing mesons is neglected. It is of advantage to distinguish three classes of decays. Decays governed by a_1 only, like $D^0 \to K^-\pi^+$ or the Cabbibo-suppressed decay $D^+ \to \bar{K}^0 K^+$, are called class I transitions. Decays governed

by a_2 only, like $D^o \to \pi^o \bar{K}^o$ or the Cabibbo-suppressed decay $D^+ \to \pi^+\phi$, are called class II. In the 3rd class are those decays, like $D^+ \to \bar{K}^o \pi^+$ or the Cabibbo-suppressed decay $F^+ \to \phi K^+$, which involve a_1 and a_2. Here the amplitudes are proportional to $a_1 + xa_2$ where x varies from process to process[4]. F5 For Cabibbo-allowed transitions $D^+ \to PP$ where the final mesons belong to the same SU3 multiplet one has $x = +1$ in the SU3 symmetry limit. $x = +1$ also holds for Cabibbo-allowed $D^+ \to PV$ transitions to members of the same collinear $SU_W(6)$ multiplet in the limit of perfect $SU_W(6)$ symmetry[4,5]. F6 Consequently, in these Cabibbo-allowed D^+-decays, an interference of two amplitudes occurs. From eq. (6) one expects $a_2/a_1 < 0$ and thus a destructive interference. These D^+-decay amplitudes are therefore very sensitive to the precise values of x which differ from 1 due to the deviation of the decay constants and form-factors from the symmetry limit. The transition $D^+ \to \bar{K}^o A_1^+$, on the other hand, is a pure class I transition and should have a large branching ratio.

The charm changing currents in (5) can turn the D or F into a final meson and, in some instances, annihilate the heavy meson. The annihilation process will be neglected here since the corresponding amplitudes are proportional to the divergence of asymptotically conserved light meson currents at $q^2 = m_D^2$ and are thus quite small. The annihilation process could, of course, be important in many-body decays or in less energetic two-body decays.

In table 1 the theoretical predictions for the widths of some important partial decay modes are displayed. They are obtained from the effective Hamiltonian using currents of the form (1) to (3). Note that final-state interactions have not yet been considered and all overlap factors h (see section 2) are boldly set equal to one.

As a first test of the effective Hamiltonian one can form the ratios of the calculated rates, separately for class I and class II transitions and compare them with the corresponding Mark III data. The agreement is good which is encouraging[6,14]. The measured ratio between class II and class I transitions then gives the additional important information: $|a_2/a_1| \approx 0.6$. Finally, a short view on the experimental rates for class III transitions shows that $a_2/a_1 < 0$ as expected. The result, $a_2/a_1 \approx -0.6$, demonstrates some interesting enhancement of the SU(3) sextet part of the non-leptonic Hamiltonian[15]. This enhancement is, however, not as dramatic as octet enhancement in strange particle decays.

The absolute values of a_1 and a_2 cannot be determined very well because of the errors in the D-lifetime and D-production cross section. Without any correction for final state interaction one finds from class I and class II transitions

$$a_1 \cong 0.9 \qquad a_2 \cong -0.6 \tag{7}$$

with an error in scale of about 15 %.

5. Final-state interaction. Final-state interactions can seriously affect the decay process[16]. The amplitude for the decay to a state of given isospin will be modified in modulus and phase. In the $D \to \bar{K}\pi$ case (and less certain in $D \to \bar{K}\rho$ decays)the relative phase ϕ between the I = 1/2 and I = 3/2 amplitude can be directly extracted from the Mark III data. An isospin analysis gives :

$$\begin{aligned} A(D^0 \to K^-\pi^+) &= \frac{1}{\sqrt{3}}(A_{3/2} + \sqrt{2}\,A_{1/2}) \\ A(D^0 \to \bar{K}^0\pi^0) &= \frac{1}{\sqrt{3}}(\sqrt{2}\,A_{3/2} - A_{1/2}) \\ A(D^+ \to \bar{K}^0\pi^+) &= \sqrt{3}\,A_{3/2} \end{aligned} \tag{8}$$

Squaring these expressions and using the Mark III and lifetime data[1,2]one finds $\phi \approx 80^0$. The final-state interaction will in addition also change the modulus of the isospin amplitudes. For the exotic I = 3/2 channel in $\bar{K}\pi$ final states, no change in modulus is expected. In the I = 1/2 channel, however, strong absorption occurs[17]. A reduction of the unperturbed I = 1/2 amplitude by $\approx$ 20 % seems plausible in this case[F7]. Using now table 1 for Cabibbo-allowed D^+-transitions, too, one obtains improved values for a_1 and a_2, namely

$$a_1 \cong 1.1 \text{ to } 1.2, \qquad a_2 \cong -0.5 \text{ to } -0.6 \tag{9}$$

instead of (7). The larger value of a_1 compensates the absorption.

An independent check on these values is obtainable from transitions where final-state interactions are likely to be negligible. Good examples are the decays $F^+ \to \phi\,\pi^+$ (for a_1) and $D^+ \to \phi\,\pi^+$ (for a_2). The measured decay rates[18,1] agree for both of these decays with the prediction for a_1 and a_2 as given in (9). Smaller experi-

mental error limits on these decays are urgently needed, however.

6. Comparison with short-distance QCD factors. In spite of the uncertainties as to the precise values of a_1 and a_2, it is tempting to compare them with the QCD prediction using (6). The value obtained for a_1 and the relative sign of a_2/a_1 agree with the expectation from QCD. The fitted ratio $|a_2/a_1|$, on the other hand, is much larger than expected from (6) for $\xi = 1/3$. Our results suggest instead to use ξ as a parameter with a value close to zero. ξ parametrizes the contribution of Fierz-transformed current products.[21] $\xi = 0$ implies that quarks associated with different colour singlet currents do not combine to form a single meson. Indeed, the saturation of a Fierz-transformed interaction composed of coloured currents is a doubtful procedure.[F8] $\xi \cong 0$ is not so surprising.

7. More about D- and F-decays. With the method presented here much more two-body decay widths than given in the table can and have been calculated[19]. Certainly, the estimate of transitions to a pair of relatively massive particles, for example $D \to K^* \omega$, is somewhat doubtful because of the limited energy release and the unknown effect of final-state interaction. Nevertheless, for an orientation it is instructive to sum up all of the theoretical two-body partial widths separately for D^0, D^+ and F-decays and to compare them with the corresponding total widths. It turns out that the two-body decay modes provide, together with the experimentally determined[1] semi-leptonic widths, for roughly $\approx$ 80 % of the branching ratios in each case. Remarkably, the ratio of summed-up non-leptonic transition rates of D^0 versus D^+ is about ≈ 3! The simple reason is that the main D^+-rates are proportional to $(a_1 + xa_2)^2$ giving the destructive interference noted before. This does not happen in allowed D^0 or F^+-decays. No annihilation contribution was used for this estimate. Thus, at least a sizeable part of the D^0-D^+ lifetime difference arises from two-body decay channels.

8. B-decays. The predictions for some important B-decay channels are displayed in the table. The decay widths are proportional to $|V_{cb}|^2$, the square of the b $\to$ c Kobayashi-Maskawa matrix element scaled here to $(0.05)^2$. The coefficient $a_1^{(b)}$ is expected to differ not much from $a_1^{(c)}$ since, according to (6), this coefficient is insensitive to the values of ξ between 1/3 and 0. Indeed, with

$a_1 = 1.2$, $|V_{cb}| = 0.05$ and $\tau_{B^-} \cong 1.5 \times 10^{-12}$ sec one obtains $BR(B^0 \to D^+\pi^-) \cong BR(B^0 \to D^{*+}\pi^-) \cong 2\,\%$, compatible with the Cleo results[20]. The magnitude and sign of $a_2^{(b)}$ cannot really be predicted apart from the inequality $|a_2^{(b)}| < |a_2^{(c)}|$. The decay mode $B^0 \to \bar{K}^0\, J/\psi$ could provide us with the necessary information. Of great interest are also those class II transitions in which a D^0-meson is directly generated by the charm carrying weak current. The quantity $\hat{a}_2 = f_D/f_K\, a_2$ introduced in the table describes these decays, with f_D denoting the D-decay constant. Interference of a_1 with $\hat{a}_2$ will occur in some B^--decays providing a possibility to obtain the sign of $a_2^{(b)}/a_1^{(b)}$ and to further check the theoretical scheme. As in the case of D-decays, the relative phase of I = 1/2 and I = 3/2 decay amplitudes can also be obtained from these measurements.

9. Conclusions. A factorized form of the weak Hamiltonian predicts two-body decay rates of heavy mesons being in good agreement with the Mark III data. This holds for Cabibbo-suppressed as well as for Cabibbo-allowed transitions. Apart from corrections for final-state interactions, two parameters related to QCD short-distance coefficients are needed and have been determined for charm decays. For each of the three mesons D^+, D^0, and F^+ the widths of the two-body hadronic channels and of the semi-leptonic mode[1] then sum up to $\approx 80\,\%$ of the total width. A destructive interference in important two-body D^+-decays is at least partly responsible for the longer lifetime of this meson. For more quantitative tests better data are urgently needed, especially the rates for decays to a single isospin state where little final-state interaction effects are expected. Decays of the B-mesons, besides giving very important information about QCD-factors, can be used to obtain the so far unknown fundamental D and F-decay constants.

It is a pleasure to thank M. Bauer for his cooperation and valuable help in the calculations and J. Björken for very stimulating remarks.

Table 1: Example of Theoretical Decay Widths of Heavy Mesons

Widths in 10^{10} sec^{-1} $a_{1,2} = a^{(c)}_{1,2}$		Widths in $\lvert V_{cb}/0.05\rvert^2$ 10^{10} sec^{-1} $a_{1,2} = a^{(b)}_{1,2}$ $\hat{a}_1 = (f_F/f_K)a_1$ $\hat{a}_2 = (f_D/f_K)a_2$	
$D^0 \to K^-\pi^+$	$17.1\ a_1^2$	$B^0 \to \bar{D}^+\pi^-$	$0.84\ a_1^2$
$D^0 \to K^-\rho^+$	$33.8\ a_1^2$	$B^0 \to D^+\rho^-$	$2.24\ a_1^2$
$F^+ \to \phi\ \pi^+$	$9.4\ a_1^2$	$B^0 \to D^{+*}\pi^-$	$0.79\ a_1^2$
$D^+ \to \bar{K}^0K^+$	$1.3\ a_1^2$	$B^0 \to D^{+*}F^-$	$0.84\ \hat{a}_1^2$
$D^0 \to \pi^0\bar{K}^0$	$16.0\ a_2^2$	$B^0 \to \bar{K}^0\ J/\psi$	$6.0\ a_2^2$
$D^0 \to \rho^0\bar{K}^0$	$7.6\ a_2^2$	$B^0 \to \pi^0D^0$	$1.04\ \hat{a}_2^2$
$D^+ \to \pi^+\phi$	$2.0\ a_2^2$	$B^0 \to \pi^0D^{*0}$	$1.46\ \hat{a}_2^2$
$F^+ \to K^+\omega$	$1.1\ a_2^2$	$B^0 \to \rho^0D^0$	$0.76\ \hat{a}_2^2$
$D^+ \to \bar{K}^0\pi^+$	$17.1\ (a_1+1.37a_2)^2$	$B^- \to D^0\pi^-$	$0.84\ (a_1+1.56\hat{a}_2)^2$
$D^+ \to \bar{K}^0\rho^+$	$34.1\ (a_1+0.69a_2)^2$	$B^- \to D^0\rho^-$	$2.24\ (a_1+0.83\hat{a}_2)^2$
$F^+ \to \phi K^+$	$0.6\ (a_1+1.72a_2)^2$	$B^- \to D^{*0}\pi^-$	$0.79\ (a_1+1.92\hat{a}_2)^2$

Pole-type formfactors are used for the hadron currents. Final-state interactions are not included. Factors h (see section 2) are set equal to 1.

Footnotes

F1 Even in strange particle decays factorization gives qualitatively acceptable results for $|\Delta I| = 3/2$ transitions[8].

F2 This gives already sufficient information for the evaluation of the non-leptonic decay amplitudes to PP and PV states given in table 1.

F3 In this determination I used constituent quark masses and scaled quark momenta ($p_c = p\, m_c/(m_c+m_u)$ etc.) in the $p \to \infty$. limit.

F4 With regard to generation mixing only the Cabibbo angle is of importance in charm decays since the cosine of the remaining mixing angles are very close to one.

F5 In table 3 of ref. 4 the combination $c_1+\tilde{x}c_2$ and $\xi=1/3$ is used. The connection with x is $x=(3\tilde{x}-1)/(3-\tilde{x})$.

F6 A statement to the contrary in ref. 13 is incorrect.

F7 Eq. (6) of ref. 6 suggests a corresponding suppression. A two-channel black sphere scattering gives a factor $1/\sqrt{2}$ for $|(S^{1/2})_{el}|$.

F8 I am indebted to R. Rückl for a discussion on this point.

References

1) R. H. Schindler, Mark III Collaboration, Proceedings XXIInd International Conference on High Energy Physics, Leipzig July 1984, V1, p. 171;
J. Hauser, Proceedings XXth Rencontre de Moriond, La Plagne Jan. 1985.
2)* R. Klanner, Proceedings XXIInd International Conference on High Energy Physics, Leipzig July 1984, V2, p. 201.
3) M. K. Gaillard, B. W. Lee, and J. L. Rosner, Rev. Mod. Phys. 47 (1975) 277;
J. Ellis, M. K. Gaillard, and D. V. Nanopoulos, Nucl. Phys. B100 (1975) 313.
4) D. Fakirov and B. Stech, Nucl. Phys. B133 (1978) 315.
5) N. Cabibbo, L. Maiani, Phys. Lett. 73B (1978) 418.
6) M. Bauer and B. Stech, Phys. Lett. 152B (1985) 380.
7) R. P. Feynman, in: Symmetries in Elementary Particle Physics, ed. Zichichi, Academic Press, N.Y. 1965, p. 167.
8) O. Haan and B. Stech, Nucl. Phys. B22 (1970) 448.
9) see e.g. V. de Alfaro, S. Fubini, G. Furlan, and C. Rosetti, Currents in Hadron Physics, North Holland 1973.
10) For a different approach see A. Ali, Z. Physik C1 (1979) 25, and literature quoted there.
11) M. K. Gaillard and B. W. Lee, Phys. Rev. Lett. 33 (1974) 108;
G. Altarelli, L. Maiani, Phys. Lett. 52B (1974) 351;
G. Altarelli, G. Corci, G. Martinelli, R. Petrarca, Nucl. Phys. B187 (1981) 461.
12) For a recent review on heavy flavour decay see:
R. Rückl, CERN preprint 1984.
13) I. I. Bigi, Z. Physik C 6 (1980) 83.

14) R. Rückl. Proceedings XXIInd International Conference on High Energy Physics, July 1984, V1, p. 135.
15) B. Guberina, S. Nussinov, R. D. Peccei, and R. Rückl, Phys. Lett. 89B (1979) 111.
16) H. J. Lipkin, Phys. Rev. Lett. 90B (1980) 710.
17) P. Estabrookds et al., Nucl. Phys. B133 (1978) 490.
18) K. R. Schubert, Proceedings XXth Rencontre de Moriond, La Plagne Jan. 1985.
19) M. Bauer and B. Stech, paper in preparation.
20) Th. Gentile, Cleo Collaboration, Proceedings XXth Rencontre de Moriond, La Plagne Jan. 1985.

* G. de Rijk (ACCMORE), P. Wright (EHS), J. Brau (SLAC HYBRID), Proceedings XXth Rencontre de Moriond, La Plagne Jan. 1985.

21) A parameter ε similar to ξ was introduced by N. Deshpande, M. Gronau and D. Sutherland in Phys. Lett. 90B (1980) 431. ε describes a complex amplitude ratio, however, while ξ as defined in (6) is a real number.

B meson Decays: Recent Results from CLEO

T. Gentile
Department of Physics and Astronomy
University of Rochester
Rochester, New York 14627
U.S.A.

Abstract

The properties of B decays are briefly reviewed. The CLEO results on the exclusive B decay modes are presented and the results of a new search for b→u 2-body transitions is reported. A novel technique for "partial" B reconstruction is presented, yielding rates for the decay modes of the form $\bar{B}^0 \to D^{*+}X^-$, where X is π, ρ, or F. The CLEO results on the ratio of the charged and neutral B lifetimes and the B^0-$\bar{B}^0$ mixing limit are also presented. Finally, future prospects with an enlarged data set are outlined.

Brief Review of Early Results: Most of what is known of B mesons has been learned through the study of the decays of the $\Upsilon(4S)$ meson. The $\Upsilon(4S)$, produced as a resonance in e^+e^- annihilation, is the first $b\bar{b}$ bound state which is above threshold for production of mesons with net beauty. The CLEO data set on which the following is based consists of 40.6 pb^{-1} of integrated luminosity taken on the $\Upsilon(4S)$ and 17.3 pb^{-1} taken on the continuum immediately below the $\Upsilon(4S)$. The data were taken at the Cornell Electron Storage Ring (CESR).

The examination of the leptons coming from $\Upsilon(4S)$ decays has been especially fruitful. In particular, the yield of prompt leptons provided the first evidence that the decay products of the $\Upsilon(4S)$, B mesons, carried a new flavor and were weakly decaying[1,2] CLEO has measured the average leptonic branching fractions[3] for B mesons to be: $Br(B\to e\nu X) = .120 \pm .007 \pm .004$ and $Br(B\to\mu\nu X) = .108 \pm .006 \pm .010$ where the first errors quoted are statistical and the second errors are systematic. A search for dilepton events of the form $B\to\ell^+\ell^-X$ yielded an upper limit for flavor changing neutral current decays of less than .31% at the 90% C.L.[4] The semileptonic charged multiplicity was measured to be $3.8 \pm .4$[5] Of more significance than the simple counting of leptons observed, however, are the shapes and endpoints of the lepton momentum spectra. Figure 1 shows the electron momentum spectrum observed in $\Upsilon(4S)$ decays. Studies of this spectrum have shown that the hadronic recoil mass in the decay $B\to e\nu X$ is approximately 2 GeV/c. The shapes and the endpoints of the lepton spectra imply that the ratio of $b\to u$ transitions to $b\to c$ transitions is $< 4\%$ at the 90% C.L.[6] It seems therefore an excellent approximation to assume that every b decay produces a charmed particle. The electron momentum spectrum is consistent with a hadronic system composed of 50% D and 50% D^* mesons. Using the measured semileptonic charged multiplicities of the D mesons, the calculated charged multiplicity resulting from such a mixture would be 2.52 which suggests that there is little, if any, additional fragmentation of the daughter c quark and the spectator anti-quark. Figure 2a schematically depicts the spectator decay of a B meson in which the

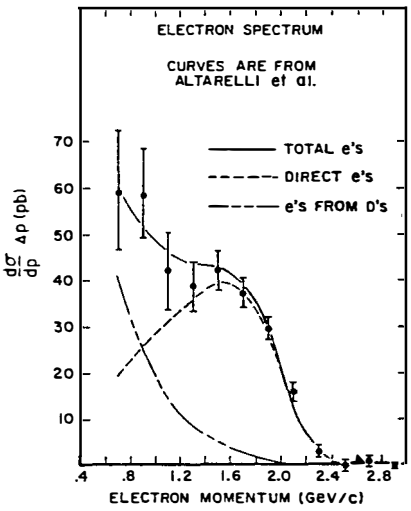

Fig. 1. Electron momentum spectrum from $\Upsilon(4S)$ decays.

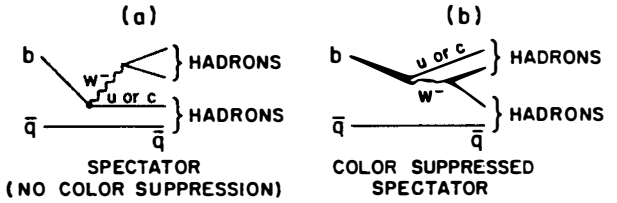

Fig. 2. Spectator decays of B mesons.

virtual W boson decay products form hadrons independent of the c quark and spectator anti-quark. Figure 2b shows a spectator decay in which one of the decay products of the W boson has the appropriate color to form a color-singlet hadron with the daughter c quark. This process is called "color-mixing". A simple argument involving the probability of producing the appropriate color anti-quark which forms a color-singlet with the daughter c quark suggests that this latter process is expected to be suppressed by approximately 1/9. Phase space calculations give a rate for $W^- \to \bar{c}s$ of ~ 15%. A search for decays of the form $B \to \psi X$ yields an upper limit for this process to be less than 1.6% at the 90% C.L.[7] in good agreement with theoretical expectations.

Figure 3 shows the observed momentum spectra of charged D^*'s and neutral D's coming from B decay. The dashed curve is a simple phase space distribution and the solid curve is obtained by using a V-A weak decay matrix element for the process $b \to ce\nu$ in which the b quark has been given the mass of the B meson and the c quark has been given the mass of the D meson. The similarity in shape between the observed momentum spectra and the $b \to ce\nu$ curve suggest that the fragmentation of the decay products of the virtual W boson emitted by the decaying b quark is nearly independent of the fragmentation of the daughter c quark and the spectator anti-quark. In summary, b decay seems well described by the spectator model with no "color mixing"; i.e. the b decays via V-A matrix element to a c quark with emmission of a virtual W boson.

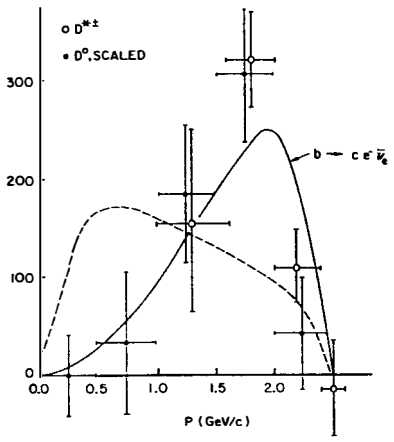

Fig. 3. D^*, D° momentum spectra.

Full B Reconstruction: Full reconstruction[7,8] of B mesons requires the detection and correct identification of all of the decay products. This is very difficult because B mesons resulting from $\Upsilon(4S)$ decays are nearly at rest in the laboratory frame ($\beta \sim .08$) producing a nearly isotropic decay. With a mean charged multiplicity in $B\bar{B}$ events of ~ 11, the combinatorial problem of correctly choosing and identifying the right set of particles corresponding to the correct B meson decay is quite formidable. The situation becomes worse when actual acceptances and efficiencies are folded in. The most viable strategy for reconstruction of B mesons with CLEO data is to search for low multiplicity decays in which a charmed particle can be reconstructed, e.g. $B^- \to D^0\pi^- \to (K^-\pi^+)\pi^-$ or $\bar{B}^0 \to D^{*+}\pi^- \to (D^0\pi^+)\pi^-$. The data were cut on the ratio of Fox-Wolfram moments[9] $H_2/H_0 = R_2 < .3$ in order to reduce the 2-jet continuum background. D^0's were made by combining identified kaons with oppositely charged tracks and required to have a momentum between 1 and 2.6 GeV/c, the kinematic maximum. Since the D^0 momentum is fairly hard, the directions of its decay products are correlated with its line of flight. A cut of $|\cos\theta| < .8$ was made for the angle of the D^0 daughter π with respect to the direction of the $K\pi$ system. For $K\pi$ combinations with a mass of 1865 ± 40 MeV/c^2, D^*'s were reconstructed by computing the $K\pi\pi - K\pi$ mass difference, which is known to be 145.4 MeV/c^2 for the decay $D^{*+} \to D^0\pi^+$. An overall energy constraint of $m_B^2 = E_{beam}^2 + (\Sigma_i \vec{p}_i)^2$ was imposed and the 4-momenta of D^0 and D^* candidates were constrained to have the correct invariant mass. Figure 4 shows the reconstruction results for events satisfying a χ^2 cut. Background estimates were made by performing the same analysis on continuum data taken below the $\Upsilon(4S)$ (no signal was observed) and by displacing the $K\pi$ mass cut ± 200 MeV/c^2 from the correct D^0 mass (known as the D^0 sidebands). The branching fractions were computed under the assumption that the $\bar{B}^0$-B^- mass difference is Eichten's[10] theoretical value of 4.4 MeV/c^2, yielding $Br(\Upsilon(4S) \to B^0\bar{B}^0) = .40$ and $Br(\Upsilon(4S) \to B^+B^-) = .60$. The results are listed in Table I.

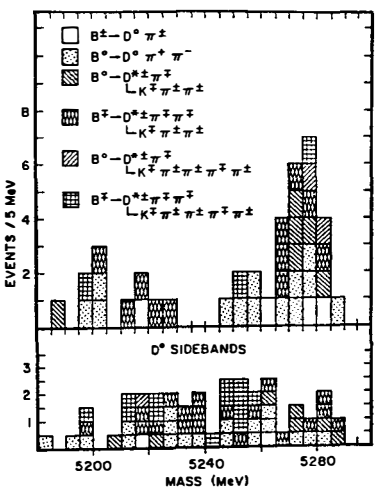

Fig. 4. B reconstruction results.

Knowledge of the B meson masses enables a precision search[7] for b→u 2-body decays such as $\bar{B}^0 \to \pi^+\pi^-$ and $B^- \to \rho^0\pi^-$.

Table I

$\langle B \rangle = 5273.0 \pm 1.3 \pm 2.0$ MeV/c^2	$B^- \to D^0 \pi^-$ = (4.2 ± 4.2)%
$B^- = 5271.2 \pm 2.2 \pm 2.0$	$\bar{B}^0 \to D^0 \pi^+ \pi^-$ = (13.0 ± 9.0)%
$\bar{B}^0 = 5275.2 \pm 1.9 \pm 2.0$	$\bar{B}^0 \to D^{*+} \pi^-$ = (2.6 ± 1.9)%
$\bar{B}^0 - B^- = 4.0 \pm 2.7 \pm 2.0$	$B^- \to D^{*+} \pi^- \pi^+$ = (4.8 ± 3.0)%

For both cases a cut was made which required the reconstructed system to be near the known beam energy within some limit: for the $\bar{B}^0 \to \pi^+ \pi^-$ case this limit was 300 MeV and for the case of $B^- \to \rho^0 \pi^-$ it was 250 MeV. A ρ^0 was defined as any $\pi^+ \pi^-$ combination with invariant mass between .5 and 1 GeV. As before, the energy of the reconstructed B meson was constrained to have the beam energy. The topology of these two-body decays is quite specific. They must have two high momentum particles with invariant mass near the beam energy and yet the sum of their momenta must be relatively small: ~ 400 MeV/c. This means that they must be energetic and nearly oppositely directed in the laboratory frame, appearing much like 2-jet continuum events. The continuum background can be greatly reduced by computing the jet axis of the event without the particles comprising the B candidate. In a true $B^0\bar{B}^0$ event the other B decay should be nearly isotropic and there should be no correlation between the computed jet axis and the direction of the other B's daughter particles. However, in a 2-jet continuum event the direction of the high momentum particles, which would normally make promising B candidates, is highly correlated with the jet axis. This point is illustrated in Figure 5. In order to reduce this background, events were rejected if at least one of the high momentum particles has $|\cos\theta| > .8$ with respect to the jet axis. For the $B^- \to \rho^0 \pi^-$ case, an additional requirement was made on the polarization of the ρ^0. CLEO finds upper limits of $Br(\bar{B}^0 \to \pi^+ \pi^-) < 0.05\%$ and $Br(B^- \to \rho^0 \pi^-) < 0.06\%$ at the 90% C.L. Since the method used here is not sensitive to the mass of the final-state particles, the lepton identification capabilities of the CLEO detector can be used to set limits on processes of the form $\bar{B}^0 \to \ell^+ \ell^-$. Upper limits for these processes are $Br(\bar{B}^0 \to e^+ e^-) < 0.03\%$, $Br(\bar{B}^0 \to \mu^+ \mu^-) < 0.02\%$, and $Br(\bar{B}^0 \to e^\pm \mu^\mp) < 0.03\%$ at the 90% C.L.[7]

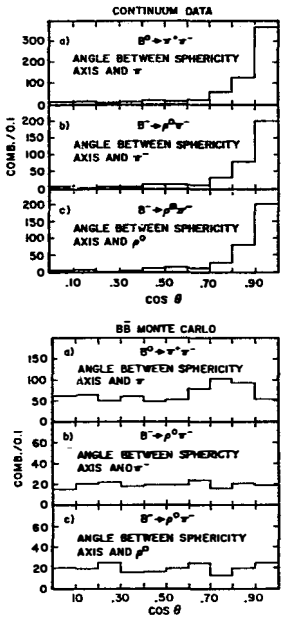

Fig. 5

Partial B Reconstruction: As evidenced in the preceeding section, full B meson reconstruction is a difficult task. From a data sample of approximately 80,000 B decays, CLEO has only been able to fully reconstruct about 25. In this section, a novel technique of "partial" B reconstruction[7] is outlined which yields measures of the branching fractions for processes of the form $\bar{B}^0 \to D^{*+} X^- \to (D^0 \pi^+) X^-$, where X can be π, ρ, or F.

The word "partial" in this case refers to the fact that the D^0 is not directly observed. To illustrate the technique, consider the decay $\bar{B}^0 \to D^{*+} \pi^-$ The objective here will be to maximally exploit the particular kinematics of this decay in order to obtain an improved signal-to-background ratio. As mentioned previously, the B mesons produced in the decay of the $\Upsilon(4S)$ are moving very slowly ($\beta \sim .08$); therefore 2-body decays of the B meson have nearly monoenergetic spectra in the laboratory frame. In particular, the π^- momentum is constrained to lie between 2 and 2.6 GeV/c. The $D^{*+} \to D^0 \pi^+$ decay has a Q value of only 145 MeV. This means that the π^+ is very soft, less than 250 MeV/c in the laboratory frame, and that it essentially retains the D^{*+} direction. Simple energy conservation gives $E_{D^0} = (E_{beam} - E_{\pi^-} - E_{\pi^+})$. This allows the calculation of the magnitude of the D^0 momentum. The angle between the D^0 and the π^+ is given by $\cos\theta = (m_{D^0}^2 + m_{\pi^+}^2 + 2E_{D^0}E_{\pi^+} - m_{D^{*+}}^2)/(2|\vec{p}_{D^0}||\vec{p}_{\pi^+}|)$. The D^0 is thus constrained to lie on a cone around the soft π^+. The only unknown left in the problem is the angle between the D^{*+} and the π^-. This angle is chosen to maximize the reconstructed B (pseudo)mass. For a genuine $\bar{B}^0$ decay there will be an angle which yields a reconstructed $\bar{B}^0$ mass within 14 MeV of the beam energy, however this will not be possible for the bulk of the fake combinations. As seen in Figure 6, Monte Carlo studies of $B^0\bar{B}^0$ events show that this technique yields a pseudomass for the B meson which peaks between the true B mass and the beam energy. The background from 3-body decays such as $\bar{B}^0 \to D^{*+} e^- \nu$ was eliminated by requiring that the hard pion from the B decay have momentum > 2.3 GeV/c. The continuum background was reduced by requiring $R_2 < .5$. The shape of the background can

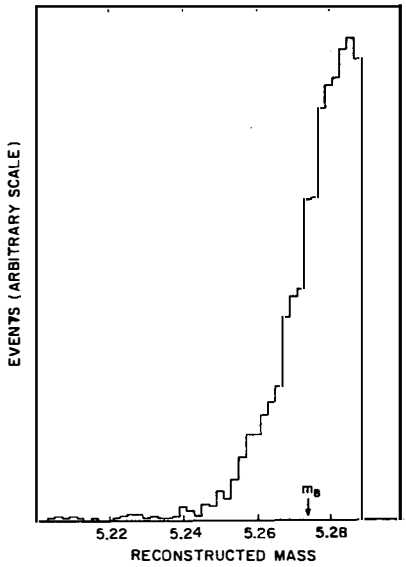

Fig. 6.

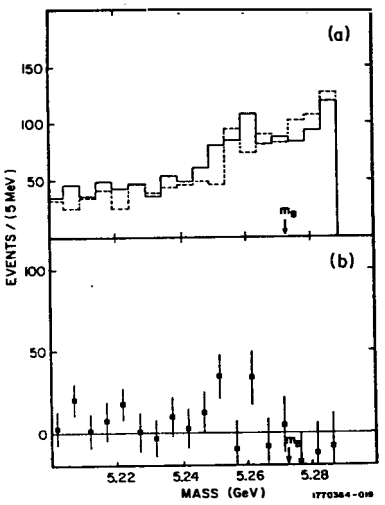

Fig. 7. (See text)

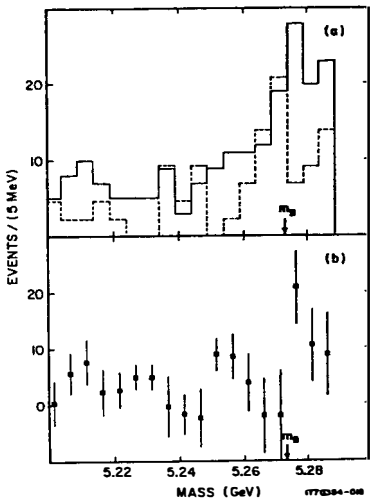

Fig. 8. (See text)

be measured in several ways. One method is to reverse the 3-momentum of the soft pion from the D^{*+} decay. The hard pion from the primary B decay and the soft pion in the D^{*+} decay should be essentially back-to-back; thus the true $\bar{B}^0$ signal should not contribute in the track-inverted analysis. Another measure of the background is the analysis of the continuum data taken below the $\Upsilon(4S)$. In this method the particle momenta are scaled by the ratio of the mass of the $\Upsilon(4S)$ and twice the actual beam energy; and in the analysis itself, the beam energy is set to be half the mass of the $\Upsilon(4S)$. Figure 7a shows the track inverted analysis on (solid) and below (dashed) the $\Upsilon(4S)$. Figure 7b shows the subtraction of the two. Figure 8a shows the partial B reconstruction pseudomass distribution (solid line) and the scaled continuum background (dashed line). Figure 8b shows the continuum subtracted signal. The analysis finds 41 ± 12 $\bar{B}^0$ events giving a value of $Br(\bar{B}^0 \to D^{*+}\pi^-) = (2.1 \pm .5 \pm .5)\%$, assuming $Br(\Upsilon(4S) \to B^0\bar{B}^0) = .4$ and $Br(D^{*+} \to \pi^+ D^0) = .60 \pm .15$.[7]

Using a similar technique[11], CLEO has measured the branching fraction for $\bar{B}^0 \to D^{*+}\rho^- \to (\pi^+ D^0)(\pi^-\pi^0)$. As in the previous example, the momentum of the ρ^- is kinematically restricted to lie between 2 GeV/c and 2.4 GeV/c. Photon showers with energies greater than 250 MeV were observed in the CLEO electromagnetic shower counters which consist of layers of proportional wire tubes interleaved with lead sheets. Pairs of showers were used to make π^0's. Figure 9 shows the

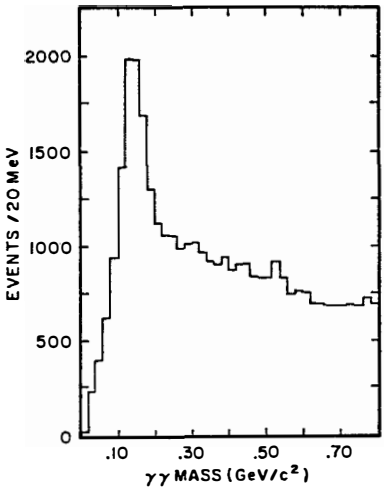

Fig. 9. γ-γ mass spectrum.

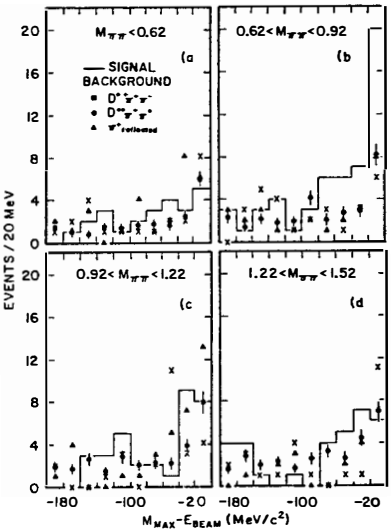

Fig. 10. Reconstructed B pseudomass.

invariant mass spectrum of photon pairs which make which make a π^0 candidate with energy greater than 1 GeV. In the analysis, a π^0 was defined as any photon pair with invariant mass between 70 MeV/c^2 and 200 MeV/c^2 and with energy greater than 1 GeV. The photon energies were then constrained to yield an invariant mass of m_{π^0}. The soft π^+ from the D^{*+} decay was required to have momentum of less than 230 MeV/c and its direction had to be within 26° of the reverse ρ^- direction. The π^0 candidates were paired with negatively charged tracks to make ρ^- candidates. The analysis was repeated for various ranges of the invariant mass of the $\pi^-\pi^0$ system; in each mass range the momentum of the $\pi^-\pi^0$ system was restricted to be less than the kinematic maximum allowed for $\bar{B}^0 \to D^{*+}(\pi^-\pi^0)$. As before, the background from 2-jet continuum events was reduced by requiring $R_2 < .3$. The results are shown in Figure 10. A clear signal is observed for $m_{\pi^-\pi^0}$ between .62 and .92 GeV. The background was estimated in three ways: by studying the process $\bar{B}^0 \to D^{*+}X^+ \to D^+(\pi^+\pi^0)$, by inverting the 3-momentum of the soft pion from the D^{*+} decay, and by studying the decay $\bar{B}^0 \to D^{*+}X^0$. Subtraction of the average of the various background estimates leaves a signal of 12.4 ± 4.5 events. Under the same assumptions used in the calculation of $Br(\bar{B}^0 \to D^{*+}\pi^-)$, this yields $Br(\bar{B}^0 \to D^{*+}\rho^-) = 7.3 \pm 2.6 \,^{+9.2}_{-2.6}\%$.

The partial reconstruction technique has also been used to search for the process $\bar{B}^0 \to D^{*+}F^- \to D^{*+}(\phi\pi^-)$[12]. Oppositely signed tracks not positively identified as pions were paired together under the

assumption that they were kaons. The K^+K^- pairs with invariant mass within 7 MeV/c^2 of the ϕ mass were then paired with negatively charged tracks to make F^- mesons. Only F^- candidates with momentum greater than 1 GeV/c and less than 2.5 GeV/c were kept. No signal was observed, implying $Br(\bar{B}^0 \to D^{*+}F^-) < 10\%$.

The Lifetime Ratio and Mixing: In semileptonic decay, only the spectator diagram contributes; thus the partial widths for $\bar{B}^0 \to \ell^- \nu X^+$ and for $B^- \to \ell^- \nu X^0$ are equal. This means that the ratio of the lifetimes of the charged and neutral B mesons is equal to the ratio of the respective semileptonic branching fractions. The experimental problem for CLEO is that only the average of the semileptonic branching fractions for B mesons is measured. If the ratio of production of neutral and charged B mesons from $\Upsilon(4S)$ decays is taken to be 4:6 as discussed earlier, then measurements of the prompt single lepton and dilepton (from parallel B decays) yields coming from B decays can be used to unravel the average B meson leptonic branching fraction into its component parts. CLEO finds 85 ± 16 dilepton events from parallel B decays yielding a limit on the ratio of neutral to charged lifetimes of $.25 < \tau^0/\tau^- < 2.9$ at the 90% C.L.[4]

As in the K^0-$\bar{K}^0$ system, mixing between B^0 and $\bar{B}^0$ is possible through the diagrams shown in Figure 11. An observable consequence of B^0-$\bar{B}^0$ mixing is the number of like sign dileptons coming from parallel B decays. A convenient parameter for measuring B^0-$\bar{B}^0$ mixing is $Y = [N(B^0\bar{B}^0) + N(\bar{B}^0\bar{B}^0)]/N(B^0\bar{B}^0)$. For complete mixing Y = 1, and for no mixing Y = 0. Experimentally, Y can be related to the numbers of observed dilepton events by $Y = [N(\ell^+\ell^+) + N(\ell^-\ell^-)]/N(\ell^+\ell^-)$. Only dileptons from parallel B decays are included; fakes and cascade contributions must be subtracted out. Unfortunately, the computation of $N(\ell^+\ell^-)$ depends strongly on the production ratio of neutral to charged B mesons on the $\Upsilon(4S)$ and on the ratio of the semileptonic branching fractions. Figure 12 shows the 90% C.L. upper limit on Y versus the ratio of semileptonic branching fractions[4].

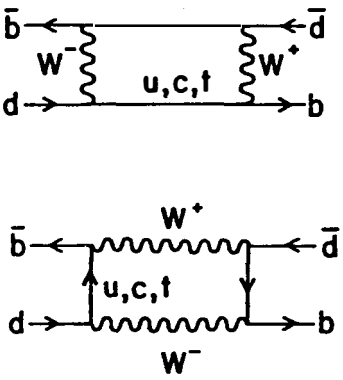

Fig. 11. B^0-$\bar{B}^0$ mixing diagrams.

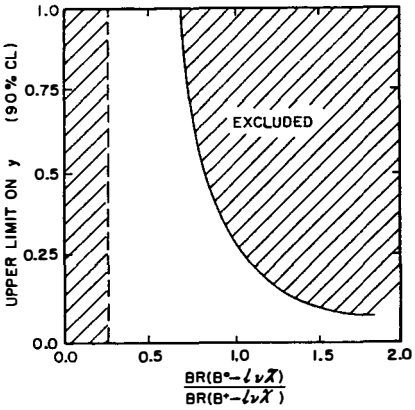

Fig. 12. Upper limit on Y.

Future Prospects: CESR has recently upgraded its LINAC to enhance its ability to produce positrons and has now moved to a seven bunch mode of operation Current running conditions now produce ~1 pb^{-1} of integrated luminosity per day at the $\Upsilon(4S)$ energy. The possibilities for tripling the CLEO B meson data set in 1985 are quite good. CLEO has also now added a high precision secondary vertex detector and installed charge sensitive electronics for dE/dx measurements on its main drift chamber, significantly enhancing CLEO's charged particle momentum resolution and identification abilities. With an enlarged data set, it seems feasible to: reduce the limit on b→u/b→c transitions by a factor of 4; reduce the limit on B°-$\bar{B}^{\circ}$ mixing and the ratio of neutral to charged lifetimes by a factor of 3; perhaps measure τ_B directly; reconstruct ~ 100 additional B mesons; and improve the measured branching fractions and the B°-B^{-} mass difference.

References:

1. C. Bebek et al., Phys. Rev. Lettr. 46, 84 (1981)
2. K. Chadwick et al., Phys. Rev. Lettr. 46, 88 (1981)
3. K. Chadwick et al., Phys. Rev. D27, (1983)
4. P. Avery et al., Phys. Rev. Lettr. 53, 1309 (1984)
5. M. S. Alam et al., Phys. Rev. Lettr. 49, 357 (1982)
6. A. Chen et al., Phys. Rev. Lettr. 52, 1084 (1984)
7. R. Giles et al., Phys. Rev. D30, 2270 (1984)
8. S. Behrends et al., Phys. Rev. Lettr. 50, 881 (1983)
9. G. C. Fox and S. Wolfram, Phys. Rev. Lettr. 41, 1581 (1978)
10. E. Eichten, Phys. Rev D22, 1819 (1980)
11. "Observation of the Decay $\bar{B}^{\circ}\to D^{**}\rho^{-}$", A. Chen et al., accepted for publication in Phys. Rev. Lettr.
12. "Upper Limit on B→F Decays", K. Berkelman et al., CBX-84-82, Cornell Laboratoty of Nuclear Studies

B LIFETIME MEASUREMENTS AT PEP

Presented by Clara Matteuzzi
for the MARK II Collaboration[1)]

INTRODUCTION

The average lifetime of b hadronic states has been measured by three detectors at the e^+e^- intersecting storage ring PEP at SLAC: DELCO[2], MAC[3], MARK II[4]. The production of heavy mesons moving relativistically in e^+e^- annihilations at a center of mass energy of 29 GeV, makes it possible to measure their lifetimes with the existing techniques. The interest of measuring b lifetime is that it is determined by the strength of weak interactions in mixing the quark generations. This means that it allows the measurement of the element of the Kobayashi-Maskawa matrix for the mixing bc or bu.

THE DETECTORS

In order to measure B hadrons lifetime, a detector must provide good lepton identification and good accuracy in particle tracking.

DELCO is a detector particularly efficient in identifying electrons over a large solid angle. The identification is achieved with a 36-cell Cerenkov counter covering 60% of the solid angle. These counters, in combination with shower counters, allow a π/e separation better than 1/1000 with high detection efficiency. The particle tracking is made by 16 layers of cylindrical drift chambers with a momentum resolution of $\sigma_p/p = \sqrt{0.06^2 + (0.02)^2}$ (p in GeV). The contribution of the drift chamber resolution to the average error on the measured distance between two tracks at the beam crossing point is $\sim 280\ \mu$m. The beam size is measured by pickup buttons located 4.5 m on either side of the beam crossing point. The horizontal size is $\sigma_x = (356 \pm 13)\ \mu$m and the vertical one is $\sigma_y = (44 \pm 51)\ \mu$m.

The tracking device of MAC consists of a cylindrical drift chamber with 10 layers of wires, immersed in a magnetic field of 5.7 KGauss. The chamber has a spatial resolution of $\sigma_p/p = 0.065\ p$ (p in GeV). The chamber is surrounded by an electromagnetic and hadron calorimeter, made of a lead-proportional wire chamber sandwich, providing a total of 16 radiation lengths of material. It allows electron identification and gives an π/e separation in the range of 0.5-1% over about 70% of solid angle and for particles with momentum larger than 1.8 GeV/c. The entire calorimeter detector is surrounded by drift chambers for identifying and tracking muons over 77% of the solid angle. The probability of misidentifying an hadron as a μ is 1.5% for particle momenta greater than 2 GeV/c. The beam position is determined for each run by a fit to Bhabha events. The rms beam size is 500 μm horizontally and 100 μm vertically.

The MARK II detector provides charged particle tracking with 23 layers of drift chambers with a resolution of $\sigma_p/p = 0.02p$ (p in GeV). The inner part of the layers is a high precision drift chamber[5] (called the vertex detector), located just outside the beam pipe. It allows an accuracy of 100 μm in the plane perpendicular to the beam. The electron identification is achieved over 65% of solid angle with a liquid argon calorimeter, rejecting hadrons at a level of 0.5% for momenta greater than 2 GeV/c. Proportional tubes interspersed with steel layers provide muon identification over 45% of solid angle, misidentifying hadrons with a probability of about 1%.

THE METHOD

The B hadron lifetime is measured from the distribution of the distance of closest approach to the interaction point of leptons coming from the semileptonic decay of B particles.

The method is carried out in the following way. First of all a sample of data enriched in $e^+e^- \rightarrow b\bar{b}$ must be selected. This is achieved selecting $q\bar{q}$ events containing leptons of high transverse momentum. A

Table I

Definition of b enriched sample

Expt	Kinematic cuts	Populations
DELCO	$p_T^e > 1$ GeV/c $p > 1$ GeV/c	0.77 $b\bar{b}$ 0.17 $c\bar{c}$ 0.06 bkg
MAC	$p > 2$ GeV/c $p_T > 1.5$ GeV/c	0.53 0.18 0.29
MARK II	$p > 2$ GeV/c $p_T > 1$ GeV/c	0.62 0.15 0.23

Monte Carlo method predicts the composition of the sample defined by the selection criteria. Table I gives the populations in terms of $e^+e^- \rightarrow b\bar{b}$, $e^+e^- \rightarrow c\bar{c}$ and background from π and K following the cuts applied and the performances of each detector. Besides the kinematical cuts each experiment selects only good quality lepton trajectories, requiring a minimum number of hits in the drift chamber layers. Then the impact parameter δ of leptons is measured. This is defined as the distance of closest approach between the lepton trajectory and the average beam position, projected in the plane perpendicular to the beam. The impact parameter (fig. 1) is a positive defined quantity in principle, but tracking and beam position errors give rise to both positive and negative values. Conventionally δ is positive if the intersection of the B trajectory (approximated by the thrust direction) with that of the lepton corresponds to a positive decay length, it is negative otherwise. The primary vertex is approximated by the average beam position. The error on δ is the sum in quadrature of the track error and the effective beam size (which is a function of the azimuthal angle). The measured distribution of δ is the superposition of three distributions, the one of B hadrons (B), the one of charmed hadrons (C), and the one of background hadrons (bkg). Therefore, to extract the average impact parameter of B hadrons, a fit is done to the distribution

$$(dN/d\delta)_{MEAS} = f_B(dN/d\delta)_B + f_C(dN/d\delta)_C + f_{bkg}(dN/d\delta)_{bkg} ,$$

where f_B, f_C, f_{bkg} are the respective frequencies of the populations predicted by Monte Carlo, $(dN/d\delta)_C$ is the impact parameter distribution of leptons from charmed hadrons, determined by Monte Carlo assuming a value of τ_C, and $(dN/d\delta)_{bkg}$ is the δ distribution for background hadrons, also determined by Monte Carlo or measured directly with a 'control' data sample.

RESULTS

Table II gives a summary of the different assumptions and results obtained in the three experiments. The lifetime t_B is fixed by how much the weak interactions mix the quark states of different generations. This means that it can be expressed[6] as a function of the Kobayashi-Maskawa matrix elements:

$$\tau_B = \tau_\mu (m_\mu/m_b)^5 [1/(2.75|U_{bc}|^2 + 7.7|U_{bu}|^2)] .$$

Using U_{bu} measurements from CESR[7] one obtains $|U_{bc}| = 0.058$ or 0.040 if one takes $\tau_B = 0.85$ or $\tau_B = 1.8$ ps.

One must stress that these measurements have a large systematica error. It comes mainly from the estimate of the beam position, the approximation of the B direction with the thrust axis, the effect of the cut on $|\delta|$ used for the fit, and also from the assumed c lifetime value and the Monte Carlo estimates of the composition of the selected data sample. It is clear that measurements with much smaller systematic errors are needed. Some checks of the method to measure lifetimes have been made by the three experiments. DELCO measures the impact parameter of leptons in the reactions $e^+e^- \rightarrow e^+e^-e^+e^-$ where no displacement from zero should be observed. They measure an average value $\langle\delta\rangle = (-10 \pm 14)\mu$m. The impact parameter method applied to a sample of events enriched in charmed hadrons (i.e. $p > 1$ GeV/c and $p_T < 1$ GeV/c) gives a charm lifetime of $(0.77 \pm^{0.50}_{0.42})$. MAC and MARK II measure separately B lifetime

Table II

Summary of the values used by the three experiments in the fit and final results on average B lifetime in picoseconds

	DELCO	MAC	MARK II
$\int \mathcal{L}dt$ (pb^{-1})	118	160	208
N_ℓ	60 e's	160 e's 238 μ's	150 e's 120 μ's
$\langle\delta\rangle_{measured}(\mu m)$	215 ± 81	120 ± 28	80 ± 17
$\langle\sigma_\delta\rangle$ (μm)	400	600	200
$\langle\delta\rangle_{bkg}$ (μm)	40 ± 8	23 ± 7	29 ± 5
$\langle\tau_c\rangle$ (10^{-12} sec)	0.64	0.55	0.60
τ_B (10^{-12} sec)	$1.16^{+0.37}_{-0.34}$ ± 0.23	1.6 ± 0.4 ± 0.4	0.85 ± 0.17 ±
Minimization method	Max likelihood	Median	Max likelihood

with electron and muons, yielding compatible values. Each detector measures by impact parameter method the τ lepton lifetime, obtaining (0.29 ± 0.08), (0.33 ± 0.04), (0.31 ± 0.02) picoseconds respectively from DELCO, MAC and MARK II. These values are in good agreement with the τ lifetime measured by MARK II[8] from the distribution of the distance of secondary verteces in the decay $\tau \rightarrow 3\pi\nu$, τ_τ = (0.286 ± 0.016 ± 0.025) × 10^{-13} sec.

CONCLUSIONS

The measurements of B hadron mean lifetime in e^+e^- annihilations at PEP yield values around 1 picosecond. Experiments at PETRA obtain very similar results[9]. It is clear however that it is necessary to perform measurements with much smaller systematic error. It must be also stressed that the measured value concerns an average over neutral and charged B hadrons, produced in e^+e^- collisions in a not yet known proportion.

REFERENCES

1) Collaboration members are: T. Barklow, A.M. Boyarski, M. Breidenbach, P.R. Burchat, D.L. Burke, J.M. Dorfan, G.J. Feldman, L. Gladney, G. Hanson, K. Hayes, R.J. Hollebeek, W.R. Innes, J.A. Jaros, D. Karlen, A.J. Lankford, R.R. Larsen, B.W. LeClaire, N.S. Lockyer, V. Lüth, C. Matteuzzi, R.A. Ong, M.L. Perl, B. Richter, K. Riles, M.C. Ross, D. Schlatter, J.M. Yelton and C. Zaiser, Stanford Linear Accelerator Center, Stanford University, Stanford, California.
G.S. Abrams, D. Amidei, A.R. Baden, J. Boyer, F. Butler, G. Gidal, M.S. Gold, G. Goldhaber, L. Golding, J. Haggerty, D. Herrup, I. Jurivic, J.A. Kadyk, M.E. Nelson, P.C. Rowson, H. Schellman, W.B. Schmidke, P.D. Sheldon, C. de la Vaissiere and D.R. Wood, Lawrence Berkeley Laboratory and Department of Physics, University of California, Berkeley, California.
M.E. Levi and T. Schaad, Department of Physics, Harvard University, Cambridge, Massachusetts.

2) D.E. Klem et al., DELCO collaboration, Phys. Rev. Lett. 53, 1873, 1984.

3) E. Fernandez et al., MAC Collaboration, Phys. Rev. Lett. 51, 1022, 1983 and W.T. Ford COLO-HEP-69, 1984.

4) N.S. Lockyer et al., Phys. Rev. Lett. 51, 1316, 1983 and J.A. Jaros, Talk given at SLAC Topical Conference, August 1984.

5) J.A. Jaros, Proceed. of the International Conference on Instrumentation for Colliding Beam Physics, SLAC Report 250.

6) M. Gaillard, L. Maiani, Proceed. of 1979 Cargese Summer Institute, ed. by M. Levy, Plenum Press, NY, p.433.

7) A. Chen et al., Phys. Rev. Lett. 52, 1084 (1984).

8) J.A. Jaros, Talk given at SLAC Topical Conference, August 1984.

9) W. Bartel et al., Phys. Lett. 114B, 71 (1982);
M. Althoff et al, TASSO Collaboration, Phys. Lett. 149B, 524, 1984.

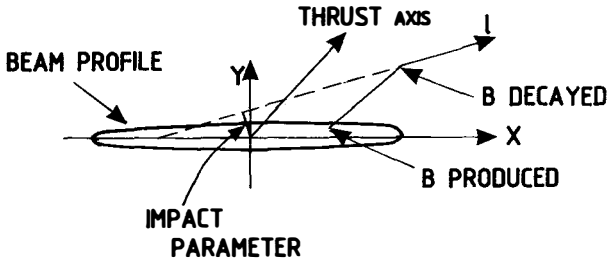

Fig. 1 Definition of impact parameter.

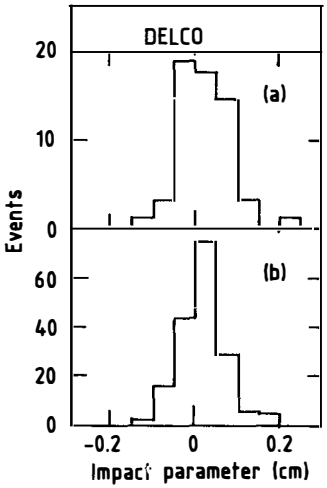

Fig. 2 Impact parameter (δ) distribution. Only those events having $|\delta| <$ 3 mm have been used in the fit. (a) b enriched region. The average value is $\langle\delta\rangle = 215 \pm 81\ \mu$m. (b) c enriched region, defined by the kinematical cuts $p > 1$ GeV/c and $p_T < 1$ GeV/c. The average value is $\langle\delta\rangle = 137 \pm 54.\mu$m

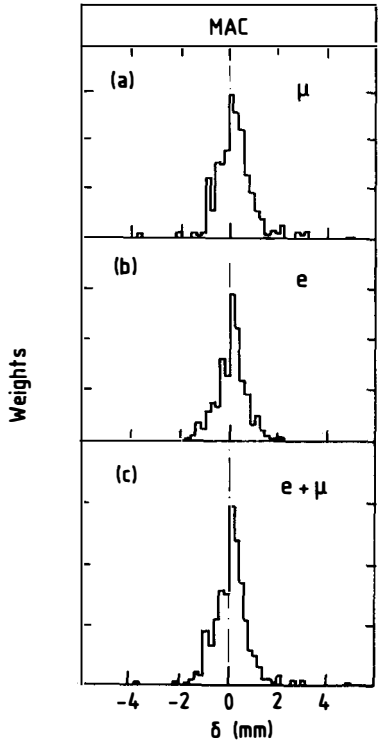

Fig. 3 Distributions of impact parameter weighted over the error, for b enriched sample. (a) For μ's only. The average value is $\langle\delta\rangle = (159 \pm 39)\mu$m considering only events with $\delta < 1$ mm. (b) For electrons only. The average value is $\langle\delta\rangle = 83 \pm 42\ \mu$m. (c) For all events.

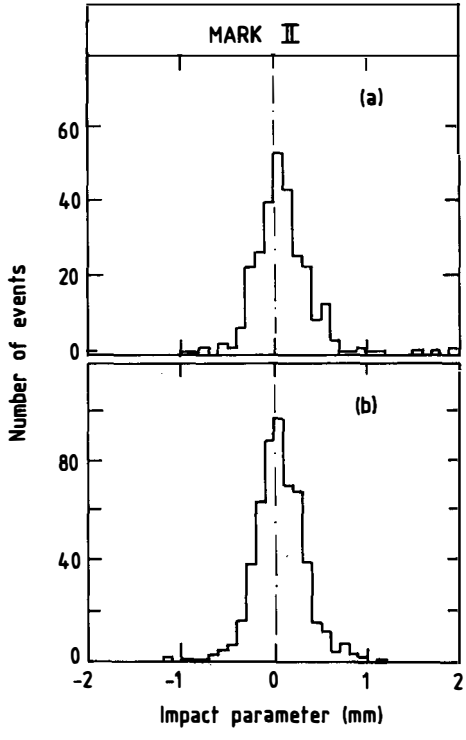

Fig. 4 Impact parameter distributions. Only events with $\sigma_\delta < 310\ \mu$m have been put in the histograms. This corresponds to exclude vertical trajectories, due to the dependence of σ on the azimuthal angle. (a) b enriched sample. The average value is $\langle\delta\rangle = 80 \pm 17\ \mu$m considering only $|\delta| < 1.2$ mm. (b) c enriched sample, defined by the kinematical cuts $p > 3$ GeV/c and $p_T < 1$ GeV/c. The average value is $\langle\delta\rangle = (59 \pm 12)\mu$m.

MEASUREMENT OF THE AVERAGE B-LIFETIME BY TASSO.

J.A.Thomas
Imperial College of Science and Technology, London

ABSTRACT

TASSO has measured the B-lifetime, averaged over all B decays using two independent data samples, each having different resolutions. The two data samples were found to yield consistent values for the B-lifetime, and the combined result is

$$1.83 \begin{smallmatrix} + 0.38 \\ - 0.37 \end{smallmatrix} \begin{smallmatrix} + 0.37 \\ - 0.34 \end{smallmatrix} \times 10^{-12} s.$$

The motivation behind measuring the B-meson lifetime comes mainly from the present status of the standard model. The fundamental mixing between quarks is not predicted and so it must be measured. The expression for the B-lifetime (τ_B) in terms of the Kobayashi-Maskawa (K-M) matrix components is[1)]

$$\tau_B = 10^{-14}\text{s}\ \{3.68\ |U_{bc}|^2 + 7.8\ |U_{bu}|^2\}^{-1}$$

and since $|U_{bu}|/|U_{bc}| < 0.11$[1)], $|U_{bu}|$ can be neglected and then a measurement of τ_B can give us a direct measurement of the K-M matrix element $|U_{bc}|$.

The method which TASSO has used measures the average lifetime of all B mesons, in contrast with other experiments which measure the lifetime of a subset of B mesons which have decayed semileptonically. This, in principle, is a different measurement. The B meson is thought to decay predominantly via the spectator model as shown in fig. 1a.

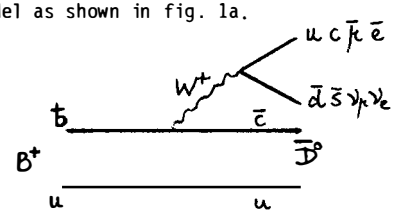

Fig. 1a

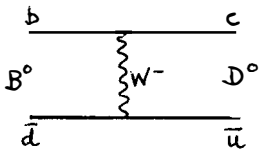

Fig. 1b

However, the decay via the exchange diagram as shown in fig. 1b is also possible in neutral B mesons and if this contribution were large, there would be a difference between the B^0 and B^+ meson lifetime (as indeed there is between D^0 and D^+ mesons) and also the semileptonic branching ratio for the B^0 would be suppressed. Thus a measurement of the B meson lifetime averaged over all B mesons might be different from that measured through the semi-leptonic channel only, if the B^0 and B^+ have different lifetimes.

To measure lifetimes in e^+e^- experiments, the usual parameter to investigate is called the 'impact parameter' d, which is the distance of closest approach of the track in question to the interaction point (I.P.). As shown in fig. 2, if we look at B mesons with a finite lifetime, the B meson will travel a distance x before it decays. The decay product tracks will then each have an impact parameter, d, assigned to them. For measuring lifetimes, it is convenient to give this value a sign as an indication of the direction of the track. In the ideal case of perfect track reconstruction, all tracks coming from the decay of a B meson will have a positive d. If we assume the B meson to be travelling

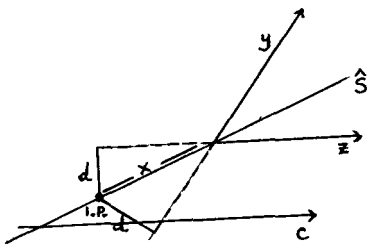

Fig. 2

in the same direction as the sphericity axis of the event, $\hat{S}$, then if the decay decay track crosses $\hat{S}$ in front of the I.P., d is called positive as shown in fig.2 by tracks y and z. If the track crosses $\hat{S}$ behind the I.P. as would be the case with a badly measured track, it will have a negative d as shown in fig. 2 by track c. If the decay tracks make an angle Ψ with the original direction of the B-meson, then

$$x = \frac{d}{\sin\Psi} \text{ and } \tau_B = \frac{1}{\gamma\beta c}\,\frac{d}{\sin\Psi}$$

Assuming zero mass decay products, a relativistic B meson and isotropic decays and averaging over the decay angular distribution

$$\tau_B \approx \frac{1}{c}\,\frac{2}{\pi}\,\langle d\rangle$$

which is independent of γ, i.e. the B meson momentum. In the TASSO detector we look at the projection of d onto the plane perpendicular to the beam pipe, and this projected impact parameter, δ, can be expressed similarly

$$\tau_B = f\,\frac{1}{c}\,\langle\delta\rangle$$

where f is a function of the projection and thus depends on the B meson production angular distribution and the detector acceptance. f was found to be ~2.0 for both bottom and charm meson decay.

In the process $e^+e^- \to q\bar{q}$ the quarks are produced in the ratio u:d:s:c:b = 4:1:1:4:1 from the squares of their charges and so if we look directly at the $\langle\delta\rangle$ of all events, it is clear that

$$\langle\delta\rangle = \frac{XT\langle\delta\rangle_{uds} + YT\langle\delta\rangle_c + ZT\langle\delta\rangle_b}{T},$$

where X is the proportion of uds tracks, Y is the proportion of charm tracks, Z is the proportion of b tracks and T is the total number of tracks. With the above proportions, it is clear that Z is 1/11 x the b event multiplicity, and $\langle\delta\rangle$ will be dominated by $\langle\delta\rangle_{uds}$ and $\langle\delta\rangle_c$. However, were we to enrich our sample such that the ratios were uds:c:b = 1:1:1, then the three separate $\langle\delta\rangle$ would have approximately equal weight in the above expression and, providing the

B lifetime were big enough, the $\langle\delta\rangle_b$ term would dominate.

To enrich our sample in b quark events, we made use of the difference in shape between b quark events and udsc events. It is expected that b quarks, having a larger mass, will produce events having high sphericity. The following procedure was adopted:
The sphericity axis of the event was required to lie with $\cos\Theta = \pm 0.7$ as shown in fig. 3, so that the event went into the detector acceptance. Then, only charged particles which fell within cones of half opening angle 41^0 about the sphericity axis were considered. The event was then divided into two hemispheres by the plane perpendicular to the sphericity axis and the tracks in each hemisphere were given a Lorenz boost towards their respective B meson rest frames. The magnitude of the boost was chosen from Monte Carlo studies to be $\beta = 0.7$ for the 34.6 GeV data and $\beta = 0.75$ for the 43.3 GeV data, which gave the largest separation between $b\bar{b}$ events and udsc events. The sphericity of each jet was calculated and then the product of S1·S2 was required to be >0.1. Using this product reduces contamination from $q\bar{q}g$ events which will have a high sphericity for one jet only. The Monte Carlo showed that the remaining sample contained 32 % $b\bar{b}$, 35 % $c\bar{c}$ and 33 % uds events.

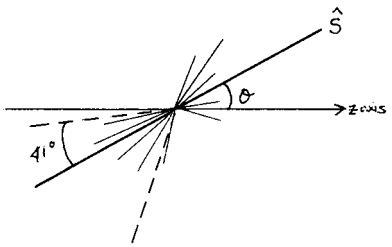

Fig. 3

Obviously, to interpret our results correctly, we need a large sample of Monte Carlo events for two reasons. Firstly to tell us the relative proportions of udsc + b in our enriched sample and secondly, to predict the $\langle\delta\rangle$ value for different values of the B lifetimes which can then be directly compared with the data.

The data were separated into two distinct samples. 22474 hadronic events were collected at an average c.m. energy of 34.6 GeV using only the central drift chamber (CDC) for tracking. A further 2001 events were collected at an average c.m. energy of 43.3 GeV after the installation of the TASSO high precision vertex chamber (VXD). The VXD has a spacial drift resolution of ~90 μ and an impact parameter resolution of ~360 μ which is dominated by the beam size. Figure 4a shows the asymmetry of the δ distribution compared with the Monte Carlo prediction for $\tau_B = 0$ and $\tau_B = 2 \cdot 10^{12}$s. Clearly the data is not in agreement with the $\tau_B = 0$ prediction. Figure 4b shows the same distribution for the second set of data.

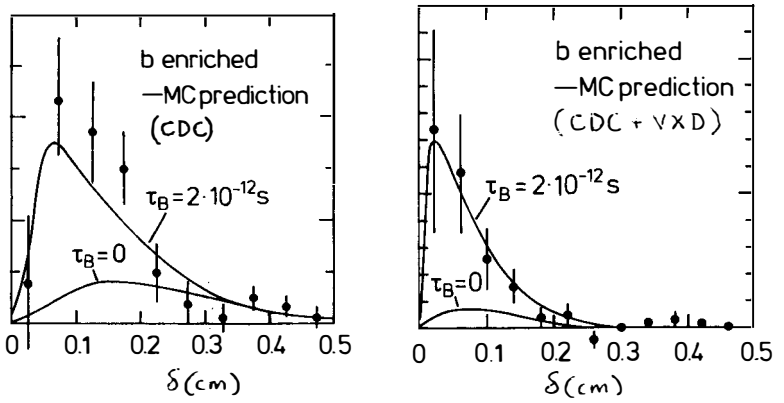

Fig. 4

To extract a lifetime, a graph was plotted of generated τ_B for the Monte Carlo vs $\langle\delta\rangle$, and the data was superimposed on the top as shown in fig. 5. It is then easy to read off the measured lifetime value and its statistical error. The two

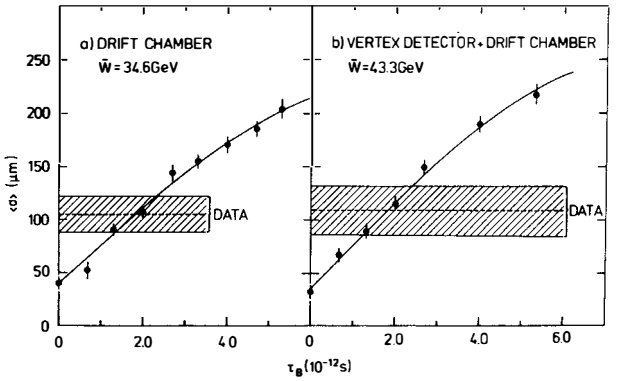

Fig. 5

lifetimes extracted in this way, corresponding to the two statistically independent data sets were

a) CDC only $1.85 \,^{+\,0.49}_{-\,0.48} \cdot 10^{-12}$s

b) CDC + VXD $1.80 \,^{+\,0.58}_{-\,0.57} \cdot 10^{-12}$s

Combining these two values gave

$$1.83 \begin{smallmatrix} + 0.38 \\ - 0.37 \end{smallmatrix} \cdot 10^{-12} s.$$

Finally, the systematic error was calculated and here are listed the separate sources and their contributions.

Tracking

. A shift in the beam position of ~200 μ changed $\langle\delta\rangle$ by less than 2 μ	⇒0.05 ps
. Choise of $\|\delta\|$ cut of ±0.5 cm	⇒0.10 ps
. Choice of $\geq$ 5 hits required for a track in the vertex detector	⇒0.10 ps

Monte Carlo.

Previously undetected systematic shifts in $\langle\delta\rangle$	⇒0.16 ps
Uncertainties in the uds + c lifetimes and multiplicity	⇒0.10 ps
Uncertainties in b multiplicity, fragmentation and decay	⇒0.15 ps
Uncertainty in the proportion of b in the b enriched sample	$\Rightarrow \begin{smallmatrix} +0.25 \\ -0.20 \end{smallmatrix}$ ps

In summary, TASSO has measured the B-meson lifetime to be

$$1.83 \begin{smallmatrix} + 0.38 + 0.37 \\ - 0.37 - 0.34 \end{smallmatrix} \cdot 10^{-12} s$$

which is the lifetime averaged over all B decays. Two independent data sets, each having very different resolutions were used and found to yield consistent values for the B meson lifetime.

REFERENCES

1. J.Lee-Franzini, invited talk at the Europhysics Study Conference on Flavour Mixing in Weak Interactions, Erice, March 1984; See also S.Stone, Proc. 1983 International Symposium on Lepton and Photon Interactions at High Energies, Cornell, ed. D.G.Cassel and D.L.Kreinick (1983).

RESULTS ON B QUARKS FROM JADE

ROGER BARLOW
Manchester University, Manchester, England

ABSTRACT

Results are presented on the lifetime and the electroweak induced asymmetry, from which a limit is obtained on the mixing of neutral B mesons. The statistical methods used to extract the b quark signal are emphasised.

1. Introduction

Events in which b quarks are produced in e^+e^- annihilation are characterised by high p_T leptons and fat event shapes. Unfortunately these do not serve to make a clean distinction between the b quark signal and the background from lighter quarks, and any cut on these variables which reduces the background to an acceptable level also reduces the signal by an undesirably large amount. We have therefore been investigating the use of techniques of extracting information from the data other than by applying cuts, and these have proved very successful; we would like to draw the attention of other experiments to the existence of such alternatives and urge their more widespread use. These techniques assume that the distributions in the indicator variables (p_T etc.) arising from various sources are predictable by Monte-Carlo programs, and have been criticised for this reason. However the programs used, both for "physics" - 4 vector generation - and for describing the apparatus, have been tried and tested and reproduce the data well. Furthermore the effects of cuts have also to be calculated using Monte-Carlo methods and also give results heavily dependent on the programs used.

2. The B lifetime

The aplanarity A of the event and the p_T of the muon are used as indicator variables. By comparing the joint distribution in A and p_T expected from b quarks to that expected from all sources, one obtains the probability $P(A,p_T)$ that an event of given A and p_T is a b quark event. This is then used as a weight to enhance the b quark signal in a plot of the impact parameter[1], δ (or any other quantity), and likewise by weighting by (1-P) one obtains a plot in which the b signal is depleted. As the effects of this enhancement and depletion on b and non-b events are known, the pure signal and background distribution can be deduced from the difference between the two weighted plots, and these are shown. All tracks in the event are used - an estimated 71% come from B mesons, this high figure being due to the hard fragmentation of b quarks.

The fact that the signal distribution is clearly skewed from zero,

(the mean is 0.195 ± 0.062 mm), whereas the background is not, should go a long way towards convincing those sceptics who still doubt whether the lifetime has been measured at all[2]. Plots using only the muon track show a similar effect.

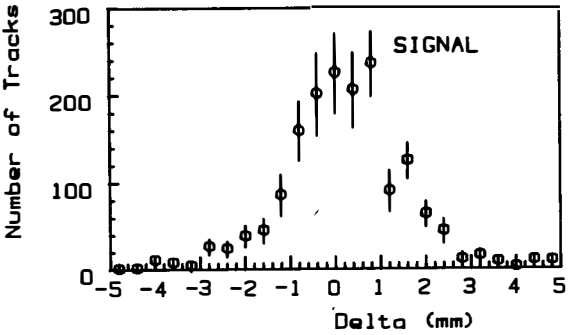

After corrections for those tracks not from the B, beam pipe interactions, and the charm lifetime, we obtain[3),4)]:

$$\tau_B = 1.7 \pm 0.6 \pm 0.4 \text{ psec}$$

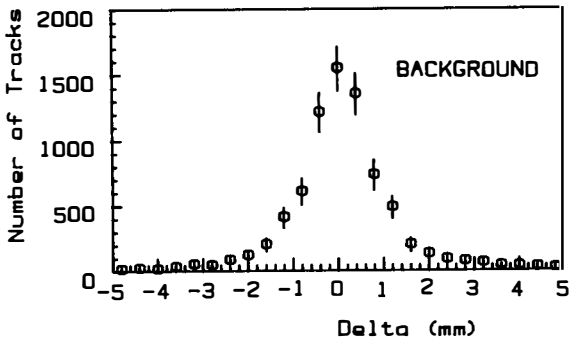

This agrees with an analysis made using the cuts method, which obtained $1.8 \begin{smallmatrix} + 0.5 \\ - 0.3 \end{smallmatrix} \pm 0.4$ psec (the smaller error being due to the use of electrons).

3. The electroweak-induced charge asymmetry

We have analysed 1780 events from 76 pb^{-1} at 35 GeV[5) 6) 7)]. Three signal variables are used: the p_T of the muon, the p_T of the neutrino, as measured by the missing momentum, and the "Jet mass" <M>. Again, Monte-Carlo events are used to find the distributions in the 3 variables, and this time the various classes of background (punch through, c quarks, etc.) are studied separately. One can then fit the joint $(<M>, P_T^{\mu}, P_T^{\nu})$ distribution by adjusting the sizes of the different contributions, and thus determine the number of b quarks in any sample. If this is done for "forward" muons (i.e. μ^+ along

the e^+ direction or μ^- along the e^- direction) one finds 114.6±12.5 events, for the "backward" muons it is 191.3±16.2. So there is obviously a large asymmetry present.

The figure shows the result of similar calculations for smaller bins in Cos θ (the outermost bins have been corrected for acceptance). The points deviate significantly from the symmetric QED curve, but agree well if a linear term is included. For maximum statistical power joint distribution in $(\langle M\rangle, p_T^{\mu}, p_T^{\nu}, \text{Cos } \theta)$ is fitted with the asymmetry as a free parameter, giving $A_B = (-22.8 \pm 6.0 \pm 2.5)\%$ which agrees well with the GWS prediction of −25.2%. Interpreting this as a measure of the axial charge of the b quark, we obtain −0.90±0.24±0.10.

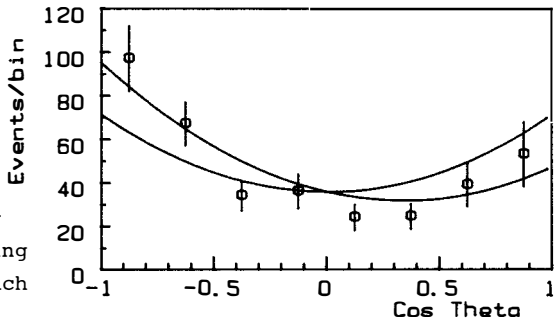

4. Limits on B-$\bar{B}$ mixing

If a B meson mixes with its antiparticle, the b quark "forgets" whether it is a quark or an antiquark, and the charge of the decay muon becomes randomised so that the asymmetry effect is reduced. The discrepancy between the observed effect and the GSW prediction is given by (assuming the leptonic branching ratios of all B hadrons to be equal)

$$\Delta = \frac{A_{pred} - A_{obs}}{A_{pred}} = \frac{2Kr}{1+r}$$

where K is the fraction of B hadrons that may mix, and r is a measure of the amount of mixing, the ratio of wrong-sign to right-sign decays. It can lie between 0 (no mixing) and 1 (full mixing).

$$r = \frac{Br(B \to \mu^+ \nu X)}{Br(B \to \mu^- \nu X)}$$

From the numbers given in Section 3, we have $\Delta = 0.10 \pm 0.24 \pm 0.10$.

The theoretical prejudice is that r will be small for B_d mesons, but may be large for B_s. First consider all B^o mesons. To find K, we need to know the probability that the b quark plucks a d or s anti-quark, rather than a u anti-quark, out of the sea. It is not clear whether for this process the appropriate u:d:s ratio is 1:1:0.3, as measured in fragmentation, or 1:1:1, which must be reached in the large q^2 limit (though the former is widely regarded as being more appropriate and is likely to be nearer the truth). Using 1:1:0.3 gives $r = 0.09 \pm 0.22 \pm 0.09$. This is significantly different from 1, and full mixing of B^o mesons is ruled out, in agreement with the CLEO result[8].

For B_s mixing even the 1:1:1 ratio only gives $r = 0.17 \pm 0.47 \pm 0.20$. This is not a meaningful measurement - but it could become so with a fairly modest increase of statistics. We therefore hope that this method will result in a measurement of this very important quantity in the not too far distant future.

5. References

1) W. Bartel et al, Physics Letters 114B 71 (1982)
2) J. D. Bjorken, these Proceedings
3) JADE collaboration, in preparation
4) P. Steffen. Proceedings of the XXII Int. Conf. on HEP, Leipzig 1984
5) W. Bartel et al, Physics Letters 146B 437 (1984)
6) R. Marshall, Report RAL-84-002 (1984)
7) R. Marshall, Report RAL-84-003 (1984)
8) P. Avery et al, CLEO preprint 84/612 (1984)

HYPERON BETA DECAYS

AND

CABIBBO MODEL

Jean-Marc Gaillard
Laboratoire de l'Accélérateur linéaire
Orsay, France

ABSTRACT

The advent of a new generation of hyperon decay experiments using high-energy hyperon beams has provided high-statistics data samples for almost every type of beta decay. Using these experimental results, combined with neutron decay measurements, an excellent fit to the Cabibbo model in its simplest original form is obtained. Effects due to the breaking of SU(3) have yet to be uncovered in the decays.

1. INTRODUCTION

Recently several high-statistics experiments have been performed with hyperon beams to measure the properties of hyperon beta decays. The results of these recent experiments allow a detailed comparison to the Cabibbo model and to its generalization to the six quarks u, d, c, s, t, b within the SU(2)XU(1) gauge group of Glashow, Weinberg and Salam for electroweak interactions.

In previous tests of the Cabibbo model it had been necessary to combine data from many different experiments. These experiments had been analysed under a variety of assumptions which affected the values obtained for the weak form factors and for the leptonic branching ratios. For the hyperon beam experiments a much better consistency of the assumptions used in the analyses has been achieved making more meaningful the comparison with the Cabibbo model.

2. RECENT EXPERIMENTAL DATA

The types of hyperon semi-letponic decays measured in each experiment and the number of events collected are given in Table 1.

TABLE 1

RECENT DATA ON HYPERON SEMILEPTONIC DECAYS

CERN SPS experiment (Ref. 1)

$\Sigma^- \to \Lambda e^- \bar{\nu}$	1649 events	$\sim$ 300
$\Lambda \to p e^- \bar{\nu}$	7111 events	$\sim$ 2000
$\Xi^- \to \Lambda e^- \bar{\nu}$	2608 events	$\sim$ 30
$\Sigma^- \to n e^- \bar{\nu}$	4456 events	$\sim$ 4000
$\Xi^- \to \Sigma^0 e^- \bar{\nu}$	154 events	-

$\Lambda \to p e^- \bar{\nu}$ with neutral beams

BNL (Ref. 2) 10^5 events	10^4 analysed
FERMILAB (Ref. 3) 50000 events	analysis in progress

Σ^- (polarized) $\to n e^- \bar{\nu}$ at FERMILAB (Ref. 4)

$\sim$ 90000 events	25000 analysed

At the SPS five types of semi-leptonic decays have been measured in a single experiment[1]. For comparison the last column gives the total number of events available for each decay prior to that experiment.

For the $\Lambda^o \to pe\bar{\nu}$ decay at BNL, results based on the analysis of 10000 decays have been published[2]. For the 50000 $\Lambda \to pe\nu$ of the Fermi Lab. experiment[3] the analysis is still in progress.

Finally for the crucial Fermi Lab. experiment[4] on polarized Σ^- beta decays, results on the electron asymmetry based on 25000 events have been obtained.

3. THEORETICAL FRAMEWORK

Weak transitions are assumed to arise from the self coupling of a single charged current J_μ^W :

$$Hw = (G/\sqrt{2})\, J_\mu^W\, J_\mu^{W+} + h.c.$$

The current J_μ^W is the sum of the current operators for the leptons J_μ^ℓ and for the strongly interacting particles J_μ^h. The explicit V-A form of the lepton current in terms of the lepton fields is :

$$J_\mu^\ell = \Sigma \left[\bar{\ell}\, \gamma_\mu\, (1+\gamma_5)\, \nu_\ell \right]$$

where the sum extends over the three types of leptons $\ell = e, \mu, \tau$, which have been observed and their associated neutrinos.

In the SU(2)XU(1) gauge theory the quark form of the hadronic current, very similar to that of the leptonic current, is given by :

$$J^h = \bar{u}\, \gamma_\mu\, (1+\gamma_5)\, d' + \bar{c}\, \gamma_\mu (1+\gamma_5)\, s' + \bar{t}\, \gamma_\mu (1+\gamma_5)\, b'$$

The weak eigenstates d', s', b' are related to the mass eigenstates d, s, b by :

$$\begin{pmatrix} d' \\ s' \\ b' \end{pmatrix} = U \begin{pmatrix} d \\ s \\ b \end{pmatrix}$$

where U is a unitary matrix first introduced by Kobayashi and Maskawa :

$$d' = \alpha\, d + \beta\, s = \gamma\, b \; ; \; |\alpha|^2 + |\beta|^2 + |\gamma|^2 = 1$$

Restricted to the known baryon states built from the u, d, s quarks, Cabibbo made the hypothesis :

$$\alpha = \cos\theta c \quad \beta = \sin\theta c \quad ; \quad |\alpha|^2 + |\beta|^2 = 1$$

This has turned out to be an excellent approximation since the (u, b) weak coupling has now been measured to be very small.

But the simple V-A expression of the weak quark current is considerably obscured due to the strong interaction dressing for real hadrons. The general form of the baryon matrix element for the decay $B_1 \to B_2\, \ell\nu$ is :

$$\langle B_2|J_\mu^h|B_1\rangle = C\bar{u}_{B_2}(p_2)\Big(f_1(q^2)\gamma_\mu + i[f_2(q^2)/M_1]\sigma_{\mu\nu}q^\nu + [f_3(q^2)/M_1]q_\mu + \Big\{g_1(q^2)\gamma_\mu + i[g_2(q^2)/M_1]\sigma_{\mu\nu}q^\nu + [g_3(q^2)/M_1]q_\mu\Big\}\gamma_5\Big)\, u_{B_1}(p_1)$$

where $u_{B_1}(p_1)$, p_1, M_1 $\left[\bar{u}_{B_2}(p_2),\ p_2,\ M_2\right]$ are the Dirac spinor, the four-momentum, and the mass of the initial [final] baryon, $q = p_2 - p_1$ and $C = \begin{bmatrix}\cos\theta_c\\ \sin\theta_c\end{bmatrix}$ for $\Delta S = \begin{bmatrix}0\\1\end{bmatrix}$ transitions.

A priori, each semileptonic decay mode depends on six independent functions of q^2, called form factors : $f_1(q^2)$, $f_2(q^2)$ for the vector part of the weak interaction, and $g_1(q^2)$, $g_2(q^2)$, $g_3(q^2)$ for the axial part.

The additional assumptions of the Cabibbo model reduce the number of independent form factors : namely, all the form factors will be a function of only three independent parameters not predicted by the theory. These assumptions make use of the identification of the $J^P = \frac{1}{2}^+$ baryon states in terms of SU(3) octet components. We will only list them (for a detailed discussion see for example Ref. (5)) :

- the components of the weak hadronic current are the charged members of a SU(3) octet
- generalization of the conserved vector current hypothesis to SU(3)
- absence of second class currents ($g_2 = o$, $f_3 = o$).

Within the model there remain only one form factor to be measured for each decay, the axial vector form factor $g_1(q^2)$. It is a linear combination of two independent parameters :

$$g_1(q^2) = a\, F(q^2) + b\, D(q^2)$$

where a and b are Clebsch Gordon coefficients.

The q^2 dependences of the form factors are inferred from the experimental information obtained from electroproduction and neutrino experiments.

Since the q^2 values involved are always small first order corrective terms are adequate (see Ref. (5)).

$$f_1(q^2) = f_1(o)\ (1 + 2q^2/m^2_V)$$

$$g_1(q^2) = g_1(o)\ (1 + 2q^2/M^2_A)$$

Neglecting the q^2 dependence is a cause of significant shifts in the values of the form factor ratio g_1/f_1.

Within the Cabibbo model the three independent parameters are thus :

$$F = F(o) \quad , \quad D = D(o) \quad \text{and} \quad \theta_c \ .$$

Experiments on several hyperon semileptonic decays have now reached a level of precision where the radiative corrections are expected to be significant

compared with the experimental errors. They are taken into account when comparing the recent experimental information with the predictions of the Cabibbo model (see Ref. (5)).

Finally effects of SU(3) breaking are expected to modify the baryon matrix element and finite g_2 terms may appear (g_2 = o within the Cabibbo model which assumes SU(3) invariance). In the analysis of recent experiments, possible effects of SU(3) breaking have been investigated.

4. FITS TO THE CABIBBO MODEL

The purpose of a Cabibbo fit is to determine the values of θc, F, and D corresponding to the best agreement between the experimental results and the theoretical expectations for all the observed decays. Conclusions about the validity of the model are inferred from the quality of the agreement, e.g. value of the χ^2 for a least square fit. With the advent of the high-statistics experiments on hyperon semileptonic decays, the complete consistency of the assumptions used in the experiment analyses (q^2 dependences, radiative corrections, ...) has become crucial for the significance of the fit procedure.

The fit shown on Fig. 1 uses only the results of the SPS experiment combined with the results of the neutron lifetime measurements :

$$|g_1/f_1|_{\tau n} = 1.239 \pm 0.009$$

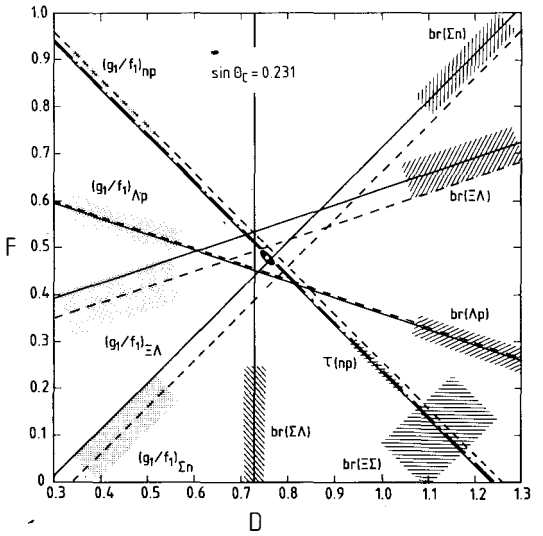

Fig. 1 A plot of allowed values of F and D showing the constraints on the Cabibbo fit imposed by the various measurements. The solid lines were obtained from the branching ratio measurements assuming $\sin\theta_C$ = 0.231, and the dashed lines correspond to the direct (g_1/f_1) determinations. The back ellipse shows the region within one standard deviation of the F and D values given by the fit (see text).

In the expression of the baryon matrix element we have used the convention that $g_1/f_1 = F + D$ is positive for the neutron decay, which fixes also all other signs. Experimentally the sign of g_1/f_1 is obtained by measuring the correlation between the polarization of the initial (final) baryon with the decay electron. In the SPS experiment this is done for all the decays involving Λ's. In the case of the $\Sigma^- \to ne\bar{\nu}$ decay the sign of the form-factor ratio is only given by the weak dependence of the electron energy spectrum. The negative sign of g_1/f_1, in agreement with the Cabibbo theory, is favoured by at least 2.6 standard deviations.

The results of the fit are :

$$F = 0.477 \pm 0.012, \quad D = 0.756 \pm 0.011,$$

and

$$\sin\theta_c = 0.231 \pm 0.003$$

with a χ^2 of 8.8 for 6 degrees of freedom.

The $\Lambda \to pe\nu$ experiment at BNL has been analysed using assumptions consistent with those of the SPS experiment analysis, except for a difference in the q^2 dependence parametrization. They give $g_1/f_1 = 0.715 \pm 0.026$, a value which is increased by 0.03 when a consistent q^2 parametrization is used. This result is in excellent agreement with the value $g_1/f_1 = 0.73$ given by the fit. The measured value of the branching ratio is only 6% lower than the fit value, which, however, amounts to three times the quoted error.

From the good fit presented above the simple Cabibbo model seems to meet with remarkable success in describing hyperon semileptonic decays. However, several low statistics experiments[6-9] attempting to measure the electron asymmetry in the decay of polarized $\Sigma^- \to ne\bar{\nu}$ had observed indications for g_1/f_1 to be positive in contradiction with the Cabibbo model. Recently the first results of the Fermilab experiment based on the analysis of 25000 polarized $\Sigma^- \to ne\bar{\nu}$ have been reported. The value[4] obtained for the electron asymmetry α_e is shown on Fig. 2 together with the results of previous experiments[6-9]. The curve represents the α_e dependence as a function of g_1/f_1 in the standard Cabibbo model. The result

$$\alpha_e = -0.53 \pm 0.14$$

is in excellent agreement with the value $\alpha_e = -0.54$ computed from the Cabibbo fit presented above. The background is very low and the large statistics allows a very detailed study of possible systematic effects of crucial importance for such an experiment. This results appears to settle the controversial question of the sign of g_1/f_1 in $\Sigma^- \to ne\bar{\nu}$ decays.

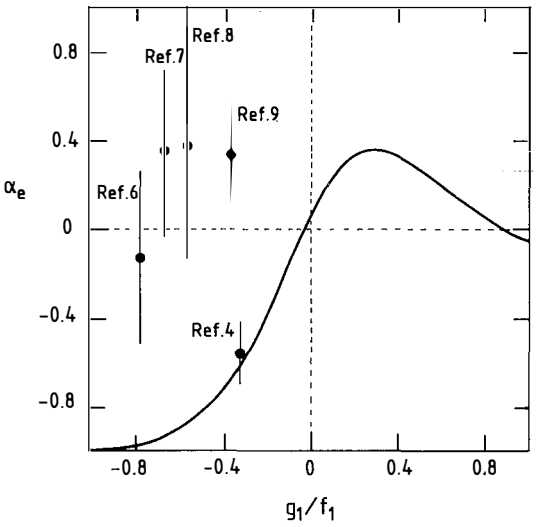

Fig. 2

Plot of the electron asymmetry α_e vs. g_1/f_1

5. DISCUSSION AND CONCLUSIONS

The results of the good fit to the hyperon data presented in the previous sections :

$$F = 0.477 \pm 0.012,\ D = 0.756 \pm 0.011 \text{ and } \sin\theta_c = 0.231 \pm 0.003$$

have been obtained within the framework of the Cabibbo model, which assumes SU(3) invariance of the strong interactions. That is already an indication that the effects of SU(3) breaking are not very large for hyperon decays. It has been shown by Ademollo and Gatto[10] that for the vector part of the baryon matrix element the first order symmetry breaking effects vanish. Therefore the effects due to the breaking of SU(3) are expected to be more important in the axial - vector terms than in the vector terms. By introducing small g_2 terms the χ^2 of the fit shows a slight improvement. However the χ^2 variation is too small to be considered significant, indicating that the data are not yet sufficiently precise to establish the presence of g_2 terms.

An independent measurement of the Cabibbo angle can be obtained from the K_{e_3} decay rates. The only contribution to these decays comes from the weak vector current. Therefore the effects of SU(3) breaking are rather small and appear to be within the reach of reliable theoretical calculations. Using the K_{e_3}

experimental data Shrock and Wang[11] derived $\sin\theta_c = 0.219 \pm 0.003$ and from a careful new analysis Leutwyler and Roos[12] have obtained $\sin\theta_c = 0.220 \pm 0.002$. Although corrections have been applied to obtain this value of $\sin\theta_c$, it is not clear at this stage whether the difference between this and the hyperon value $\sin\theta_c = 0.231 \pm 0.003$ comes from SU(3) - breaking effects in the meson or in the baryon decays. An obvious question is what is the "true" value of the bare Cabibbo angle ?

As an example of a theoretical attempt to calculate the effects of SU(3) breaking in hyperon decays, one can take the results of Donoghue and Holstein[13]. Using their prescriptions for the modifications to f_2, f_1 and g_1 and for the predicted values of g_2/g_1, the fit to the hyperon data is very poor ($\chi^2/DOF = 21.8/6$), showing a strong disagreement between the data and this particular model of SU(3) breaking.

In conclusion although the good fit obtained to the simple Cabibbo model does not call for sizeable SU(3) - breaking effects, there is certainly room for such effects. However the theoretical ground rules for hunting the SU(3) - breaking game seem far from being established.

Finally, the hyperon data can be used to set an upper limit on the mixing angle θ_3 of the Kobayashi - Maskawa matrix. With their parametrization, $\sin\theta_c = \sin\theta_1 \cos\theta_3$ and $\cos\theta_c = \cos\theta_1$. Nuclear beta-decay data are used to impose a futher constraint on θ_1 in the four parameter fit : F, D, θ_1 and θ_3. The result is :

$$| \sin\theta_3 | < 0.20$$

This upper limit is in agreement with the more stringent limits on $\sin\theta_3$ which have been obtained from beauty decay measurements.

REFERENCES

1. M. Bourquin et al., Z. Phys. C12, 307 (1982) ; Z. Phys. C21, 1 (1983) ; Z. Phys. C21, 17 (1983) ; Z. Phys. C21, 27 (1983).

2. J. Wise et al., Phys. Lett. 91B 165 (1980) and 98B, 123 (1980) ; D. Jensen et al., Proc. Int. Conf. High-Energy Physics, Brighton, 255 (1983).

3. J.S. Dworkin, A High-Statistics Study of Lambda Beta-Decay (thesis), Univ. Michigan, Ann Arbor, MI 48109 (1983).

4. S.Y. Hsuch et al., Measurement of the Electron Asymmetry in the Beta Decay of Polarized Σ^- Hyperons, to be published in Phys. Rev. Letters.

5. J-M. Gaillard and G. Sauvage, Ann. Rev. Nucl. Part. Sci. 34, 351 (1984).

6. L.K. Gershwin et al., Phys. Rev. Lett. 20, 1270 (1968).

7. D. Bogert et al., Phys. Rev. D2, 6 (1970).

8. R.J. Ellis et al., Nucl. Phys. B29, 77 (1972).

9. P. Keller et al., Phys. Rev. Lett. 48, 971 (1982).

10. M. Ademollo and R. Gatto, Phys. Rev. Lett. 13, 264 (1964).

11. R.E. Shrock and L.L. Wang, Phys. Rev. Lett. 41, 1692 (1978).

12. H. Leutwyler and M. Roos, Z. Phys. C25, 91 (1984).

13. J.F. Donoghue and B.R. Holstein, Phys. Rev. D25, 206 (1982).

MEASUREMENT OF THE A^+ LIFETIME AT THE CERN SPS HYPERON BEAM

H.W. Siebert *)
Physikalisches Institut, Universität Heidelberg,
Fed. Rep. Germany

ABSTRACT

The lifetime of the charmed strange baryon A^+ has been determined at the CERN SPS hyperon beam from tracks measured in proportional wire chambers. The result is $\tau = (4.8^{+2.9}_{-1.8}) \times 10^{-13}$ s.

*) Member of the WA62 Collaboration: Bristol-Geneva-Heidelberg-Lausanne-London(QMC)-RAL.

Two years ago, the WA62 Collaboration[1] reported the first observation of the charmed strange baryon A^+, produced at the CERN SPS hyperon beam by Σ^- of 135 GeV/c in a beryllium target[2]. The A^+ was observed as a narrow peak in the $(\Lambda K^-\pi^+\pi^+)$ effective mass distribution at 2460 MeV/c^2, i.e. 180 MeV/c^2 above the Λ_c^+ mass. The peak width was 21 MeV/c^2 (FWHM), compatible with the resolution of the apparatus. The interpretation of this state as a Cabibbo-allowed decay of the A^+ was based on its charge and strangeness and on its narrow width. We have now determined the lifetime of this state[3] from the same data.

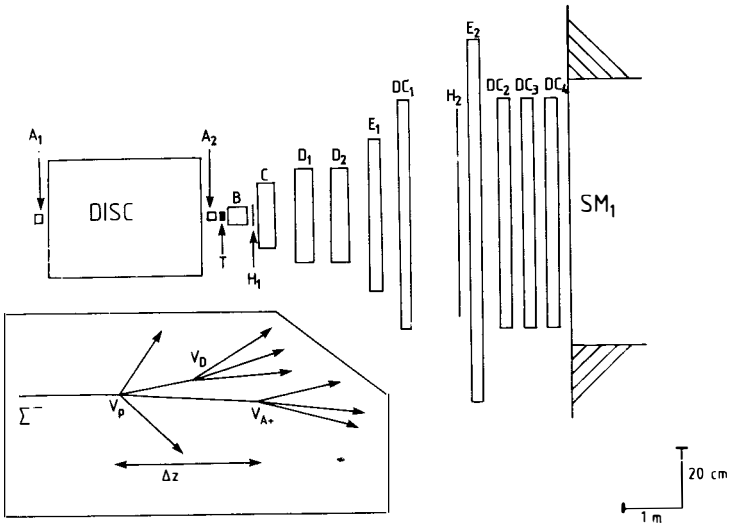

Fig. 1 Plan view of apparatus. A–E: MWPC sets. T: target. DC: drift chamber sets. H: scintillator hodoscopes. SM1: first spectrometer magnet. The inset shows a schematic view of charged tracks from associated A^+,D^- production inside the target. V_p: production vertex. V_{A^+}: A^+ decay vertex with $K^-\pi^+\pi^+$ tracks. V_D: D decay vertex.

A general description of the apparatus is given in the talk by R.M. Brown in these Proceedings. The observed A^+ had a mean momentum of 90 GeV/c, resulting in decay lengths of a few mm for typical charm lifetimes. Using proportional chambers with 0.5 mm wire pitch (A and B in Fig. 1), the tracks of incoming Σ^- and outgoing secondary particles could be extrapolated into the target with sufficient precision for a lifetime measurement.

The A^+ decay vertex V_{A^+} (see inset in Fig. 1) was reconstructed from the K^- and π^+ tracks. The production vertex V_p was reconstructed from the tracks of the incoming Σ^- and of any additional charged particle coming from the target and seen in chambers B to D_1. The determination of the production vertex could possibly be distorted by secondary interactions in

the target or by decays of short-lived particles produced in the primary interaction, e.g. D mesons (V_D). Errors arising from these sources will be discussed below.

For the lifetime determination, we restricted the sample used for the A^+ observation[2] by using only events with exactly one A^+ candidate, with more stringent geometrical criteria applied to the A^+ decay vertex. For the reconstruction of the production vertex, we used only tracks with an angle of more than 20 mrad with respect to the beam axis. These requirements improved the signal/background ratio from 82/147 to 53/59, while the statistical significance of the signal did not change. The distribution of the effective $(\Lambda K^-\pi^+\pi^+)$ mass for this sample is shown in Fig. 2.

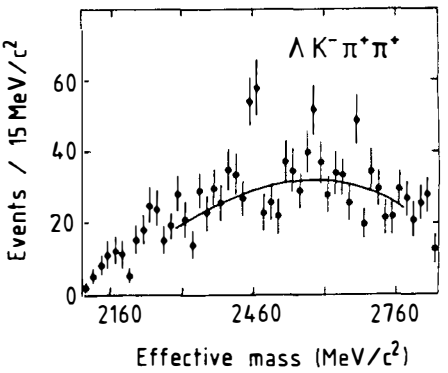

Fig. 2 Distribution of the effective $(\Lambda K^-\pi^+\pi^+)$ mass. The curve shows a second-order polynomial fit excluding the A^+ peak.

The resulting distributions of Δz, the distance between production and decay vertex, are shown in Fig. 3. Positive Δz means decay vertex downstream of the production vertex. Figure 3a contains the "far sample", i.e. all events outside the candidate and "near sample" intervals [$m(\Lambda K^-\pi^+\pi^+) <$ 2370 MeV/c^2 or $>$ 2550 MeV/c^2]. This distribution is centred at zero and has a r.m.s. of 6 mm. Figure 3b shows the Δz distribution of the A^+ candidates in the two signal bins [2445 $< m(\Lambda K^-\pi^+\pi^+) <$ 2475 MeV/c^2], which is shifted to positive Δz values. Figure 3c shows the distribution of the "near sample", which is again centred at zero. Subtracting this distribution, suitably normalized, from the Δz distribution of the candidates, one obtains the distribution in Fig. 3d for the A^+ signal. This distribution is clearly shifted to positive Δz values.

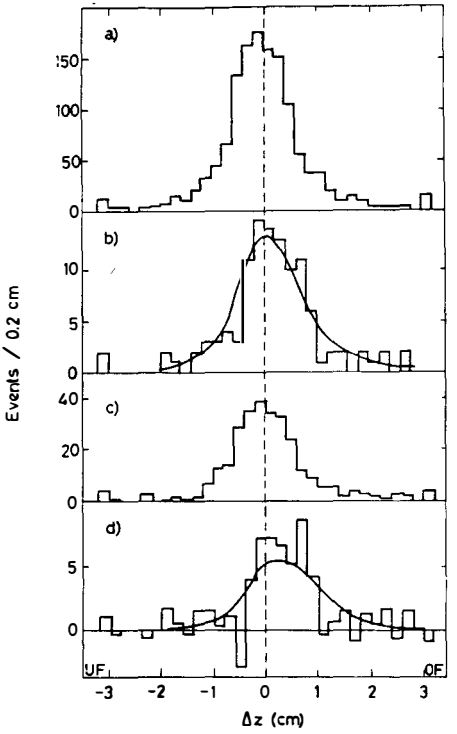

Fig. 3 Distributions of Δz. a) "Far sample", 1329 events. b) A^+ candidates, 112 events. The curve shows the best fit to the data. c) "Near sample", 295 events. d) A^+ signal after background subtraction, 53 events. The curve shows the Monte Carlo calculation for $\tau = 4.8 \times 10^{-13}$ s.

The A^+ lifetime was determined by a maximum likelihood analysis of the Δz spectrum of the A^+ candidates, using the observed Δz spectrum of the background to describe the apparatus resolution. That way, we automatically took into account the effects of secondary interactions, which should be the same for A^+ and background events. The result was $\tau(A^+) = (4.8^{+2.1}_{-1.5}) \times 10^{-13}$, where the error is the statistical error of the fit. The log likelihood curve for the fit is shown in Fig. 4. The difference between the values for $\tau = 0$ and $\tau = 4.8 \times 10^{-13}$ s is 6.0, corresponding to an effect of 3.5 standard deviations.

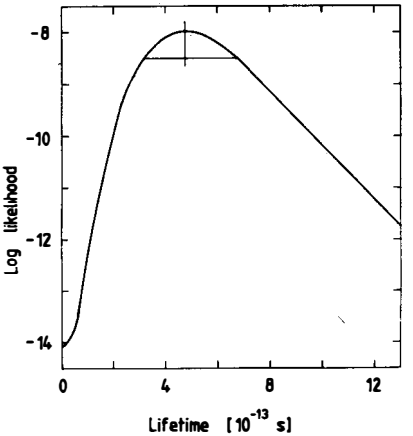

Fig. 4 Likelihood curve resulting from the lifetime fit. The thin lines show the central value and the fit error.

Uncertainties arising from the background subtraction were estimated to be $\pm 1.0 \times 10^{-13}$ s. It was not possible to determine which, if any, of the additional tracks in the candidate events came from $\overline{D}$ decays. Such tracks would tend to give smaller Δz values, as determined by a Monte Carlo calculation. The relatively small momenta expected for associated $\overline{D}$ limited the possible effect on the lifetime measurement to $\Delta\tau = -1.7 \times 10^{-13}$ s. As we found no direct proof for the existence of this effect, we did not change the observed lifetime, but added the value 1.7×10^{-13} s to the error on the positive side. The final result then was

$$\tau(A^+) = (4.8^{+2.1\ +\ 2.0}_{-1.5\ -\ 1.0}) \times 10^{-13} \text{ s} ,$$

keeping statistical and systematic errors separate. Adding them in quadrature leads to

$$\tau(A^+) = (4.8^{+2.9}_{-1.8}) \times 10^{-13} \text{ s} .$$

The order of magnitude of the measured lifetime is strong support of the identification of the observed state as the charmed strange baryon A^+.

The Λ_c^+ is the only other charmed baryon, whose lifetime has been measured. The average of three experiments[4] with a total of 19 observed events is $\tau(\Lambda_c^+) = (2.2^{+0.7}_{-0.4}) \times 10^{-13}$ s. The Λ_c^+ is expected to decay considerably faster than the A^+, because W-exchange processes (cd → su) can contribute to Λ_c^+ decays, but not to A^+ decays. Two theoretical estimates for the ratio $\tau(A^+)/\tau(\Lambda_c^+)$ are 2.5 [5] and 4 [6]. Our result supports this tendency.

REFERENCES

1) Members of the WA62 Collaboration: S.F. Biagi, M. Bourquin, A.J. Britten, R.M. Brown, H.J. Burckhart, A.A. Carter, Ch. Doré, P. Extermann, M. Gailloud, C.N.P. Gee, W.M. Gibson, J.C. Gordon, R.J. Gray, P. Igo-Kemenes, P. Jacot-Guillarmod, W.C. Louis, T. Modis, Ph. Rosselet, B.J. Saunders, P. Schirato, H.W. Siebert, V.J. Smith, K.-P. Streit, J.J. Thresher, S.N. Tovey and R. Weill.

2) S.F. Biagi et al., Phys. Lett. 122B (1983) 455.

3) S.F. Biagi et al., Phys. Lett. 150B (1985) 230.

4) N. Ushida et al., Phys. Rev. Lett. 51 (1983) 2362.
C.M. Fisher et al., Contr. no. 788, Int. Conf. on High-Energy Physics, Paris (1982).
M.I. Adamovich et al., Phys. Lett. 140B (1984) 119.

5) J.G. Körner, G. Kramer and J. Willrodt, Z. Phys. C2 (1979) 117.

6) R. Rückl, Weak decays of heavy flavours, Habilitationsschrift, Universität München (October 1983), and CERN preprint (1983).

WEAK DECAYS OF HEAVY BARYONS

D. Ebert
Institut für Hochenergiephysik der
Akademie der Wissenschaften der DDR,
DDR, 1615 Berlin-Zeuthen

Abstract

A brief survey of inclusive as well as exclusive weak decays of heavy baryons is given. Particular emphasis will be put on the discussion of explicit model estimates of weak matrix elements and their comparision with experiments.

1. Introduction

Heavy hadrons with open flavour represent an interesting system whose weak decays are determined by an interplay of strong and weak interactions. In particular, the surprising nonspectator role of the light quarks in charmed-meson decays makes especially interesting the prediction of lifetimes or decay rates of charmed baryons. In this talk I want to give a brief survey of Cabibbo-favoured inclusive as well as exclusive weak decays of charmed baryons. For definiteness I shall consider the charmed baryons $\Lambda_c^+ = c[u,d]$, $A^0 = c[s,d]$, $A^+ = c[s,u]$ and $T^0 = css$ with masses $m_{\Lambda_c^+} = (2282 \pm 3)$ MeV/c^2 [1], $m_{A^+} = (2460 \pm 15)$ MeV/c^2 [2] and $m_{T^0} = (2740 \pm 25)$ MeV/c^2 [2] which are expected to be stable under strong and electromagnetic interactions. Among them the A^+ and T^0 have been detected recently at the CERN SPS hyperon beam [2]. Bottom baryons can be treated analogously.

2. Inclusive decays

Weak decays of charmed baryons may proceed via the weak decay $c \to s(u\bar{d}$ or $\nu_l l)$ of the c-quark inside the baryon, with light quarks acting as inert spectators (spectator model [3]) and by the annihilation process $cd \to su$ via W-boson exchange. Calculating the corresponding spectator and annihilation diagrams one obtains the lifetime relation $\tau(B_c) = \tau_c \times [1 + \Gamma_{ns}(B_c)\tau_c]^{-1}$. Here τ_c is the lifetime of the c-quark calculated from the spectator diagram and $\Gamma_{ns}(B_c)$ the rate associated to the annihilation diagram. Straightforward calculation gives (we set here $\cos\theta_c \approx 1$)

$$\Gamma(c \to \text{all}) = \tau_c^{-1} = \left\{(2f_+^2 + f_-^2) + 2\right\}\left(\frac{m_c}{m_\mu}\right)^5 0.7 \times \Gamma(\mu \to \nu_\mu e \bar{\nu}_e) \qquad (1)$$

where $f_- \sim 2$, $f_+ = 1/\sqrt{f_-} \sim 0.7$ are the usual QCD short-distance factors of the effective weak Hamiltonian H_W, $m_c = 1.5$ GeV is the c-quark mass and 0.7 is a phase space correction factor. One

then predicts $\tau_c \sim 7 \cdot 10^{-13}$ sec [+]. For illustration let us consider the Λ_c^+ decay. The rate $\Gamma_{ns}(\Lambda_c^+)$ for the nonspectator process $\Lambda_c^+ \to suu$ has been calculated by Barger et al [4] in a nonrelativistic quark model, $\Gamma_{ns}(\Lambda_c^+) = \frac{G_F^2}{2\pi} \cos^4\theta_c f_-^2 |\psi(0)|^2 m_c^2$.

Estimating $|\psi(0)|^2$ from $\Sigma_c^+ - \Lambda_c^+$ hyperfine mass splitting they obtained $\Gamma_{ns}(\Lambda_c^+) \sim 0.3 \cdot 10^{13}$ sec^{-1}. This leads to the lifetime prediction $\tau(\Lambda_c^+) \sim 2.1 \cdot 10^{-13}$ sec. Moreover, there are Pauli interference contributions due to identical quarks in the final state leading to an effective reduction $\Gamma_{ns}(\Lambda_c^+) \to 0.7\,\Gamma_{ns}(\Lambda_c^+)$ and thus to a somewhat larger value $\tau(\Lambda_c^+) \sim 2.7 \cdot 10^{-13}$ sec [5]. The corresponding experimental value is $\tau(\Lambda_c^+) = (2.3\,^{+1.0}_{-0.6}) \cdot 10^{-13}$ sec [1]. Note that nonspectator (annihilation) diagrams contribute to the nonleptonic weak decays of the Λ_c^+, A^0 baryons but not to A^+ or T^0 decays. Thus one expects the following inequalities for lifetimes and semileptonic branching ratios: i) $\tau(\Lambda_c^+, A^0) < \tau(T^0, A^+)$ and ii) $B(\Lambda_c^+ \to e^+\nu_e X) \approx B(A^0 \to e^+\nu_e X) < B(A^+ \to e^+\nu_e X) \approx B(T^0 \to e^+\nu_e X) \approx 1/5 = 20\,\%$. This pattern is indicated by recent experiments yielding $\tau(\Lambda_c^+) < \tau(A^+) = (4.8\,^{+2.9}_{-1.8}) \cdot 10^{-13}$ sec [2] and $B(\Lambda_c^+ \to e^+\nu_e X) = (4.5 \pm 1.7)\,\%$ [6] Better data are urgently needed.

3. Exclusive decays

Exclusive weak two-body decays $B_\alpha^c \to B_\beta + M_K$ of charmed baryons have been recently discussed in the framework of the MIT-bag model [7,8]. Using current algebra techniques one represents the (parity-violating) S-wave and (parity-conserving) P-wave amplitudes A and B as a sum of so-called commutator terms, baryon pole terms and factorizable contributions. For example [8],

$$A = -\frac{1}{\sqrt{2}F_k}\left(I^k_{\beta\gamma}\, a_{\gamma\alpha} - I^k_{\gamma\alpha}\, a_{\beta\gamma}\right) - \frac{1}{\sqrt{2}F_k}\left(M_\alpha - M_\beta\right)\left[\frac{g^A_{k\beta\delta}\, b_{\delta\alpha}}{M_\alpha + M_\delta} - \frac{g^A_{k\gamma\alpha}\, b_{\beta\gamma}}{M_\beta + M_\gamma}\right] + A^{fac} \qquad (2)$$

[+] Since the expression for τ_c is very sensitive to a change of m_c this absolute prediction should not be taken too seriously. The following considerations are, however, assumed to give a correct picture of the relative decay pattern of charmed baryons.

where F_k is the meson decay constant, M_α etc. are baryon masses, $I^k_{\beta\gamma}$ are unitary-spin matrix elements and g^A are axial vector coupling constants. $a_{\beta\alpha}$ and $b_{\beta\alpha}$ are baryon-baryon matrix elements $\sim \langle\beta|H_w^{PC,PV}|\alpha\rangle$ of the parity-conserving (PC) or parity-violating (PV) part of H_W. (Note that in contrast to hyperon decays the PV-matrix elements b are no longer negligible for charmed baryon decays due to the large SU(4) breaking.) Finally, the factorizable term A^{fac} corresponds to the usual quark decay (spectator) diagrams. The quantities g^A and $a_{\beta\alpha}$, $b_{\beta\alpha}$ in eq (2) are given in terms of two-quark or four-quark overlap integrals, respectively. Our estimates based on the use of MIT-bag wave functions yield a ratio $|b/a|$ which is larger than the value 0.1 obtained for hyperon decays but smaller than the value 1 anticipated in ref /9/. Generally, the PV-matrix elements $b_{\beta\alpha}$ lead to corrections at the 20 % level in partial rates. They cause, in particular, sensitive changes in the asymmetry parameter α, e.g. $\alpha(\Lambda_c^+ \to \Xi^0 K^+)$ = -0.1 (b neglected) $\to$ -0.9 (b included) [8]. Moreover, non-spectator contributions lead to large differences in the A^+ and A^0 partial rates. Notice that the MIT-bag prediction for the ratio $\Gamma(\Lambda_c^+ \to \Sigma^0\pi^+)/\Gamma(\Lambda_c^+ \to p\bar{K}^0)$ = 0.71 is consistent with the data of the Fermilab bubble chamber [10]. Unfortunately, the absolute predictions $\Gamma(\Lambda_c^+ \to \Lambda\pi^+)$ = 3.8 and $\Gamma(\Lambda_c^+ \to p\bar{K}^0)$ = 1.7 (in units of 10^{11} sec^{-1}) are, however, too large when compared with the recent data [1] $\Gamma(\Lambda_c^+ \to \Lambda\pi^+) = (0.26\ ^{+0.24}_{-0.23})$ and $\Gamma(\Lambda_c^+ \to p\bar{K}^0) = (0.48\ ^{+0.32}_{-0.37})$. This discrepancy may possibly be resolved by making use of more realistic hydrogen-like bag models with localized c-quarks [11]. In fact, localized c-quark wave functions are expected to reduce the size of overlap integrals. Applying a modified bag model of this type we found $\Gamma(\Lambda_c^+ \to \Lambda\pi^+)$ = 0.21 and $\Gamma(\Lambda_c^+ \to p\bar{K}^0)$ = 0.1 [12]. Thus the MIT-bag results are reduced by about an order of magnitude (ratios of rates remain almost unchanged). This change is welcomed for the modes $\Lambda_c^+ \to \Lambda\pi^+$, $p\bar{K}^0$. To decide whether a corresponding suppression of other decay modes is likewise welcomed or not one needs more data with better statistics.

References

1) Particle Data Group, Rev. Mod. Phys. 56, No 2, II (1984).

2) S.F. Biagi et al., CERN-EP/84-76 and 84-154 (1984)

3) J. Ellis, M.K. Gaillard and D.V. Nanopoulos, Nucl. Phys. B100, 313 (1975); D. Fakirov and B. Stech, Nucl. Phys. B133, 315 (1978); N. Cabibbo and L. Maiani, Phys. Lett. 79B, 109 (1978)

4) V. Barger, J.P. Leveille and P.M. Stevenson, Phys. Rev. Lett. 44, 226 (1980)

5) R. Rückl, Phys. Lett. 120B, 449 (1983)

6) E. Vella et al., SLAC-PUB-2898 (1982)

7) B. Guberina et al., Z. Phys. C-Part. Fields C13, 251 (1982)

8) D. Ebert and W. Kallies, Phys. Lett. 131B, 183 (1983); Yad. Fiz. 40, 1250 (1984)

9) E. Golowich and B.R. Holstein, Phys. Rev. D26, 182 (1982)

10) T. Kitagaki et al. Phys. Rev. Lett. 45, 955 (1980); ibid. 48, 299 (1982)

11) D. Izatt, C. De Tar and M. Stephenson, Nucl. Phys. B199, 269 (1982)

12) D. Ebert and W. Kallies, Proceedings of the XVIII International Symposium Ahrenshoop, p. 197 (1984)

A MEASUREMENT OF $\frac{\epsilon'}{\epsilon}$ AT FERMILAB

BY THE CHICAGO-SACLAY COLLABORATION *

Presented by B. PEYAUD

ABSTRACT : The direct CP violation parameter $\frac{\epsilon'}{\epsilon}$ of the Ko-$\bar{K}$o system has been measured through the study of the 2π decays of K_S and K_L. The use of a double beam was essential for reducing the systematic errors on the result which is $\frac{\epsilon'}{\epsilon}$ = -0.0046 $\pm$ 0.0053 (statistical) $\pm$ 0.0024 (systematic) compatible with previous measurements but close to the edge of current predictions made in the framework of the Kobayashi Maskawa (K.M.) model.

R.H. BERNSTEIN, G.J. BOCK, D. CARLSMITH, D.P. COUPAL, J.W. CRONIN,
G.D. GOLLIN, Wen KELING, K. NISHIKAWA, H.W.M. NORTON, B. WINSTEIN
The Enrico Fermi Institute, CHICAGO.

B. PEYAUD, R. TURLAY, A. ZYLBERSTEJN
C.E.N. SACLAY.

The complex parameter $\epsilon = (2.274 \pm 0.022)\ \exp i\ (43.7^{o} \pm 0.2^{o})$ that measures the mixing of K_1 (CP odd) and K_2 (CP even) in the K^{o}_{L} and K^{o}_{S} states accounts for all the CP nonconserving effects that have been seen in the K_0 - $\bar{K}_0$ system since the observation of $K_L \rightarrow \pi^+ \pi^-$ in 1964 (1).

The superweak interpretation of CP violation (2) results solely from a small $\Delta S = 2$ interaction ($K_0 \leftrightarrow \bar{K}_0$ transitions) giving rise to the small (ϵ) impurity of K_1 (resp. K_2) in the physical K_L (resp. K_S) state. Another possible source of CP violation is the direct decay $K_2 \rightarrow 2\pi$ ($\Delta S = 1$ transitions) whose amplitude is given by the parameter $\epsilon' = \frac{1}{\sqrt{2}} \mathrm{Im} \left(\frac{a_2}{a_0}\right) \exp i\,(\pi/2 - \delta_2 - \delta_0)$ where a_0 (resp. a_2) is the amplitude $K_0 \rightarrow 2\pi$ in the I = 0 (resp. I = 2) final state.

Models with CP violating phases have been constructed either as a result of complex mixing of $(u, c, t)_L$ and $(d, s, b)_L$ of quarks through the K.M. matrix (3) or as a consequence of the exchange of scalar Higgs particle in the K_0 - $\bar{K}_0$ diagrams (4). The K.M. predictions still have large uncertainties and range from 10^{-3} to 10^{-2} and the Higgs contribution to ϵ'/ϵ has been estimated to be of order -0.05 to - 0.02.

The experiment E617 carried out at Fermilab by the Chicago-Saclay collaboration was designed to observe both decays modes $K_{L,S} \rightarrow 2\pi^0$ and $K_{L,S} \rightarrow \pi^+ \pi^-$ whose amplitudes define the ratios :

$$\eta_{00} = \frac{\text{amp}\ (K_L \rightarrow 2\pi^0)}{\text{amp}\ (K_S \rightarrow 2\pi^0)} = \epsilon - 2\epsilon'$$

$$\eta_{+-} = \frac{\text{amp}\ (K_L \rightarrow \pi^+ \pi^-)}{\text{amp}\ (K_S \rightarrow \pi^+ \pi^-)} = \epsilon + \epsilon'$$

Where in the superweak hypothesis $\eta_{00} = \eta_{+-}$ i.e. $\frac{\epsilon'}{\epsilon} = 0$

Two K_L beams were produced in the forward direction by 400 GeV protons. A 1m long carbon regenerator inserted in one of the beams produced the $K_S \rightarrow 2\pi$ decays whereas the free beam produced the K_L decays that were observed and accepted by our detector over 14m of vaccum following the regenerator. The charged tracks were analysed in momenta by a drift chamber spectrometer thus allowing the reconstruction of the invariant mass of the two pions as well as the decay point in the vaccum pipe. The $2\pi^0$ modes were triggered on a single conversion of one of the 4 photons in a 0.1 r.l. lead converter installed at the end of the decay region. The $e^+ e^-$ pair was then tracked by the spectrometer as well as with a 804 lead glass block array together with the 3 photons (Fig. 1). The vertex position along the beam

resulted from the best pairing of the e.m. clusters in the lead glass. The intersection of this longitudinal plane with the $e^+ e^-$ common path from the conversion point to the spectrometer magnet would then delineate in which beam the decay occured. Finally the P_T of an event could be measured by the angle between the measured momentum of the kaon and the line between target and regenarator.

The dual beam arrangement is a practical tool which allows to measure in the same apparatus both K_L and K_S decays. The acceptances being the same in a given (P_K, Z) bin (P_K is kaon momentum and Z is the position of vertex) there is a large cancellation of both acceptances, live-time, and regeneration power in the ratios :

$R^{00} = N^{00}$ vaccum/N^{00} regenerator and $R^{+-} = N^{+-}$ vaccum/N^{+-} regenerator

Where the N are the numbers of events for each mode.

Explicitly one has for the neutral mode

$$N^{00}\ \text{vac} = |\epsilon - 2\epsilon'|^2 \text{ in the vaccum beam}$$

and

$$N^{00}\ \text{reg} = |\rho e^{i\Delta m t - t/2} + \epsilon - 2\epsilon'|^2 \text{ in the regenerated beam}$$

And similarly for the charged mode.

$$N^{+-}\ \text{vac} = |\epsilon + \epsilon'|^2$$

$$N^{+-}\ \text{reg} = |\rho e^{i\Delta m t - t/2} + \epsilon + \epsilon'|^2$$

The use of a thick regenerator giving $\rho \gg \epsilon$ leads to $R = R^{00}/R^{+-} = 1 - 6\frac{\epsilon'}{\epsilon}$

Each of the 4 modes has a specific background that must be understood in order to be substracted (Fig. 2). This was done in the charged mode by the study of K_{e3} and $K_{\mu 3}$ events and inelasticaly produced K_S in the regenerator. The main background in the $K_L \to 2\pi^0$ mode is from $K_L \to 3\pi^0$ where photons are lost or from a single cluster in the lead glass. The $K_S \to 2\pi^0$ had a small inelastic component that was corrected for.

After all substractions have been made the total number of events are given in Table 1.

MODE	NUMBER OF EVENTS
$K_L \to 2\pi^0$	3152 ± 61
$K_S \to 2\pi^0$	5663 ± 84
$K_L \to \pi^+ \pi^-$	10638 ± 106
$K_S \to \pi^+ \pi^-$	25751 ± 163

Table 1 : Events totals for the Chicago-Saclay Experiment.

Comparison of data with Monte-Carlo is shown in Fig. 3 and 4.

Different methods were developed for the analysis in order to extract ϵ'/ϵ. The Monte Carlo free method makes use of the double ratio $R = 1 - 6\,\epsilon'/\epsilon$ that translates directly into the physical quantity ϵ'/ϵ. Several (P_K, Z) bins were chosen for dividing the different modes and ϵ'/ϵ was then measured from a bin to bin ratio of ratios. The final result needs a small correction resulting from the dilution of K_S in the regeneration beam.

The value obtained is $\frac{\epsilon'}{\epsilon} = -0.0044 \pm 0.0062$

A statistically more powerfull method was also developed for the extraction of ϵ'/ϵ from the data. It involves a fit of $(f - \bar{f})/k$, which governs the regeneration amplitude same for neutral and charge mode, together with ϵ'/ϵ. The phase of $(f - \bar{f})/k$ and that on carbon are well known (5) and the result of the fit gives : $(f - \bar{f})/k = P_K(-0.610 \pm 0.023)$ (charged mode) and $(f - \bar{f})/k = P_K(-0.572 \pm 0.072)$ (neutral mode) in very good agreement with previous results (6)

The result of the fit on $\frac{\epsilon'}{\epsilon}$ is then

$$\frac{\epsilon'}{\epsilon} = -0.0046 \pm 0.0053$$

in good agreement with the result from the double ratio method.

The systematic errors on this result originate dominantly from uncertainties on the different backgrounds and at some lower level from uncertainties in the ratio of Monte Carlo acceptances. The overall systematic error has been estimated to be 1.3 % in the double ratio resulting then as 0.0024 on ϵ'/ϵ.

The result of this experiment is then

$$\frac{\epsilon'}{\epsilon} = -0.0046 \pm 0.0058$$

when we combine the statistical and systematic errors in quadrature.

It is consistent with the value reported by the BNL-YALE collaboration of 0.0017 ± 0.0082 (7). This result does not give full support for the K.M. model which still have large theorical uncertainties.

REFERENCES :

1. J.H. CHRISTENSON et al., Phys. Rev. Lett. 13, 138 (1984)

2. L. WOLFENSTEIN, Phys. Rev. Lett. 13, 562 (1964)

3. M. KOBAYASHI, K. MASKAWA, Prog. Theor. Phys. 49, 652 (1973)
   F. GILMAN and J. HAGELIN, Phys. lett. 133 B, 443 (1983)
   for a review see also A.J. BURAS MPI-PAE/PTh 46/84
   B. GUBERINA, this conference

4. S. WEINBERG, Phys. Rev. Lett. 37, 657 (1976)
   A.I. SANDA, Phys. Rev. D23, 2647 (1981)
   N.G. DESHPANDE, Phys. Rev. D23, 2654 (1981)

5. J. ROEHRIG et al., Phys. Rev. Lett. 38, 1116 (1977)
   A. GSPONER et al., Phys. Rev. Lett. 42, 13 (1979)

6. A. GSPONER et al., Phys. Rev. Lett. 42, 13 (1979)

7. Talk by M. SCHMIDT, this conference.

FIGURES :

Fig. 1 Schematic diagram of the apparatus.

Fig. 2 Plots of events versus vertex position for $K_{L,S} \to \pi^+ \pi^-$ in different momentum bins.

Fig. 3 Plots of events versus vertex position for $K_L \to \pi^0 \pi^0$ and $K_S \to \pi^0 \pi^0$ in different momentum bins.

Fig. 4 Plots of events versus M $\pi^0 \pi^0$ for the $K_L \to \pi^0 \pi^0$ in different momentum bins with $P_T^2 < 2500$ $(MeV/c)^2$. The background is shown as a solid line.

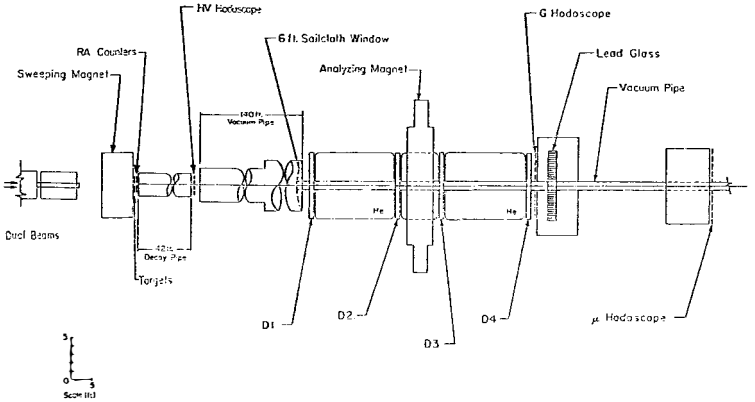
HV Hodoscope
6 ft. Sailcloth Window
G Hodoscope
RA Counters
Analyzing Magnet
Lead Glass
Sweeping Magnet
Vacuum Pipe
Decay Pipe
Targets
D1
D2
D3
D4
μ Hodoscope

Fig. 1

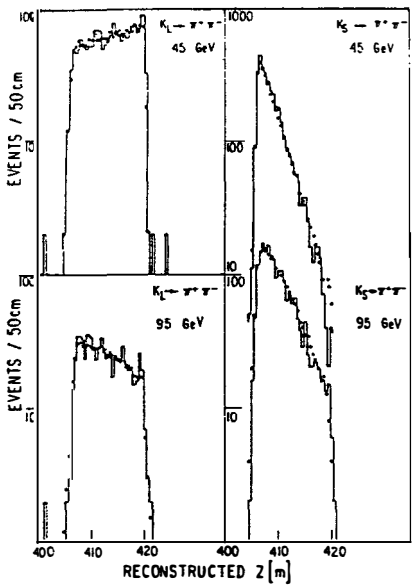
EVENTS / 50cm
45 GeV
95 GeV
RECONSTRUCTED Z [m]

Fig. 2

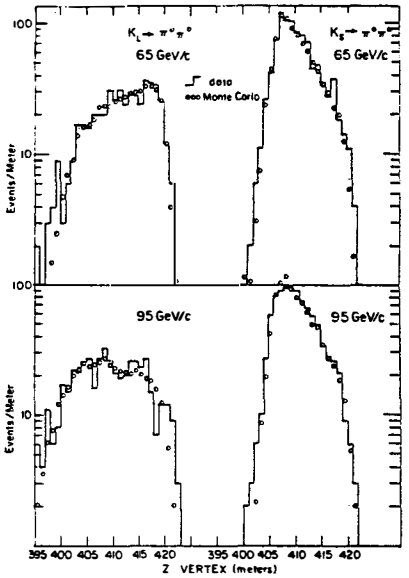
$K_L \to \pi^+\pi^-\pi^0$
65 GeV/c
data
Monte Carlo
$K_S \to \pi^+\pi^-\pi^0$
65 GeV/c
95 GeV/c
95 GeV/c
Events/Meter
Z VERTEX (meters)

Fig. 3

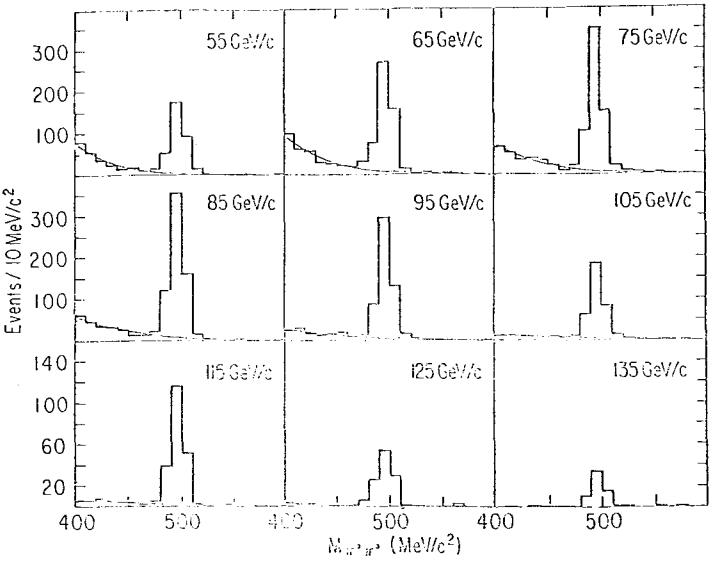
55 GeV/c
65 GeV/c
75 GeV/c
85 GeV/c
95 GeV/c
105 GeV/c
115 GeV/c
125 GeV/c
135 GeV/c
Events/10 MeV/c²

Fig. 4

A Measurement of ε'/ε

Michael P. Schmidt
Yale University

ABSTRACT

Results are presented for the recent Yale-BNL measurement of the ε'/ε at the Brookhaven AGS.

INTRODUCTION

After twenty years of intense scrutiny, CP violation is apparently still well described, if not explained, by the "superweak" hypothesis[1], in which $|\Delta S| = 2$, T-violating transitions between the K^0, $\bar{K}^0$ states induce CP violating impurities in the K^0_L, K^0_S states. CP-violating effects observed in the $K^0 - \bar{K}^0$ system can be described in terms of one parameter, $|\varepsilon| \simeq 2 \times 10^{-3}$, which defines the portion of the CP-even state K^0_1 found in the predominantly CP-odd K^0_L state: $K^0_L \propto K^0_2 + \varepsilon K^0_1$. The phase of ε itself is determined from CP conserving considerations $\arg(\varepsilon) = \tan^{-1}(2\Delta m/\Gamma_S)$, where Δm is the $K_L - K_S$ mass difference and Γ_S is the K_S decay rate. Despite sensitive searches for effects in other systems, such as the electric dipole moment of the neutron or T-odd correlations in nuclear beta decay and $K_{\mu 3}$ decays, the observation of CP violation is as yet confined to the $K^0 - \bar{K}^0$ system.

A precise measurement of the relative rates for the CP-violating decays $K^0_L \to \pi^+\pi^-$ and $K^0_L \to \pi^0\pi^0$ in principle provides a test for $|\Delta S| = 1$, CP-violating decay amplitudes which result in deviations from the "superweak" prediction: $\eta^{+-} = \eta^{00} = \varepsilon$, where η^{+-} and η^{00} are the ratios of K_L to K_S decay amplitudes into $\pi^+\pi^-$ and $\pi^0\pi^0$ final states. Gauge theory models of CP violation are in general constructed to nearly mimic the "superweak" predictions by having the dominant contribution to CP violation arise from complex terms in the $K^0 - \bar{K}^0$ mixing amplitudes. However, there are usually additional contributions in the form of direct CP violating $|\Delta S| = 1$ decay amplitudes, parametrized by ε', which are not identical for the weak transitions into $\pi\pi$ isospin I = 0 and 2 final states. One can write $\varepsilon' \simeq \mathrm{Im}A_2/\sqrt{2}\,\mathrm{Re}A_0 \exp\left(i(\pi/2 + \delta_2 - \delta_0)\right)$ in terms of the $\pi\pi$ isospin (I = 0,2) decay amplitudes A_I and final state interaction phase shifts δ_I. The effect of the direct amplitude is apparent from the relations $\eta^{+-} \simeq \varepsilon + \varepsilon'$ and $\eta^{00} \simeq \varepsilon - 2\varepsilon'$, yielding $R = |\eta^{+-}|^2/|\eta^{00}|^2 = 1 + 6\,\mathrm{Re}(\varepsilon'/\varepsilon)$. It is fortuitous that nature has conspired to have $\arg(\varepsilon') \approx \arg(\varepsilon)$ providing

experimentalists with the possibility of detecting a nonvanishing value for ε'.

THE EXPERIMENT

The Yale-BNL[2] group has recently completed a measurement of R and thus ε'/ε at the Brookhaven AGS. The experiment is conceptually simple, involving a neutral beam passing through the center of a dual spectrometer (Fig. 1) consisting of multiwire proportional chambers and scintillation counter arrays placed about a spectrometer magnet (61 cm gap, Δp_t = 150 MeV/c) followed by a large lead glass array. The detector was simultaneously sensitive to charged and neutral decays through different regions of solid angle. The relative intensities for $K^0 \to \pi^+\pi^-$ and $K^0 \to \pi^0\pi^0$ decays were

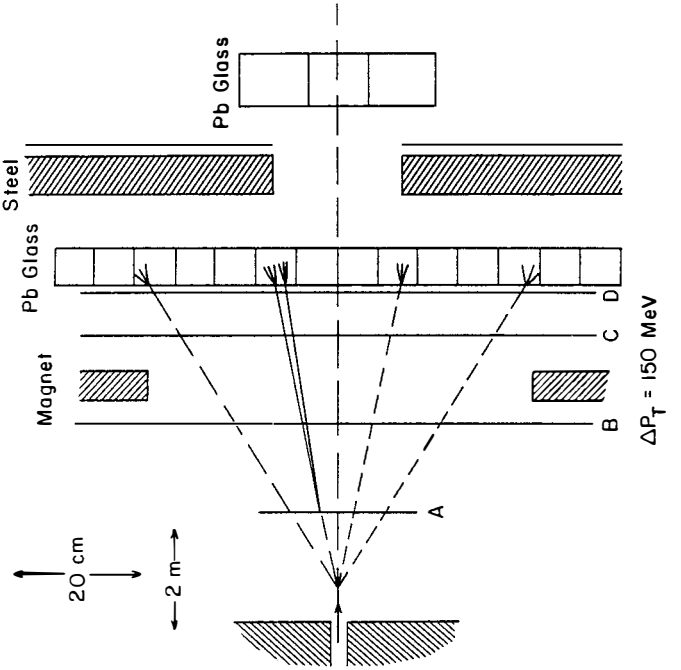

Figure 1. Schematic representation of the detector (elevation view) illustrating a $K^0 \to \pi^0\pi^0$ decay in the non-bending plane. Proportional wire chambers are shown as A, B, C and D. A 1 mm lead sheet is placed just upstream of the A plane. Scintillation counters used to define the trigger are not shown.

determined under two beam conditions: first, a K^0_L beam and second, a predominantly K^0_S beam as afforded by a removable 80 cm long reactor graphite (p = 1.72) regenerator, which was placed with the exit face 120 cm upstream of the beginning of the 120 cm fiducial decay volume.

The determination of R is obtained by taking the ratio of intensity ratios $R = R_L/R_S$ where $R_L = I(K_L \to \pi^+\pi^-)/I(K_L \to \pi^0\pi^0)$ and $R_S = I(K_S \to \pi^+\pi^-)/I(K_S \to \pi^0\pi^0)$. With neutral $(\pi^0\pi^0)$ and charged $(\pi^+\pi^-)$ decay modes detected simultaneously the measurement is self normalizing. The detector acceptance and efficiency also cancels if the ratios are computed within K^0 energy (E_K) and decay position (Z_K) intervals for which the differential intensity variations are small. The beam condition, K_L or K_S, was changed several times per shift, to reduce possible biases associated with long term variations in the detector response. Trigger and veto logic, constructed with 100K ECL circuitry, was carefully designed to avoid dead time biases between the event types[3].

The detector operated in a zero degree neutral beam line (Fig. 2), with an acceptance of 3.5 μsr, derived from 28 GeV/c protons incident on a 20 cm long copper target. The proton beam dump was situated in the first sweeping

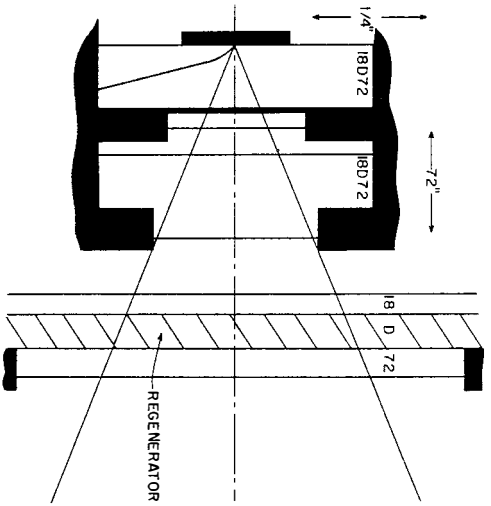

Figure 2. Schematic representation of the zero degree neutral beam line.

magnet. A 3 cm lead plug upstream of the first brass collimator converted gamma rays from the target. In the K^0_L running mode about 10^{12} protons/pulse (< 1 sec) were put on target generating about 3×10^8 neutrons and 4×10^6 K^0_L. This resulted in about 4×10^6 counts/sec in the large PWC upstream of the spectrometer magnet (B). We note that this rate is nearly 10 times that expected from K decays and neutron interactions in the detector region. These rates were found to drop by a factor of 2 when the primary beam was steered off target.

Neutral event triggers were required to have one and only one gamma ray (from the π^0 decays) convert in a 1 mm thick lead sheet at the end of the decay volume. In addition the energy deposited in the lead glass array, as determined from a fast analog sum, was required to be greater than 6 GeV, with at least 1.5 GeV deposited in the upper and lower halves of the array. Neutral events were required to have 7 GeV < E_K < 14 GeV, and 1 GeV < E_i < 8 GeV for each of the unconverted gamma rays. The converted pair trajectories in combination with the narrow neutral beam ($\sigma_r \approx 0.5$ cm, in the decay zone) allowed a determination of the decay vertex ($\sigma_z \approx 13$ cm). The energies and positions of the unconverted gamma rays were determined in 208 elements (SF2, 6.5 cm × 6.5 cm × 51 cm) of lead glass arranged in a roughly 90 cm × 90 cm array with a 13 cm × 13 cm hole for passing the neutral beam. Backgrounds for $K^0_L \to 2\pi^0$ due to $K^0_L \to 3\pi^0$ were largely suppressed by the detection of extra gamma rays outside the lead glass array. This was accomplished by lead-scintillator veto counters upstream of the spectrometer magnet and an additional small array (30 cm × 30 cm) of lead glass (8 elements) downstream of the main array. The 10 cm × 10 cm hole in this small array subtended a solid angle from the decay region of only 10^{-4} sr.

Charged event triggers required two charged particles on opposite sides of the neutral beam as defined by scintillation counters, beginning with a set located in a 4 cm high horizontal gap in the gamma converter. The

charged events were reconstructed from the trajectories found in the proportional wire chambers which consisted of 4 arrays: A(X,Y; 2 mm pitch; 128 wires each), B (X,X' (in vernier), & Y; 3 mm pitch; 256 wires each), C (X,Y & θ; 3 mm pitch, 256 wires each) and D (X,X' (in vernier), & Y; 3 mm pitch; 256 wires each). Backgrounds due to $K_{\mu 3}$ decays were largely suppressed by vetos from a scintillation counter array behind a 60 cm steel wall following the lead glass array. K_{e3} backgrounds were largely eliminated (on-line) by the electron identification afforded by the lead glass array. Charged events were required to have 7 GeV < E_K < 14 GeV and 2 GeV/c < p_i < 8 GeV/c for the charged secondaries.

Data acquisition was accomplished via our Brookhaven Fastbus system.[4] This is a 32 bit multiplexed (address/data) system sporting ECL circuitry transaction speeds (≈ 100 nsec), logical addressing, and water cooled devices (< 70 WATTS; < 250 IC per card). The system consisted of three FASTBUS crate segments, two FASTBUS cable segments with three segment interconnects, an interface to the PDP11-44 on-line computer, and about 25 data acquisition and control cards.

Roughly 200 triggers per pulse were processed on-line, with about 3 events per pulse written to tape. About 30 tapes (800 bpi) were written during the February-March 1984 run. This event sample includes momentum analyzed electrons used for the lead glass calibration.

RESULTS

Figure 3 shows the mass plot distributions for events accepted by the off-line analysis. Charged events were required to fit, in addition to particle identification criteria, kinematics expected of a two body decay. Events were selected with "χ_c^2" = $(\Delta\theta/0.75\ \text{mr})^2 + (\Delta p_t/20\ \text{MeV/c})^2 < 3$, where $\Delta\theta$ and Δp_t measure the acoplanarity and transverse momentum imbalance for the event. Neutral events were required to have the topology of a $2\pi^0$ event with "χ_n^2" = $(\bar{X}/2\text{cm})^2 + (\bar{Y}/2\text{cm})^2 + (\Delta Q_1/10\ \text{MeV})^2 + (\Delta Q_2/10\ \text{MeV})^2 < 10$, where $\bar{X}$ and

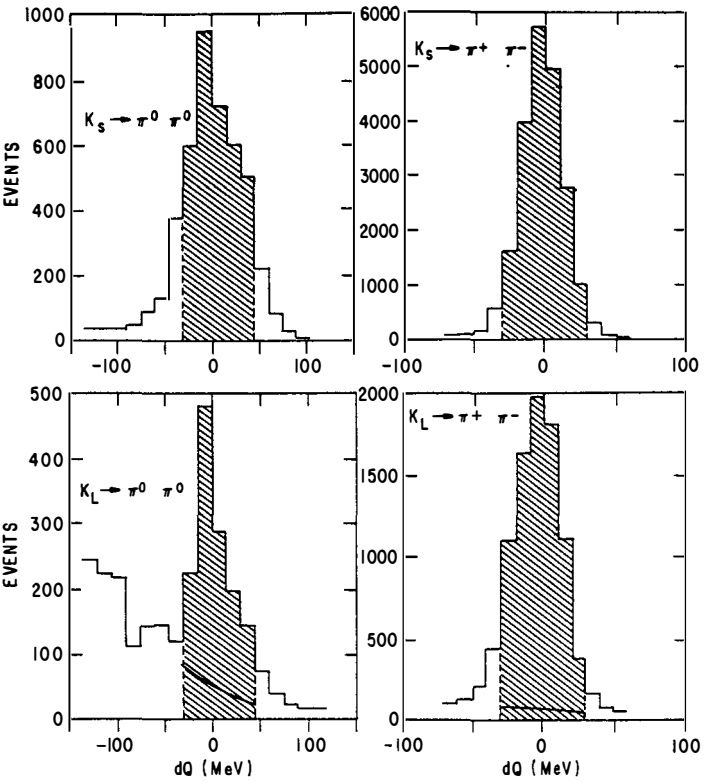

Figure 3. Measured invariant mass distributions for the four event types. Fiducial regions used in the analysis are cross hatched.

$\bar{Y}$ are the first moments of energy in the lead glass array, and ΔQ_1, ΔQ_2 are the differences between the reconstructed and true π^0 mass for the two best gamma pair combinations.

The final event sample (cross hatched in Fig. 3) contains 1361 $K^0_L \to 2\pi^0$, 3537 $K^0_S \to 2\pi^0$, 8680 $K^0_L \to \pi^+\pi^-$ and 20963 $K^0_S \to \pi^+\pi^-$ events. A value for R was found through a statistically weighted mean of values of R determined for 42 data bins defined by seven 1 GeV intervals of energy (E_K) and six 20 cm intervals of the fiducial decay space (Z_K). This

allowed the required cancellation of acceptance factors, despite the differences in energy and decay position distribution for the four event types. Explicit dependence on Monte Carlo results was not required although such calculations agreed with the observed distributions. The background for $K^0_L \to 2\pi^0$, primarily due to $K^0_L \to 3\pi^0$ decays (and neutron interactions with helium in the decay volume), is found to be 17.5 ± 3.0% of the signal (-30 MeV $< \Delta Q <$ + 45 MeV in Fig. 3) when averaged over the 42 data bins. Monte Carlo calculations show that the shape of the 3 π^0 background does not vary appreciably over different sectors of E_K and Z_K. Further small corrections of the order of 2% are required for backgrounds in the other modes, for incoherent K_S production and for K_L dilution of the nominal K_S decays. Applying these corrections we obtain R = 1.010 ± 0.043 (stat) ± 0.026 (sys), and compounding the errors we find ε'/ε = 0.0017 ± 0.0082 consistent with zero, with previous results[5,6], and with the recent value obtained at Fermilab[7] of $\varepsilon'/\varepsilon = -0.0046 \pm 0.0058$ (again, errors have been compounded). If we permit ourselves to combine these two most recent results (note that the systematic errors in the two experiments are dominated by different sources) we find $\varepsilon'/\varepsilon = -0.0025 \pm 0.0047$, a value which is not in agreement with the expectations of milliweak Higgs models ($\varepsilon'/\varepsilon < -0.02$) or the KM 6-quark model ($\varepsilon'/\varepsilon > 0.01$; for $m_t < 60$ GeV/c, $\tau_B > 1$ psec and the bag factor B ≈ 1/3) of CP violation.[8]

This work is supported in part by the U.S. Department of Energy under Contract Numbers DE-AC02-76ER03075 and DE-AC02-76CH00016

REFERENCES

1. L. Wolfenstein, Phys. Rev. Lett. 13, 562 (1964).
2. J.K. Black, R.K. Adair, S.R. Blatt, M.K. Campbell, H. Kasha, M. Mannelli, M.P. Schmidt, C.B. Schwarz, R.C. Larsen, L.B. Leipuner, and W.M. Morse, to be published in Phys. Rev. Lett.
3. J.K. Black, Yale University Doctoral Thesis (1984, unpublished).
4. L.B. Leipuner, et al., IEEE Trans. on Nucl. Sci. NS-30, 3733 (1983); G. Benenson, et al., ibid, 3958; and W.M. Morse, et al., ibid, 3964; M.P. Schmidt, et al., IEEE Trans. on Nucl. Sci. NS-31, 203 (1984); J.K. Black, et al., ibid, 201 (1984), and reference 3.
5. M. Banner, et al., Phys. Rev. Lett. 28, 1597 (1972); M. Holder, et al., Phys. Lett. 40B, 141 (1972).
6. W.M. Morse, Proceedings, Conference on "Flavor Mixing in Weak Interactions", Erice, March 1984 (BNL-35087), and reference 3.
7. K. Nishikawa, et al., Proceedings XXIII International Conference on High Energy Physics, Leipzig (1984).
8. A.J. Buras, Proceedings, Workshop on the Future of Intermediate Energy Physics in Europe, Freiburg, April 1984, and references therein.

CURRENT SEARCHES FOR THE ELECTRIC DIPOLE MOMENT OF THE NEUTRON

Pedro C. Miranda
Institut Laue-Langevin
156X, Grenoble Cedex, France

ABSTRACT

The two most sensitive experiments currently searching for a neutron electric dipole moment (ILL, France and LNPI, USSR) are described. The present upper limit on the neutron EDM is $|d_n| \leq 4 \times 10^{-25}$ e.cm at the 90% confidence level. An improvement on this limit by about one order of magnitude is expected in the near future.

INTRODUCTION

The existence of an electric dipole moment (EDM) of the neutron would be direct evidence of both P and T violation and, by implication, CP violation. The table below, taken from "CP Violation in the Standard Model and Beyond"[1] shows a few theoretical

Model	d_n
STANDARD (3 generations)	$<10^{-30}$ e.cm
MORE HIGGS DOUBLETS	$(0.3\text{-}1.0)\times10^{-25}$ e.cm
HORIZONTAL INTERACTIONS	$>10^{-28}$ e.cm
LEFT-RIGHT SYMMETRIC MODELS	3×10^{-27} e.m
SUSY	$<10^{-25}$ e.cm

predictions for the value of the neutron EDM, d_n. The present experimental upper limit: $|d_n| < 4\times10^{-25}$ e.cm at the 90% confidence level has already eliminated some calculations. Improving this limit by one order of magnitude will exclude some more calculations and further constrain some models' parameters, especially if a non-zero value of d_n is measured.

THE EXPERIMENTS

One experiment is situated at the Institut Laue-Langevin (ILL), Grenoble, France and the other at the Leningrad Nuclear Physics Institute, Gatchina, USSR.

The two experiments have important common features. They both use ultra-cold neutrons (UCN), neutrons that are so slow ($v \leq 6$ m/s) that they are reflected by many material surfaces for all angles of incidence and can therefore be contained in a neutron bottle for many seconds. They both use, also, the principle of magnetic resonance to detect shifts in the Larmor precession frequency of the neutron in a static magnetic field B_o when an electric field, parallel or antiparallel to B_o, is applied. Since $h\nu = -\vec{\mu}_B\cdot\vec{B} - \vec{d}_n\cdot\vec{E}$, the shift in the precession frequency on reversing the direction of the electric field is $\Delta\nu = 4|d_n|E/h$, provided B_o remains constant.

The apparatus set up at the ILL by the Harvard-Sussex-RAL-ILL collaboration is shown in figure 1[2]. The storage volume consists of a BeO cylinder 25 cm in diameter and 10 cm long separating two Be plates, one of them being grounded and the other kept at ± 120 kV. A coil is used to generate a steady field B_o perpendicular to the Be plates, which is usually set at 10 mgauss corresponding to a neutron precession frequency of 30 Hz. The magnetic field is monitored by 3 Rb optical pumping magnetometers scattered about the storage volume. Surrounding

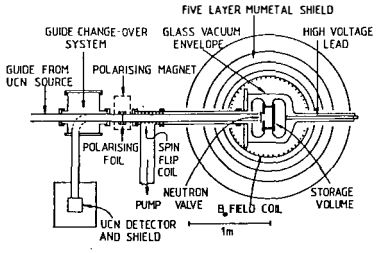

Fig. 1

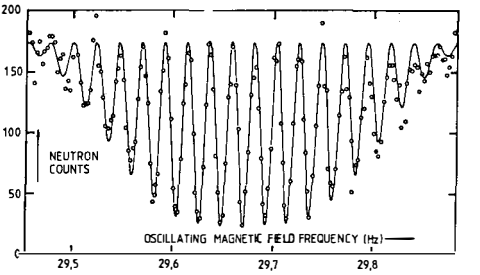

Fig. 2

the whole is a 5-layer mu-metal shield ensuring a high uniformity and time stability of the field.

Ultra-cold neutrons from a water converter at 320K are brought to the experiment via a Ni-coated glass guide and are directed towards a transmission polarizer. At the entrance of the change-over system the UCN density is $\sim$ 1.5 UCN/cm^3. The density of polarized UCN in the storage volume is allowed to build up for 10 sec and reaches the value of 0.2 polarized UCN/cm^3 detected by the counter. The neutron valve is then closed and an oscillating magnetic field applied for 2 sec in order to flip the spins from the B_o direction into the perpendicular plane where they are left to precess for typically 80 sec. During this storage time the number of UCN decays exponentially with a time constant of 70 sec because of losses due to collisions with the walls. Meanwhile the change-over system has switched over allowing the neutrons in the guide tube outside the storage volume to fall down into the ^{3}He proportional counter. A second 2 sec burst of oscillating field coherent with the first one is applied, the neutron valve is opened and the neutrons with the right spin-state diffuse past the polarizer into the detector. At resonance, i.e. when the frequency of the oscillating field is exactly equal to the average neutron precession frequency, the net effect of the two pulses is a 180° flip of the spin and so very few neutrons are counted. A typical resonance curve is shown in figure 2[2)]. After a counting time of 12 sec an adiabatic 180° spin flip coil is energised and the neutrons which couldn't previously pass through the polarizer are also counted for 12 sec. The storage volume is then filled again to start another cycle.

In practice the resonant frequency is determined by counting neutrons at the half-height, first on one side then on the other of the center valley of the resonance curve, as these are the points of greatest slope. Such pairs of neutron counts are accumulated for approximately one hour, then the direction of the electric field is reversed and more pairs of neutron counts accumulated, and so

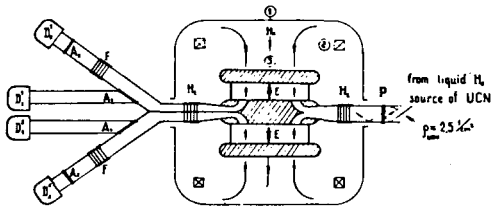

Fig. 3

on. In the data analysis one looks for a correlation between the resonance frequency and the direction of the electric field; the analysis of the data collected so far has yielded the result $d_n = (-3.2 \pm 3.5) \times 10^{-25}$ e.cm or $|d_n| < 8 \times 10^{-25}$ e.cm at the 90% confidence level. At present the experimental sensitivity is limited only by counting statistics, as no systematic errors have been detected. During the last half of the data taking period the neutron density available was down by a factor of 4 on the value mentioned earlier.

The experimental set up at Gatchina is shown schematically in figure 3[3]. UCN are confined in two chambers, 55 cm in diameter and 7 - 10 cm high, with oppositely directed fields of about 15 kV/cm. It is a "continuous flow" type spectrometer, i.e. the UCN simply diffuse from the input to the output guide spending on average some 5 sec in the chambers. The stability of the 28 mgauss uniform static field is achieved by using a 3-layer magnetic shield. In addition, Helmholtz coils and a fluxgate are used to compensate for fluctuations in the external field, while a Cs optical pumping magnetometer is used to lock the field inside the shield to a constant value.

A neutron guide extracts UCN from a liquid hydrogen moderator and transports them towards the entrance of the spectrometer where the UCN density is 2 UCN/cm^3. A transmission polarizer then selects one spin orientation. The coil wound around the input guide superimposes an oscillating magnetic field on a static inhomogeneous field and flips the spins adiabatically through 90°. Thus the neutrons wander through the chambers precessing in a plane perpendicular to the direction of the static fields B_o,E. On leaving the chambers they are subjected to another adiabatic 90° spin flip. There are two sets of two detectors so that the neutron counts from the upper and lower chambers can be monitored independently. A combination of analysis polarizers and 180° spin flippers enables both spin components to be monitored simultaneously on two different detectors.

Frequency shifts are detected by setting the frequency to its resonance value and introducing a ± 90% phase difference between the two adiabatic spin flips, which amounts to working on the points of steepest slope of the UCN

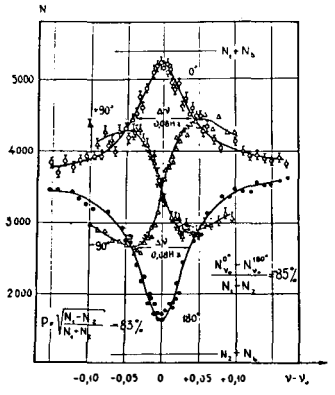

Fig. 4

count vs frequency curves shown in figure 4[4]. The sign of ± 90° phase difference is reversed every 100 sec and the electric field polarity is reversed every 200 sec; hence a basic set of measurements lasts 400 sec. Again, the principle of data analysis is to look for a correlation between the resonance frequency and the electric field direction. This experiment led to the result $d_n = (-2 \pm 1) \times 10^{-25}$ e.cm or $|d_n| < 4 \times 10^{-25}$ at the 90% confidence level[5].

In this type of experiment there are 3 major sources of spurious EDM signals. The $\vec{v} \times \vec{E}$ effect, whereby a neutron travelling with velocity v in an electric field E experiences a magnetic field proportional to $\vec{v} \times \vec{E}$, was the main reason for abandoning beam experiments in favour of UCN storage ones where the effective v is much smaller. For the ILL experiment the $\vec{v} \times \vec{E}$ effect contribution to the EDM signal is estimated at $\sim 10^{-27}$ e.cm, but this could be as much as 10^{-25} e.cm for the Gatchina experiment. Leakage currents are another source of spurious signals since currents leaking from the high voltage plate to the grounded one will produce local magnetic fields which would be correlated to the electric field direction. At ILL, the leakage current is kept under 50 nA, ensuring that any contribution to the EDM signal is $< 10^{-26}$ e.cm. The leakage currents probably exceed 100 nA at Gatchina, where higher currents are perhaps tolerable because of partial cancellation of spurious fields in a double chamber arrangement. A third source of spurious signals are any changes in the static magnetic field correlated with the high voltage polarity. In the ILL set-up three Rb magnetometers are used to monitor the field and check that its contribution to the EDM signal is $\leq 10^{-25}$ e.cm. In the Gatchina set-up a real EDM signal will have opposite signs on the upper and lower chamber whereas a signal due to fluctuations in the magnetic field will have the same sign in both chambers. On the whole, we believe that the two apparatuses have similar intrinsic sensitivities but that the ILL's is less suject to systematic errors.

PROSPECTS

Both teams are now working at improving their equipment. At ILL new UCN sources are being developed and by the end of 1985 the UCN flux available should be 50 - 200 times greater than that used towards the end of the last data taking period. The magnetometers, which measure the field only 4 - 5 times more accurately than the neutrons themselves, are being rebuilt in order to reduce their

noise. With these improvements the error on the EDM should be brought down to $\sim 3 \times 10^{-26}$ e.cm by the end of 1986. At Gatchina more radical changes are under way: the continuous flow spectrometer has been replaced by a storage bottle type experiment, most likely in an attempt to overcome $\vec{v} \times \vec{E}$ effects. This should result in a gain in sensitivity of a factor 2 - 3. A superconducting shield will be used to achieve the required increase in time stability of the magnetic field. Improvements in the liquid hydrogen UCN source should enhance the flux by a factor of 5 - 6 and it is therefore expected that the error on the EDM will decrease to $\sim 2 \times 10^{-26}$ e.cm in one or two years' time.

REFERENCES

1) A.J. Buras, MPI-PAE/PTH 46/48. Invited talk presented at the "Workshop on the future on medium energy physics in Europe", 10 - 13 April 1984, Freiburg. To appear in the Proceedings.
2) J.M. Pendlebury et al., Phys. Lett. 136B (1984) 327.
3) I.S. Altarev et al., Phys. Lett. 102B (1981) 13.
4) I.S. Altarev et al., Nucl. Phys. A341 (1980) 269.
5) V.M. Lobashev, A.P. Serebrov, Journal de Physique C3 45 (1984) 11.

WHERE ARE CP-VIOLATING EFFECTS LARGE?

Lincoln Wolfenstein
Physics Department
Carnegie-Mellon University

ABSTRACT

The Kobayashi-Maskawa (KM) model of CP violation requires a large phase in the quark mixing matrix in order to agree with present data. The question of whether CP violation is in some sense maximal is discussed. As a result of the large phase there should be large CP-violating effects observable and these are shown uniquely to occur in the B°-$\overline{B}^\circ$ system.

Twenty years after the discovery of CP violation there still is only one CP-violating effect that has been measured. The effect is given by the parameter ε with a magnitude of 2.3×10^{-3}. Thus empirically CP violation appears to be a small effect. Here we wish to look at the possibility that in some sense CP violation is large and that there may be large effects observable (in principle, at least) in other processes.

The most conservative model of CP violation is that of Kobayashi and Maskawa (KM) who ascribe all CP violation to a phase in the quark mixing matrix within the standard SU(2) x U(1) electroweak theory. Recent data on B decays leads to the conclusion that in order to obtain a large enough value for ε in this model it is necessary that the phase be large. This leads us to the question whether the phase is 90°, corresponding in some sense to maximal CP violation. As we shall see this question cannot be phrased unambiguously and probably has a negative answer when posed in the most straightforward way. A more interesting question is whether the mass matrix in some sense violates CP maximally and this is possible.

Given the large phase in the KM matrix it is natural to ask whether this leads to large CP violating effects in some cases. It is easy to identify the processes where this is possible; they turn out to be in B° decays. Unfortunately the proposed experiments are extremely difficult.

It is convenient on purely empirical grounds to expand the KM matrix in powers of a parameter λ, which is equal to the Cabibbo angle. To order λ^3

$$\begin{pmatrix} V_{ud} & V_{us} & V_{ub} \\ V_{cd} & V_{cs} & V_{cb} \\ V_{td} & V_{ts} & V_{tb} \end{pmatrix} = \begin{pmatrix} 1-\lambda^2/2 & \lambda & A\lambda^3(\rho-i\eta) \\ -\lambda & 1-\lambda^2/2 & A\lambda^2 \\ A\lambda^3(1-\rho-i\eta) & -A\lambda^2 & 1 \end{pmatrix} \tag{1}$$

From the rates of semi-leptonic K and B decays[1]

$$\begin{aligned} \lambda &= .22 \\ A &= 1 \pm 0.2 \\ \rho^2 + \eta^2 &\lesssim 0.3 \end{aligned} \tag{2}$$

The phase convention I use emphasizes the fact that CP violation enters only at the order λ^3. A reduction of the uncertainty in the lifetime of B mesons will help to constrain A, although there remains a theoretical uncertainty that may be 10% in A. The observation of the decay $b \to ue\nu$ would allow a determination of $\rho^2 + \eta^2$. Any additional information on the parameters must come from analyzing CP-violating effects.[2] We assume throughout only three generations;

the possibility of additional generations could seriously modify our discussion.[3]

The standard evaluation of ε using the box diagram is well approximated for m_t around 45 Gev by[4]

$$\varepsilon = 3.1 \times 10^{-3} A^2 \eta B [1 + (1/2) A^2 (1-\rho) (m_t/42\text{Gev})^2] \qquad (3)$$

While there are some uncertainties relative to strong-interaction corrections in this evaluation, by far the main uncertainty concerns B which parameterizes the matrix element

$$\langle \bar{K}^0 | \bar{S}_L \gamma^\lambda d_L \; \bar{S}_L \gamma_\lambda d_L | K^0 \rangle$$

where S_L, d_L are left-handed quark field operators. The value B=1 corresponds to the insertion of the vacuum in all possible ways as originally done by Gaillard and Lee.[5] The bag model gives |B| of the order of one-third but is very sensitive to bag model parameters in part because V and A contributions cancel. The use of the soft pion approximation plus SU(3) provides a relation[6] between B and the rate for the $\Delta I=3/2$ K^+ decay yielding B=1/3. This approximation is precarious because the expansion parameter is $(M_K/\Lambda)^2$ where Λ is of the order of 1Gev so that one is at the mercy of numerical coefficients. Using SU(3) x SU(3) chiral perturbation theory Mark Wise has calculated the correction to this approximation and found it to be 100% because of a large numerical coefficient. (Note that soft pions plus SU(2) is much more reliable because the expansion parameter is $(M_\pi/\Lambda)^2$.) His conclusion is that the approximation is invalid in this case.[7]

Even with B=1 if we set A=1 and M_t=45Gev the values of η and ρ are highly constrained. From Eqs. (2) and (3) we have

$$\eta = 0.4 \text{ to } 0.55 \qquad (4)$$
$$\rho = -0.4 \text{ to } 0.2$$

The corresponding values of the phases of the corner elements of the KM matrix are

$$|\text{phase of } V_{ub}| = 45^\circ \text{ to } 110^\circ$$
$$|\text{phase of } V_{td}| = 15^\circ \text{ to } 30^\circ$$

Thus the phase of V_{ub}, which is the same as the phase δ in the Maiani

representation of the KM matrix, can be 90° but the phase of V_{td} cannot.

In order to treat all three generations symmetrically in the parameterization of the KM matrix we have suggested the following form[8]

$$V = \exp i\,(H_1 + H_2 + H_3) \tag{5}$$

$$H_1 = \begin{pmatrix} 0 & -i\theta_1 e^{-i\phi_1} & 0 \\ i\theta_1 e^{i\phi_1} & 0 & 0 \\ 0 & 0 & 0 \end{pmatrix}$$

$$H_2 = \begin{pmatrix} 0 & 0 & 0 \\ 0 & 0 & -i\theta_2 e^{-i\phi_2} \\ 0 & i\theta_2 e^{i\phi_2} & 0 \end{pmatrix}$$

$$H_3 = \begin{pmatrix} 0 & 0 & -i\theta_3 e^{-i\phi_3} \\ 0 & 0 & 0 \\ i\theta_3 e^{+i\phi_3} & 0 & 0 \end{pmatrix}$$

It is easy to show that by a choice of phase convention one can set two of the ϕ_i equal to zero but that the combination

$$\Phi = \phi_3 - \phi_1 - \phi_2 \tag{6}$$

is invariant.[9] Our form Eq. (1) is reproduced by choosing $\phi_1 = \phi_2 = 0$ and

$$\begin{aligned} \sin\theta_1 &= \lambda \\ \theta_2 &= A\lambda^2 \\ \theta_3 e^{i\Phi} &= \theta_3 e^{i\phi_3} = A\lambda^3\,(\rho - 1/2 + i\eta) \end{aligned} \tag{7}$$

Of course, Eq. (5) is exactly unitary whereas Eq. (1) is only unitary to order λ^3. A natural way to define maximum CP violation is to choose the invariant phase Φ as $\pm 90°$; this requires $\rho = 1/2$, which is inconsistent with the solution (4), and is barely consistent with the constraint (2). Thus we conclude that the most straightforward unambiguous criterion for maximum CP violation of the KM matrix is probably not satisfied. Gronau and Schechter and independently Roos[9] have suggested an alternative

$$V = \pi_{ijk} \; e^{iH_i} \; e^{iH_j} \; e^{iH_k}$$

where (i,j,k) represent some permutation of (1,2,3) and the result now depends on the ordering because the H_i do not commute. As a result the relation between $\theta_3 e^{i\phi 3}$ and ρ is not that of Eq. (7) but depends on the ordering with $(\rho - 1/2)$ in Eq. (7) replaced either by ρ or $(\rho - 1)$. The condition for maximum CP violation is therefore ambiguous corresponding either to $\rho=0$ (phase $V_{ub} = 90°$) or $\rho=1$ (phase $V_{td} = 90°$). The first of these is consistent with present data.

The mass matrix itself is more fundamental than the KM matrix. Our empirical knowledge of the mass matrix is much less than that of the KM matrix, however. It is nevertheless interesting to consider possible forms for the mass matrix with the idea of maximal CP violation in mind. One possibility suggested by Stech[10] has the following form

$$M_d = kM_u + M_1 \tag{8}$$

where M_u is the up mass matrix in diagonal form, k is a number, and M_1 is an antisymmetric hermitean matrix. This form of M_1 may be considered as the assumption of maximal CP violation because M_1 has only imaginary elements. This means that all the quark mixing is associated with a CP-odd term in the mass matrix. This is quite similar in spirit to our previous assumption that $\phi = 90°$ in Eq. (6) corresponding to all $\phi_i = 90°$. A detailed calculation shows that Stech's assumption can be satisfied if

$$\rho \simeq -\frac{\lambda^4 m_b}{m_s}\eta^2 \simeq 0 \tag{9}$$

Thus this version of maximal CP violation predicts ρ close to zero which is consistent with present empirical constraints.

An alternative considered by Michael Shin[11] and collaborators can be based on the ansatz

$$\begin{aligned} M_u &= M_o + iM_1 \\ M_d &= kM_o + k'M_1 \end{aligned} \tag{10}$$

with M_o, M_1 having the Fritzsch form

$$M_o = \begin{pmatrix} 0 & 0 & 0 \\ 0 & 0 & b \\ 0 & b & c \end{pmatrix} \quad M_1 = \begin{pmatrix} 0 & a & 0 \\ a & 0 & 0 \\ 0 & 0 & 0 \end{pmatrix}$$

The i in the form of M_u represents Shin's assumption for maximal CP violation. This can be shown also to correspond to $\rho \simeq 0$.

Since the KM matrix appears to have a large CP-violating phase we now turn to the question of where this phase could produce large CP-violating observables. We note first that a CP-odd intensity term must be proportional to

$$I = \theta_1\ \theta_2\ \theta_3\ \sin\Phi = \imath/2 \det(H_1 + H_2 + H_3) = A^2\lambda^6\eta \tag{11}$$

The reason is that if one of the θ's, say θ_k, is chosen equal to zero it is possible by a choice of phase convention to set $\Phi = \phi_k$ but clearly ϕ_k is meaningless if $\theta_k = 0$. The CP-violating effect is given by (I/R) where R is a CP-even intensity. In order to get a large CP violating observable it is necessary that R also be of order λ^6. On the other hand if R is of order λ^n with $n < 6$, the CP violating effect is of order λ^{6-n}.

To illustrate what I mean let me first look at the K° system. The decay amplitude in terms of quarks is dominated by

$$s \to u + \bar{u} + d \tag{12}$$

which is CP-even in our phase convention. The CP-violating effect ϵ is well-described by the K°-$\bar{K}^\circ$ mixing due to the box diagram:

$$\epsilon = \frac{\text{(CP-odd) Box}}{\text{(CP-even) Box}}$$

Let us look at one side of the box diagram. There are CP-even contributions from intermediate u or c quarks proportional to

$$\text{Re (Side)} \sim V_{du} V_{su} \quad \text{or} \quad V_{dc} V_{sc} \sim \lambda \tag{13a}$$

On the other hand the CP-odd contribution from the intermediate t is proportional to

$$\text{Im (Side)} \sim \text{Im} V_{dt} V_{st}^* = A^2\lambda^5\eta \tag{13b}$$

It follows that

$$\varepsilon \sim \frac{\text{Im(Side) Re(Side)}}{\text{Re(Side) Re(Side)}}$$

$$\sim \frac{A^2\lambda^6\eta}{\lambda^2} = 2.3 \times 10^{-3} A^2\eta \qquad (14)$$

Thus the small value of ε in the standard model as given in Eq. (3) is due to the smallness of the mixing angles given by the factor λ^4 rather than the smallness of the CP-violating factor η. [Eq. (13) is slightly misleading because the dependence on quark masses is missing; actually the numerator factor λ^6 should be multiplied by $\ln(m_t/m_c)^2$ and there is an additional term in the numerator of order $A^4\lambda^{10}(m_t/m_c)^2$; for $m_t \sim 45$Gev the qualitative conclusion is unchanged.]

A similar analysis for the heavier analogues of the K° is shown in Table 1. It is seen that there are two systems, $(\bar{d}b)$ and $(\bar{t}u)$, for which the CP-violating effects are of order 1, that is, λ°. Note that in all cases Re(Side) Im(Side) $\sim A^2\lambda^6$; the large CP-violating effects come when all terms contributing to Re(Side) are of order λ^3. The two examples can be identified by inspection looking at Eq. (1). In order for these effects, which are associated with the mass matrix to be useful, it is necessary that the two mass eigenstates can be distinguished during the meson's lifetime. In the case of the K° this can be done in two different ways. Because $\Gamma_S \gg \Gamma_L$ it is possible to obtain a beam of pure K_L to study. Also because $\Delta m \sim \Gamma_S$ it is possible to observe the effects of oscillations before the K_S has disappeared.

TABLE 1

Box diagrams for K°-$\bar{K}^\circ$ mixing and analogous systems. Products of KM elements contributing to the real or imaginary part of a side are indicated. When all intermediate states give the contributions of the same order the symbol j is used; this is the case for Re(Side) for B° and T_u. For the other cases two intermediate states give the same order and the other is different; in these cases just one intermediate quark is noted.

	Re(Side)	Im(Side)	ε/η
$\bar{K}^\circ(\bar{d}s)$	$V_{cd}V_{cs}^* \sim \lambda$	$V_{td}V_{ts}^* \sim \eta A^2\lambda^5$	$A^2\lambda^4$
$\bar{B}^\circ(\bar{d}b)$	$V_{jb}V_{jd}^* \sim A\lambda^3$	$V_{tb}V_{td}^* \sim \eta A\lambda^3$	1
$\bar{B}_s^\circ(\bar{s}b)$	$V_{tb}V_{ts}^* \sim A\lambda^2$	$V_{ub}V_{us}^* \sim \eta A\lambda^4$	λ^2
$D^\circ(\bar{c}u)$	$V_{cs}V_{us}^* \sim \lambda$	$V_{cb}V_{ub}^* \sim \eta A^2\lambda^5$	$A^2\lambda^4$
$T_u(\bar{t}u)$	$V_{tj}V_{uj}^* \sim A\lambda^3$	$V_{tb}V_{ub}^* \sim \eta A\lambda^3$	1
$T_c(\bar{t}c)$	$V_{tb}V_{cb}^* \sim A\lambda^2$	$V_{td}V_{cd}^* \sim \eta A\lambda^4$	λ^2

In the case of the heavy quark systems one expects $\Delta\Gamma$, the difference in the two decay rates, to be small[12] compared to the mean rate Γ so that one cannot separate the eigenstates. Thus the main hope is to find a system for which $\Delta m/\Gamma$ is large enough to see effects generated by oscillations. In Table 2 rough orders of magnitudes for $\Delta m/\Gamma$ are given. It is clear that the systems involving the t quarks are hopeless, since the lifetimes are very short due to the large mass while Δm is of order m_b^2. Thus the system $(\bar{d}b)$ is uniquely signaled as the place to look for large CP-violating effects.

TABLE 2

Average decay widths and mass differences for K° and analogue systems. Values of Δm, except for the K° system are rough estimates, based (except for the D° system) on scaling from the K° case.

	$\Gamma(\sec^{-1})$	$\Delta m(\sec^{-1})$	$\Delta m/\Gamma = x$
K_s°	10^{10}	$1/2\ 10^{10}$	1/2
B_d°	10^{12}	$\sim\lambda^6 m_t^2 \sim 2\cdot 10^{11}$	0.2
B_s°	10^{12}	$\sim\lambda^4 m_t^2 \sim 3\cdot 10^{12}$	3
D°	$2\ 10^{12}$	$\sim 10^9$	$\sim 10^{-3}$
T_u	10^{19}	$\sim\lambda^6 m_b^2 \sim 10^9$	10^{-10}
T_c	10^{19}	$\sim\lambda^4 m_b^2 \sim 10^{11}$	10^{-8}

What CP-violating effects can we look for?[13] Returning to the K° system we note there are two different kinds of experiments that depend on K°-$\bar{K}^\circ$ mixing: (1) The charge asymmetry in $K_L \to \pi^\pm e^\mp \nu$ depends on Re ε. (2) The Fitch-Cronin effect

$$|\eta_{+-}| = \left|\frac{A(K_L \to \pi^+\pi^-)}{A(K_S \to \pi^+\pi^-)}\right|$$

on the other hand depends primarily on the magnitude of the mixing parameter ε. This last statement really depends on the phase convention we use in which the decay amplitude (11) is real. In the case of the B°-$\bar{B}^\circ$ system for the favored decays (amplitude $\sim A\lambda^2$)

$$b \to c + \bar{u} + d \qquad (14a)$$

$$b \to c + \bar{c} + s \qquad (14b)$$

the decay amplitudes are also real. If we now calculate the mixing parameter

ε_B we find it is almost purely imaginary. As a result the CP-violating charge asymmetry in semi-leptonic B decays which depends on Re ε_B is extremely small, whereas analogs of the Fitch-Cronin experiment can show large, passibly maximal, CP violation.

What are these experiments? They involve decays to final states which are CP eigenstates and were first analyzed by Sanda and collaborators.[14][15] The idealized experiment involves the associated production of $b+\bar{b}$ and by observing $b(\bar{b})$ decay at t=0 tagging $\bar{B}^\circ$ (B°). One then looks for the decay into a CP eigenstate such as ΨK_S° (CP odd) or $D + \bar{D}+K_S^\circ$ (CP even). The decay probability displays an oscillation for the $\bar{B}^\circ$ case given by

$$\text{Prob}\ (\pm) = \text{const}\ [\ 1 \pm \sin\theta\ \sin(\Delta m)\ t]\ e^{-\Gamma t} \tag{16a}$$

$$\tan\theta/2 = \eta/(1-\rho) \tag{16b}$$

where (±) corresponds to the CP eigenvalue of the final state. From Eq. (4) the amplitude of the oscillation sin θ is expected to be between 0.5 and 0.85, thus close to the maximum possible. The CP violation is also shown by the reversal of the ± sign on the right hand side of Eq. (16a) when $\bar{B}^\circ$ is replaced by B°. Without seeing the time dependence a measure of CP violation is given by the total rate asymmetry[14]

$$r_\pm = \frac{\Gamma(B^\circ \to \pm) - \Gamma(\bar{B}^\circ \to \pm)}{\Gamma(B^\circ \to \pm) + \Gamma(\bar{B}^\circ \to \pm)} \tag{17a}$$

$$r_\pm = \pm \frac{(\Delta m/\Gamma)\ \sin\theta}{1 + (\Delta m/\Gamma)^2} \tag{17b}$$

While Δm has a large range of uncertainty (due to the problems of evaluating the analogue of the parameter B for the B° system) reasonable parameters yield the result $r_\pm \approx .10$ to .15, thus 20 to 30 percent of the maximum possible. Unfortunately these experiments involve exclusive decays any one of which is likely to have a very low branching ratio.

So far we have considered CP-violating effects that are associated with mass mixing, in particular, B°-$\bar{B}^\circ$ mixing. In so far as CP violation can entirely be blamed on mixing there is no way of distinguishing the KM model from a superweak model. As is well known, in the K° system a distinction occurs because the KM model predicts a difference between $\eta_\pm$ and η_{00} (described by the parameter ε') whereas these are equal in the superweak model. The difference is associated with the existence of CP-violating decay amplitudes, in particular, those associated with penguin graphs. This CP-violating effect

is of the same order λ^4 as the mass matrix effect; however, for dynamical reasons (the $\Delta I = 1/2$ rule, the smallness of penguins) we expect ε'/ε to be of the order 10^{-3} to 10^{-2}. In the B°-$\overline{B}^\circ$ system the situation is different. For the favored decays corresponding to the CP-conserving quark amplitudes (14) there are no interfering CP-violating amplitudes until you go to order $A\lambda^4$. Thus for the most probable decays CP-violating effects in the decay amplitude are of order λ^2 and may be further suppressed for dynamical reasons.

It is possible, however, to obtain large CP-violating effects in B decay amplitudes by looking at unfavored B decays for which the amplitude is of order $A\lambda^3$ instead of $A\lambda^2$. At the quark level there are five possibilities shown in Table 3. Let us first look at the same experiment we have discussed before described by the parameter $r_\pm$ defined by Eq. (17a), but now with the final states being of the form $n\pi$. Then Eq. (17b) no longer holds because in our phase convention the predominant decay amplitude (A in Table 3) violates CP. The difference in the result for $r_\pm$ for this unfavored decay from the result for favored decays shows clearly that the theory is not superweak.

Effects due to CP-violating decay amplitudes can also show up in $B^\pm$ decays.[15][16] Two conditions must be met in this case: (1) More than one quark amplitude must contribute or else the CP-violating phase can be rotated away; (2) Final state interactions must be significant or else the effects will vanish as a consequence of CPT invariance. For example in the decay $B \to n\pi$

TABLE 3

UNFAVORED B DECAYS

	Quark Amplitude	Coupling	Typical Final States
A.	$b \to u + \bar{u} + d$	$A\lambda^3(\rho - i\eta)$	$n\pi$
B.	$b \to c + \bar{c} + d$	$A\lambda^3$	$\Psi\pi$
C.	$b \to t + \bar{t} + d$	$A\lambda^3(1 - \rho + i\eta)$	$D\bar{D}\pi$
D.	$b \to c + \bar{u} + s$	$A\lambda^3$	$D\bar{K}^\circ$
E.	$b \to u + \bar{c} + s$	$A\lambda^3(\rho - i\eta)$	$\bar{D}K^\circ$

the dominant quark amplitude A may interfere with penguin graphs induced by B and C. This can cause a rate difference between $B^+ \to \pi^+\pi^\circ$ and $B^- \to \pi^-\pi^\circ$. The interference between D and E can produce rate differences between

$$B^- \to \underset{\downarrow K_S}{D^\circ} + \bar{K}^\circ + X^- \quad \text{and} \quad B^+ \to \underset{\downarrow K_S}{D^\circ} + K^\circ + X^+$$

These experiments seem even more difficult than those based on B°-$\bar{B}^\circ$ mixing. Furthermore whereas $r_\pm$ depends only on the KM matrix parameters (by Eqs. (17b) and (16b) assuming $\Delta m/\Gamma$ is measured) the rate difference between B^+ and B^- depends on complicated dynamical calculations. Another example in which a large CP-violating effect is possible is the highly suppressed decay $B \to K+n\pi$. At the spectator level this requires the quark amplitude $b \to u+s+\bar{u}$ of order $A\lambda^4$, but there exist non-spectator contributions (penguins, for example) of order $A\lambda^2$ as $b \to t+\bar{t}+s$. Thus it may turn out that the two amplitudes are comparable yielding large CP violation but a very low branching ratio.

We have emphasized here the unique role of the B°-$\bar{B}^\circ$ system in testing the large CP-violating phase the KM model seems to require. It should, of course, be emphasized that it is quite possible that the KM model does not provide the explanation of CP violation in K° decay. The observation of a large CP-violation in a system for which the KM model predicts a small effect would obviously be extremely important and therefore it is equally important to study those systems.

This work has been supported in part by the U.S. Department of Energy.

REFERENCES

1. The value of λ is from H. Leutwyler and M. Roos, Zeits f. Physik C25, 90 (1984). The values of A is based on $[\Gamma(B \to Xe\nu)] = (.12)\ (1.2 \times 10^{-12}\ \text{sec})^{-1}$. The limit on $\rho^2+\eta^2$ comes from $\Gamma(b \to ue\nu)/\Gamma(b \to ce\nu) < .03$.
2. For a more detailed review of CP violation in K° decay in the KM model see L. Wolfenstein, Comments on Particle and Nuclear Physics (to be published), CERN-TH3925/84.
3. For a discussion see M. Gronau and J. Schechter, SLAC preprint 3451, Sept., 1984; E. Paschos in these proceedings and references therein.
4. Eq. (3) is "exact" for m_t=45Gev in the sense that it does not assume m_t/m_W small. "Exact" results are given by A. J. Buras et al, Nuc. Phys. B238, 529 (1984) and by M. Shin, Harvard preprint HUTP-84-A024. Eq. (3) is within 10% of "exact" for m_t between 35 and 60 Gev.
5. M. K. Gaillard and B. W. Lee, Phys. Rev. D10, 897 (1974).
6. J. F. Donoghue et al, Phys. Lett. 119B, 412 (1982).
7. J. Bijnens, H. Sonoda, and M. B. Wise, Phys. Rev. Lett. 53, 2367 (1984).
8. L. Wolfenstein, Phys. Lett. 144B, 425 (1984) and CMU preprint HEP84-20.
9. The importance of such a combination has been pointed out by M. Gronau and J. Schechter, Syracuse University preprint COO-3533-299 and by M. Roos, Physica Scripta, to be published.
10. B. Stech, Phys. Lett 130B, 189 (1983).
11. M. Shin, Phys. Lett. 145B, 285 (1984); H. Georgi, A. Nelson, and M. Shin, Harvard preprint HUTP-84/A071.
12. For a discussion of the B system see J. S. Hagelin, Nuc. Phys. B193, 123 (1981).
13. This discussion closely parallels L. Wolfenstein, Nuc. Phys B246, 45 (1984).

14. I. I. Bigi and A. I. Sanda, Nuc. Phys. B 193, 85 (1981).

15. A. B. Carter and A. I. Sanda, Phys. Rev. Lett. 45, 952 (1980); Phys. Rev. D23, 1567 (1981).

16. S. Barshay and J. Geris, Phys. Lett 84B, 319 (1979), J. Bernabeu and C. Jarlskog, Z. Phys. C8, 233 (1981).

MAXIMAL CP VIOLATION

M. Gronau
Department of Physics, Technion-Israel Institute of Technology,
Haifa, Israel

ABSTRACT

An ambiguity in the definition of the concept of maximal CP violation in the standard model is resolved by identifying in the quark mixing matrix U a rephasing-invariant quantity ϕ. All lowest order CP violating amplitudes become maximal for $\phi = \pi/2$ when $|U_{us}|$, $|U_{cb}|$, $|U_{ub}|$ are fixed. A model of the quark mass matrix is presented, in which the maximal CP phase is correlated with the quark mass spectrum. The mixing matrix is completely determined in terms of quark mass ratios in excellent agreement with experiments.

Up to now the only manifestation of CP violation in nature is the observed CP impurity in the neutral kaon system. In the standard SU(2)xU(1) three generation model the CP impurity parameter ε is proportional to $\sin\theta_1 \sin\theta_2 \sin\theta_3 \sin\delta$, the product of the sines of the three mixing angles θ_i and of the CP violating phase δ of the Kobayashi-Maskawa (KM) matrix[1]. With the measurements of the very small angles θ_2 and θ_3 it became evident that, to account for the measured value of ε, δ must be quite large, possibly as large as $\pi/2$. This raises the interesting possibility of maximal CP violation, an extension of the separate maximal P and C violations exhibited by the weak interactions.

The concept of maximal CP violation suffers, however, from an ambiguous definition. To this ambiguity and to some resolution I wish to address this talk.[2,3] I shall also discuss some models of the quark mass matrix which may give rise to maximal CP violation.

The K-M matrix is a unitary matrix U which relates the quark mass eigenstates to the weak eigenstates. It may be described in terms of three angles and a phase in many different ways. In principle each of these different descriptions may be used to define maximal CP violation when the corresponding phase becomes "maximal", i.e. an odd integer product of $\pi/2$. Moreover, there is another apparent ambiguity related to the freedom of phase convention for the quark fields.[4] As an example, it may seem that U would describe maximal CP violation (in a given phase convention) if it were to have large real diagonal elements and small pure imaginary off-diagonal elements.[5] But it is obvious that this particular form is modified when choosing a different phase convention for the quark fields.

Any plausible definition of maximal CP violation requires the use of a phase which is independent of one's phase convention. We start by proving the existence of such a phase and by identifying it.
The quark mixing matrix is a 3x3 unitary matrix, which in general may be expressed in terms of 3 angles (θ_{ij}) and 6 phases (β_i, ϕ_{ij}), $i < j = 1,2,3$:

$$U = \begin{pmatrix} e^{i\beta_1} & & \\ & e^{i\beta_2} & \\ & & e^{i\beta_3} \end{pmatrix} \omega_{23}\, \omega_{12}\, \omega_{13} \qquad (1)$$

where ω_{ij} is a complex rotation in the ij plane, e.g.

$$\omega_{12}(\theta_{12},\phi_{12}) = \begin{pmatrix} \cos\theta_{12} & e^{i\phi_{12}}\sin\theta_{12} & \\ -e^{-i\phi_{12}}\sin\theta_{12} & \cos\theta_{12} & \\ & & 1 \end{pmatrix} \qquad (2)$$

The most general phase transformation on the six mass eigenstates may be written in terms of six phases α_i, γ_i (i = 1,2,3) in the form:[6]

$$U \to \begin{pmatrix} e^{i(\alpha_1-\gamma_1)} & & \\ & e^{i(\alpha_2-\gamma_2)} & \\ & & e^{i(\alpha_3-\gamma_3)} \end{pmatrix} U \begin{pmatrix} e^{-i\alpha_1} & & \\ & e^{-i\alpha_2} & \\ & & e^{-i\alpha_3} \end{pmatrix} =$$

$$= \begin{pmatrix} e^{i(\beta_1-\gamma_1)} & & \\ & e^{i(\beta_2-\gamma_2)} & \\ & & e^{i(\beta_3-\gamma_3)} \end{pmatrix} \prod_{i<j} \omega_{ij}(\theta_{ij},\phi_{ij}+\alpha_i-\alpha_j) \qquad (3)$$

Since the three differences $\alpha_i - \alpha_j$ are not mutually independent, two things become immediately obvious:

a. One of the six phases of U is unavoidable, which just reproduces the original argument of Kobayashi and Maskawa.[7]

b. There is one combination of the three phases ϕ_{ij}, namely $(\phi_{31} = -\phi_{13})$

$$\phi \equiv \phi_{12} + \phi_{23} + \phi_{31} \qquad (4)$$

which is invariant under all phase transformations on the quark fields.

Physics is independent of one's phase convention. Therefore all physical quantities must depend on the sum of phases ϕ rather than on the values of the separate phases ϕ_{ij}. Since in Eqs. (1) (2) each of the separate phases $e^{\pm i\phi_{ij}}$ multiplies $s_{ij} \equiv \sin\theta_{ij}$, ϕ will always appear in the product $s_{12}s_{23}s_{13}e^{i\phi}$. All CP violating amplitudes (in strange, charmed, b-like and t-like systems) are proportional to the imaginary part of this product. This proves a general theorem that <u>any CP violating amplitude must be proportional to $s_{12}s_{23}s_{13}\sin\phi$.</u>[8] As it turned out from measurements of the two mixing angles θ_{23} and θ_{13}, this product is extremely small ($<10^{-4}$) even if $\sin\phi$ is as large as it could possibly be.

It is instructive to mention the origin of the invariance property of $s_{12}s_{23}s_{13}\sin\phi$:

$$\text{Im Tr } (\omega_{23}\omega_{12}\omega_{13}) = -s_{12}s_{23}s_{13}\sin\phi \tag{5}$$

Being the imaginary part of the trace of the mixing matrix, this product is invariant under the nontrivial unitary phase transformations given by the parameters α_i.

The invariant phase may be generalized to any number of generations in a rather straightforward manner.[2,9] Here we shall restrict our attention to the presently realistic case of three generations focussing on the question of maximal CP violation. The latter concept may be naturally defined by

$$\phi = (\text{odd integer})\ \frac{\pi}{2} \tag{6}$$

However, an immediate question comes up as to other possible definitions of invariant phases. For instance, if instead of Eq. (1) one defines the mixing matrix in an Euler-like manner (as done originally by Kobayashi and Maskawa[7])

$$U_{KM} = \omega_{23}\omega_{12}\omega'_{23} \tag{7}$$

the invariant phase becomes

$$\phi_{KM} = \phi_{23} - \phi'_{23} \tag{8}$$

An alternative definition of maximal CP violation besides Eq. (6) may then be $\phi_{KM} = (\text{odd integer})\ \pi/2$. Since in the representation of Eq. (7) ϕ_{KM} is the only phase-convention-independent CP violating parameter in the Lagrangian, it may in principle provide a legitimate definition of maximal CP violation.

To single out one of the possible definitions we shall have to go beyond general considerations of the quark mixing matrix. An assumption will be made that the underlying theory of quark masses, mixing and CP violation does not single out one generation when introducing the phase. This eliminates ϕ_{KM} of Eq. (8) which singles out the first generation.

The above assumption leaves us with presentations such as Eq. (1), which treat all three generations on equal footing. There are altogether six products of the three ω_{ij} written in different orders. To first order in all θ_{ij} these six presentations become identical. However, empirically the three θ_{ij} of Eq. (1) may be represented by different powers of a small parameter - the Cabibbo angle:[10]

$$|U_{us}| = s_{12} \simeq \theta_c \qquad |U_{cb}| \simeq s_{23} \simeq \theta_c^2 \qquad |U_{ub}| \simeq s_{13} < \theta_c^3 \tag{9}$$

When these empirical observations are taken into account it is found[2] that the six orders devide into two equivalence classes. The first consists of $\omega_{23}\omega_{12}\omega_{13}, \omega_{23}\omega_{13}\omega_{12}$[11] and $\omega_{13}\omega_{23}\omega_{12}$ in all of which Eq. (9) holds. The magnitudes of the above-diagonal elements of U are essentially independent of the CP violating phase. The presentations of the second class[12] are basically the hermitian conjugates of the above (with mixing angles $-\theta_{ij}$). Here the three below-diagonal elements are given approximately by the sines of the mixing angles. The above-diagonal elements have more complicated expressions and, moreover, depend crucially on the corresponding CP-violating phase ϕ'. It is a matter of simple algebra[3] to show that the choice $\phi' = \pi/2$ would lead to $r \equiv |U_{us}U_{cb}/U_{ub}| < 1$. Since experimentally this ratio is larger than one, this class is ruled out (by CP conserving observables!) as a viable definition of maximal CP non-conservation.

An alternative presentation was recently suggested[13], in which the product of ω_{ij} was made symmetric in the order by using the complex rotation group generators. Maximal CP violation in this scheme requires $r < 2$, which is barely consistent with present observations. This possibility is, however, ruled out by the value of ε.[13]

We may therefore conclude that maximal CP violation as a viable choice of nature, consistent with our assumption that the phase does not single out one generation, must be based on the class of presentations of Eq. (1) and is described by Eqs. (4), (6). In this presentation all (lowest order) CP-violating amplitudes are approximately proportional to $|U_{us}U_{cb}U_{ub}|\sin\phi$. When fixing the magnitudes $|U_{us}|$, $|U_{cb}|$ and $|U_{ub}|$ this product is obviously maximized at $\phi = \pi/2$. Since experiments do focus on these three CP conserving observables, CP amplitudes become numerically largest with this definition of maximality. Any other definition of maximality, which sometimes may already be ruled out by these CP conserving observables, would lead to smaller CP violating amplitudes. An amusing example is $\phi_{KM} = \pi/2$, which with the (unrealistic) choice $r \simeq 1$ (corresponding to $s_2 = 0$ in the KM notation) would mean no CP violating effects at all.

With the above definition of maximal CP violation one is tempted to search for an underlying theory of the fermion masses, which may explain the origin of the possibly maximal phase $\phi = \pi/2$ as well as the empirical values of the three mixing angles θ_{ij}. One may hope to be able to express all the four KM

parameters in terms of the given quark masses. Two such schemes have recently been studied, independently motivated by grand unified SO(10) theories. Here I wish to briefly discuss the salient features and limitations of these two models. I shall also present a scheme which combines the two models into a single more predictive framework, which correlates the maximal CP phase with the quark mass spectrum. The reader is referred to the original work for more details.

One of these schemes is based on complex Fritzsch-type up and down quark mass matrices:[14]

$$M = \begin{pmatrix} o & a & o \\ a' & o & b \\ o & b' & c \end{pmatrix}, \quad |a'| = |a| \quad |b'| = |b| \tag{10}$$

This model uses six real parameters and two phases to describe the six quark masses and the four KM parameters. The three mixing angles θ_{ij} and the CP phase ϕ may be expressed in terms of quark mass ratios and the two extra arbitrary phases.[16] The empirical values of the mixing angles[1] and the theoretically most acceptable values of the quark masses[15] constrain these two phases. These constraints indicate the interesting possibility that $\phi \simeq \pi/2$.[16] However, due to the two extra parameters neither the CP phase nor the mixing angles may be determined uniquely in terms of quark mass ratios alone. Very recently a model was suggested,[17] in which the two phases in the Fritzsch-type quark mass matrices were produced to correspond to $\phi \simeq \pi/2$.

A second model, proposed by Stech,[18] assumes a real symmetric form (S) for the up quark mass matrix M_u, whereas the down quark matrix M_d is made up of a piece proportional to M_u and a pure imaginary antisymmetric part (A):

$$M_u = S, \quad M_d = \alpha S + A \tag{11}$$

This model contains (after diagonalization of M_u) seven parameters and allows expressing the three mixing angles and the CP phase in terms of given quark mass ratios and a single arbitrary parameter. The three relations among the four KM parameters are consistent with the measured values of the mixing angles. Using the latter as input leads to a maximal CP phase $\phi \simeq \pi/2$. However, here again the KM matrix cannot be completely determined in terms of quark masses alone.

A model of the quark mass matrices, suggested by R. Johnson, J. Schechter and myself,[19] incorporates both the Fritzsch-type and the Stech schemes simultaneously. This is achieved by choosing the matrices S and A (with $A_{13} = 0$) in Eq. (11) to be of a Fritzsch-form. This model has six parameters, just as many as there are quark masses, and consequently the KM matrix is completely

determined in terms of quark mass ratios. Using the theoretically most acceptable values of the latter, the three mixing angles are predicted in excellent agreement with their measured values. An interesting aspect of this scheme is that it predicts maximal CP violation. The maximal CP phase is correlated with the quark mass spectrum. It follows from the anomalously small u quark mass:

$$\frac{m_u}{m_d} \ll \frac{m_c}{m_s}\ ,\ \frac{m_t}{m_b} \tag{12}$$

In particular, in the limit $m_u \to 0$ the model predicts $\phi = \pi/2$ and no strong CP violation.

Finally, maximal CP violation may be the support by which the standard model will stand the test of CP violation. The calculation of the CP impurity parameter ε within the standard KM model is still in agreement with experiment.[1] The most uncertain factors in the calculation are $|U_{ub}|$ and the theoretical estimate (B) of the K^o-$\bar{K}^o$ matrix element.[20] A crucial test of the model relies on measuring a nonzero value of $|U_{ub}|$, not too far below the present experimental bound, and on a better theoretical determination of B. The lower these two parameters are pushed (and the lower the values of m_t and $|U_{cb}|$) the closer the model gets into jeopardy. Maximal CP violation $\phi = \pi/2$, for which ε is maximized, has the best chance to survive.

ACKNOWLEDGEMENT

This talk is based on work (refs. 2,19) done with Robert Johnson and Joseph Schechter, to both I am grateful for an enjoyable collaboration. I wish to thank A. Davidson, H. Fritzsch, M. Roos, B. Stech and L. Wolfenstein for useful discussions. It is a pleasure to acknowledge the warm hospitality of J. Tran Thanh Van at the Moriond Meeting.

REFERENCES

1. For a review of the present status of the KM matrix with further references see E.A. Paschos, these proceedings.

2. This discussion follows closely M. Gronau and J. Schechter, Phys. Rev. Lett. 54, 385 (1985).

3. For a somewhat longer pedagogical presentation see M. Gronau, talk at the Third Telemark Conference on Neutrino Mass and Low Energy Weak Interactions, Cable, Wisconsin, 25-27 October 1984 (to appear in the proceedings).

4. L. Wolfenstein, Phys. Lett. 144B, 425 (1984).

5. This example is borrowed from ref. 4.

6. J. Schechter and J.W.F. Valle, Phys. Rev. D21, 309 (1980); D22, 2227 (1980).

7. M. Kobayashi and K. Maskawa, Prog. Theoret. Phys. 49, 652 (1973).

8. A similar result, claimed to hold as an approximation, was obtained through direct inspection by L.L. Chau and W.Y. Keung, Phys. Rev. Lett. 53, 1802 (1984).

9. M. Gronau and J. Schechter, SLAC-PUB-3451 (1984), to be published in Phys. Rev. D.

10. L. Wolfenstein, Phys. Rev. Lett. 51, 1945 (1983).

11. This is essentially the representation introduced by L. Maiani, Phys. Lett. 62B, 183 (1976), with the notations $\theta = \theta_{12}$, $\beta = \theta_{13}$, $\gamma = \theta_{23}$, $\phi_{12} = \phi_{13} = 0$, $\phi = \phi_{23}$.

12. One of these presentations was considered by M. Roos, University of Helsinki Report HU-TFT-84-38 (1984).

13. L. Wolfenstein, Carnegie-Mellon University Report CMU-HEP-84-20 (1984).

14. H. Fritzsch, Phys. Lett. 73B, 317 (1978). Nucl. Phys. B155, 189 (1979). L.F. Li, Phys. Lett. 84B, 461 (1979).

15. J. Gasser and H. Leutwyler, Phys. Reports 87, 77 (1982). For the t-quark mass one takes the tentative value $m_t = 30\text{-}50$ GeV.

16. M. Shin, Phys. Lett. 145B, 285 (1984). This paper contains references to previous work on the complex Fritzsch-type mass matrix.

17. H. Georgi, A. Nelson and M. Shin, Phys. Lett. 150B, 306 (1985).

18. B. Stech, Phys. Lett. 130B, 189 (1983). See also G. Ecker, Zeit. f. Phys. C24, 353 (1984).

19. M. Gronau, R. Johnson and J. Schechter, Syracuse University Report SU-4222-312 (1985).

20. For a critical discussion of the uncertainty in estimates of B see E. Golowich, these proceedings.

$B^{o}\bar{B}^{o}$ MIXING PERSPECTIVES

Juliet Lee-Franzini
SUNY at Stony Brook, Stony Brook, NY, USA

ABSTRACT

The perspectives for measuring mixing in the B system, for normal ($b\bar{d}$), strange ($b\bar{s}$) and excited B's (B^{*}) are reviewed. One needs to weigh the relative merits of using copiously produced normal B's at the T(4S) with their anticipated minute mixing, against using strange B's possibly produced infrequently at the T(5S) which however are expected to mix 100%. Enhanced mixing is also expected near the threshold of $B^{*}B$ production, but the magnitude of the enhancement is not sufficiently large to compensate for the decreased hadronic cross section. Experiments at accelerators which are not predominantly "B-factories" are also considered. The prognosis reached is that we will not see definitive results until ≈ Moriond 89.

INTRODUCTION

The present paper, whose purpose is to crystal gaze the perspectives of measuring B^oB^o mixing in the near future, is organized in three sections. In the first a series of terms are defined such that one can discuss the "standard model" predictions for mixing in the B-meson system, and the dependences of such predictions on various parameters including the B decay constant (f_B), mass of the top quark (M_t), the B parameter (B_B) and the K-M matrix elements. After obtaining some most optimistic values for mixing for the various B-mesons (B_d's, mesons containing a b-quark and a light antiquark, B_s's, mesons containing a b-quark and a strange antiquark, B^*'s, excited B-mesons of either variety whose transition to the ground state B-mesons is via a photon), one indicates where these mesons are most likely produced in greatest profusion and estimate a most optimum signal to background ratio. Due to the smallness of said ratio, the traditional method of measuring mixing by counting excess same sign dileptons needs to be supplemented by those where the B(ness) or $\bar{B}$(ness) of a $B\bar{B}$ pair is known, posing stringent requirements on the B reconstruction efficiency of a detector. The second section closes with a forecast of 1989 for when "B-factories" such as CESR and DORIS are likely to have definitive results. The third section examines some prospects of seeing B^oB^o mixing at other types of accelerators, including non e^+e^- machines such as TEV-I, TEV-II and SSC. The conclusion is that they will have to be second generation experiments at these accelerators, and will not yield definitive results in the near future.

B^oB^o mixing can be parametrized by a quantity x ($=\Delta M \times \tau_B$) which is the product of the computed mass difference ΔM of the mass eigenstates M_1 and M_2, and the measured B-meson lifetime, τ_B. We have assumed that $\tau_1 \approx \tau_2 \approx \tau_B$, that is, $\Delta\Gamma$ is very small and thus is negligible. Pais and Treiman[1] have defined the following mixing parameters in terms of the partial rates of a B^o ($\bar{B}^o$) changing into a $\bar{B}^o$ (B^o) or remaining a B^o ($\bar{B}^o$) after creation:

$$r=\Gamma(B^o\to\bar{B}^o)/\Gamma(B^o\to B^o); \qquad \bar{r}=\Gamma(\bar{B}^o\to B^o)/\Gamma(\bar{B}^o\to\bar{B}^o).$$

For small CP violations r and $\bar{r}$ are $\approx$ equal, and using $\Delta\Gamma \ll \Delta M$, we write

$$r \approx [(\Delta M/\Gamma)^2]/[2+(\Delta M/\Gamma)^2] = x^2/[2+x^2].$$

Since the B^o and $\bar{B}^o$ are produced together, the "experimentally" measured mixing parameter r_2 is given by[2]:

$$r_2 = \frac{\Gamma(B^o\to B^o)\Gamma(\bar{B}^o\to B^o) + \Gamma(\bar{B}^o\to\bar{B}^o)\Gamma(B^o\to\bar{B}^o)}{\Gamma(B^o\to B^o)\Gamma(\bar{B}^o\to B^o)+\Gamma(B^o\to B^o)\Gamma(\bar{B}^o\to\bar{B}^o)+\Gamma(B^o\to\bar{B}^o)\Gamma(\bar{B}^o\to B^o)+\Gamma(\bar{B}^o\to\bar{B}^o)\Gamma(B^o\to\bar{B}^o)}$$

In terms of r and $\bar{r}$,

$$r_2 = [\bar{r}+r]/[\bar{r}+1+r\bar{r}+r] = [2x^2+x^4]/[2(1+2x^2+x^4)].$$

For $B_d\bar{B}_d$ mixing, $x \ll 1$,

$$r_2 \approx x^2/[1+2x^2] \approx x^2 .$$

Traditionally r_2 is usually written in terms of sums of same sign dileptons where one of the two leptons acquired a "wrong" sign due to mixing, divided by the total number of dileptons:

$$r_2 = [\ell^+\ell^+ + \ell^-\ell^-]/[\ell^+\ell^+ + \ell^+\ell^- + \ell^-\ell^+ + \ell^-\ell^-]$$

because one historically tags the B(ness) of a B^0 by the sign of the lepton from its semileptonic decay. Specifically, if we define the $\bar{B}^0$ to be $(\bar{d}b)$, $B^0 \to \ell^+\nu X$ and $\bar{B}^0 \to \ell^-\bar{\nu}X$. However, in the case of B's (unlike the case for D's), wrong sign dilepton can arise from the semileptonic decay of the daughter heavy quark (D's) as can be seen from the following decay chain: $\bar{B}^0 \to D^+ \to \ell^+$ and $B^0 \to D^- \to \ell^-$. This complication is always present in using lepton sign for B(ness) tagging, and is minimized at different machines by restricting the kinematic regions examined to favor leptons from direct B semiletponic decays.

STANDARD MODEL PREDICTIONS

In the standard model ΔM is calculated using "box diagrams" which involve K-M matrix elements[3]. Following Gilman and Hagelin's notation[4], we write:

$$\Delta M = 2|M_{12}| = \eta_{QCD} G_F^2 f_B^2 B_B M_B M_t^2/6\pi^2 \times |V_{tb}^2 V_{td}^{*2}| \quad \text{or} \quad |V_{tb}^2 V_{ts}^{*2}|$$

where η_{QCD}=0.85 as calculated by Hagelin[3], f_B is the decay constant of the B's and B_B parametrizes the ΔB(ness)=2 amplitudes. The V_{tq}'s are the quark-mixing matrix elements which in terms of the original K-M angles are given by[5]:

$$\begin{vmatrix} V_{ud} & V_{us} & V_{ub} \\ V_{cd} & V_{cs} & V_{cb} \\ V_{td} & V_{ts} & V_{tb} \end{vmatrix} = \begin{vmatrix} c_1 & -s_1c_3 & -s_1s_3 \\ s_1c_2 & c_1c_2c_3 - s_2s_3e^{i\delta} & c_1c_2s_3 + s_2c_3e^{i\delta} \\ s_1s_2 & c_1s_2c_3 + c_2s_3e^{i\delta} & c_1s_2s_3 - c_2c_3e^{i\delta} \end{vmatrix}$$

where $c_1 = \cos\theta_1$, $s_1 = \sin\theta_1$ etc.

To obtain $x_{q(=d,s)}$ one multiplies the appropriate ΔM with the measured lifetime of the meson. In the following we discuss the present knowledge of some of the quantities which enter in the expression for x_q and how they affect the predicted values for the mixing parameter r_2.

Masses

Two kinds of masses enter in the evaluation of x_q, that of the decaying mesons containing the b quark (M_B's), and that of the top quark (M_t). The former (which are quite well known) enter quadratically in the expression for r_2 while the latter (ironically considering its uncertainty) enters in the fourth power. The mass of the B_d is measured by CLEO to be 5.272 ±0.003. GeV[6]. The mass difference between B^*s and B's was measured by CUSB to be 50±4

MeV[7]. The mass difference between B_s and B_d can be inferred either by using the Eichten-Gottfried mass splitting formulae[8] or taken to be the same as the F-D mass difference, both methods give $M_s-M_d \sim 103$ MeV. For the mass of the top quark, the best at present that one can do is to take the central value from the 40 to 60 GeV range given by UA1[9].

Lifetimes

In the past year the lifetime of the B_d has been remeasured by several groups. At this workshop we heard over four new determinations[10] from which P. Cooper has obtained an "on line" (using my pocket calculator) best fit of τ_B of 1.16±0.18 psec. Assuming the validity of the spectator model, the lifetime of the heavy meson cannot depend on the flavor of the light spectator quark. We thus expect the B_d's and B_s's to have very similar lifetimes.

B-Parameter

While infinite controversy surrounds the contribution of long distance effects to the $\Delta S=2$ amplitudes parametrized by B_K[11], the consensus is that due to the massiveness of the b-quark the $\Delta B(ness)=2$ amplitude is well represented by the vacuum insertion values, i. e. , $B_B \simeq 1$.

Decay Constants

In the non relativistic approximation where $f_B^2=[12|\psi(0)|^2]/M_b$ and $\psi(0)$ is the wave function at origin of the bound $b\bar{q}$ state, the weak decay constant f_B can be interpreted to give a measure of the size of the B meson[12]. In the same approximation the mass difference between B^* and B (hyperfine splitting due to one gluon exchange) can be expressed as: $\Delta M=[32\pi\alpha_s|\psi(0)|^2]/[9M_b m_q]$[13]. Using the measured ΔM[7] and α_s[14] (~ 0.2), and the m_q value favored from spectator model studies[15,16] of 150 MeV, one find f_B to be ~200 MeV, a value not very different from the theoretical estimates obtained using potential models, QCD sum rules and Bag models (ranging from 120 to 140 MeV[12]. One sees that much uncertainty surrounds f_B, as we saw from the the discussion at this workshop where we could not even agree on the appropriate value for m_q to insert into the non relativistic f_B formula.

The decay constant f_B enters to the fourth power in r_2, and is one of the crucial parameters to be determined in the B system. In principle one could obtain it from measuring the rate of $B\to\tau\nu$ which is proportional to f_B^2 and $|V_{ub}|^2$, this rate is expected to be woefully small ($\simeq 10^{-5}$). Leveille[17], in the 1982 Moriond Heavy Flavors Workshop, had made an estimate of the effects of W exchange and gluon enhanced diagrams which contribute only to the B^o hadronic decay rate and obtained the result that the ratio of the charged B's to neutral B's semileptonic decay rates is (f_B in GeV):

$$BR^{\pm}/BR^{o} = [1+2.2|V_{ub}/V_{cb}|^2+1.2f_B^2]/[1+2.2|V_{ub}/V_{cb}|^2]$$

From our current knowledge of the quark mixing matrix, the above expression

reduces to $BR^{\pm}/BR^{o} \approx [1+1.2f_B^2]$ (≈ 1.05 for f_B=200 MeV). Therefore I expect that this type of measurements will eventually yield a better estimate of f_B. For the present, I will adopt f_B=160 MeV for predicting r_2.

K-M Matrix Elements

From inspection of the K-M matrix

$$|V_{tb}^2 V_{td}^{*2}| = |(c_1 s_2 s_3 - c_2 c_3 e^{i\delta})^2| \, |s_1 s_2|^2 \approx s_1^2 s_2^2,$$

$$|V_{tb}^2 V_{ts}^{*2}| = |(c_1 s_2 s_3 - c_2 c_3 e^{i\delta})^2| \, |(c_1 s_2 c_3 + c_2 s_3 e^{-i\delta}| \approx (s_2^2 + s_3^2 + 2 s_2 s_3 \cos\delta)$$

As I reported at last year's Moriond meeting[18] the mixing matrix elements can be expressed in terms of the B lifetime and semileptonic decay parameters as

$|V_{cb}| = \{[BR(B\to Xe\nu)/\tau_B] \times [K_{cb}/(1+R_B)]\}^{1/2}$ where

$R_B = \Gamma(B\to X_u \ell\nu)/\Gamma(B\to X_c \ell\nu)$ and $K_{cb} = (2.35 \pm 0.13) \times 10^{-14}$ sec from fitting the CUSB B β-decay spectrum. Using the world average value for the BR(B→e or μ,νX) of (11.8±0.35±0.75)%, I obtained:

$|V_{cb}|^2 = (2.78\pm0.18)\times10^{-15}\,\text{sec}/[(1+R_B)\tau_B]$,

$|V_{ub}|^2 = R_B(1.23\pm0.09)\times10^{-15}\,\text{sec}/[(1+R_B)\tau_B]$.

Since $s_3 = |V_{ub}|/s_1$, $s_3 = [3.5\times10^{-8}\ \text{sec}^{1/2}]/s_1 \times [R_B/(1+R_B)\tau_B] \approx 0.0238$

for τ=1.16 psec, s_1=0.231±0.003[19] and R_B=0.03 [the 90%c. l. [16,18)].

From $|V_{cb}|^2 = c_1^2 c_2^2 s_3^2 + s_2^2 c_3^2 + 2c_1 c_2 s_3 s_2 c_3 c_\delta$, one obtains

$s_2 = |V_{cb}|[\sqrt{(1-8.06 R_B s_\delta^2)} - 2.84\sqrt{R_B} c_\delta]$, by using c_1=0.9737±0.0025[20].

In figure 1 we show this relation evaluated for δ=0 to π, the curve is for R_B=0.03 and the line for R_B=0. We note that s_2 is bounded between 0.022 and 0.047 for δ =0 to about 105° and between 0.047 and 0.070 for δ>105°.

For optimistic estimates, I use the values of s_2 and s_3 obtained from R_B=0.03 and $\delta=\pi$ obtaining $|V_{tb}^2 V_{td}^{*2}| = 2.6\times10^{-4}$ and $|V_{tb}^2 V_{ts}^{*2}| = 2.1\times10^{-4}$. Note that the latter is ≈8 times larger than the former.

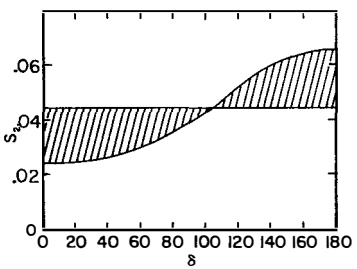

Figure 1 s_2 vs δ, the allowed region is shaded.

Predicted Mixing Parameters

In summary, $x_q = 770\times(f_B/0.16)^2 (B_B/1)^2 (M_t/45)(\tau_B/1.16)|V_{tb}^2 V_{tq}^{*2}|$ and

For B_d: $x_d \approx 0.2$; $r_d \approx 0.02$; $r_{2,d} \approx 0.04$.

For B_s: $x_s \approx 1.66$; $r_s \approx 0.58$; $r_{2,s} \approx 0.58$.

Note that mixing in the B_s is at least 15 times larger than in the B_d system.

Non-standard models, for ex. Gronau and Schechter[21]'s, allow for the possibility that $x_d = 1$, hence $r_d \approx 0.33$ and $r_{2,d} \approx 0.38$.

The above values of r's are derived using the relationship between r and x which only apply to $B^0\bar{B}^0$ produced in an odd L state, as for example in T(4S) decays where no B^*'s are produced. Bigi and Sanda[22] noted (and L. Wolfenstein clarified for me) that when the B pairs are in an even L state, $r=[3x^2+x^4]/[2+x^2+x^4]$, yielding: $r_{d,even} \approx 0.06$, three time larger than for the odd L case.

One does not gain much using B_s^*'s because r_s was so large to begin with, i. e. $r_{s,even} \approx 0.67$ (as compared to 0.58).

The B pair would be in an even L state if they are produced near a $B^*\bar{B}$ (or $B\bar{B}^*$) threshold where the B^* decays into a γ and the ground state B meson, at higher energies all partial waves enter and the enhancement due to the L-even states is diluted. Therefore experimentally one searches for evidence of the onset of B^* production and hope that the cross section is fortuitously large.

$B^0\bar{B}^0$ MIXING AT B FACTORIES

Present Status

Two accelerators in the world today, CESR and DORIS, are dubbed B-factories, not because they produce the most B's, but because they produce mostly B's. CLEO has detected 162 known sign dilepton pairs out of ≈50,000 produced $B\bar{B}$ pairs. They determine the amount of mixing by dividing the number of same sign dileptons by the total dilepton count[23]. They see 34 like sign dileptons which can be fully accounted from parallel and cascade decays. The interpretation of these results depends on the ratio of the lifetimes of the neutral and charged B's (present limits are 0.25 to 2.9) and on their relative production in T(4S) decays. Assuming 6:4 production CLEO obtains -2.6 ± 4.6 excess same sign dileptons, or less than 6.1 at 90% confidence level. For equal semileptonic BR's, the 90% c. l. upper limit is ≈30%, for lifetime ratios ($B^0/B^\pm$) less than 0.58 they can not rule out complete mixing.

Future Prospects

The above illustrates the difficulties involved in measuring $B\bar{B}$ mixing using the dilepton method at the T(4S). The resonant cross section there is ≈1 nb, which is some 30% of the total hadronic cross section. No B^*s are produced[24], and only about forty percent of the B pairs produced are neutral. Therefore one is trying to measure a (2-4)% mixing effect from 15% of the

hadronic events. One possible tack is to hunt for possible sources of resonant B^* and/or B_s production. Figure 2 shows the CUSB scan at CESR above the T(4S) region[25]. The top figure shows $R_{visible}$ for all hadronic events, the bottom figure is R_{vis} for events which passed a thrust cut, note the suppressed zero in both figures. Both show complicated structures, which survive the thrust cut ($B\bar{B}$ events are less "thrusty" than continuum events) and therefore are resonance associated. The tall peak on the left of the figures is the T(4S), which lies below the B^* production threshold[24]. Since the mass difference between B and B^* is ≈50 MeV and the mass difference between the strange and normal B's are expected to be ≈100 MeV (see section on masses), 6 thresholds (indicated by arrows in figure 4): $B_{d(u)}\bar{B}_{d(u)}$, $B_{d(u)}\bar{B}^*_{d(u)}$, $B^*_{d(u)}\bar{B}^*_{d(u)}$, $B_s\bar{B}_s$, $B^*_s\bar{B}_s$, $B^*_s\bar{B}^*_s$, occur within the W range of 10.55 and 10.85 GeV. Furthermore, all potential models[26] indicate that three higher T resonances, T(4S), T(5S) and T(6S) are expected to be present in the W range 10.5 to 11.5 GeV. The question is whether one is fortunate enough to have the resonance poles and the thresholds related in such a way as to have strongly enhanced production of specific decay channels, as for ex. in the case of the T(4S) decaying exclusively into $B_{d(u)}\bar{B}_{d(u)}$'s. CUSB has performed an analysis of their data by performing a coupled

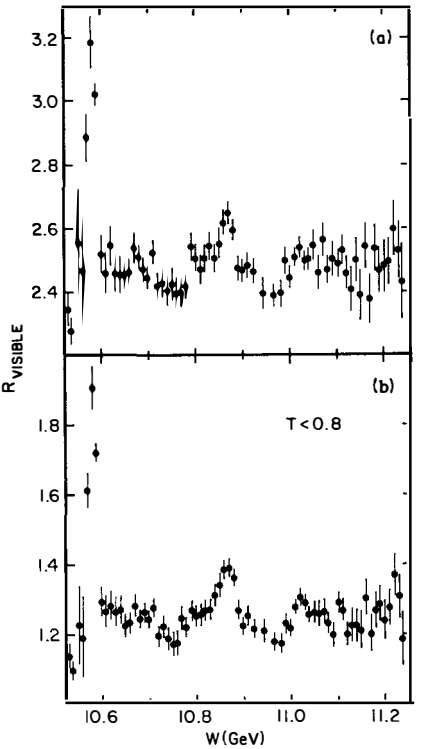

Figure 2 $R_{visible}$ vs E_{cm}.

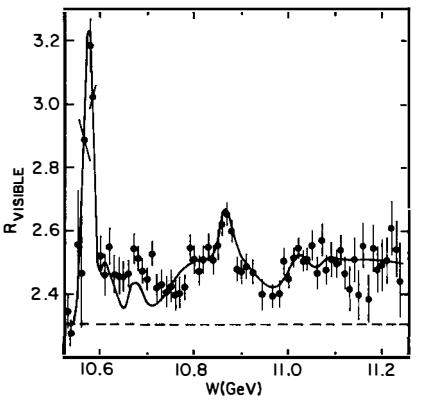

Figure 3 CUSB Computation superimposed over data.

channel calculation using the Eichten et al[27] potential model, assuming only four T(nS) states and the six thresholds. In figure 3 the CUSB computed curve is shown superimposed over their data, the agreement between them is remarkable, especially considering the simplifying assumptions made. In the top half of figure 4 the separate contribution from each T resonance is shown. Note that aside from the major peak the T(4S) has two secondary peaks due to the opening of the $B_{d(u)}\bar{B}^{*}_{d(u)}$ and $B^{*}_{d(u)}\bar{B}^{*}_{d(c)}$ channels. What is not shown is that in fact the $T(4S)\rightarrow B_{d(u)}\bar{B}_{d(u)}$ amplitude is negligible for W=10.62 to 10.73 GeV. Therefore at W=10.62 GeV, at the first secondary peak of the T(4S), the $B_d\bar{B}_d$ are produced only in an L=even state (thus the mixing effect is expected to be three times larger). However, at 10.62 GeV, the resonant cross section is ≈1/5th of that at the T(4S) peak, or ≈6% of the total hadronic cross section. Therefore it is not clear that one would lose rather than gain by running at the tail rather than on peak of the T(4S).

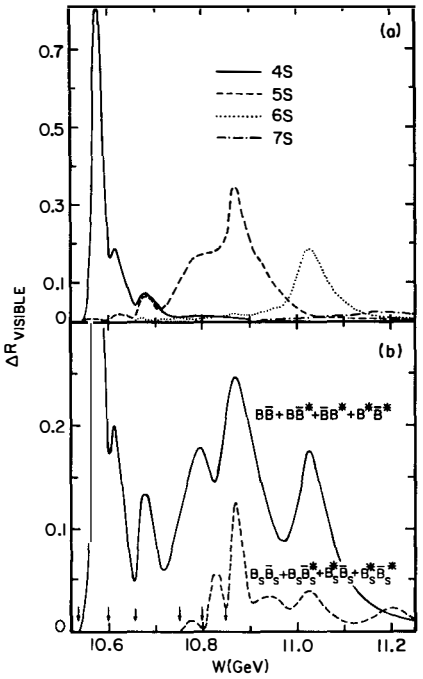

Figure 4 CUSB decompositions, (top) contributions from T(nS)s, (bottom) as a function of light quark content.

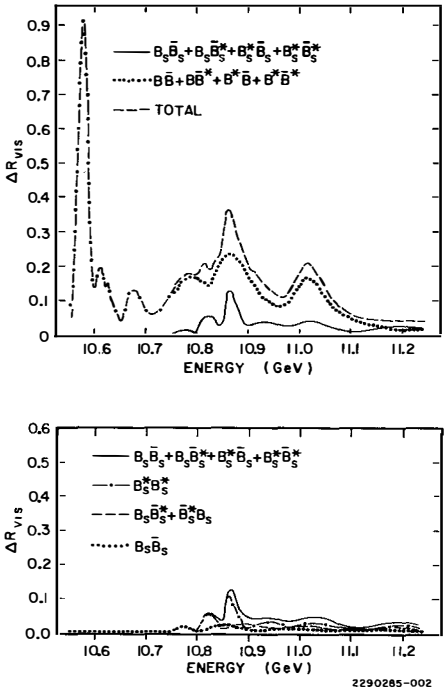

Figure 5 CUSB decompositions, (top) subcomponents: $B_{d(u)}$ and B_s, (bottom) subcomponents of B_s contributions.

A more promising prospect is to look for B_s production. The CUSB decomposition (shown in the bottom half of figure 4) indicates that 1/4 of the total resonant cross section above ≈10.8 GeV results in B_s's. In particular, the narrow peak of the T(5S) is apparently due to the $B^*_s\bar{B}^*_s$ decay channel (see figure 5 bottom) and whose cross section is ≈ 1/8th that of the T(4S) peak (see figure 5, top). Since $r_{2,s}$ is at least 15× larger than $r_{2,d}$, one could conceivably try to measure mixing at T(5S) peak. It is still a very difficult experiment because while the expected mixing is ≈100%, only (2-3)% of the total hadronic events produced at that energy decays into the desired channels (states containing $B_s\bar{B}_s$'s).

Using Tagged B's

Since the dilepton method is particularly vulnerable to backgrounds of wrong sign leptons from non mixing sources, despite the notorious difficulty in reconstructing B's, we consider the advantage of using B(ness) tagged events in mixing measurements. This method has been used extensively in the $D^o\bar{D}^o$ mixing searches. Ideally, one fully reconstructs one of the B's through its hadronic decay modes, (say it is a B^o), then one can predict the sign of the lepton (or kaon) in the decay of its partner (the $\bar{B}^o$) and check whether it has undergone (CP) change. At the T(4S), one further gains using reconstructed B's since one removes continuum D events which are 60% of all D's, and one removes charged B pairs which are ≈60% of all B pairs. The signal to background ratio from using the two methods are summarized below.

Table Maximal mixing signal: Number of events per T(4S) decay.

Method	Signal	Background/Signal
dielectron, E_e> 1 GeV	10^{-2}	130 %
dielectron, E_e> 1.5 GeV	4×10^{-3}	55 %
dilepton, E_ℓ> 1 GeV	4×10^{-2}	103 %
dilepton, E_ℓ> 1.5 GeV	1.6×10^{-4}	37 %
tagged B, E_ℓ> 1 GeV	$3.3\times10^{-2}\times\varepsilon$	8 %
tagged B, E_ℓ> 1.5 GeV	$2.1\times10^{-2}\times\varepsilon$	2 %

ε = B reconstruction efficiency

We can make an estimate of how many events one could collect per year. CESR now delivers > 1 pb^{-1}/day with three bunches in the ring. With the anticipated machine upgrade of going to 7 bunches and implementing μbeta insertions, CESR expects to deliver ≈3-5 pb^{-1}/day. The branching ratio of

B's→decay modes without ν's is approximately 48%. Thus one expects (0.7to 1.5)×10^6×ε reconstructed B-mesons per year. The question is what is ε? CLEO, using only low multiplicity, charged final states and the "M(Dπ)-M(D^*)" trick, achieves an ε of 0.03%[28]. Mark III, using full particle identification and high multiplicity final states, achieves an ε for D reconstruction of ≈10%[29]. At CESR, if one had superb low energy photon energy resolution, one could also add the "M(Dγ)-M(D)" trick. Therefore, despite the higher B multiplicity, with an ideal detector at CESR one may reach B reconstruction efficiencies of the order of 3% to 10%, yielding 50,000 to 150,000 reconstructed B's per year!

What are the requirements for such an ideal detector? In tracking it must have high efficiency and high resolution over 4π solid angle, which implies a superb central drift chamber. In electromagnetic calorimetry it must have high efficiency, excellent energy resolution over a wide range of photon energies, and complete 4π coverage, which implies it must reside inside the magnetic coil. In particle identification it must have full π/K separation up to 2.5 GeV. A detector which purports to fulfill these requirements is being designed and constructed at CESR. It is called CLEO-II. The em calorimetry is done with $15 Million of Cesium Iodide crystals surrounding time of flight counters, central trackers, encased within a superconducting magnetic coil[30].

A realistic forecast for 1988 is to use a reconstruction efficiency of 2% during CLEO-II's learning period, and an integrated luminosity of 5000 pb^{-1} for the first year (or 10^7 $B\bar{B}$ events). Then 80,000 neutral B's will have been reconstructed, half of which will have a charged K, 22% of these will have the B partner decaying semileptonically. In summary, we expect 8,800 reconstructed neutral B's with $K^{\pm}$ and their B partner decaying semileptonically with E_{ℓ}>1 GeV, which for 100% mixing would yield 4,400 events, or some 90 wrong sign K-ℓ final states (with some seven background events) for 2% mixing. This would certainly constitutes a definitive measurement.

$B^0\bar{B}^0$ MIXING AT OTHER MACHINES

I. At Higher Energy e^+e^- Machines

A new trick suggested by R. Barlow[31] at this workshop is to supplement the dilepton method at high energy e^+e^- machines such as LEP and SLC by measuring the deviation of the observed asymmetry from the one predicted by Glashow-Weinberg-Salem and attributing it to mixing. My question is if such a deviation were found, would the interpretation be unique? It would be an interesting result in any case.

II. AT TEV-I, TEV-II,.....SSC

TEV-II

At TEV-II there is certainly no dirth of B production. In fact it is a true B-factory. The problem is identifying the B's amongst the infinite number of other particles produced. One needs a good fast trigger, precise vertex reconstruction, short dead time and the ability to accept high incident flux [$\approx 10^6$/sec] in the detector. One prototype of such a design which capitalizes on the relatively long B lifetime is described to me by Jean Slaughter[32]. This design proposes their high resolution streamer chamber as the vertex detector (it has enough length for tracks to separate so one could reconstruct vertices), to be followed by a magnet then by TRD's and em calorimetry. The trigger (TRD) ask for $p_T > 1$ GeV, tracks are then searched for in the calorimeter. They assume 50 nb B production cross section at 800 GeV, for a 1000 hour run will obtain 218 $B\bar{B}$ triggered hologram pictures. While it would not be sufficient to measure mixing, a second generation experiment of this type seem hopeful.

TEV-II

J. Rosner[33] has computed the ($p\bar{p} \to Q\bar{Q}$+other particles) cross section at $p\bar{p}$ colliders. The rates are reasonable to consider measuring $B\bar{B}$ mixing at TEV-I. In the following we discuss a prototype set up designed by P. Franzini[34] within the DO calorimeter[35] which is not in the original proposal but could be added on later. At TEV-I, $\sqrt{s} = 2$ TeV, $\sigma(b\bar{b}) \approx 0.25$ μb. Assuming a luminosity of 10^{30}/sec/cm^2 this implies ≈20,000 $B\bar{B}$/day. In the rapidity range $|y_{b\bar{b}}| < 1.5$ and for $p_t(b) > 15$ GeV, one can collect ≈300 dimuons from $B\bar{B}$ semileptonic decay, or 30,000 μμ's/100 days at full TEV-I luminosity. $\gamma c\tau \approx 1$ mm, therefore we assume a vertex detector with vertex resolution ≈50μm (or 15μ in space). Imposing that the two B decay lengths each be greater than 200 μ and that they be azimuthally separated by 45° (cleanliness cuts) reduces the above numbers to ≈5000 μμ events/run.

The event identification would require: a) two vertices, b) two muons identified by eight dE/dx measurements in 6-8 nuclear interaction lengths of uranium liquid argon calorimeter, c) two muons with distinct vertices, d) two well measured momenta in magnetized iron. The backgrounds which come from sequential decays, punch through from fast prompt pions (≈0.3% in DO) are removed by vertex association. Statistical analyses used to isolate the $B\bar{B}$ signal (P_t to B direction cuts) will dilute some the measurement, mixing to a few per cent is detectable.

SSC

As long as one is crystal gazing, it should be mentioned that at high energies $B\bar{B}$ mixing can be measured, in principle, considerably better at the SSC using a dedicated detector for this purpose. One such prototype design[36] involves a two armed spectrometer, each arm containing vertex tracking, TRD's for electron identification and trigger, followed by tracking

chambers and calorimetry. One sure forecast is that we won't hear results from them at Morion 1989.

CONCLUSIONS AND EXHORTATIONS

The obvious conclusion is that definitive $B\bar{B}$ mixing measurements are difficult because of the smallness of the expected effect. Nevertheless, the experiments should be done not only "because it COULD BE there!", but one could also be lucky and find a large effect and go beyond the "standard model". At the very least, this provides a new way to measure f_B. Moreover, CP violation effects are expected to be on the order of 10^{-4}, 10^{-5} from virtual transitions in both the B_d and B_s systems. One has to go to exclusive channels (on mass shell, $B^o/\bar{B}^o \to f+X$ processes where f is a common final state for B^o and $\bar{B}^o$ and X stands for other particles)[22] to perhaps detect CP violation. Therefore the more practice one has in reconstructing B's, the better the future prospects.

Therefore, Good luck to CLEO and ARGUS, and Good Hunting to Everybody.

ACKNOWLEDGEMENTS

The author thanks P. Franzini, J. Rosner and L. Wolfenstein for discussions during preparation of this paper. She thanks L. Montanet for this chance at playing prophet (an enjoyable role which could become addictive) and the organizers of this workshop where numerous stimulating discussions between participants took place. The author's research is supported in part by the U. S. National Science Foundation.

REFERENCES

1. A. Pais and S. B. Treiman, Phys. Rev. D12 (1975) 2744.
2. L. B. Okun, V. I. Zhakarov and B. M. Pontecorvo, Nuovo Cimen. Lett. 13 (1975) 218.
3. See for example J. S. Hagelin, Nuc. Phys. B193 (1981) 123.
4. F.J. Gilman and J.S. Hagelin, Phys. Lett. 133B (1983) 443; SLAC-PUB-3226 (1983).
5. M. Kobayashi and T. Maskawa, Prog. Theor. Phys. 49 (1973) 652.
6. S. Behrends et al., Phys. Rev. Lett. 50 (1983) 881.
7. J. Lee-Franzini, in Proceedings of the 22nd International Conference on High Energy Physics, edited by A. Meyer and E. Wieczorek (Karl Marx Univ., DDR, 1985) in press.
8. E. Eicthen and K. Gottfried, Phys. Lett. 66B (1977) 286.
9. P. Ermard, reported at this workshop.

10. C. Matteuzzi, J. Thomas and R. Barlow, reported at this workshop.
11. P. Colic et al., Phys. Rev. D26 (1982) 2286;
J. Donaghue et al., Phys. Lett. 119B (1982) 412;
N. Cabibbo, private communication.
12. L. Maiani, Jour. de Phys. Coll. C-3 (1982) 631.
13. J. M. Richard, review talk at this workshop.
14. R. D. Schamberger et al., Phys. Lett. 138B, 225 (1984).
15. G. Altarelli et al., Nucl. Phys. B208 (1982) 365.
16. J. Lee-Franzini, in Proc. of the Europhysics Conf. "Flavor Mixing in Weak Interactions" ed. L.L. Chau (Plenum, N.Y., 1984) to be published.
17. J.P. Leveille, in Proc. Moriond Workshop on New Flavor, ed. J. Tran Than Van and L. Montanet (Gif-sur-Yvette, Editions Frontieres, 1982) 191.
18. J. Lee-Franzini, in Proceedings of the XIXth Rencontre de Moriond - Phenomenology of Gauge Theories, ed. by J. Tran Thanh Van (Editions Frontieres, Gif sur Yvette, 1984) p477.
19. M. Bourquin et al., Rutherford Lab preprint RL-83-054 (1983).
J. M. Gaillard, reported at this workshop.
20. Particle Data Group, Phys. Lett. 111B (1982) 1.
21. M. Gronau and J. Schechter, SLAC preprint PUB-3451.
22. I.I. Bigi and A.I. Sanda, Phys. Rev. D29 (1984) 1393;
23. P. Avery et al., Phys. Rev. Lett. 53 (1984) 1309.
24. R.D. Schamberger et al., Phys. Rev. D26 (1982) 720;
D30 (1984) 1985.
25. D. M. J. Lovelock et al., Phys. Rev. Lett. 54 377 (1985).
26. See P. Franzini and J. Lee-Franzini, Phys. Rep. 81 (1982) 239 and references therein.
27. E. Eichten, Phys. Rev. D22 (1980) 1819.
28. T. Gentile, reported at this workshop.
29. J. Hauser, reported at this workshop.
30. CLEO-II Collaboration, Cornell University preprint CLNS 85/634.
31. R. Barlow, reported at this workshop.
32. J. Slaughter, private communication.
33. J. Rosner, Phys. Lett. 146B (1985).
34. P. Franzini, private communication.
35. DO Collaboration, Fermilab E-740 Design Report.
36. D. Loveless et al., in Proc. of "$P\bar{P}$ Options for the Super Collider", DPF Workshop, ed. by J. E. Pilcher and A. R. White (1984) 294.

MIXING ANGLES AND CP VIOLATION IN THE KM MODEL

E.A. Paschos
Institut für Physik, Universität Dortmund
4600 Dortmund 50, West-Germany

Abstract

We summarize the constraints for the mixing angles and the CP-violating phase and discuss their implications for the ε'/ε ratio, which is at the edge of the KM model prediction. The extension to an eight quark model is briefly discussed.

Basic Constraints

During the past two years considerable progress was made in the determination of the charged current couplings. In fact the accumulated information allows us to pose precise questions on the origin of the mixing angles and CP non-conservation of K^o and other meson decays.

In the standard model the couplings are defined by the equation

$$\bar{\psi}^u_L V_{KM} \psi^d_L = [\bar{u}\ \bar{c}\ \bar{t}]_L \begin{bmatrix} V_{ud} & V_{us} & V_{ub} \\ V_{cd} & V_{cs} & V_{cb} \\ V_{td} & V_{ts} & V_{tb} \end{bmatrix} \begin{bmatrix} d \\ s \\ b \end{bmatrix}_L \tag{1}$$

The determination of the above matrix elements draws from many experiments described below.

1) From beta decay one determines the ratio

$$(G_V/G_\mu)_{exp} = |V_{ud}|\{1 + \delta_R\} \tag{2}$$

where G_V is the vector coupling occuring in $0^+ \to 0^+$ transitions, and G_μ the Fermi coupling constant measured in μ-decay. The quantity δ_R represents the radiative corrections whose contributions are essential. The most accurate values come from the ft-values of $A\ell^{26}$ and O^{14}. The average value[1] over many nuclei is

$$|V_{ud}| = 0.9733 \pm 0.0024 \tag{3}$$

2) From strange particle decays there are two independent determinations of V_{us}. The first is from $K \to \pi e \nu$ where only the vector current contributes. An extensive study of this process gives the value[2,3]

$$|V_{us}| = 0.220 \pm 0.002 \quad . \tag{4}$$

An alternative determination of V_{us} is from hyperon decays. Here there are many decays, the range of extrapolation in q^2 is smaller, but there are contributions from vector and axial couplings. The experimental colleagues have done a χ^2-fit of their data and obtained[4] the very precise value

$$|V_{us}| = 0.231 \pm 0.003 \tag{5}$$

Obviously with the small errors, equations (4) and (5) are not compatible. At the moment it is hard to pinpoint the origin of this difference, but for lack of better ideas I shall use a range of values

$$0.218 \leq |V_{us}| \leq 0.235 \tag{6}$$

which spans both reactions. Future analyses must also include new results on neutron life-time and $\Sigma^- \to n + e + \nu$ decay.[5]

3) Results on the B-meson decays provided a crucial link by measuring the absolute value of the V_{cb} element. The weighted average of the data presented at this workshop is[6]

$$\tau_B = (1.20 \pm 0.17) \times 10^{-12} \text{ sec} \tag{7}$$

and the branching ratios

$$\begin{aligned} \frac{Br(b \to ue\nu)}{Br(b \to ce\nu)} &\leq 0.04 \quad \text{CLEO}^{7)} \\ &\leq 0.045 \quad \text{CUSB}^{8)} \end{aligned} \tag{8}$$

giving a ratio for the matrix elements

$$\left|\frac{V_{ub}}{V_{cb}}\right| \leq 0.14 \tag{9}$$

The absolute value of the element is determined from the decay rate (or together with studies of the leptonic spectrum)

$$|V_{cb}| = 0.053 \pm 0.004 \tag{10}$$

There is some theoretical uncertainty on this value coming from corrections to the decay formulas and this could bring the total error to 15 %. Evidently the percentage error in V_{bc} is considerably bigger than in the previous two elements.

The results in equs. (3), (6), (9) and (10) together with the unitarity of the KM matrix restrict all elements as follows

$$V_{KM} = \begin{bmatrix} 0.973 \pm 0.002 & 0.226 \pm 0.009 & |V_{ub}| \leq 0.008 \\ -0.226 \pm 0.009 & |V_{cs}| \geq 0.970 & 0.053 \pm 0.004 \\ |V_{td}| \leq 0.013 & |V_{ts}| \leq 0.057 & |V_{tb}| \geq 0.998 \end{bmatrix} \tag{11}$$

Two other elements were independently determined in neutrino experiments[9,1,10)]

$$\begin{aligned} |V_{cd}| &= 0.25 \pm 0.04 \\ |V_{cs}| &= 0.9 \pm 0.1 \end{aligned} \tag{12}$$

and are consistent with the values given in eq. (11). Finally the values for V_{ud}, V_{us}, V_{ub} and V_{cb} do not use the unitarity of the KM matrix and they are useful in models with more quarks where the matrices are larger. I must also admit that I have been more conservative on the errors than other authors, but even the larger errors do not crucially affect the rest of the article.

The mixing matrix can be parametrized in terms of three angles, the real parameters of O(3), and a phase factor which cannot be eliminated by redefining the phases of the quarks fields or the overall phase of the amplitudes. The angles generalize the Cabibbo angle and the phase produces CP non-conservation in several processes. Kobayashi and Maskawa[11)] were the first to make this observation in the standard model.

There are several parametrizations of the flavor mixing matrix. Some authors prefer to use the original parametrization of Kobayashi-Maskawa,[11)] others prefer a form introduced by Maiani[12)] and still others a form introduced by Wolfenstein.[13)] The physics of course remains the same no matter which parametrization is used. Each of the parametrizations has its advantages. For instance the matrix introduced by Wolfenstein expands the matrix elements in terms of a small parameter $\lambda = \sin\theta_c$ and determines the remaining structure by the unitary nature of the matrix, but at this time there is no deeper theoretical understanding on the origin of a small expansion parameter. Maiani's parametrization has the advantage that it is easy to incorporate the experimental results in equ. (11). The small values of the off-diagonal elements justify a small angle approximation where the matrix takes the form

$$V_{KM} = \begin{bmatrix} \cos\theta & \sin\theta & \beta \\ -\gamma\beta e^{i\delta} & -\sin\theta & c_\theta & \gamma e^{i\delta} \\ -\beta+\gamma\theta e^{-i\delta} & -\beta\theta - e^{-i\delta}\gamma & 1 \end{bmatrix} \qquad (13)$$

with $|\beta| = |V_{ub}|$ and $|\gamma| = |V_{cb}|$. The experimental results are now summarized by the relations[14)]

$$\sin\theta_c = 0.226 \pm 0.009$$

$$0.049 \leq \gamma \leq 0.057 \qquad (14)$$

$$\beta \leq 0.008$$

Since phases are important for the rest of this article I discuss them in some detail. It is possible to change the phase of the elements in eq. (13) by redefining the phases of the quark fields. For instance,[14b)]

$$\bar{\psi}^u_L \tilde{V}_{KM} \psi^d_L = [\bar{u}\ \bar{c}\ \bar{t}e^{-i\delta}] \begin{bmatrix} \cos\theta & \sin\theta & \beta e^{-i\delta} \\ -\gamma\beta e^{i\delta}-\theta & \cos\theta & \gamma \\ -\beta e^{i\delta}+\gamma\theta & -\beta\theta e^{i\delta}-\gamma & 1 \end{bmatrix} \begin{bmatrix} d \\ s \\ be^{i\delta} \end{bmatrix} \qquad (15)$$

This change modifies the phases of the decay amplitudes and of the mass matrices, but physical observables are invariant to these changes. In fact, we need two measurements in order to determine if CP violation originates in the mass matrix or the decay amplitude.

Once a phase convention is adopted we can trace its effects through Feynman diagram and determine the imaginary parts of amplitudes. Finally, one of the phases in the problem can be identified with the overall phase of the hadronic states, i.e., we can use $|K^o\rangle$ and $|\bar{K}^o\rangle$ or new states defined through a U(1) transformation

$$|\tilde{K}^o\rangle = e^{-i\xi}|K^o\rangle \quad \text{and} \quad |\tilde{\bar{K}}^o\rangle = e^{i\zeta}|\bar{K}^o\rangle \quad . \qquad (16)$$

Later on, we shall find these properties useful in discussing the K^o system.

Constraints from the K-mesons

The results summarized in eqs. (14) are incomplete in two respects
(i) the angle β is not bounded from below and
(ii) there are no limitations on the phase δ.
In order to limit these parameters it is necessary to consider the CP-violating parameters of the K^0 system. The mass difference $\Delta M = M_{K_S} - M_{K_L}$ will not be used because as demonstrated by several authors[15] it receives a substantial contribution from long distances and we do not know for sure which fraction of the mass difference can be attributed to the box diagrams.

The ε parameter, however, which measures the deviation of K_S and K_L from CP eigenstates, originates from diagrams where W's and heavy quarks (charm and top) are exchanged and a short distance dominance is very plausible. The off diagonal elements of the mass matrix acquire an imaginary part with

$$\sqrt{2}|\varepsilon| = \frac{\mathrm{Im}M_{12}}{(M_L - M_S)_{exp}} \tag{17}$$

Since the first row of (13) is real an imaginary part for the dispersive part of the mass matrix is produced from couplings to heavy quarks. They can come either from the box diagrams (fig. 1) or from Penguin like diagrams (fig. 2).

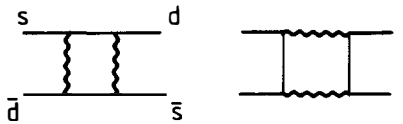

Fig. 1

Box Diagrams

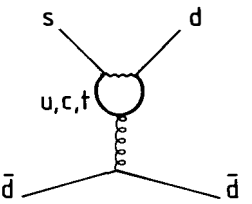

Fig. 2

Penguin Diagrams

The effect of the Penguin diagrams is relevant to the discussion of the ε'-parameter. They can also occur in the decays

$$K \to 2\pi \tag{18}$$

where long distance contributions are also important. Their effect to $|\varepsilon|$ is an overall phase ξ' which can be eliminated by a U(1) transformation defined in equ. (16). Then

$$\sqrt{2}|\varepsilon| = \frac{\mathrm{Im}\tilde{M}_{12}}{(M_L - M_S)_{exp}} + O\left(\frac{1}{15.5}\,\varepsilon'/\varepsilon\right) \quad . \tag{19}$$

The last term, in view of the experimental value reported for ε'/ε, is small and will be neglected. The term $\mathrm{Im}\tilde{M}_{12}$ comes from the box diagrams with the formula

$$\sqrt{2}|\varepsilon| \approx \frac{G^2 f_K^2 M_K B_K}{12\pi^2 (M_L - M_S)}\,\eta_1 |V_{ub}||V_{cb}||V_{us}|\sin\delta \;\times$$

$$\left\{\frac{\eta_2}{\eta_1} m_t^2 \left(|V_{cb}|^2 - \frac{|V_{cb}||V_{ub}|}{|V_{us}|} c_\delta\right) + m_c^2 \left(\frac{\eta_3}{\eta_1} \ln\frac{m_t^2}{m_c^2} - 1\right)\right\} \tag{20}$$

giving an accurate approximation for $m_t \lesssim 60$ GeV and with

$\beta \simeq |V_{ub}|$, $\gamma \simeq |V_{cb}|$, $\theta \simeq |V_{us}|$

Most of the terms in this expression were already defined, except for B_K which is defined in terms of the matrix element

$$\langle K^o | \bar{s}\,\gamma^\mu (1-\gamma_5) d\; \bar{s}\,\gamma_\mu (1-\gamma_5) d | \bar{K}^o \rangle = \frac{4}{3} B_K f_K^2 M_K \quad \text{and} \tag{21}$$

η_i's are QCD correction factors. Given that the mass m_t is between 40 and 60 GeV we can limit the ranges of the other parameters. Fig. 3 shows the range of B_K which is allowed by the data. Alternatively, if we select values for $m_t = 40$ and $\gamma = 0.057$, as suggested by the data, and set $B_K = 1$, then $\beta = |V_{ub}|$ and δ are restricted to lie in the shaded region of fig. 4. Obviously for $\beta = |V_{ub}| = 0$ there is no CP violation. When the B_K factor

is decreased, the shaded area moves upwards. We shall use these regions later for the predictions of ε'/ε. It is also evident that the main uncertainty is the B_K factor for which I refer to other theoretical talks.[16]

Recent results

In the decays

$$K^o \to 2\pi \tag{22}$$

the final states can have isospin zero or two and the transition amplitudes are denoted by A_o and A_2. When CP is conserved a relative phase between the amplitudes is produced by final state interactions through the phase shifts δ_o and δ_2. Using again the U(1) transformation of equ. (16) we can make the A_o amplitude real, then CP-violation is controlled by the parameter

$$\varepsilon' \equiv i \frac{\mathrm{Im}\, A_2}{A_o} e^{i(\delta_2 - \delta_o)} \tag{23}$$

This parameter is obtained from the measurable quantities n_{+-} and n_{oo} defined as

$$n_{+-} \equiv \frac{\langle \pi^+\pi^- | \; | K_L \rangle}{\langle \pi^+\pi^- | \; | K_S \rangle} = \varepsilon + \varepsilon' + \left(\begin{matrix}\text{smaller} \\ \text{terms}\end{matrix}\right) \tag{24}$$

$$n_{oo} \equiv \frac{\langle \pi^o\pi^o | \; | K_L \rangle}{\langle \pi^o\pi^o | \; | K_S \rangle} = \varepsilon - \varepsilon' + \left(\begin{matrix}\text{smaller} \\ \text{terms}\end{matrix}\right) \tag{25}$$

Two measurements were reported at this Workshop

$$\varepsilon'/\varepsilon = -0.0046 \pm 0.0024 \text{ (syst.)} \pm 0.0053 \text{ (stat.)} \quad \text{(Chicago-Saclay)}^{17)}$$
$$\varepsilon'/\varepsilon = +0.0017 \pm 0.0084 \text{ (stat. + syst.)} \quad \text{(Yale-BNL)}^{18)} \tag{26}$$

Evidently these measurements are consistent with zero (superweak theory) or small positive or negative values.

Beyond the final state interactions a relative phase between A_o and A_2 is produced by the Penguin diagrams (fig. 2). As discussed at the end of the first section the phase occurs in diagrams with heavy intermediate states where a short distance expansion is justified. It is generally accepted that the Penguin diagrams are enhanced[19] relative to other diagrams and was also argued[20] that the value for ε'/ε should be large and measurable. In the Wu-Yang convension the phase is transfered into the A_2 amplitude by applying the U(1) transformation already mentioned. Then

$$A_o \text{ is real}$$
$$A_2 = |A_2|e^{-i\xi} \qquad \text{and} \tag{27}$$
$$\varepsilon'/\varepsilon = -15.5\xi$$

This much is general. In the rest of this section I will describe the results of computing the penguin diagrams for 3 and 4 generations and then compare their predictions.

The extension to more generations introduces in fig. 2 additional heavy quarks in the intermediate state. The heavy quarks decouple and their end effect is to modify the structure of the charged current coupling by introducing additional angles. For instance, the final expression[21], with the standard assumptions, is

$$\varepsilon'/\varepsilon \cong \{40.7\beta\gamma\sin\delta_1 - 52.0\sigma\tau\sin\delta_2\} \frac{\langle 2\pi, I=0|Q_6|K_o\rangle}{1.4\ \text{GeV}^3} \tag{28}$$

The angles β, γ and the phase δ_1 are those used earlier. The new angles σ, τ and the phase δ_2 are new angles[21,22] introduced by the new generation. Finally, the dominant operator is

$$Q_6 = \sum_{\alpha,\beta} \bar{s}_\alpha \bar{d}_\beta (V-A) [\bar{u}_\alpha u_\beta + \bar{d}_\alpha d_\beta + \bar{s}_\alpha s_\beta] (V+A) \tag{29}$$

with indices α and β denoting color and the subscripts (V-A) and (V+A) the chiral structure of the operators. A major uncertainty is still the value of the matrix element for this operator.

In the limit $\sigma = \tau = 0$ the fourth generation decouples and equ. (28) reduces to the standard result. When the sign of the matrix element is chosen such that it constructively interferes with the rest of the $\Delta I = 1/2$

amplitude ($\Delta I = 1/2$ enhancement), then ε'/ε is positive. The matrix element is calculated either by a vacuum insertion method or by a combination of current algebra and the bag model. For the value

$$\langle 2\pi, I=0 | Q_6 | K \rangle = 1.4 \text{ GeV}^3 \tag{30}$$

the present ranges of β, γ and δ_1 restrict the ratio as follows

$$0.008 < \varepsilon'/\varepsilon < 0.012 \tag{31}$$

It has been pointed out[23], however, that the recent calculations allow values for the matrix element smaller by a factor of three. In addition factorization gives[24] a similar result. Thus I believe that the lower bound

$$0.002 < \varepsilon'/\varepsilon \tag{32}$$

is more realistic.

In four generations there are three more mixing angles and two new phases. We studied[21] this model with the intent not to derive bounds for the mixing angles, but rather to find some typical solutions characterizing the different predictions for ε'/ε. We found solutions which satisfy all previous constraints and in addition the predictions for ε'/ε are in the range of the measurements in equ. (26). Whereas ε'/ε is positive definite in the six quark model, the eight quark model can account for negative values and should be considered seriously if the experimental value for ε'/ε is restricted to lie below the bound in equ. (32).

Outlook

In the Moriond meeting in 1980 Jim Cronin asked which measurements were useful order to determine the elements of the Kobayashi-Maskawa matrix. The answer at that meeting was[25] "A crucial input, which is still missing, is the absolute normalization of a matrix element in the second or third row of V_{KM}. Two measurements are very relevant to the determination of the angles in the charged currents. The first involves the decay chain of the b-quark: Which decay is the dominant

$$b \to c \quad \text{or} \quad b \to u \qquad \text{and by how much?}$$

The second concerns the mixing phenomena of states with heavy quarks, like D^o-$\bar{D}^o$, B_d-$\bar{B}_d$ and B_s-$\bar{B}_s$." We saw in this Workshop that some of these goals have been achieved and the KM-matrix is precisely known, except for a lower bound of the V_{ub} element whose importance can not be overestimated.

Today we are in a position to pose precise questions. The following is a shopping list to occupy us for the next few years

i) It is very likely that theorists will obtain better estimates of matrix elements quadrilinear in the fermion fields, like B_K and Q_6. Such an advancement will make a precise measurement of ε'/ε even more important.

ii) A measurement of $|V_{ub}| = \beta$ is important because a zero value implies that CP-violation in the KM model is excluded.

iii) We need better identification of Bd and Bs decays, as well as their decay properties,[26] mixing properties, time development and CP-violation.

iv) A magnitude of V_{tb} less than one requires additional quarks.

v) The easiest search for a fourth generation is a heavy lepton[26] with mass $\approx$ 60 GeV.

Finally we need a deeper theoretical understanding for the origin of the fermion mass matrices, which in turn determine the quark masses and mixing angles.

Acknowledgement

The work was supported in part by a grant from the Bundesministerium für Forschung und Technologie.

Figure Captions

Fig. 3: Allowed range for B_K as a function of m_t.

Fig. 4: Allowed ranges for the angles β and δ for $\gamma = 0.057$ and $B_K \approx 1$ for two values of m_t.

References

1. E.A. Paschos and U. Türke, Phys. Lett. 116B, 360 (1982).
2. R.E. Shrock and L.-L. Wang, Phys. Rev. Lett. 41, 1692 (1978).
3. H. Leutwyler and M. Roos, CERN preprint 3830 (1984).
4. J.M. Gaillard, these proceedings.
5. Remark by P. Cooper at this meeting; see contribution by J.D. Bjorken (ref. 32).
6. Cl. Matteuzzi (SLAC experiments); J. Thomas (TASSO); R. Barlow (JADE), these proceedings.
7. A. Chen et al., Phys. Rev. Lett. 52, 1084 (1984).
8. C. Klopfenstein et al., Phys. Lett. 130B, 444 (1983); J. Lee Franzini, Moriond (1984), pg. 477.
9. S. Pakvasa, J.J. Sakurai and S.F. Tuan, Phys. Rev. D23, 2799 (1981).
10. K. Kleinknecht and B. Renk, Z. Phys. C16, 7 (1982); C20, 67 (1983); K. Kleinknecht, Moriond (1984), pg. 541.
11. M. Kobayashi and K. Maskawa, Prog. Theor. Phys. 49, 652 (1973).
12. L. Maiani, Proc. Int. Symp. on Lepton and Photon Int., Hamburg 1977, pg. 877.
13. L. Wolfenstein, Phys. Rev. Lett. 51, 1945 (1983).
14. The constraints on the element` or the angles have been checked by many groups and are now universall› cepted.
E.A. Paschos, B. Stech and U. Türke, Phys. Lett. 128B, 240 (1982);
P. Ginsparg, S.L. Glashow and M. Wise, Phys. Rev. Lett. 50, 1415 (1983); erratum 51, 1395 (1983); ref. 10;
L.-L. Chau, W.Y. Keung and M.D. Tran, Phys. Rev. D29, 592 (1984);
A. Buras, W. Slominski and H. Steger, Nucl. Phys.B238, 529 (1984); B245, 369 (1984);
I. Bigi and A.I. Sanda, Phys. Rev. D29, 1393 (1984);
E.A. Paschos and U. Türke, Nucl. Phys. B243, 29 (1984);
M. Lusignali and A. Pugliese, Phys. Lett. 144B, 110 (1984);
T. Brown and S. Pakvasa, UH-511-1984.

14b. L.L. Chau and W.Y. Keung, Phys. Rev. Lett. 53, 1802 (1984).

15. L. Wolfenstein, Nucl. Phys. B160, 501 (1979);
C. Hill, Phys. Lett. 97B, 275 (1980);
I.I. Bigi and A.I. Sanda, RU preprint 84/13/82.
16. J.F. Donohue, UMHEP-196 (1984);
B. Guberina, G. Nardulli, D.G. Sutherland, E. Golowich, these proceedings.
17. B. Winstein, Proc. Neutrino Conf., pg. 627 (1984);
B. Pejaud, these proceedings.
18. M. Schmidt, these proceedings.
19. M.A. Shifman, A.J. Vainshtein and V.I. Zakharov, Nucl. Phys. B120, 316 (1977);
F.J. Gilman and M.B. Wise, Phys. Rev. D20, 2392; Phys. Lett. 83B, 83 (1979);
B. Guberina and R.D. Peccei, Nucl. Phys. B163, 289 (1983).

20. F.J. Gilman and J.S. Hagelin, Phys. Lett. 126B, 111 (1983); J.S. Hagelin, Proc. Moriond 1984, pg. 533.

21. U. Türke, E.A. Paschos, H. Usler and R. Decker, DO-TH 84/26.

22. M. Gronau and J. Schechter, SLAC-PUB 3451 (1984).

23. L. Wolfenstein, CERN-TH.3925/84.

24. B. Stech, Note added to Contribution at the Proc. of Eur. Conf. "Flavour Mixing in Weak Int.", Erice (1984).

25. E.A. Paschos, Electroweak Interactions and Unified Theories, pg. 255 (Moriond 1980).

26. J.D. Bjorken, these proceedings.

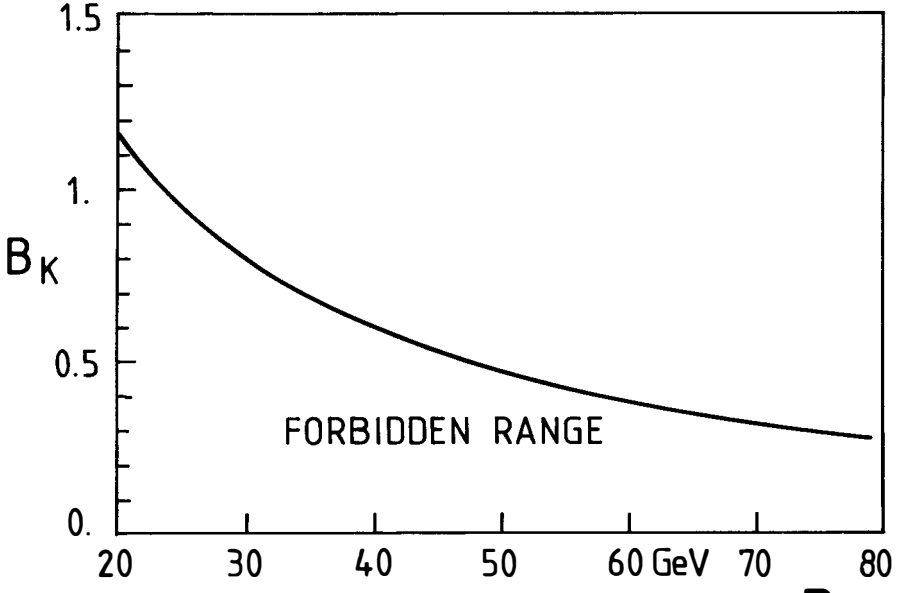
1.5
1.
B_K
0.5
0.
FORBIDDEN RANGE
20
30
40
50
60 GeV
70
80
m_t

Fig. 3

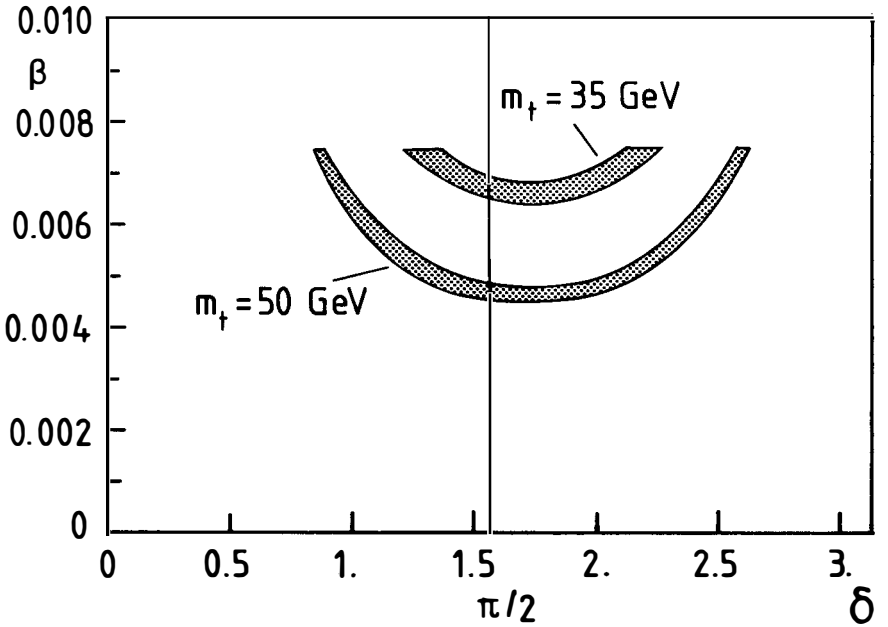
0.010
β
0.008
0.006
0.004
0.002
0
$m_t = 35$ GeV
$m_t = 50$ GeV
0
0.5
1.
1.5
2.
2.5
3.
π/2
δ

Fig. 4

THE NEUTRON ELECTRIC DIPOLE MOMENT IN THE STANDARD MODEL

J. O. Eeg
Institute of Physics, University of Oslo

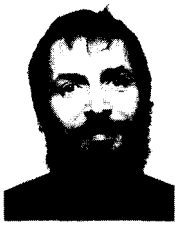

I give a short review of Neutron Electric dipole calculations based on the assumption that the only source of CP-violation is the Kobayashi-Maskawa phase. The numerical estimates for the biggest contributions are in the range (10^{-32} to 10^{-30}) e·cm, depending on quark model parameters.

1. Introduction. I will give a short review of calculations on the Neutron Electric Dipole Moment (NEDM - or "DEMON") in the Standard Model. That is, it is assumed that the only source of CP-violation is the Kobayashi-Maskawa (KM)[1] phase. Results on experiments and more exotic CP-violating models are covered by other speakers.

At three level fermions do not have electric dipole moments (EDM). But higher order diagrams in electroweak theory generate a CP-violating piece of the electromagnetic current for the neutron

$$J_\mu^{NEDM} = D_n \, \partial^\nu \, [\bar{\psi}_n \, \gamma_5 \, \sigma_{\mu\nu} \, \psi_n] \, , \tag{1}$$

where D_n is the NEDM and ψ_n the Dirac-field for the neutron. Within the KM-model [1] contributions to NEDM always have the form

$$D_n = e \, G_F^{\,2} \, F_{KM} \, \hat{D}_n \, , \tag{2}$$

where e is the electric charge, G_F the Fermi coupling constant, and

$$F_{KM} = s_1^{\,2} \, s_2 \, s_3 \, c_1 \, c_2 \, c_3 \, \sin\delta \tag{3}$$

In (3) $s_i \equiv \sin\theta_i$ and $c_i \equiv \cos\theta_i$, θ_i ;i = 1,2,3 being the generalized Cabbibo angles of the KM-model. δ is the KM phase angle. $\hat{D}_n$ in (2) has dimension mass in third power and is otherwise dependent on the specific mechanism for NEDM. The results obtained for the biggest contributions are of order

$$\left| \frac{D_n}{e \cdot cm} \right| \sim 10^{-32} \quad \text{to} \quad 10^{-30} \tag{4}$$

depending on the specific choice of quark model with appurtenant parameters. (4) corresponds to 10^{-16} to 10^{-18} in Bohr magnetons.

There are in general two main mechanisms for NEDM: a) An EDM for a single quark can be generated through higher loop diagrams in electroweak interactions. b) The NEDM can be generated by interplay of two or more quarks in the neutron. In the following a brief survey of quark diagrams for NEDM and the corresponding estimates will be given.

2. EDM for a single quark. Typical lowest order loop diagrams generating an EDM of a single quark are shown in Fig. 1 (Note that one loop diagrams for diagonal transitions like $d \to \gamma d$ and $u \to \gamma u$ are not CP-violating). While individual diagrams of this type give [2] contributions to NEDM of order 10^{-31} (- in the units of eq.4 -), it was later shown [3] that the sum of all pure

electroweak diagrams (like Fig. 1a) is zero. With a gluon interaction added as in Fig. 1b, one obtains [4]

$$D_n \sim e\, G_F^2\, F_{KM}\, m_{u,d}^{(c)}\, \frac{\alpha_s}{\pi^5}\, \frac{m_q^4}{M_W^2} \quad , \tag{5}$$

where $m_{u,d}^{(c)}$ denotes the constituent quark mass for u- and d-quarks, and α_s is the strong coupling constant. m_q^4 symbolizes a product (of fourth order) of quark masses involving GIM factors like $(m_t^2 - m_c^2)$ and $(m_b^2 - m_s^2)$. Numerically one finds from (5) a NEDM of order 10^{-34} in the same unit as in (4). This is far below the experimental limit $\sim 10^{-25}$.

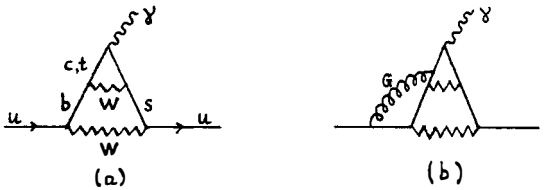

Fig. 1. Electric dipole moment of a single quark. (a) Pure electroweak diagram. (b) Same diagram as 1a with gluon interaction added.

3. NEDM due to electroweak interplay of two or three quarks in the neutron. The NEDM can also be generated by a non-diagonal one-loop CP-violating electroweak transition, d → γs say, combined with W-exchange between two quarks, as visualized in Fig. 2a. This mechanism has been considered by several authors [5,6,7], and the numbers obtained are in the range 10^{-32} to 10^{-34} depending on the assumptions. Interpreting the quark diagram in Fig. 2a as a pole diagram on baryon level, as in Fig. 2b, one finds an expression for the NEDM of the form [7]

$$D_n \sim e\, G_F^2\, F_{KM}\, \frac{(m_t^2 - m_c^2)}{\pi^2\, M_W^2} \cdot \frac{m_s}{\Delta M}\, |\psi(0)|^2\, (QMP)_1 \quad , \tag{6}$$

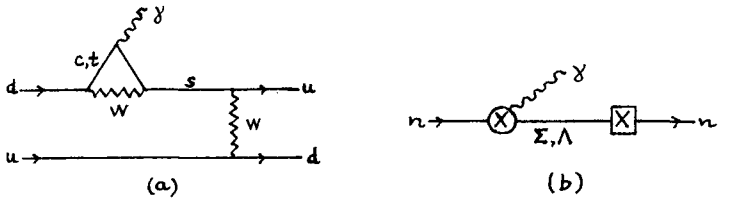

Fig. 2. (a) NEDM generated by a d → γs loop combined with W-exchange between two quark lines. (b) Same diagram as in 2a intepreted as a pole diagram on baryon level.

where ΔM is the strange to non-strange baryon mass difference, $|\psi(0)|^2$ is the square of the wave function at the origin, and $(QMP)_1$ symbolizes quark model parameters. 10^{-34} seems to be [6,7] the best estimate obtained for NEDM within the mechanism shown in Fig. 2.

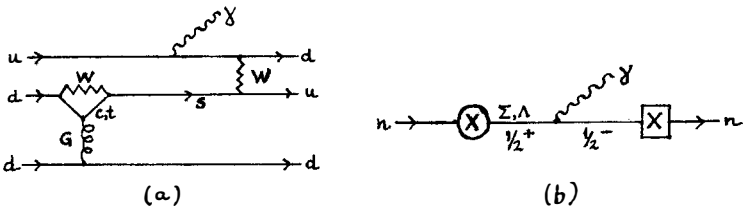

Fig. 3. Diagram for NEDM due to interplay of three quarks in the neutron. (a) On quark level. (b) Intepreted as a pole diagram on baryon level. The cross within the circle (square) represents the penguin interaction (ordinary W exchange).

Then it was realized [8,9] that if the γ in Fig. 2a is replaced by a virtual gluon (G) (subsequently attached to another quark line), thus making a penguin diagram, one gains a factor $\sim 10^2$ to 10^3. The γ has then to be emitted from another quark line, like in Fig. 3a. Intepreting this quark diagram in terms of baryon poles, as in Fig. 3b, one obtains [8]

$$D_n \sim e\, G_F^2\, F_{KM}\, \frac{\alpha_s}{\pi}\, \ell n\left(\frac{m_t^2}{m_c^2}\right) \cdot \frac{|\psi(0)|^4}{(\Delta M)^2}\, (QMP)_2 \ , \qquad (7)$$

where $(QMP)_2$ is a factor containing quark model parameters. (Note that in order to obtain a NEDM, one of the intermediate strange baryons must be a negative parity resonance). From (7) Gavela et al.[8] made the estimate 10^{-31} to 10^{-30} for NEDM, which is the biggest one obtained within the KM-model. One should note that two loop diagrams for $ud \to du\gamma$ of the type in Fig. 4a are partly included in (7). Namely, when the horizontal intermediate quark lines in Fig. 4a have quark momenta $\lesssim 1$ GeV, Fig. 4a can be intepreted as a pole diagram as in Fig. 3b.

The diagram in Fig. 4a can also be intepreted as an ordinary Feynman diagram potentially containing short distance effects [10]. The horizontal quark lines in the box loop are then expected to have quark momenta between ~ 1 GeV and M_W before the GIM-mechanism is taken into account. Considering CP-violating Feynman diagrams for $ud \to du\gamma$, γ can also be emitted inside the penguin loop in Fig. 4b [8,10,11]. Elementary processes like $d \to q'\gamma G$ ($q' = s,b$) and $u \to q\gamma G$ ($q = c,t$) we have baptized "photopenguin" [10]. They can in the limit $M_W \to \infty$

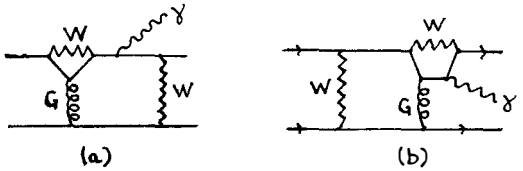

Fig. 4. Two loop Feyman diagrams for NEDM due to interplay of two quarks in the neutron. (a) Containing an ordinary penguin loop. (b) Containing a photopenguin loop. Note that also (s,b) quarks can enter the (photo)penguin loop and (c,t) quarks the upper part of the box loop.

be represented by the triangle diagram [12]. One must also take into account diagrams like those in Fig. 4, but with crossed gluon (G) and W lines. These latter diagrams can not be intepreted in terms of baryon poles like in Fig. 2b and 3b. The sum of all Feynman two loop diagrams for $ud \to du\gamma$ can be written as a CP-violating effective interaction which gives a contribution to NEDM of the form [10]

$$D_n \sim e\, G_F^2\, F_{KM}\, \frac{\alpha_s}{\pi^3}\, \ell n \left(\frac{m_b^2}{m_c^2} \right) \cdot I_{Bag} \,, \qquad (8)$$

where I_{Bag} is an integral over bag wave functions corresponding to the hadronic quantity $|\psi(0)|^2$ in (6) and (7). For individual diagrams, $\ell n(M_W^2/m_q^2)$ terms are present. But after the two-fold GIM-mechanism (- one in the box - and one in the penguin loop) has been taken into account, we are left with contributions $\sim \ell n(m_b^2/m_c^2)$ which we call "relics of short distance effects" [10]. The numerical estimate obtained from (8) is $\sim 10^{-32}$.

The diagram 4b has recently been interpreted and calculated as a pole diagram (like in Fig. 2b) and the following NEDM obtained [11]:

$$D_n \sim e\, G_F^2\, F_{KM}\, \frac{\alpha_s}{\pi} \left(\frac{1}{m_c^2} - \frac{1}{m_t^2} \right) \frac{|\psi(0)|^4}{\Delta M} \cdot (QMP)_3 \,, \qquad (9)$$

which gives the numerical estimate $\sim 10^{-32}$ to 10^{-31}.

4. Conclusion. The biggest contributions to NEDM within the KM model comes from diagrams like those in Figs. 3 and 4. It should, however, be emphasized that the "long distance" contributions (7) and (9) obtained by Gavela et al. [8,11] and the "short distance" contribution (8) obtained by Eeg & Picek [10] are complementary. Although the contributions (7) and (9) contain short distance effects through the penguin loop and W-exchange, they are cruically dependent on long distance effects due to intermediate baryon poles. For this reason (7)

and (9) contain $|\psi(0)|^2$ in second power, while (8) contains the corresponding quantity I_{Bag} in first power. Thus the "long distance" contributions (7) and (9) are more model dependent than the "short distance" contribution (8). If $|\psi(0)|^2$ is overestimated [10,13] in Refs. 8,11 and I_{Bag} is underestimated [11] in Ref. 10, then both "long" and "short" distance contributions are roughly of the same order of magnitude 10^{-32} to 10^{-31} (However, the "long distance" contribution from 4a is bigger than from 4b, while the opposite is the case for "short distance" contributions [10]).

In conclusion, the value of NEDM within the KM model is ~ 10^{-32} to 10^{-30}, that is, at least five order of magnitude below the experimental value. This result is welcome in the sense that it keeps the KM value of the NEDM well separated from the corresponding values obtained in more exotic models like Left-Right symmetric- and Higgs-exchange models, which give bigger numbers.

Refereces

1) M. Kobayashi and K. Maskawa, Prog. Theor. Phys. 49 (1973) 652
2) J. Ellis, M.K. Gaillard and D.V. Nanopoulos, Nucl.Phys. B109 (1976) 213
   J. Ellis and M.K. Gaillard, Nucl. Phys. B150 (1979) 141
3) E.P. Shabalin, Yad. Fiz. 28 (1978) 151 [Sov. J. Nucl. Phys. 28 (1978) 75]
4) E.P. Shabalin, Yad. Fiz. 31 (1980) 1665 [Sov.J. Nucl. Phys. 31 (1980) 864]
5) D.V. Nanopoulos, A. Yildiz and P.H. Cox, Phys. Lett. 87B (1979) 53;
   Ann. Phys. 127 (1980) 126
   B.F. Morel, Nucl. Phys. B157 (1979) 23
   N.G. Deshpande, G.Eilam and W.L. Spence, Phys. Lett. 108B (1982) 42
6) E.P. Shabalin, Yad. Fiz. 32 (1980) 443 [Sov. J. Nucl. Phys. 32 (1980) 228]
7) M.B. Gavela, A. Le Yaouanc, L. Oliver, O. Pène, J.C. Raynal, T.N. Pham,
   Phys. Lett. 109B (1982) 83
8) M.B. Gavela et al. Phys. Lett. 109B (1982) 215
9) I.B. Khriplovich and A.R. Zhitnitsky, Phys. Lett. 109 (1982) 490
   E. Golowich and B.R. Holstein, Phys. Rev. D26 (1982) 182
10) J.O. Eeg and I. Picek, Phys. Lett. 130B (1983) 308;
    Nucl. Phys. B244 (1984) 77
11) M.B. Gavela et al., Z. Phys. C23 (1984) 251
12) L. Rosenberg, Phys. Rev. 129 (1963) 2786
    S.L. Adler, Phys. Rev. 177 (1969) 2426
13) E. P. Shabalin, Usp. Fiz. Nauk 139 (1983 561 [Sov. Phys. Usp. 26
    (1983) 297]

MASS MIXING AND CP VIOLATION IN THE $D^0\bar{D}^0$ SYSTEM

P. VERRECCHIA

Département de Physique des Particules Elémentaires,
CEN-Saclay, 91191 Gif-sur-Yvette Cedex, France.

ABSTRACT

We present here a review of experimental upper limits on $D^0\bar{D}^0$ transitions (mixing). A new upper limit obtained with the BCDMS spectrometer will be discuted in more details and compared to the expected value from the standard six quarks model.

Kobayashi - Maskawa matrix and CP violation in $K^{\circ}\bar{K}^{\circ}$ system

The mixing of quarks through the weak interaction is described by a unitary matrix V_{ij} conventionally known as the Kobayashi - Maskawa matrix which can be parametrised by 3 angles and 1 phase δ possibly related to CP violation.

It is remarkable that so far the only CP violation observed is still the originally observed system of $K_S - K_L$ in 1964 [1].

The available experimental informations on the K_S^o K_L^o mas difference Δm and the CP violation parameter ϵ do not constrain δ.

Δm is given by the relation [2] :

$$\Delta m = 2\ \mathrm{Re}(M_{12}) = 2\ \mathrm{Re}\left(-\frac{G_F^2}{12\pi^2} m_W^2\ B_K\ f_K^2\ m_K\ \left(\sum_{ij} \lambda_i\ \lambda_j\ A_{ij}\right)\right)$$

where $\lambda_i = V_{id}\ V^*_{is}$

ϵ is given by the relation [3] :

$$|\varepsilon| = 2 \left|\frac{m_t - m_c}{m_c}\right| \frac{s_2\ c_2\ t_3}{2\sqrt{2}\ c_1}\ s_\delta$$

Since δ is closely related to the CP violation phenomenology, the confirmation of the Kobayashi - Maskawa model must come from the observation of CP violation in other system.

Theoretical predictions on $D^{\circ}\bar{D}^{\circ}$ system

The box graph calculation of Δm and ϵ in the $K^{\circ}\bar{K}^{\circ}$ system can be adapted for the heavy quark $D^{\circ}\bar{D}^{\circ}$ system.

The transition matrix M_{12} and the absorptive amplitude Γ_{12} of $D^{\circ}\bar{D}^{\circ}$ transitions are given by the following relation [2] :

$$M_{12} = \frac{G_F^2\ B_D\ f_D^2\ m_D\ m_W^2}{12\ 2} \sum_{i,j} \lambda_i\ \lambda_j\ A_{ij} \qquad \text{where} \qquad \lambda_i = V_{ci}\ V^*_{vi}$$

indices i, j run through the d,s allowed channel

$$\Gamma_{12} = - \frac{G_F^2 \, B_D \, f_D^2 \, m_D}{\pi} \sum_{\pm, i, j} \frac{1}{(8 \pm 16)} \lambda_i \lambda_j C_{ij}$$

where positive and negative sign gives the contribution of W emission and W exchange graph. A_{ij} and C_{ij} are expressed in terms of quark's mass m_c, m_d, m_s, m_u ; D meson and W boson mass.

The mass difference Δm and the width difference $\Delta\Gamma$ are given by the relation [2] :

$$\Delta m - i \frac{\Delta\Gamma}{2} = 2 \left[(M_{12} - i \frac{\Gamma_{12}}{2}) (M_{12}^* - i \frac{\Gamma_{12}^*}{2}) \right]^{1/2}$$

The dependence of δ upon Δm and $\Delta\Gamma$ is shown in the figure 1.

a) computed value of $\Gamma(D^\circ)$ is found to be compatible with the experimental measure [4]

b) the total width of the D meson is much larger than Δm and $\Delta\Gamma$: as the D° decays are Cabibbo favored, the life time is much shorter than the oscillation period, so that there is no observable interference.

The mixing parameter r(D) and the experimental signature of $D^\circ\bar{D}^\circ$ transition

The experiments do not measure directly Δm or $\Delta\Gamma$ but the mixing parameter r(D) which is the probability that a D° state should evolve into a $\bar{D}^\circ$ state.

The D° meson can decay into hadronic or semi leptonic final states like $D^\circ \to K^- x$ and $D^\circ \to e^+ \nu_e x$, if a $D^\circ\bar{D}^\circ$ transition occurs we can expect forbidden final state such as $D^\circ \to K^+ x$ and $D^\circ \to e^- \bar{\nu}_e x$. The experiments measure the fraction of such forbidden channels i. e.

$$r(D) = \frac{D^\circ \to K^+ X \ (\text{or } \ell^- \bar{\nu}_\ell \, X)}{D^\circ \to \text{anything}}$$

The mixing parameter r(D) is related to Δm, $\Delta\Gamma$ and Γ [2]

$$r(D) \# \frac{(\Delta m)^2 + (\frac{\Delta\Gamma}{2})^2}{2\Gamma^2 + (\Delta m)^2 - (\frac{\Delta\Gamma}{2})^2}$$

In the standard Kobayashi-Maskawa framework, we expect : $r(D) < 10^{-3}$.

Previous experimental results

A) e^+e^- collider : in e^+e^- interaction, the experiments study the charmed particle prediction via the $D^\circ\bar{D}^\circ$ pair production or inclusive D^* production. In the $D^\circ\bar{D}^\circ$ channel, the normal final state obtained by the decays of both D's is :

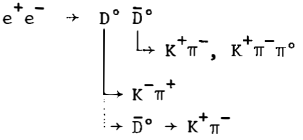

The signature of a $D^\circ\bar{D}^\circ$ transition is a $(K^+K^-)\,K^+$ final state where the $(K^+\pi^-)$ system comes from a D meson.

Alternatively, the decay cascade of a D^* is :

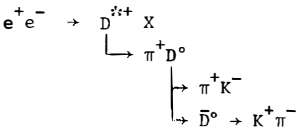

The signature of a $D^\circ\bar{D}^\circ$ transition is a $\pi^+\,(K^+\pi^-)$ final state where the $(K^+\pi^-)$ system comes from a $\bar{D}^\circ$ decay and the mass of the $\pi^+\,(K^+\pi^-)$ system is the D^{*+} mass.

As shown by table 1, no significant signal has been found in e^+e^- interactions. Some of the experiments give upper limit at 90 % CL on the mixing parameter r(D).

B) Hadroproduction

- The ACCMOR collaboration [5] studies the $D\bar{D}$ pair production and the inclusive D^* production in π^- Be interaction with a 200 GeV π^- beam. They search for e^+K^- and e^-K^+ pairs. In a statistic of 60 D^* and 320 D, they obtain an upper limit of 7 % on r(D).

- A beam dump experiment [6] performed at Fermilab in 1982 looks for charmed particle pairs produced in π^-Fe interaction. $D^\circ\bar{D}^\circ$ transitions are detected as final states with like sign dimuons. They have 1 $\mu^+\mu^+$ and 2 $\mu^-\mu^-$ events, while 154 $\mu^+\mu^-$ are observed. The same sign dimuon events are consistent with the expected background from π/K decays, which gives an upper limit on r(D) of 4.4 % at 90 % CL. This experiment gives at present the best limit in $D^\circ\bar{D}^\circ$ mixing.

C) Photoproduction

An experiment [7] performed at Fermilab in 1979 with a 50 GeV incident photon beam has reported the observation of inclusive D^{*+} and D^{*-} production and decays. Their statistic is based on 200 D but no enhancement was observed in the $\pi^+ (K^+\pi^-)$ channel. They correspond to an upper limit on r(D) of 11 % at 90 % CL.

D) Neutrino scattering

In neutrino-Iron or Neon interaction, a D° can be produced by the diagramm :

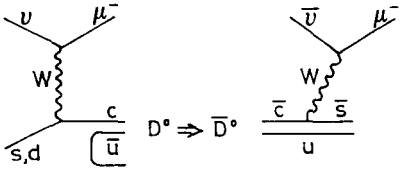

In the presence of $D^\circ\bar{D}^\circ$ transitions, the ν_μ beam induces $\mu^-\mu^-(e^-)$ final states and $\bar{\nu}_\mu$ induces $\mu^+\mu^+(e^+)$ final states. As summarized in table 3 like sign dileptons has been observed in several counters experiments and in a few bubble chamber experiments. However, the situation is unclear mostly because of large uncertainties in substracting background in counter experiment and because of poor statistic in bubble chamber experiments.

E) Muoproduction

These experiments measure the production of additional muons in the interaction of muons with nuclei. If $D^\circ\bar{D}^\circ$ transitions occurs, like sign dimuons are obstained when both D's decay simileptonically.

For instance $\mu^+ N \rightarrow \mu^+ (D^\circ, D^+ \ldots)(\bar{D}^\circ, D^- \ldots) X$

$\bar{D}^\circ \rightarrow \mu^- \bar{\nu}_\mu X$; $\rightarrow \mu^- \bar{\nu}_\mu X$

a) EMC [8] observe 2 $\mu^+\mu^+\mu^+$ and 1 $\mu^+\mu^-\mu^-$ final states in muon-Fe interaction at 250 GeV. They deduce an upper limit of 20 % on the mixing parameter r(D) with 90 % CL.

b) We present now, the result of our study of wrong sign dimuons in deep inelastic interactions of 200 GeV muons with a carbon target obtained in the BCDMS spectrometer.

Apparatus and data taking : The experiment was performed at the CERN SPS muon beam. The apparatus [9] is a 50 m long toroidal iron magnet, centered on the beam axis and instrumented with scintillation counters and multiwire proportional chambers to detect the scattered muons. The central hole of the magnet contains a 40 m long carbon target.

The data presented here were obtained with μ^+ and μ^- beams of 200 GeV energy, and are selected from a data sample that was used to study electroweak effects in deep inelastic muon-nucleon scattering [10]. The total number of incoming muons is $1.75\ 10^{12}$, corresponding to an integrated luminosity of $9.17\ 10^{39}\ cm^2$. The spectrometer magnetic field was reversed with each change of the beam polarity in order to always focus muons of the same sign as the incoming beam muon towards the spectrometer axis. 165 candidate events with two wrong sign (defocused) muon tracks were found in the raw data sample ; the interacting beam muon escapes, in general, through the central hole of the spectrometer without being detected. Of these candidates, 114 were retained as good events after visual scanning by physicists. To ensure a good momentum determination, each track was required to have at least 4 points in each of the two projections recorded by the MWPC's. To suppress spurious triggers from hadronic punch-through and to allow a computation of the acceptance, the reconstructed muon tracks had to fulfill the trigger requirement of the experiment. Since the spectrometer is designed to measure focused tracks but has a poor acceptance for defocused muons which rapidly escape the magnet volume, these cuts reduce the final data sample to only 17 events.

background from π/K decays : The main background in the selected data sample is due to ordinary π and K decays. It is computed with a Monte-Carlo programm which simulates the multiplicities charged π's and K's in the final state, their distributions in transverse momentum P_T, and their fractional energy z as measured by the EMC [11]. The simulation takes into account the correlation between these variables and the asymetry between π^+ and π^- production. Primary hadrons are allowed to decay in the target region before entering the iron toroids ; the development of hadronic showers due to secondary interactions inside the carbon target is ignored. We also neglect the effect of K^o, vector meson (ρ, ω, ϕ) and strange baryon (Λ, Σ) production. Decay muons are tracked throught the detector, simulating multiple scattering and energy loss ; they are reconstructed and the events are selected in exactly the same way as the experimental data. We find a background from double hadron decay of 15.5 ± 2.8 events which is compatible with the 17 events observed. The figure 2 indicates a good agreement of the kinematic distributions of experimental data and simulated background, justifying a posteriori the above sim-

plifications. We gain additional confidence in this simulation programm from the good background description which is observed for other multimuon topologies as shown in table 4.

Production of $c\bar{c}$ quarks pairs : to compute the acceptance of the apparatus for muon pairs from charmed quaks decays, the kinematics of $c\bar{c}$ pairs was calculated in the framework of the photon gluon fusion [12] model as in our study of muons pairs at 200 GeV energy [13]. The gluon distribution $G(\eta)$ and the QCD parameters of the γGF model were taken from the EMC adjustements of their open charm data [14].

Upper limit on $D^0\bar{D}^0$ transitions : We use the total difractive charm production cross section of $\sigma(c\bar{c}) = 6.9^{+1.9}_{-1.4}$ nb measured by the BFP collaboration at 209 GeV beam energy [15] which is in good agreement with the EMC result $\sigma(c\bar{c}) = 9.8 \pm 3.3$ nb at 250 GeV [14] when the difference in beam energy is taken into account. We then assume the c quark to fragment with aqual probabiity in charged and neutral D's [16], i. e. a cross section of $\sigma(D^0\bar{c}) = 3.4$ nb for the production of $D^0\bar{D}^0$ and D^0D^- pairs. With the known semileptonic branching ratios of the D^0 (5 %) and the $D^{\pm}$ (19 %) [17] this corresponds to an effective cross section for μ pair production of $\sigma(D^0\bar{c}) \times B_{sl}^2 = 20$ pb. To this, we assign a global systematic error of % 50 % which accounts for the quoted error of the charm cross section, the uncertainty of the charged to neutral D production ratio, and a possible contribution of F and Λ_c production to the measured charm cross sections. Assuming a flat fragmentation function of the c quark in the $c\bar{c}$ c.m. system, we find an acceptance for wrong sign dimuon final states of $A = (2.9 \pm 0.3) \times 10^{-13}$. The use of the other fragmentation functions compatible with EMC open charm data [14], i.e. flat fragmentation or fragmentation like exp (-3.6 z) in the laboratory frame, has only little effect on our acceptance ; on the basis of such studies, we estimate a systematic error of the acceptance calculation of 15 %. The signal which we should expect for an (unphysical) mixing probability $P(D^0 \leftrightarrow \bar{D}^0) = 1$ is $L \times \sigma(D^0\bar{c}) \times B_{sl}^2 \times A = 542 \pm 60$ events, where the error accounts for the Monte-Carlo statistics of the acceptance calculation and a systematic uncertainty of the luminosity calibration. Figure 3 shows the simuated distribution of the sum of transverse momenta of muons from double charm decays. Since the shape is very simular to the corresponding spectrum of hadronic background, we calculate the upper limit in the mixing probability directly from the statistical error on 17 events and find $r(D) \equiv P(D^0 \leftrightarrow \bar{D}^0) < 2.5$ % at 90 % CL.

Conclusions

1) Combining all experimental upper limits summarized in tables 1 and 2 we can extract new upper limit on probability transitions, we find $r(D) = P(D^\circ \leftrightarrow \bar{D}^\circ) <$ 1.90 % at 90 % CL. The limit on $D^\circ\bar{D}^\circ$ mixing is still far above the prediction of the standard six quarks model but rules out alternative models in which the mixing is predicted to be larger [18].

2) From the expression which connect the mixing parameter r(D) to the mass and width difference of the $D^\circ\bar{D}^\circ$ system we can deduce, if $\Delta\Gamma << \Gamma$ the expression of the mass difference of the $D^\circ\bar{D}^\circ$ system :

We have $$\Delta m^2 \# \frac{2\ r\ \Gamma^2}{1 - r}$$

If we take the average value of the D° life time [4]

$$\tau(D^\circ) = \frac{\hbar}{\Gamma} \# (3.6 \pm 0.35) 10^{-13} \text{ sec.}$$

We find $\Delta m < 0.36\ 10^{-3}$ eV with 90 % CL.
This can be compared with the measured $K^\circ\bar{K}^\circ$ mass difference of 0.352×10^{-5} eV. If we report this upper limit on figure 1 we see that we cannot use this experimental information to put constraints on δ.

References

[1] J.H. CHRISTENSON, J.W. CRONIN, V.L. FITCH and R. TURLAY, Phys. Rev. Lett. 13 (1962) 138

[2] LING LIE CHAU, quark mixing in weak interactions, Phys. Rep. 95 (1983) 1

[3] S. PAKVASA and H. SUGAWARA, Phys. Rev. D14 (1976) 305

[4] K. SCHUBERT, 11th International Conference on Neutrino Physics and Astrophysics, Dortmund, June 11-16 1984

[5] R. BAILEY et al., Phys. Lett. 132B (1983) 237

[6] A. BODEK et al., Phys. Lett. 113B (1982) 82

[7] P. AVERY et al., Phys. Rev. Lett. 44 (1980) 1309

[8] J.J. AUBERT et al., Phys. Lett. 106B (1981) 419

[9] D. BOLLINI et al., Nucl. Instr. Methods, 204 (1982) 333

[10] A. ARGENTO et al., Phys. Lett. 120B (1983) 245

[11] J.J. AUBERT et al., Phys. Lett. 95B (1980) 306
J.J. AUBERT et al., Phys. Lett. 100B (1981) 433

[12] For a review and full bibliography of the γGF model, see
R.J.N. PHILLIPS, Proc. XX Int. Conf. on high energy physics,
Madison, Wisconsin 1980, L. DERRAND and L.G. PONDROM ed., p. 1470

[13] D. BOLLINI et al., Nucl. Phys. B199 (1982) 27

[14] J.J. AUBERT et al., Nucl. Phys. B213 (1983) 31

[15] G.D. GOLLIN et al., Phys. Rev. D24 (1981) 559

[16] R. BAILEY et al., Phys. Lett. 132B (1983) 230

[17] Particle Data Group, review of particle properties, Rev. Mod. Phys.
56 (1984) 51

[18] E. PASCHOS, Phys. Rev. D15 (1977) 1966

[19] J.G.H. de GROOT et al., Phys. Lett. 86B (1979) 103

[20] T. TRINKO et al., Phys. Rev. D23 (1981) 1889

[21] V.V. AMMOSOV et al., Phys. Lett. 105B (1981) 151

[22] A. HAATUFT et al., Nucl. Phys. B222 (1983) 365

[23] to be published in Phys. Lett. B

experiments	e(D)
MARK I	0.18
MARK II	0.16
TASSO	0.23
ARGUS	0.12

TABLE 1. Upper limit obtained by experiments at e+e- collider.

experiments	r(D)
Ref. 6)	0.044
Ref. 7)	0.11
EMC	0.20
BCDMS	0.025

TABLE 2. Upper limit obtained by other kind of experiment.

Experiments	Beam	Number of like sign dimuons	Cuts (GeV)	Expected backgr. from π/K decays	r(D)
CDHS	ν_μ	(290±17)$\mu^-\mu^-$	$p_\mu > 6.5$	207±33	4.1±2.2
	$\bar{\nu}_\mu$	(53±7)$\mu^+\mu^+$		31±7	4.2±2.3
Reference 19) (Fermilab)	ν_μ	(149±20)$\mu^-\mu^-$	$p_\mu > 5$	97±24	7±4
15 ft BC (Ne,H2) Reference 20)	$\bar{\nu}_\mu$	4 μ+e+	$p_\mu > 4$ and $p_e > 0.4$	1.1	13^{+15}_{-9}
GGM BC (propane-fréon) Reference 21)	ν	10 μ- e-	p_μ >4.5 and p_e >0.5	4.1	20±11
		7 μ-e-	p_μ >4.5 and p_e >0.8	2.1	22±12
BEBC (WA 59) Reference 22)	ν_μ	9 μ-μ-	p_{μ_1} >4 and p_{μ_2} >3	7	0.22 (*)
	$\bar{\nu}_\mu$	5 μ+μ+		7	0.12 (*)
	ν_e	3 μ+e+	p_μ >4 and p_e >0.8	1.7	0.06 (*)

TABLE 3. Experimental results from neutrino scattering.

r(D) is just the ratio (number of like sign dimuons)/(opposite sign dimuons). It's not claimed by the authors to be $D^\circ\bar{D}^\circ$ mixing.

(*) upper limit at 90 % CL.

Type of multimuons	Kinematic range of muons arising from π/K decays		$\sigma_{seen} - \sigma_{other\ chan.}$	σ_{MC}
	momentum	transverse momentum		
Opposite sign dimuons $\mu N \to (\mu)\mu^+\mu^- X$	10 to 60 GeV	0.3 to 3 GeV	0.14 pb ± 0.02 pb	0.14 pb ± 0.01 pb
Same sign dimuons $\mu^\pm N \to \mu^\pm\mu^\pm X$	10 to 40 GeV	1.6 to 3 GeV	$3.7\ 10^{-3}$ pb ± $0.8\ 10^{-3}$ pb	$4.8\ 10^{-3}$ pb ± $0.6\ 10^{-3}$ pb
Single defocused $\mu^\pm N \to \mu^\mp X$	40 to 80 GeV	0.6 to 4.5 GeV	0.82 pb ± 0.4 pb	0.81 pb ± 0.17 pb
Wrong sign dimuons $\mu^\pm \to \mu^\mp\mu^\mp X$	10 to 60 GeV	0.5 to 3 GeV	$1.85\ 10^{-3}$ pb ± $0.6\ 10^{-3}$ pb	$1.7\ 10^{-3}$ pb ± $0.3\ 10^{-3}$ pb

TABLE 4

FIG.1

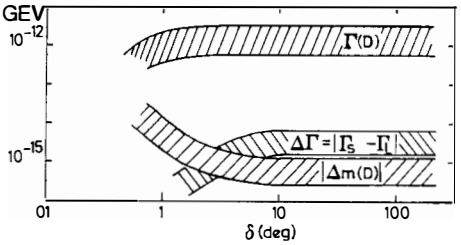

FIG. 2

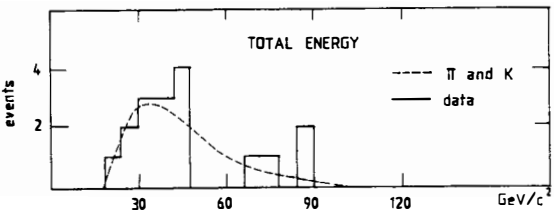

FIG. 3

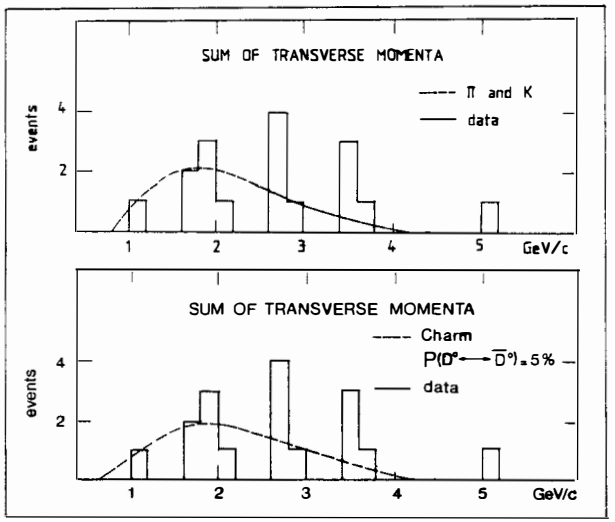

BOUNDS ON ε'/ε IN THE STANDARD MODEL VIA QCD SUM RULES

Branko Guberina
Rudjer Bošković Institute[+]
Zagreb, Croatia, Yugoslavia
and
Max-Planck-Institut für Physik und Astrophysik
— Werner-Heisenberg-Institut für Physik —
D-8000 München 40, Germany

The lower bound on ε'/ε is obtained by deriving an upper bound on the K-π transition amplitude of the penguin operator via QCD sum rules. The uncertainties which enter into this and alternative calculations are discussed.

[+]Permanent address

Our starting point* is the lower bound on ε'/ε derived recently by Gilman and Hagelin[3] using the measured B lifetime

$$\left|\frac{\varepsilon'}{\varepsilon}\right| \geq 8.4\,(s_2c_2s_3s_\delta)\,(\mathrm{Im}\ c_5)\,(\langle\pi^0\pi^0 \quad |4\mathcal{O}_5|K^0\rangle)\,(0.14\ \mathrm{GeV}^3)^{-1} \qquad (1)$$

The first parenthesis on the r.h.s. is the lower bound on the product of Kobayashi-Maskawa (K-M) parameters given as a function of the B-meson lifetime τ_B, the K^0-$\bar{K}^0$ mixing parameter B and the top-quark mass m_t. The bound increases with increasing τ_B, but increasing B and m_t decreases the bound significantly.

The second parenthesis is the QCD "renormalized" Wilson coefficient of the penguin operator, calculated by using the renormalization group techniques in the leading log approximation[4,5].

The third parenthesis in (1) is the matrix element of the penguin operator. The calculation of the matrix element is subject to uncertainties due mainly to our lack of knowledge of the true hadronic wave functions. It may be estimated by using the vacuum saturation or directly calculated in quark models[6,7] (bag model, oscillator model). In our approach we derive the bound on the matrix element by using the techniques of QCD sum rules[8]. We start[9] with a $K \to 2\pi$ transition amplitude

$$a^{\mathrm{peng}}(K^0 \to \pi^+\pi^-) = \kappa\,\frac{1}{f_\pi}\,(\sqrt{2}\,G_F\cos\theta_C\sin\theta_C)\,\mathrm{Re}\,c_5 \times \{\langle\pi^+|\mathcal{O}_5|K^+\rangle + \langle\pi^+|\mathcal{O}_5^{(c)}|K^+\rangle\} \qquad (2)$$

obtained via soft-pion limit (PCAC). The second term in (2) arises from the commutator of the normal-ordered operator $\mathcal{O}_5$ with an axial charge Q^5

$$[Q^5, \mathcal{O}_5] = -[Q, \mathcal{O}_5] + \frac{32}{9}\langle 0|\bar{d}d|0\rangle :\bar{s}(1+\gamma_5)d: \quad , \qquad (3)$$

the last term being the so-called anomalous term[6]. Its matrix element is given by

$$\mathcal{M}^{(c)} = \langle\pi^+|\mathcal{O}_5^{(c)}|K^+\rangle = \left(1 - \frac{1}{N_c^2}\right)\frac{f_\pi m_\pi^2}{m_u+m_d}\,\frac{f_K m_K^2}{m_s+m_u} \qquad (4)$$

and is sensitive to the choice of current quark masses.

The coefficient κ in (2), which takes care of the continuation to the physical momentum, is obtained under the assumption that the momentum dependence is quadratic in meson momenta. At the physical

*For recent reviews on the subject, see refs. 1 and 2.

point, κ is given by

$$\kappa = \frac{1}{(k\cdot p)} (m_K^2 - m_\pi^2) , \tag{5}$$

where k and p are momenta of π and K, respectively, in the matrix elements in (2).

In our approach, we put the bound on the matrix element by relating it to the two-point function

$$\psi(q^2) = i\int d^4x\, e^{iq\cdot x} \langle 0|T(\mathcal{O}_5(x)\mathcal{O}_5^\dagger(0)|0\rangle \tag{6}$$

which gives the bound in the form

$$|F(0)| \leq \mathcal{A}(Q^2) , \tag{7}$$

where $|F(0)| \equiv \langle\pi^+|\mathcal{O}_5|K^+\rangle$ can be viewed as the value of a scalar form factor F(t) at t=0 which is a real analytic function in the complex t-plane with a cut $(m_K+m_\pi)^2 \leq t < \infty$. The function $\mathcal{A}(Q^2)$ is obtained from the $\psi(q^2)$ by saturating the absorptive part, Im $\psi(t)$, by lowest hadronic states. It follows from QCD that $\psi(t)$ obeys a dispersion relation defined up to an arbitrary polynomial in $Q^2=-q^2$ of degree four at most. To get rid of this arbitrariness, we actually work with $\mathcal{F}(Q^2)$ which is a fifth derivative of $\psi(q^2)$ with respect to q^2.

In calculating the bound, we make an Ansatz for the spectral function $\frac{1}{\pi}$ Im $\psi(t)$ and then calculate $\mathcal{F}(Q^2)$

$$\frac{1}{\pi}\,\text{Im}\,\psi(t) = \text{sum of low-energy hadronic contributions} + \text{QCD-continuum} . \tag{8}$$

The last term in (8) is given by the asymptotic behavior of $\frac{1}{\pi}$ Im $\psi(t)$ which can be obtained from the QCD calculation of $\psi(q^2)$. Obviously, $\mathcal{F}(Q^2) \to \mathcal{F}(Q^2)_{\text{asym QCD}}$ for large Q^2. However, since the bound in (7) grows as $(Q^2)^{5/2}$, it is not very restrictive for large Q^2. Therefore, one also needs to calculate the first term in (8). This we do by making use of the following Ansatz:

$$\psi(q^2) \simeq i\int d^4x\, e^{iq\cdot x} \langle 0|T(J^\pi(x)J^{\pi\dagger}(0)|0\rangle\langle 0|T(J^K(x)J^{K\dagger}(0)|0\rangle ; \tag{9}$$

this corresponds to summing a class of hadronic contributions which are leading in the $1/N_c$ expansion plus some nonleading contributions, but not all the subleading ones.

The upper bound obtained can be significantly improved under

certain assumptions about the analytic structure of the F(t). F(t) should be i) polynomially bounded (and this is proved from QCD) and ii) should have no zeros in the complex plane. Unfortunately, we have no control of the second requirement, although it is a usual Ansatz in the calculation of form factors.

It turns out [9] that the low Q^2 behavior for $\Psi(Q^2)$ is completely saturated by π and K contributions at the point Q_o^2 where the bound is optimal. Besides, the asymptotic part at Q_o^2 is completely negligible. This enables us to factorize out the vacuum-saturation result for the matrix element:

$$\mathcal{T}^{tot}(Q^2) = (\mathcal{M}^{(c)})^2 \cdot I(Q^2, m_K^2, m_\pi^2) \quad . \tag{10}$$

By numerical evaluation of the integral I in (10) we find* that

$$|\langle\pi^+|\mathcal{O}_5|K^+\rangle| \leq 0.9\,\mathcal{M}^{(c)} \quad . \tag{11}$$

The bound (11) is independent of the values of quark masses, or any other input parameter except m_π and m_K. From (11) the following constraints are obtained:

$$0.1\,\mathcal{M}^{(c)} \leq |\langle\pi^+|\mathcal{O}_5 + \mathcal{O}_5^{(c)}|K^+\rangle| \leq \mathcal{M}^{(c)} \quad . \tag{12}$$

Obviously, the lower limit in (12) is obtained by subtracting two large numbers and is therefore sensitive to the approximations used. Fortunately, <u>both</u> normal and anomalous matrix elements are proportional to $\mathcal{M}^{(c)}$ and, consequently, the sensitive quark mass dependence is factorized out. This virtue is not achieved in quark model calculations. Besides, the N_c dependence, at least in the asymptotic limit, is also factorized, and being given by the factor $(1-N_c^{-2})$, it amounts to a correction of about 10%.

Numerically, we find that with $B = \frac{2}{3}$, $\tau_B = 0.9\times10^{-12}$ sec, $m_t = 40$ GeV and Im $c_5 = 0.1$

$$\left|\frac{\varepsilon'}{\varepsilon}\right| \geq 8\times10^{-4} \quad , \tag{13}$$

i.e. an order of magnitude smaller than the Gilman-Hagelin result in ref. 3.

---

*For the bounds on the other operators that contribute to the $K \to 2\pi$ amplitudes, see ref. 10.

D i s c u s s i o n: The following comments are in order:

i) Current quark mass dependence. In their paper[3] Gilman and Hagelin used the bag estimate of $\langle\pi^+|\mathcal{O}_5|K^+\rangle$ of ref. 6, but neglected the anomalous term, which was estimated by Donoghue et al.[6] to be rather small. In expression (4) they used the unusually large values of current quark masses obtained via bag model calculation. In our approach we use the running quark masses at 1 GeV^2 obtained from the QCD sum rules: m_s = 160 MeV, m_d = 11 MeV and m_u = 5 MeV. Using our values of quark masses + anomalous term would reduce the Gilman-Hagelin estimate by a factor of three.

ii) Continuation to the physical point. There is some ambiguity as to what value to use for $(k\cdot p)$ in eq. (5), since $k_\pi = p_K$. Of course, the sum of matrix elements in (2) should exhibit the same momentum dependence, which cancels the factor $(k\cdot p)$ in κ. Unfortunately, this cannot be extracted explicitly from the calculation. We have consistently used $(k\cdot p) = m_K^2$, which gives κ = 0.923. If there were no continuation, κ would be equal to 1/2.

iii) μ dependence. The Im c_5 has been calculated by summing up the leading logs via the renormalization group equation[4,5] and depends on the choice of the renormalization point μ. This μ dependence should cancel with a μ dependence of the matrix element. However, the latter cannot be calculated in quark models. In our approach, we could explicitly calculate the μ dependence for the asymptotic $\psi(q^2)$, but not the μ dependence for low Q^2. Although the μ dependence of Im c_5 is rather modest, it is still a serious source of uncertainty, as was explicitly shown recently by Buras and Słominski[8].

Finally, we would like to point out that all ambiguities discussed above may be avoided if one combines the effective chiral lagrangian technique with the QCD-duality approach of ref. 12. It has been successfully applied[13] to the calculation of the parameter B and may also be applied to the calculation of ε'/ε. The work on this is in progress[14].

Acknowledgments. I would like to acknowledge the pleasant collaboration with N. Bilić and very useful discussions with B. Machet A. Pich and E. de Rafael. This work was partially supported by the SIZ I of S.R. Croatia and the U.S. National Science Foundation unde Grant No. YOR 82/051. The hospitality at the Werner-Heisenberg-

Institut is greatly acknowledged.

References

1. A.J. Buras, in Proc. Workshop on the Future of Intermediate Energy Physics in Europe, Freiburg im Breisgau, 10-13 April 1984, p. 53
2. E. de Rafael, Lectures on Quark-Flavor Mixing in the Standard Model, MPI-PAE/PTh 72/84.
3. F.J. Gilman and J.S. Hagelin, Phys. Lett. 133B (1983) 443.
4. F.J. Gilman and M.B. Wise, Phys. Rev. D20 (1979) 2392.
5. B. Guberina and R.D. Peccei, Nucl. Phys. B163 (1980) 289.
6. J.F. Donoghue, E. Golowich, W.A. Ponce and B.R. Holstein, Phys. Rev. D21 (1980) 186.
7. P. Colić, D. Tadić and J. Trampetić, Phys. Rev. D26 (1982) 2286.
8. B. Guberina, B. Machet and E. de Rafael, Phys. Lett. 128B (1983) 269.
9. N. Bilić and B. Guberina, Phys. Lett. 150B (1985) 311.
10. N. Bilić and B. Guberina, Z. für Phys. to be published.
11. A.J. Buras and W. Słominski, MPI-PAE/PTh 68/84, Nucl. Phys. B, to be published.
12. R.A. Bertlmann, G. Launer and E. de Rafael, Nucl. Phys. B250 (1985) 61.
13. A. Pich and E. de Rafael, to be published.
14. B. Guberina, A. Pich and E. de Rafael, work in progress.

COMMENTS ON CP-VIOLATION IN RARE KAON DECAYS AND ON THE STATUS OF THE B-PARAMETER

Eugene Golowich
Department of Physics and Astronomy
University of Massachusetts
Amherst, MA 01003
U.S.A,

Abstract

Following some introductory remarks reviewing the current status of the KM model in the study of CP-violations, we consider prospects for observing CP-violating effects in rare kaon decay modes. The $K \to \gamma\gamma$ mode provides an illustration. Then the separate matter of attempts to determine the B-parameter is addressed. Emphasis is placed on recent developments on this topic.

(i) CP-Violation in Rare Kaon Decay Modes

In the twenty years since CP-violation in the kaon complex was discovered, a number of theoretical mechanisms have been proposed. Among them are superweak, Higgs, KM mixing, left-right symmetric, etc. In the following we shall restrict ourselves solely to KM mixing (i.e., CP $\leftrightarrow \delta = 0$). However, the author must admit to a growing feeling that CP-violation is a more pervasive phenomenon than commonly thought and may well enter the fabric of theory at more than one location.

CP-violations in $K\pi\pi$ interactions are expressible in terms of two complex numbers, ε and ε'. In magnitude ε' is no more than a few thousandths of ε [data presented at this Conference implies $\varepsilon'/\varepsilon = (-2.6 \pm 4.8) \times 10^{-3}$], where $|\varepsilon| \simeq 2.3 \times 10^{-3}$. Physically, ε can feel the presence of CP impurities in the kaon mass matrix and the $K \to (\pi\pi)_{I=0}$ decay amplitude, while ε' probes I=2 $\pi\pi$ decay.

Next, recall how the KM-angle δ, which is restricted to the heavy-quark sector of the weak-mixing matrix, can affect $K\pi\pi$ physics. There are the 'box-diagrams', which are believed to be the dominant contributors to $\mathrm{Im}M_{12}$ which

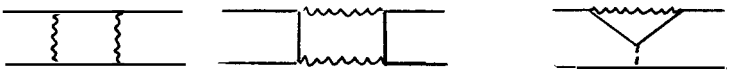

BOX PENGUIN

itself is thought to dominate other contributions to ε, and the 'penguin' diagrams which contribute to ε'. One numerical analysis yields the results[1] $|\varepsilon| \simeq 4 s_1 s_2 s_3 s_\delta B/0.33$, $|\varepsilon'| \simeq s_1 s_2 s_3 s_\delta P/40$, where B is the much discussed B-parameter (see the second part of this report) and $P \equiv \langle \pi^+\pi^- | O_{peng} | K \rangle / (0.43\ \mathrm{GeV})^3$ is a $K\pi\pi$ penguin matrix element in units of a bag model estimate. If these estimates are not unreasonable, then a value of ε'/ε at the level of a few parts per thousand is a natural consequence of the model. Clearly however the tiny values of s_2, s_3 imply that δ must not be too far from $\pi/2$ and/or B must not be too small if the KM model is to remain a candidate as the sole source of CP-violation. At any rate even if the KM model of CP-violation is not yet ruled out, it is nonetheless true that the $K\pi\pi$ CP-violating effects are almost entirely 'ε-physics' which in turn is 'mass-matrix physics'.

Is this always the case? Let us consider rare kaon decay modes such as $K \to \gamma\gamma$, $K \to \pi\pi\gamma$, $K \to \pi\nu\bar{\nu}$ etc. for which it might be possible to observe CP-violating effects which are not directly associated with the mass matrix. Correspondingly let us characterize CP-violations in such experiments in terms of two parameters, ε which we define to arise solely from the mass matrix, and $\bar{\varepsilon}$ which is defined to represent any 'other' source. Of interest is the ratio $\bar{\varepsilon}/\varepsilon$.

Such a study is not motivated by intellectual curiosity alone. After a high level of activity in the late 1960's, there was a relative lull in experimental studies of kaon decays in recent times. An exception is of course the

effort to measure ε'/ε as motivated by the work of Gilman and Wise.[2] However advances in beam energy and detection technology have led to a revived interest in the subject and a number of experiments are either in the proposal stage or even underway.

For the rest of this section we concentrate on $K \to \gamma\gamma$ transitions. The Review of Particle Properties lists $BR(K_L \to \gamma\gamma) = (4.9 \pm 0.4) \times 10^{-4}$ and $BR(K_S \to \gamma\gamma) < 4. \times 10^{-4}$. If $K_S \to \gamma\gamma$ predominantly arises from the $\pi\pi$ intermediate state, then $\Gamma(K_S \to \gamma\gamma)/\Gamma(K_L \to \gamma\gamma) \simeq 2$ so that roughly a factor of 10^2 improvement is needed in the $K_S \to \gamma\gamma$ branching ratio before a signal will be seen.

In kaon decay the $\pi\pi$ final state can have only CP = +1. The $\gamma\gamma$ final state is richer in that both CP = $\pm$1 configurations can occur. Thus even if CP-violation is absent, the K_S and K_L components of K^o will decay separately into the CP = +1,-1 $\gamma\gamma$ final states. The associated photon polarization vectors occur as $\vec{\varepsilon}(1)\cdot\vec{\varepsilon}(2)$ for CP = +1 and $\vec{\varepsilon}(1) \times \vec{\varepsilon}(2)\cdot\vec{p}(1)$ for CP = -1. Corresponding to these are the Lorentz invariant combinations of field operators $F_{\mu\nu}F^{\mu\nu}$ and $\varepsilon_{\mu\nu\alpha\beta}F^{\mu\nu}F^{\alpha\beta}$ respectively (denoted hereafter as FF and $F\tilde{F}$). Let us concentrate in the following on the $F\tilde{F}$ amplitude, which can in principle give rise to interesting CP-violating effects. We begin by defining a $K_L\gamma\gamma$ phenomenological Lagrangian, $L(K_L\gamma\gamma) = (g/m_K)K_L\varepsilon_{\mu\nu\alpha\beta}F^{\mu\nu}F^{\alpha\beta}$. The associated decay width is $\Gamma(K_L\gamma\gamma) = g^2 m_K/\pi$. From the measured K_L-lifetime and $K_L \to \gamma\gamma$ branching ratio, we thus infer the empirical amplitude

$$M = 1.6 \times 10^{-9}\ \varepsilon_{\mu\nu\alpha\beta}p_1^{\mu}\varepsilon^{\nu}(1)\ p_2^{\alpha}\varepsilon^{\beta}(2)/m_K \quad . \tag{1}$$

A venerable description for this process has been the pseudoscalar-meson pole model, which we depict as

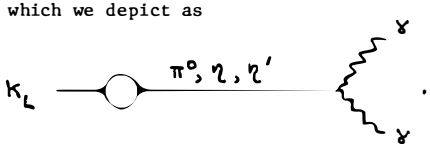

In this approach, the K_L mixes weakly with a spinless meson which then propagates and finally decays into a pair of photons. Other contributions to $K_L \to \gamma\gamma$ are of course possible but in view of our limited time, we focus our attention here on this one mechanism. The $\gamma\gamma$ decays of π^o, η, and η' can be read off from experimental data. For the weak mixing vertex we can use a chiral SU(3) Lagrangian (see part (ii) of this report), with the experimental $K \to \pi\pi$ amplitude as input, to determine the $K_L \to \pi^o$, η transitions, and separately, the quark-penguin approach to characterize $K_L \to \eta'$. One concludes from all this that the model can do a reasonable job of reproducing the experimental amplitude. The η-pole is dominant (due to enhancement from the small energy denominator), followed by the π^o pole, with the smallest contribution being the η' pole. Roughly speaking the

10^{-9} amplitude arises from a 10^{-7} weak-mixing factor and a 10^{-2} propagation and photon-decay factor.

CP-violation can occur in the $K_L \to \eta'$ amplitude. It is convenient to express this transition as [3]

$$\langle \eta' | H_w | K_L \rangle = \sqrt{\frac{2}{3}}\, F \langle \pi^o | H_w | K_L \rangle \qquad (2)$$

where we ignore $\eta_o - \eta_8$ mixing, $F \equiv 1 - 3f - 3i\xi(1-f)$ contains the CP-violating parameter $\xi = \mathrm{Im}A_o/\mathrm{Re}\,A_o$ and f is the fraction in $K \to \pi\pi$ due to the penguin interaction. We refer the interested reader to Ref. 3 for details. A measure of CP-violation in the $F\tilde{F}$ two-photon state is given by

$$\frac{\cancel{CP}}{CP} = \frac{A(K_S \to F\tilde{F})}{A(K_L \to F\tilde{F})} = \varepsilon + \bar{\varepsilon} \qquad (3)$$

where the contribution to ε comes from the CP-odd impurity in K_S. As indicated above, our simple pole model for $K_L \to \gamma\gamma$ contains a contribution to $\bar{\varepsilon}$ arising from the $K_L \to \eta'$ vertex and we find

$$\left|\frac{\bar{\varepsilon}}{\varepsilon}\right| \sim \frac{3}{2}(1-f)\frac{\xi}{\varepsilon} \sim 30\,\frac{\varepsilon'}{\varepsilon} \qquad (4)$$

i.e. there is no $\Delta I = 1/2$ rule suppression here.

The phenomenology of CP-violation in radiative kaon decays has been worked out in Ref. 4. For the $K \to \gamma\gamma$ system, CP-violation can manifest itself via interference and/or circular polarization effects. For example detection of circular polarization in $\gamma\gamma$ decay of a pure K_L beam would be an unambiguous signal for CP-violation. However, in this case the effect would be predominantly ε-physics. Details will be presented in a future publication. In conclusion then, we are in the process of carrying out a study of CP-violations in rare kaon decays with an emphasis on 'non-ε' physics. We have seen how such effects can be relatively larger in $K \to \gamma\gamma$ than in $K \to \pi\pi$. Although experiments on this subject are not likely to be simple, the time has come to seriously address the subject.

(ii) Current Status of the B-Parameter

The 'B-parameter' is defined as

$$B = \frac{\langle K^o | \bar{d}\Gamma_L^\mu s \bar{d}\Gamma_{L\mu} s | \bar{K}^o \rangle}{\langle K^o | \bar{d}\Gamma_L^\mu s \bar{d}\Gamma_{L\mu} s | \bar{K}^o \rangle_{vac}} \qquad (5)$$

where $\Gamma_L^\mu \equiv \gamma^\mu(1+\gamma_5)$ and the subscript 'vac' denotes evaluation in the vacuum saturation approximation. Thus B is a dimensionless number, whose determination involves a $\Delta S=2$ local four-quark operator.

There have been many purely theoretical attempts to calculate B, including bag, oscillator, lattice, dispersion relation, sum rule, etc. methods. Values with which the author is personally acquainted cover a distressingly wide range,

$-0.4 \lesssim B \lesssim 3$. To usefully constrain models of CP-violation, B would need to be known with substantially more precision. This state of affairs is not entirely surprising. B is dependent on quark wave functions within hadrons. Unfortunately QCD, the model of strong interactions, has not yet attained calculational status.

Several years ago an alternative determination, relying upon experimental data, was carried out.[5] The chain of reasoning proceeded as follows. First we infer the $K^- \to \pi^-\pi^o$ amplitude from the associated decay rate, then employ current algebra to find the $\bar{K}^o \to \pi^o$ matrix element, and finally use SU(3) to obtain the B-parameter. A somewhat novel feature of this analysis is that the SU(3) quantities of interest transform as members of a 27-plet.

The method just outlined yielded the value $B \simeq 0.33$, substantially below the vacuum saturation estimate. Two crucial assumptions underlay the calculation - the momentum dependence of the current algebra extrapolation from $K^- \to \pi^-\pi^o$ to $\bar{K}^o \to \pi^o$ and the SU(3) relation between $\bar{K}^o \to \pi^o$ and $\bar{K}^o \to K^o$.

At this point we momentarily digress to cast this phenomenological determination in the language of 'chiral Lagrangians'. These are quantities which allow the chirally symmetric interactions of the light mesons to appear in a natural and almost automatic fashion. In our case the 'field variable' is $U = \exp(i\vec{\lambda}\cdot\vec{\phi}/F)$ where $\vec{\lambda},\vec{\phi}$ are the eight SU(3) matrices and pseudoscalar fields respectively and F is the pseudoscalar meson decay constant (we take $F=F_\pi$). Under chiral transformations of $SU(3)_L \times SU(3)_R$, U transforms as $U \to LUR^+$. It is useful to define $X_\mu = U\partial_\mu U^+$ which transforms as $(8_L,1_R)$. Interactions involving the pseudoscalar mesons and transforming as $(27_L,1_R)$ under thiral $SU(3)_L \times SU(3)_R$ are then given by

$$L_{27}^{(2)} = g_{27}^{(2)}\, C\begin{pmatrix} 8 & 8 & 27 \\ i & j & 6 \end{pmatrix} \mathrm{Tr}(\lambda_i X_\mu \lambda_j X^\mu) \qquad (6)$$

where the C-symbol is an SU(3) Clebsch-Gordan coefficient. This Lagrangian describes a hierarchy of vertices involving two or more pseudoscalar mesons. The coupling constant $g_{27}^{(2)}$ can be fixed from the $K^- \to \pi^-\pi^o$ width and the evaluation $B \simeq 0.33$ then follows upon direct calculation. This determination is entirely equivalent to the 'phenomenological' method described earlier - only the language is different.

The chiral Lagrangian formalism is convenient for analyzing uncertainties in the $B \simeq 0.33$ determination. Several possibilities come to mind. For example, $L_{27}^{(2)}$ is not the unique Lagrangian transforming as $(27_L,1_R)$. There are an infinity of others, containing more derivatives than the two in $L_{27}^{(2)}$. Their amplitudes contain higher powers of particle momentum p relative, presumably, to some scale Λ appropriate to chiral symmetry. It was shown recently,[6] at least for $\Delta I = 1/2$ transitions, that $m_K/\Lambda < 1$. Hence it is unlikely higher order Lagran-

gians would affect the $B \simeq 0.33$ value appreciably.[7]

The type of correction just considered involves the momentum dependence of the meson amplitudes. It is also possible to consider the effect of SU(3) symmetry breaking by computing amplitudes to 'one-loop' order in $L_{27}^{(2)}$. This matter is somewhat subtle in that each chiral Lagrangian is nonrenormalizable, and thus is typically analyzed only in the context of 'tree-approximation'. Indeed power-law corrections appear in the one-loop calculations, and these renormalize parameters occurring in the higher-order Lagrangians just discussed. However logarithmic corrections also appear, and their effect is to modify the tree-level amplitudes. Such corrections do not generally change the qualitative nature of the tree-level results. For example, the one-loop logarithmic correction to the tree-level result for the pion decay constant is about twelve per cent in magnitude.

The one-loop logarithmic corrections to the chiral determination of the B-parameter have recently been computed.[8] They turn out to be surprisingly large,

$$B = 0.33\left(1 - \frac{55}{6}\left(\frac{m_K}{4\pi f_\pi}\right)^2 \ln\left(\frac{m_K}{\mu}\right)^2\right) \qquad (7)$$

where $f_\pi \simeq 130$ MeV and μ is the renormalization scale. The value $\mu \simeq 1$ GeV is chosen in Ref. 8. If so, the correction is of the same order as the tree-level result and the chiral perturbation theory is seen to break down in this case.

We would seem to be back where we started as regards a meaningful attempt to pin down the elusive B-parameter! Certainly this is so if the chiral perturbation theory is stopped at second order. Perhaps, however, a leading-log summation to all orders would ameliorate the large radiative correction and thus render a reliable estimate of B. Time will tell, as always, with the B-parameter.

References

1. J. Donoghue, UMass preprint UMHEP-215 (1984).
2. F. Gilman and M. Wise, Phys. Lett. 93B, 129 (1980).
3. J. Donoghue and B. Holstein, Phys. Rev. D29, 2088 (1984).
4. L. Wolfenstein and L. Sehgal, Phys. Rev. 162, 1362 (1967).
5. J. Donoghue, E. Golowich, and B. Holstein, Phys. Lett. 119B, 412 (1982).
6. J. Donoghue, E. Golowich, and B. Holstein, Phys. Rev. D30, 587 (1984).
7. E. Golowich, Phenomenology of Gauge Theories, 19th Rencontre de Moriond, p. 571 (1984).
8. J. Bijnens, H. Sonoda, and M. Wise, Phys. Rev. Lett. 53, 2367 (1984).

ENERGY DEPENDENCE OF THE K^{O}-$\overline{K^{O}}$ PARAMETERS – THEIR RÉDEI BEHAVIOUR AND LONG- VERSUS SHORT-DISTANCE PARTS

I. Picek
Rudjer Bošković Institute, Zagreb, Croatia, Yugoslavia

If the recently reported energy dependence of the K^{O}-$\overline{K^{O}}$ parameters is true, the K^{O}-$\overline{K^{O}}$ system turns out to be an even more special system than found previously. Specifically, it might signal some new physics manifested by a change in the flat Minkowski metric. Also, such Rédei behaviour gives insight into the relative importance of long- versus short-distance contributions to the matrix elements related to the K^{O}-$\overline{K^{O}}$ parameters. In view of this possible valuable information, an independent experimental check on the reported energy dependence is strongly encouraged.

The neutral $K^o-\overline{K^o}$ meson system has played a distinguished role in particle physics in the past twenty years. There is no evidence for any other CP measurement that could be comparable with the accuracy of measurement in this system. Moreover, the K^o-K^o system seems to provide somewhat unexpected additional information, the recently reported energy dependence[1] (table 1) representable in the form

$$x = x_o[1 + b_x\gamma^2] , \quad \gamma = \frac{E_K}{m} = (1-\beta^2)^{-1/2} . \tag{1}$$

This result conforms to "the Rédei behaviour" obtained previously[2] for some weak particle decays, provided weak interactions have a special metric originating from the Higgs sector of the standard model. In fact, the change in the Minkowski metric

$$g_{\mu\nu} \to g_{\mu\nu} + \chi_{\mu\nu} \tag{2a}$$

with a simple deviation $\chi_{\mu\nu}$ characterized by a single parameter α,

$$\chi_{\mu\nu} = \mathrm{diag}(\alpha, \alpha/3, \alpha/3, \alpha/3) , \tag{2b}$$

gives the Rédei behaviour of weak decaying particle lifetimes. However, the Rédei coefficients $b_x \sim 10^{-5}$ in table 1, although rather small, exceed by many orders of magnitude the values expected in the particular model of Lorentz non-invariance[2,3].

As well as indicating a deviation from Lorentz invariance, eq. (1) might also signal the sensitivity of the $K^o-\overline{K^o}$ system to interactions with some new, otherwise unobserved fields. The analysis of ref. 1 indicates the interaction with a C-even tensor field (which agrees with the model of Lorentz non-invariance). Whatever "new physics" might exist in the $K^o-\overline{K^o}$ system, we suppose that it manifests itself by the change in the Minkowski metric (eq. 2). For example, such a change in the flat Minkowski metric $g_{\mu\nu}$ may stem from strong gravity[4]. The same effect might result from some other, yet unknown mechanism, relevant to the $K^o-\overline{K^o}$ system. We therefore take under scrutiny[5] a whole class of models characterized by (2), in order to extract some information on both the "new physics" and the $K^o-\overline{K^o}$ system.

The parameters of the K^o-$\overline{K^o}$ system, being typical hadronic quantities, suffer from a common "disease". The share of short- (SD) versus long-distance (LD) contributions to these quantities is poorly known. Here we show that the Rédei behaviour might be helpful in shedding light on the relative importance of SD and LD effects. In this respect, we start from the existing experience in calculating the $K_S \to 2\pi$ matrix element, in order to extract the parameter α in (2b). In this treatment, the SD (vacuum saturation) part, which exhibits the Rédei behaviour, is extracted from the total amplitude. The SD amplitude (where the penguin mechanism is important[6]))

$$A_{SD} \equiv \langle \pi^+(k)\pi^-(q)|H_W|K_S(p)\rangle_{SD} = \tilde{c}_{SD}(2p^2-k^2-q^2) \ , \tag{3a}$$

implemented by (2), takes the form

$$A_{SD}^{\text{Rédei}} = c_{SD}(1 + \tfrac{4}{3}\,\alpha\gamma^2) \ . \tag{3b}$$

Since the SD contribution ($A_{SD} = (13.25\pm5.3)\times10^{-8}\ m_K$) gives only a part of the measured amplitude ($A_{exp} = \pm77.8\times10^{-8}\ m_K$), the total amplitude also contains the long-distance part d_{LD} (for which there is no reliable calculation at present),

$$A_{tot}^{\text{Rédei}} = c_{SD}(1 + \tfrac{4}{3}\,\alpha\gamma^2) + d_{LD} \ . \tag{4a}$$

Then, matching the expression for the $K_S \to \pi^+\pi^-$ lifetime[5]

$$\tau(K_S \to \pi^+\pi^-) = (c_{SD} + d_{LD})^{-2}\left[1 - \frac{2}{1 + \dfrac{d_{LD}}{c_{SD}}}\,\frac{4}{3}\,\alpha\gamma^2\right] \tag{4b}$$

with the second row of table 1, we obtain

$$\alpha = (-3.90 \pm 1.98)\times10^{-6} \ . \tag{5}$$

Once we have estimated α, which should be universal for the K^o-$\overline{K^o}$ system, we can evaluate the LD and SD parts of the quantities from table 1, as given in table 2.

For example, the K_L-K_S mass difference Δm contains the purely SD contribution Δm_{box} calculated in terms of the quark box diagram[7] and the LD non-box dispersive contribution parametrized by

Table 1. K^o-$\overline{K^o}$ parameters and their Rédei behaviour[1)]

Parameter	Energy dependence at Fermilab energies ($30 \leq E_k \leq 130$ GeV)	
	x_o	$10^6\, b_x$
Δm ($10^{10}\ \hbar\ \mathrm{sec}^{-1}$)	0.557 ±0.036	-8.48 ±2.89
τ_S (10^{-10} sec)	0.880 ±0.015	1.77 ±0.90
$\lvert\eta_{+-}\rvert$ (10^{-3})	2.14 ±0.04	-2.01 ±0.86
$\tan\phi_{+-}$	1.276 ±0.499	-33.7 ±12.3

Table 2. SD and LD parts of the K^o-$\overline{K^o}$ parameters

Parameters related to x_o in table 1	SD part	LD part
$\Delta m = 0.557$ ($10^{10}\ \hbar\ \mathrm{sec}^{-1}$)	$a_{SD} = 0.907$	$b_{LD} = -0.350$
$A(K_S \to \pi^+\pi^-)$ ($10^3\ \hbar^{1/2}\mathrm{sec}^{-1/2}$)	$c_{SD} = 15$	$d_{LD} = 73.3$
$A(K_L \to \pi^+\pi^-)$ ($10^3\ \hbar^{1/2}\mathrm{sec}^{-1/2}$)	$e_{SD} = 0.11$	$f_{LD} = 0.09$

a quantity D[8)]

$$\Delta m = (\Delta m)_{box} + (\Delta m)_{LD} \,, \tag{6a}$$

where

$$(\Delta m)_{box} = B(\Delta m)^{VSA}_{box} \,, \quad (\Delta m)_{LD} = D\Delta m \,. \tag{6b}$$

While the factor B is estimated to be of the order of one, the value of D is not reliably calculable. Let us quote the values from

refs. 9 and 10, respectively:

$$-0.7 < D < 3 \ , \tag{7a}$$

$$D = 0.10 \pm 0.41 \ . \tag{7b}$$

The Rédei behaviour of the SD part Δm_{box} has already been calculated in the vacuum-saturation approximation[3]:

$$\Delta m_{box}^{VSA} = \frac{G_F^2}{6\pi^2} m_c^2 \cos^2\theta_C \sin^2\theta_C f_K^2 m_K \left[1 + \frac{4}{3}\alpha(\gamma^2 - \tfrac{1}{4})\right] . \tag{8}$$

Then the full mass difference has the form

$$\Delta m = a_{SD}\left[1 + \frac{4}{3}\alpha(\gamma^2 - \tfrac{1}{4})\right] + b_{LD}$$

$$\simeq (a_{SD} + b_{LD})\left[1 + \frac{4}{3}\frac{a_{SD}}{a_{SD} + b_{LD}}\alpha\gamma^2\right] . \tag{9}$$

Substituting (5) in (9) and matching it with the measured curve (table 1), we obtain the first row in table 2.

Similarly, the last row in table 2 corresponds to the amplitude

$$A(K_L \to \pi^+\pi^-) = e_{SD}(1 + \frac{4}{3}\alpha\gamma^2) + f_{LD} \ . \tag{10}$$

A common feature of the results given in table 2 is that the SD and LD matrix elements for the K^o-K^o parameters are of equal importance. Using table 2 to calculate the quantity displayed in (7), we obtain

$$D = (1 - \frac{\Delta m_{SD}}{\Delta m}) \simeq -0.63 \ ,$$

which is in the range of (7a), but contradicts (7b).

To summarize, we have considered the K^o-K^o system to illustrate the role which the Rédei behaviour might have in providing additional information about some physical quantities and, simultaneously, in shedding light on the possible new physics beyond the standard model. There are already two interrelated subjects at the border of the standard model:

i) explanation of CP violation

ii) the Higgs sector.

In view of i), the Rédei behaviour in the K^o-$\overline{K^o}$ system (to which CP violation has so far been restricted) might open a new

window onto the physics behind CP violation.

As regards ii), the existing attempts to parametrize CP violation rely on the arbitrariness in the Higgs sector of the standard model (e.g. the standard Kobayashi-Maskawa model is due to the arbitrariness in the Yukawa Higgs couplings). It has been noticed[2,3] that another freedom left over in the Higgs kinetic term, namely the freedom to perform the transformation (2) without spoiling gauge invariance, may result in the Rédei behaviour. However, the presently reported[1] Rédei behaviour does not fit in with the model of refs. 2 and 3. Faced with this situation, we encourage an independent experimental check on the reported energy dependence. Only an independent confirmation of the Rédei behaviour would allow one to draw firm conclusions about its origin and consequences.

I would like to thank J.O. Eeg for useful discussions and H.B. Nielsen for continuous interest.

REFERENCES

1) S.H. Aronson et al., Phys. Rev. Lett. 48 (1982) 1306; Phys. Lett. 116B (1982) 73; Phys. Rev. D28 (1983) 476, 495; V.K. Birulev et al., Nucl. Phys. B115 (1976) 249
2) H.B. Nielsen and I. Picek, Phys. Lett. 114B (1982) 141
3) H.B. Nielsen and I. Picek, Nucl. Phys. B211 (1983) 269, Add. B242 (1984) 542
4) M. Gasperini, Phys. Lett. 141B (1984) 369
5) I. Picek, RBI-TP-1-84 preprint
6) M.A. Shifman, A.I. Vainstein and V.I. Zakharov, Nucl. Phys. B120 (1977) 316; ZhETF (USSR) 22 (1975) 123 |JETP (Sov. Phys.) 22 (1975) 55|; ZhETF (USSR) 72 (1977) 72 |JETP (Sov. Phys.) 45 (1977) 670|
T.N. Pham, Phys. Lett. 145B (1984) 113
B. Gavela, A. Le Yaouanc, L. Oliver, O. Pène and J.C. Raynal, Phys. Lett. 148B (1984) 225
J.F. Donoghue, Phys. Rev. D30 (1984) 1499
7) M.K. Gaillard and B.W. Lee, Phys. Rev. D10 (1974) 897
8) L. Wolfenstein, Nucl. Phys. B160 (1979) 501; C.T. Hill, Phys. Lett. 97B (1980) 275
9) I.I. Bigi and V.I. Sanda, Phys. Lett. 148B (1984) 205
10) P. Cea and G. Nardulli, CTP-84/P.1698 preprint

LONG RANGE EFFECTS IN THE K^{o}-$\bar{K}^{o}$ SYSTEM

Giuseppe Nardulli
Dipartimento di Fisica dell'Università, Bari
I. N. F. N. Sezione di Bari, Italy

ABSTRACT: A recent calculation of the factors B, D defined by the formula: $\Delta m = B\ (\delta m) + D\ (\Delta m)$, where Δm is the K_L-K_S mass difference and δm is the result of the box diagram in the vacuum approximation, is presented. Results are $B = 1.05 \pm 0.15$ and $D = 0.10 \pm 0.41$.

Long range, i.e. low mass, effects in the K^o-$\bar{K}^o$ system are twofold: first of all they appear in the evaluation of the famous B factor that relates the full box diagram calculation of the K^o-$\bar{K}^o$ matrix element to the vacuum approximation[1]; secondly, they are present in the so-called dispersive contributions[2] obtained by inserting low-lying states between two $\Delta S=1$ weak non leptonic hamiltonians H_w. In this paper I shall consider the K_L-K_S mass difference which is related to the real part of the K^o-$\bar{K}^o$ matrix element, but similar effects appear also in the imaginary part that governs CP violations in the kaon system[3].

To begin with, we write the following formula for the K_L-K_S mass difference Δm:

$$\Delta m = (\Delta m)_{BOX} + (\Delta m)_{LD} \tag{1}$$

$(\Delta m)_{LD}$ contains the long-distance dispersive contributions to Δm and is usually parametrized as follows:

$$(\Delta m)_{LD} = D\ \Delta m \tag{2}$$

As for the box diagram contribution, in a six-quark scheme, including QCD corrections[4] one has

$$\begin{aligned}(\Delta m)_{BOX} &= 2\ \mathrm{Re}\langle \bar{K}^o \mid H_{eff}^{\Delta S=2} \mid K^o\rangle = \\ &= G_F^2 M_W^2 / (16\pi^2)(\alpha(\mu^2))^{-6/27} F(x_j,\theta_j)\langle \bar{K}^o \mid \bar{s}\gamma_\mu(1-\gamma_5)d\ \bar{s}\gamma^\mu(1-\gamma_5)d \mid K^o\rangle \\ &= G_F^2/(6\pi^2)\ (\alpha(\mu^2))^{-6/27}\ F(x_j,\theta_j)\ B\ f_K^2\ m_K\ M_W^2\end{aligned} \tag{3}$$

where $\alpha(\mu^2)$ is the strong coupling constant, the B factor ($B=B(\mu)$) will be defined below, $f_K = 163$ MeV ,

$$F(x_j,\theta_j) = \mathrm{Re}(\ \lambda_c^2\ S(x_c)\ \eta_1 + \lambda_t^2\ S(x_t)\ \eta_2 + 2\ \lambda_c\lambda_t\ S(x_c,x_t)\ \eta_3) \tag{4}$$

$x_j = m_j^2/M_W^2$, $\lambda_i = V_{id}^* V_{is}$ (V_{ij} are the elements of the KM matrix[5]) and the functions S are given by:

$$S(x) = x\ (\ 1/4 + 9/4\ (1-x)^{-1} - 3/2(1-x)^{-2}) + 3/2\ x^3/(x-1)^3\ \ln x \tag{5}$$

$$\begin{aligned}S(x_i,x_j) \simeq x_i x_j((1/4 + 3/2(1-x_i)^{-1} - 3/4(1-x_i)^{-2})\ln x_i/(x_i-x_j) + \\ (i\leftrightarrow j) - 3/4(1-x_i)^{-1}(1-x_j)^{-1})\end{aligned} \tag{6}$$

The QCD coefficients η_j are given by $\eta_1 \simeq 0.7$ (for $\Lambda \simeq 100$ MeV; for $\Lambda \simeq 200$ MeV one has $\eta_1 \simeq 0.8$), $\eta_2 \simeq 0.6$, $\eta_3 \simeq 0.4$; other coefficients are as follows (by making the hypothesis, experimentally acceptable, that $\sin\theta_3 \simeq 0$ and $\sin\theta_2 << \sin\theta_1$)

$$\mathrm{Re}\ \lambda_c^2 \simeq s_1^2 c_1^2\ , \qquad \mathrm{Re}\ \lambda_t^2 \simeq s_1^2 c_1^2 s_2^4\ , \qquad \mathrm{Re}\ \lambda_c\ \lambda_t \simeq s_1^2 c_1^2 s_2^2 \tag{7}$$

where $s_j = \sin\theta_j$ and $c_j = \cos\theta_j$. Assuming $s_2 \simeq 0.1$ (it may be smaller, but terms containing s_2 contribute by less than 15% to the final result), we obtain

$$(\Delta m)_{BOX} \simeq 3.2 \cdot 10^{-15}\ B \tag{8}$$

where we have used $m_t \simeq 40$ GeV and $m_c \simeq 1.5$ GeV. By using Eqs. (1) and (2) and the experimental value of Δm we obtain

$$1 \simeq B + D \tag{9}$$

Eq.(9) represents an experimental constraint on the values of the parameters B, D; we shall now summarize results of a calculation of these parameters[6),7)] based on dispersion relations (D.R.'s) and hadronic phenomenology. In order to compute B we consider its definition

$$B = M / M_{VAC} \tag{10}$$

where $(J_\mu^{6-i7} = \bar{s}\gamma_\mu(1-\gamma_5)d)$

$$M = <\bar{K}^o|: J_\mu^{6-i7}(0) J^{\mu 6-i7}(0):|K^o> \tag{11}$$

is the full matrix element and M_{VAC} is obtained by inserting the hadronic vacuum between the two currents

$$M_{VAC} = 2 f_K^2 m_K^2 \tag{12}$$

As for the full matrix element M, we proceed as follows: we evaluate the currents in two different space-time points: x, y such that $x-y = (\vec{0}, \vec{n}/\mu)$ where $\vec{n}$ is a unity vector, μ is the onset of the scaling ($\mu \simeq 1$ GeV) and an average over spatial directions is understood. This procedure is allowed owing to the precocity of the short-distance behaviour. The result is [8)]:

$$M_{conn} = M - M_{VAC} = \int d^4q/(2\pi)^4 \; j_o(|\vec{q}|/\mu) \;\; T_{conn}(q) \tag{13}$$

where the function $j_o(x)=(\sin x)/x$ cuts off the integral for large momenta and

$$\begin{aligned} T_{conn}(q) &= g^{\mu\nu} \; (\; T_{\mu\nu}(q) + \hat{T}_{\mu\nu}(q) \;) \\ T_{\mu\nu}(q) &= \int d^4x \; \exp(iqx) \; <\bar{K}^o|T(V_\mu^\alpha(x) \; V_\nu^\alpha(0))|K^o>_{conn} \\ \hat{T}_{\mu\nu}(q) &= \int d^4x \; \exp(iqx) \; <\bar{K}^o|T(A_\mu^\alpha(x) \; A_\nu^\alpha(0) \; |K^o>_{conn} \end{aligned} \tag{14}$$

($\alpha = 6-i7$) . The tensors $T_{\mu\nu}$ and $\hat{T}_{\mu\nu}$ can be decomposed in invariant amplitudes $T_j(q^2,\nu=pq)$ and $\hat{T}_j(q^2,\nu)$ that obey unsubtracted D.R.'s. The reason is that, assuming Regge behaviour for fixed q^2 and $|\nu|\to\infty$, one has $\alpha_{\Delta S=2}(0) < 0$, because a $\Delta S=2$ Regge trajectory is exotic and one faces a situation similar to the $\pi^+-\pi^o$, $\Delta I=2$ electromagnetic mass difference[9)]. As a consequence, the D.R.'s will be saturated by a few low-lying poles: π^o, η, ω, ρ^o, ϕ . The relevant form factors can be extracted from hadronic phenomenology, while the exact value of the μ parameter can be fixed by the $\Delta I = 3/2$ amplitude in the $K\to\pi\pi$ decay; notice that $B(\mu)\cdot(\alpha(\mu^2))^{-6/27}$ should be independent on μ (we shall discuss this point later).

An analogous calculation of $A_{3/2}(K\to\pi\pi)$ was performed some time ago[8)] and recently improved [6)]; it must be stressed that, if one uses PCAC and Current Algebra, one reduces to the calculation of a matrix element of the type $<\pi|O_{3/2}|K>$

which is similar to (11). As a matter of fact this argument has been used, together with $SU(3)_{flav}$ symmetry, to give an estimate of B [10]; however one may expect important $SU(3)_{flav}$ breaking effects in the pseudoscalar octet and this is why our calculations for $K \to \pi$ and $K^o \to \bar{K}^o$ transition amplitudes contain symmetry breaking.

Our results can be summarized as follows:

1) The value $\mu \simeq 0.8$ GeV gives $A_{3/2}(K \to \pi\pi) = 0.84 \cdot 10^{-8}$ GeV (exp.: $A_{3/2} = 0.86 \cdot 10^{-8}$ GeV); with the same value of μ and using a Regge parametrization for the continuum [8] one obtains for the $\Delta I = 1/2$ amplitude : $A_{1/2} = 2.5 \cdot 10^{-7}$ GeV (exp. : $A_{1/2} = 2.7 \cdot 10^{-7}$ GeV).

2) The factor $B = B(\mu)$ turns out to be in the range

$$0.9 < B < 1.2 \tag{15}$$

for μ in the range 0.5 - 1.2 GeV; in the same range of values of μ also $(\alpha(\mu^2))^{-6/27}$ is rather independent on μ, so that $\bar{B} = B(\mu) \cdot (\alpha(\mu^2))^{-6/27} \simeq 1.4$ is (approximately) μ-independent [11]; notice that for larger values of μ this is not true, which is not surprising as our calculated $B(\mu)$ depends on some assumptions on the form factors which turn out to be accurate only for moderate values of q^2.

An approach similar to the one described above can be used to estimate the D factor in Eq.(2) [7]. We write

$$(\Delta m)_{LD} = (\delta m_L)_{LD} - (\delta m_S)_{LD} \tag{16}$$

where $(\delta m_j)_{LD}$ is the long-distance contribution to the self energy of K_j (j= L, S), and introduce self energy functions $\Pi_j(s)$ normalized as follows:

$$\begin{aligned} \mathrm{Re}\ \Pi_j(m_K^2) &= 2\, m_K\, \delta m_j \\ \mathrm{Im}\ \Pi_j(m_K^2) &= -\, m_K\, \Gamma_j(m_K^2) \end{aligned} \tag{17}$$

where $\Gamma_j(m_K^2) = \Gamma_j$ is the K_j width. $\Pi_j(s)$ satisfies an unsubtracted DR [12]:

$$\mathrm{Re}\ \Pi_j(s) = 1/\pi\ \ P\int \mathrm{Im}\Pi_j(s')/(s'-s)ds' \tag{18}$$

In the case of K_L, Eq. (18) reduces to

$$\mathrm{Re}\ \Pi_L(s) = \sum_n |a_{K_L n}|^2/(s-m_n^2) + 1/\pi\ P \int_{9m_\pi^2}^{m_c^2} \mathrm{Im}\ \Pi_L(s')/(s'-s)\ ds' \tag{19}$$

wher m_c is the mass of the charmed quark which is an adequate energy scale for long distance contributions, the sum runs over the low mass mesons $n = \pi^o, \eta, \eta', \rho^o, \omega$ and

$$a_{K_L n} = \langle n\ |H_w|K_L\rangle \tag{20}$$

The continuum contribution in (19) can be evaluated using a smooth form-factor describing the decay of an off-shell kaon into three pions; we get

$$\left.\frac{\delta m_L}{\Gamma_S}\right|_{3\pi} = -0.02 \pm 0.01 \tag{21}$$

which is rather small as compared to the experimental $K_L - K_S$ mass difference (its magnitude is determined by the ratio $\Gamma(K_L \to 3\pi)/\Gamma_S \simeq 10^{-3}$) :

$$\Delta m / \Gamma_S = 0.48 \pm 0.02 \tag{22}$$

The pseudoscalar meson contribution can be calculated by using a technique similar to the one employed in the evaluation of the B factor. One finds

$$\begin{aligned} &\langle \pi^o | H_w | K^o \rangle = -4.06\ 10^{-8}\ \text{GeV}^2 \\ &\langle \eta_8 | H_w | K^o \rangle = \beta/\sqrt{3}\ \langle \pi^o | H_w | K^o \rangle \quad , \quad \beta = 1.08 \\ &\langle \eta_o | H_w | K^o \rangle = -\frac{2\sqrt{2}}{\sqrt{3}}\ \langle \pi^o | H_w | K^o \rangle \quad , \rho = 0.74 \end{aligned} \tag{23}$$

where ($\theta \simeq -10.4^o$)

$$\begin{aligned} |\eta\rangle &= \cos\theta\ |\eta_8\rangle - \sin\theta\ |\eta_o\rangle \\ |\eta'\rangle &= \sin\theta\ |\eta_8\rangle + \cos\theta\ |\eta_o\rangle \end{aligned} \tag{24}$$

On the other hand the ρ , ω contribution turns out to be negligible and, by summing up all the long-distance contributions to the K_L self energy one obtains

$$(\delta m_L)_{LD} / \Gamma_S = -0.51 \pm 0.13 \tag{25}$$

where the quoted error takes into account experimental uncertainties on θ and an overall normalization uncertainty on the matrix elements (23).

Finally we consider the K_S case. Eq.(18) becomes

$$\text{Re}\ \Pi_S(s) = 1/\pi\ P \int_{4m_\pi^2}^{m_c^2} \text{Im}\ \Pi_S(s')/(s'-s)ds' \tag{26}$$

We identify $\Gamma_S(s) = -1/\sqrt{s}\ \text{Im}\ \Pi_S(s)$ with the decay width of an off-shell K_S into two pions; thus we have

$$\Gamma_S(s) = \text{const} \left[\frac{s - 4m_\pi^2}{s^2}\right]^{1/2} |F(s)|^2 \tag{27}$$

where the constant is fixed by the normalization condition $\Gamma_S(m_K^2) = \Gamma_S$ and F(s) is a form factor. Using an old suggestion by Nishijima[13], we suppose that F(s) be dominated by an I=0 scalar resonance, having mass m_R and width Γ_R:

$$F(s) = \text{const} / (m_R^2 - s - i\ \Gamma_R\ m_R) \tag{28}$$

Data on I=J=0 $\pi\pi$ phase shift can be fitted by such a resonance with m_R = 800 MeV and a width (a= 0.3 GeV^2, b=0.8) [14] given by : $\Gamma_R = 1/(2m_R)(1-4m_\pi^2/s)^{1/2}(a+bs)$. Using such assumptions we obtain the result (the error arises from uncertainties in the fit; our integral converges rapidly so that uncertainties arising from the region $\sqrt{s'}$ = (1 GeV, m_c) are negligible)

$$\delta m_S/\Gamma_S\big|_{2\pi} = -0.56 \pm 0.07 \tag{29}$$

Summing up results contained in Eqs. (25) and (29) we obtain the result

$$(\Delta m)_{LD}/\Gamma_S = + 0.05 \pm 0.20 \qquad (30)$$

which gives

$$D = 0.10 \pm 0.41 \qquad (31)$$

In conclusion the D parameter turns out to be rather small, owing to a cancel= lation between the long distance contributions to the self energies of K_L and K_S. D contains a large error that cannot be reduced at the present level of develop= ment of the theory; nevertheless Eq.(31) is able to give some informations; for example it excludes too small values of B if the constraint (9) has to be implemen= ted. Let us finally mention some other calculations: the result (31) is compatible with the findings of Ref.(15), where, however, the assumption of SU(3) chiral sym= metry may introduce large uncertainties; our method of dealing with the 2π continu= um has been also used by Bigi and Sanda[16], but their parametrization of the 2π phase shift lead to large errors in D; finally, a recent calculation by Penning= ton [17] of the 2π contribution gives a result sensibly lower than our outcome (29): such a smaller value is obtained by assuming a subtracted DR instead of Eq. (26), which in our opinion is not justified.

REFERENCES

1) M. K. Gaillard and B. W. Lee, Phys. Rev. D10 (1974) 897
2) L.Wolfenstein, Nucl.Phys.B160 (1979) 501; C.T.Hill,Phys.Lett.97B (1980) 275
3) J. F. Donoghue and B. R. Holstein, Phys. Rev. D29 (1984) 2088
4) F. J. Gilman and M. B. Wise, Phys. Rev. D27 (1983) 1128
5) M. Kobayashi and T. Maskawa, Prog. Theor. Phys. 49 (1973) 652
6) P. Cea, G. Nardulli and G. Preparata, Phys. Lett. 148B (1984) 477
7) P. Cea and G. Nardulli, preprint CPT-84/P.1698 (Marseille), Phys.Lett.B(in press)
8) G. Nardulli, G. Preparata and D. Rotondi, Phys. Rev. D27 (1983) 557
9) H. Harari, Phys. Rev. Lett. 17 (1966) 1303
10) J. F. Donoghue, E. Golowich and B.R. Holstein, Phys. Lett. 119B(1982) 412
11) A. J. Buras, W. Slominski and H. Steger, Nucl. Phys. B238 (1984) 529
12) R. Marshak, Riazuddin and C. P. Ryan, Teory of weak interactions in particle physics, Wiley and sons Ed. (New York, 1969)
13) K. Nishijima, Phys. Rev. Lett. 12 (1964) 6
14) G. Mennessier, Zeits. f. Phys. C16 (1983) 241 ; N. M. Cason et al., Phys. Rev. D28 (1983) 1586
15) J. F. Donoghue, E. Golowich and B. R. Holstein, Phys. Lett. 135B (1984) 481
16) I. I. Bigi and A. Sanda, Phys. Lett. 148B (1984) 205
17) M. R. Pennington, preprint DTP/85/2 (University of Durham)

EXACT CALCULATION OF FLAVOUR-CHANGING TRANSITIONS

Swee-Ping CHIA
Physics Department, University of Malaya
Kuala Lumpur, Malaysia

ABSTRACT

Exact renomalised expressions for flavour-changing quark self-energy, flavour-changing quark-gluon vertex function and flavour-changing quark-photon vertex function are presented within the framework of standard $SU(3)_C$ x SU(2) x U(1) theory with six quark flavours. Applications to physical processes such as nonleptonic decays of neutral kaons, flavour-changing radiative decays and the electric dipole moment of neutron are discussed.

I. Introduction

The standard $SU(3)_C \times SU(2) \times U(1)$ theory is now firmly established after the observation of gluon jets[1] and discovery of the W and Z weak bosons.[2] There is, however, a particular aspect of the theory that still remains a mystery, namely the mixing of quark flavours.[3] With six quark flavours, the flavour mixing can be parametrized with the 3x3 Kobayashi-Maskawa (KM) mixing matrix.[4] Besides three mixing angles θ_1, θ_2 and θ_3, the KM matrix also contains a phase angle δ that would give rise to CP violating effects in a natural way. One consequence of this flavour mixing is the neutral conversion of quark flavours, such as from a s-quark to a d-quark, either directly,[5)-7)] or with the emission of a gluon[6),8),9)] or a photon.[9),10)] Although such conversions are prohibited at the tree level, it is nevertheless possible at high orders in the weak coupling constant g.

In order to probe into the finer details of the standard theory, it is necessary to carry out accurate calculations of these flavour-changing (FC) neutral transitions. We present here the exact calculations, to order g^2, of the FC quark self-energy,[7] FC quark-gluon vertex[6] and FC quark-photon vertex, in the unitary gauge.[11] The top-quark mass is not assumed to be small compared to M_w. Although the expressions are derived for $s \to d$ transitions, they are however quite general, and are easily adaptable to other FC transitions.

II. Direct Flavour Conversion

The Feynman diagram for the $s \to d$ self-energy is as shown in Fig. 1. The calculation is straight forward.[7] The self-energy is renormalized so that the the renormalized self-energy $\Sigma_R(p)$ vanishes when one of the external quark is on mass-shell.[5] For $p^2 \ll M_w^2$, we obtain[7]

$$\Sigma_R(p) = \frac{G_F}{4\sqrt{2}\pi^2}\{(p^2-m_d^2-m_s^2)\not{p}L+m_d m_s(-\not{p}R+m_d R+m_s L)\}G_C \qquad (1)$$

where $L, R = \frac{1}{2}(1 \pm \gamma_5)$ and

$$G_C = -2c_1 s_1 c_3(m_u^2-m_c^2)/M_w^2 + s_1 s_2(-c_1 s_2 c_3+c_2 s_3 e^{i\delta})(C_t+2m_c^2/M_w^2) \qquad (2)$$

$$C_t = -\tfrac{1}{2}\mu^2\{(4-\mu^2)(1-\mu^4)+\mu^2(9-4\mu^2+\mu^4)\ell n\mu^2\}/(1-\mu^2)^4, \quad \mu = m_t/M_w \qquad (3)$$

As expressed in Eq. (1), Σ_R is important only when both external quarks are far off mass-shell, and is thus applicable to processes involving the K-meson. It is especially suitable for calculating the $\bar{K}^o \to$ vacuum transition amplitude, $\langle 0|H_w|\bar{K}^o\rangle$,[7),12)] which can occur via an internal $s \to d$ conversion as depicted in Fig. 2. Approximating the $Kq\bar{q}$ binding by an effective constant γ_5 coupling, we obtain

$$\langle 0|H_w|\bar{K}^o\rangle = i\frac{3G_F g_{Kqq}}{128\pi^4}(m_s-m_d)M^4 G_C \lesssim 7\times 10^{-11}\ \text{GeV}^3, \tag{4}$$

where M is the relevant QCD renormalization point, and is taken to be 2 GeV. We can use Eq. (4) to estimate the contribution to the $\Delta I = \frac{1}{2}$ amplitude, $a_{\frac{1}{2}}$, of K^o decays that arises from $\bar{K}^o \to$ vacuum transition. Using PCAC analysis, we have[12),7)]

$$a_{\frac{1}{2}} = -\frac{i}{2f_\pi^2}\left(1-\frac{m_\pi^2}{m_k^2}\right)\langle 0|H_w|\bar{K}^o\rangle \lesssim 4\times 10^{-9}\ \text{GeV} \tag{5}$$

This is at least two orders of magnitude smaller than the experimental value of 3.53×10^{-7} GeV. Our result therefore disagrees with that of McKellar and Scadron.[12)]

Using pion PCAC, we can give an estimate of $K_L \to \pi^o$ transition amplitude $\langle \pi^o|H_w|K_L\rangle$ in terms of $\langle 0|H_w|\bar{K}^o\rangle$,[12),7)]

$$\langle \pi^o|H_w|K_L\rangle = \frac{1}{\sqrt{2}f_\pi}\langle 0|H_w|\bar{K}^o\rangle \lesssim 5\times 10^{-10}\ \text{GeV}^2 \tag{6}$$

The $K_L \to \pi^o$ amplitude can be used to relate $K_L \to \gamma\gamma$ to $\pi^o \to \gamma\gamma$ be assuming pion-pole dominance,[12),7)]

$$\Gamma(K_L \to \gamma\gamma) = \Gamma(\pi^o \to \gamma\gamma)\left|\langle \pi^o|H_w|K_L\rangle/(m_k^2-m_\pi^2)\right|^2 \lesssim 5\times 10^{-2}\,s^{-1} \tag{7}$$

This is again too small when compared to the experimental value of $0.945\times 10^4\,s^{-1}$. We therefore conclude that $K_L \to \gamma\gamma$ cannot be explained by pion-pole dominance.[7)]

III. Flavour Conversion with One Gluon Emission

Figure 3 shows the Feynman diagram for the FC quark-gluon vertex, or the penguin vertex. The vertex function $\Gamma_\mu^a(p,k)$ is renormalized by requiring that Ward-Takahashi identity is satisfied by the renormalized quantities:[6)]

$$k^\mu \Gamma_{R\mu}^a(p,k) = g_s \tfrac{1}{2}\lambda^a\{\Sigma_R(p) - \Sigma_R(p-k)\}. \tag{8}$$

We give here the on-shell vertex function[6)] for the case $k^2 << M_w^2$:

$$\Gamma_{R\mu}^a(\text{on-shell}) = \frac{g_s G_F}{4\sqrt{2}\pi^2}\tfrac{1}{2}\lambda^a\{G_A(k_\mu \not{k} - k^2\gamma_\mu)L + iG_B\sigma_{\mu\nu}k^\nu(m_d L + m_s R)\} \tag{9}$$

where

$$G_A = \frac{2}{3}c_1 s_1 c_3 \ell n(m_u^2/m_c^2) + s_1 s_2(-c_1 s_2 c_3 + c_2 s_3 e^{i\delta})\{A_t - \frac{2}{3}\ell n(m_c^2/M_w^2)\} \tag{10}$$

$$G_B = \frac{1}{2}c_1 s_1 c_3(m_u^2-m_c^2)/M_w^2 + s_1 s_2(-c_1 s_2 c_3 + c_2 s_3 e^{i\delta})(B_t - \tfrac{1}{2}m_c^2/M_w^2) \tag{11}$$

$$A_t = -\frac{1}{12}\{\mu^2(1-\mu^2)(18-11\mu^2-\mu^4) - 2(4-16\mu^2+9\mu^4)\ell n\mu^2\}/(1-\mu^2)^4 \tag{12}$$

$$B_t = -\frac{1}{4}\mu^2\{(1-\mu^2)(2+5\mu^2-\mu^4) - 6\mu^2\ell n\mu^2\}/(1-\mu^2)^4 \tag{13}$$

Our expressions, Eqs. (10) - (13), agree completely with the calculation of Deshpande and Nazerimonfared.[9] It is noted that G_A dominates over G_B because the ratio of $A_t - \frac{2}{3}\ell n(m_c^2/M_w^2)$ to $B_t - \frac{1}{2} m_c^2/M_w^2$ is about 70 at $m_t = 40$ GeV.

The main application of the FC quark-gluon vertex is in the penguin diagram[8] as shown in Fig. 4. The effective Hamiltonian for the penguin diagram is

$$H_w(\text{penguin}) = - \frac{\alpha_s G_F}{\sqrt{2}\pi} G_A (\bar{d}\gamma_\mu L \tfrac{1}{2}\lambda^a s)(\bar{u}\gamma^\mu \tfrac{1}{2}\lambda^a u + \ldots) \tag{14}$$

The contribution of the penguin diagram in the electric dipole moment of neutron has been estimated previously.[13] Our new expression for G_A allows us to improve on this estimate.[6] However, the improve is only slight; for $m_t = 40$ GeV, we get only a factor of 1.2 over the old estimate. Thus the contribution of the penguin diagram to the electric dipole moment remains of order 10^{-30} e-cm or 10^{-32} e-cm, depending on the specific mechanism.[13]

The penguin diagram also contributes to the parameter ξ given by[6]

$$\xi = \text{Im}(K^0 \to 2\pi) \,/\, \text{Re}(K^0 \to 2\pi)$$

$$= \text{Im}\, G_A / \text{Re}\, G_A \approx - 5.60 \times 10^{-4} \quad \text{for} \quad m_t = 40 \text{ GeV} \tag{15}$$

This gives a value for ε'/ε of[6]

$$\varepsilon'/\varepsilon = 2.75 \times 10^{-3} \quad \text{for} \quad m_t = 40 \text{ GeV}, \tag{16}$$

which is in agreement with recent experimental values of $- 0.0046 \pm 0.0053 \pm 0.0024$[14] and $+ 0.0017 \pm 0.0084$.[15]

IV. Flavour Conversion with One Photon Emission

The Feynman diagrams for the FC quark-photon vertex $\Gamma_\mu^{(\gamma)}(p,k)$ are as shown in Fig. 5.[11] Renormalization is performed by requiring that the renormalized quantities satisfy the Ward-Takahashi identity.[11] For $k^2 \ll M_w^2$, the on-shell vertex function is given by[11]

$$\Gamma_{R\mu}^{(\gamma)}(\text{on-shell}) = \frac{eG_F}{4\sqrt{2}\pi^2}\{G_A^{(\gamma)}(k_\mu \not{k} - k^2\gamma_\mu)L + iG_B^{(\gamma)}\sigma_{\mu\nu}k^\nu(m_d L + m_s R)\} \tag{17}$$

where

$$G_A^{(\gamma)} = \tfrac{4}{9}c_1 s_1 c_3 \ell n(m_u^2/m_c^2) + s_1 s_2 (-c_1 s_2 c_3 + c_2 s_3 e^{i\delta})\{\tfrac{2}{3}A_t - \tilde{A}_t - \tfrac{4}{9}\ell n(m_c^2/M_w^2)\} \tag{18}$$

$$G_B^{(\gamma)} = - \tfrac{7}{8}c_1 s_1 c_3 (m_u^2 - m_c^2)/M_w^2 + s_1 s_2 (-c_1 s_2 c_3 + c_2 s_3 e^{i\delta})(\tfrac{2}{3}B_t - \tilde{B}_t + \tfrac{7}{8} m_c^2/M_w^2) \tag{19}$$

A_t and B_t are as given in Eqs. (12) and (13), and $\tilde{A}_t$ and $\tilde{B}_t$ are given by

$$\tilde{A}_t = \tfrac{1}{16}\mu^2\{(1-\mu^2)(14-41\mu^2+21\mu^4) + 2\mu^2(4-16\mu^2+9\mu^4)\ell n\mu^2\}/(1-\mu^2)^4 \tag{20}$$

$$\tilde{B}_t = \tfrac{1}{48}\mu^2\{(1-\mu^2)(58-31\mu^2+27\mu^4) + 2\mu^2(48-40\mu^2+19\mu^4)\ell n\mu^2\}/(1-\mu^2)^4. \tag{21}$$

Equations (20) and (21) for $\tilde{A}_t$ and $\tilde{B}_t$ are different from those obtained by Deshpande and Nazerimonfared.[9] Since our calculation is performed in the unitary gauge in which only observed particles are present, we are confident that our expressions are the correct ones.

From Eqs. (18) and (19), we can see that $G_A^{(\gamma)}$ is more dominant than $G_B^{(\gamma)}$. In fact, for m_t = 40 GeV,

$$\mathrm{Re}G_A^{(\gamma)}/\mathrm{Re}G_B^{(\gamma)} \sim 10^3, \qquad \mathrm{Im}G_A^{(\gamma)}/\mathrm{Im}G_B^{(\gamma)} \sim 20 \tag{22}$$

But for the emission of real photon, only $G_B^{(\gamma)}$ contributes because the $G_A^{(\gamma)}$ term vanishes. Real photon emission processes are therefore strongly suppressed. This is well illustrated by comparing the decay rates for $s \to d\gamma$ and $s \to de^+e^-$. The computations are straight-forward, and we obtain

$$\Gamma(s \to d\gamma) \sim (\alpha G_F^2/128\pi^4) m_s^5 |G_B^{(\gamma)}|^2 \sim 7 \times 10^{-15} \text{ eV} \tag{23}$$

$$\Gamma(s \to de^+e^-) \sim (\alpha G_F^2/1536\pi^6) m_s^5 |G_A^{(\gamma)}|^2 \sim 2 \times 10^{-11} \text{ eV} \tag{24}$$

where we have assumed that the $s \to de^+e^-$ decay occurs via an intermediate virtual photon which subsequently decays into e^+e^-. The decay rate of 2×10^{-11} eV for $s \to de^+e^-$ appears to be in the right ball-park for describing the decay $\Sigma^+ \to pe^+e^-$:

$$\Gamma(\Sigma^+ \to pe^+e^-)_{\text{expt}} < 6 \times 10^{-11} \text{ eV} \tag{25}$$

But the rate of 7×10^{-15} eV appears to be too small for describing the FC radiative decays of Σ^+, Ξ^o, Ξ^- and Ω^-:

$$\left.\begin{aligned}
&\Gamma(\Sigma^+ \to p\gamma)_{\text{expt}} = (0.99 \pm 0.11) \times 10^{-8} \text{ eV} \\
&\Gamma(\Xi^o \to \Lambda^o\gamma)_{\text{expt}} = (1.1 \pm 1.1) \times 10^{-8} \text{ eV} \\
&\Gamma(\Xi^o \to \Sigma^o\gamma)_{\text{expt}} < 1.6 \times 10^{-7} \text{ eV} \\
&\Gamma(\Xi^- \to \Sigma^-\gamma)_{\text{expt}} < 4.8 \times 10^{-9} \text{ eV} \\
&\Gamma(\Omega^- \to \Xi^-\gamma)_{\text{expt}} < 2.5 \times 10^{-8} \text{ eV}
\end{aligned}\right\} \tag{26}$$

But we are reminded that the FC radiative decays of these strange hyperons also receive contribution from the penguin diagram such as Fig. 6. This diagram will give a more dominant contribution to the radiative decay because the gluon involved at the penguin vertex is in the virtual state, and is therefore enhanced. To obtain a rough estimate of the magnitude of this contribution, we merely replace $G_B^{(\gamma)}$ in Eq. (23) by G_A. The resultant estimate is

$$\Gamma(sq \to sq\ \gamma)_{\text{penguin}} \sim 2 \times 10^{-9} \text{ eV} \tag{27}$$

which comes quite close to the experimental decay rates.

It is interesting to speculate on the possibility of bare top-flavour production from the process

$e^+e^- \to \gamma^* \to t\bar{c}$.

A quick estimate gives a cross-section for such a process of

$$\sigma \sim \alpha^2 G_F^2 \sin^2\theta_3 \, m_b^4 E_{tot}^2 / M_w^2 . \tag{28}$$

For E_{tot} = 30 - 40 GeV, $\sigma \sim 10^{-9}$ pb, which is probably too small to be measurable. The possibility of electro-production of bare top-flavour by the process

$e^- u \to e^- t$

via one virtual photon exchange is even less likely because of the further suppression.

Let us now turn to the CP violating effects arising from the sdγ vertex. Besides the pengiun diagram contribution, the electric dipole moment of neutron also receives contribution from diagram of Fig. 7,[16] which involves the sdγ vertex. Such contribution gives[16]

$$D_n = (G_F^2/8\pi^2)\,|\psi(o)|^2 \, (c_1 s_1^2 c_2 s_2 c_3 s_3 \sin\delta)(\tilde{B}_t - \tfrac{2}{3} B_t) , \tag{29}$$

where

$$|\psi(o)|^2 \approx 3 \times 10^{-3} \text{ GeV} \tag{30}$$

Using our expressions for B_t and $\tilde{B}_t$, we obtain, for m_t = 40 GeV,

$$D_n \sim 10^{-33} \text{ e-cm}. \tag{31}$$

This is improved by one order of magnitude, but is still smaller than the penguin contribution.

We have argued previously that the FC radiative decays of strange hyperons, and possibly those of K-mesons, might be accounted for by processes involving the sdγ vertex or the sdg vertex. If this is so, we would then be in a position to estimate the CP violating effects in such decays. For FC decays that involve a virtual photon, the relevant quantity for measuring the CP violating effect is $\mathrm{Im}G_A^{(\gamma)}/\mathrm{Re}G_A^{(\gamma)}$,

$$\mathrm{Im}G_A^{(\gamma)}/\mathrm{Re}G_A^{(\gamma)} \sim 5 \times 10^{-4}. \tag{32}$$

It is therefore too small an effect. For decays involving a real photon, we have seen that it is the pengiun diagram involving the penguin vertex that gives the dominant contribution. The relevant quantity here is $\mathrm{Im}G_A/\mathrm{Re}G_B$, which is again $\sim 10^{-4}$. The CP violating effects in FC radiative decays of strange particles are therefore too small to be observable.

V. Conclusion

We have presented exact calculations of Flavour-changing quark transitions, which involve direct conversion of flavour, or conversion with the emission of a gluon or a photon. Estimates are made on the contributions of these transitions to various processes. Direct flavour conversion is used to compute the $\bar{K}^o \rightarrow$ vacuum transition amplitude and is found to be too small to explain the $\Delta I = \frac{1}{2}$ rule or the $K_L \rightarrow \gamma\gamma$ decay. The gluon-emitting flavour conversion is applied to the penguin diagram. It is found that the penguin contribution to the electric dipole moment of neutron remains at 10^{-30} e-cm or 10^{-32} e-cm. It also gives an estimate of 2.75×10^{-3} for the parameter ϵ'/ϵ which is in agreement with recent experimental values. Photon-emitting flavour conversion is applied to various processes. Flavour-changing radiative decays of strange particles appears to be explanable in terms of the flavour-changing quark transitions. But the CP violating effects in such decays are estimated to be too small to be measurable. Photon-emitting quark flavour transition gives a value of 10^{-33} e-cm to the electric dipole moment of neutron, which is still smaller than the penguin contribution. Finally, the possibility of bare top-flavour production from the processes $e^+e^- \rightarrow t\bar{c}$ or $e^-u \rightarrow e^-t$ is shown to be very unlikely.

References

1. R. Brandelik et al., Phys. Lett. 86B (1979) 243; D.P. Barber et al., Phys. Rev. Lett. 43 (1979) 830; C. Berger et al., Phys. Lett. 86B (1979) 418; W. Bartel et al., Phys. Lett. 91B (1980) 142.

2. G. Arnison et al., Phys. Lett. 122B (1983) 103; 126B (1983) 398; 129B (1983) 273; G. Banner et al., Phys. Lett. 122B (1983) 476; P. Bagnaia et al., Phys. Lett. 129B (1983) 130.

3. N. Cabibbo, Phys. Rev. Lett. 10 (1963) 531; S. Glashow, J. Iliopoulos and L. Maiani, Phys. Rev. D2 (1970) 1285.

4. M. Kobayashi and T. Maskawa, Prog. Theor. Phys. 49 (1973) 652.

5. E.P. Shablin, Sov. J. Nucl. Phys. 28 (1978) 75; D.V. Nanopoulos, A. Yildiz and P.H. Cox, Ann. Phys. 127 (1980) 126; S.P. Chia and S. Nandi, Phys. Lett. 117B (1982) 45.

6. S.P. Chia, Phys. Lett. 130B (1983) 315.

7. S.P. Chia, Phys. Lett. 147B (1984) 361.

8. A.I. Vainshtein, V.I. Zakharov and M.A. Shifman, JETP Lett. 22 (1975) 55; M.A. Shifman, A.I. Vainshtein and V.I. Zakharov, Nucl. Phys. B120 (1977) 316; M.B. Wise and E. Witten, Phys. Rev. D20 (1979) 1216; S.P. Chia and S. Nanadi, Phys. Rev. D27 (1983) 1654.

9. N.G. Deshpande and M. Nazerimonfared, Nucl. Phys. B213 (1983) 390.

10. T. Inami and C.S. Lim, Prog. Theor. Phys. 65 (1981) 297; A.J. Buras, Phys. Rev. Lett. 46 (1981) 1354; N.G. Deshpande and G. Eilam, Phys. Rev. D26 (1982) 2463.

11. S.P. Chia and G. Rajagopal, University of Malaya Preprint, UMKL-85-1 (unpublished).

12. B.H.J. Mckellar and M.D. Scadron, Phys. Rev. D27 (1983) 157.

13. M.B. Gavela et al., Phys. Lett. 109B (1982) 215; I.B. Khriplovich and A.R. Zhitnitsky, Phys. Lett. 109B (1982) 490.

14. B. Peyand, this proceedings.

15. M. Schmidt, this proceedings.

16. N.G. Deshpande, G. Eilam and W.L. Spence, Phys. Lett. 108B (1982) 42.

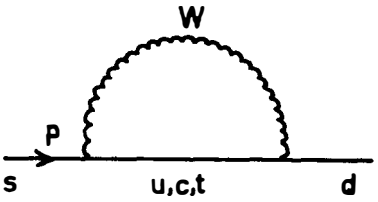

Fig. 1 Feynman diagram for the s - d self-energy.

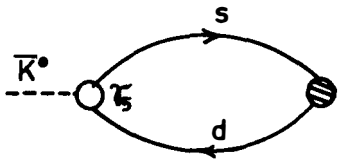

Fig. 2 Quark-loop diagram for $\bar{K}^o \to$ vacuum transition.

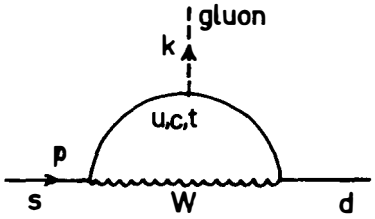

Fig. 3 Feynman diagram for the sdg vertex.

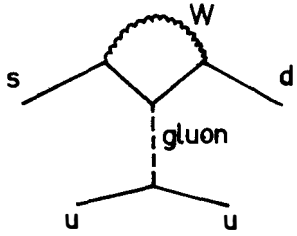

Fig. 4 The penguin diagram.

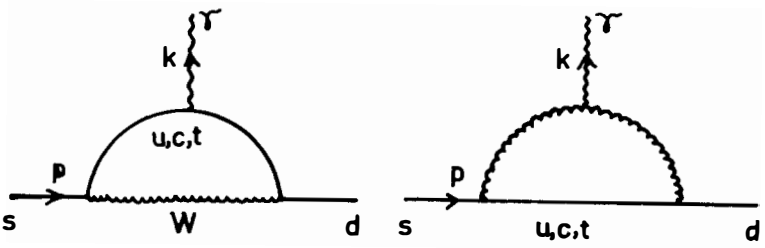

Fig. 5 Feynman diagrams for the sdγ vertex.

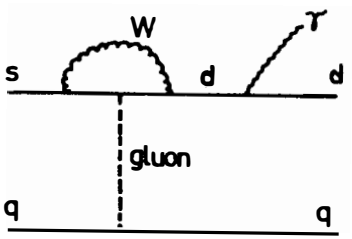

Fig. 6 Penguin diagram contribution to the FC radiative decay of strange hyperons.

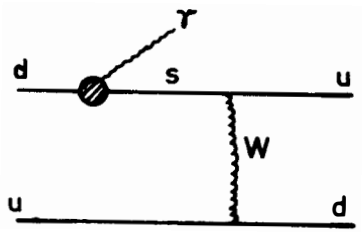

Fig. 7 Diagram involving the sdγ vertex that contributes to the electric dipole moment of neutron.

$\Delta I=\frac{1}{2}$ RULE, HEAVY QUARKS, AND CP VIOLATION

D. G. SUTHERLAND
UNIVERSITY OF GLASGOW, GLASGOW G12 8QQ

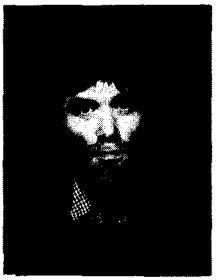

ABSTRACT

The $\Delta I=\frac{1}{2}$ rule for K decays is discussed in an approach emphasising long distance aspects of the matrix elements. Large contributions from t quark states are found necessary. Consequent discrepancy with the KM model for CP violating amplitudes is explained. The relationship to the standard short distance estimates is discussed.

I present a brief account of a recent attempt with Pham[1] to understand the $\Delta I=\frac{1}{2}$ rule in K decay. The relevance of this to the Workshop is that, upon using improved experimental and theoretical input, we find much sharper disagreement with data in the KM model of CP violation than in previous analyses.

Our motivation derived from dissatisfaction with the orthodox treatments of the $\Delta I=\frac{1}{2}$ rule. The original calculations[2] of hard gluon corrections gave an enhancement of only ~ 5 as opposed to experimental ~ 22 of $\Delta I=\frac{1}{2}$ over $\Delta I=\frac{3}{2}$, while the hopes expressed for penguin operators introduced by SVZ[3] seem unfulfilled. Recently several authors[4] have estimated, with perturbative estimates of C_5, that only 10-20% of the $\Delta I=\frac{1}{2}$ amplitude comes from penguin operators. Guberina has discussed here a hadronic sum rule and concludes also that penguin operators do not adequately explain the $\Delta I=\frac{1}{2}$ rule.

It is disturbing that after 25 years we still cannot understand the $\Delta I=\frac{1}{2}$ rule for K decay. Furthermore, as similar operators appear in estimates of ε', doubt is cast on these by our failure. Our feeling was that the most serious omission in the usual analysis was the effect of soft gluons. An interesting paper is this spirit by Nardulli et.al.[5] argued that the $\Delta I=\frac{1}{2}$ rule could be attributed to the K^* Regge Pole in the weak virtual Compton amplitude -clearly a soft effect.

Our treatment differs in several respects from that of Nardulli et.al., but it shares the essential feature of focussing on the relatively low q^2 behaviour of the virtual Compton amplitude. The relation of this to the usual short distance analysis we discuss below.

We make essential use of the chiral SU(3) x SU(3) result that $\langle\pi(p)|H_{WK}|K(k)\rangle \propto p.k$[6] Any momentum independent piece should vanish with m_s. It is not clear how the SU(3) invariant and momentum independent K^* contribution can satisfy this and we believe it contributes only to the $K\pi$ mixing, which should be rotated away, and not to the $K\to\pi\pi$ amplitude. We see no such reason to rotate away p.k piece, and we compute this by inserting intermediate states $|M\rangle$ in the chiral limit with vector dominance for $\langle\pi|J_\mu|M\rangle$.

We find $\langle\pi^+|H_{WK}^{\Delta I=i}|K^+\rangle = 2^{-\frac{1}{2}}G_F\sin\theta_c\cos\theta_c p.k\, f_\pi^2 x1.3$, for $i=\frac{1}{2}; x(-0.07)$ for $i=\frac{3}{2}$ the main contributions coming from intermediate π, K, vacuum, ω and K^* states with very small additions from higher states (thus far only 3 light quarks appear in the currents). One sees a large enhancement of $\Delta I=\frac{1}{2}$ over $\Delta I=\frac{3}{2}$ by ~ 20, though one should be aware that the $I=\frac{3}{2}$ amplitude involves cancellations and is very sensitive to assumptions on input; it may also receive substantial contributions from mixed weak and isospin violating effects.

The magnitude of $\langle\pi^+|H_{WK}^{\Delta I=\frac{1}{2}}|K^+\rangle$ can be estimated as $2^{-\frac{1}{2}}G_F\sin\theta_c\cos\theta_c f_\pi^2 p.k \times 3$ from $\Gamma(K_s\to\pi^+\pi^-)$ and a soft pion theorem with a correction[7] from final state interactions of the pions. Before comparing this

with our estimate above, we should include the effects of hard gluons, though we expect (from eg. refs.2) and 6)) that these will be modest. Since our emphasis is on soft gluons we accept our treatment of hard gluons may be approximate, but we do not believe this should lend to serious errors.

We use a method similar to one discussed by Wilson.[8] Write

$$T(J_\mu(x)J_\nu(0) = \sum_n C_n(x)\ O_n + R(x) \qquad (1)$$

where R(x) is a remainder $\to 0$ as $x \to 0$, to obtain a sum rule

$$\int d^4q\ (M_{AB}(q) - \sum_n \tilde{C}_n(q) \langle A|O_n|B\rangle) = 0 \qquad (2)$$

where $$M_{AB}(q) = \langle A|\int d^4x\ e^{iqx} T(J_\mu(x)\ J_\nu(0)|B\rangle \qquad (3)$$

and $$\tilde{C}_n(q) = \int d^4x\ e^{iqx} C_n(x) \qquad (4)$$

We hope that the rapidly converging integral (as a reflection of precocity of scaling) gives a good approximation if we cut off the integral at moderate q_{max}, around 2 GeV. say, so that

$$\int_o^{q_{max}} d^4q\ M_{AB}(q) = \sum_n \tilde{C}_n(q_{max})\ \langle A|O_n|B\rangle \qquad (5)$$

Since the operators O_1, O_5 and O_6 have similar ratios $\tilde{C}_i(q_{max})/\tilde{C}_i(M_W) \simeq 0.7$ for $q_{max} \simeq 2$ GeV, we can relate the short distance result to our long distance estimates to obtain $\langle\pi^+|H_{WK}^{\Delta I=\frac{1}{2}}|K^+\rangle \simeq 2^{-\frac{1}{2}} G_F \sin\theta_c \cos\theta_c f_\pi^2 p.k \times 1.9$

Thus we find a discrepancy of 50% with our estimated phenomenological value above. Several attitudes to this can be adopted. One might try to reduce q_{max} to 1 GeV, but the change in $\tilde{C}_n$ induced is largely compensated by a reduction in $\int_o^{q_{max}} d^4q\ M_{AB}(q)$ - a nice feature of our approach. Our feeling was that the discrepancy was too large to be due to chiral symmetry breaking, but a recent calculation[9] of the $\langle K^+|O_4|\pi^+\pi^o\rangle$ in chiral perturbation theory finds 50% corrections as discussed here by Golowich. Until a similar calculation is made and assessed for the $\Delta I=\frac{1}{2}$ amplitude, we cannot rule out chiral symmetry breaking as the source of discrepancy. As in the orthodox treatments[10] there is only approximate matching of long and short distance effects and this is made worse by the appearance of O_5 and O_6 for which the soft gluon corrections to the perturbative operators can not be taken as local operators when only u quarks appear in the loop.[11]

Thus from phenomenology we are probably not forced to have a larger contribution from heavy quarks than the orthodox $\sim$ 10% penguin estimate. We do not believe, however, that it is consistent with our treatment of the long distance effects for light quarks to take this estimate. Rather we calculate the effects of D, D^* intermediate states using F^* and D^* dominance of the currents. Of course, larger uncertainties enter here, especially for the D^* intermediate states, but we note that a similar model seems rather successfull in describing D semi-leptonic decays, as discussed here by Stech. We then obtain an almost

total cancellation (of GIM type) with our previous three quark contribution. Only modest short distance enhancement is expected (see below).

Within the KM model we are left with only the possibility of including the effect of states including t quarks. A calculation analogous to that for D, D^* intermediate states gives a contribution $\sim m_t^2 |U^*_{ts} U_{td}|/\cos\theta_c \sin\theta_c$ of that from the D, D^* states. With present data on the 3 generation KM model we find $m_T \simeq (40 \pm 8)$ GeV is needed to fit $K_S \to \pi^+\pi^-$ rate. In our estimates we generalised the model of Stech and collaborators and the errors from this e.g. T^* dominance, at least out to $q^2 \simeq m_T^2$, are hard to assess and are probably no smaller than those from the KM matrix elements. Nevertheless it is gratifying that our central mass estimate is close to that reported here by UA1 collaboration.

Before discussing further these uncertainties and the relation of these estimates to the short distance analysis, we show how we encounter a serious disagreement with data if our estimates are even approximately valid. Since the $K_S \to \pi^+\pi^-$ amplitude is essentially all due to intermediate states with t quarks, $|\varepsilon'| \lesssim 10^{-5}$ requires a KM phase $\delta \lesssim O(10^{-4})$. In consequence the box diagram gives $\varepsilon_m << \varepsilon_{empirical}$ ($=2.3\ 10^{-3}$ in modulus) provided only that the B parameter is $\lesssim O(1)$ as indicated by bounds of Guberina et.al.[12] Thus we have a situation where, in the standard notation[13], $\xi/\varepsilon_m >> 1$.

It is known that this can be made compatible with data on ε'/ε if large dispersive correction to the box diagram occurs; in the notation of Wolfenstein[13] $D<-10$ is required. In ref. 1 we took the view that this might allow agreement with the KM model. This was based on a related calculation by Dupont and Pham[14] which found $D \sim -6$ in a model and thereby gave agreement with the earlier data on ε/ε. As we now explain, we now believe, on re-analysis and on using new data on ε'/ε, that $D \sim -2$ is very unlikely and thus the 3 quark KM model is in strong disagreement with data.

There are three elements in our re-analysis and all tend to increase D. The most important is the use of the final state interaction correction[7] in estimating $\langle K|H_{WK}^{\Delta I=\frac{1}{2}}|\pi\rangle$. This reduces the magnitude of D by $\simeq 3$. Secondly the positive contribution to D from 2π intermediate states, while still rather uncertain,[15] is probably O(1) rather than negligibly small. Finally the SU(3) violation in $\langle K|H_{WK}^{\Delta I=\frac{1}{2}}|M\rangle$, ($M=\pi,\eta,\eta'$)was probably as large as feasible and the use of a nonlinear chiral Lagrangian[16] with SU(3) breaking give $|D|$ much smaller than in Ref. 14). To avoid confusion we emphasise that these remarks apply to D within the KM model only, and not to D within the multi-Higgs models of CP violation discussed here by Sanda and by Pham.

Is there a relatively modest change in the standard model that would restore agreement with data or are we forced to new physics such as that dis-

cussed here by Mohapatra and Gerard? One possibility might be a fourth generation of quarks, but we do not find this very plausible, since it would require apparently very conspirational cancellations of the imaginary parts of t and t′ contributions.

Because of the importance of our conclusion, it behoves us to explain further the assumption underlying it and its connection with the short distance approach. Repeating our use of the sum rule of Wilson[8] for heavy quarks, we expect only O_5 and O_6 penguin operators to be significant. The coefficient functions will be modified by soft gluonic effects, but, for c or t in the loop, the penguin operators are still effectively local four fermion operators.[11] Usually these soft gluonic modifications seem to be taken small, but we are lead to doubt this from the sum rule. Note that for heavy quark Q of mass m_Q it is appropriate to take $q_{max} \approx m_Q$ on the ground that only then can scaling be expected from the currents containing Q. Consequently we expect only a most enhancement ($\simeq$ 1.2) from hard gluons.

Our other assumption of vector dominance for heavy vector mesons is hard to justify but it appears reasonable and to have some support from semi-leptonic D decay as well as being testable in T decay Theoretically QCD sum rules might be used to investigate this. While uncertain for T decay, we recall that its validity of D decay would leave us with a lack of understanding of $\Delta I=\frac{1}{2}$ rule in the standard model if the T contribution is small.

It seems worthwhile to give a diagrammatic interpretation of the difference from the usual approach. The soft gluons in the diagram build the resonances in the intermediate state and in the formfactors.

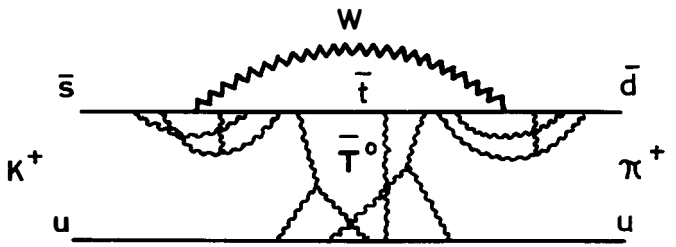

As discussed by Isgur and Llewellyn Smith,[17] it appears that soft effects in the π wavefunction are much larger than the perturbative effects at $q^2 \simeq$ few GeV^2 and we believe a similar effect is at work here; further study of this for heavy quarks, perhaps in a Bethe-Salpeter equation approach, could be helpful.

Galic[18] has recently put forward a similar explanation of the $\Delta I=\frac{1}{2}$ rule in terms of a heavy quark in interaction with soft gluons. His approach is an effective theory and he makes no calculation of the size of the effect and does not treat CP effects, so that it is difficult to compare with our approach. A

treatment with affinities to ours has been advocated by Donoghue[19] and implemented recently by Eeg.[20] They use bag model states and we feel uneasy on the chiral properties of such calculations.

Finally we stress again the dramatic conflict with the standard model that arises in our attempt to explain the $\Delta I=\frac{1}{2}$ rule. We emphasise that this is not a conflict dependent on delicate details. If our calculation is even approximately correct, the conflict persists. We feel that serious efforts to justify or to vitiate our computation are, therefor, required.

References:

1) T.N.Pham and D.G.Sutherland, Phys. Lett. 135B (1984) 209.
2) M.K.Gaillard, and B.W.Lee, Phys. Rev. D10 (1974) 897 ; G.Altarelli and L. Maiani, Phys. Lett. 52B (1974) 351.
3) M.A.Shifman, et.al. Nucl. Phys. B120 (1977) 315 ; JETP 45 (1977) 670.
4) Y.Dupont and T.N.Pham, Phys. Rev. D29 (1984) 1368 ; J.F.Donoghue, Phys. Rev. D30 (1984) 1499 ; T.N.Pham, Phys. Lett. 145B (1984) 113 ; M.B.Gavela, et.al. Phys. Lett. 148B (1984) 225.
5) G. Nardulli, et.al. Phys. Rev. D27 (1983) 557.
6) J.A.Cantor, Phys. Rev. D3 (1971) 3205.
7) I.Antoniadis and T.N.Truong, Phys. Lett. 109B (1982) 67.
8) K.G.Wilson, Phys. Rev. 179 (1969) 1499.
9) J. Bijnens, et.al. Phys. Rev. Lett. 53 (1984) 2367.
10) A.J.Buras and W.Slominski, Munich preprint MPI-PAE/PTh 68/84 (1984).
11) M.B.Wise and E.Witten, Phys. Rev. D20 (1979) 1216.
12) B.Guberina, et.al. Phys. Lett. 128B (1983) 269.
13) See e.g. L.Wolfenstein, CERN preprint, CERN-TH.3925/84 (1984)
14) Y.Dupont and T.N.Pham, Phys. Rev. D28 (1984) 2169.
15) I.I.Bigi and A.Sanda, Phys. Lett. 148B (1984) 205 ; M.B.Pennington, Durham Univ. preprint,DTP/85/2 (1985) ; T.N.Pham and D.G.Sutherland in preparation.
16) T.N.Pham, Phys. Rev. D30 (1984) 234.
17) N.Isgur and C.H.Llewellyn Smith, Phys. Rev. Lett. 52 (1984) 1080.
18) H.Galic, SLAC preprint, SLAC-PUB-3383 (1984).
19) J.F.Donoghue, in 'Phenomenology of Unified Theories' Ed. H.Galic, et.al. (World Scientific, 1984).
20) J.O.Eeg, University of Oslo preprint (1984).

ON THE PREDICTION FOR ε'/ε IN MODELS WITH SPONTANEOUS CP VIOLATION AND NATURAL FLAVOR CONSERVATION

A.I. Sanda
Rockefeller University, New York, New York 10021

The result $|\varepsilon'/\varepsilon| \approx .05$ in models with spontaneous CP violation with natural flavor conservation was obtained using the vacuum saturation approximation. This approach has been criticized as the vacuum saturation approximation, as used here, does not show any remnant of chiral SU(3) x SU(3) symmetry. Assuming that this objection is relevant,(i.e. chiral perturbation theory converges for matrix elements in question), $|\varepsilon'/\varepsilon| \approx .006$ was obtained following wisdom of chiral symmetry. It is pointed out that the latter calculation ignores η-η' mixing. If the mixing is included $|\varepsilon'/\varepsilon| \approx .016$ results. While this is too large compared to experimental result, it is not possible to put a theoretical error on this result. As the validity of vacuum saturation approximation is an important question, a serious attempt to understand the prediction of chiral perturbation theory is worthwhile.

Work supported in part by the Department of Energy under Contract Grant Number DE-AC02-81ER40033B.000.

At this time, the origin of CP violation is completely open. Grand unified theories or super symmetric theories which incorporate a mechanism for generating baryon asymmetry may lead to the explanation of phenomena observed in K meson decays. One might, however, search for theories which accommodate CP violation within the context of the SU(2)xU(1) electroweak gauge theory. In this case various possibilities and their consequences can be mapped as shown in Fig. 1

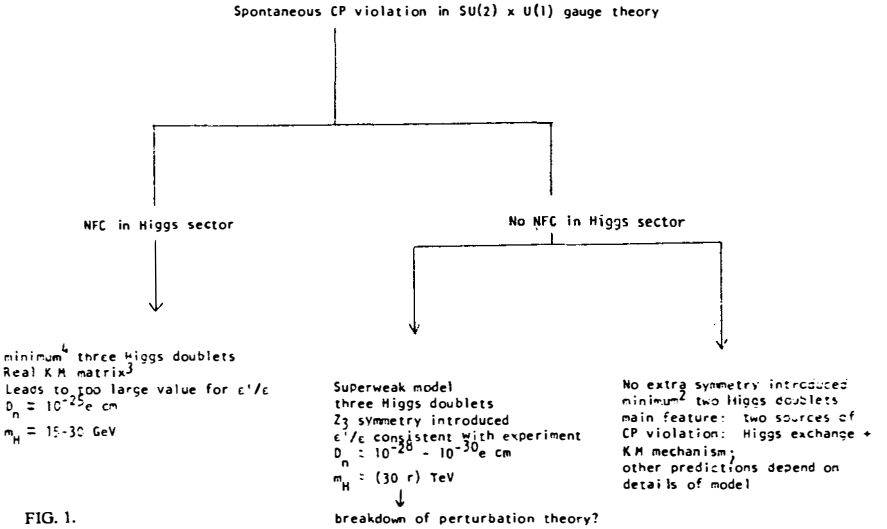

FIG. 1.

As it can be seen in Fig 1, vacuum saturation approximation (VSA) used to evaluate $\langle K^0 | H | \bar{K}^0 \rangle$ matrix element lead to the prediction[2]

$$\left|\frac{\varepsilon'}{\varepsilon}\right| = .05 \qquad (1)$$

for the spontaneous CP violation with natural flavor conservation (NFC) . Result of recent experimental measurements[3] are

$$\varepsilon'/\varepsilon = -.0046 + .0053 \pm .0024 \quad \text{Chicago - Saclay}$$
$$+.0017 \pm .0084 \quad \text{Yale - BNL} , \qquad (2)$$

The prediction seems to contradict experiments. In this talk, I shall briefly review various contributions to the subject with main emphasis in exposing all assumptions which goes into the prediction.

I. Spontaneous CP violation and NFC.

Spontaneous symmetry breaking is extremely elegant in that there is natural explanation for symmetry breaking and avoid having to introduce such breaking by hand. To illustrate this for CP violation, I will consider a simple example: Consider a Higgs potential

$$V = -\mu \sum |\phi_i|^2 + \sum \lambda |\phi_i|^4 + C[(\phi_1^\dagger \phi_2)(\phi_1^\dagger \phi_3) + (\phi_2^\dagger \phi_1)(\phi_2^\dagger \phi_3) + (\phi_3^\dagger \phi_1)(\phi_3^\dagger \phi_2)] \text{ H.C.} \quad (3)$$

where three scalar fields ϕ_1, ϕ_2, and ϕ_3 have been introduced and the specific form may be due to some discrete symmetry.

If $\langle \phi_i \rangle = v\, e^{i\alpha_i}$,

$$V = -3\mu v^2 + 3\lambda v^4 + v^4 C[\cos(2\alpha_1-\alpha_2-\alpha_3)+\cos(2\alpha_2-\alpha_1-\alpha_3) + \cos(2\alpha_3-\alpha_1-\alpha_2)]. \quad (4)$$

This potential has a minimum at $\alpha_1-\alpha_3$, $\alpha_2-\alpha_3 = \frac{2\pi}{3} + 2n\pi$.

Non-trivial phase α_i will lead to observable CP violation. If one wishes to consider a model with light scalar particles ($\sim$10GeV), the transition $s\bar{d} \to \phi \to \bar{s}d$ must be avoided as it will predict large ΔM for $K^\circ\bar{K}^\circ$ system. This can be achieved by, for example, coupling only ϕ_1 to down quarks and ϕ_2 to up quarks:

$$\phi^\circ = g^1_{ij}\, \bar{d}_{iL} d_{jR} v\, e^{i\alpha_1} + g^2_{ij} \bar{u}_{iL} u_{jR} v\, e^{i\alpha_2} + g^1_{ij}\, \bar{d}_{iL} d_{jR} H^\circ_1 + g^2_{ij} \bar{u}_{iL} u_{jR}\, H^\circ \quad (5)$$

where we have written $\phi_i{}^\circ = v e^{i\alpha_i} + H^\circ{}_i$. $g^1{}_{ij}$, and $g^2{}_{ij}$ are real as required by the condition for spontaneous CP violation, Eq.5 has two important consequences: (1) The phase in the mass matrix can be eliminated by the rotation $d_{jR} \to e^{-i\alpha_1} d_{jR}$, $u_{jR} \to e^{i\alpha_1} u_{jR}$. Thus the resulting KM mixing matrix is real. (2) The H° couplings to quarks are proportional to corresponding mass matrix. Thus in terms of mass eigenstates, H° coupling is diagonal $s\bar{d} \to \phi^\circ \to \bar{s}d$ transition is, therefore, avoided.

II. ε'/ε

Diagonalizing the mass matrix for the K°-$\bar{K}^\circ$ system we obtain in the Wu-Yang phase convention

$$\varepsilon = \frac{1}{\sqrt{2}} e^{+i\pi/4} \frac{\mathrm{Im}M_{12}}{\Delta M}$$

and

$$\varepsilon' = \frac{i}{\sqrt{2}} e^{i(\delta_2-\delta_o)} \frac{\mathrm{Im}A_2}{A_o} \tag{6}$$

where

$$2\mathrm{Re}M_{12} = \Delta M \tag{7}$$

Denoting

$$A_I e^{i\delta_I} = \langle (2\pi)_I | H | K^\circ \rangle \tag{8}$$

we note that

$$A_o = |A_o| e^{i\xi} \tag{9}$$

where the phase $e^{i\xi}$ arises from the complex KM angles in the coefficient of O_5 and O_6 operators responsible for the $\Delta I = 1/2$ transition. Rotating the phase $|K^\circ\rangle \to e^{-i\xi}|K^\circ\rangle$ to comply with the Wu-Yang phase convention, the expression for ε becomes[5]

$$\varepsilon = \frac{1}{2\sqrt{2}} e^{i\pi/4} \left[\frac{\mathrm{Im}\, M_{12}}{\mathrm{Re}\, M_{12}} + 2\xi \right] \tag{10}$$

and

$$\frac{\mathrm{Im}\, M_{12}}{\mathrm{Re}\, M_{12}} = (1-D) \frac{\mathrm{Im}(M_{12})_{SD}}{\mathrm{Re}(M_{12})_{SD}} + D \frac{\mathrm{Im}(M_{12})_{LD}}{\mathrm{Re}(M_{12})_{LD}} \tag{11}$$

where we have used the notation[6]

$$M_{12} = (M_{12})_{SD} + D(M_{12})_{LD}$$

$$\text{and } (M_{12})_{LD} = D\, M_{12}. \tag{12}$$

It has long been assumed that the long distance contribution $(M_{12})_{LD}$ was real in the Wu-Yang phase convention, i.e. had a phase -2ξ in the perturbation expansion with the KM matrix. We parametrize the deviation from this by introducing an extra parameter[7] κ:

$$\mathrm{Im}(M_{12})_{LD} = (-2\xi + \kappa)\, \mathrm{Re}(M_{12})_{LD}$$

and obtain

$$\varepsilon = \frac{1-D}{2\sqrt{2}} e^{i\pi/4}\left\{ \varepsilon_m + 2\xi + \frac{D}{1-D} \kappa\right\}, \qquad (14)$$

where $\varepsilon_m = \dfrac{\mathrm{Im}(M_{12})_{SD}}{\mathrm{Re}(M_{12})_{SD}}$.

The value of ε' is not affected by these considerations. Performing the phase rotation explained above (9), we obtain

$$\frac{\varepsilon'}{\varepsilon} = -e^{i(\pi/4 + \delta_2 - \delta_o)} \frac{2\xi}{20\ (1-D)\left[\varepsilon_m + 2\xi + \frac{D\kappa}{1-D}\right]} \qquad (15)$$

III. Prediction:

In the Higgs model, the dominant contribution to $\mathrm{Im}M_{12}$ and ImA° comes from Figs 2a, and 2b, respectively.

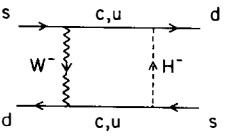

a

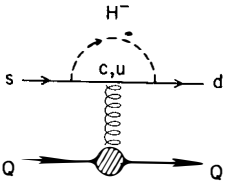

b

FIG. 2.

These interactions have been computed and the matrix elements were estimated using VSA with a result[2]

$$\varepsilon/\varepsilon m \gg 1. \qquad (16)$$

This result was subsequently checked by replacing VSA by the MIT bag model for matrix element evaluation[9]. With Eq. 13, Eq. 1 naturally follows from Eq. 15 if $D \simeq 0$ and $\kappa \simeq 0$. Dupont and Pham has raised an objection to using VSA in evaluating the matrix element depicted in Fig.2b. they point out that the effective hamiltonian from Fig 2b has the transformation property

$$H \sim (8,1) + e^{i\zeta}(3,3)$$

under chiral SU(3) x SU(3). Furthermore, the matrix element $\langle K^\circ \left| (3,3) \right| \pi^\circ \rangle$ vanish in the symmetry limit. Perturbation expansion in the symmetry breaking parameter should lead to a result for $\langle K^\circ \left| (3,3) \right| \pi^\circ \rangle$ which is considerably smaller than that obtained

using the VSA. At present, convergence of such expansion for the matrix element under consideration has not been verified. In fact there are some examples of matrix elements for which the chiral perturbation expansion diverge.[11] It may be that the result obtained by summing the chiral perturbation expansion is closer to the result of heuristic VSA than to its leading term.

For now, however, I shall stick to the contention of Donoghue and Holstein[12] who emphasized the point made by Dupont and Pham and estimated ε'/ε taking into account of the suppression factor for $\langle K^\circ \left| (3,3) \right| \pi^\circ \rangle$. They estimate

$$\langle K^\circ \left| (3,3) \right| \pi^\circ \text{ or } \eta_8 \rangle \approx \langle K^\circ \left| (8,1) \right| \pi^\circ \text{ or } \eta_8 \rangle \times \left(\frac{M_k}{\Lambda} \right)^2 \qquad (17)$$

$$\langle K^\circ \left| (3,3) \right| \eta_o \rangle \quad \approx \quad \langle K^\circ \left| (8,1) \right| \eta_o \rangle$$

where η_8 and η_o are octect and singlet component of η, respectively. The factor $(M_k/\Lambda)^2$ where $\Lambda = 1\text{GeV}$ is introduced in order to have an expression which vanishs in the chiral limit. In spite of the suppression factor in Eq. (17) which decreases previous estimate of ξ by the factor $(M_k/\Lambda)^2$, ε_m in Eq. 15 does not play an important role in reducing the value for ε'/ε. Note, however that Eq. 17 leads to

$$\text{Im}(M_{12})_{\eta_o} \gg \text{Im}\,(M_{12})_{2\pi,\ \pi^\circ,\ \eta_8} \qquad (18)$$

while the same can not be said for the real parts. Donoghue and Holstein claims that η_o contribution to $(M_{12})_{LD}$ leads to a sufficiently large κ so that

$$\varepsilon'/\varepsilon \approx -.006$$

with about a factor of 3 error in both directions. Frère, Hagelin and I have studied the same effect while we were in Moriond last year.[7] Our result is

$$\left| \varepsilon'/\varepsilon \right| \approx .016 \qquad (19)$$

with about a factor of 3 error in both directions.

The difference in our result and that of Ref. 12 is that they have identified η_o with $\eta'(958)$ and ignored η-η' mixing.

IV. Conclusion.

The vacuum saturation approximation leads to a clean prediction, Eq.(1). With this assumption the model with spontaneous CP violation and natural flavor conservation is ruled out. The vacuum saturation approximation, however, is not consistent with the constraints from chiral SU(3) x SU(3) symmetry. It may be that when

chiral perturbation series is summed, the heuristic vacuum saturation result may be recovered. Within the framework of chiral perturbation theory, ε'/ε turns out to be anywhere from $.002 \sim .045$. There is no prediction. It is however a viable warning against accepting the conclusion drawn from the analysis using vacuum saturation approximation. It is extremely important to understand the predictions and limitations of chiral perturbation theory in the K meson systems.

References and Footnotes

1. G.C. Branco and A.I. Sanda, Phys. Rev. D26, 3176 (1982).
2. A.I. Sanda, Phys. Rev. D23, 2647(1981);
   N.G. Despande Phys. Rev. D23,2654 (1981).
3. For the result of both experiments, see K. Nishikawa, lecture given in XXII International Conference in High Energy Physics, Leipzig, 1984 edited by A. Meyer and E. Wieczorek.
4. S. Weinberg, Phys. Rev. Lett. 31, 657(1976);
   G.C. Branco, Phys. Rev. Lett. 44, 504 (1980).
5. F. Gilman and M.B. Wise, Phys. Lett. 83B, 83(1979).
6. L. Wolfenstein, Nucl. Phys. B160, 501 (1979);
   C.T. Hill, Phys. Lett. 97B, 275 (1980).
7. J.M. Frere, J. Hagelin, and A.I. Sanda, Phys. Lett. 151B, 161(1985).
8. D. Chang, Phys. Rev. D25, 1318 (1982) has discussed a possibiity that D is large and negative.
   The value of $D<-2$ needed seems to be ruled out. I. Bigi and A.I. Sanda, Phys. Lett. 148B, 205 (1984) M.R. Pennington DTP/85/2 preprint used more recent $\pi\pi$ phase shift to obtain 2π contribution to $D_{2\pi} = .46 + .13$.
9. J.F. Donoghue, J. Hagelin, and B.R. Holstein, Phys. Rev. D25, 195 (1982).
10. Y. Dupont and T.N. Pham Phys. Rev. D28, 2169, (1983).
11. J. Bijnens, H. Sonoda and M.B. Wise, Calt. 68-1193.
12. J.F. Donoghue and B.R. Holstein, UMHEP - 213.

ε'/ε IN THE HIGGS BOSON EXCHANGE MODEL OF CP VIOLATION

T.N. PHAM

Centre de Physique Théorique* de l'Ecole Polytechnique
Plateau de Palaiseau - 91128 Palaiseau - Cedex - France

ABSTRACT

Recent analyses of ε'/ε in the Higgs boson exchange model of CP violation is reviewed and discussed. In this model, $SU(3) \times SU(3)$ chiral symmetry suppresses the direct CP violating $K_L \to 2\pi$ amplitude but not the $K^o - \bar{K}^o$ mass matrix which gets most of the contribution from the η' - pole and higher intermediate states. This reduces considerably previous estimates of ε'/ε which could still be made compatible with present data barring strong cancellations between various dispersive contributions.

* Laboratoire Propre du CNRS n° 14

The physics of the Higgs model of CP violation [1] has been discussed by several authors [2-6] in the past. Recently there has been attempt to make a better estimate of ε'/ε in this model. In this talk, I would like to discuss a new estimate of ε'/ε by Donoghue and Holstein [7]. I shall put particular emphasis on the constraints imposed on the $K_L \to 2\pi$ amplitude by Current Algebra and chiral symmetry which play an important role in our understanding of the physics of K decays. This has been overlooked in the past and has only been stressed recently beginning with the works of Dupont and myself [5,8]. It turns out that, in the Higgs model, the direct CP violating $K_L \to 2\pi$ decay is suppressed relative to the $K^o - \bar{K}^o$ transition so that ε'/ε can be considerably smaller than previous estimates unless there are cancellations between various contributions to the $K^o - \bar{K}^o$ mass matrix. As details of the model are given by Sanda in the preceding talk, I shall concentrate on the physics of CP violation in K decays. Following standard analysis [9], we have

$$\frac{\varepsilon'}{\varepsilon} = -\left(\frac{1}{20}\right) \frac{2\xi}{\varepsilon_m + 2\xi} \tag{1}$$

where

$$\varepsilon_m = \frac{\mathrm{Im} < K^o | \mathcal{L}_w | \bar{K}^o >}{\mathrm{Re} < K^o | \mathcal{L}_w | \bar{K}^o >} \tag{2}$$

$$\xi = \frac{\mathrm{Im} < \pi\pi(I=0) | \mathcal{L}_w | K^o >}{\mathrm{Re} < \pi\pi(I=0) | \mathcal{L}_w | K^o >} \tag{3}$$

The ratio ε_m/ξ is a measure of the importance of the transition mass matrix relative to the direct interactions. The new measurements of ε'/ε at Fermilab reported here by the Chicago-Saclay and by the Brookhaven-Yale groups give respectively

$$\begin{aligned} \varepsilon'/\varepsilon &= -0.0046 \pm 0.0053 \\ &= +0.0017 \pm 0.0084 \end{aligned} \tag{4}$$

which implies a very small value for ξ/ε_m and tells us that CP-violating effects are almost exclusively due to the $\Delta S = 2$ $K_S - K_L$ transition. We seem to be closer than ever to the super weak model [10]. On the other hand both the Kobayashi-Maskawa (KM) model [11] and the Higgs model predict a nonvanishing value for ε'/ε, the latter however qualitatively produces a larger ε'/ε than the KM model. Before getting to the Higgs model, it is useful to note that the estimate of

ε'/ε in the KM model is also subjected to large uncertainties, mostly due to lack of a correct explanation for the $\Delta I = \frac{1}{2}$ rule in nonleptonic K decays and the KM model could be in difficulty as discussed by Sutherland at this meeting.

In the Higgs model, the main contribution to the CP violating $K^o - \bar{K}^o$ transition comes from the dispersive part[5] (the so-called long distance part), the short-distance part or the box diagram makes only a small contribution to ε_m/ξ as found[2] by Deshpande and Sanda and subsequently by Donghue, Hagelin and Holstein[3]. The dispersive part is given by

$$<K^o|i\mathcal{L}_w|\bar{K}^o> = (i)^2 \int d^4x <K^o|T\{\mathcal{L}_w(x)\mathcal{L}_w(o)\}|\bar{K}^o> \tag{5}$$

Expanding (5) in terms of intermediate states we have [4, 5, 12]

$$\mathrm{Im}<K^o|\mathcal{L}_-^{\Delta S=2}|\bar{K}^o> = \mathrm{Im} \sum_n \frac{<K^o|\mathcal{L}_-^{\Delta S=1}|n><n|\mathcal{L}_+^{\Delta S=1}|\bar{K}^o>}{m_K^2 - m_n^2} \tag{6}$$

where n runs over the single particle intermediate states $(\pi^o, \eta, \eta'$ etc...) as well as the $(2\pi, 3\pi)$ continuum. We see immediately from (6) that ε_m/ξ is of the order O(1). The Higgs model is then clearly not of the superweak theories and qualitatively, seems to be incompatible with experiment. However a careful estimate shows that the π^o, η, η' terms make a large contribution to ε_m/ξ as pointed out by Dupont and myself[5]. More recently, Donoghue and Holstein[7] have reanalysed ε'/ε and showed that the real source of enhancement for ε_m/ξ is the suppression of the CP-violating $K \to 2\pi$ in the chiral symmetry limit and ε'/ε can be made compatible with data for $\varepsilon_m/\xi \sim 5 - 10$. To show this, notice that the CP violating $\Delta S=1$ Penguin transition operator is of the form[2,3]

$$\mathcal{L}_-^{\Delta S=1} = i\tilde{f}\,\bar{d}_R \sigma_{\mu\nu} \lambda_a s_L F^a_{\mu\nu} \tag{7}$$

($\tilde{f}$ is the strength of the $s \to d +$ gluon transition and $F^a_{\mu\nu}$ is the gluon field strength tensor) which is a left-right operator and transforms as a $(3,\bar{3})$ representation under $SU(3) \times SU(3)$. As pointed but by Dupont and myself, the matrix element of $\mathcal{L}_-^{\Delta S=1}$ have a momentum independent piece which behaves as the usual meson mass term and can be diagonalised away[5]. From an effective Lagrangian stand point, they are given as

$$\begin{aligned} u_7' &= \mathrm{Tr}[\lambda_7(M + M^+)] \\ v_6' &= \mathrm{Tr}[\lambda_6(M - M^+)] \end{aligned} \tag{8}$$

in the standard non-linear realization of chiral symmetry. M takes the exponential form [13]

$$M = \exp(2if\phi) \ , \quad f = f_\pi^{-1} \ , \quad f_\pi \simeq m_\pi \ .$$

$$(\phi = \sum_i \lambda_i \frac{\phi_i}{\sqrt{2}})$$

u_7' and v_6' are proportional to the divergences of the vector and axial vector currents and are changes of the strong interaction Lagrangian induced by a small $SU(3) \times SU(3)$ rotation. Hence by the same rotation these momentum independent $(3,\bar{3})$ terms can be eliminated without affecting other terms by any appreciable amount [14].

Thus the $K \to 2\pi$, $K - \pi$ and $K - \eta$ transitions vanish in the chiral symmetry limit. Explicit calculation shows that cancellations indeed occur [7]. For example in the $K \to 2\pi$ amplitude, the direct term v_6' is cancelled by a $\Delta S=1$ term induced by the chiral invariant $K \to \pi\pi K$ transition followed by a $K \to$ vacuum amplitude which comes also from v_6' .

However the matrix elements of $\mathcal{L}_-^{\Delta S=1}$ can also have a momentum dependent part given by [7,15]

$$\mathcal{L}_-^{\Delta S=1} = \frac{a}{\Lambda^2} \mathrm{Tr}[(\lambda_6 + i\lambda_7) M \partial_\mu M \partial_\mu M^+] \qquad (9)$$

which cannot be rotated away and give rise to $K \to 2\pi$ amplitudes of the order $O(k^2/\Lambda^2)$ relative to the momentum independent terms. The suppression of the $K \to 2\pi$ amplitudes well as the $K^o - \pi^o$ and $K^o - \eta$ transition leaves the η'-pole and higher intermediate states (σ , S^* etc...) as the dominant contribution to the dispersive part of the $K^o - \bar{K}^o$ transition. In particular the $K^o - \eta'$ transition can be written as

$$\mathcal{L}_{K^o\eta'} = a\phi_{\eta'} \mathrm{Tr}[(\lambda_6 + i\lambda_7) M] \qquad (10)$$

which cannot be rotated away and give a $K^o\eta'$ mixing much larger than the $K_L \to 2\pi$ amplitude. Hence

$$\frac{\xi}{\varepsilon_m} \sim O(k^2/\Lambda^2)$$

A quantitative estimate for ξ/ε_m is more difficult. However if we

assume that $\Lambda \simeq 1\text{GeV}$ as in the case of the derivative coupling $(3,\bar{3})$ mass term[15] for SU(3) breaking effects in f_K/f_π, then a rough estimate by Donoghue and Holstein gives[7]

$$\frac{\varepsilon'}{\varepsilon} \simeq -0.006 \tag{11}$$

which is still consistent with present data.

If we now include $\eta-\eta'$ mixing and other SU(3) violation effects in the $K^o-\pi^o$ and $K^o-\eta$ mixing, then the π^o,η and η' pole terms tend to cancel out resulting in a small value for ε_m. The extent of this cancellation depends on the way various SU(3) breaking effects are handled. If such a cancellation does occur then higher intermediate states (e.g. $S^*,\delta,\varepsilon,\kappa$, etc...) must be included. These contributions, like the η'-pole terms, do not vanish in the chiral symmetry limit and could give a large contribution to ε_m in the same way as the η'-pole terms. In any case ε_m/ξ can be large. Because of the large theoretical uncertainties, it is too early to rule out the Higgs model at the moment but the situation may change with a more precise measurement of ε'/ε in the near future.

I thank A. Sanda, D.G. Sutherland, L. Wolfenstein for useful discussions ; L. Oliver, Tran thanh Van and the organizers of this workshop for the warm hospitality at Moriond.

REFERENCES

[1] S. Weinberg, Phys. Rev. Lett. 37,657(1976).
T.D. Lee, Phys. Rev. D8, 1226(1973).
[2] N. Deshpande, Phys. Rev. D23,2654(1981).
A. Sanda, Phys. Rev. D23,2647(1981).
[3] J.F. Donoghue, J. Hagelin and B.R. Holstein, Phys. Rev. D25,195(1982).
[4] D. Chang, Phys. Rev. D25,1318(1982).
[5] Y. Dupont and T.N. Pham, Phys. Rev. D28,2169(1983).
[6] J. Hagelin, Phys. Lett. 117B,441(1982).
[7] J.F. Donoghue and B.R. Holstein, Amherst preprint UMHEP-213(1984).
[8] Y. Dupont and T.N. Pham, Phys. Rev. D29,1369(1984).
[9] F.J. Gilman and M.B. Wise, Phys. Rev. D20, 2392(1979).
[10] L. Wolfenstein, Phys. Rev. Lett. 13,180(1964).
[11] M. Kobayashi and T. Maskawa, Prog. Theor. Phys. 49,652(1973).
[12] L. Wolfenstein, Nucl. Phys. B160,501(1979).
C. Hill, Phys. Lett. 97B,275(1980).
[13] J. Cronin, Phys. Rev. 161,1483(1967).
S. Coleman, J. Wess and B. Zumino, Phys. Rev. 177,2239(1969).
[14] S. Coleman and S.L. Glashow, Phys. Rev. 134,B671(1964).
[15] T.N. Pham, Phys. Rev. D30,234(1984).

ε'/ε IN A MODEL WITH SPONTANEOUS P AND CP VIOLATION*

G. Ecker and W. Grimus
Institut für Theoretische Physik
Universität Wien
(presented by G. Ecker)

ABSTRACT

ε'/ε, the $K_L K_S$ mass difference and the neutron electric dipole moment are calculated in a minimal left-right symmetric gauge model. A distinctive feature of the model are the constraints on quark masses and mixing angles implied by CP invariance of the Lagrangian. For M_{W_2} in the several TeV range the model satisfies all experimental constraints. ε'/ε may be negative and is found to be less than 10^{-2} in absolute magnitude.

*) Partially supported by "Fonds zur Förderung der wissenschaftlichen Forschung", Project Nr. 5444.

I. CP Violation in the Standard Model

In order to motivate our work[1] let me summarize very briefly the theoretical and phenomenological status of CP violation in the standard model with three fermion generations.

The mechanism of breaking CP explicitly via complex Yukawa couplings provides a possible parametrization, but not a fundamental understanding of CP violation. The situation is much improved in models with spontaneous CP violation where both the gauge symmetry breaking and CP violation have a common origin. In addition, such a scenario is almost unavoidable[2] if the Higgs fields are envisaged as composite fields in an underlying purely fermionic gauge theory.

To implement spontaneous CP violation the scalar sector must be enlarged beyond the single Higgs doublet of the standard model. Moreover, if we insist on spontaneous P violation as well we also need a larger gauge group, the minimal extension[3] being $SU(2)_L \times SU(2)_R \times U(1)$.

Much of the current theoretical activity in this field is due to two recent measurements of ε'/ε:

$$\varepsilon'/\varepsilon = \begin{cases} (-4.6 \pm 5.3 \pm 2.4)\cdot 10^{-3} & \text{Chicago-Saclay}^{4} \\ (1.7 \pm 8.4)\cdot 10^{-3} & \text{BNL-Yale}^{5}. \end{cases}$$

Using the constraints on weak mixing angles implied by the measured bottom lifetime and the upper bound on the semileptonic branching ratio $\bar{R} = \Gamma(b \to ue\nu)/\Gamma(b \to ce\nu)$ one finds[6] that the standard six-quark model is still compatible with experiment. However, with only a little imagination the following two possible problems for the standard model may be foreseen:

i) ε problem: even allowing for reasonable long-distance contributions ε comes out too small for $m_t \leq 50$ GeV and $\bar{R} < 0.01$.

ii) ε'/ε problem: the standard model predicts[6] a positive lower bound $\varepsilon'/\varepsilon \gtrsim 0.002$.

II. Spontaneous CP Violation in Left-Right Symmetric Models

Gauge models based on $SU(2)_L \times SU(2)_R \times U(1)$ have the attractive feature[3] of allowing for spontaneous P and CP violation already with a minimal Higgs sector consisting of a single scalar multiplet

$$\Phi = \begin{pmatrix} \Phi_1^0 & \Phi_2^+ \\ \Phi_1^- & \Phi_2^0 \end{pmatrix} \quad \begin{matrix} \downarrow SU(2)_L \\ \leftarrow SU(2)_R \end{matrix} \qquad (1)$$

coupling to quarks. CP violation is due to the Higgs phase $\alpha = \arg(\langle\Phi_1^0\rangle_0 \langle\Phi_2^0\rangle_0)$.

From a complete classification[7] of P and CP invariant Yukawa interactions

$$-\mathcal{L}_Y = \bar{q}_L \Gamma \Phi q_R + \bar{q}_L \Delta \tilde{\Phi} q_R + \text{h.c.}$$
$$\tilde{\Phi} = \tau_2 \Phi^* \tau_2 \qquad (2)$$

for three generations one concludes that P invariance implies hermitian Yukawa coupling matrices Γ, Δ with a certain choice of phases whereas the additional requirement of CP invariance leads to the following two cases.

a) Manifest CP: Γ, Δ are symmetric so that the left- and right-handed mixing matrices may be chosen to obey $K_R = K_L^*$, but there are no further constraints on the quark mass matrices. A general analysis of CP violation in such models can be performed in the small-phase (α) approximation.[8]

b) Non-manifest CP: The concept[7] of non-aligned P and CP transformations allows for a single additional model with coupling matrices

$$\Gamma = \text{diag}(g_1, g_2, g_3) \qquad \Delta = i \begin{pmatrix} 0 & h_1 & h_2 \\ -h_1 & 0 & h_3 \\ -h_2 & -h_3 & 0 \end{pmatrix} . \qquad (3)$$

g_i, h_i real

In the following, only this specific model will be considered which possesses the distinctive property that P and CP invariance alone give rise to the following constraints[1),7)] for quark masses and mixing angles.

i) $$s_1^2 \simeq \frac{m_d}{m_s}\left(1 \pm s_3^2 \frac{m_b}{m_s}\right) \simeq \frac{m_d}{m_s} . \qquad (4)$$

ii) $K_R \neq K_L^*$ except for $h_2 = 0$ which corresponds to the unique model from horizontal symmetries.[9]

iii) $$\left|\frac{m_s}{m_b} - \frac{m_c}{m_t}\right| \lesssim |K_{L,cb}|^2 \leq 4 \cdot 10^{-3} \qquad (5)$$

implying $m_t \simeq m_b m_c / m_s$. This approximate relation is due to the small mixing parameters s_2, s_3 in contrast to the much bigger s_1 which allows for

$m_c \gg m_s m_u / m_d$.

iv) The left-right mixing angle ξ_{LR} is determined as

$$\xi_{LR} \simeq \frac{2m_b}{m_t} \frac{M_{W_1}^2}{M_{W_2}^2} \simeq 2 \cdot 10^{-3} \, (M_{W_2}/\text{TeV})^{-2} \, . \qquad (6)$$

We have performed detailed calculations of the effective $|\Delta S| = 1,2$ interactions including QCD corrections (for previous work cf. Ref. 1). The QCD corrections turn out to enhance the effective weak Hamiltonians and they are larger than in the standard model for two reasons: four-quark operators with bigger anomalous dimensions are involved and there are larger masses (M_{W_2}, M_{Higgs}) in the theory. For the numerical calculations we take $\Lambda_{\overline{MS}} = 200$ MeV for four flavours. To evaluate quark operator matrix elements between hadronic states the vacuum insertion technique is used throughout.

Turning first to $|\Delta S| = 2$, one finds in contrast to the standard model a tree-level contribution induced by neutral Higgs exchange. In the minimal model under consideration the Higgs couplings are uniquely specified in terms of quark masses and mixing angles and only the Higgs mass M_H enters as an additional free parameter. At the one loop level, the effective $|\Delta S| = 2$ interaction is dominated by the usual box diagrams with left- and right-handed gauge bosons and with Higgs bosons being exchanged.

The real part of the $|\Delta S| = 2$ $K^0\bar{K}^0$ transition amplitude determines the $K_L K_S$ mass difference Δm_{LS}. Unlike in the case of manifest left-right symmetry[3] with $K_L = K_R$, the genuine left-right contributions to Δm_{LS} have the same sign as Δm_{LS}^{EXP} and therefore increase the standard model prediction. Keeping in mind possible long-distance contributions we require $\Delta m_{LS}^{THEORY} \leq 2 \cdot \Delta m_{LS}^{EXP}$ leading to the lower bounds

$$M_{W_2} \geq 2.2 \text{ TeV} \, , \qquad M_H \geq 8.6 \text{ TeV} \, . \qquad (7)$$

The $|\Delta S| = 1$ effective Hamiltonian is mainly determined by W_1 and W_2 exchange and QCD corrections must again be included. The dominant contributions are proportional to the left-right mixing angle ξ_{LR}.

To calculate ε, ε' we fix $m_t(m_t) = 35$ GeV and consider three values of the free parameter $p := h_2/h_1$ corresponding to $\bar{R} \lesssim 10^{-4}$ ($p = 0$) and $\bar{R} \simeq 0.005$ ($|p| = 1/2$). For such small values of $\bar{R}$ the standard model mechanism is clearly insufficient to explain CP violation. For given M_{W_2}, M_H we determine the allowed values of the Higgs phase α which yield $\varepsilon_{THEORY} = \varepsilon_{EXP} \pm 30\%$ to account again for possible long-distance contributions to ε. For such α we then calculate both ε'/ε and the neutron electric dipole moment d_n including both[10] one-loop and

exchange contributions to d_n. Typical results are displayed in Figs. 1, 2 with M_H = 15 TeV. The absolute values for ε'/ε and d_n increase somewhat with M_H but the limiting values for $M_H \to \infty$ are not too much different from the ones shown in the figures.

III. Conclusions

The following conclusions apply a priori only to the specific model (3), but as far as the CP violating aspects are concerned they remain true for a generic minimal left-right symmetric model with spontaneous CP violation.

1) Left-right symmetry provides an attractive scenario for CP violation.
2) Spontaneous P and CP violation may imply constrained quark mass matrices.
3) Left-right contributions enhance the standard model value for Δm_{LS} in the specific model under consideration.
4) In contrast to the standard model, the correct value of ε can be obtained even with $m_t < 50$ GeV, $\bar{R} < 0.01$ if M_{W_2} is in the several TeV range.
5) ε'/ε may have either sign and $|\varepsilon'/\varepsilon| < 10^{-2}$.
6) The neutron electric dipole moment satisfies the experimental upper bound[11] $4 \cdot 10^{-25}$ e.cm, but it may reach the same order of magnitude.

References

1) G. Ecker and W. Grimus, Univ. Wien preprint UWThPh-1984-47 (Dec. 1984), to appear in Phys. Lett. B.
2) A. Masiero, R.N. Mohapatra and R.D. Peccei, Nucl. Phys. B192 (1981) 66.
3) R.N. Mohapatra and G. Senjanović, Phys. Rev. Lett. 40 (1980) 912; Phys. Rev. D23 (1981) 165.
4) B. Peyaud, these Proceedings.
5) M. Schmidt, these Proceedings.
6) e.g., E. Paschos, these Proceedings.
7) G. Ecker, W. Grimus and H. Neufeld, Nucl. Phys. B247 (1984) 70.
8) D. Chang, Nucl. Phys. B214 (1983) 435;
   G. Ecker and W. Grimus, in preparation.
9) G. Ecker, W. Grimus and W. Konetschny, Phys. Lett. 94B (1980) 381; Nucl. Phys. B177 (1981) 489.
10) G. Ecker, W. Grimus and H. Neufeld, Nucl. Phys. B229 (1983) 421.
11) P. Miranda, these Proceedings.

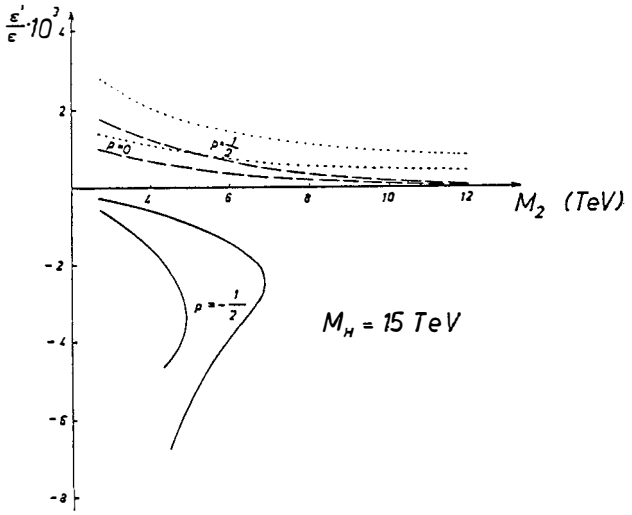

Fig. 1: Allowed domains for ε'/ε as functions of M_{W_2} with M_H = 15 TeV for the three values of the parameter p: p = 0 (dashed curves), p = 1/2 (dotted curves) and p = - 1/2 (full curves).

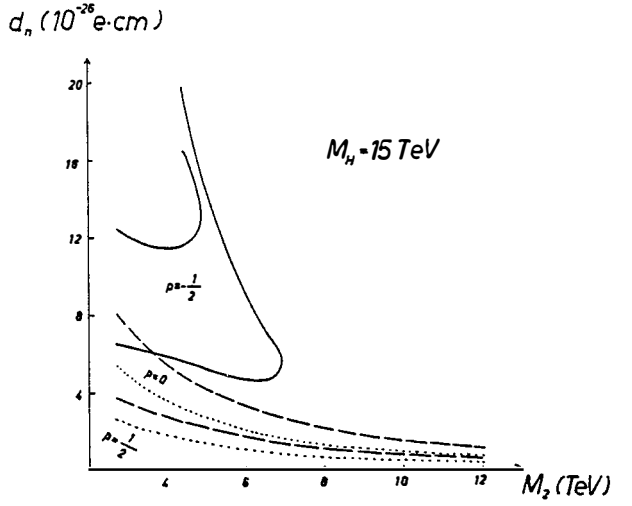

Fig. 2: Allowed domains for d_n (notations as in Fig. 1).

CP-Violation and Left-Right Symmetry[†]

Rabindra N. Mohapatra
Department of Physics and Astronomy
University of Maryland
College Park, MD 20742

ABSTRACT

We show that in the left-right symmetric models of CP-violation with 3 generations, ϵ' vanishes in the limit of the Kobayashi-Maskawa angle $s_3 = 0$ and W_L-W_R mixing $\zeta = 0$. This model would appear to be better suited for the description of CP-violating phenomena, if the upper limits on the branching ratio for $b \to ue\bar{\nu}$ (which is proportional to s_3^2) as well as ϵ'/ϵ keeps getting smaller.

[†]Work supported by the National Science Foundation Grant No. PHY-82-18338.

1. Introduction

Even though the phenomenon of CP-violation was discovered nearly twenty years ago, its origin remains a mystery. With the advent of gauge theories, it was realized that for two generations of quarks and leptons, the V-A gauge interactions are always CP-conserving.[1,2] In ref. 1 and 3 it was proposed that the CP-violation may have its origin in yet unobserved new physics such as possible right-handed weak currents. On the other hand, Kobayashi and Maskawa[2] proposed that the V-A gauge interactions can accomodate CP-non-conservation for three generations of quarks and leptons. The Kobayashi-Maskawa model, has become the focus of a great deal of theoretical activities, following the discovery of the b-quark and the τ-lepton, that indicated the existence of the third generation.

The KM model is described by the following Lagrangian:

$$\mathcal{L}_{WK} = \frac{ig}{\sqrt{2}} W^{+}_{\mu} \bar{P}_L \gamma_\mu U_{KM} N_L + h.c. \tag{1}$$

where P = (u,c,t,...) and N = (d,s,b,...) and

$$U_{KM} = \begin{pmatrix} c_1 & -s_1c_3 & -s_1s_3 \\ s_1c_2 & c_1c_2c_3 - s_2s_3e^{i\delta} & c_1c_2s_3 + s_2c_3e^{i\delta} \\ s_1s_2 & c_1s_2c_3 + c_2s_3e^{i\delta} & c_1s_2s_3 - c_2c_3e^{i\delta} \end{pmatrix} \tag{2}$$

with $s_i = \sin\theta_i$ and $c_i = \cos\theta_i$. Of the three angles the first one, θ_1 is the Cabibbo angle and is determined to be .229. The recent results on the b-quark lifetime and decays[4] have implied considerable restriction on the other angles θ_2 and θ_3 . More quantitatively,[5] one finds.

$$s_2^2 + s_3^2 + 2s_2s_3c_\delta \approx 4\times10^{-3}\left(\frac{10^{-12}\,\text{sec.}}{\tau_b}\right)B(b\to c)$$

$$\approx 3 \times 10^{-3}(10^{-12}\,\text{sec.}/\tau_b) \tag{3}$$

and

$$s_3^2 \approx 4 \times 10^{-2}(10^{-12}\ \text{sec.}/\tau_b)\cdot B(b \to u)$$

$$\leq 10^{-3}\ (10^{-12}\text{sec.}/\tau_b)\ . \tag{4}$$

Here we have used the experimental information that the ratio $r = B(b \to u)/B(b \to c)$ is less than 5%. The implications of eqn. (3) and (4) for CP-violation have been extensively studied in literature (for original references, see ref. 5). A consensus seems to be emerging that unless the $\Delta S = 2$ hadronic matrix element (the B-parameter) is large, the magnitude of the CP-violating parameter $\varepsilon(\varepsilon \simeq 2.3 \times 10^{-3})$, can not be understood for the s_3 parameter less than 1% (or $r < .01$). Thus, if r_{expt} gets smaller than 1% there must be new contributions to CP-violation in K^o-decays.

A second prediction of the KM model is that the ratio ε'/ε is bigger than[6] $(2\text{-}3) \times 10^{-3}$, although uncertainties exist here too. The most recent experimental search for ε'/ε has led to the result

$$\varepsilon'/\varepsilon = (-4.6 \pm 5.3 \pm 2.4) \times 10^{-3} \ . \qquad (5)$$

It is thus clear that, if experimental value of ε'/ε goes below 2×10^{-3} or so the KM model will be ruled out and other sources for CP-violation must be looked for. The reason for this lower bound on ε'/ε is the fact that in the K-M model both ε' and ε parameters owe their origin to a common source.

In this lecture, we argue that the left-right symmetric model of CP-violation provides a natural framework for accomodating arbitrarily small ε'/ε as well as a small value of the parameter r while at the same time explaining the magnitude of the ε-parameter. This happens because ε' and ε receive dominant contributions from different sources: ε arises from the right-handed currents whereas ε' owes its origin to the s_3-parameter of KM-model as well as the left-right mixing.[3,7] The model requires an upper bound on the W_R-mass of about 65 Tev.

2. CP-Violation and Left-Right Symmetry

It was suggested in ref. 3 that CP-violation is associated primarily with the V+A currents. This general idea has two immediate conceptual advantages:

(a) the smallness of CP-violating parameter ε, ε' , etc. gets related to the suppression of V+A currents, i.e.

$$\varepsilon, \varepsilon' \approx (m_{W_L}/m_{W_R})^2 \qquad (6)$$

thereby explaining why ε and ε' are small.

(b) The gauge interactions can be CP-violating even for two generatios of fermions. Thus, the magnitude of CP-violating is not dependent on the mixing angles of the third generation with the first two.

Furthermore, the sources of ε and ε' can be separated from each other.

Let us start our discussion by writing down the modified charge current interaction in the left-right symmetric models:

$$\mathcal{L}_{wk}^{LRS} = \frac{ig_L}{2\sqrt{2}} W^+_{\mu,L} \bar{P} \gamma_\mu (1+\gamma_5) U_{KM} N + \frac{ig_R}{2\sqrt{2}} W^+_{\mu,R} \bar{P} \gamma_\mu (1-\gamma_5) V N$$

$$+ \frac{1}{2} m^2_{W_R} \zeta W^+_{\mu_L} W^-_{\mu_R} + h.c. \qquad (7)$$

The appearance of the second and third terms in eqn. (7) are characteristic of the left-right synmmetric models and is due to the fact that under the gauge group, $SU(2)_L \times SU(2)_R \times U(1)_{B-L}$ the quarks and leptons are assigned to doublets in a left-right symmetric manner.[8,9] The third term that mixes the left and right gauge bosons arises when the Higgs mechanism generates mass for the fermions. The gauge couplings in (7) g_L and g_R are equal due to left-right symmetry.

We now discuss the question of phases in the mixing matrices U_{KM} and V. This counting has been carried out in the literature[10,11] and it depends on the structure of the quark mass matrices $M_{u,d}$. Two distinct cases arise from the constraints of left-right symmetry.

Case A. Hermitean Quark Mass matrices:

$$M_q = M_q^\dagger \qquad (8)$$

Since a hermitean mass matrix is diagonalized by unitary transformations, the mixing matrices of the left and right-handed sectors are identical and one obtains

$$U_{KM} = V \qquad (9)$$

This case is called manifest left-right symmetry.

Case B. Symmetric Quark Mass Matrices:

This arises in left-right-symmetric grandunified models such as SO(10) or from spontaneous CP-violation.[10] In this case

$$V = K_u U^*_{KM} K_d \tag{10}$$

where K_u and K_d are diagonal unitary matrices. Thus the real mixing angles are the same in the left and right-handed currents, which helps keep the number of real mixing parameters same as in the KM model. But due to the presence of $K_{u,d}$, it has more CP-violating phases than the KM model. For instance, for two generations, K_i's are 2 × 2 matrices and there are three non-trivial phases. For three generations, this number goes up to six.[12] It therefore follows from this that, even if the third generation was completely decoupled from the first and second, there would be CP-violation in weak interactions. In fact, the model of ref. 3 only used two generations of fermions, to generate CP-violation. In this lecture, we will discuss the model with three generations and study its properties. This model has six phases but we will see that if the left-right mixing term is neglected, there are only two of whom appear in the CP-violating $K^o \to 2\pi$ decay processes. Of them one is the KM phase δ, whose effect on ε and ε' are controlled by the KM mixing angles s_2 and s_3. If s_3 turns out to be smaller than 10^{-2} due to the fact that r becomes smaller than 10^{-2}, the effect of this phase on ε and ε' will be insignificant and then only one phase will govern the ε parameter in K^o decay.

To start our discussion, we write (in eqn. (7))

$$V = \begin{pmatrix} e^{i\alpha_1} & & \\ & e^{i\alpha_2} & \\ & & e^{-i(\alpha_1+\alpha_2)} \end{pmatrix} U^*_{KM} \begin{pmatrix} e^{i\beta_1} & & \\ & e^{i\beta_2} & \\ & & e^{-i(\beta_1+\beta_2)} \end{pmatrix} \tag{11}$$

and replace $\zeta \to \zeta e^{i\gamma}$. Thus, $\alpha_1, \alpha_2, \beta_1, \beta_2$, δ and γ are the six physical phases in question. We divide our general discussion of CP-violating effects into two parts. In the first part (sec. 3) we let $\zeta \to 0$ and in the second part, we take the nonvanishing ζ into account.

3. CP-Violation without Left-Right Mixing: ($\zeta = 0$)

The effective $\Delta S = 1$ Hamiltoninan receives two contributions: W_L, W_R exchange graphs shown in fig. 1 and Penguin diagrams involving both W_L and W_R bosons as shown in fig. 2. The first kind of contribution leads to a $\Delta S = 1$ Hamiltonian, $\mathcal{H}_W$.

$$\mathcal{H}_W = \frac{4G_F}{\sqrt{2}}\Big[\sum_{q=u,c,t}\lambda_q\{\bar{s}_L\gamma_\mu q_L\bar{q}_L\gamma_\mu d_L + \eta e^{i(\beta_1-\beta_2)}\bar{s}_R\gamma_\mu q_R\cdot\bar{q}_R\gamma_\mu d_R\}$$

$$\{-c_2s_1s_2s_3e^{-i\delta}(\bar{s}_L\gamma_\mu c_L\bar{c}_L\gamma_\mu d_L - \bar{s}_L\gamma_\mu t_L\bar{t}_L\gamma_\mu\delta_L) +$$

$$+ \eta e^{i(\beta_1-\beta_2)}c_2s_1s_2s_3e^{+i\delta}(\bar{s}_R\gamma_\mu c_R\bar{c}_R\gamma_\mu d_R - \bar{s}_R\gamma_\mu t_R\bar{t}_R\gamma_\mu d_R)\Big] \tag{12}$$

where $\lambda_u = -c_1s_1c_3$; $\lambda_c = +s_1c_2(c_1c_2c_3)$; $\lambda_t = +s_1s_2(c_2s_2c_3)$;

and $\eta = (m_{W_L}/m_{W_R})^2$. (13)

The penguin diagram contributions coming from fig. 2 give rise to the effective $\Delta S = 1$ Hamiltonian $\mathcal{H}_p$:

$$\mathcal{H}_p = \sqrt{2}\,G_F\,[\bar{u}\gamma_\mu\lambda^a u + \bar{d}\gamma_\mu\lambda^a d]\,\frac{\alpha_2(\mu)}{12\pi}$$

$$\times\Big[\{\bar{s}_L\gamma_\mu d_L + \eta e^{i(\beta_1-\beta_2)}\bar{s}_R\gamma_\mu d_R\}\sum_{q=u,c,t}\lambda_q \ell n\,\frac{m_q^2}{\mu^2}$$

$$+ c_2s_1s_2s_3\,\ell n\,m_c^2/m_t^2\,\{-e^{-i\delta}\bar{s}_L\gamma_\mu d_L + e^{i(\beta_1-\beta_2)+i\delta}\bar{s}_R\gamma_\mu d_R\}\Big] \tag{14}$$

If we separate each of $\mathcal{H}_w$ and $\mathcal{H}_p$ into two parts, denoting the parts in curly brackets in eqn. (12) and (13) by $\mathcal{H}_\omega^{(o)}$ and $\mathcal{H}_p^{(o)}$ and the remainder as $\mathcal{H}_w'$ and $\mathcal{H}_p'$, we can write the effective $\Delta s = 1$ weak Hamiltonian H_{wk} into two parts:

$$H_{wk} \equiv H_{wk} + H_p \equiv H_{wk}^{(o)} + H_{wk}' \tag{15}$$

where $H_{wk}^{(o)} = H_w^{(o)} + H_p^{(o)}$; $H_{wk}' = H_w' + H_p'$. (16)

Separating it into parity conserving and parity violating pieces denoted by $S^{(o)}$ and $P^{(o)}$, one can show that CP-conserving $S_+^{(o)}$ and $P_+^{(o)}$ CP-violating pieces $S_-^{(o)}$ and $P_-^{(o)}$ pieces satisfy the following relations:

$$[I_3, S_-^{(o)}] \simeq -i\sin(\beta_1-\beta_2) S_+^{(o)} \tag{17a}$$

and

$$[I_3, P_-^{(o)}] \simeq i\sin(\beta_1-\beta_2) P_+^{(o)} \tag{17b}$$

These relations were called Iso-conjugate relations[3] and imply special relations between the $\Delta I = 3/2$ and $\Delta I = 1/2$, $K^o \to 2\pi$ and 3π amplitudes. For our purpose, it suffices to note that, eqn. (17b) implies that,

$$\frac{\mathrm{Im}A_2}{\mathrm{Re}A_2} = \frac{\mathrm{Im}A_o}{\mathrm{Re}A_o} \,. \tag{18}$$

This leads to $\varepsilon' = 0$. This point was noted[3] to hold exactly in the case of two generations as is obvious from eqn. (12) and (14) by setting $s_3 = 0 = s_2$. Coming to the case of three generations, we note that if we set $s_3 = 0$, H_p' and H_w' vanish and eqn. (17b) holds and we get $\varepsilon' = 0$ (of course, in the limit of vanishing ζ) and yet the third generation is not fully decoupled. This, we believe, is an important new result; clearly, the third generation is not totally decoupled from the first two as is evidenced by the observed decay mode $b \to ce\bar{\nu}$; on the other hand, $b \to ue\bar{\nu}$ has not been observed yet. Therefore, it may very well be that s_3 is very small (even much less than 10^{-2}) in which case KM model will be inadequate to explain CP-violation. The left-right model then has just the right property to explain ε as we will see below. Let us proceed to the calculation of ε and ε'. To calculate ε, we need $\mathrm{Im}M_{12}$. The $\Delta S = 2$ effective operator receives contribution from W_LW_L, W_LW_R and W_RW_R as well as the neutral Higgs exchange diagrams. Neglecting the Higgs contributions and keeping terms to order η, we get[13]

$$\mathrm{Im}M_{12} = \frac{G_F^2}{12\pi^2} s_1^2 F_K^2 m_K m_c^2 B\Big[2s_2 s_3 s_\delta \Big\{-\eta_1 + \eta_2 K \frac{m_t^2}{m_c^2} + \eta_3 \ell n \frac{m_t^2}{m_c^2}\Big\} + 8\rho(m_{W_L}^2/m_{W_R}^2)(\beta_1-\beta_2)\{1 + \ell n\, x_c\} \times I_{LR}\Big] \tag{19}$$

where I_{LR} represents the QCD correction to the L-R box graph estimated to be[14] about 3 for $\Lambda_{QCD} \simeq 100$ Mev. ρ is defined by $\langle \bar{K}^o | \bar{s}_L d_R \bar{s}_R d_L | K^o \rangle = \rho \langle \bar{K}^o | \bar{s}_L \gamma_\mu d_L \bar{s}_L \gamma_\mu d_L | K^o \rangle$. We take a digression here to remark that, real part of M^{12} also receives a contribution from the box graph, which has opposite sign to the LL box graph

and must therefore be less than it in magnitude. This sets a lower bound[15] on the mass of the right-handed W_R-boson of about 2.8 Tev (after QCD effects are taken into account.

From eqn. (19), it follows that, if the mass of W_R is not too heavy, the second term can dominate under certain circumstances. For instance if $s_3 < .02$ corresponding to $B(b\to u)/B(b\to c) < 10^{-2}$, then even for $s_\delta \approx 1$, the first term can not account for the magnitude of ε-parameter if $B \approx 1/2$. In this case (letting $s_3 \approx 0$), we find, for $\rho B \approx 8$

$$\varepsilon \approx (1.4)10^3 \sin(\beta_1-\beta_2)(m_{W_L}/m_{W_R})^2 . \tag{20}$$

Two points are worth noting here: first that, as claimed earlier, $\varepsilon \to 0$ as $m_{W_R} \to \infty$ this relating P and CP-violation; secondly, for $\sin(\beta_2-\beta_1) \approx 1$, to explain ε, we must have $m_{W_R} < .78 \times 3\ 10\ m_{W_L} \approx 65$ Tev. This provides an upperbound on the mass of the W_R-boson.

Let us now proceed to the discussion of ε'. For this purpose, we need to calculate $\mathrm{Im}A_o/\mathrm{Re}A_o$ and $\mathrm{Im}A_2/\mathrm{Re}A_2$. This can be done by looking at eqn. (15), (16), (12) and (14) and we get, (assuming Penguin dominance for the real part)

$$\frac{\mathrm{Im}A_o}{\mathrm{Re}A_o} \approx \sin(\beta_1-\beta_2) + s_2 s_3 s_\delta \cdot \frac{\ell n\ m_c^2/m_t^2}{\ell n\ m_c^2/\mu^2 + s_2^2 \ell n\ m_t^2/\mu^2} f + O(\eta s_3) \tag{21}$$

$$\frac{\mathrm{Im}A_2}{\mathrm{Re}A_2} \approx \eta(\beta_1-\beta_2) . \tag{22}$$

where

$$f = \frac{\langle \pi\pi(I=0)\,|\,\bar{s}\gamma_\mu(1+\gamma_5)\lambda^a d \Sigma \bar{q}\gamma_\mu(1-\gamma_5)\lambda^a q\,|\,K^o\rangle}{\mathrm{Re}\langle \pi\pi(I=0)\,|\,H_{WK}^{(o)}\,|\,K\rangle}$$

This implies that, for $s_3 < .01$

$$\frac{\varepsilon'}{\varepsilon} \approx \frac{\omega\, s_2 s_3 s_\delta \cdot f \cdot \ell n(m_c^2/m_t^2)}{10^3 \sin(\beta_1-\beta_2)(m_{W_L}/m_{W_R})^2 \{\ell n\ m_c^2/\mu^2 + s_2^2 \ell n\ m_t^2/\mu^2\}} \tag{23}$$

It is clear that ε'/ε in this case can be of arbitrarily small magnitude and either sign (by adjusting sign of s_δ).

Thus, if ε'/ε continues to escape detection and the b-decay to u-quarks also is tiny, the left-right symnmetric models pro-

vides a more natural framework too explain the various CP-violation parameters without relying on unknown hadronic parameters nor long distance effects.

4. Effect of W_L-W_R mixing

So far in our discussion of CP-violation in left-right symmetric models, we ignored the effect of W_R-W_L mixing parameter ζ. This parameter is experimentally known to be small:[16] $\zeta \lesssim 10^{-2}$. Its effect on the $\Delta S = 2$ transition operator is small. We, therefore, focus on its effect on the $\Delta S = 1$ operator. In the presence of W_L-W_R mixing graphs as in fig. 4, the H_{WK} in eqn. (15) gets modified to the following form:

$$H_{WK} = H_{WK}^{(o)} + H'_{WK} + H_{WK,LR} \cdots \tag{24}$$

where

$$H_{WK,LR} = \frac{G_F \zeta}{\sqrt{2}} \sum_{a=u,c,t} e^{i\gamma} \bar{s}_R \gamma_\mu q_R \bar{q}_L \gamma_\mu d_L U_{qd} U_{qs} e^{i\sigma_q}$$

$$+ \text{ similar terms} \tag{25}$$

The Penguin diagram contributions in this case are negligible. The first thing to note is that $H_{WK,LR}$ does not satisfy the isoconjugate relations in eqn. (17). Therefore, it will make different contributions to $\mathrm{Im}A_o/\mathrm{Re}A_o$ and $\mathrm{Im}A_e/\mathrm{Re}A_2$ as follows:

$$\frac{\mathrm{Im}A_o}{\mathrm{Re}A_o} \simeq \eta(\beta_1-\beta_2) - \frac{s_2 s_3 s_\delta \ell n\, m_c^2/m_t^2 f + \zeta \sin(\gamma+\beta_1-\beta_2) g_o}{\ell n\, m_c^2/\mu^2 + s_2^2 \ell n\, m_t^2/\mu^2} \tag{26}$$

and $$\frac{\mathrm{Im}A_2}{\mathrm{Re}A_2} \simeq \eta(\beta_1-\beta_2) - \zeta \sin(\gamma+\beta_1-\beta_2) g_2 \tag{27}$$

where

$$g_I = \frac{\langle 2\pi' I | H_{WK,LR}^{PV} | K^o \rangle}{\langle 2\pi, I | H_{WK}^{(o),PV} + H_{WK,LR}^{PV} | K^o \rangle} \,. \tag{28}$$

From this, we find that

$$\frac{\epsilon'}{\epsilon} \simeq \omega \left\{ \frac{s_2 s_3 s_\delta f \ell n\, m_c^2/m_t^2 + \zeta \sin(\gamma+\beta_1-\beta_2) g_o}{\ell n\, m_c^2/\mu^2 + s_2^2 \ell n\, m_t^2/\mu^2} \right.$$

$$\left. -\zeta \sin(\gamma+\beta_1-\beta_2) g_2 \right\} / 10^3 \sin(\beta_1-\beta_2)\eta \,. \tag{29}$$

Several points are worth noting in this expression; first that even in the limit of $s_3 \to 0$, ε'/ε is non-vanishing and is proportional to ζ and we get:

$$\frac{\varepsilon'}{\varepsilon} \simeq \omega \cdot \frac{\zeta \sin(\gamma+\beta_1-\beta_2)}{\eta 10^3 \sin(\beta_1-\beta_2)} \, x \tag{30}$$

where x denotes the hadronic factors. If all phases are assumed to be of the same order, we expect $\varepsilon'/\varepsilon \simeq \omega\zeta \lesssim 5 \times 10^{-4}$ for x of order 1. This value can, however, be tuned down by arbitrary amount without effecting any other physics by "dialing" ζ to smaller values. In fact any sign can also be obtained for ε'/ε .

An important point to note here is that in the limit of $\zeta \to 0$, the electric dipole moment of the neutron has the same value as in the Kobayashi-Maskawa model and is extremely small, ($d_n^e \simeq 10^{-30}$ ecm). However, for $\zeta \neq 0$, new contributions of the type shown in fig. 5 to d_n^e arise.[3,7] These and the Higgs contributions have been extensively studied in ref. 17 and one finds for W_L-W_R mixing contribution:

$$d_n = \frac{G_F e}{3\sqrt{2}\pi^{3/2}} \zeta \, m_q \sin(\gamma+\beta_1-\beta_2)$$

$$\simeq 10^{-21} \zeta \sin(\gamma+\beta_1-\beta_2) \text{ ecm} . \tag{31}$$

From eqn. (34) and (36), we see that, for $s_3 = 0$,

$$10^{-20}\varepsilon' \simeq d_n(\text{in ecm}) \times h' \tag{32}$$

where h' is a hadronic factor of order 1 to 10. For the present upper limit on ε' of about 10^{-6}, we find, $d_n \lesssim (10^{-25}\text{-}10^{-26})$ ecm. Thus, ε' and d_n get linked to each other and could provide a test of this model of CP-violation.

5. Constraints of Spontaneous CP-Violation

It is known that in the left-right symmetric model with the minimal set of Higgs bosons,[18] i.e. triplets $\Delta_L(3,1,+2)$ + $\Delta_R(1,3,+2)$ and one mixed doublet $\phi(2,2,0)$, if the Lagrangian is assumed to be CP-conserving prior to spontaneous breakdown, then there can be a minimum where $\langle\phi\rangle_{diag} = (\kappa, \kappa' e^{i\alpha})$ which breaks CP-symmetry spontaneously. It has been shown by Chang[11] that, in this case all phases in the weak current, i.e. $\gamma, \alpha_1, \alpha_2, \beta_1, \beta_2$ and δ can be expressed in terms of this single phase α , making this

model more predictive. For instance, the KM phase δ is given by[11]

$$\delta \simeq r \sin\alpha \frac{m_c}{m_s}\left(\frac{s_2+s_3}{s_3}\right)\left\{1 + s_3(s_2+s_3)\frac{m_t}{m_c}\right\} . \qquad (33)$$

Since $\zeta \simeq r\eta$, ($\gamma = \mathcal{K}'/\mathcal{K}$) given ζ and η , r can be determined. All other phases (except γ) are also related in a similar manner to r sin α . The phase γ is directly proportional to α (i.e. $\gamma = \alpha$). In this case all CP-violating effects arise from the W_L-W_R mixing effect and leads to a lower bound on ε'/ε :

$$\frac{\varepsilon'}{\varepsilon} \simeq \omega\cdot x\cdot\frac{\zeta\sin(\gamma+\beta_1-\beta_2)}{10^3\eta\sin(\beta_1-\beta_2)} \simeq \omega x \frac{r\eta\sin\alpha}{10^3\eta r\sin\alpha f(m_c m_s)} \simeq \frac{\omega x}{10^3 f(m_c,m_s)} \qquad (34)$$

Using $f(m_c,m_s) \simeq \frac{m_c}{m_s} \simeq 10$ and $x \simeq 10$. There are also QCD enhancement effects in ε' of order 3 to 4 and putting all these together, we conclude that, we expect $\varepsilon'/\varepsilon \simeq 10^{-4}$ to 10^{-3}.

Another point of interest in this model is that, if we assume $r \ll 10^{-1}$, we expect the KM phase $\delta \ll 1$ in which case, ε is dominated completely by the right-handed contribution regardless of the magnitude of s_3.

6. Conclusion

In conclusion, two crucial tests for the KM model are: (a) discovery of $b \to ue\nu$ decay with $B(b\to ue\bar{\nu})/B(B\to ce\bar{\nu}) \geq .01$ and (b) a nonvanishing positive $\varepsilon'/\varepsilon \gtrsim 10^{-3}$. Both these are within the reach of current experiments. Should either of these predictions of KM model run into conflict with experiment, a viable alternative is provided by the left-right symmetric model with $m_{W_R} \leq 65$ Tev, with a small left-right mixing, ζ . ε'/ε is correlated with s_3 and ζ and could take either sign where ε is dominated by the right-handed current effects and goes down like $(m_{W_L}/m_{W_R})^2$. Observation of ε'/ε would then predict observable electric dipole moment of the neutron, which will constitute a test of the model.

I wish to thank D. Chang for many discussions on CP-violation.

Figure Captions

Fig. 1. Typical box graph contribution to $\Delta s = 2$ matrix element in gauge theories.

Fig. 2. Tree level Feynman diagram involving $W_{L,R}$ exchange that contributes to $\Delta s = 1$ weak Hamiltonian.
Fig. 3. Typical Penguin diagram contribution to $\Delta s = 1$ weak Hamiltonian.
Fig.4. Typical left-right W_L-W_R mixing contribution to $\Delta s = 1$ weak Hamiltonian.
Fig. 5. Typical W_L-W_R mixing contribution to electric dipole moment of the neutron.

Footnotes and References

1. R.N. Mohapatra, Phys. Rev. D6, 2023 (1972).
2. M. Kobayashi and T. Maskawa, Prog. Theor. Phys. 49, 652 (1973).
3. R.N. Mohapatra and J.C. Pati, Phys. Rev. D11, 566 (1975).
4. N.S. Lockyer et. al., Phys. Rev. Lett. 51, 1316 (1983); E. Fernandez et. al., Phys. Rev. Lett. 51, 1022 (1983).
5. See excellent recent reviews by: L.L. Chau, Phys. Rep. 95C, 1 (1983); A.J. Buras, Max Planck Preprint (1984); B. Holstein, Univ. of Mass. Preprint (1984); L. Wolfenstein, CERN Preprint (1984).
6. F. Gilman and M. Wise, Phys. Lett. 83B, 83 (1979); Phys. Rev. D20, 2392 (1979); B. Guberina and R.D. Peccei, Nucl. Phys. B163, 289 (1980); F. Gilman and J. Hagelin, Phys. Lett. 126B, 111 (1983).
7. G. Beall and A. Soni, Phys. Rev. Lett. 47, 552 (1981).
8. J.C. Pati and A. Salam, Phys. Rev. D10, 275 (1974); R.N. Mohapatra and J.C. Pati, Phys. Rev. D11, 566, 2558 (1975); G. Senjanović and R.N. Mohapatra, Phys. Rev. D12, 1502 (1975).
9. For a recent review see, R.N. Mohapatra, Lectures at the NATO Advanced Summer Institute on Particle Physics, Münich (1983).
10. R.N. Mohapatra, F.E. Paige and D.P. Sidhu, Phys. Rev. D17, 2642 (1978).
11. R.N. Mohapatra and D.P. Sidhu, Phys. Rev. D17, 1876 (1978); P. Herczeg, Phys. Rev. D28, 200 (1983); D. Chang, Nucl. Phys. B214, 435 (1983).
12. For arbitrary number of generations, the number of physical phases $N_D = N_L + 2N_g - 1$ where N_L is the corresponding number for $SU(2)_L \times U(1)$ theories, i.e. $N_L = 1/2(N_g-1)(N_g-2)$.
13. R.N. Mohapatra, G. Senjanović and M.D. Tran, Phys. Rev. D28, 546 (1983).
14. I.I. Bigi and J.M. Frere, Phys. Lett. (1983)
15. G. Beall, M. Bender and A. Soni, Phys. Rev. Lett. 48, 848 (1982).
16. M.A.B. Bég, R. Budny, R.N. Mohapatra and A. Sirlin, Phys. Rev. Lett. 38, 1252 (1977); I.I. Bigi and J.M. Frere, Phys. Lett. 110B, 255 (1982); J. Donoghue and B. Holstein, Phys. Lett. 113B, 383 (1982); E. Masso, Phys. Rev. Lett. 52, (1984).
17. G. Ecker, W. Grimus and H. Neufeld, Nucl. Phys. (1983).
18. R.N. Mohapatra and G. Senjanovic, Phys. Rev. Lett. 44, 912 (1980); Phys. Rev. D23, 165 (1981).

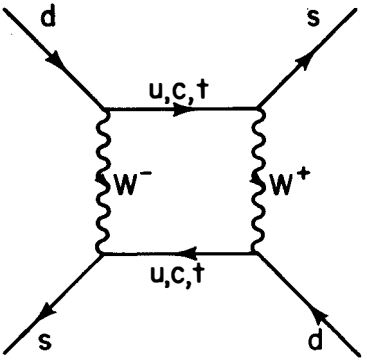

fig. 1

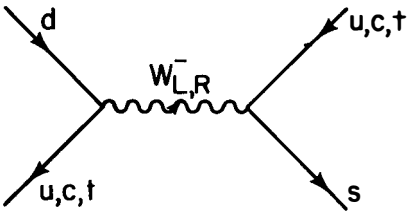

fig. 2

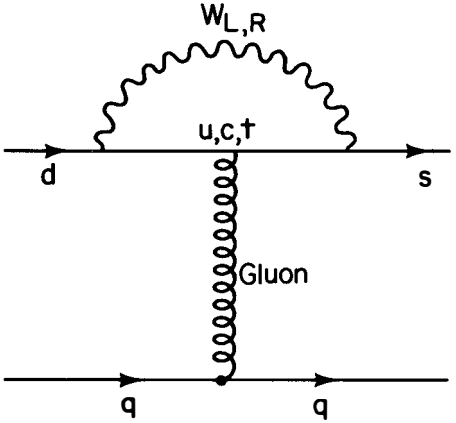

fig. 3

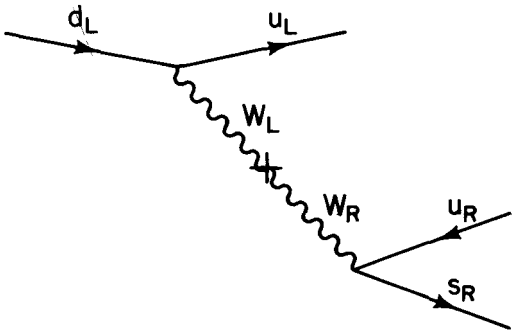

fig. 4

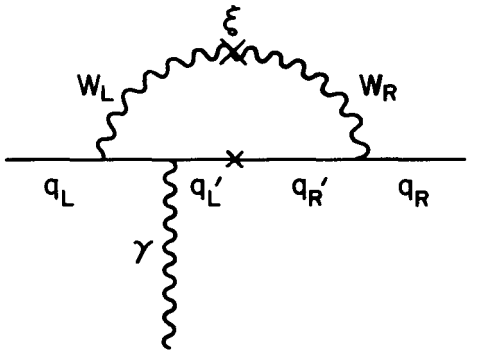

Fig. 5

SPONTANEOUS CP BREAKING

J.-M. Gérard
Max-Planck-Institut für Physik und Astrophysik
- Werner-Heisenberg-Institut für Physik -
Föhringer Ring 6, D 8000 München 40
Federal Republic of Germany

Abstract:

The new measurements of ε'/ε require an interesting hierarchy among the vacuum expectation values present in the three scalar doublet model with natural flavor conservation and spontaneous CP breaking.

The possible ways to implement CP breaking in an $SU(2)_L \times U(1)$ electroweak model with n scalar doublets can be classified according to the nature of this breaking (i.e. whether spontaneous (SCPB) or explicit) and the properties of the neutral scalar sector with respect to flavor violation (i.e. whether the principle of natural flavor conservation (NFC) is extended to the non gauge sector or not).

Table 1: Classification of the various CP violation sources

n	NFC	SCPB	Sources
1	Yes	Yes	-
	Yes	No	$W_L^{\pm}$
2	Yes	Yes	-
	Yes	No	$W_L^{\pm}$
	No	Yes-No	$W_L^{\pm}$, H^o
>2	Yes	Yes	$H^{\pm}$
	Yes	No	$W_L^{\pm}$, $H^{\pm}$
	No	Yes-No	$W_L^{\pm}$, $H^{\pm}$, H^o

In the minimal model with only one scalar doublet responsible for the $SU(2)_L \times U(1)$ breaking and the fermion masses, one needs complex Yukawa couplings to ensure an (explicit) CP breaking. As we know this Kobayashi-Maskawa (KM) mechanism[1] could fail to reproduce the CP violating parameters ϵ and ϵ'/ϵ[2]. It is, therefore, of importance to look for a simple extension of the standard model with a new CP breaking mechanism.

The introduction of a second scalar doublet allows such a new mechanism if we release the scalar sector from the NFC constraint[3]. In this case, CP violation is carried by both charged gauge bosons $W_L^{\pm}$ and physical neutral scalars H^o. However the latter have to be rather heavy (5-10 TeV) in order to avoid too large a tree-level contribution to the K^o-$\bar{K}^o$ mass difference ΔM. The CP violation due to scalar exchange is therefore superweak and implies a positive sign for ϵ'/ϵ, as in the standard model. The presence of free Yukawa parameters does not allow definite predictions about the magnitude of the various CP violating quantities[4]. From Table 1 the most interesting candidate seems therefore to be a three scalar doublet model[5] with NFC and SCPB such that all CP violating processes are induced by charged scalar $H^{\pm}$ exchanges[6].

In this model, NFC is ensured by requiring that each quark charge sector couples to only one scalar doublet and we obtain the following Yukawa interactions:

$$L_Y = (\bar{u}^o, \bar{d}^o)^i_L \left\{ \frac{M_d^{ij}}{\upsilon_1} d_R^{oj} \Phi_1 + \frac{M_u^{ij}}{\upsilon_2^*} u_R^{oj} \tilde{\Phi}_2 \right\} + \text{h.c.} \qquad (1)$$

where υ_i is the vacuum expectation value (υ.e.υ.) associated to the doublet Φ_i ($i = 1,2,3$). At this stage, the Yukawa couplings for the leptons are not specified while the down and up quark mass matrices $M_{d,u}$ are proportional to υ_1 and υ_2^* respectively. The constraint of NFC obviously implies that all the Yukawa couplings in Eq. (1) can be reexpressed in terms of the fermion masses and the KM mixing matrix K, in the physical basis for the quarks. In particular, for the interactions with the physical charged scalars H_a^+ ($a = 1,2$) we obtain

$$L_Y(H_a^+) = \bar{u} \left\{ K \begin{pmatrix} m_d & & \\ & m_s & \\ & & m_b \end{pmatrix} \left(\frac{1+\gamma_5}{2} \right) \frac{\gamma_a}{\gamma_a} + \begin{pmatrix} m_u & & \\ & m_c & \\ & & m_t \end{pmatrix} K \left(\frac{1-\gamma_5}{2} \right) \gamma_a \right\} d\, H_a^+ \qquad (2)$$

The remaining free parameters in Eq. (2) arise from the diagonalization of the 3 x 3 charged scalar mass matrix by means of an unitary matrix U^H characterized[7] by three angles and one phase δ^H:

$$\begin{pmatrix} \Phi_1^+ \\ \Phi_2^+ \\ \Phi_3^+ \end{pmatrix} = U^H \begin{pmatrix} G^+ \\ H_1^+ \\ H_2^+ \end{pmatrix} \qquad (3)$$

where G^+ is the Goldstone boson associated to W_L^+. However, the unknown γ_a and γ_a couplings are related to the various υ.e.υ.'s as follows:

$$|\gamma_a| \simeq \left| \frac{\upsilon}{\upsilon_2} \right| \; ; \gamma_a \simeq \left| \frac{\upsilon\, \upsilon_3}{\upsilon_1 \upsilon_2} \right| e^{i\delta^H} \qquad (4)$$

with $\upsilon \equiv (\Sigma\, \upsilon_i^2)^{1/2} = 2^{-3/4}\, G_F^{-1/2}$.

The constraint of SCPB means that CP violation is only induced by complex υ.e.υ's:

$$\upsilon_i \equiv |\upsilon_i| \, e^{i\sigma_i} \tag{5}$$

From Eq. (1) we conclude that the KM mixing matrix K is orthogonal ($\delta_{KM} = 0$) since the phases associated to the υ.e.υ.'s υ_1 and υ_2 are rotated away by a simple re-definition of the right-handed down and up quark fields respectively. A careful analysis of the scalar potential V indicates that these phases can be spontaneously generated by the following self-interaction coupling:

$$V(\Phi_i) \ni \lambda_{ij} \{(\Phi_i^+ \Phi_j)(\Phi_i^+ \Phi_j) + h.c.\} \tag{6}$$

After the minimalization of the potential, we indeed obtain:

$$\left(\frac{M_2^2 - M_1^2}{\upsilon^2}\right) \mathrm{Im}\, \gamma_a = \lambda_{12} \sin 2(\sigma_1 - \sigma_2) \tag{7}$$

which simply relates the unique CP violating phase δ^H to the relative phase between υ_1 and υ_2. From relation (7) we conclude that the model is still CP invariant in the limit of degenerate physical charged scalar masses ($M_1 = M_2$).

We are now in position to compute the short-distance (SD)[8] charged scalar contribution to the off-diagonal element M_{12} of the K^0-$\bar{K}^0$ mass matrix. Naively the main contributions come from the scalar-gauge boson (H-W) exchange box-diagrams which only contain two (small) Yukawa couplings.

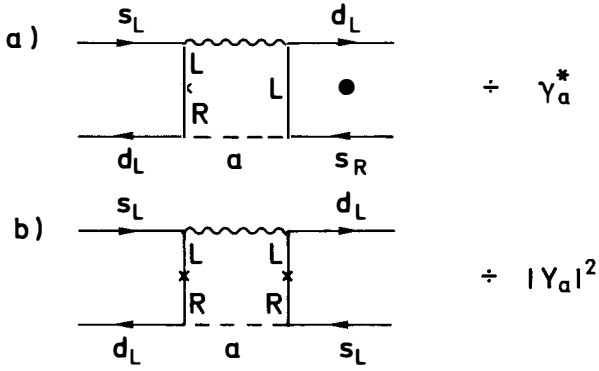

Fig. 1: H-W exchange diagrams in the limit $m_d = 0$. Crossed diagrams are understood.

However the contribution to the imaginary part of M_{12} (Fig. 1a) is GIM suppressed and, in addition, vanishing in the limit where the external momenta are neglected (we mark this latter suppression with a black dot). It is, therefore, of relevance to consider also the scalar-scalar (H-H) exchange box-diagrams.

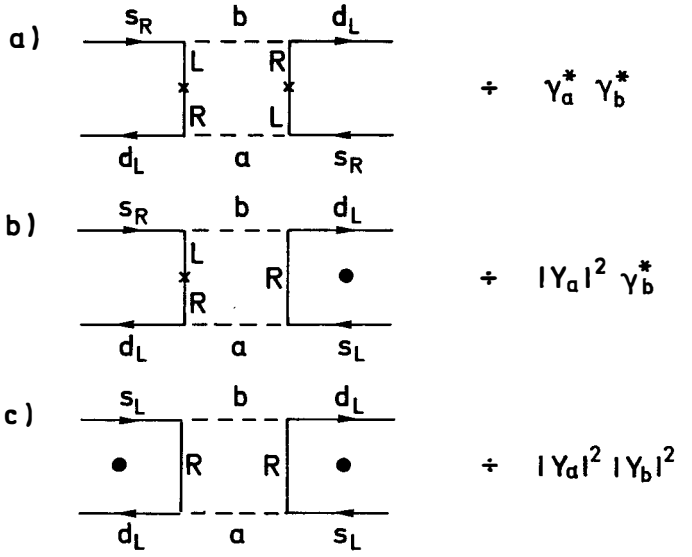

Fig. 2: H-H exchange diagrams in the limit $m_d = o$. Crossed diagrams are understood.

Let us now estimate the ratio ε'/ε defined as follows:

$$\varepsilon'/\varepsilon \simeq - \frac{1}{20} \frac{\xi^H \cdot \Delta M}{\text{Im } M_{12}^{SD} + 2\, \xi^H \, \text{Re} M_{12}^{SD}}, \quad \xi^H \equiv \frac{\text{Im } A_o^H}{\text{Re} A_o} \tag{8}$$

where $\text{Im } A_o^H$ is the imaginary part of the ($\Delta I = 1/2$) K-decay amplitude arising from the Penguin diagram with charged scalar exchange. If we assume order-one scalar couplings in (2), namely (4):

$$|v_1| \sim |v_2| \sim |v_3| \tag{9}$$

all the diagrams (Figs. 1-2) contribute with the same weight[4,9] and we recover the usual result[10]:

$$2\,\xi^{H}\ \mathrm{Re}\ M_{12}^{SD} \gg \mathrm{Im}\ M_{12}^{SD} \tag{10}$$

which implies:

$$\tilde{\varepsilon}'/\varepsilon \simeq -0.05\ \frac{\Delta M}{2\mathrm{Re}\ M_{12}^{SD}} \tag{11}$$

Moreover Re M_{12}^{SD} is dominated by the standard W-W exchange diagram which turns out to be smaller than $\frac{\Delta M}{2}$ for a Bag factor B smaller than 3/2. This is clearly incompatible with the experimental measurement[11] of ε'/ε:

$$(\varepsilon'/\varepsilon)_{exp} = (-4.6 \pm 5.3 \pm 2.4)\ 10^{-3}. \tag{12}$$

How could we increase Im M_{12}^{SD}? A first and obvious possibility consists in increasing the value of Im γ_a to enhance the contribution of the diagram in Fig. 1a. However, in this case, we obtain too large an electric dipole moment for the neutron (d_n). On the other hand, if we increase the value of $|\gamma_a|$ (see Fig. 2b) then, we are in conflict with ΔM (see Fig. 1b). So the unique way to consistently decrease $|\varepsilon'/\varepsilon|$ is to assume a large value for the Re γ_a (Re γ_a = (10^2))[4,9]. In this limit, we find that Im M_{12}^{SD} is mainly induced by the diagram of Fig. 2a while the contribution to Re M_{12}^{SD} is still dominated by the diagrams of Figs. 1b and 2a in such a way that

$$\mathrm{Im}\ M_{12}^{SD} \gg \xi^{H}\ (2\ \mathrm{Re}\ M_{12}^{SD}). \tag{13}$$

This implies that ε'/ε, whose sign is determined by the sign of $\sin(\sigma_1-\sigma_2)$, is compatible with the experimental result (12). Moreover the K^o-$\bar{K}^o$ mass difference ΔM can be reproduced without having to invoke large long distance effects.

Table 2: Values of ε'/ε, d_n and $(\Delta M)^{SD}/\Delta M$, for M_1 = 25 GeV

B	M_2(GeV)	$\varepsilon'/\varepsilon.10^3$	$d_n.10^{25}$	$(\Delta M)^{SD}/\Delta M$	($\lvert\upsilon_1\rvert$, $\lvert\upsilon_2\rvert$, $\lvert\upsilon_3\rvert$) (GeV)
1	58	-5.9	-1.3	1.3	(1, 71, 174)
2/3	66	-6.2	-1.3	0.9	"
1/2	74	-5.6	-1.2	1.1	(1.2, 56, 180)
1/2	106	-5.6	-1.1	1.1	"
1/3	106	-5.2	-1.0	1.8	(1.7, 41, 183)

From Eq. (4) we derive that Re γ_a = O(10²) and Im γ_a, $|Y_a|$ = O(1) require the following hierarchy among the υ.e.υ.'s (see Table 2):

$$|\upsilon_1| \ll |\upsilon_2| < |\upsilon_3| \tag{14}$$

which is shielded from large radiative corrections by the NFC condition. The hierarchy $\left|\frac{\upsilon_1}{\upsilon_2}\right| \ll 1$ is suggested by the existing mass spectrum for the heavy quarks. Indeed, the KM mixing matrix structure provides us with an intriguing picture for the Cabibbo-like mixing angle dependence on fermion masses and strongly supports the idea of an almost unmixed third generation. In the three scalar doublet model (see Eq. (1)), this decoupling implies:

$$\frac{m_b}{m_t} \simeq \left|\frac{\upsilon_1}{\upsilon_2}\right| \tag{15}$$

if we assume same-order Yukawa couplings for the members of the generation. Moreover, the υ.e.υ's presented in Table 2 suggests order-one Yukawa couplings for this heavy generation. In this model, the various υ.e.υ.'s fix therefore the typical scales[12] for the $SU(2)_L \times U(1)$ mass spectrum:

$$\begin{aligned} m_b,\ m_\tau &= O(\upsilon_1) \\ m_t &= O(\upsilon_2) \\ M_W &= O(\upsilon_3) \end{aligned} \tag{16}$$

We conclude that $SU(2)_L \times U(1)$ is mainly broken by the υ.e.υ. of the scalar doublet Φ_3 uncoupled to matter fields and the lepton sector only couples to Φ_1 at the tree-level. This nicely illustrates how important new experimental informations on CP violation are for an analysis of the unknown scalar sector of the electroweak model.

Acknowledgements

The work reported here was done in collaboration with G.C. Branco and A.J. Buras. I thank J. Bjorken for his comment on monojet events which led to Ref. 12).

References

1) M. Kobayashi and T. Maskawa, Prog. Theor. Phys. 49 (1973) 652.

2) For a review see E. Paschos, talk presented at this workshop.

3) T.D. Lee, Phys. Rev. D8 (1973) 1226.

4) G.C. Branco, A.J. Buras and J.-M. Gérard, MPI preprint (1985) MPI-PAE/PTh 4/85.

5) S. Weinberg, Phys. Rev. Lett. 37 (1976) 657.

6) G.C. Branco, Phys. Rev. Lett. 44 (1980) 504.

7) C.H. Albright, J. Smith and S.-H.H. Tye, Phys. Rev. D21 (1980) 711.

8) For a discussion on the possible long-distance effects see T. Pham and A. Sanda, talks presented at this workshop.

9) G.C. Branco, A.J. Buras and J.-M. Gérard, MPI preprint (1985) MPI-PAE/PTh 1/85.

10) A.I. Sanda, Phys. Rev. D23 (1981) 2647;
N.G. Deshpande, Phys. Rev. D23 (1981) 2654;
J.F. Donoghue, J.S. Hagelin and B.R. Holstein, Phys. Rev. D25 (1982) 195.

11) B. Winstein (Chicago-Fermilab-Saclay Coll.) Proc. Neutrino Conference 84, Dortmund.

12) The very light neutral scalar associated to the scale v_1 allows Z-decays into light particles and could explain the monojet events seen at CERN:
S.L. Glashow and A. Manohar, Harvard preprint HUTP-84/A080.

SUSY AND KOBAYASHI-MASKAWA

J.-M. Gérard
Max-Planck-Institut für Physik und Astrophysik
- Werner-Heisenberg-Institut für Physik -
Föhringer Ring 6, D 8000 München 40
Federal Republic of Germany

Abstract:

A supersymmetric extension of the Kobayashi-Maskawa mechanism to strong interactions gives interesting predictions for the CP violating parameters ε and ε'/ε.

In N = 1 supersymmetric Yang-Mills theories[1], the spin 1 gauge particles (weak W^+, gluon G, ...) have fermionic partners (wino $\tilde{W}$, gluino $\tilde{G}$, ...) while the spin 1/2 matter fields (quark q, ...) are associated with scalar companions (squark $\tilde{q}$, ...). This well-known "correspondence principle" implies new gauge couplings in the supersymmetric extension of the $SU(3)_c \times SU(2)_L \times U(1)$ standard model. Let us first consider the charged weak gauge coupling:

$$g_W \bar{u}^o_L \gamma_\mu d^o_L W^+_\mu \tag{1}$$

where internal indices are understood. In the physical basis for the quarks, we obtain

$$g_W \bar{u}_L U^u U^{d\dagger} \gamma_\mu d_L W^+_\mu \tag{2}$$

where U^u and U^d are the unitary matrices which diagonalize the up and down quark mass matrices M_u and M_d respectively. The product $U^u U^{d\dagger}$ is the so-called Kobayashi-Maskawa (KM) mixing matrix K. From the "correspondence principle", supersymmetry (SUSY) induces the new gauge coupling

$$g_W \tilde{u}^{o*} d^o_L \tilde{W}^+ \tag{3}$$

which can also be rewritten in terms of the physical squarks and quarks as follows:

$$g_W \tilde{u}^* \tilde{U}^u U^{d\dagger} d_L \tilde{W}^+ \tag{4}$$

where $\tilde{U}^u$ is the unitary matrix needed to diagonalize the up squark mass matrix. We therefore observe a slight departure from the usual weak interactions if $\tilde{U}^q$ is different from U^q. However, the appearance of $\tilde{U}^q$ modifies the usual picture of the strong interactions. Whereas the strong coupling of quarks to gluons is flavor-blind, namely

$$g_s \bar{q}^o \gamma_\mu q^o G_\mu = g_s \bar{q} \gamma_\mu q G_\mu \tag{5}$$

the one associated to the gluino is in general not:

$$g_s \tilde{q}^{o*} q^o \tilde{G} = g_s \tilde{q}^* \tilde{U}^q U^{q\dagger} q \tilde{G} \tag{6}$$

if $\tilde{U}^q \neq U^q$.

In a class of models based on N = 1 supergravity[1], SUSY is softly broken

and the down squark mass matrix reads

$$M^2_{\tilde{d}^0} \simeq \begin{pmatrix} m^2_{3/2}\, 1 + M_d M_d^\dagger + c M_u M_u^\dagger & A^* m_{3/2} M_d \\ A m_{3/2} M_d^\dagger & m^2_{3/2} 1 + M_d^\dagger M_d \end{pmatrix} \tag{7}$$

where $m_{3/2}$ is essentially the gravitino mass, A is the order-one coefficient in front of the Yukawa-like soft-breaking terms and c, generated from radiative corrections[2], is a measure of the one-loop flavor violation induced by the charged Higgs sector. If we try to diagonalize this mass matrix by means of the matrix U^d, we obtain:

$$M^2_{\tilde{d}} \simeq \begin{pmatrix} m^2_{3/2} 1 + \hat{M}_d^2 + c K^\dagger \hat{M}_u^2 K & |A| m_{3/2} \hat{M}_d \\ |A| m_{3/2} \hat{M}_d & m^2_{3/2} 1 + \hat{M}_d^2 \end{pmatrix} \tag{8}$$

where $\hat{M}_{u,d}$ denote the diagonal up and down quark matrices respectively. The squark mass matrix (8) is obviously not diagonal in the flavor-space. We, therefore, have to consider $\tilde{U}^d \neq U^d$ and we conclude (see Eq. (6)) that there are flavor as well as CP violations in strong interactions which are also controlled by the KM mixing matrix and the magnitude of the parameter c. The latter is of order-one[2] in models where $SU(2)_L \times U(1)$ is broken via radiative corrections. Moreover it is negative, a consequence of the fact that the top is the heaviest quark. From (8) this requires $m_t \lesssim (-c)^{-1/2}\, m_{3/2}$ in order to keep color and electric charges unbroken.

Let us now briefly review the predictions of the supersymmetric extension of the KM mechanism. First of all, the off-diagonal element M_{12} of the K^o-$\bar{K}^o$ mass matrix gets an additional contribution from the gluino-squark exchange box-diagram.

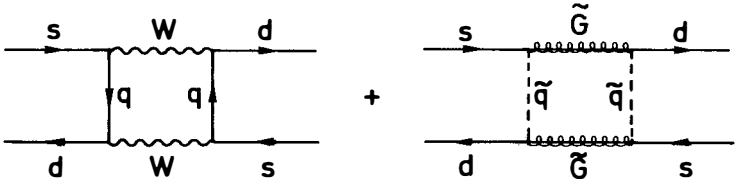

Fig. 1: Box-diagram contributions to the $\Delta S = 2$ matrix element M_{12}.

The experimental value of the K^o-$\bar{K}^o$ mass difference ΔM provides us with a constraint on the real part of M_{12}. This only corresponds to a weak bound[3] on the squark and gluino masses.

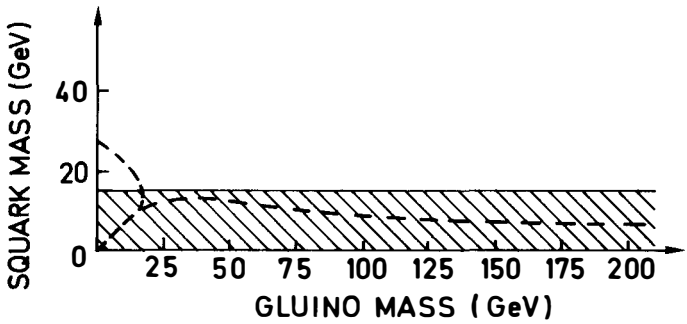

Fig. 2: Bounds on squark and gluino masses. The region above the broken curve is allowed by ΔM and the shaded region is ruled out by experiments.

On the other hand, the imaginary part of M_{12}, responsible for the CP violating impurity ϵ in the K^o-$\bar{K}^o$ mass matrix gives rise to an important improvement[4] with respect to the standard model.

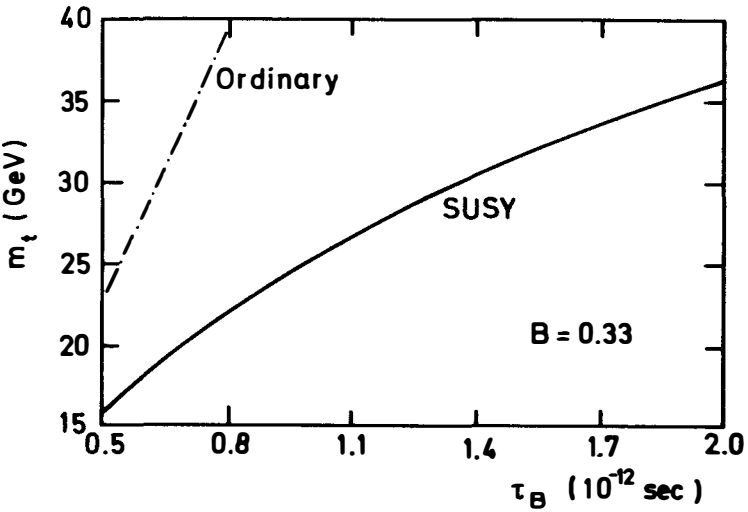

Fig. 3: The lower bound on the top quark mass as a function of the B-lifetime for 40 GeV squark and gluino masses (A = 3, c = -1).

For reasonable masses of squark and gluino (~40 GeV), the experimental value of ϵ allows for a 40 GeV top quark even if the Bag parameter B is one third of its value

predicted by the vacuum insertion approximation. This of course allows more freedom than in the ordinary theory, in spite of the smallness of the KM mixing angles ϑ_2 and ϑ_3.

The CP violation in the ($\Delta S = 1$) K-decay also gets an additional contribution due to the appearance of the supersymmetric Penguin, namely the Pengluino[5].

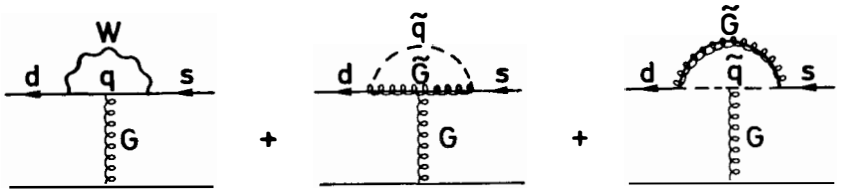

Fig. 4: Penguin and Pengluino contributions to ε'.

It results a smaller ε'/ε parameter[5] than in the ordinary standard model.

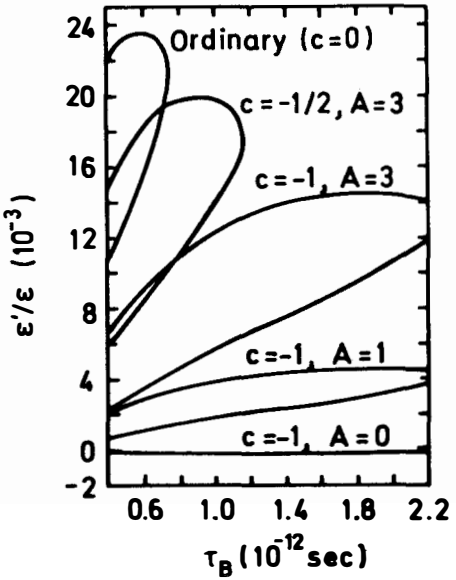

Fig. 5: ε'/ε as a function of the B-lifetime for a top quark mass equal to 40 GeV.

This in fact reflects the freedom we gain in fitting the ε parameter which allows smaller values for the KM CP violating phase δ. Let us note that one can even mimic the superweak CP violation feature ($\varepsilon' = 0$). But is it a surprise in the frame-

work of a super(electro)weak model?

To sum up, the extension of the KM mechanism to the supersymmetric $SU(3)_c \times SU(2)_L \times U(1)$ model certainly helps the electroweak theory which is confronted to drastic experimental constraints. SUSY, however, introduces additional CP violation sources[6].

A first important CP violating phase can be induced if the soft-breaking A parameter turns out to be complex, $A = |A| e^{i\xi}$. In such a case, an electric dipole moment of the neutron (EDMN) arises at the one-loop level[7] (Fig. 6) and obviously dominates over the three-loop contribution appearing in the standard KM model.

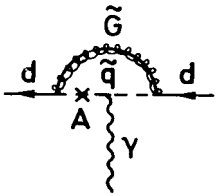

Fig. 6: One-loop gluino-squark contribution to EDMN.

The experimental bound on the EDMN provides us therefore with a rather strong constraint on the magnitude of the ξ-angle[7,3]:

$$\xi \lesssim 10^{-2} \qquad (9)$$

The smallness of this angle leaves the KM predictions presented before almost unchanged[3]. Let us also point out that in a large class of models, the A parameter arising from the so-called hidden sector of the theory (responsible for the local SUSY breaking) is naturally real.

Another CP violating phase is induced by the wino-Higgsino mixing. However, the weak and Yukawa couplings associated with these new fermions imply too small a value of ε[8] or too large of value of $|\varepsilon'/\varepsilon|$[9].

These additional sources of CP violation being unable to substitute for the KM mechanism, we conclude that:

SUSY NEEDS KM, BUT IS IT MUTUAL?

Acknowledgements

I thank W. Grimus, A. Masiero, D. Nanopoulos, Amitava Raychaudhuri and G. Zoupanos for their most enjoyable collaborations.

REFERENCES

1) For a review, see e.g. H.P. Nilles, Phys. Rep. 110 (1984) 1.

2) M.J. Duncan, Nucl. Phys. B221 (1983) 285;
J.F. Donoghue, H.P. Nilles and D. Wyler, Phys. Lett. 128B (1983) 55.

3) J.-M. Gérard, W. Grimus, Amitava Raychaudhuri and G. Zoupanos, Phys. Lett. 140B (1984) 349.

4) J.-M. Gérard, W. Grimus, A. Masiero, D. Nanopoulos and Amitava Raychaudhuri, Phys. Lett. 141B (1984) 79.

5) J.-M. Gérard, W. Grimus and Amitava Raychaudhuri, Phys. Lett. 145B 400.

6) For a review, see e.g. J.-M. Gérard, W. Grimus, A. Masiero, D. Nanopoulos and Amitava Raychaudhuri, CERN preprint TH.3920/84, to appear in Nucl. Phys. B.

7) W. Buchmüller and D. Wyler, Phys. Lett. 121B (1983) 321;
J. Polchinski and M.B. Wise, Phys. Lett. 125B (1983) 393;
D.V. Nanopoulos and M. Srednicki, Phys. Lett. 128B (1983) 61.

8) F. del Aguila, J.A. Grifols, A. Méndez, D.V. Nanopoulos and M. Srednicki, Phys. Lett. 129B (1983) 77.

9) J.-M. Frère and M.B. Gavela, Phys. Lett. 132B (1983) 107.

MUON DECAY

Herbert Steiner
Lawrence Berkeley Laboratory and Department of Physics
University of California, Berkeley, California 94720, U.S.A.*

ABSTRACT

Improved searches for rare processes in muon decay have substantially improved existing limits, but no evidence for any non-standard behavior has been found. The result of a recent sensitive search for right-handed currents indicates that the ratio (V+A)-amplitude/(V-A)-amplitude $\leq$ 0.029. This experiment also imposed new limits on non-standard couplings and on the energy scales where lepton substructure and family symmetry breaking effects might manifest themselves.

Although muon decay has been studied extensively for more than 30 years there have been several interesting new experiments during the last year or two. I have chosen to subdivide these new experiments into two classes: (1) standard decay (e.g. $\mu^+ \rightarrow e^+\nu_e\bar{\nu}_\mu$), where the objectives were to improve our understanding of the Lorentz structure of the interaction, to search for right handed currents, and to search for lepton substructure, and (2) searches for rare processes such as the decays $\mu^+ \rightarrow e^+\gamma$, $\mu^+ \rightarrow e^+e^-e^+$, $\mu^+ \rightarrow e^+ + f$ (f is an axion-like scalar) and the conversion process $\mu^- + (A,Z) \rightarrow e^- + X$, where the goals were to explore new physics.

These and the other new results can be summarized by the somewhat disappointing statement that nothing unusual was seen. An LBL/TRIUMF/Northwestern collaboration found no evidence for right-handed currents. No evidence was seen for S, T or P couplings nor was there any indication that leptons have substructure below a composite mass scale of 2400 GeV. No experiment has found any evidence for any of the rare processes mentioned previously. The present limits on the relevant branching ratios are:

B.R. $(\mu^+ \rightarrow e^+e^-e^+) \leq 2.4\times10^{-12}$	(SIN)[2]
B.R. $(\mu^- + (A,Z) \rightarrow e^- + X) \leq 2\times10^{-11}$	(TRIUMF)[3]
B.R. $(\mu^+ \rightarrow e^+ + f) \leq 6\times10^{-5}$	(LBL/TRIUMF/NW)[4]
B.R. $(\mu^+ \rightarrow e^+ + \gamma) \leq 1.7\times10^{-10}$	(PDG World Average)

Despite the lack of unexpected new results it is important to realize that the frontiers continue to be pushed back significantly, and that possible subtle deviations from expectations based on the Standard Model may only manifest themselves experimentally as measurements of ever increased refinement and precision are made. I think the recent muon decay experiments constitute very meaningful steps in that direction. Other experiments at TRIUMF, LAMPF and SIN are underway to further improve this situation.

As an illustration of the present generation of muon decay experiments I would like to discuss in more detail our Search for Right-Handed Currents in Muon Decay at TRIUMF.[1] In particular I will present the current (essentially final) status of the results and discuss their significance in terms of right-handed currents, limits on non-(V,A) couplings, the existence of axion-like scalars, and lepton substructure.

When we embarked on this search all weak interaction experiments were consistent with a pure (V-A) interaction. They still are. However, an admixture of up to 13% (V+A)-amplitude also fit the data. Equivalently the right-handed gauge boson, W_R, had to be at least twice as massive as its standard left-handed counterpart, W_L. In the meantime, theoretical analysis of the K_1^0–K_2^0 mass difference strongly suggests that $M(W_R) > 1.6$ TeV.[5] However, such analyses are at least weakly model-dependent and therefore an independent measurement is useful. Furthermore, the only previous measurement made in the late 1960's yielded a result which was 2 standard deviations away from the pure V-A prediction.

The method used in our search was to study the decay $\mu^+ \rightarrow e^+\nu_e\bar{\nu}_\mu$ for fully polarized muons when the positrons are emitted with maximum energy; i.e. when $x = p_e/p_e(\max) \cong 1$. One produces fully polarized μ^+ from pion decay at rest, stops them in a non-depolarizing target, and then

looks for $x = 1$ positrons emitted in a direction opposite to that of the muon's spin. By angular momentum conservation these positrons must have negative helicity. This is forbidden for a pure (V-A)-interaction, and therefore any such positrons would signal the presence of a (V+A) interaction. Unfortunately the finite energy and angular acceptances of the apparatus allow tails of the (V-A) positron distributions to be detected as well, and suitable extrapolations are necessary to cleanly isolate the (V+A)-contribution.

The shape of the expected V-A spectrum is shown in figure 1. It can be written:

$$\frac{d^2\Gamma}{x^2 dx d(\cos\theta)} \propto \left\{ \left[(3-2x) + \left(\frac{4}{3}\rho - 1 \right)(4x-3) + 12 \left(\frac{m_e}{m_\mu} \right) \left(\frac{1-x}{x} \right) \eta \right] + \left[(2x-1) + \left(\frac{4}{3}\delta - 1 \right)(4x-3) \right] \xi P_\mu \cos\theta \right\}.$$

Here $\pi-\theta$ is the angle between $\vec{S}_\mu$ and $\vec{p}_e$; ρ, η, δ, ξ are the usual muon decay parameters, and P_μ is the polarization of the muon.

$$\text{When } x = 1, \quad \frac{d^2\Gamma}{dx d(\cos\theta)} \propto \left\{ 1 - \frac{\delta\xi}{\rho} P_\mu \cos\theta \right\}.$$

For a pure V-A interaction $\xi = 1$, $\rho = \delta = 3/4$, $P_\mu = 1$. When $\cos\theta = 1$ the rate vanishes. In the experiment we measure $P_\mu \delta\xi/\rho$. In a separate experiment with the same apparatus we were also able to make an improved measurement of the parameter δ.

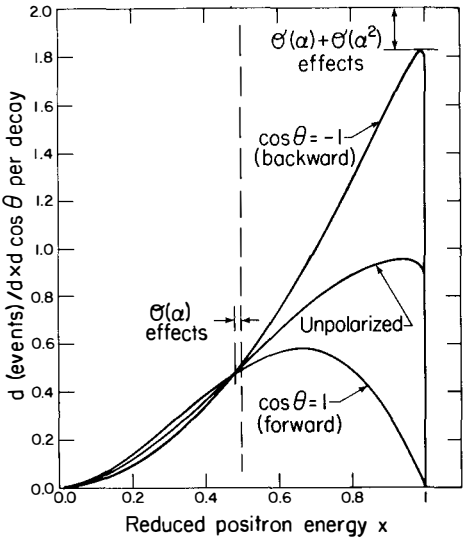

Fig. 1. Positron momentum spectrum from completely polarized μ^+ decay at rest for a V-A interaction.

The experimental method had three essential ingredients:

(1) *A 100% polarized μ^+ beam.* This was done by using the so-called surface muon beam at TRIUMF. The basic idea is to first produce positive pions with 500 MeV protons. The pions of interest stop and decay into muons near the surface of the production target. These fully polarized muons are then transported by a system of magnets and quadrupoles to the stopping target without depolarizing them.

(2) *Stopping the muons without depolarizing them.* To do this thin metal foil targets (Al, Au, Ag, Cu) were used. A longitudinal magnetic field, $B_{\parallel} \cong 1.1T$, was usually applied as an additional safeguard against depolarization. Alternatively the longitudinal field could be replaced by a weak transverse magnetic field ($B_{\perp} \sim 100$ gauss) which was used to precess the muon spins. The data taken in this mode were used both for purposes of calibrating the $x = 1$ edge of the decay spectrum and for a largely independent measurement of $P_{\mu}\xi\delta/\rho$ based on the magnitude of the μSR precession amplitude.

(3) *Determining the momentum and angle of the decay positron with good resolution.* To do this we used a focusing spectrometer with momentum resolution ($\Delta p/p \cong 0.002$). The absolute calibration of the spectrum end point was based on the spin precessed data discussed in (2).

The experiment is essentially complete. Preliminary results obtained with the longitudinal field configuration have been published,[6] and the more recent μSR analysis has been submitted for publication[7] and reported at last summer's Leipzig Conference.[4] An example of the shapes of the spin-held and spin-precessed data near $x = 1$ is shown in figure 2. The characteristic oscillations in the rate of detected positrons as a function of time for the μSR data is shown in figure 3. Here the exponential decay with μ^+ lifetime has been factored out.

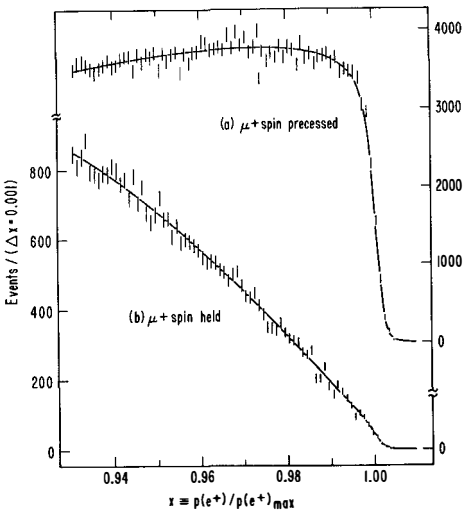

Fig. 2. Distributions (uncorrected for acceptance) in reduced positron momentum with the μ^+ spin (a) precessed and (b) held.

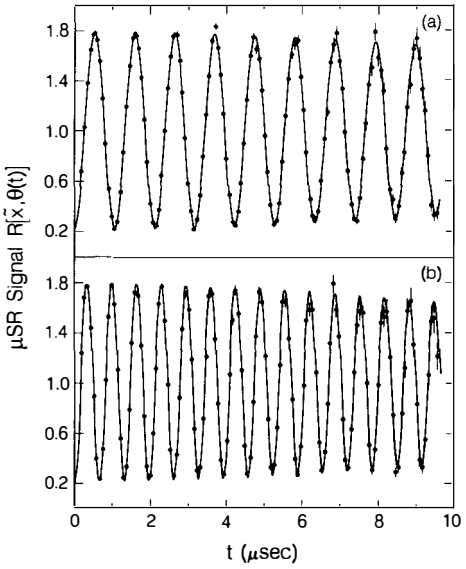

Fig. 3. Data constituting 73% of the total μSR data, with (a) 70-G, and (b) 110-G transverse fields.

In the space available here it is not possible nor appropriate to describe in further detail either the experimental method or the various systematic checks that played essential roles in these measurements. The interested reader is referred to the references just cited.[6,7]

Let me turn next to the results. It is important to note that the (V+A) limits obtained in this experiment are only valid if the mass of the heavy right-handed neutrino is less than about 10 MeV/c^2. Our result $P_\mu \xi\delta/\rho \geq 0.9966$ (90% CL) places the following limit on the contribution of a possible (V+A) interaction to muon decay:

$$\frac{\text{(V+A) Amplitude}}{\text{(V–A) Amplitude}} \leq 0.029 \qquad \text{(90\% CL)}.$$

In terms of mass limits on a right-handed gauge boson which could mediate such an interaction it is necessary to introduce two parameters--a mass and a mixing angle. This is because the mass eigenstates (W_1,W_2) are not necessarily the same as the charged gauge boson eigenstates (W_L,W_R).

Writing $W_1 = W_L\cos\zeta - W_R\sin\zeta$ and $W_2 = W_L\sin\zeta + W_R\cos\zeta$, we find $M(W_2) \geq 470$ GeV/c^2 if ζ is constrained to be zero whereas $M(W_2) \geq 400$ GeV/c^2 if ζ is free.

In general the Lorentz structure of the interaction admits the possibility of S, T, and P couplings in addition to the dominant V-A term. Let us write

$$L_{int} = -\frac{G}{\sqrt{2}} \sum_{i=1}^{5} [(\bar{e}\Gamma_i\nu_e)(\bar{\nu}_\mu\Gamma_i(G_i+G_i'\,\gamma_5)\mu) + \text{h.c.}] \qquad \text{where } \Gamma_i = 1,\ \gamma_\alpha,\ \sigma_{\alpha\beta},\ \gamma_\alpha\gamma_5,\ i\gamma_5.$$

Then the results of this experiment can be used to obtain the following limits:

(1) If the interaction is (V–A) + T (no S and P) $(G_T + G_T')^2 \leq 0.027$.

(2) If the interaction is (V–A) + S + P (no T) $(G_S - G_{P'})^2 + (G_S' - G_P)^2 \leq 0.054$.

With the same apparatus we obtained an improved value for the muon decay parameter δ. If only (V,A) couplings contribute to muon decay $\delta = 3/4$. Deviation from this value would signal something new, and can be used to further constrain S, T, and P contributions. Our very preliminary result is

$$\delta = 0.748 \pm 0.004 \text{ (statistical)} \pm 0.003 \text{ (systematic)}.$$

This should be compared with the world average value $\delta = 0.755 \pm 0.009$ listed in the latest Particle Data Group compilation.

The fact that our value of $P_\mu \xi\delta/\rho$ is very close to 1 can be used to set a limit on the mass scale above which composite lepton structure might manifest itself.[8] If leptons are composite there should be a contact interaction contribution to the Lagrangian describing muon decay. Following Peskin let us write

$$L = L_{V-A} + L_{contact}$$

where L_{V-A} is the usual V-A Lagrangian, and

$$\begin{aligned} L_{contact} = g^2/\Lambda^2\{ & \eta_1(\overline{\nu}_{\mu_L}\gamma^\mu\mu_L)(\overline{e}_L\gamma_\mu\nu_{e_L}) + \eta_2(\overline{\nu}_{\mu_R}\gamma^\mu\mu_R)(\overline{e}_R\gamma_\mu\nu_{e_R}) + \eta_3(\overline{\nu}_{\mu_L}\gamma^\mu\nu_{e_L})(\overline{e}_R\gamma_\mu\mu_R) \\ & + \eta_4(\overline{e}_L\gamma^\mu\mu_L)(\overline{\nu}_{\mu_R}\gamma_\mu\nu_{e_R}) + \eta_5(\overline{\nu}_{\mu_L}\mu_R)(\overline{e}_L\nu_{e_R}) + \eta_6(\overline{\nu}_{\mu_L}\nu_{e_R})(\overline{e}_L\mu_R) \\ & + \eta_7(\overline{\nu}_{\mu_R}\mu_L)(\overline{e}_R\nu_{e_L}) + \eta_8(\overline{\nu}_{\mu_R}\nu_{e_L})(\overline{e}_R\mu_L)\} \end{aligned}$$

Here g is a coupling constant of hadronic strength, Λ is the mass scale for compositeness, and the η_i are couplings of order unity. This is the most general SU(2)×U(1) invariant contact interaction. Using this Lagrangian to calculate the decay rate near $x = 1$ and $\cos\theta = +1$ we find

$$1 - \frac{\xi\delta}{\rho} P_\mu = 2\left(\frac{620}{\Lambda}\right)^4 \frac{g^2}{4\pi}\left(\eta_2^2 + \eta_3^2 + \frac{\eta_5^2}{4}\right) \leq 0.0034$$

or that $\Lambda^2 > (3050 \text{ GeV})^2 \frac{g^2}{4\pi}\left(\eta_2^2 + \eta_3^2 + \frac{\eta_5^2}{4}\right)$. If we make the not unreasonable assumption that $\frac{g^2}{4\pi} = 2.1$ and $\eta_i > 0.2$, then $\Lambda \geq 2400$ GeV. This value of Λ should be compared with limits deduced from other experiments using the same kind of model:

Experiment	Λ lower limit
$(g-2)_e$	$\sim$ 30 GeV
$(g-2)_\mu$	$\sim$ 750 GeV
$e^+e^- \rightarrow e^+e^-$	$\sim$ 2000 GeV

Finally we use the vanishing of the rate at $x = 1$ and $\cos\theta = +1$ to set a limit on the energy scale at which flavor symmetry could be spontaneously broken. The specific familon model discussed here is due to Wilczek.[9] Suppose muons could decay via the mode $\mu^+ \rightarrow e^+ + f_{\mu e}$, where $f_{\mu e}$

is an axion-like scalar called the familon. The contribution to the Lagrangian can be written:

$$\Delta L = \frac{1}{F_{\mu e}} \bar{\mu}\gamma_\rho e \partial_\rho f_{\mu e}.$$

and the branching ratio is

$$\frac{\Gamma(\mu^+ \to e^+ + f)}{\Gamma(\mu^+ \to e^+\nu\bar{\nu})} \cong \frac{2.5\times10^{14}}{F_{\mu e}^2} (\text{GeV})^2.$$

Here $F_{\mu e}$ is the energy scale at which flavor symmetry is spontaneously broken.

Because $\mu^+ \to e^+ + f$ is isotropic it should cause monoenergetic positrons to be emitted at $x = 1$ and $\cos\theta = 1$. We see no such peak, and consequently set the limit:

$$\frac{\Gamma(\mu^+ \to e^+ + f)}{\Gamma(\mu^+ \to e^+\nu\bar{\nu})} \leq 6\times10^{-6}.$$

This translates to $F_{\mu e} \geq 6.5\times10^9$ GeV (90% CL).

I think this example illustrates how muon decay experiments address a variety of issues of current interest in particle physics. It would be nice if one of these days a new generation of even more refined measurements would actually show some unpredicted behavior and thereby allow us to probe the next level of understanding of elementary processes.

REFERENCES

* This work was supported in part by the Director, Office of Energy Research, Office of High Energy and Nuclear Physics, Division of High Energy Physics of the U.S. Department of Energy under contracts DE-AC03-76SF00098 and AC02-ER02289.

1] Berkeley-LBL/Northwestern/TRIUMF Collaboration: B. Balke, J. Carr, G. Gidal, B. Gobbi, A. Jodidio, C.J. Oram, K.A. Shinsky, H.M. Steiner, D.P. Stoker, M. Strovink, and R.D. Tripp.

2] H.K. Walter, ETHZ-IMP-P84/4, August 1984 (unpublished), invited talk at 10th Int. Conf. on Particles and Nuclei (PANIC), Heidelberg, West Germany, July 30 - August 3, 1984.

3] D.A. Bryman et al., TRI-PP-84-59, July 1984 (unpublished), invited talk at 10th Int. Conf. on Particles and Nuclei (PANIC), Heidelberg, West Germany, July 30 - August 3, 1984.

4] B. Balke et al., "Search for Right-Handed currents in Muon Decay", contribution to XXII Int. Conf. on High Energy Physics, Leipzig, East Germany, July 19-25, 1984.

5] G. Beall, M. Bander, and A. Soni, Phys. Rev. Lett. **48,** 848 (1982).

6] J. Carr et al., Phys. Rev. Lett. **51,** 627 (1983).

7] D.P. Stoker et al., "Search for Right-Handed Currents Using Muon Spin Rotation", LBL-18935, submitted for publication.

8] M.E. Peskin, private communication.

9] F. Wilczek, Phys. Rev. Lett. **49,** 1549 (1982).

SEARCH FOR HIGGS IN UPSILON DECAYS WITH CUSB 1.5†

Paolo Franzini
Columbia University New York, N. Y. 10027

ABSTRACT

We have searched for Higgs produced via the reaction $T \to H + \Upsilon$ in a sample of 400,000 decays. No monochromatic photon lines are observed. We obtain upper limits for Higgs production in T decay which are lower than the minimal standard model prediction for Higgs' masses in the range 2 to 5 GeV.

The search for Higgs scalars in radiative decays of heavy vector mesons was first suggested by Wilczek[1] and Weinberg[2] in conjunction with the possible existence of the "axion", a very light Higgs postulated to avoid the problem of strong CP violation[3]. The decay rate for $V \to \Upsilon + H$, where V is a 1^{--} bound state of a heavy $Q\bar{Q}$ pair is given in terms of the two muon rate by $\Gamma(V \to \Upsilon + h)/\Gamma(V \to \mu\mu) = G\alpha M_Q^2/(\pi\sqrt{2}) \times (1 - M_H^2/M_V^2)x^2$ exhibiting the coupling of Higgs to the quark mass M_Q. x is unity in the standard model where only one physical, neutral Higgs state survives. For models with more Higgs', where the two fields ϕ_1 and ϕ_2 correspond to two neutral physical Higgs states, $x = \langle\phi_1\rangle/\langle\phi_2\rangle$ is unknown, where $\langle\phi\rangle$ is the field vacuum expectation value. Moreover if x is the factor for

up-like quarks, the same factor, or its inverse, appears for down-like quarks depending on the particular model. Interest in the search for Higgs' in T (and ψ) decays was stimulated by supersymmetric models in which it appears natural to have Higgs' with a few GeV mass[4]. The above formula for Γ gives, for the case of T decays, $BR(T\to H+\gamma) \approx 2.5\times10^{-4}(1-M_H^2/89.5)x^2$, M_H in GeV. Tantalizing experimental results were presented sometime ago by the Mark III collaboration[5], suggesting the existence of a Higgs candidate of 2.2 GeV mass, hastily christened $\xi(2.2)$. More recently the Crystal Ball collaboration reported evidence[6] for $T\to\gamma+X$, with a branching ratio around 0.5% and an x mass of 8.3 GeV. This state, named ζ, was also considered as a possible candidate for the Higgs' vacuum. The CUSB collaboration had also searched for $T\to\gamma+X$ with null result[7]. They obtain an upper limit for the branching ratio of $\approx$0.1% for Higgs' masses between 2.5 and 5 GeV and from a new analysis[8] a limit of $\approx$ 0.2% for M=8.3 GeV. One should note that if ξ and ζ were indeed Higgs' they require x^2 factors of >10 and >100 respectively.

It clearly appears worthwhile to reexamine the whole situation, both with respect to whether these objects exists at all and are indeed Higgs mesons, and improve the sensitivity of Higgs searches untill the standard model branching ratio is reached. This in general requires vastly increased statistics and improved detector performance. CESR provided us last fall with 400,000 T's, the largest single sample collected to date and we significantly improved the performance of CUSB over part of its coverage. CUSB has underway an upgrade program (CUSB II) which consists of inserting a cylindrical array of bismuth germanate, BGO, 12 radiation lengths (λ_o) thick, subdivided into 2×36×5 elements in θ,ϕ and r. Since only a fraction of the BGO crystals were available to us in Summer '84, we installed a partial array covering 110 degrees in ϕ and only 8 λ_o thick. Also thin scintillator were installed in front of all BGO and NaI sectors of the detector to provide additional charged particle veto. The whole BGO array is supposed to improve the CUSB energy resolution by as much as factor 3.5. The limited array used gave us an improvement of $\approx$ 2.3, consistent with the limited thickness and coverage. We wish to point out that at 4.7 GeV (electron from Bhabha scattering) we have measured a resolution σ_E/E of 1%. This is the best resolution achieved yet by any detector in actual running of a high energy physics experiment. This partial upgrade is called CUSB 1.5.

In the analysis of the data collected we arranged the photon search codes so that for 1/4 of the solid angle photon energies are measured in BGO. The collected sample is equivalent therefore to 100,000 upsilon decays having their decay photons detected in BGO and 300,000 in NaI. Because of the superior resolution in BGO, the present sample is equivalent to 530,000 upsilon decays

collected with the old CUSB detector. The search codes used with the present data are mostly adaptation of the ones used previously. In addition to clustering and isolation criteria used to reject merged π^o we require that the shower centroids measured in the four BGO layers and the 5 NaI layers agree within the expected spread. This requirement is very efficient in removing shower contaminated by other close-by photons and nuclear interactions, particularly in BGO, because of true projective boundaries and absence of azimuthal cracks and is responsible for different shape of the photon spectra at high energy.

Figures 1 and 2 show most of the inclusive photon spectra form T decays (including ≈15% continuum events) as observed in BGO and NaI.

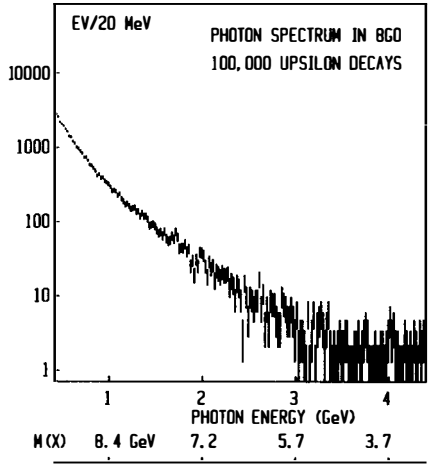

Figure 1

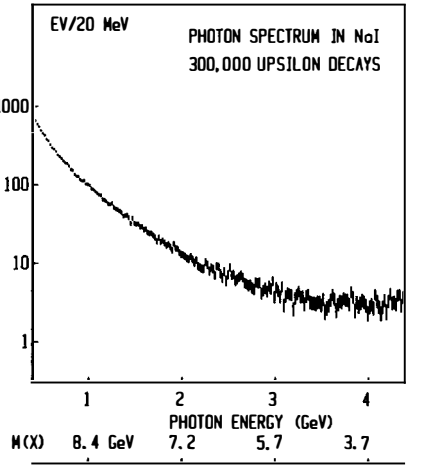

Figure 2

Both spectra are smooth, featureless and in good agreement with what one expect: mostly photons from π^o decays with small contaminations from hadronic interactions. In the absence of any monochromatic signal one cannot prove the existence of any Higgs'. Worse yet one cannot disprove their existence either and all that's left is to give upper limits for BR(T→γ+x) at some confidence level, like 90%. Figures 1 and 2 do not show fine details. The data has been however scrutinized in fine detail and fitted in various energy regions with polynomials plus gaussians with the proper, energy dependent, resolution given by: $\sigma_E/E=0.0039/\sqrt[4]{E}$ for NaI and by $\sigma_E/E=0.0018/\sqrt[4]{E}$ for BGO. No signal (positive or negative) of significance greater than one standard deviation is observed in this way. Nor is a one standard deviation signal ever observed at the same energy in the two samples. Figure three shows an example of such fits where a

negative signal of 47±51 counts is observed at 1090 MeV, corresponding to M_X=8300 MeV. Since the spectra are so smooth we feel it is appropriate to apply the procedure described to the locally averaged count. This is equivalent to computing the error of the (vanishingly small) area of the gaussian as $\delta N(\text{counts})=[(\text{counts/MeV})\times\sigma_E(\text{MeV})\times 3.7]^{1/2}$. Finally the 90% C.L. upper limit to the branching ratio is given by $BR<\delta N\times 1.65/N_T/\varepsilon$ where ε is the (energy dependent) photon finding efficiency. Note that it is common practice to use 2.36 and 1.28 instead of 3.7 and 1.65 respectively resulting in upper limits which are optimistically lowered by a factor 0.62. The results of this negative labor are shown in figure 4. For the first time upper limits lower than the minimal standard model predictions have been obtained for masses between 2 and 5.5 GeV. Strictly speaking, the computed limit applies to BR(T→Y+X)×BR(X→anything detectable).

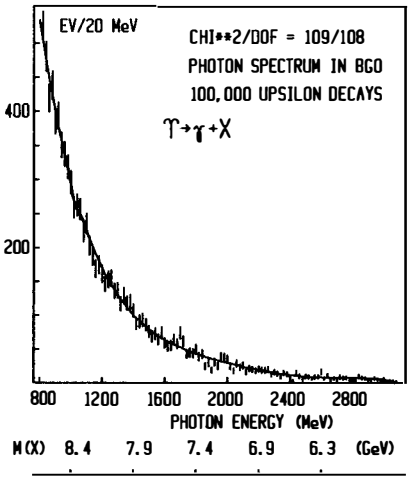

Figure 3

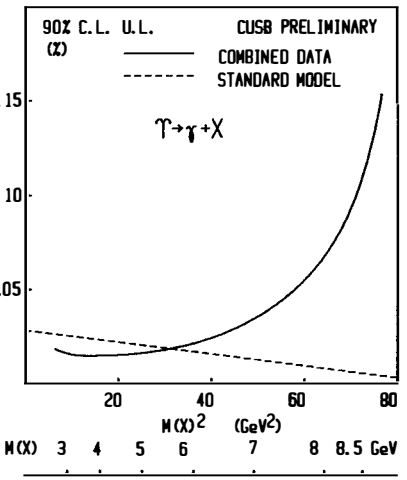

Figure 4

For Higgs' of coventional properties and the data analyzed, the second BR is unity. The present data were collected with a trigger threshold of ≈500 Mev and we used very loose event selection criteria, essentially satisfied by the presence in the detector of two energy clusters or one energy cluster plus one track. It would indeed be quite feasible for the completed CUSBII detector and with modest running at the improved CESR to reach the standard model level for masses up to 7-8 GeV. Results in this mass range would be of significance to supersymmetric models with very light Higgs whether they are found or not. Concerning the ζ(8.3) our limit for its BR in T decays is 0.09%. Conversely had the branching ratio been ≈0.5% as claimed by the Crystal Ball we should have

observed a signal of 660±72 counts while we observe ~40. Our upper limit for ξ production in T decay is ≈0.02%. Scaling only according to the c- and b-quark mass ratio our limit is more than an order of magnitude less than the BR obtained by Mark III. Scaling from T to ψ is of course a bit murky.

In conclusion Higgs scalars still elude us, at least for very low masses. The standard model expected BR value has just been passed and it is possible to do still better in T decays.

Acknowledgements. The absolute faith of J. L-F. in our data always spurred us to better results. The successful operation of the first BGO array in a high energy physics experiment was in large part due to Zhao, Michael Tuts and Dean Schamberger.

References and footnotes.

† The member of the CUSB 1.5 collaboration are P. Franzini, P. M. Tuts, D. Son, S. Youssef and T. Zhao, Columbia University; J. Lee-Franzini, R. D. Schamberger, C. Klopfenstein, T. Kaarsberg, M. Lovelock and S. Yoakum, SUNY at Stony Brook.

1). F. Wilczek, Phys. Rev. Lett. 40 (1978) 220.
2). S. Weinberg, Phys. Rev. Lett. 40 (1978) 223.
3). R. Peccei and H. Quinn, Phys. Rev. Lett. 38 (1977) 1440.
4). D. Nanopolous, Cargese Summer Institute Lectures, 1983.
5). D. Hitlin, Proc. Int. Symp. on Lepton and Photon Interactions, eds. D. Cassel and D. Kreinick. Cornell, 1983.
6). C. Peck et al. DESY84-064, SLAC-PUB-3380 (1984).
7). S. Youssef et al., Phys. Lett. 139B (1984) 332.
8). P. Franzini, Proc. XXII Int. Conf. on High Energy Physics, Eds A. Meyer and E. Wiecxorek, Leipzig.

SEARCHING FOR NEW NEUTRAL PARTICLES

Jonathan L. Rosner
Enrico Fermi Institute and Department of Physics
University of Chicago, Chicago, IL 60637

ABSTRACT

Searches are reviewed and suggested for certain types of new neutral particles. (a) Extra Z's are expected if the electroweak group is extended beyond SU(2) x U(1). Masses above 140 GeV/c^2 are ripe for exploration. (b) Neutral heavy leptons above 2 GeV/c^2 are possible in a wide range of contexts. (c) Higgs bosons beyond the first doublet can be produced at tree level in Z° decays, with an intrinsic rate of $\Gamma(Z^\circ \to \nu\bar{\nu})/2$ for each such "extra" doublet. Exotic e^+e^- and $\bar{p}p$ events are discussed in the light of these last two (and other) possibilities.

I. INTRODUCTION

At present the "standard" SU(2) X U(1) electroweak model describes a wealth of data in quantitative detail. But are we sure it is the whole story, even at energies accessible today? In this brief review I wish to make the case for neutral particle searches as the most effective way of probing beyond the standard model with the comparatively modest means at our disposal within the next decade. Neutral particles are the most elusive initially, but their signatures may be the most spectracular when finally identified. We shall be concerned with only a few examples.

A. Extra Z's are expected whenever the electroweak gauge symmetry is larger than SU(2) X U(1). They affect low-energy electroweak phenomena indirectly, and can be searched for directly in high-energy collider data. The mass range $M_{Z'} \geq$ 140 GeV/c^2 is open for hunting.

B. Neutral heavy leptons are also expected if the electroweak group is larger than SU(2) X U(1). They correspond to right-handed neutrinos. Searches for such objects also are capable of discovering heavy fourth generation neutrinos and mirror neutrinos (coupling right-handedly to electroweak $SU(2)_L$). Wide gaps exist in our knowledge about neutral heavy leptons above 2 GeV/c^2.

C. Higgs bosons beyond the minimum number (one needed in $SU(2)_L$ X U(1)) can be produced copiously in Z decays if they are members of doublets, triplets, or higher representations of $SU(2)_L$. Many models predict such bosons; the only question is whether they are light enough to be seen in Z decays.

D. Photinos (supersymmetric partners of the photon) are expected to be emitted in almost all processes in which supersymmetric partners of ordinary particles are produced. Some of the signatures for neutral leptons or new Higgs bosons are related to those for photinos.

In Sec. II we motivate the introduction of new neutral particles, concentrating on neutral leptons and Higgs bosons. Sec. III is devoted to searches for heavy neutral leptons via heavy flavor production in beam dumps, and via Z^0 decays. This leads us to a discussion of exotic events (Sec. IV), particularly from the CELLO and UA1 collaborations. The events found by UA1 consisting of one or more jets and large missing transverse momentum, if not due to conventional background sources, suggest the existence of neutral particles which escape the detector. One class of possibilities involves the decay of Z^0 to (seen particle [s]) + (unseen particle [s]). Tests of this hypothesis (including production of virtual Z^0's in present e^+e^- experiments) are mentioned in Sec. V. A final section summarizes.

II. MOTIVATIONS

A. Extra U(1). In $SU(2)_L$ X $U(1)_Y$, the electric charge Q is written as the sum of I_{3L} and Y/2, both of which are gauged. The resulting mixtures are the

photon and a "standard" Z°. If, instead, one writes

$$Q = I_{3L} + I_{3R} + (B-L)/2 \ , \qquad (1)$$

where B and L are baryon and lepton numbers, and gauges I_{3L}, I_{3R}, and B-L separately, the resulting mixtures are γ, Z°, and a new boson Z_χ. This boson couples (when the Z° is affected little by mixing with it) to a charge

$$Q_\chi = \frac{1}{\sqrt{10}} [5I_{3R} + 3\,(I_{3L} - Q)]. \qquad (2)$$

The Z_χ can be as light as 140 GeV/c without having notably affected low-energy electroweak phenomena. At this mass, it probably wouldn't have been seen directly yet, but would be accessible in future CERN or Fermilab searches. We refer to a recent review[1] for further discussion of this boson; for present purposes it is mainly of interest with regard to right-handed neutrinos, discussed below.

B. Neutral heavy leptons N are expected in several contexts. They are all able to mix with ordinary neutrinos ν_e, ν_μ, and ν_τ, and then can decay by conventional neutral- and charged-current processes, such as $N \to e^- u\bar{d}$, $N \to \nu\, u\bar{u}$, and so forth. If neutral-current decays are not suppressed, one expects[2,3]

$$B(N \to \nu\nu\bar{\nu}) \simeq 10\% \qquad B(N \to \ell\ell'\nu) \simeq 20\%$$
$$B(N \to \nu + \text{hadrons}) \simeq 20\% \qquad B(N \to \ell + \text{hadrons}) \simeq 50\% \ . \qquad (3)$$

Specific types of neutral leptons include the following:

1. Right-handed neutrinos N suffice to cancel anomalies when I_{3L}, I_{3R}, and B-L are all gauged. A fermion generation then consists of $(u, d, e, \nu)_L$ and $(u, d, e, N)_R$. If only I_{3L} and Y were gauged, N_R could be omitted. A typical N mass only has to be less than $\simeq M_{Z_\chi}/g$, where g is the gauge coupling of Z_χ to $N\bar{N}$. It could be much less, though. Right-handed neutrinos can be either of Dirac[2-5] or Majorana[5,6] type. In the former case, the neutrino mass m_ν can vanish while M_N is free. In the latter, $(m_\nu M_N)^{1/2}$ is a typical Dirac mass, $\lesssim$ (MeV to GeV).

2. Fourth generation neutrinos[7] ν_4 belong to conventional $SU(2)_L$ doublets $(\nu_4, L^-)_L$, and are produced in Z° decays: $B(Z^\circ \to \nu_4\bar{\nu}_4) \simeq 6\%$. The GIM mechanism ensures that their neutral-current decays are suppressed.

3. Mirror neutrinos[8] of right-handed helicity belong to an $SU(2)_L$ doublet $(\nu_M, L^-)_R$. Again, $B(Z^\circ \to \nu_M\bar{\nu}_M) \simeq 6\%$, but the GIM mechanism is now frustrated, and neutral-current decays occur.

C. Higgs doublets beyond the first are expected in a wide range of theories, such as SU(2) X U(1) X U(1), technicolor, supersymmetry, or composite-Higgs models. A complex doublet contains two charged and two neutral (scalar and pseudoscalar) bosons. In a one-doublet model, the charged bosons become the longitudinal components of $W^\pm$, the pseudoscalar becomes the longitudinal component of Z°, and only the scalar remains as a distinct particle. In a model with more than one doublet, both the scalar S and pseudoscalar P of the additional doublets are

physical particles. A tree-level Z°-S-P coupling exists, with

$$\Gamma(Z^\circ \to SP) = \frac{1}{2}\,\Gamma(Z^\circ \to \nu\bar{\nu}) \simeq 90\ \text{MeV} \qquad (4)$$

for each additional doublet, as long as the decay is kinematically allowed.[9,10] Thus, the decays of Z° can be a copious source of nonstandard Higgs bosons.

D. Photinos and other supersymmetric partners of ordinary neutral particles can be produced copiously in pairs when energies approach typical supersymmetry-breaking scales. This is thought to be possible at the CERN $\bar{p}p$ collider.[11]

III. NEUTRAL LEPTON SEARCHES

We concentrate here on searches devoted to those $SU(2)_L$-singlet leptons which mix weakly with ordinary neutrinos and must be produced via this mixing. More direct searches are possible when these leptons are not $SU(2)_L$ singlets; these are discussed in Secs. IV and V.

A. Beam dump limits. The copious production of heavy quarks in hadronic experiments ($\gtrsim 10^{15}$ $c,\bar{c}$ and 10^{12} $b,\bar{b}$ in a typical fixed-target beam dump experiment at Fermilab or the SPS) permits the search for new heavy leptons N in such decays as $c \to sN\ell$, $b \to cN\ell$. The N production rate is proportional to the square of a ν_ℓ-N mixing amplitude $U_{N\nu_\ell}$. One searches for the subsequent decay of N downstream of the beam dump.[3] Large mixing amplitudes imply short lifetimes, requiring the detector to be as close as possible to the beam dump. The lifetime has been estimated:[3]

$$\tau_N \simeq (5 \times 10^{-12}\,\text{s})\,|U|^{-2}(M_N/1\ \text{GeV})^{-5.2}\ , \qquad (5)$$

if neutral current decays are allowed (leading to the branching ratios (3)). Slightly longer lifetimes are expected for fourth generation neutrinos, whose neutral-current decays are suppressed. A typical value of U is (Dirac mass)/M_N, where the numerator may range from MeV to tens of GeV in specific models.[2]

The CHARM beam dump experiment[12] places a 35m long detector 480 m downstream of a dump in which we estimate[3] 10^{15} $D^\pm$ mesons to have been produced by 400 GeV/c protons. The branching ratio for $D^\pm \to N\ell^\pm$ can be calculated in terms of $|U_{N\nu_\ell}|^2$. The absence of a signal for N decay in the detector then allows one to exclude the vertically shaded region in Fig. 1.[13] Hypothetical additional limits obtained from an "ideal dump" experiment[3] are shown by the diagonally shaded regions. Here the protons are assumed to have p=800 GeV/c, and the detector is placed only 50 m from the dump, but all other parameters are the same as in the CHARM experiment. A larger $|U|^2$ range can be excluded via charm decay, and an analysis in terms of $b \to cN\ell$ allows one to exclude M_N values up to $2\frac{1}{2}$ - 3 GeV for certain ranges of mixing parameters.

B. Rare Z or W decays can act as a source of new neutral leptons mixed with ordinary neutrinos through the processes $Z \to (N\bar{\nu}$ or $\nu\bar{N})$, or $W \to N\ell$. The rate is

again proportional to $|U|^2$. (The rare Z decays only produce neutral leptons in this way if neutral-current couplings are not suppressed by the GIM mechanism). As an example of the M_N-$|U|^2$ range accessible to such searches, we show in Fig.1 contours of $B(Z \to N\bar{\nu}$ or $\nu\bar{N})P_d$, where P_d is the probablity of detecting a secondary vertex due to N decay between 100 μm and 2 m from the Z production point.[13] (We assume Z to be produced at rest, as in e^+e^- collisions. Longitudinal motion, as in $\bar{p}p$ collisions, doesn't change the argument much.) Even the observation of one rare Z decay in 100 ($BP_d=10^{-2}$) can provide useful information, since weak universality upper limits on $|U_{N\nu_\tau}|^2$ are around 15% (the accuracy to which the τ lifetime has been measured[14]). For $|U_{N\nu_\ell}|^2$and $|U_{N\nu_\mu}|^2$, the upper limits are around[2-4] 10^{-2}, requiring observation of one rare decay in 1000 to set useful bounds. Very similar arguments apply to rare W decays.[13] If levels of $BP_d=10^{-6}$ can be examined (this should be possible for Z's at SLC or LEP), neutral leptons above M_N=10 GeV will be accessible via this technique for a substantial range of $|U|^2$.

IV. EXOTIC EVENTS

It is useful to consider unusual events as illustrations of the types of particle searches that are possible at present. We discuss just two: the CELLO 2μ+2 jet event,[15] and events with unbalanced $p_\perp$ obtained by UA1.[16]

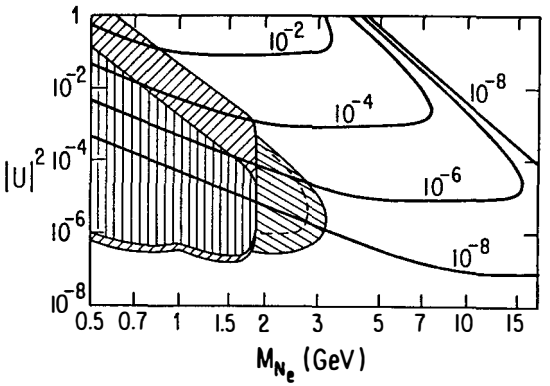

FIG 1. Comparison of regions in heavy lepton mass (M_{N_ℓ}) and square of mixing amplitude ($|U|^2$) excluded or excludable by beam dump and rare-Z decay searches. The shaded regions correspond to beam dump experiments. Region ▥: already excluded from $D \to N\ell$, $N\ell$+... (see calculation of Ref. 3 based on data of Ref. 12). Region ▨: excludable from $D \to N\ell$, $N\ell$+... in an "ideal" beam dump experiment Ref. 3). Region ▧: excludable from $b \to cN\ell$ in an "ideal dump " experiment. Solid line: $\sigma(b)=10^{-31}cm^2$; dashed line: $\sigma(b)=10^{-32}cm^2$. The contours, labeled by detection probabilities $BP_d=10^{-2}$, 10^{-4}, 10^{-6}, 10^{-8}, correspond to rare-Z-decay searches, in which a decay is detected between ℓ_1=100μm and ℓ_2=2m from a Z produced at rest.

A. The CELLO collaboration[15] has reported an event obtained at $\sqrt{s}$=43.45 GeV consisting of two muons, each approximately back-to-back with a jet of about 10 GeV, and with little missing energy. Interpretations[17] include the following:

1. Quantum electrodynamics, such as $e^+e^- \to \gamma^*\gamma^* \to \mu^+\mu^- q\bar{q}$, was originally deemed an unlikely source of the CELLO event. As more high-energy data are gathered without a repetition of it, it becomes less singular.

2. Scalar neutrinos could be produced in pairs from a virtual Z, but with a β^3 threshold factor that makes them improbable in the CELLO experiment.

3. Leptoquarks[18,19] of $\lesssim$ 20 GeV could in principle decay to μ + (jet). They can also be produced in pairs in $\bar{p}p$ collisions; data on $\bar{p}p \to \mu^+\mu^-$ + (jets)[20] may be capable of setting limits on them.

4. Neutral leptons[15,21] could be produced in pairs, via a virtual Z (for weak isodoublet members) or a light, weakly coupled Z_χ (for right-handed neutrinos). This last possibility looks less likely in view of new data[22,23] which show no unusual e^+e^- peaks below the Z°. The mass of each μ + jet combination is compatible with 20.5 ± 1 GeV/c^2. Each jet must be interpreted as an unresolved quark-antiquark pair. Similar events should occur in further PETRA data now being obtained at $\sqrt{s}$ 44=GeV, but have not appeared so far. Signatures in $\bar{p}p \to \mu^+\mu^-$ + jets)[20] should be visible, and are discussed further in Ref. 21.

B. The UA1 collaboration published evidence for events with missing transverse energy opposite one or more jets, based on 1983 data.[16] Some properties of these events are summarized in Table 1.

TABLE 1. UA1 monojet properties from 1983 data

	Event	E_T(jet) (GeV)	ΔE_M (GeV)	$m_T(j,\Delta E_M)$ (GeV/c^2)
jet	A	71[a]	66±8	130±16
	B	48	59±7	106±12
	C	52	46±8	97±17
	D	43	42±6	85±12
	E	46	41±7	87±14
	F[b]	39	34±7	73±14
γ	G[c]	44	40±6	84±6
	H	54	40±4	93±5

a) μ of 46 GeV/c included.

b) consistent with $W \to \tau\nu$

c) could be $W \to e\nu$

Suggestive features of the 1983 data include a preponderance of jet (E_T) and missing (ΔE_M) transverse energies in the 40-60 GeV range and of transverse masses (m_T) in the 80-100 GeV range, and a tendency for the jets to be "skinny," with low effective masses and charged particle multiplicities ($n_{ch} \leq 4$).

The 1984 run finds similar events, at about the same rate. The total integrated luminosities were 113 nb^{-1} for the 1983 data and about 280 nb^{-1} (on tape) for the 1984 sample. In about 2/3 of this last sample, four monojet and four dijet events have been reported.[23] These events have missing transverse energies rather similar to those of Table 1. The jet energies and total transverse masses appear to be more spread out.

Some interpretations of these events include the following.

1. Calorimeter leaks, though frequently discussed, appear not to be a serious problem for UA1. However, a cross-check by UA2 would be quite helpful. Some statement for energetic monojets[24] (say, above 50 GeV) or dijets might be possible, even though the UA2 calorimeter does not cover the full solid angle.

2. Z + jet(s), followed by $Z \to \nu\bar{\nu}$, is considered unlikely both on experimental[25] and theoretical[26] grounds. More data on visible high-$p^{\perp}$ Z decays (to e^+e^- or $\mu^+\mu^-$) will be available soon.

3. $W \to \tau\nu$ decays would look like some monojet candidates. The observed events ($p^{\perp} \geq 40$ GeV/c) are more energetic than expectations for $W \to \tau\nu$ ($\langle p^{\perp} \rangle \simeq 28$ GeV/c). Quantitative differences of opinion exist regarding this background.[16,27] It can probably be reduced substantially by choosing events with $n_{ch} \geq 4$ and $m_T > m_W$.

4. Supersymmetry provides several possible explanations for mono-and dijets with missing $p^{\perp}$. Pairs of 40 GeV gluinos[28,29] would decay to photinos and visible jets, giving transverse momentum imbalance some of the time. Pairs of 40 GeV squarks[29] would give stiffer and skinnier monojets than gluino pairs. A 100 GeV squark[30-32] $\tilde{q}$ produced off a sea of 5 GeV gluinos $\tilde{g}$ via the reaction (e.g.) $q\tilde{g} \to \tilde{q}g$ could decay via $\tilde{q}(100) \to \tilde{\gamma}q$, though this would not be its dominant decay. The quarks in this last process would yield monojets with a Jacobian peak structure, possible smeared out by the dynamics of quark fragmentation.[33] The production of 5 GeV gluinos in pairs will contribute additional events with jet(s)+ missing $p^{\perp}$, whose structure is expected to be distinct from $\tilde{q} \to \tilde{\gamma}q$. Specific details are just now being worked out.[32]

5. Leptoquarks of 40 GeV,[19] produced in pairs and decaying to $q + \nu$, can yield identical signatures to squarks of 40 GeV decaying to $q + \tilde{\gamma}$.

Monojets, both in old and new data, appear to have low effective masses and charge multiplicities. This trend, if confirmed, could suggest they are light, color-singlet objects. If not τ's, what could they be? There are several models in which they are products of unusual Z^0 decays:

6. $Z^\circ \to$ pairs of neutral heavy leptons; [34-36]

or

7. $Z^\circ \to$ pairs of scalar particles. [10,36,37]

These suggestions can be tested quite soon, as we now show.

V. UNUSUAL Z° DECAYS

Two types of Z° decays can lead to interesting signatures which are already visible, several years before the advent of "Z° factories" at SLC and LEP.

A. $Z^\circ \to N\bar{N}$, where N is a neutral heavy lepton, can occur with a 6% branching ratio if N is an $SU(2)_L$ isodoublet member. A fourth-generation neutrino or mirror neutrino satisfies this criterion. For the latter, the branching ratios (3) are expected. If one N decays to $\nu\nu\bar{\nu}$ and the other to visible particles, an event with unbalanced transverse momentum can result. [34,35]

The effective mass of the particles seen in UA1 monojets would suggest $M_N \lesssim$ (few GeV) if this mechanism is to explain the monojets. One would expect a Jacobian peak for $N \to \ell$ + (hadrons), corresponding to half the monojet events, on the basis of the ratios (3). This model predicts

$$B(Z^\circ \to [\text{seen N}] + [\text{unseen N}]) \simeq 6\% \times 2 \times (0.9) \times (0.1) \simeq 1\% \quad . \tag{6}$$

Only half these will look like two-body Z decays since $B(N \to \ell + \text{hadrons}) \simeq 0.5$. Thus a) neutral leptons probably cannot explain all the UA1 monojets unless more than one lepton family is involved, and b) a search for "monojet" decays of Z° should be sensitive at the $B(Z^\circ \to \text{monojet}) \gtrsim 1/2\%$ level to rule out even the most prominent heavy-lepton possibilities. One should see final states rich in leptons, which does not seem to be the case for the typical UA1 events with missing $p_\perp$.

B. $Z^\circ \to SP$ decays, where S and P are scalar and pseudoscalar members of each new Higgs doublet, are expected with a typical rate of $\frac{1}{2}\Gamma(Z^\circ \to \nu\bar{\nu}) \simeq 90$ MeV, or branching ratio of about 3% for $\Gamma_Z = 3$ GeV, as mentioned in Sec. II. A model whereby this process can account for the UA1 monojets has been constructed. [10] The pseudoscalar P weighs a few GeV and gives the jet; the scalar S escapes unseen, living a least a nanosecond. It is probably light ($\gtrsim$ 200 MeV) and weakly coupled to fermions. If, instead, S were required to give the jet and P to be very light and escape, the decay $S \to PP$ would be kinematically allowed. One then would expect $B(S \to PP) \simeq 100\%$, so S would escape too.

One would like a natural way to keep S and P light and weakly coupled to fermions. One example, probably not minimal, may be an $SU(2)_L \times SU(2)_R \times U(1)_{B-L}$ model [38] with charge assignment (1), in which Higgs fields transform under $SU(2)_L \times SU(2)_R$ as $(\frac{1}{2}, \frac{1}{2})$ (conventional), $(\frac{1}{2}, 0)$ (new), and $(0, \frac{1}{2})$ (new). The last two don't couple directly to fermions except via mixing, but the $(\frac{1}{2}, 0)$

can be produced in pairs in Z decays.

What are some early signatures of unusual Z° decays? We shall mention two.

C. $e^+e^- \to Z°(\text{virtual}) \to (\text{any})$ reactions are accessible at present PEP and PETRA energies and luminosities. The cross section for production of any final state f via a virtual Z is

$$\sigma(e^+e^- \to Z_{virt} \to f) = \frac{G_F M_Z \Gamma_Z s}{\sqrt{2}\,(M_Z^2 - s)^2} B(Z \to f)(1-4x+8x^2), \qquad (7)$$

where Γ_Z=3 GeV, $x=\sin^2\theta$=0.22, M_Z=94 GeV, and G_F=1.166 x 10^{-5} Gev^{-2}. This implies the event rates shown in Table 2.

TABLE 2. Events obtainable via virtual Z° decays at e^+e^- machines.

	PEP	PETRA	TRISTAN	
	($\sqrt{s}$ = 29 GeV)	($\sqrt{s}$ = 44 GeV)	($\sqrt{s}$ = 60 GeV)	($\sqrt{s}$ = 70 GeV)
σ/B (pb)	6	19	61	148
Assumed $\int L\,dt(pb^{-1})$	200	100	100	100
Events:				
B= 1%:	12	19	61	148
B= 6%	72	112	366	888

The Mark II detector, as an example, has accumulated 220 pb^{-1} at $\sqrt{s}$ = 29 GeV in four years of running. This has enabled it to perform useful searches for Z° decays to heavy neutral leptons[39] or other unusual final states[40] at a level of $B(Z \to f)$ of a few percent or less.

If unusual Z° decays were responsible for the UA1 monojets, one would see "spread-out" unbalanced jets at PEP or PETRA (since E_{jet} here may not be so much larger than m_{jet}). These would be distributed as $1+\cos^2\theta^*$ (for fermions) or $\sin^2\theta^*$ (for bosons), where θ^* is the angle with respect to the beam. It appears, in fact, that for a wide range of jet masses around 5 GeV, unusual Z° decays already can be ruled out as a source of the UA1 monojets by a search at Mark II.[40]

D. Angular and $p^\perp$ distributions in $\bar{p}p$ collisions. In $\bar{p}p$ collisions, though the Z° is moving, the distribution in laboratory angle θ and transverse momentum $p^\perp$ of its decay products still reflects the underlying θ^* distribution: $1+\cos^2\theta^*$ for fermions (not distinguishing particle and antiparticle) and $\sin^2\theta^*$ for bosons.

Here θ^* is the angle of the Z° decay product in the parton-parton center of mass. For two-body Z° decays, the exact shape of the Jacobian peak will reflect the spin of the decay products.[36] Two θ-$p^\perp$ distributions are compared in Fig. 2.

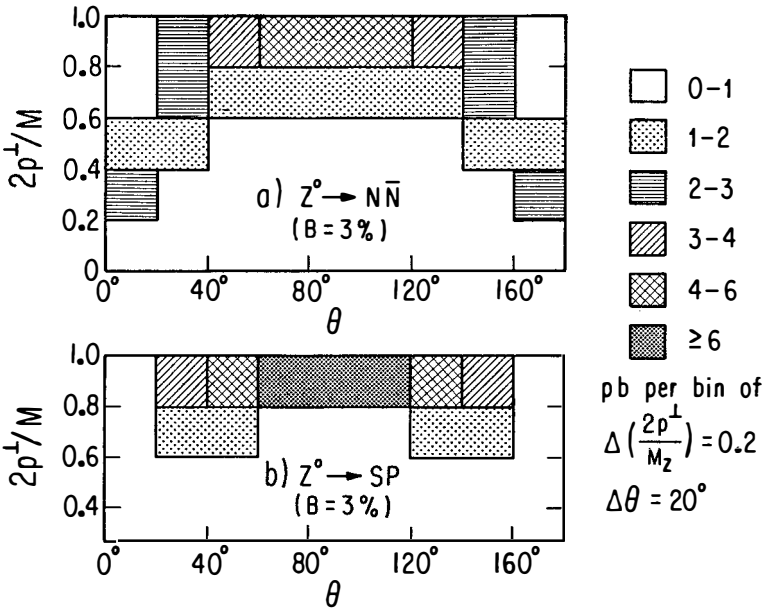

FIG. 2. Distributions in laboratory angle θ and transverse momentum $p^\perp$ of decay products in $\bar{p}p \rightarrow Z^\circ \rightarrow$ a) $N\bar{N}$ (fermions), b) SP (bosons), at $\sqrt{s}$ = 630 GeV. Structure functions and other assumptions are described in Ref. 36.

VI. PROSPECTS AND CONCLUSIONS

Many interesting effects (CELLO event, radiative Z decays, "noisy" Z°'s, jet-jet mass bumps, high-transverse-momentum W's, to name a few) present in 1983 data appear in 1984 to have been tails of conventional distributions.[22,23] So far, the UA1 mono-and dijets with missing $p^\perp$ remain potential signatures of new physics. They are in urgent need of confirmation from some other source. We have suggested some searches that may bear indirectly on the monojets, but are of interest in their own right.

Search for new heavy Z's will rely in the next couple of years both on precision tests of SU(2) x U(1) (as in electroweak asymmetries) and on direct searches, which may be possible up to nearly $M_{Z'}$ = 400 GeV at the Fermilab collider.

Neutral heavy leptons can be produced in pairs at many e^+e^- machines, up to M_N = 35 GeV at TRISTAN. Signatures such as monojets or $\mu\mu$ + (jets) at $\bar{p}p$

colliders are useful in looking for these objects. Improved beam-dump experiments are possible. There exist wide gaps in experimental bounds, which are only just now starting to be filled.

New Higgs bosons will be visible, if they are light enough and are not $SU(2)_L$ singlets, in the decays $Z \to (\text{scalar}) + (\text{pseudoscalar})$. Each such isodoublet beyond the first corresponds to a partial width $\Gamma(Z \to SP) \simeq 90$ MeV, or half the width for a neutrino species. Whether Nature makes use of this interesting source of spinless particles remains to be seen.

ACKNOWLEDGMENTS

I wish to thank M. Gronau, L. Hall, R. Jaffe, Y. Kitazawa, P. Langacker, C.N. Leung, and R. Robinett for enjoyable collaborations on some of the work mentioned here, and K. Eggert, G. Feldman, S. Glashow, H. Kowalski, S. Nussinov, F. Pauss, M. Perl, J. Rohlf, C. Rubbia, X. Tata, R. Thun, and L. Wolfenstein for useful discussions. I am grateful to the theory groups of Tel Aviv University and CERN for their hospitality, and to members of the UA2 collaboration for conversations and for the use of their VAX 11/780 for computations. This work was supported in part by the United States Department of Energy under Contract No. DE-AC02-82ER 40073.

REFERENCES

1] Jonathan L. Rosner, CERN report TH.3998/84, to appear in Comments on Nuclear and Particle Physics.

2] C. N. Leung and J.L. Rosner, Phys. Rev. D28 (1983) 2205.

3] M. Gronau, C.N. Leung, and J.L. Rosner, Phys. Rev. D29 (1984) 2539.

4] D. Wyler and L. Wolfenstein, Nucl. Phys. B218 (1983) 205.

5] C.N. Leung and S.T. Petcov, Phys. Lett. 125B (1983) 461.

6] M. Gell-Mann, P. Ramond, and R. Slansky, in Supergravity, D.Z. Freedman and P. van Nieuwenhuizen eds., (North-Holland, Amsterdam, 1979), p. 315; T. Yanagida, Proc. of Workshop on Unified Theory and Baryon Number in the Universe, O. Sawada and A. Sugamoto, eds., (KEK, Tsukuba, Japan, 1979); Rabindra N. Mohapatra and Goran Senjanovic, Phys. Rev. Lett. 44 (1980) 912; Phys. Rev. D23 (1981) 165.

7] R. Thun, Phys. Lett. 134B (1984) 459; V. Barger et al., ibid. 133B (1983) 449; ibid. 141B (1984) 126; Phys. Rev. D29 (1984) 2020; ibid. D30 (1984) 947.

8] J.C. Pati and A. Salam, Phys. Lett. 58B (1975) 333; J. Maalampi and K. Enqvist, Phys. Lett. 97B (1980) 217; K. Enqvist, K. Mursala, and M. Roos, Nucl. Phys. B226 (1983) 121; K. Enqvist and J. Maalampi, Z. Phys. C21 (1984) 345; M. Roos, Phys. Lett. 135B (1984) 487; F. Wilczek and A. Zee, Phys. Rev. D25 (1982) 553; G. Senjanovic, F. Wilczek, and A. Zee, Phys. Lett. 141B (1984) 389; J. Bagger and S. Dimopoulos, Nucl. Phys. B244 (1984) 247.

9] K. Lane, Proc. of the 1982 DPF Summer Study on Elementary Particles and Future Facilities, ed. R. Donaldson et al., Fermilab, 1983, p. 222; H. Hüffel and G. Pocsik, Z. Phys. C8 (1981) 13; G. Pocsik and G. Zsigmond, Z. Phys. C10 (1981) 367; A. Grau et al., Phys. Rev. D25 (1982) 165; N.G. Deshpande, X. Tata, and D.A. Dicus, Phys. Rev. D29 (1984) 1572; P. Langacker, Proc. of 1984 DPF Summer Study on Elementary Particles and Future Facilities, Snowmass, CO, to be published.

10] S.L. Glashow and A. Manohar, Phys. Rev. Lett. 54 (1985) 526. See also S. F. King, ibid. 528.

11] John Ellis, lectures at Advanced Study Inst., Whitehorse, Canada, Aug., 1984, CERN report TH.4017/84, to be published.

12] F. Bergsma et al., Phys. Lett. 128B (1983) 361; K. Winter in Proc. 1983 Int. Symp. on Lepton and Photon Interactions at High Energies, Ithaca, New York, D. Cassel & D. Kreinick eds., (Lab of Nucl. Studies, Cornell U., Ithaca, 1983), p. 177.

13] J.L. Rosner, E. Fermi Inst. report EFI 84/40 to appear in Phys. Rev. D.

14] D.E. Amidei, Ph.D. Thesis, U. of Calif., LBL report 17795, 1984.

15] H. J. Behrend et al., Phys. Lett. 141B (1984) 145.

16] G. Arnison et al., Phys. Lett. 139B (1984) 115.

17] L.J. Hall, R.L. Jaffe, and J.L. Rosner, CERN report TH.3991/84, to be published in Phys. Reports.

18] R.N. Mohapatra, G. Segre, and L. Wolfenstein, Phys. Lett. 145B (1984).

19] B. Schrempp and F. Schrempp, DESY report 84-117, Dec., 1984.

20] G. Arnison et al., CERN report EP/85-xxx, in preparation.

21] J.L. Rosner, Nucl. Phys. B248 (1984) 503.

22] D. Froidevaux, this conference.

23] J. Rohlf, talks given at conferences in Berkeley and Aspen, Jan., 1985.

24] P. Darriulat, private communication.

25] C. Rubbia, invited talk at Div. of Particles and Fields Meeting, APS, Santa Fe, NM, Oct. 31 - Nov. 3, 1984, to be published.

26] G. Altarelli, R.K. Ellis, M. Greco and G. Martinelli, Nucl. Phys. B246 (1984) 12; G. Altarelli, R.K. Ellis and G. Martinelli, FNAL-Pub 84/107-T., 1984.

27] P. Aurenche and R. Kinnunen, Annecy, LAPP-TH-108 (1984); R. Odorico, U. of Bologna report IFUB 85/1 (1985).

28] E. Reya and D.P. Roy, Phys. Lett. 141B (1984) 442; Phys. Rev. Lett. 53 (1984) 881.

29] J. Ellis and H. Kowalski, Phys. Lett. 142B (1984) 441; Nucl. Phys. B246 (1984) 180; CERN rep. TH.4072 (1984), in preparation.

30] M.J. Herrero et al., Phys. Lett. 132B (1983) 199; ibid. 145B (1984) 430.

31] V. Barger, K. Hagiwara, J. Woodside and W.-Y. Keung, PRL 53 (1984) 641.

32] A. De Rújula and R. Petronzio, in preparation.

33] I thank D. Froidevaux for this observation.

34] L. M. Krauss, Phys. Lett. 143B (1984) 248.

35] M. Gronau and J. Rosner, Phys. Lett. 147B (1984) 217.

36] J. Rosner, CERN report TH.4086/85, to be published in Phys. Lett. B.

37] S.F. King, Harvard report HUTP-84/A084, 1984.

38] G. Senjanovic, Nucl. Phys. B153 (1979) 334.

39] M. Perl, SLAC-PUB-3515 and LBL-18707, 1984, submitted to Phys. Rev. D. Earlier searches for neutral leptons in e^+e^- annihilations have been performed by W. Bartel et al., Phys. Lett. 123B (1983) 353, and by D. Errede et al., Phys. Lett. 149B (1984) 519.

40] G. Feldman, private communication of work in progress.

SEARCH FOR THE TOP QUARK IN W-DECAY

Aachen - Annecy(LAPP) - Birmingham - CERN - Harvard - Helsinki - Imperial College, London - Queen Mary College, London - Kiel - NIKHEF, Amsterdam - Padua - Paris (Coll. de France) - Riverside - Rome - Rutherford Appleton Lab. - Saclay (CEN) - Victoria - Vienna - Wisconsin Collaboration

presented by

Peter Erhard
III.Phys.Inst.A, RWTH Aachen

A clear signal is observed for the production of events containing an isolated lepton and two or more jets. Six events with exactly two jets have an effective mass around the mass of the charged IVB and are consistent with a hadronic decay of the W. Rates and features of the events are incompatible with charm and beauty production. They are, however, consistent with the process $W \to t\bar{b}$, followed by $t \to bl\nu$, where t is the sixth quark of the Cabibbo current. If this is indeed so, the mass of the top quark is bounded between 30 and 50 GeV/c^2.

1. Introduction

In the running period of 1983 with an integrated luminosity of 120 nb^{-1}, the UA1 Collaboration has recorded 68 events with $e\nu_e$ decays[1] of the charged Intermediate Vector Boson (IVB), and a more restrictive sample of $W \to \mu\nu_\mu$ decays[2] (14 events). The charged IVB is expected to couple to charge 2/3 quarks and to the Cabibbo-rotated charge 1/3 quarks with the same strength as to leptons. From the number of observed decays to electrons, taking into account detection efficiency and colour factor, we expect that (255±30) $W \to ud_c$ and the same number of $W \to cs_c$ must also have been produced in the same running period. Unfortunately, the detection of these decays is made very difficult by the presence of a large QCD background.

The decay $W^+ \to t\bar{b}_c$ (and also $W^- \to \bar{t}b_c$), however, where (tb_c) is the third weak isospin doublet of quarks, can provide a clean signature, if the t-quark decays semileptonically:

$$W^+ \to t\bar{b}_c \quad (t \to l^+\nu b_c) \qquad l=(\text{electron,muon})$$

Since previous, unsuccessful searches for the t-quark in e^+e^- colliding beams[3] have established a mass limit of $m_t \geq 22$ GeV/c^2, the t-quark will be relatively slow in the laboratory, and the angles between decay particles will be large. These events will contain two jets, an isolated lepton, and some missing energy. For m_t = 40 GeV/c^2 the number of events is reduced by a factor of 0.71 with respect to massless quarks, giving a total of (181±20) $W \to t\bar{b}_c$ decays from our data sample. Assuming a semileptonic branching ratio of 1/9, as expected from naive quark and lepton counting, we expect (20 ± 2.2) electrons (both signs) and an equal number of muons. With the cuts necessary to ensure good lepton and jet identification and to enhance the signal above the background ($E_T(\bar{b}_c) > 8$ GeV; $E_T(b_c) > 7$ GeV; $p_T(l) > 12$ GeV/c) we arrive at (4 ± 0.3) events in each leptonic channel, before geometrical and track isolation cuts. In order to separate this small signal from the background arising from $(b\bar{b})$ and $(c\bar{c})$ production, a parallel analysis must be performed to extract the properties and magnitude of this

background from the data.

2. The electron sample

Electron identification in the UA1 detector[4] is based on the measurement of momentum (p) from the magnetic curvature in the central detector and on absorption in the 27 X_0 of a 4π lead/scintillator calorimeter hodoscope segmented four times in depth, followed by a hadron calorimeter, in which only a small residual energy E_{had} is expected. Each of the four segments of the lead/scintilator calorimeter cells is read out by four independent photomultipliers in a way that permits the determination, by pulse division, of the centroid of the energy deposition in two orthogonal directions.

In the case of the decay $W \rightarrow e\nu_e$[1], very generous selection criteria were sufficient to obtain an essentially pure event sample, namely:

(i) a charged track of p_T 7 GeV/c, of projected length > 30 cm and at least 20 digitizings,

(ii) an energy deposition of E_T>15 GeV in two adjacent EM cells,

(iii) a match within 5 SD between the impact of the track and the centroid of the energy depositions in the calorimeter,

(iv) an energy deposition E_{had}<600 MeV in the subsequent hadronic calorimeter,

(v) electron isolation, namely no more than 10% of the electron energy is allowed for any additional energy deposited in a cone around the electron track $\Delta R=(\Delta\eta^2 + \Delta\varphi^2)^{1/2}$, where φ is the azimuthal angle measured in radians and η is the rapidity,

(vi) no jet back-to-back in φ with respect to the electron within 30°.

In this way, we have detected **49** $W \rightarrow e\nu_e$ decays, completely background free and satisfying the additional condition $\Delta E_m > 15$ GeV. These events give us an ideal electron calibration sample for the present search.

However, as soon as the limitation on the jet activity and the missing-energy requirement are dropped, we find a much larger sample of presumably heavily contaminated events. Requiring the electron transverse energy $E_T > 12$ GeV and tightening the E_{had} condition to $E_{had} < 200$MeV leaves us with 152 events. A first reduction of the sample can be achieved by removing photon conversions in the beam tube and in the walls of the central detector. These events can easily be recognized, by scanning or program, by looking for tracks which have a small minimum distance D from the electron track. As one can see from fig. 1, there is a large peak centered around D=0, mostly from track pairs having charges of opposite signs. Applying a cut on D at 3σ, forty-three conversions are removed.

The remaining 109 events are still largely contaminated by multiple particle overlaps, namely jets with one charged energetic hadron and one or several π^0's simulating the EM behaviour. In order to eliminate this background, we raise the electron transverse energy threshold to 15 GeV and make use of the full rejection power of the detector, demanding

(i) a good match between momentum measurement and the energy deposition in the calorimeters, $|(1/p)-(1/E)| < 3\sigma$,

(ii) a good electromagnetic shape in the energy deposition in the four EM segments, charactarized[5] by $\chi^2_R < 20$,

(iii) a stricter isolation requirement for the electron track, namely that the $\sum p_T$ of all other tracks and the energy deposited in all calorimeters $\sum E_T$ be less than 1 GeV in a cone of $\Delta R < 0.4$ around the track.

This new selection leads to twelve events, namely seven events with electrons and one jet and five events with at least two jets. Forty-four out of the forty-nine W events survive these cuts. One can compare the distributions of $\sum E_T$ versus χ^2_R for the calibration sample of $W \to e\nu_e$ decays (fig. 2a), the sample of single jets (fig. 2b), and the sample of events with at least two jets (fig. 2c). While both the ≥ 2 jet events and the $W \to e\nu_e$ events have a cleanly isolated electron and small values of χ^2_R,

the single jet events are more widely distributed, indicating that they are not truly isolated. We concentrate on the five events with ≥ 2 jets. Their electron properties closely resemble the ones of the W calibration sample (fig.3).

The shape of the QCD background is obtained from an isolated π^0 + ≥ 2 jet data sample. In fig. 4 E_T^{out}, the transverse energy component of the π^0 perpendicular to the plane formed by the $p\bar{p}$ axis and the highest E_T jet (j1) is plotted as a function of $\cos \theta^*_{j2}$. The angle θ^*_{j2} is between the average ($p\bar{p}$) beam axis and the lowest E_T jet (j2) in the (π^0 j1 j2) rest frame. The five electron + ≥ 2 jet events (fig. 5) are all contained within a region RI=($E_T^{out} > 8$ GeV, $|\cos \theta^*_{j2}| < 0.73$), whereas the majority of background QCD events lie in the complementary region RII. Comparison of shape with the Kolmogorov test gives a proability that the QCD background events have a distribution identical to the five electron + ≥ 2 jet events of $5.2*10^{-4}$, which corresponds to a 3.5 σ difference.

To determine the absolute magnitude of the background from $\pi^{\pm}$+ 2 jet events, we use a $\pi^{\pm}$+ jet data sample and estimate the probability that a $\pi^{\pm}$ satisfies the isolated electron selection criteria. Of the 169 $\pi^{\pm}+\geq 2$ jet events originally selected, 68 satisfy the electron trigger requirement of $E_T > 12$ GeV. The probability that these charged pions fake an isolated electron is estimated to be $1.5*10^{-3}$ (based on test beam measurements), yielding a total of 0.1 background events[6].

3. The muon sample

The set of cuts used to arrive at a sample of isolated muons with one or more jets is as follows:

(i) a track in the muon chambers with a matching track in the central detector, having $p_T > 12$ GeV/c, projected length ≥ 40 cm, and at least 30 digitizings,

(ii) isolation, namely $\sum p_T < 0.1\ p_T(\mu)$, $\sum E_T < 0.2\ p_T(\mu)$, where the sum extends to all tracks and calorimeter hits in a cone of $\Delta R \leq 0.4$.

Forty events survive these cuts. The dominant source of background comes from the decays of pions and kaons in the central detector drift volume. In the case of slow kaons, parent and daughter tracks may form a kink in the track digitizings in a configuration which is reconstructed as a single fake high-momentum track. After visual scanning and rejection of obvious $K \rightarrow \mu \nu_\mu$ decays, and an enhanced isolation requirement of no jet within a distance $\Delta R=1$ around the muon we are left with twelve events, seven with one jet, four with two jets, and one with three jets. Again, we concentrate on the ≥ 2 jet events.

The residual decay background has been determined from a 5 nb^{-1} data sample collected with a low threshold ($E_T > 15$ GeV) jet trigger. This trigger requirement is satisfied by the five muon + ≥ 2 jet events. We wish to estimate the probability that decaying hadrons pass our track-quality cuts and are reconstructed with $p_T > 12$ GeV/c. The background rate is then the convolution of this probability (per decaying hadron) with the measured p_T spectrum of the 5 nb^{-1} sample. For a mixture of 50% pions and 25% kaons, the probability is typically $4*10^{-5}$ for a hadron with a p_T of 8 GeV/c to be reconstructed with $p_T > 12$ GeV/c.

We find that the corresponding number of decay muon + ≥ 2 jet events is 0.4, giving less than 0.1 background events for $|\cos \theta^*_{j2}| < 0.8$. In fig. 5 E_T^{out} is plotted versus $\cos \theta^*_{j2}$ for the five muon + ≥ 2 jet events and the five electron + ≥ 2 jet events. Of the four muon + two jet events, one event is most likely a QCD background event since the lowest E_T jet lies close to the beam axis with $\cos \theta^*_{j2} = 0.93$. This event is removed from the data sample.

4. Backgrounds due to beauty and charm pair production

Having concluded that the signal events are indeed events with genuine leptons, we will now consider the possibility that they are due to the semileptonic decay of b-quarks or c-quarks.

Events with the topology of the signal events occur if the lepton is the leading particle (thus suppressing the isolation veto) and another central jet is produced by higher-order QCD processes, namely

$$\begin{aligned} gg &\rightarrow gb\bar{b}(gc\bar{c}), \\ q\bar{q} &\rightarrow gb\bar{b}(gc\bar{c}), \\ qg &\rightarrow qb\bar{b}(qc\bar{c}). \end{aligned} \qquad (1)$$

In order to estimate this type of background, a direct method has been used, which relies on isolation and topology to distinguish signal from background. To this purpose events containing a muon of $p_T > 12$ GeV/c and at least one jet of E_T 8 GeV have been selected inclusively. In order to evaluate the effect of the isolation cut, we have neglected all particles within a cone of $\Delta R=1$ around the muon. Events with a clear two-jet topology outside this cone have been selected and carefully scanned. In addition to the known, isolated events, 17 other events have been found, in which the muon is accompanied by hadronic activity. These events have all the properties expected from the QCD background processes (1), namely:

(i) the higher E_T jet tends to be back-to-back with the muon in the transverse plane, $\Delta\varphi(\mu j1) \simeq 180°$,
(ii) the soft jet is sharply collimated around the incoming beam directions $|\cos \theta^*_{j2}| \simeq 1$, as expected for gluon jets from initial state bremsstrahlung (fig 6a).

These distributions are completely different from the ones for the isolated events (fig. 6b), which are broader in $\Delta\varphi(\mu j1)$ and flat in $\cos \theta^*_{j2}$. The probability that the two samples have an identical source, is $3*10^{-4}$, equivalent to a 3.6 SD effect. Therefore we conclude that b and c associated processes cannot be the origin of the observed signal.

5. Interpretation of the events

To examine the physical origin of the six events with an

isolated lepton and two jets (one of the events is shown in fig. 7), we have plotted in figs. 8, 9 the invariant mass of the system consisting of the lepton, the jets, and the transverse component of the neutrino. A peak is observed at a value corresponding to the W mass, indicating that the events are compatible with a new, semileptonic decay of the W particle.

In order to test the hypothesis that the events are due to $W \to t\bar{b}$ decays, we evaluate the invariant mass of the system consisting of the lepton, the transverse component of the neutrino, and one of the jets (fig. 9). Choosing the lower-energy jet, we observe a peak around 40 GeV/c^2, whereas the system with the higher E_T jet has a broader distribution extending to higher mass values. We prefer the choice of the lower-energy jet, because Monte Carlo studies have shown that this is the right choice in the majority of $W \to t\bar{b}$ events. These distributions differ strongly from those for non-isolated muons and two central jets ($|\cos \theta^*_{j2}| \leq 0.8$), which are flat for both four-body and three-body mass combinations (fig. 10).

The decay hypothesis $W \to t\bar{b}$ with $m_t \simeq 40$ GeV/c^2 describes all kinematical distributions[7] very well, as shown in fig. 11. We quote a systematic error of ±10 GeV/c^2 in the evaluation of masses from jets, primarily due to uncertanties in the reconstruction of jet energies. Therefore the isolated lepton + 2 jet events are compatible with $W \to t\bar{b}$ decays, with a top quark mass between 30 and 50 GeV/c^2. Combining the number of these events, the number of $W \to e\nu_e$ decays, and the Monte Carlo determined detection efficiency, we evaluate a top semileptonic branching ratio of 0.23±0.09.

6. Conclusions

A clear signal is observed for the production of events containing an isolated lepton and two or more jets. These events are not due to trivial non-leptonic background. Six events with exactly two jets have an effective mass around the mass of the charged IVB and are consistent with a hadronic decay of the W.

Rates and features of the events are incompatible with charm and beauty production. They are, however, consistent with the process $W \to t\bar{b}$, followed by $t \to bl\nu$, where t is the sixth quark of the Cabibbo current. If this is indeed so, the mass of the top quark is bounded between 30 and 50 GeV/c^2.

References

1) UA1 Collaboration, G. Arnison et al., Phys.Lett. 122B (1983); 129B (1983) 273;
C. Rubbia, Experimental observation of events with large missing transverse energy accompanied by a jet or photon(s) in $p\bar{p}$ collisions at $\sqrt{s}$ = 540 GeV, talk 4th Topical Workshop on Proton=Antiproton Collider Physics (Berne, 1984).
2) UA1 Collaboration, G. Arnison et al., Phys.Lett.134B (1984) 469.
3) TASSO Collaboration, M. Althoff et al., Phys.Lett. 138B (1984) 441;
S. Yamada, Proc. 1983 Intern. Symp. on Lepton and Photon interactions at high energies (Cornell, 1983); and DESY report 83-100 (1983).
4) M. Barranco-Luque et al., Nucl.Instrum.Methods 176 (1980) 175;
M. Calvetti et al., Nucl.Instrum.Methods 176 (1980) 255;
IEEE Trans.Nucl.Sci. NS-30 (1983) 71;
M. Corden et al., Phys.Scr. 25 (1982) 5, 11;
K. Eggert et al., Nucl.Instrum.Methods 176 (1980) 217.
5) E. Eisenhandler et al., CERN UA1-TN/84-64 (1984).
6) M. N. Minard, B. Sadoulet and I. Wingerter, Background Study to e + jet events, CERN UA1-TN/84-77 (1984).
7) V. Barger et al., CERN preprint Ref. TH 3972(1984), submitted to Phys.Lett.
8) UA1 Collaboration, S. Geer, Hadronic jet activity associated with intermediate vector boson production at the SPS collider, presented at the 19th Recontre de Moriond (La Plagne, 1984).
9) R. Kinnunen, private communication; and Ph.D. thesis, University of Helsinki (1984), to be published.

Figure Captions

Fig. 1: Identification of π^0 conversions
The minimum distance D (at the point where the tracks are parallel) between the energetic electron candidate and the nearest track in the drift plane of the central detector is shown normalized by the error on this quantity.

Fig. 2: Electron isolation
The electron quality parameter X_R^2 [5] is shown as a function of the energy accompanying the electron in a cone of $\Delta R \leq 0.4$ around the track. This is shown for a) $W \to e \nu_e$ events; b) e + single jet events; c) e + $\geq$ 2 jet events.

Fig. 3: Electron quality
The quality of the electrons in the e + $\geq$ 2 jet sample (shaded) is compared with the control sample of $W \to e \nu_e$ decays. The quality variables shown are: a) the matching between the momentum measurement and the energy deposition in the calorimeters; b) the quality of the matching between the track measured in the central detector and the direction measured by pulse division in each of the four segments of the e.m. calorimeter; c) an over-all quality parameter X_R^2 [5] measuring the electromagnetic shape of the longitudinal shower profile and the pulse sharing between the different calorimeter samples; d) the energy deposited in the hadron calorimeter behind the electromagnetic shower.

Fig. 4: Measured shape of expected QCD background extracted from π^0 + $\geq$ 2 jet events. The transverse energy component of the isolated π^0 perpendicular to the plane formed by the $p\bar{p}$ axis and the highest-E_T jet, E_{T*}^{out} is plotted as a function of cos θ_{j2}^*. The angle θ_{j2} is between the average beam axis in the three-body rest frame and the lowest-E_T jet (j2).

Fig. 5: As fig. 4, but for the isolated electron + $\geq$2 jet events (open circles) and the isolated muon + $\geq$ 2 jet events (full circles).

Fig. 6: Lepton + 2 jet event shape for a) the non-isolated muon sample, and b) the isolated electron and isolated muon samples. The angle in the transverse plane between the lepton and the highest E_T jet, $\Delta\varphi(lj1)$, is shown as a function of cos θ_{j2}^* (see fig. 4). The curves show the expectations[8] for (a) QCD background events from process (1), and (b) $W \to t\bar{b}$ events with a top quark mass m_t = 40 GeV/c^2.

Fig. 7: Graphic display of calorimeter cells ($E_T > 2$ GeV) and charged tracks ($p_T > 1.5$ GeV/c) observed in the UA1 detector for event 7443/509, a $W \to t\bar{b}$ candidate. a) general view, b) view looking along the beam direction

Fig. 8: Four-body versus three-body mass distribution for the six $W \to t\bar{b}$ candidate events. The effective mass of the lepton, the lower-E_T jet, and of the transverse component of the neutrino is plotted against the mass of the lepton, two-jet, transverse neutrino system. The curves show the expected[9] distribution, taking into account the experimental resolution.

Fig. 9: The two solutions for the three-body mass distribution $m(l\nu_T j)$. The mass of the system with the higher E_T jet $m(l\nu_T j2)$ is plotted against the mass of the system containing the lower E_T jet $m(l\nu_T j2)$.

Fig.10: As fig. 8, but for the non-isolated muon events, in which the lower-E_T jet is central ($|\cos\theta^*_{j2}| \leq 0.8$).

Fig.11: Kinematic distributions for the six $W \to t\bar{b}$ candidates, compared with theoretical expectations[7] for a top mass $m_t = 40$ GeV/c^2. (a) Mass distributions for (i) the lepton two-jet system m(j1j2l); ii) the lepton highest-E_T system m(j1l); and (iii) the lepton lowest-E_T jet system m(j2l). (b) Transverse mass distributions defined in ref.7): (i) $m_T(1)$, $m_T^2(1) = m_W^2 + m_b^2 - 2m_W(m_b^2 + \bar{b}_T^2)^{1/2}$, where $\bar{b}_T$ is the transverse momentum of the highest E_T jet, (ii) $m_T(2) = m_T(bl,\nu)$, where $m_T^2(c\nu) = (c_T^0 + \nu_T)^2 - (\underline{c}_T + \underline{\nu}_T)^2$ and $c_T^0 = (\underline{c}_T^2 + m_c^2)^{1/2}$. (iii) $m_T(3) = m_T(\bar{b}bl;\nu)$.

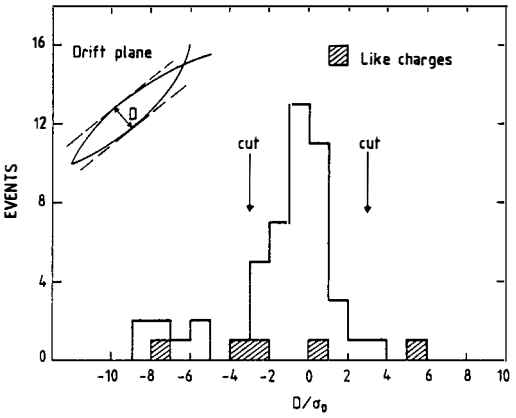
Drift plane
D
Like charges
cut
cut
EVENTS
16
12
8
4
0
-10
-8
-6
-4
-2
0
2
4
6
8
10
D/σD

Fig.1

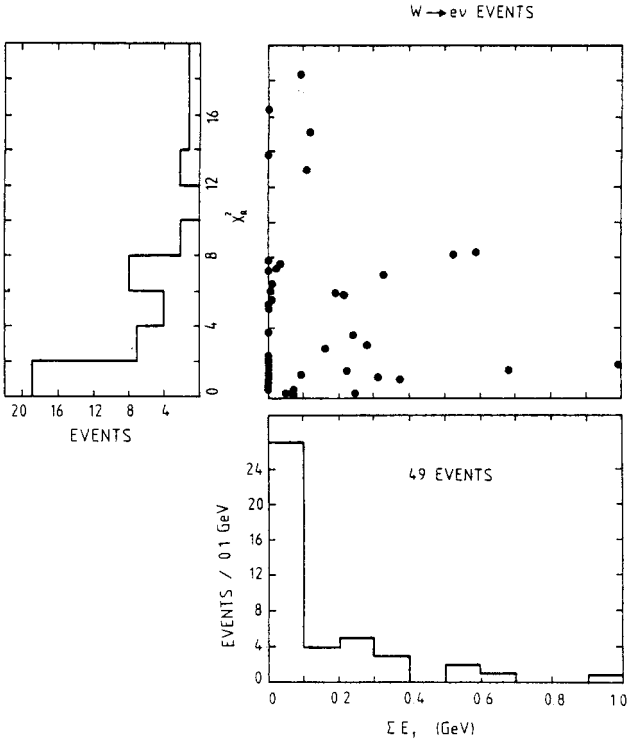
W→eν EVENTS
χ²a
EVENTS
20
16
12
8
4
0
49 EVENTS
EVENTS / 0.1 GeV
24
20
16
12
8
4
0
0.2
0.4
0.6
0.8
1.0
ΣE, (GeV)

Fig. 2a

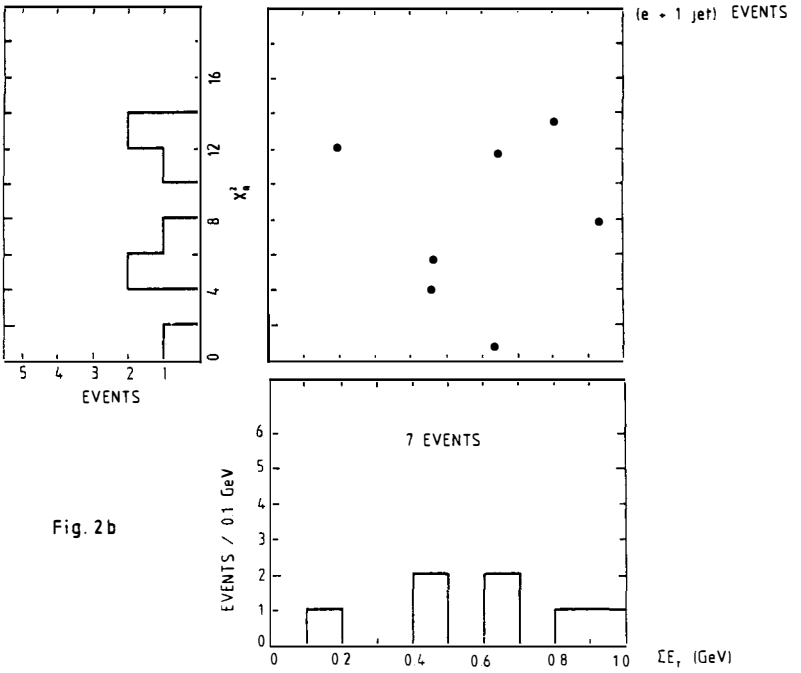
(e + 1 jet) EVENTS
χ^2_n
EVENTS
7 EVENTS
EVENTS / 0.1 GeV
ΣE_T (GeV)

Fig. 2b

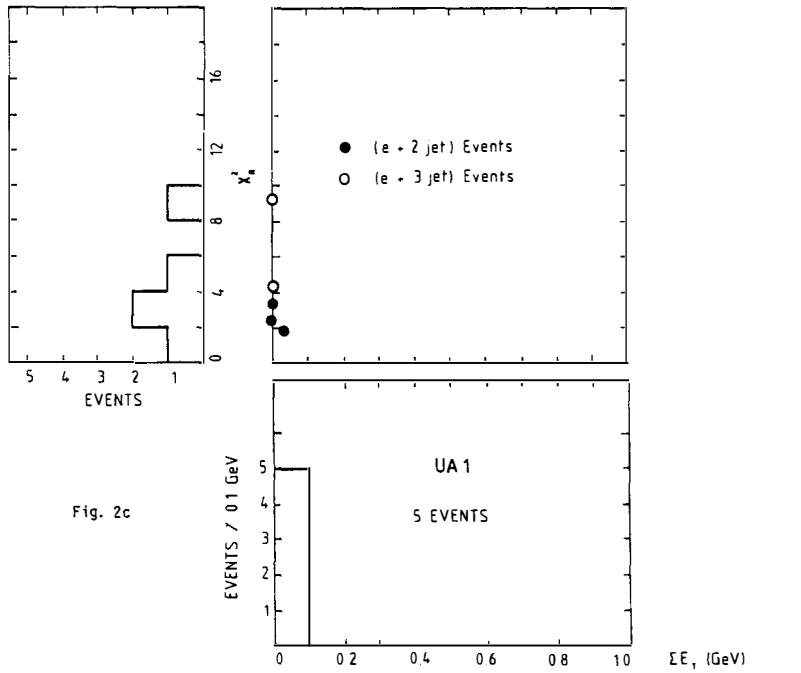
(e + 2 jet) Events
(e + 3 jet) Events
χ^2_n
EVENTS
UA 1
5 EVENTS
EVENTS / 0.1 GeV
ΣE_T (GeV)

Fig. 2c

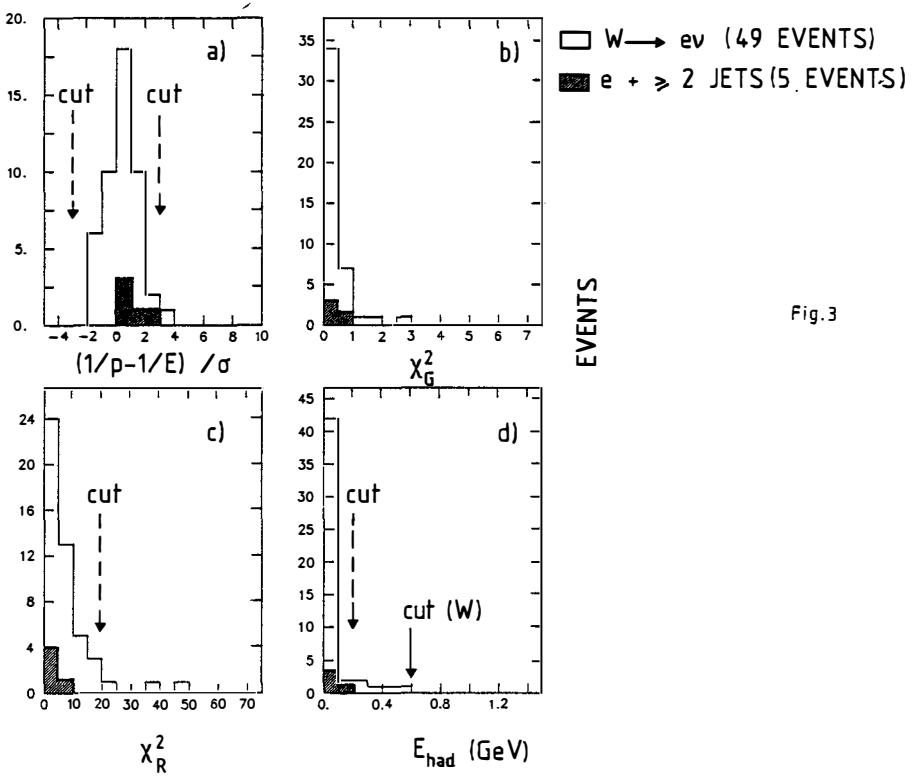
a)
cut
cut
(1/p-1/E) /σ
b)
χ^2_G
c)
cut
χ^2_R
d)
cut
cut (W)
E_{had} (GeV)
W → eν (49 EVENTS)
e + ≥ 2 JETS (5 EVENTS)
EVENTS

Fig.3

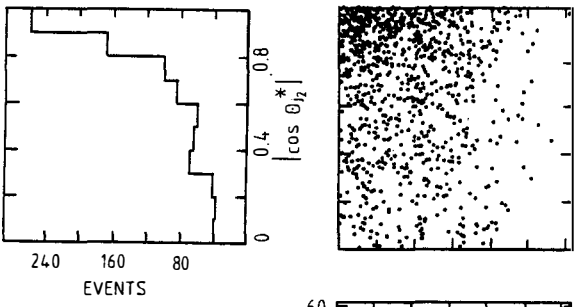
EVENTS
$|\cos\theta^*_{12}|$

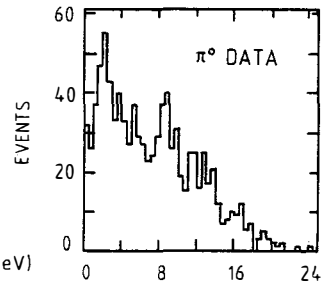
π° DATA
EVENTS
E_T^{out} (GeV)

Fig.4

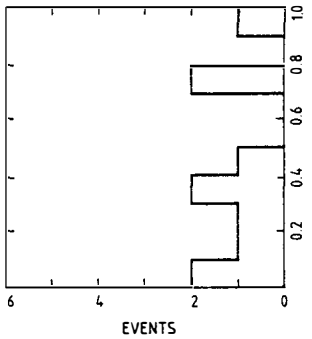

Fig.5

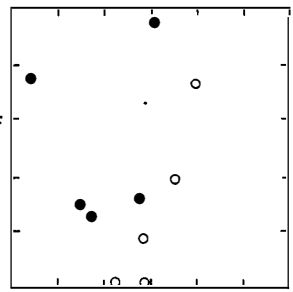

○ e + ⩾ 2 jets

● μ + ⩾ 2 jets

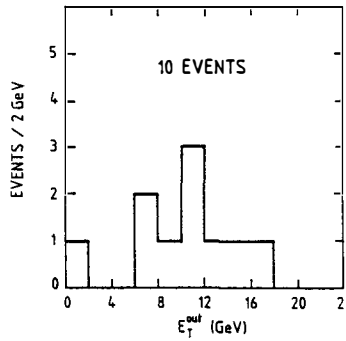

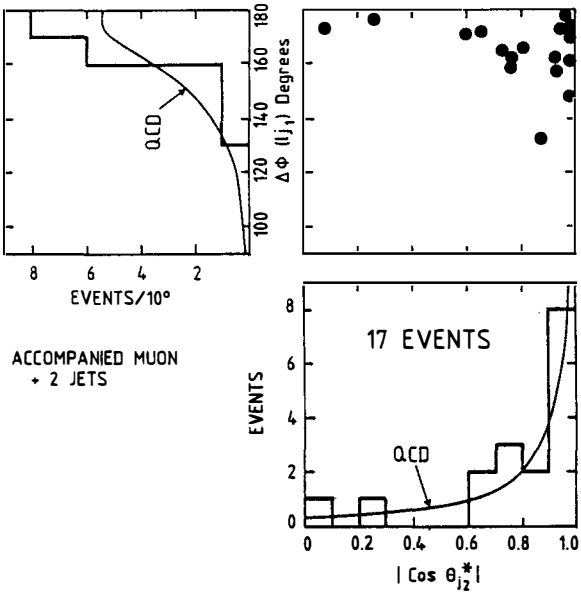

Fig.6a

Fig. 6b

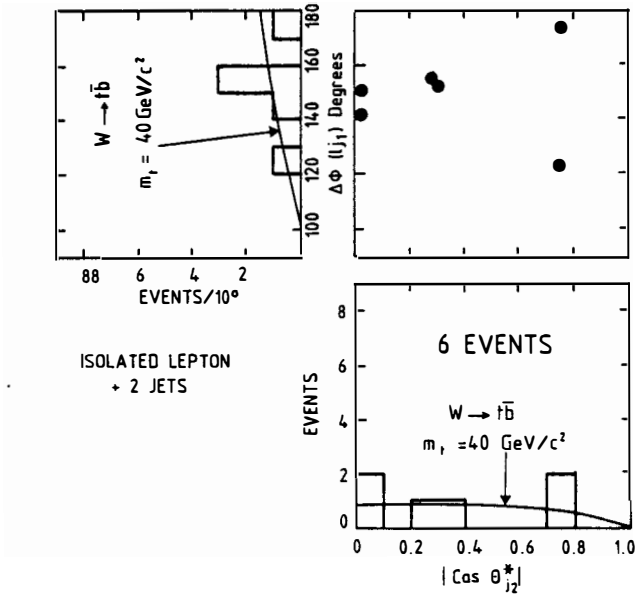
W → tb̄
m_t = 40 GeV/c²
EVENTS/10°
88 6 4 2
100 120 140 160 180
Δφ (l j1) Degrees
ISOLATED LEPTON
+ 2 JETS
6 EVENTS
W → tb̄
m_t = 40 GeV/c²
EVENTS
0 2 4 6 8
0 0.2 0.4 0.6 0.8 1.0
| Cos θ*j2 |

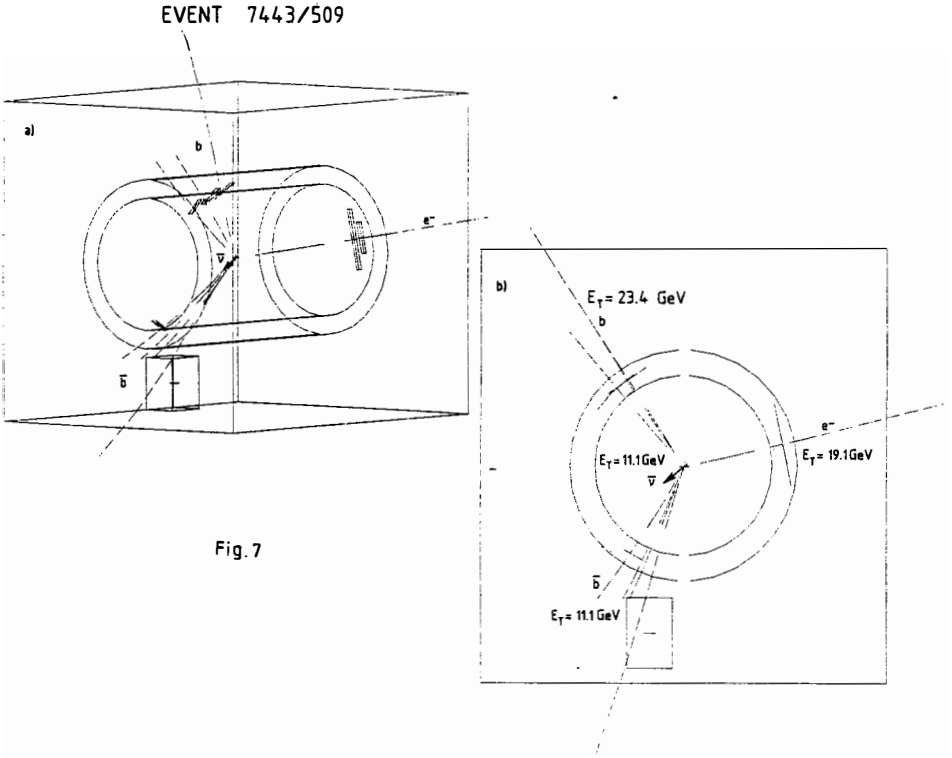
EVENT 7443/509
a)
b
e⁻
ν
b̄
b)
E_T = 23.4 GeV
b
e⁻
E_T = 19.1 GeV
E_T = 11.1 GeV
ν
b̄
E_T = 11.1 GeV

Fig. 7

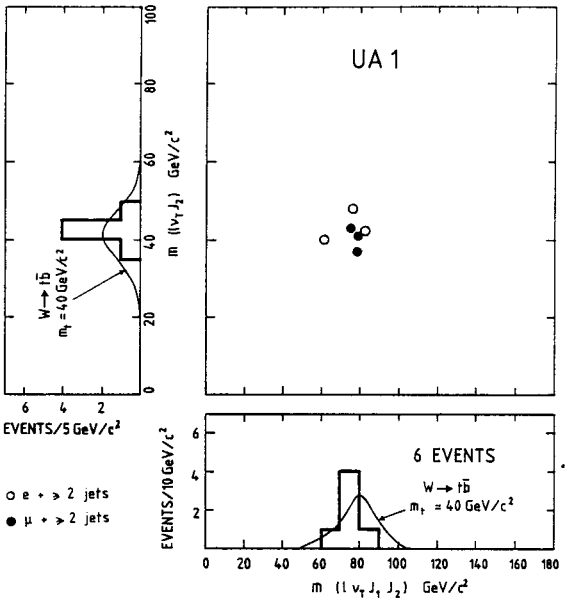
UA 1
m (lν_T J_2) GeV/c²
W → tb̄
m_t = 40 GeV/c²
EVENTS/5 GeV/c²
○ e + ⩾ 2 jets
● μ + ⩾ 2 jets
EVENTS/10 GeV/c²
6 EVENTS
W → tb̄
m_t = 40 GeV/c²
m (l ν_T J_1 J_2) GeV/c²

Fig.8

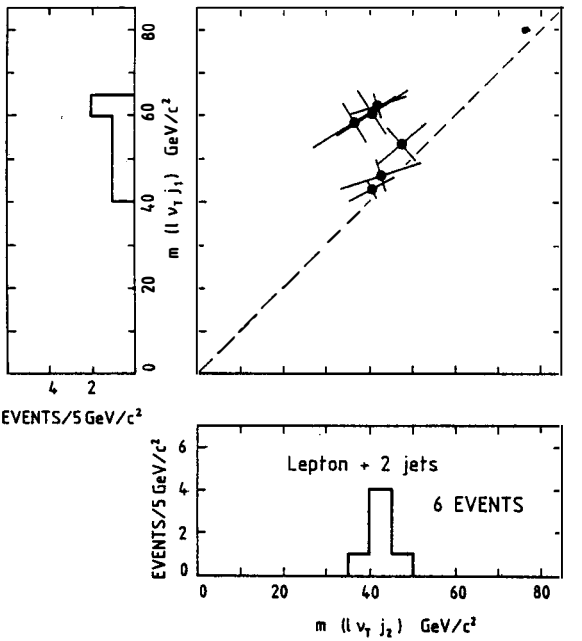
m (l ν_T j_1) GeV/c²
EVENTS/5 GeV/c²
Lepton + 2 jets
6 EVENTS
EVENTS/5 GeV/c²
m (l ν_T j_2) GeV/c²

Fig.9

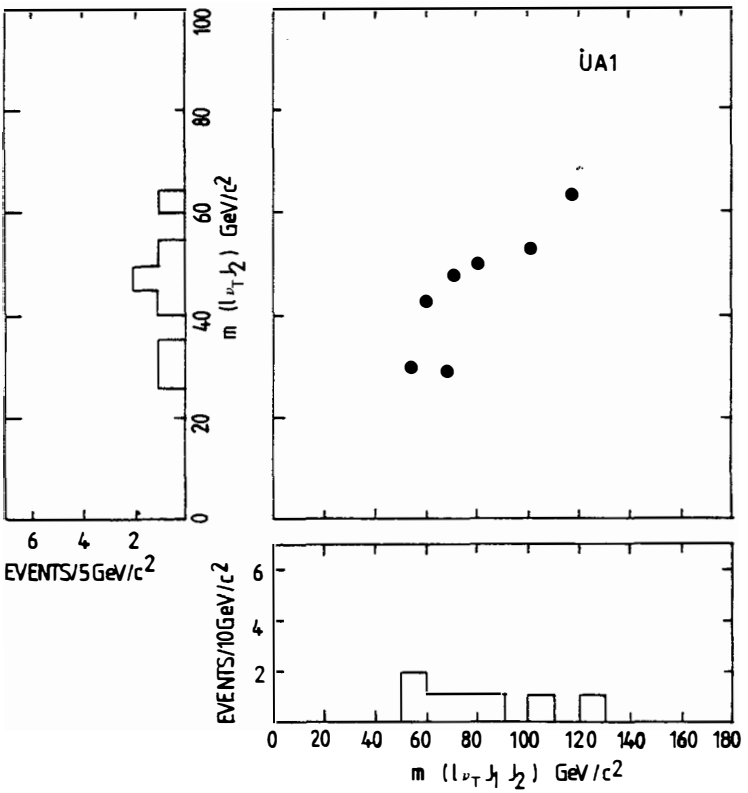
UA1
m (l ν_T J_2) GeV/c²
EVENTS/5GeV/c²
EVENTS/10GeV/c²
m (l ν_T J_1 J_2) GeV/c²

Fig.10

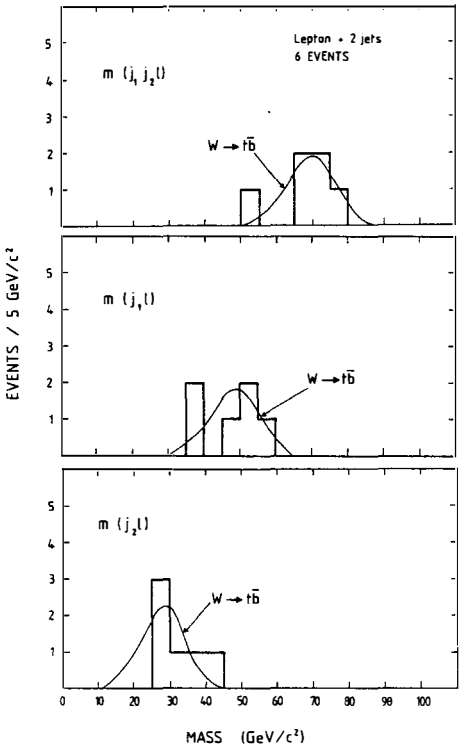

Fig.11a

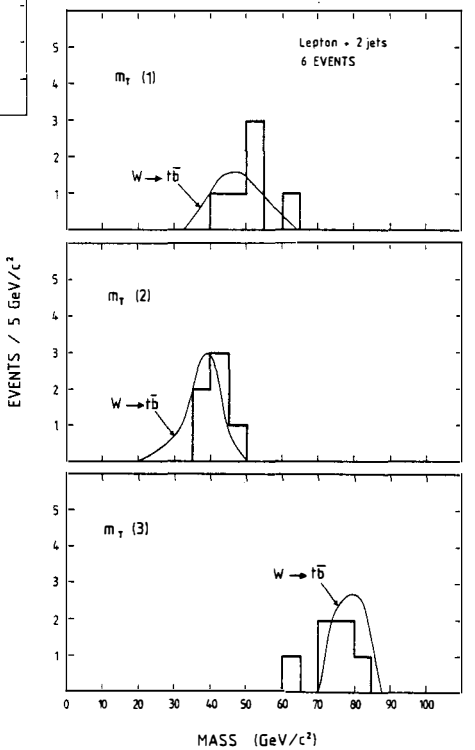

Fig.11b

TOP FLAVOUR PRODUCTION AT $\bar{P}P$ COLLIDER ENERGY

D.P. Roy*
Institut für Physik, Universität Dortmund
4600 Dortmund 50, West-Germany

Abstract

We discuss the question of top flavour production at the $\bar{p}p$ collider energy - first the theoretical expectations based on various top production mechanisms, and then their comparison with the top candidate events recently reported by the UA1 experiment.

*On sabbatical leave from Tata Institute of Fundamental Research, Bombay 400005, India.

Theoretical Expectations

There has been a good deal of interest over the past two years on the question of heavy flavour (particularly top) production at the $\bar{p}p$ collider[1-10]. The main points of interest are (1) what is the most effective signature for heavy flavours - especially top; and (2) what sort of event rates does one expect?

The best way to look for heavy flavour events is to look for large p_T electrons or muons coming from their semileptonic decay. I shall often generically call them electrons. Let us recall that the Kobayashi-Maskawa favoured decays are $T \to Be\nu$, $B \to Ce\nu$ and $C \to Se\nu$. It has been long recognized[11] that for electron $p_T \simeq 15 - 20$ GeV the dominant contributions should come from heavy flavours - charm, bottom and a possible top in the mass range of 30 - 40 GeV. Each of these is expected to be over an order of magnitude larger than the W and the electromagnetic contributions. However, bottom and charm contributions are expected to be somewhat larger than top and hence a serious background to a possible top signal. Several ways to distinguish the top from the lighter flavour contributions have been suggested over the years; but it is generally recognized now that the best signature for top is provided by the track isolation criterion, first suggested in ref. 1.

For the semileptonic decay $Y \to e\nu X$, if the parent mass m_Y is significantly larger than the electron p_T (as in the case of top) then it should come out as an isolated electron; and if the parent mass is significantly smaller (as in the case of bottom) then it should emerge together with the decay hadron jet X within a very small angle.

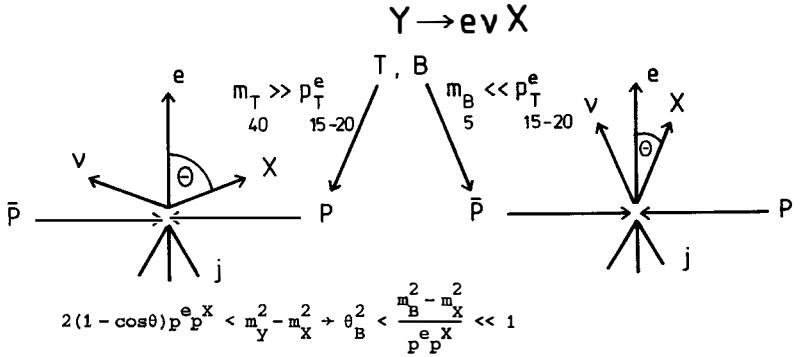

The reason is simply that the eX invariant mass must be less than the parent mass, which is easily satisfied for top ($m_T >> p_T^e$). But for bottom ($m_B << p_T^e$) it means that the opening angle $\theta << 1$ rad for p^X of a few GeV.

For a more quantitative estimate, let us do a simple calculation for electrons coming at 90^o - i.e. in the transverse direction. For the 3 body decay $Y \to e\nu X$, the electron decay momentum in the Y rest frame is $\simeq m_Y/3$. And the large p_T^e cut ensures leading particle configuration for the electron, where both the electron decay momentum and Y production momentum are alligned in the transverse direction. Thus the electron lab. momentum is simply related to its decay momentum by a boost in the transverse direction, i.e.

$$p_T^e \equiv p_e = (m_y/3)[p_y/m_y + \sqrt{1 + (p_y/m_y)^2}]$$

This leads to entirely different configurations for a 40 GeV top and a bottom decay.

Y	m_Y	p_e	p_Y	$p_X^{\parallel} \simeq p_\nu^{\parallel}$	$p_X^{\perp} \simeq p_\nu^{\perp}$
T	40	20	16	-2	~ 10
B	5	20	30	5	~ 4/3

A p_e of 20 GeV corresponds to a p_Y of 16 GeV for top and 30 GeV for bottom, which means that the other two decay particles carry very little (in fact negative) momentum along the electron direction for top but a significant positive momentum (~ 5 GeV) for bottom. In contrast, their momenta in the perpendicular direction ($\simeq \sqrt{2/3} \cdot m_Y/3$) is quite large for top decay and only ~ 4/3 GeV for bottom. Thus for top decay the hadron jet and the neutrino should emerge roughly perpendicular to the electron; whereas for bottom decay they should emerge within roughly 15^o of the electron. And what is true for bottom is of course even more true for charm. We shall see that these features are borne out by detailed calculation involving a variety of heavy flavour production mechanisms.[3,4]

As we have just seen, large p_T electrons correspond to heavy flavour production at large p_T, where perturbative QCD should hold. The relevant production mechanisms are flavour creation, by quark-antiquark and gluon-gluon fusion (Fig. 1a); and flavour excitation, where a perturbatively

evolved heavy quark is stripped off by the hard scattering process (Fig. 1b).[12] We shall consider 2 models for the heavy quark distribution function - (I) a soft distribution function, as given by perturbative QCD[12] and (II) a hard one, as assumed by Barger et al.[13] to account for the diffractive charm production data. The latter is a phenomenological model. To see the uncertainty in these production mechanisms we shall compute the flavour creation contribution for fixed α_s and structure functions ($Q^2 = Q_o^2 \simeq 10\ GeV^2$) as well as those evolving with quark mass ($Q^2 = 4m_Y^2$). For the flavour excitation models the minimum t (which is expected to be of the order M_Y^2 from perturbative QCD) will be varied between $\frac{1}{2}m_Y^2$ and m_Y^2. Finally we consider the heavy flavour production from W decay (Fig. 1c), which should have no major uncertainty, given the phenomenological input of the K factor ($\simeq 2$).

Model	C	B	T(40)
Fl.Cr. Fixed - Evolved	.26 - .30	.60 - .25	.35 - .03
Fl.Ex. I	.28	.35	.15 - .03
Fl.Ex. II	.44	.36	.25 - .08
$-t_o = \frac{1}{2}m_Y^2 - m_Y^2$			
$W \to C\bar{S}$, $T\bar{B}$ (K=2)	.05	.03 - .04	.03 - .04
No. of Events-FC	≥ 25	≥ 25	≥ 3
FE	"	"	"
(L=100/nb) W	5	3-4	3-4

Table I. Charm, Bottom & Top cont. to $p_T^e > 15$ GeV cross-section (nb)

We see from Table I that the flavour creation contribution has typically a factor of 10 uncertainty for top of mass 40 GeV. The flavour excitation contribution for top lies in the same ball park as flavour creation, and similarly for the lighter flavours. The weak production of top is comparable to the conservative estimates of flavour creation and excitation, which correspond however to the canonical choice of model parameters. For a total luminosity of 100 events/nb, characteristic of the presently available collider data, one expects at least 10 top events and a top to bottom (or charm) ratio of 1 to 5. We shall see below that (1) unlike the event

rate, the distinctive configurations of top events are quite model independent; and (2) they can be used to suppress the bottom and charm background by two orders of magnitude without affecting the top signal.

Fig. 2 shows the distribution in the azimuthal opening angle between e and X. Irrespective of the production mechansim, the bottom and charm decay electrons are always accompanied by the decay hadron jet within an azimuthal angle of 15°, whereas they come out with a large opening angle of $\approx 90^{\circ}$ for top. Fig. 3 shows the distributions in the corresponding opening angle in the event plane. The bottom and charm decay electrons are always accompanied by the decay hadron jet X within a rapidity interval of 0.3 units whereas for top the relative rapidity could be anywhere up to 1.5 units. Thus the lighter flavour background can be effectively suppressed by making sure that the electron is isolated to within a $\Delta\phi$ of $\pm 15^{\circ}$ and $\Delta\eta$ of $\pm .3$ units. They can simulate such an isolated electron only if the decay jet X is soft. However, only about 3 - 4 % of bottom and charm events give a $p_T^X < 2$ GeV (Fig. 4). Thus ensuring the accompanying p_T to be less than 2 GeV in the above cone (which corresponds to the isolation cut of the UA1 expt.[14]) should convert the 1 to 5 disadvantage for top to a 5 to 1 advantage. To confirm the top signal, of course, one must see the decay hadron jet of $p_T \sim 8$ GeV coming out at a fairly large angle with respect to the electron. Although the bottom and charm events can simulate such an extra jet through hard gluon emission, it further suppresses the rate by an order of magnitude resulting in a net background $\lesssim 1$ % of the expected signal.[10] Thus an isolated electron plus two jets constitutes a pretty unambiguous signature for top. The instrumental background - i.e. hadrons misidentified as electrons and muons coming from π, K decay in flight - are also estimated to be at the level of a few percent of the signal, thanks again to the track isolation criterion.

The azimuthal separation between the electron and the opposite side jet ϕ_{ej} can be used as a further check on the top signal (Fig. 5). Whereas they emerge essentially back to back for bottom and charm, the top decay events can show a greater deviation from the back to back configuration because of its large Q value. This may be translated into the aplanarity parameter $p_{out}^e = p_T^e \sin\phi_{ej}$, which is bounded by $m_Y/2$ (i.e. ≤ 2 GeV for the lighter flavour background).[5] With precise measurement of missing p_T, the neutrino p_T distribution relative to the electron can also be used as an additional check (Fig. 6). For top the neutrino p_T perpendicular to the

electron is large, and in the parallel direction it can take both positive and negative values. For bottom (and charm) the perpendicular p_T is small and the parallel p_T is positive definite. The $B\bar{B}$ flavour creation followed by simultaneous semileptonic decays can sometimes simulate a missing p_T antiparallel to the electron[8] (dot-dashed line); but there is still an appreciable difference between the top and the bottom configurations. Finally the installation of the UA1 vertex detector, should enable one to identify the 2nd jet as a bottom jet, as expected from top decay.

Table II. Model Independence of Top Events Configuration (m_T = 35). Upper (lower) entries correspond to $p_T^e \geq 15(10)$, relevant for electron (muon) events[4]. m_T = 40 gives similar result.

Average Value	Flav.Cr.	Flav.Ex.I	$W \to T\bar{B}$
p_T^e	20.7- 20.6 16.3- 16.2	20.2- 21.4 16.3- 17.9	20.5 16.5
$p_T^T (=p_T^j)$	31.7- 30.8 26.4- 25.4	26.8- 34.1 25.o- 33.0	27.9 25.9
p_T^X	11.5- 11.3 11.9- 11.6	9.5- 11.3 10.8- 12.3	9.7 11.3
$p_T^{\nu\parallel}$	4.0- 3.6 2.8- 2.4	2.0- 4.8 2.1- 5.1	2.4 2.6
$p_T^{\nu\perp}$	6.4- 6.3 6.9- 6.7	6.4- 7.0 6.8- 7.5	6.5 7.0
ϕ_{eX}	75^o - 77^o 82^o - 84^o	80^o - 67^o 82^o - 67^o	80^o 82^o
ϕ_{ej}	160^o -159^o 147^o -146^o	159^o -161^o 150^o -155^o	159^o 148^o
$M_T(e\nu X)$	28.4- 28.5 28.3- 28.4	28.8- 27.8 28.2- 27.5	29.0 28.8
$M_T(e\nu Xj)$	92.4- 91.3 85.7- 84.5	66.8- 78.7 63.4- 76.6	69.1 65.9
η_{e^-}	o o	o o	0.3 0.4

Table II shows that all the kinematic quantities for top events are practically independent of the production model and choice of model parameters. The eνX transverse mass shows the Jacobian peak near the parent top mass, which can be used to estimate it. For $W \to T\bar{B}$ events, there is a Jacobian peak in the overall 4 body (eνXj) transverse mass near m_W. But this may not be able to distinguish the weak from the strong production events since the latter also show peaks in the same region. Similarly the weak production has a finite electron positron asymmetry; but the effect is too small to be able to distinguish the weak from the strong production events, at least with the present statistics. By far the best distinction between the different production mechanisms is provided by the opposite side jet topology. For flavour creation, the 3 body decay of the recoiling $\bar{T}$ is expected to sometimes simulate an additional jet, resulting in a lepton plus 3 jets. One expects no such events for weak production or flavour excitation. (For flavour excitation, the associated $\bar{T}$ is expected to emerge along the beam line; but some of its decay fragments should show hits in the forward detectors.)

In summary: (1) Isolated large p_T electrons and muons provide effective signature for a top particle of mass ~ 40 GeV. Demanding the accompanying p_T to be < 2 GeV, within a cone of $\Delta\phi = \pm 15^o$ and $\Delta\eta = \pm 0.3$, reduces the total bottom and charm background to less than half the size of the expected top signal. (2) To confirm the signal, of course, one must see the decay hadron jet X, emerging at a moderately large angle with respect to the electron, in addition to the opposite side jet. (3) Further tests are provided by the azimuthal correlation between p_T^e and p_T^j (opposite side jet p_T) as well as between p_T^e and p_T^ν (missing p_T). (4) Top mass can be estimated from the Jacobian peak in the eνX transverse mass. (5) The opposite side jet topology can distinguish between the different production mechanisms.

Comparison with the UA1 Data

Table III. No. of isolated lepton plus n-jet events, with $p_T^{\ell} \geq 15$ GeV and $p_T^{j} \geq 8(10)$ GeV

No. of jets (n)	No. of Pred. Events (m_T=40) $W \to T\bar{B}$	Flav.Cr.	Flav.Ex. I	No. of Exptl. Events
1	1·1 (1·7)	·6 (1·0)	1·6 (1·9)	-
2	2·6 (2·0)	2·6 (2·8)	2·8 (2·5)	6
3	-	1·6 (1·1)	-	3
4	-	·2 (·1)	-	-

Table III compares the 6 isolated lepton plus 2-jet events and 3 isolated lepton plus 3-jet events, recently reported by UA1 (the latter have not been subjected to as detailed a background analysis as the former),[14] with the corresponding predictions from various top production mechanisms with canonical choice of model parameters.[15] The $W \to T\bar{B}$ rate, which is fairly reliable, can account for about half the observed lepton plus 2-jet events, but no lepton plus 3-jet event. Hard gluon radiation can give an extra jet; but the rate is about 10 % - i.e. < 0.3 event. The flavour creation rate is less certain; but the predicted ratio of 2 to 3 jet events ($\simeq$ 2:1) should be quite reliable. If one assumes the 3 lepton plus 3-jet events to be genuine top events and allows for a fluctuation of at most a factor of 2, then at least half the lepton plus 2-jet events should come from flavour creation. The flavour excitation has of course even a larger uncertainty; but one already sees from comparing the other two with data that there is not a very large room for flavour excitation. Within the uncertainties, it can be anywhere between 0 and the listed value.

One sees from Figs. 7-11 that the kinematic distributions of the 6 lepton plus 2-jet events are in reasonable agreement with the theoretical expectations for top from either production mechanism - weak or flavour creation[15] (see also refs. 16,17). The 3 lepton plus 3-jet events are also compatible with the flavour creation predictions. The azimuthal separation between the lepton and the hardest jet shows a broad backward peak as expected from either production model of top (Fig. 7). Fig. 8 shows the

corresponding lepton p_{out} distribution. One may note that all but one event have $p^{\ell}_{out} > m_B/2$. The hardest jet p_T distribution agrees with the theoretical expectations (Fig. 9), bearing in mind a 20 % uncertainty in the jet p_T measurement. The distribution in mass of the 3 body system - lepton, lower p_T jet (j_2) and missing $p_T(\nu_T)$ - shows the characteristic peak at $m_T \simeq 40$ GeV, again in agreement with either production model (Fig. 10). There is however an uncertainty of ±10 GeV in the mass measurement arising from that of the jet p_T measurement, which simplies $m_T = 40 \pm 10$ GeV. The corresponding mass distribution of the overall 4-body system, $m(\ell j_1 j_2 \nu_T)$, peaks around m_W as expected from the weak production model (Fig. 11). One should note however that the flavour creation contribution also peaks in the same region. The difference between the two peak positions is compatible with the measurement uncertainty of ±10 GeV; and even the apparently substantial difference between the two widths can not be discriminated by the present data at a 1σ level. In any case, an equimixture of the two contributions would give a perfectly satisfactory bit.

In summary: The kinematic features of the 6 isolated lepton plus 2-jet events from UA1 are in good agreement with the theoretical expectations of a 40 ± 10 GeV top, for either weak ($W \to T\bar{B}$) or strong (flavour creation) production mechanism. The 3 isolated lepton plus 3-jet events are also compatible with the flavour creation prediction. The relative size of the two contributions may be estimated from the event rate as well as the relative number of 2 to 3 jet events. Both seem to suggest roughly equal contributions from the two mechanisms to the lepton plus 2-jet events.

References

1. R.M. Godbole, S. Pakvasa, D.P. Roy, Phys. Rev. Lett. 50, 1539 (1983).
2. V. Barger, A.D. Martin, R.J.N. Phillips, Phys. Lett. 125B, 339, 343 (1983); Phys. Rev. D28, 145 (1983).
3. D.P. Roy, Z. Phys. C21, 333 (1984).
4. J. Lindfors, D.P. Roy, Z. Phys. C24, 271 (1984).
5. B.R. Desai, J. Lindfors, Phys. Lett. 131B, 217 (1983).
6. L.M. Seghal, P.M. Zerwas, Nucl. Phys. B234, 61 (1984).
7. R. Horgan, M. Jacob, Nucl. Phys. B238, 221 (1984).
8. G. Ballocchi, R. Odorico, Phys. Lett. 136B, 126 (1984).
9. V. Barger, H. Baer, A.D. Martin, R.J.N. Phillips, Phys. Rev. D29, 887 (1984);

F. Halzen, D.M. Scott, Phys. Lett. 129B, 341 (1983);
K. Hagiwara and W.F. Long, Phys. Lett. 132B 202 (1983);
I. Crewther-Rose, Phys. Lett. 140B, 101 (1984);
R. Odorico, Nucl. Phys. B242, 297 (1984);
M Chaichian et al., Phys. Rev. D30, 1894 (1984);
J.H. Kühn, Fermilab Pub. 83/79 (1983);
P. Aurenche, R. Kinnunen, K. Mursula, LAPP-TH-106 (1984).

10. V. Barger et al., Phys. Rev. D29, 1923 (1984);
I. Schmitt et al., Phys. Lett. 139B, 99 (1984).

11. S. Pakvasa, M. Dechantsreiter, F. Halzen, D.M. Scott, Phys. Rev. D20, 2862 (1979).

12. B. Cambridge, Nucl. Phys. B151, 429 (1979).

13. V. Barger, F. Halzen, W.Y. Keung, Phys. Rev. D24, 1428 (1981).

14. UA1 Coll.: G. Arnison et al., Phys. Lett. 147B, 493 (1984);
C. Rubbia, Proceedings of the 11 Intl. Conf. on Neutrino Physics and Astrophysics, Dortmund 1984 (ed. K. Kleinknecht and E.A. Paschos), p.1.

15. R.M. Godbole, D.P. Roy, DO-TH 84/25 (1984).

16. V. Barger, A.D. Martin, R.J.N. Phillips, CERN.TH.3972 (1984).

17. R. Kinnunen, Helsinki Univ. Ph.D. thesis, HU-P-D41 (1984).

Figure Captions

1. Typical (a) flavour creation and (b) flavour excitation contribution to heavy flavour production. (c) Heavy flavour production via W decay.

2. Relative azimuthal distribution between the electron and the decay hadron jet X for charm, bottom and top. The normalizations correspond to the canonical choice of model parameters. The solid, long dashed and short dashed lines correspond to flavour creation, flavour excitation model I and weak production. The flavour excitation model II gives similar distributions.[3]

3. Relative pseudorapidity distribution between the electron and the decay hadron jet X for charm, bottom and top, with the line convention of Fig. 2 and free normalization.

4. Decay hadron jet p_T distribution for charm, bottom and top, with the line convention of Fig. 2. The flavour excitation contribution for charm (not shown) is very similar to the flavour creation.

5. Relative azimuthal distribution between the electron and the opposite side jet ϕ_{ej} for bottom, charm and top, with the line convention of Fig. 2.

6. The missing p_T (p_T^{ν}) distribution (a) parallel and (b) perpendicular to the electron in the flavour creation model (other models give similar result). The effect of the simultaneous semileptonic decay of the anti-bottom is shown by the dot-dashed line.

7. Comparison of weak (W) and flavour creation (FC) model predictions with the distribution of the isolated lepton plus 2-jet events in $\phi_{\ell j_1}$ - azimuthal angle between lepton and the hardest jet. The isolated lepton plus 3-jet events (arrows) are also compared with the corresponding flavour creation prediction (dashed line). The same conventions

are followed in the following figures.

8. Distributions in p_{out}^{ℓ} - lepton momentum normal to the beam and hardest jet plane.
9. Hardest jet p_T distributions.
10. Mass distribution of the 3-body system - lepton, softer jet (j_2) and missing $p_T(\nu_T)$.
11. Distribution in the overall 4-body mass $m(lj_1j_2\nu_T)$ [5-body mass $m(lj_1j_2j_3\nu_T)$ for the lepton plus 3-jet events].

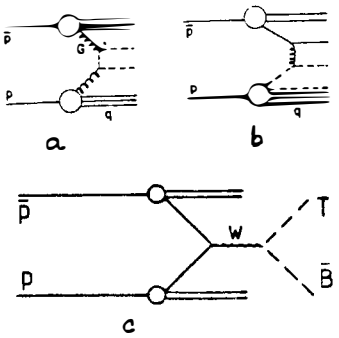

Fig. 1

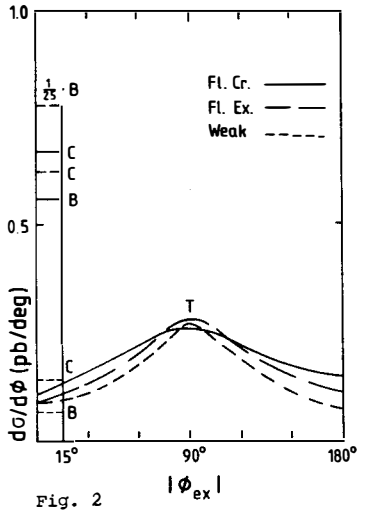

Fig. 2

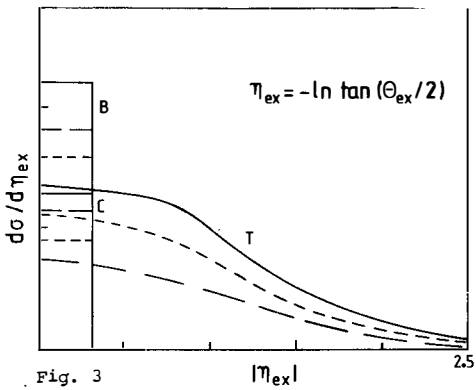

Fig. 3

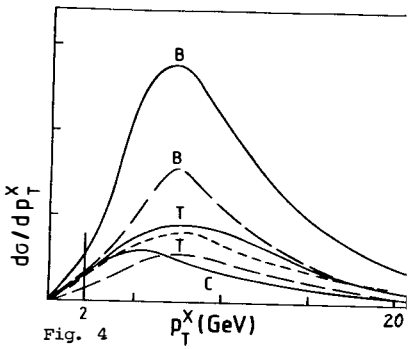

Fig. 4

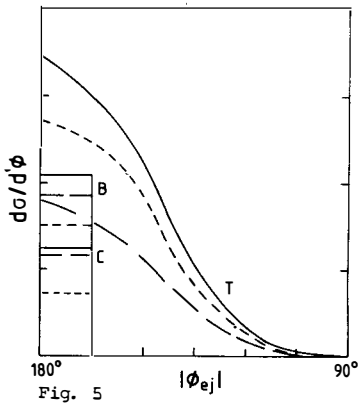

Fig. 5

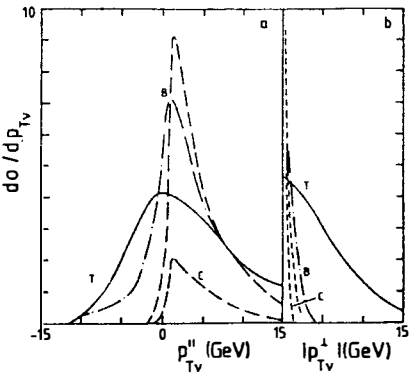

Fig. 6

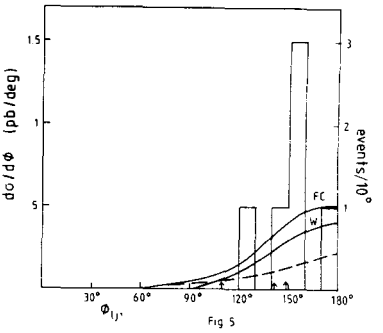

Fig. 7

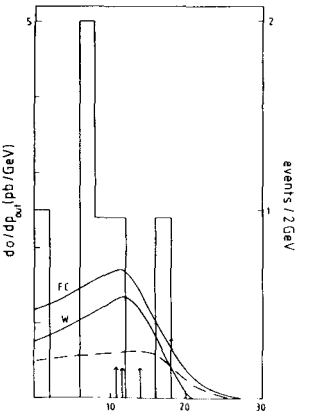

Fig. 8 P_{T}^{l} (GeV)

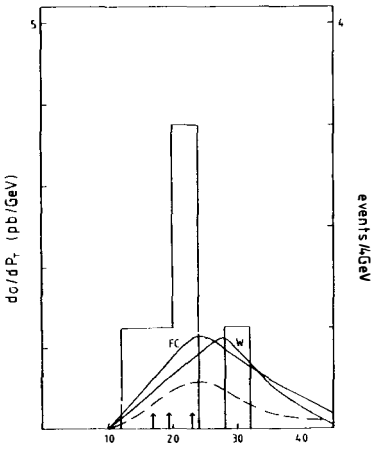

Fig. 9 $P_T^{j_1}$ (GeV)

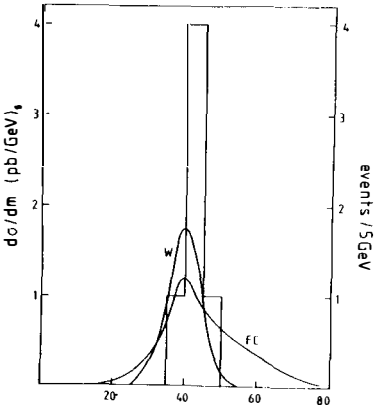

Fig. 10 $m(l j_2 \nu_T)$ in GeV

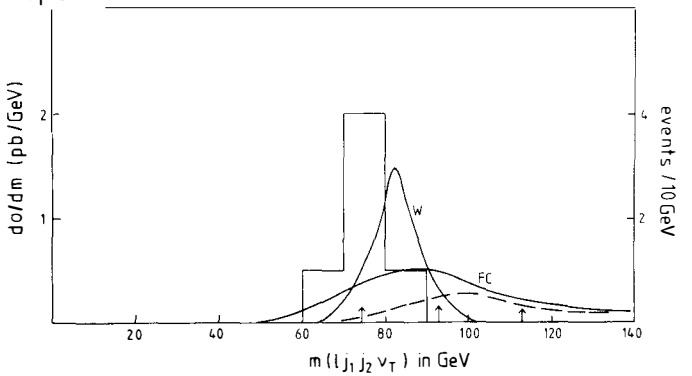

Fig. 11

HEAVY QUARKS AND CP: MORIOND '85

J. D. Bjorken
Fermi National Accelerator Laboratory
Batavia, Illinois 60510

Abstract

The presentations at the Fifth Moriond Workshop on Heavy Quarks, Flavor Mixing, and CP Violation (La Plagne, France, January 13-19, 1985) are summarized. The table of contents is as follows:

CONTENTS

I. INTRODUCTION

The task of this report is to summarize the many excellent contributions to this workshop. As is usually the case, a summarizer carries this through in accordance with biases based on his or her personal experience. This case is no exception, and I shall begin by explicitly stating a bias of my own, a bias influential in my wanting very much to participate in this meeting.

At present Fermilab is beginning the experimental program with its new superconducting accelerator, the Tevatron. There exist several fixed-target experiments devoted to the subject matter of this workshop. Beyond them, I believe there exists much future potential in this field--although any future generations of experiments are sure to be quite difficult. Herein lies the problem: Fermilab--and the experimental community itself--must project its plans well into the future. The question of program balance--in particular, fixed-target experiments versus colliding-beam facilities--becomes an important one. It is not only the laboratory priorities and those of the national funding agencies that enter, but those of the physicists themselves: is there the interest, and especially the necessary manpower, in the community to do this kind of work? And underlying all these questions is the most important one: how important are the physics goals themselves? The physics goals are the subject of this workshop, and one which therefore especially commands my interest.

This summary will be divided into three parts: "What's New?", "Why is All This Being Done?", and "What Next?".

II. WHAT'S NEW?

We classify this section according to quark type, beginning with the heaviest, and ending with the lightest.

A. Beyond the Top

Alas, nothing experimental was reported to this meeting. We perhaps must await the TeV I collider--or later--for that. However, there seems to be a

revival of interest in the 4th generation by theorists.[1] As best as I can tell, this comes from two sources. The first is the diminished confidence in "naive SU(5)" (proton-decay is behind schedule) which argues for no more than 3 generations. The other is the squeeze (more later) on the parameters of the Kobayshi-Maskawa matrix from measurements of B lifetime, ε'/ε, $b \not\to u l \nu$, and m_t. There may need to be a position of retreat for the standard model. An extra generation, with its extra degrees of freedom, can provide this.

B. Top Quarks

There is as yet nothing new experimentally on the status of the top from the latest $S\bar{p}pS$ running period. Both Erhard[2] and Roy[3] displayed confidence in the interpretation of the original events as being evidence of t quark production, with Roy emphasizing that roughly half of the six events could be from strong production of $t\bar{t}$. Meanwhile theorists[4] anticipate with pleasure the observation of toponium in e^+e^- collisions at LEP. In Europe the emphasis naturally rests on interpretation of LEP-induced phenomena. However, SLAC's SLC will be there sooner, and may be occasionally obliged to run below the Z° if its klystrons have trouble living long enough under the high-powered operating conditions required of them. Toponium searches (even with poorer resolution) would then be an especially attractive way to pass the time. The method of choice would seem to be to look for non-collinear events from single-quark decays of toponium as well as from open $t\bar{t}$ production. Any discontinuity in phenomenology (even without resolution of individual levels) in onium vis-a-vis open $t\bar{t}$ production will be of special interest for that application.

C. Bottom Quarks

There is no shortage of rather fresh data on bottom. These data may be classified into several categories:

1. Onium properties

Other than the absence[5],[6] of $\Upsilon(1S)$ decay into γ plus higgs, I did not discern much new news on properties of $\Upsilon(nS;\ n \leq 3)$. But major news exists beyond the 4S, where much structure in the total cross-section (Fig. 1) is observed[7] at CESR. At the minimum the 5S and 6S seem to be seen, with perhaps more levels present. Ono[8] prefers an interpretation which includes a "hybrid" $Q\bar{Q}g$ state (string vibration?) while others claim such a state is not necessary. In general, it must be agreed by all that coupled-channel analyses involving the open $B\bar{B}$, $B\bar{B}^*$ channels as well as the usual "theorists'" $b\bar{b}$ channel are mandatory. This leads to unitarity corrections[9] to levels and potential as well. I am loath here to suggest any critical judgment. The job is in good hands and needs some maturation.

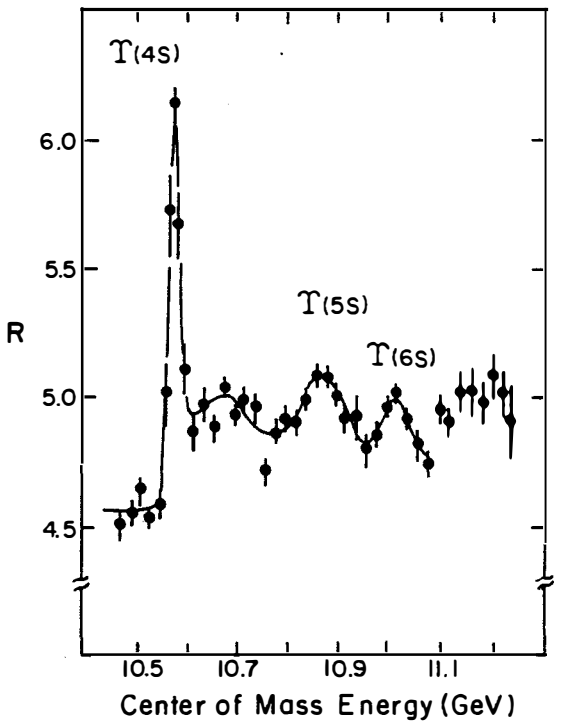

Fig. 1. Total e^+e^- cross-section in the energy region at and above $\Upsilon(4S)$. (From Ref. 7).

2. $B^* \to B\gamma$

Along with the 5S and 6S resonances has come the observation of γ-rays clearly associated with production of B^* ($J = 1^-$) and its radiative decay into B. The mass difference[10]

$$M(B^*) - M(B) = 52 \pm 2 \pm 4 \text{ MeV}$$

is a value not unwelcome to theorists.[11]

3. Semileptonic B decays

While there is nothing very new here, the well-established data on $B \to 0,0^*l\nu$ (with little if any excitation of charm states more massive than D^*) is most important in establishing expected partial semileptonic widths. The 4% limit on $\Gamma(b\to u)/\Gamma(b\to c)$ is likewise central to much of the material of this workshop. Since both measurements, along with those of the B lifetime, impact directly on the experimental determination of the Kobayashi-Maskawa parameters, it is clear that improvement of these measurements remains of high priority.

4. Inclusive decays $B \to D,D^* + \text{"W"}$

While not given much emphasis at the workshop, CLEO measurements[12] of D,D^* inclusive spectra at the T(4S) are of special interest. They indicate consistency with a "factorization" model

$$B \to D,D^* + \text{virtual } W \longrightarrow \text{hadrons}$$

with the mass-spectrum of virtual W the same as that of the $l\nu_l$ system produced in semileptonic decays. For the record, Fig. 2 shows a sketch of that spectrum. Simulation of the non-leptonic events under this hypothesis shows consistency of event properties (e.g., multiplicity) with this model. These observations are especially relevant to properties of exclusive decays of charm and bottom mesons, as analyzed by Bauer & Stech.[13]

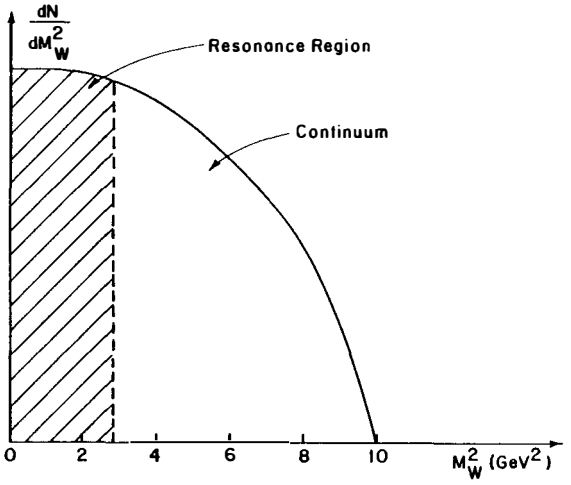

Fig. 2. Expected mass-spectrum of "virtual W" in B → D,D* + "W" decays.

5. Exclusive B-decays

It is a happy circumstance that, with such a large parent mass, exclusive B decay channels have been found,[14] such as

$B^+ \to D^0\pi^+$ 4.2 ± 4.2 %

$B^0 \to D^0\pi^+\pi^-$ 13 ± 9%

Also noteworthy is the determination of

$\bar{B}^0 \to D^{*+}\pi^-$ 2.1 ± .6 ± .5%

by indirect means utilizing the special kinematic properties of D* cascade decay and $B\bar{B}$ production at the T(4S). The limit

$\Gamma(B \to \psi x) < 1.6\%$

may portend[15] small branching ratios for exclusive channels such as

$B \to \psi K$

ψK^*

6. B lifetime

By now there are (at least) 5 measurements of the B-lifetime[16] in e^+e^- collisions at PEP/PETRA energies. All of them rely on a statistical analysis of many events, i.e., a shift from zero of an impact parameter distribution by an amount small compared to the width but the results are consistent with each other. Peter Cooper has at this meeting combined the newest results, giving a weighted average of impressive accuracy:

$$\tau_B = (1.26 \pm 0.19) \times 10^{-12}\text{sec.}$$

Nevertheless, residual discomfort exists. A cynic may point out that experiments with better resolution tend to give smaller values for the lifetime. Peter Cooper has kindly analyzed the data as function of σ_δ, the resolution in impact parameter. The results are shown in Fig. 3. Fits linear in σ_δ extrapolate to a lifetime value $(0.79 \pm 0.23) \times 10^{-12}$sec. A super-cynical fit constrained to $\tau_B = 0$ at $\sigma_\delta = 0$ is not ruled out either. These fanciful excursions probably should not be taken too seriously. But a few individual bubble-chamber quality events with "visual" B-decays would be very reassuring.

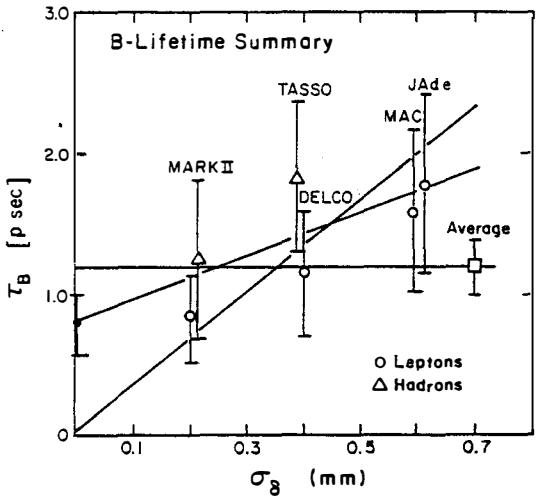

Fig. 3. B-lifetime versus impact-parameter resolution σ_δ.

D. Charm Quarks

1. D decays

Appropriate to this mountain setting (except, alas, for the paucity of new snow) was the avalanche of new D-decay properties provided by[17] the Mark III group at SPEAR. This experimental avalanche was met by a theoretical one of Bauer & Stech,[13] who provided a catalogue of predictions which seem to work quite well (cf Table I), to which we return later. The systematics of D-decays is reaching a new level of maturity.

Table I

A sampler of predicted F and D decay branching ratios (from Ref. 13).

Cabibbo Allowed		Cabibbo Suppressed	
$D^0 \to K^{*-}\rho^+$	9.2%	$D^0 \to \eta\omega$	0.55%
		$\eta'\omega$	0.55%
$F^+ \to \eta\rho^+$	6.7%	$\eta\eta$	0.1%
$\eta'\rho^+$	3.7%		
$K^+\bar{K}^{0*}$	4.9%	$D^+ \to K^+\bar{K}^{0*}$	0.7%
$K^{+*}\bar{K}^{0*}$	4.3%	$K^{+*}\bar{K}^0$	1.5%
$\bar{K}^0K^{+*}$	1.9%	$K^{+*}\bar{K}^{0*}$	0.9%
$\bar{K}^0K^+$	3.6%		
$\phi\rho^+$	8.1%		
$\phi\pi^+$	3.2%		

2. F and F*

At long last, the clouds of uncertainty surrounding existence and mass of F seem to have lifted and both the TPC at PEP and ARGUS at DORIS see evidence[18] for $F^* \to F + \gamma$ with

$$M_{F^*} - M_F = \begin{cases} 139.5 \pm 8.3 \pm 9.7 \text{ MeV} & \text{TPC} \\ 144 \pm 9 \pm 7 \text{ MeV} & \text{ARGUS} \end{cases}$$

Again (since $F^*-F \approx D^*-D$) these results are highly agreeable to theorists.

Also important is the existence,[19] with estimated branching ratio $4 \pm 3\%$ (the error estimate is mine alone), of the decay $F^+ \to \phi\pi^+$. The uncertainty in branching ratio occurs because only $\sigma B(e^+e^- \to F \to \phi\pi)$ is known, while $\sigma(e^+e^- \to F+...)/\sigma(e^+e^- \to D+...)$ is known only by the inhabitants of Lund. It will be nice to remove the uncertainties. Mark III eventually should be able to do the job.

3. D-$\bar{D}$ Mixing

New limits on D-$\bar{D}$ mixing come[20] from an interesting source: deep inelastic muon scattering via

$$\mu^+ N \to \mu^+\mu^-\mu^- + \ldots$$

The phenomenon

$$\mu^+ N \to \mu^+\mu^+\mu^- + \ldots$$

is well-interpreted in terms of charmed meson pair-production. Hence the mixing phenomenon can be limited with relatively little uncertainty; the result is

$$r(D) = \frac{\sigma(DD)+\sigma(\bar{D}\bar{D})}{2\sigma(D\bar{D})} \leq 1.8\% \ (90\%)$$

This limit will make more difficult the interpretation of ν-induced same-sign dileptons via pair production of charm.

4. Fragmentations $c \to D,F +...$

On the dynamical side, impressive progress has been made in determining the fragmentation function of charmed quarks into mesons--both D^* and F^*.

Examples from ARGUS are presented[21] in Fig. 4. Such quantitative determinations will be extremely important in all observations which need the connection between dynamics at the charmed-parton and the charmed-meson levels. These include leptoproduction processes as discussed above.

A missing piece of the puzzle is the fragmentation function of c (and/or b!!) into charmed baryons; maybe the increased luminosity of Z° factories is needed for such a study.

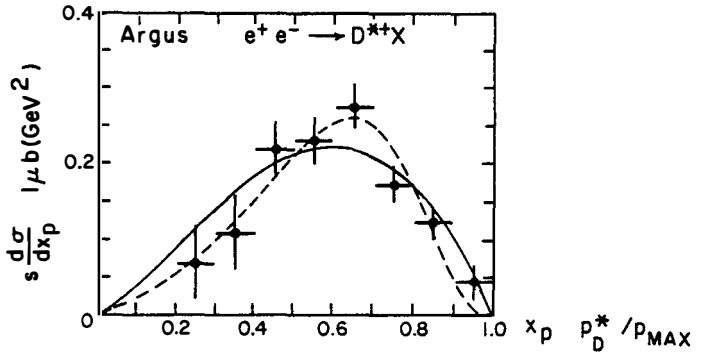

Fig. 4. Fragmentation function for $C \rightarrow D^*$, as inferred[21] from inclusive D^* production in e^+e^- annihilation.

5. Production of $A^+(usc)$ and $T^o(ssc)$

Hadroproduction of the charmed baryons $A^+_{usc}(2460\pm15)$ and $T^o_{ssc}(2740\pm25)$ by hyperon beams[22] has been surprisingly "easy"; the production is diffractive and relatively copious (σB for A^+ is quoted to be ~5 μb(!) for $x_F > 0.65$). A lifetime[23] for the A^+

$$\tau_A = 4.8^{+2.9}_{-1.8} \times 10^{-13} \text{ sec}$$

is also quoted, which helps dispel doubts held by the incredulous casual observer.

6. Lifetimes of D Mesons

Entries to the compendium of D lifetimes were reported here by high resolution rapid-cycling bubble chamber experiments at SLAC[24] and at CERN.[25] I shall not attempt here to review the situation other than pointing out that there is observed in each experiment a long-lived $\bar{D}^o$ (55×10^{-13} sec and (28 ± 9) $\times 10^{-13}$ sec respectively). My own response to those is placid discomfort.

7. $D,F \rightarrow \phi\pi$

The $\phi\pi$ channel offers great opportunities for comparison of production ratios of F^+ and D^+ in a bias-free way. In general the signal strength is

$$\frac{(\phi\pi)_{D^+}}{(\phi\pi)_{F^+}} \approx \frac{[\sigma(D^+)+1/2\sigma(D^{+*})]}{[\sigma(F^+)+\sigma(F^{*+})]} \quad \frac{B(D^+\rightarrow\phi\pi^+)}{B(F^+\rightarrow\phi\pi^+)}$$

As already mentioned, Lund tradition puts $(c\bar{s})/(\text{all charm}) \sim 1/7$, rather large, leading to a D^*/F^* ratio of somewhere between 4 and 2, depending upon the fraction of feedthrough via parent D^* production (and always assuming $D^0/D^+ \approx D^{0*}/D^{+*} \approx 1$). The ratio of branching ratios, on the other hand, favors the Cabibbo-allowed F over Cabibbo-forbidden D. The $D^+ \rightarrow \phi\pi^+$ branching ratio is measured to be 0.6%, while that for F is estimated, as mentioned earlier, to be a few percent. It is therefore reasonable to expect comparable $\phi\pi$ mass peaks at F and D. If the $F \rightarrow \phi\pi$ branching ratio is well-determined, and if, in a given experiment, the D*/D ratios can be determined via the cascading trick, the production ratios can be obtained in a splendidly bias-free way.

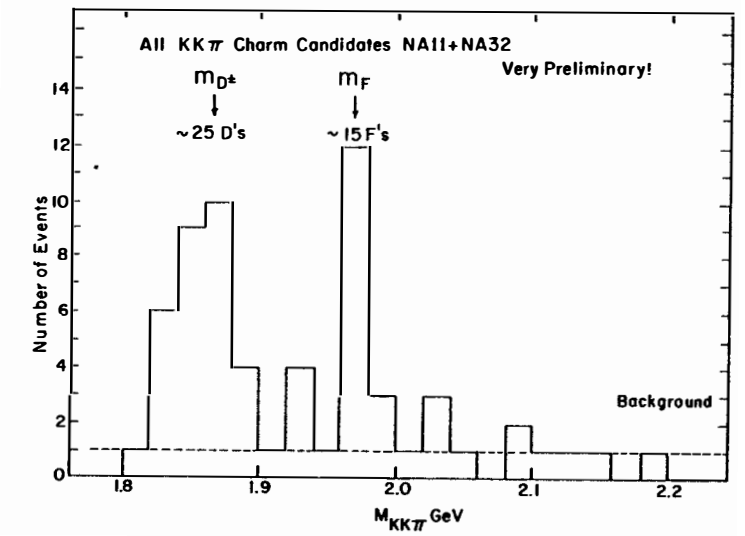

Fig. 5. Very preliminary NA11/NA32 (ACCMOR) data indicating hadroproduction of both F^+ and D^+, with decay into $\phi\pi^+$.

As yet, experiment shows no universal behavior. In e^+e^- collisions F^+, and not D^+, is seen.[26] At CERN, the NA11/NA32 data indicates[27] (Fig. 5), as yet in only the most preliminary way, comparable D^+ and F^+ signals. At Fermilab, a strong Cabibbo-forbidden $D^+ \to \phi\pi^+$ signal (~240 signal events!) has been seen[28] (Fig. 6) with no trace of an F^+. However, the experiment was designed to search for $\eta_c \to \phi\phi$ with a specialized multi-$K^\pm$ trigger. The sample is so badly biased by the trigger that the experimentalists neither dare to quote D cross sections nor F/D ratios. There is clearly something interesting here to pursue further.

This situation is indicative of the abysmal status of our understanding of the dynamics underlying hadronic production of charm. This includes normalization, energy dependence, beam dependence, x_F dependence, A-dependence, F/D ratios, D^*/D ratios, baryon/meson ratios, charm-anticharm correlations in produced phase-space--almost everything. The situation is not hopeless. There is good reason to believe that in a few years these questions will be well resolved. The LEBC program[29]--including their new experiment at Fermilab--is a good example of the progress to be expected.

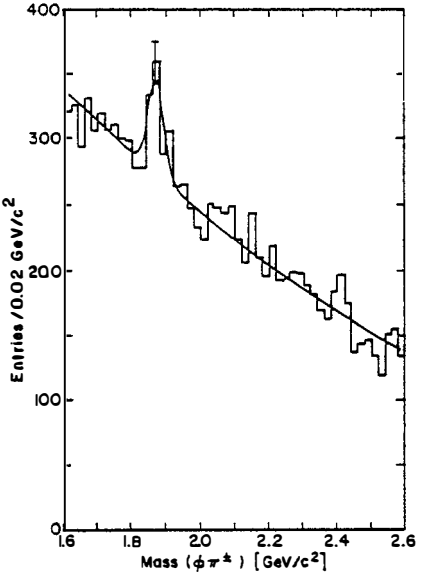

Fig. 6. Observation[28] of Cabibbo-forbidden $D^+ \to \phi\pi^+$ decay in hadroproduction.

E. Strange Quarks

Is the strange quark heavy? Hardly, although the ϕ is sometimes considered to be incipient onium. But s quarks have much to do with CP and hence this workshop.

Beautiful measurements of the CP-violating parameter ε'/ε were presented[30],[31] -

$$\frac{\varepsilon'}{\varepsilon} = \begin{cases} -.0046 \pm .0053 \pm .0024 & \text{Chicago-Saclay} \\ +.0017 \pm .0084 & \text{Yale-BNL} \end{cases}$$

These lie below the previsioned standard-model expectations--although, as we discuss later, standard-model theory can still accommodate the results.

Cabibbo theory of semileptonic $\Delta S = 1$ decays are a prototype of what one might hope for in c (and b?) decays. As reviewed by J.M. Gaillard here, the experimental situation is in excellent condition. This is especially the case, given the new measurement[32] at Fermilab of the electron asymmetry in polarized Σ^- beta decay. This measurement (Fig. 7) removes a serious discrepancy between theory and experiment.

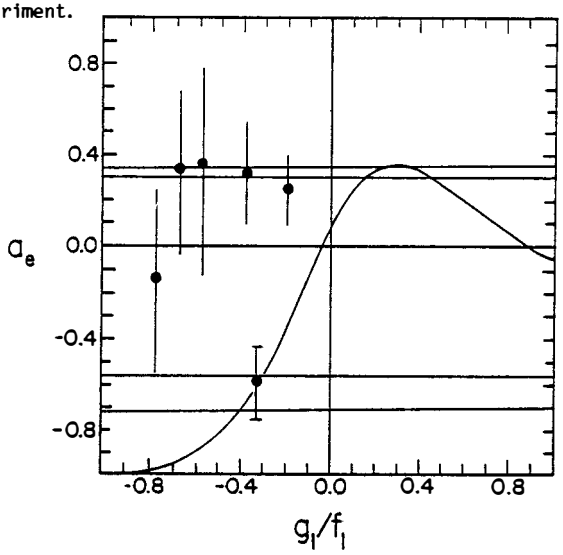

Fig. 7. Measurement[32] of electron asymmetry parameter in polarized Σ^- β decay.

F. Others

In terms of quark content, the neutron definitely does not qualify for admission to this workshop. Nevertheless, its electron dipole moment--if any--does. The measurements[33] are especially beautiful.

$$d_n \leq \begin{cases} (-2 \pm 1) \times 10^{-25} \text{ e-cm} & \text{Leningrad} \\ (-3.2 \pm 3.5) \times 10^{-25} \text{ e-cm}, & \text{ILL} \end{cases}$$

It is a pity that nature does not honor these efforts with something other than a null measurement. It is up to us therefore to provide the honors so well-deserved.

We heard from Steiner[34] of other beautiful, albeit null results in searches for anomalies in μ decay. Especially impressive to me was the limit placed on $\mu \to e + f$, with f a conjectured axion-like "familon". The limit on its decay constant is

$$F_{\text{familon}} \geq 6 \times 10^9 \text{ GeV}$$

Low energy muon decay is probing dynamics at an extraordinary energy scale.

III. WHY IS ALL THIS BEING DONE?

To this question there are many good answers, which we classify starting from the more mundane and leading to the more profound:

A. Strong Interactions and Hadron Structure

1. Onium

Heavy-quark bound states have given us a simple picture of hadron structure and confinement. Onium is the simplest case. One might expect, therefore, the $t\bar{t}$ system to be cleanest. It is thus ironic[35] that the greatest residual uncertainty in the $Q\bar{Q}$ potential still lies at the shortest distance (Fig. 8).

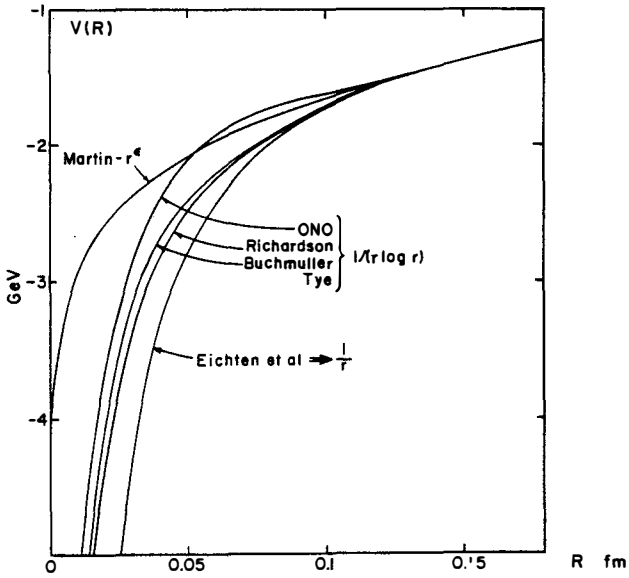

Fig. 8. Theoretical models[35] for the toponium potential.

The low lying level structure of toponium will test models, not QCD fundamentals. Measurements of α_s and how it runs are possible, however, from study of decay widths.

The overall properties of onia are in quite good shape in general, although, as already mentioned, the 5S-6S region of $(b\bar{b})$ and the 3S-4S region of $c\bar{c}$, difficult regions, are fertile areas. These are also curious puzzles, e.g., the ratio $\Gamma(\psi'\to\pi\rho)/\Gamma(\psi\to\pi\rho) \leq .02$ discussed by Karl.[36] But there ought to be a better answer.

2. $Q_1\bar{Q}_2$

The other pure heavy-quark mesons, such as $t\bar{b}$, $t\bar{c}$, $t\bar{s}$, $b\bar{c}$, $b\bar{s}$, are also interesting. $B_s(b\bar{s})$ should not be too hard; why not $b\bar{c}$? The properties of these states deserve to be fully documented.[37] This is gaining significance as the spectroscopic as well as decay systematics mature. We can guess production ratios. But what are the optimal detection signatures?

3. $Q\bar{q}$

As discussed by Richard,[38] these mesons are especially challenging: the q is more relativistic than in mesons made of light quarks. It appears that, while hyperfine structure is in reasonable condition, higher excited states need work. One might well attain experimental information about higher (e.g., p wave) excitations of D and F before long.

4. QQQ and QQq baryons

This must be the dream of QCD lattice theorists, etc. In the absence of light-quark corrections,

$$\frac{m(QQQ)}{m(Q\bar{Q})} = \frac{3}{2}\left[1+f\left(\frac{\Lambda}{M}\right)\right]$$

and the function f should be calculable from first principles. Seeing the ttt and bbb appears hopeless. Even seeing ccc is marginal at best. But, given the observation already of (ssc), the (scc) must be regarded as accessible in the long run, perhaps again in hyperon beams:

$$\frac{\sigma(\Sigma n \to ssc)}{\sigma(\Sigma n \to sss)} \sim \frac{\sigma(\Sigma N \to (scc)+\ldots)}{\sigma(\Sigma N \to (ssc)+\ldots)} \sim 10^{-2} \text{ ??}$$

Thus, as with mesons, the systematics of QQq baryons--and QQQ baryons as well (they should be an easier case)--deserve a full explication. Up-to-date wisdom on these states, which should incorporate the recent, remarkable progress in the "QCD-inspired" understanding of S = 0,1 baryons and their excitations,[39] would be most welcome.[40] This should include the gross level structure, fine and hyperfine intervals and candidates for narrow excitations with characteristic decays to the ground state. (How about, e.g., $(QQ)^*q \to QQq + \pi^+\pi^-$, with $(QQ)^*$ a radial excitation?)

5. Qqq baryons

Most of the experimental action probably will remain with the Qqq baryons. Many potential-model approaches for these, as discussed by Taxil,[41] exist. Thus far, general guidelines exist via level-ordering theorems. However, these are based on two-body interactions, which in a world of QCD strings (despite good arguments for the approximate validity of a two-body potential approach) may still hold surprises. Clearly the next steps will require stronger injections of good data on (qqc) baryons.

6. QCD dynamics

We have already mentioned the central problems. Other than the question of baryon production, e^+e^- dynamics is in rather good condition. For hadron-induced processes, everything needs work. I find especially urgent the question of diffractive mechanisms, prominent at the ISR and in the A^+ and T^0 production, and occasionally claimed elsewhere.[42] But contrary evidence, especially from direct-lepton production experiments, also exists.[43] If the diffractive mechanisms seen in A^+ and T^0 production are universal for incident baryons, the "devil's pitchfork" dissociation mechanism mentioned by Brown[22] (Fig. 9) would seem to provide a reasonable gauge for estimating yields. Some guesses are given in Table II.

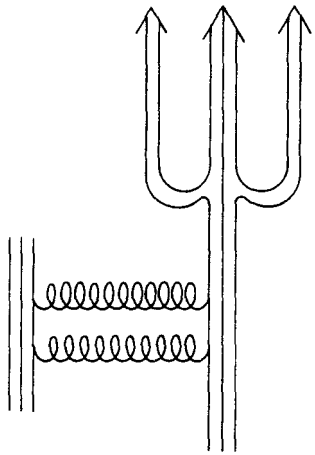

Fig. 9. "Diffraction-dissociation" or "flavor excitation" diagram for production of leading baryons containing heavy quarks.

B. Electroweak Properties

1. Bread-and-butter SU(2)×U(1) tests

As the energy scale increases, especially in e^+e^- processes, weak effects enter more prominently. The angular asymmetry reported here[44] in $B\bar{B}$ production at PEP and PETRA is a typical example. Toponium polarization,[45] as discussed by Kuhn, is another. All these tests are fundamental, so fundamental in this day and age that an experimental disagreement with theory would be a real shocker.

Table II

Some guesses for production cross-sections of leading baryons containing heavy quarks ($\sqrt{s}$ = 40 GeV; $x > 0.4$) by incident hadrons. The substitution $c \to b$ may cost a factor ~100 in cross-section at this energy.

	n,p incident	π incident	Σ^- incident	K^- incident
Σ^-(dds)	500 μb	50 μb	--	500 μb
Ξ^-(dss)	25 μb	5 μb	--	50 μb
Ω^-(sss)	0.5 μb	0.5 μb	--	5 μb
Λ_c(cud)	50 μb	5 μb	--	--
A(cus)	2.5 μb	500 nb	50 μb	5 μb
T(css)	100 nb	50 nb	2 μb	500 nb
(ccd)	10 nb	20 nb	--	--
(ccs)	500 pb	500 pb	10 nb	5 nb
(ccc)	3 pb	10 pb	3 pb	10 pb

2. Weak decay dynamics

It is gratifying that, given the challenge of new data on D and B decay properties, a theoretical response[13] exists which may suffice to meet the challenge. The approach, well-supported from first principles, boils down to simply calculating, modulo smallish corrections and additions, the amplitude for

with relatively small corrections from $q\bar{q}$ annihilation, "color-rearrangement" terms (i.e., Fierz-transformed 4-fermion couplings) and mundane final-state interactions. While - such a picture is not out of line with QCD expectations, additional phenomenological tinkering may be, not unexpectedly, in order. Figure 10 shows a general comparison of observed with calculated branching ratios. A very large collection of channels has been calculated by Bauer and Stech, and a sample is given in Table I. Not-as-yet observed modes with large branching fractions, e.g., $D \to K^*\rho$, await testing.

As mentioned before, the "factorization" picture seems also to work well for B-meson decays. It is important to sharpen this assertion; steady progress can be expected on this from CESR and DORIS.

An outstanding problem remaining is to generalize the apparent successes in interpreting D, F, B meson decays to the decays of baryons containing heavy quarks. This may be quite nontrivial; just hyperon nonleptonic decays (especially p-wave) have resisted theoretical analysis more than their mesonic counterparts. Also, the observed decay modes of A^+ ($\Lambda K^-\pi^+\pi^+$) and $T^0(\equiv^-K^-\pi^+\pi^+)$, which would seem to require assignment of sizeable branching ratios (for reasons of normalization of production cross-section), do not seem to me to invite an easy interpretation in terms of "factorization".

In addition to the need for a thorough analysis of Qqq baryon decays, an equally thorough study should be made of decay modes of $Q_1\bar{Q}_2$ mesons (e.g., $b\bar{s}$, $c\bar{b}$, $t\bar{s}$, $t\bar{c}$); they are now amenable to sound theoretical attack via the successful methods used for D, F, and B. Such mesons will someday be seen; we should know <u>now</u> the most favorable signatures.

This remark also applies to QQq baryons. In addition to the fact that such baryons will be observed, the theoretical properties of these systems (as well as QQQ baryons) might be simpler and help shed light on their counterparts containing more light quarks.

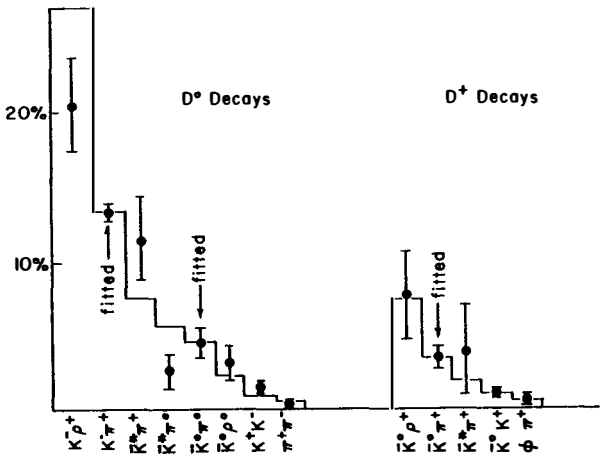

Fig. 10. Comparison of predicted[13] and measured branching ratios of D mesons.

3. Determination of the Kobayashi-Maskawa parameters

The determination of the elements of the Kobayashi-Maskawa mixing matrix is clearly a very fundamental issue (although, I think, not as fundamental as those of the quark mass matrix, from whence they come.[46]) Clearly the limits on $|V_{bu}|$ should be pushed if at all possible; the leverage there on constraining the standard picture of CP violation is as great as improving limits on ε'/ε. Both study of the end point of the semileptonic-decay spectrum and the search for exclusive uncharmed B-decay channels can be pushed further (although null results for the latter are more difficult to interpret).

4. Weak mixings

The standard model predicts very small $D\bar{D}$ mixings. Nevertheless, it was encouraging to hear that reaching the $\theta_c^4 \sim 10^{-3}$ level of sensitivity[47] is not out of the question if one can obtain a clean sample of D^*'s and measure

$$\frac{\Gamma(D^* \to \pi^+ \bar{D})}{\Gamma(D^* \to \pi^+ D)}$$

The soft π^+ tags the charm quantum number of the parent. To get an adequate sample may require not only the standard D^* kinematic trick, but also clean vertex information. Weilhammer suggests use of hadron beams in fixed target experiments for meeting these specifications.

The best system for study of $B\bar{B}$ mixing seems to be[48] the B_s, inviting long runs at $\Upsilon(5S)$. It looks to be a long and arduous task to reach the expected sensitivity.

However, for both $B\bar{B}$ and $D\bar{D}$ systems, one should keep in mind that much of the interest in the measurement lies in the possibility of severe disagreement of experiment with theory: this phenomenon seems (instinctively) to me to be sensitive to unexpected effects. Hence experimentalists should not be hung up on the parameters suggested by the standard model; the effect should be energetically searched for in all accessible channels at all levels of sensitivity.

5. CP violation

As emphasized by Wolfenstein,[49] probably the best way to improve our knowledge of CP violation is to continue pushing on the $K\bar{K}$ system: it is an exquisitely sensitive channel. At the workshop variants going beyond the standard phenomenology were discussed.

a) Measurement of η^{+-o} at Fermilab, possibly to the 10^{-3} level, is underway; theorists therefore should anticipate a result and quote their predictions. It will be good fortune in that experiment to see CP violation in the mass matrix. Deviations to my knowledge are expected in general to be small--I heard nothing to the contrary at this workshop.

b) $K_{S,L} \to \gamma\gamma$ is being examined in fine detail by Golowich.[50] The returns are not all in. In particular, what is the measurement to be done? Photon polarizations? Or $\Gamma(K\to\gamma\gamma)/\Gamma(K\to\pi^+\pi^-)$ as function of proper time?

c) Other options. There are ideas for using LEAR, as discussed in Turlay's talk. These still lie within the $K^\circ\bar{K}^\circ$ system, but complement the usual methods and may also attack the $K \to 3\pi$ system.

Various ideas are extant at Fermilab, such as improving T-violation limits in Σ β-decay, or searching for T-violation in Ξ° and $\bar{\Xi}^\circ$ decays by comparing their asymmetry parameters $\alpha_\Xi \alpha_\Lambda$. However, the question is whether there is any hope that these effects are large in comparison with $\varepsilon'(\lesssim 10^{-6}!)$? One would seem to need a $\Delta S = 1$ effective interaction which for some reason (selection rules, dynamical suppression, etc.) is highly suppressed in the K_L, K_S system but not in the baryon system. I do not know of such an option.

d) CP violation in the B_d-$\bar{B}_d$ system: Wolfenstein[49] and Sanda[51] argue this is an optimal channel where CP violating effects may be large (~20%). However, one needs to compare partial widths of B_d and $\bar{B}_d$ into exclusive final states which are CP eigenstates, e.g.,

$B_d \rightarrow$ ψK_S

$D^+ D^- \pi^\circ$

$D^\circ \pi^\circ$

$\hookrightarrow K_S \pi^\circ$

This is, clearly, not at all easy, if at all possible. (More about this later.)

6. Searches beyond the standard model

To explore phenomena beyond the standard model, as well as to understand once and for all the origin of mass and of CP violation, the method of choice is higher energy. But in the meantime there exist many opportunities. Possible foci of effort are higgs (and/or axions) and supersymmetry. We again catalogue by quark:

a) Beyond the top: The most accessible 4th generation particles may be the leptons. Searches[52] for the charged lepton in W decay and the neutral one everywhere (beam dumps?) are appropriate.

b) Top. If open channels

$t \rightarrow b h^+$, etc.

exist, they would be sensational sources. For neutral higgs, the classic method via onium radiative decay

$$(t\bar{t}) \rightarrow \gamma + h^{\circ}$$

is well suited[53] to a top mass of 40 ±10 GeV.

c) Bottom. Because of the long b-quark lifetime, bottom decays are beautiful ways to search for rare phenomena; branching ratios are enhanced. Also, anomalous $B\bar{B}$ mixing may be another sensitive measure of new physics.

d) Charm. Again, the $O\bar{D}$ mixing phenomenon, because it is expected to be small, may be a sensitive means of seeing a surprise.

e) Other. There are of course a variety of rare decays of K, μ, etc. which are a rich source of possible surprises.

7. Comments on theoretical models of CP violation

In this workshop, considerable time was devoted to the status of the theory of CP-violating effects. This is as good a place to comment on this subject as anywhere. However, I am hardly expert enough to distinguish boxes from penguins and can only view the subject as an outsider. In terms of status of the models, however, some things seemed clear to me:

a) Standard (Kobayashi-Maskawa phase) model:[54] The model appears embattled, as the data on ε'/ε, $b \not\rightarrow u l \nu$, and m_t constrain ever more tightly the phenomenology. Theorists' hubris on how well the difficult parts of the phenomenology could be controlled (the parameter B in particular) has largely disappeared, and the old sense of humility in the face of computational difficulty has re-emerged. Based on the evidence presented at this workshop[55] on how really embattled theorists (those defending the Higgs models) respond, it seems to me that new limits on ε'/ε or modest improvements in bounding V_{bu} will not destroy the KM picture. New positions of retreat will be constructed. Instead there remains the assertion that in the KM picture it is probable that a measurement of nonvanishing ε'/ε is within experimental reach--but never at the 90% confidence level.

b) Higgs model.[56] The generic prediction for these models is that ε'/ε is ~5%. As I understand it, this occurs because intrinsic $\Delta S = 2$ local operators which induce CP violation are in this model strongly suppressed. This leaves iteration of $\Delta S = 1$ CP violation via low-mass intermediate states as the source of $\Delta S = 2$ mixing. The consequence is that ε'/ε is largely determined by the Wu-Yang phenomenology alone. Efforts to push down the generic prediction follow two lines: one is to exploit--rather radically--the aforementioned uncertainties in strong-interaction effects. The other (which I find more attractive) is tuning parameters of the model as discussed by Gerard.[57] This seems not unnatural in the light of higgs models[58] of UA1 monojet phenomena ($Z^\circ \to h_1 h_2$).

c) Left-right symmetric models.[59] By default, these appear to me ascendant. The parametrization of CP violation in these models is sufficiently flexible that they can accommodate vanishing ε'/ε and V_{bu}. There are some esthetic arguments going for them as well. Nevertheless, it would be nice to have some positive indicators that this is the right direction to pursue. Solid ones seem hard to find.

In summary, measurements so far have tested the elasticity of the various models. This is indeed a very useful test; the result is that they are quite elastic. Again, while ε'/ε is an obvious parameter to improve, so also is V_{bu}. We may hope to see in the not-too-distant future a considerably more constrained situation.

IV. WHAT NEXT?

In looking at the future, all will agree that a primary goal is to understand the origin of mass and mixings, along with the CP phenomenon. The means for doing this must include the push to higher energy. In addition, it will be of great importance to examine at much greater depth the phenomena at existing energies. In addition to the discovery potential inherent in such a "low-energy" program, it also provides the solid base of information vital in interpreting what is going on at the higher energies.

A. Facilities

Among the high-energy facilities, proton-antiproton colliders will hold the lead in energy-scale for a long time. Anticipation of new-particle production in $p\bar{p}$ collisions is a common pastime.[60] Especially relevant for this workshop is the remarkable yield of soft D* 's in gluon jets, of order[61] one D*/jet when $p_\perp$ exceeds ~20 GeV. This could imply[62] enormous heavy quark yields at these colliders, with a favorable signal/noise ratio.

For example, the TeV I collider will, in a run with $\int \mathcal{L} dt = 10^{36} cm^{-2}$, produce of order 10^7 jets with $p_\perp > 20$ GeV. This is a splendid source of charmed hadrons, one which may even have decent signal/noise. Likewise, using a scaling argument, one might anticipate of order one B* per jet for $p_\perp > (m_b/m_c)$ 20 GeV $\approx$ 70 GeV. There would be over a billion such jets produced per year at an SSC.

These yields are much greater than what e^+e^- colliders provide. The Z° factories do promise to increase by a factor of at least 100 the yield of heavy quarks. Also the sophistication of the new detectors at LEP and SLC is much greater (or at least ought to be, considering the money being spent on them) than what now exists. Hence these facilities should be superb, not only for top-quark studies, but for charm and bottom as well. And, of course, SPEAR and DORIS/CESR will continue to produce additional clean new results, with the main limitation simply being integrated luminosity. (If only e^+e^- machines could make a great leap forward in luminosity!)

HERA seems to me less competitive for heavy-quark physics. However, discovery potential is high--especially if the mass scale relevant to the monojet phenomenon is $\lesssim$150 GeV.

This leaves fixed-target machines (admittedly my preoccupation) as a remaining source--and it is a rich one. In every Tevatron spill (once a minute), about 10^8 $b\bar{b}$ pairs are produced in the beam dump. That is, of course, hardly the point: signals are generally buried in heavy background. Nevertheless, the long-range potential may be extremely good, as refinement of

technique and better knowledge of production properties and decay signatures become available. I will close with a very speculative example.

B. Can One See CP Violation in the B-$\bar{B}$ System??

We already mentioned the method suggested by Sanda,[63] as discussed in the workshop by Wolfenstein.[49] Upon comprehending the prospects, the first question to ask is "Should one even try?" In what follows, we assume the answer to this highly nontrivial query is "Yes". We then ask how many $B\bar{B}$ pairs are needed to do the job. For measuring

$$\frac{\Gamma(B \to \text{f.s.}) - \Gamma(\bar{B} \to \text{f.s.})}{\text{sum}}$$

to $\ll 20\%$ or so we need at least 100 B and $\bar{B}$ decays to "f.s.", which stands for an exclusive final state which is a CP eigenstate. In addition, the flavor (b-number) of the spectator must be tagged in order to label the parent B ($\bar{B}$). This gives, very roughly (and optimistically?), for the bookkeeping

10^2 statistics (no background subtraction!!)

10^{2+2} decay branching ratios $B \to DX \to Y$

10^1 efficiency in tagging spectator.

10^1 geometrical and reconstruction efficiency(!)

This implies we need at least 10^8 produced $b\bar{b}$ quarks per experiment--probably out of reach of LEP/SLC, but perhaps not SSC.

Fixed-target experiments are at least thinkable (not for now, but maybe in 1992±4). With a 50 nb production cross section and 10^{14} interacting protons per experiment, one can produce 10^8 $b\bar{b}$ pairs for study. To get 10^{14} interacting protons into a powerful open-geometry spectrometer requires high rates. At the Tevatron a 50 MHz interaction rate (one interaction/RF bucket) translates into a reasonable 2000 hours of running to accumulate the 10^{14} interacting protons. While running at 50 MHz may seem over-optimistically high, data acquisition and

processing rates even higher are contemplated for open-geometry detectors at the SSC.

What about the other numbers? Are they conservative or optimistic? The cross-section may be conservative[64] by a factor 10-100. Also, there may be, for a canny choice of beam, kinematic regions where B_d production dominates $\bar{B}_d$ (and vice versa), so that the tagging requirement might be finessed. On the other hand, the factor 10^4 for decay branching ratios can hardly be avoided; it may be mildly optimistic. And by present standards the factor of 10% for detection and reconstruction efficiency may look wildly optimistic. However, to do this job at all requires great advances in technology. It is reasonable to posit for this purpose a spectrometer with full acceptance, resolution, particle identification, sophisticated vertex detection, and advanced on-line trigger processing capability--something nonexistent today. Thus I do not know how to balance optimism with pessimism in these estimates.

Should one think about following such a path? I don't know. A decision to do so requires a better understanding of how far spectrometer technology, etc. can be pushed. It needs better physics inputs as well: understanding of B production rates and dynamics, of B spectroscopy and of B decay rates and branching ratios. All of this should be known better in a few years.

But the real decision to follow such a path must come from those who would do the work. The task is a very long and arduous one and, even for those who would have doubts, the homework should be done. That alone leaves a lot to do for everyone.

V. THANK YOU

Thank you to Tran Than Van and the organizers for another excellent Moriond meeting. Also I thank E. Paschos and L. Oliver for help in preparing this manuscript.

REFERENCES

1. E. Paschos, these proceedings; also S.K. Bose and E.A. Paschos, Nucl. Phys. B169, 384 (1980); M. Gronau and J. Schechter, SLAC-PUB 3451 (1984); U. Türke et al., Dortmund preprint DO-TH 84/26 (1984); J.S. Hagelin, preprint MIU-THP-84/010; I. Bigi, preprint PITHA 84/19.
2. P. Erhard, these proceedings; also C. Rubbia, Proc. of Inter. Conf. on Neutrino Phys. and Astrophysics, edited by K. Kleinknecht and E.A. Paschos (World Scientific Press, 1984), p. 1; G. Arnison et al., Phys. Lett. 147B, 493 (1984).
3. D. P. Roy, these proceedings; also R. Godbole and D.P. Roy, DO-TH 84/25 (1984); V. Barger, A. Martin and R. Phillips, CERN-TH 3972 (1984); R. Kinnunen, HU-P-D 41 (1984).
4. J. Kühn, these proceedings and Acta Physica Polonica B12, 347 (1981); L.M. Sehgal and P.M. Zerwas, Nucl. Phys. B183, 417 (1981); A. Martin, Toponium Physics 1984 Evice Lectures, CERN-TH 4060/84; J. Kühn, CERN-TH 4089/85.
5. P. Franzini, these proceedings; also F. Wilczek, Phys. Rev. Lett. 39, 1304 (1977).
6. K. Schubert, these proceedings.
7. T. Jensen, these proceedings; also D. Besson et al., Phys. Rev. Lett. 54, 381 (1985); D. Lovelock et al., Phys. Rev. Lett. 54, 377 (1985).
8. S. Ono, these proceedings and LPTHE report (Orsay) 84/13 (1984).
9. N. Törnquist, these proceedings; also K. Heikkilä, S. Ono and N. Törnquist, Phys. Rev. D29, 110 (1984); N. Törnquist, Phys. Rev. Lett. 53, 878 (1984).
10. P. Franzini, these proceedings.
11. S. Ono, these proceedings; also K. Igi and S. Ono, Univ. of Tokyo preprint UT-446 (1984).
12. T. Jensen, these proceedings.
13. B. Stech, these proceedings; also M. Bauer and B. Stech, Heidelberg preprint HD-THEP 84-22 (1984); R. Rückl, CERN preprint, CERN-TH 4013 (1984).
14. T. Gentile, these proceedings.
15. R. Rückl (private communication) disagrees; he argues that phase space favors K,K* over higher mass S = 1 configuration. Maybe he's right. On $\psi K\bar{s}$ branching ratio, see also M.B. Gavella et al., LPTH (Orsay) 85/11.
16. C. Matteuzi, J. Thomas, R. Barlow, these proceedings; also K. Hayes, DESY Workshop, DESY T-84-02, 41 (1984); D. Klem et al., Phys. Rev. Lett. 53, 1873 (1984).
17. J. Hauser, these proceedings; also Mark III Collaboration presented by R. Schindler at Leipzig Conf. (1984).
18. H. Aihara, these proceedings and H. Aihara et al., Phys. Rev. Lett. 53, 2465 (1984); K. Schubert, these proceedings; also H. Albrecht et al., Phys. Lett. 146B, 111 (1984).
19. K. Schubert, I. Beltrami, these proceedings; also CLEO Collab., A. Chen et al., Phys. Rev. Lett. 51, 634 (1983); TASSO Collab., M. Althoff et al., Phys. Lett. 136B, 130 (1984); ACCMOR Collab., R. Bailey et al., Phys. Lett. 139B, 320 (1984); ARGUS Collab., H. Albrecht et al., to appear in Phys. Lett.
20. P. Verrecchia, these proceedings.
21. K. Schubert, these proceedings; also Neutrino '84 Conference Proceedings (op. cit. ref 2), Fig. 7, p. 678.
22. R. Brown, these proceedings; also S. Biagi et al., Phys. Lett. 122B, 455 (1983); CERN preprint.
23. H. Siebert, these proceedings.
24. J. Brau, these proceedings; also K. Abe et al., SLAC-PUB 3493 (1984); J. Yelton et al., Phys. Rev. Lett. 52, 2019 (1984).
25. P. Wright, these proceedings; also M. Aguilar-Benitez et al., Phys. Lett. 146B, 266 (1984).

26. K. Schubert, these proceedings; also Neutrino '84 Conference Proceedings (op. cit., ref. 2), p. 670 (1984); J. Beltrami, these proceedings.
27. G. De Rijk, these proceedings.
28. C. Georgiopoulos et al., Fermilab preprint FERMILAB PUB-84/113-E.
29. P. Wright, these proceedings; also M. Aguilar-Benitez et al., (ibid., ref. 25).
30. B. Peyaud, these proceedings; also B. Winstein, Neutrino '84 Conference Proceedings (op. cit., ref. 2), p. 627 (1984).
31. M. Schmidt, these proceedings.
32. J-M. Gaillard and G. Sauvage, Ann. Rev. Nucl. Part. Sci. 34, 351 (1984).
33. P. Miranda, these proceedings; also I.S. Altarev et al., reported by V. Lobashev at Neutrino Conf. 1982 (Hungary); I.S. Altarev et al., JETP Lett. 29, 730 (1979); N.F. Ramsey, Ann. Rev. Nucl. Sci. 32, 211 (1982).
34. H. Steiner, these proceedings; also J. Carr et al., Phys. Rev. Lett. 51, 627 (1983).
35. J. Kuhn, these proceedings; S. Ono, these proceedings; also A. Martin (ibid. ref. 4).
36. G. Karl, these proceedings; also G. Karl and W. Roberts, Phys. Lett. 144B, 263 (1984).
37. I am informed that studies have been made by S. Nussinov. I do not know the reference.
38. J. M. Richard, these proceedings; also S. Godfrey, Univ. of Toronto Ph.D. Thesis (1983); S. Godfrey and N. Isgur, Univ. of Toronto preprint (1983).
39. N. Isgur and G. Karl, Phys. Lett. 72B, 109 (1977); Phys. Rev. D18, 4187 (1978); D. Gromes and I. Stamatescu, Nucl. Phys. B112, 213 (1976).
40. No doubt there is already literature about which I am unaware. I welcome it being brought to my attention.
41. P. Taxil, these proceedings; also J.M. Richard and P. Taxil, Ann. Phys. 150, 267 (1983); Phys. Lett. 128B, 453 (1983).
42. For example, neutron production of Λ_c at 40 GeV (IHEP) with a large cross-section; A. Aleev et al., Yad. Fiz. 35, 1175 (1982) [Sov. J. Nucl. Phys. 35 (5), 687 (1982)].
43. A. Bodek, Neutrino '84 Conference Proceedings, p. 643 (1984).
44. H. Aihara, these proceedings; R. Barlow, these proceedings.
45. J. Kuhn, these proceedings.
46. For this reason, I worry that schemes (M. Gronau, these proceedings and Technion-PH 84-53; M. Gronau and J. Schechter, Phys. Rev. Lett. 54, 385 (1985); L. Wolfenstein, Ref. TH 3880-CERN (1984) and CMU-HEP 84-20; M. Roos, Helsinki preprint, HU-TFT 84-38) defining maximal CP violation via KM-matrix properties may be too superficial. Even use of the mass-matrix to define "maximal CP" may suffer the same defect: it too may still be too far removed from the intrinsic source of CP violation.
47. P. Weilhammer, these proceedings.
48. J. Lee-Franzini, these proceedings; also J. Ellis, M.K. Gaillard, D.V. Nanopoulos, Nucl. Phys. B109, 213 (1976); J.S. Hagelin, Nucl. Phys. B193, 123 (1981); A. Ali and Z.Z. Aydin, Nucl. Phys. B148, 165 (1979); A.J. Buras, W. Slominski and H. Steger, Nucl. Phys. 245B, 369 (1984) and ref. therein.
49. L. Wolfenstein, these proceedings and Nucl. Phys. 246B, 45 (1984); CERN-TH 3925/84.
50. E. Golowich, these proceedings; also R. Decker, P. Pavlopoulos and G. Zoupanos, CERN preprint (1984); J. Ellis, M.K. Gaillard, D.V. Nanopoulos, Nucl. Phys. B109, 213 (1976).
51. A. Sanda, these proceedings; also A.B. Carter and A.I. Sanda, Phys. Rev. D23, 1567 (1981); I.I. Bigi and A.I. Sanda, Nucl. Phys. B193, 85 (1981).
52. J. Rosner, these proceedings; also C. Hill, Phys. Rev. 240, 691 (1981); J.W. Halley et al., DO-TH 84/24; M. Gronau and J. Rosner, CERN-TH 3911 (1984).

53. J. Kuhn, these proceedings; also F. Wilczek, Phys. Rev. Lett. 39, 1304 (1977).
54. E. Paschos, these proceedings; also E.A. Paschos and U. Türke, Nucl. Phys. 243B, 29 (1984); B. Guberina, these proceedings; S.-P. Chia, these proceedings and Phys. Lett. 147B, 361 (1984); E. Golowich, these proceedings; J. Donoghue, E. Golowich, B. Holstein, Phys. Lett. 119B, 412 (1982); G. Nardulli, these proceedings; P. Cea, G. Nardulli and G. Preparata, Marseille preprint CPT-84, p. 1626; A. Pugliese, these proceedings; M. Lusignoli and A. Pugliese, Phys. Lett. 144B, 110 (1984); J.S. Hagelin, Proc. Moriond Conf. 1984; F. Gilman and J. Hagelin, Phys. Lett. 126B, 111 (1983); P. Ginsparg and M. Wise, Phys. Lett. 127B, 265 (1983).
55. A. Sanda, these proceedings; T. Pham, these proceedings; S. Weinberg, PRL 31, 657 (1976); A.I. Sanda, Phys. Rev. D23, 2647 (1981); N. Deshpande, Phys. Rev. D23, 2654 (1981); Y. Dupont and T.N. Pham, Phys. Rev. D28, 2169 (1983).
56. A. Sanda, these proceedings; T. Pham, these proceedings.
57. J.-M. Gerard, these proceedings; also A. Buras and J.-M Gerard, MPI preprint (1985).
58. J. Rosner, these proceedings; also S.L. Glashow and A. Manohar, PRL 54, 526 (1985).

(1984); R. Mohapatra, these proceedings; F.I. Olness and M.E. Ebel, Phys. Rev. 30D, 1034 (1984) and references therein; G. Ecker, W. Grimus and H. Neufeld, Nucl. Phys. B229, 421 (1983); G. Ecker et al., Phys. Lett. 94B, 381 (1980); Nucl. Phys. B177, 489 (1981); Nucl. Phys. B247, 70 (1984); R. Mohapatra and J.C. Pati, Phys. Rev. D11, 566, 2557 (1975); R. Mohapatra, "Left-Right Symmetry and CP Violation", College Park (Maryland) preprint (1984); R. Mohapatra, Maryland preprint 85-124 (1985).
60. R. Rückl, J. Rosner, these proceedings; G. Altarelli and R. Rückl, Phys. Lett. 144B, 126 (1984); S.L. Glashow and A. Manohar, (ibid., ref. 58); L.E. Ibanez and C. Lopez, B233, 511 (1984); J. Ellis and M. Sher, PL 148B, 309 (1984); E. Reya and D.P. Roy, PRL 53, 889 (1984).
61. G. Arnison et al., Phys. Lett. 147B, 222 (1984). This needs confirmation; some trigger bias, albeit unlikely, may exist.
62. J. Lee Franzini, these proceedings.
63. A. Sanda, these proceedings; also see ref. 51; E. Paschos and U. Türke, Nucl. Phys. B243, 29 (1984).
64. R. Rückl, these proceedings.

LIST OF PARTICIPANTS

AIHARA Hiroaki	Physics Dept.- Univ. of Tokyo 7-3-1. Hongo Bunkyo-ku 113 TOKYO JAPAN
AUGE Etienne	L.A.L. - Bat. 200 Université Paris Sud 91405 ORSAY Cedex FRANCE
BALAND Jean-François	Serv. de Phys. des Part. Elem. Fac. Scie-Av. Maistriau 19 7000 MONS BELGIUM
BARLOW Roger	Dept. of Physics Manchester University M13 9PL MANCHESTER UNITED KINGDOM
BAUER Manfred	Inst. f. Theoretische Physik Heidelberg University 6900 HEIDELBERG FEDERAL REP. GERMANY
BELTRAMI Ivano	c/o SLAC - Bin 37 P. O. Box 4349 94305 STANFORD CA USA
BJORKEN James	FERMILAB P.O. Box 500 60510 BATAVIA IL USA
BRAU James E.	Dept. of Physics University of Tennessee 37996 KNOXVILLE TN USA
BROWN Robert M.	Rutherford and Appleton Lab. Chilton OX11OQX DIDCOT UNITED KINGDOM
CALVETTI Mario	Lab. di San Piero-Univ.di Pisa San Piero a Grado 56010 PISA ITALY
CASO Carlo	INFN - Genova Via Dodecaneso 33 16146 GENOVA ITALY

CHARDIN Gabriel	D.Ph.P.E CEN Saclay 91191 GIF/YVETTE Cedex FRANCE
CHIA Swee-Ping	Physics Dept. University of Malaya 22-11 KUALA LUMPUR MALAYSIA
COIGNET Guy	L.A.P.P. B. P. 909 74019 ANNECY LE VIEUX Cedex FRANCE
COOPER Peter	Physics Dept - Yale University 260 Whitney Ave.- Box 6666 06511 NEW HAVEN CT USA
CUNDY Donald	C.E.R.N. EP Division 1211 GENEVA 23 SWITZERLAND
DALITZ Richard	Dept of Theoretical Physics Oxford Univ.- Keble Rd OX1 3RH OXFORD UNITED KINGDOM
DE RIJK Gijsbert	NIKHEF - H & (CERN EP) Kruislaa 409, Box 41882 1009 AMSTERDAM NETHERLANDS
DE VINCENZI M.	INFN - di Roma Viale Regina Elena 299 00161 ROMA ITALY
DUMARCHEZ Jacques	LPNHE - Univ. P. et M. Curie Tour 32, 4 Place Jussieu 75230 PARIS Cedex 05 FRANCE
EBERT Dietmar	Inst. fur Hochenergiephysik Akademie Wissenschaften 1615 ZEUTHEN DEMOC. REP. GERMANY
ECKER Gerhard	Institut f. Theor. Physik Vienna Univ.-Boltzmanng 5 1090 WIEN AUSTRIA
EEG Jan O.	Theory Group - Inst of Physics Univ. of Oslo - Blindern 0316 OSLO 3 NORWAY

ERHARD Peter
RWTH Aachen - III Physik. Inst
Physikzentrum (& CERN)
5100 AACHEN
FEDERAL REP. GERMANY

FORDEN Geoffrey
Rutherford and Appleton Lab.
Chilton
OX11OQX DIDCOT
UNITED KINGDOM

FRANZINI Paolo
Dept. of Physics
Columbia Univ. - Box 133
10027 NEW YORK NY
USA

FRERE Jean Marie
Service de Physique Théorique
ULB -Campus Plaine- CP225
1050 BRUXELLES
BELGIUM

FROIDEVAUX Alain
L.A.L. - Bat. 200
Université Paris Sud
91405 ORSAY Cedex
FRANCE

GAILLARD Jean Marc
L.A.L. - Bat. 200
Université Paris Sud
91405 ORSAY Cedex
FRANCE

GENTILE Simonetta
Dipt di Fis., Univ delgi Studi
Pzale A. Moro 2
00185 ROMA
ITALY

GENTILE Thomas
Dept. of Physics
Rochester University
14627 ROCHESTER NY
USA

GERARD Jean-Marc
MPI f. Physik & Astrophysik
Werner-Heisenberg Inst.
8000 MUNCHEN 40
FEDERAL REP. GERMANY

GERKE Christian
C.E.R.N.
EP Division
1211 GENEVA 23
SWITZERLAND

GILSON Hervé
Inst. de Physique Théorique
Chemin du Cyclotron 2
1348 LOUVAIN LA NEUVE
BELGIUM

GOLOWICH Eugene
Dept. of Physics - GRT-C
Univ. of Massachusetts
01002 AMHERST MA
USA

GRONAU Michel	Dept. of Physics - Technion Israel Inst. of Technology 32000 TECHNION CITY HAIFA ISRAEL
GUBERINA Branko	Rudjer Boskovic Institute P.O. Box 1016 41 001 ZAGREB Croatie YUGOSLAVIA
GUYOT Claude	D.Ph.P.E CEN Saclay 91191 GIF/YVETTE Cedex FRANCE
HAUSER Jay	Lauritsen Lab. of Physics California Inst. of Techn 91125 PASADENA CA USA
HAYOT Fernand	SPh-T CEN Saclay 91191 GIF/YVETTE Cedex FRANCE
HEIMLICH Friedrich	Inst. f. Experimental Physik Univ. Hamburg, Luruper Ch. 2000 HAMBURG 50 FEDERAL REP. GERMANY
HEYLAND Dietmar	Univ. Siegen - Inst. f. Physik Gesamthochschule 5900 SIEGEN 21 FEDERAL REP. GERMANY
JARFI Mohamed	Lab. de Phys. Théor.-Dept Phys Ave Ibn Batouta - BP 1014 RABAT MAROC
JARLSKOG Cecilia	Physics Dept.- Stockholm Univ. Vanadisvagen 9 11346 STOCKHOLM SWEDEN
JARLSKOG Goran	Dept. of Physics - Lund Univ. Solvegatan 14 223 62 LUND SWEDEN
JENSEN Terrence	Dept. of Physics Ohio Sate University 43210 COLUMBUS OHIO USA
KALMUS George	Rutherford and Appleton Lab. Chilton OX11OQX DIDCOT UNITED KINGDOM

KARL Gabriel
Dept. of Physics
University of Guelph
N1G 2W1 GUELPH
CANADA

KITAMURA Shoichi
Physics Dept.- Faculty of Scie
Fukazawa 2-1-1 Setagaya-Ku
158 TOKYO
JAPAN

KUHN Johann H.
C.E.R.N
TH Division
1211 GENEVA 23
SWITZERLAND

LEE-FRANZINI Juliet
Dept. of Physics
SUNY at Stony Brook
11794 STONY BROOK NY
USA

LONGO Michael
Dept. of Physics
Univ. of Michigan
48104 ANN ARBOR MI
USA

LUTZ Anne-Marie
L.A.L. - Bat. 200
Université Paris Sud
91405 ORSAY Cedex
FRANCE

MACHET Bruno
L.A.P.P.
B.P. 909
74019 ANNECY LE VIEUX CEDEX
FRANCE

MANNELLI Italo
C.E.R.N.
EP Division
1211 GENEVA 23
SWITZERLAND

MATTEUZZI Clara
C.E.R.N.
EP Division
1211 GENEVA 23
SWITZERLAND

MERONI Chiara
INFN - Sezione di Milano
Univ. di Milano-Celoria 16
20133 MILANO
ITALY

MIRANDA Pedro
Inst. Langevin (ILL) - 156 X
Ave des Martyrs
38042 GRENOBLE CEDEX
FRANCE

MOHAPATRA Rabindra
Dept. of Physics and Astronomy
Univ. of Maryland
20742 COLLEGE PARK MD
USA

MONTANET Lucien	C.E.R.N. EP Division 1211 GENEVA 23 SWITZERLAND
NARDULLI Giuseppe	INFN - Univ. di Bari Via Amendola 173 70126 BARI ITALY
NISHIKAWA Koichiro	Physics Dept-EFI Chicago Univ. 5640 S. Ellis Ave. 60637 CHICAGO IL USA
OLIVER Luis	L.P.T.P.E. - Bat. 211 Université Paris Sud 91405 ORSAY Cedex FRANCE
ONO Seiji	Physics Dept.- Univ. of Tokyo 7-3-1 Hongo-Bunkyo-Ku 113 TOKYO JAPAN
ORR Robert S.	Dept. of Physics Toronto University M5S 1A7 TORONTO CANADA
PASCHOS Emmanuel A.	Institut fur Physik Dortmund Univ, Box 500500 4600 DORTMUND 50 FEDERAL REP. GERMANY
PATEL Girish Dahyabhai	Physics Dept. - Liverpool Univ Oliver Lodge Lab, Box 147 L69 3BX LIVERPOOL UNITED KINGDOM
PEACH Ken	C.E.R.N. EP Division 1211 GENEVA 23 SWITZERLAND
PETROFF Pierre	L.A.L. - Bat. 200 (& CERN EP) Université Paris Sud 91405 ORSAY Cedex FRANCE
PEYAUD Bernard	D.Ph.P.E CEN Saclay 91191 GIF/YVETTE Cedex FRANCE
PHAM Trinang	Centre de Physique Théorique Ecole Polytechnique 91128 PALAISEAU FRANCE

PICEK Ivano	Dept. of Physics - Box 1016 Rudjer Boskovic Inst 41 001 ZAGREB YUGOSLAVIA
PIERAZZIMI Giuseppe	INFN - Sezione di Pisa Via Livornese 582/A 56010 PISA ITALY
PUGLIESE Alessandra	Dipt di Fis.-Univ. degli Studi Piazzale Aldo Moro 2 00185 ROMA ITALY
RICHARD Jean Marc	Inst. Laue Langevin - 156 X Ave des Martyrs 38042 GRENOBLE CEDEX FRANCE
ROOS Matts	High Ener. Phys.-Helsinki Univ Siltavuorenpenger 20 C 00170 HELSINKI 17 FINLAND
ROSNER Jonathan L.	Enrico Fermi Inst-Chicago Univ 5640 S. Ellis Avenue 60637 CHICAGO IL USA
ROY D. P.	Lehrstuhl Exp. & Theor. Physik Dortmund Univ, Box 500500 4600 DORTMUND 50 FEDERAL REP. GERMANY
RUBINSTEIN Hector	Physics Dept.- Stockholm Univ. Vanadisvagen 9 113 46 STOCKHOLM SWEDEN
RUCKL Reinhold	Max Planck Inst. Kernphysik Postfach 40 12 12 8000 MUNCHEN 40 FEDERAL REP. GERMANY
RUGGIERI Federico	INFN - Dipt. di Fisica Via Amendola 173 70126 BARI ITALY
SANDA Anthony I.	Physics Dept.-Rockefeller Univ 66th Street York Ave 10021 NEW YORK NY USA
SANDER Heinz Georg	C.E.R.N. EP Division 1211 GENEVA 23 SWITZERLAND

SCHMIDT Michael	Physics Dept - Yale University P.O. Box 6666 06510 NEW HAVEN CT USA
SCHOBERL Franz	Inst. f. Theorestische Physik Boltzmangasse 5-Wien Univ. 1090 WIEN AUSTRIA
SCHUBERT Klaus R.	Inst. f. Hochenergiephysik Univ Heidelberg-Shroderstr 6900 HEIDELBERG FEDERAL REP. GERMANY
SCIUBBA Adalberto	Ist. di Fisica, Univ di Roma Pzale A. Moro 2 00185 ROMA ITALY
SEEBRUNNER Hansjorg	Max Planck Inst. Kernphysik Postfach 40 12 12 8000 MUNCHEN 40 FEDERAL REP. GERMANY
SIEBERT Hans Wolfgang	Physikalisches Inst-Heidelberg Philosophenweg 12 6900 HEIDELBERG FEDERAL REP. GERMANY
SILVERMAN Albert	Lab. of Nuclear Studies Cornell University 14853 ITHACA NY USA
SLAUGHTER Anna Jean	FERMILAB - E630-Yale - MS 219 P.O. Box 500 60510 BATAVIA IL USA
SMADJA Gérard	D.Ph.P.E CEN Saclay 91191 GIF/YVETTE Cedex FRANCE
SQUARCIA Sandro	INFN - Dipt di Fisica Via Dodecaneso 33 16146 GENOVA ITALY
STECH Berthold	Theor. Physik Inst.-Heidelberg Philosophenweg 16 6900 HEIDELBERG FEDERAL REP. GERMANY
STEINER Herbert	LBL & Dept of Physics Univ. of California 94720 BERKELEY CA USA

SUTHERLAND David George
Dept of Natural Philosophy
Glasgow University
G128QQ GLASGOW
UNITED KINGDOM

TAXIL Pierre
Centre Phys. Theor - CNRS
U.E.R. de Luminy-Case 907
13288 MARSEILLE Cedex 02
FRANCE

THOMAS Jenny A.
High Energy Nucl. Phys. Group
Imperial College
SW7 2BZ LONDON
UNITED KINGDOM

THRESHER John James
Rutherford and Appleton Lab.
Chilton
OX11OQX DIDCOT
UNITED KINGDOM

TORNQVIST Nils A.
Dept of High Energy Physics
Siltavuorenpenger 20 C
00170 HELSINKI 17
FINLAND

TRAN THANH VAN Jean
LPTPE - Bat. 211
Université Paris Sud
91405 ORSAY CEDEX
FRANCE

TURKE Ulrich
Theoretische Physik III
Dortmund Univ, Box 500500
4600 DORTMUND 50
FEDERAL REP. GERMANY

TURLAY René
D.Ph.P.E
CEN Saclay
91191 GIF/YVETTE Cedex
FRANCE

USLER Harald
Theoretische Physik III
Dortmund Univ, Box 500500
4600 DORTMUND 50
FEDERAL REP. GERMANY

VERRECCHIA Patrice
D.Ph.P.E
CEN Saclay
91191 GIF/YVETTE Cedex
FRANCE

VILAIN Pierre
Inst f. High Energ - (ULB-VUB)
Bruxelles Univ-Pleinlaan 2
1050 BRUSSELS
BELGIUM

VONCK Bertold
IIHE - VUB
Pleinlaan 2
1040 BRUSSELS
BELGIUM

WAHL Heinrich	C.E.R.N. EP Division 1211 GENEVA 23 SWITZERLAND
WEILHAMMER Peter	C.E.R.N. EP Division 1211 GENEVE 23 SWITZERLAND
WIRBEL Manfred	Inst. f. Theoretische Physik Heidelberg Universitat 6900 HEIDELBERG FEDERAL REP. GERMANY
WOLFENSTEIN Lincoln	Dept. of Physics Carnegie Mellon University 15213 PITTSBURGH PA USA
WRIGHT Peter R. S.	Nuclear Physics Lab. Oxford Univ., Keble Road OX1 3RH OXFORD UNITED KINGDOM